

APPENDIX A
DEMONSTRATION and SENSITIVITY STUDIES

The material in Appendix A is from demonstration and sensitivity studies performed and documented to support the methodology and NRC review and approval of Revision 0 of this EM. Only acknowledged error corrections have been incorporated into Revision 2 along with pointers to other material that changes, amends, or provides additional information deemed important to define the methodology.

This page is intentionally left blank.

A.1. Introduction

Numerous sensitivity studies were performed with the evaluation model to demonstrate its acceptability to analyze LOCA, to provide a basis for the selection of input parameters, and to satisfy the requirements of Appendix K. These studies were performed with RELAP5/MOD2-B&W (Ref. A-1) to determine the magnitude of the variations on key results. They were also used to demonstrate compliance and convergence of the EM methods given in Section 4 of this topical text volume. The results of these studies, and the conclusions reached, are described in this appendix.

A.1.1. SBLOCA Transient Progression

The transient progression is briefly summarized here to identify the key phenomena and controlling thermal-hydraulic behavior during each phase of the event. The results of the sensitivity studies will refer to this information to avoid repeating the text required for each section.

The SBLOCA generally progresses through five phases: (1) subcooled depressurization, (2) pump and loop flow coastdown and natural circulation, (3) loop draining, (4) boiling pot, and (5) refill and long-term cooling. The subcooled depressurization phase begins at leak initiation. Subcooled reactor coolant system (RCS) liquid exits the break, and the pressurizer begins to empty. The RCS depressurizes quickly to the low pressure reactor trip setpoint, and then to the low pressure engineered safety features actuation setpoint (ESFAS) trip. High pressure injection (HPI) flow begins after a conservatively long ECCS delay time. When the low fluid subcooling setpoint is reached, and ESFAS has occurred, the RC pumps trip and begin to coast down. MFW pump coastdown begins on turbine trip plus a reasonable delay time. The MFW flow is terminated following a

typical pump coastdown. Total loss of the MFW flow occurs shortly after ESFAS. The subcooled depressurization phase ends when the hot leg liquid saturates.

Following RCP trip, the RCS flow transitions to a natural circulation flow condition. The continued RCS depressurization initiates liquid flashing in the hot legs and the upper plenum, allowing a steam bubble to form in the upper head and hot leg U-bends. Natural circulation ends when the U-bend steam bubble displaces the hot leg mixture levels below the hot leg spillover elevation. The hot leg containing the pressurizer surge line connection generally loses flow first because of the additional flashing of the saturated pressurizer liquid that enters during the subcooled depressurization. Intermittent hot leg spillovers can cause alternating periods of RCS repressurization and depressurization for the smaller break sizes.

As the entire RCS approaches saturated conditions, the onset of subcooled and saturated nucleate boiling occurs in the core because of the high decay heat levels. The fuel stored energy is removed via the steam generators during this RCS flow coastdown period. The core steam production, combined with the eventual loss of SG heat removal, interrupts the RCS depressurization. In the reactor vessel (RV), the steam bubble in the upper head displaces enough liquid to uncover the RVVs creating a manometric imbalance between the core and the downcomer. The imbalance forces the RVVs to open and pass steam into the downcomer. The downcomer steam volume grows until the cold leg nozzle is exposed to steam. As soon as the downcomer liquid level reaches the cold leg nozzle spillover elevation, a core steam venting path is created, allowing continuous RCS depressurization.

During the loop draining phase, the steam bubble becomes large enough in the hot legs that the primary liquid level is displaced into the SG tube region below the secondary-side auxiliary feedwater (AFW) nozzles. A boiler-condenser mode (BCM) of heat

transfer is initiated if the AFW is flowing. Periods of BCM cooling, in addition to the HPI-leak cooling, allow the RCS pressure to decrease more rapidly.

The trapped hot leg liquid mass continues to decrease due primarily to flashing. If the RV outlet annulus mixture level decreases below the hot leg nozzle spillunder elevation, steam will pass up the hot leg, and liquid will drain back into the vessel. This allows the mixture level in the outlet annulus to remain near the top of the hot leg nozzle until the hot leg is completely empty. A loop seal exists in the cold leg pump suction piping. (For a raised-loop plant, the elevation of the cold leg pump suction (CLPS) spillover is approximately the same elevation as the top of the core.) Larger breaks continue to rapidly depressurize the RCS and flash the liquid in this region.

If the levels descend to the CLPS spillunder elevation (particularly in raised-loop analyses), the loop seal clears, and another steam relief path, in addition to the RVVVs, is established between the core and the break.

At the end of the loop draining period, the only system inventory available for core cooling is the emergency core cooling system (ECCS) injection and the remaining liquid in the reactor vessel. This portion of the transient is characterized as the boiling pot mode. The RV levels will decrease if the ECCS injection cannot match the liquid vaporization due to core decay heat, passive metal heat, and flashing. Continued voiding at the break site allows continuous system depressurization until the core flood tank (CFT) fill pressure is reached or the ECCS injection matches liquid boil-off and flashing rates. During this period, the RV mixture levels may descend into the core heated region resulting in cladding temperature excursions.

An increasing RV liquid inventory signals the end of the transient. At this point, the ECCS flow heat removal exceeds the core boiling, wall energy addition, and liquid flashing

contributions. The suppression of core steam production, or the continuation of operator-controlled secondary depressurization, further depressurizes the RCS. This continued RCS depressurization supports higher ECCS injection rates. The additional ECCS flow assures that the core can be refilled, and all cladding temperature excursions quenched. Once the core has been completely refilled, a path to long-term cooling is established.

A.1.2. Base Model and Description of Studies

The first step to completing the studies in this appendix was the selection of a base or reference case. A break in the bottom of the cold leg piping between the reactor vessel inlet nozzle and the pump discharge nozzle was chosen. This break geometry and location were chosen based on the most severe SBLOCA reported in previous licensing calculations for a B&W raised-loop plant (Ref. A-2) and a preliminary spectrum analysis performed before any sensitivity studies were begun. This break size represents a reasonable starting point from which to begin sensitivity studies. The possible variation of the worst break size and location will be encountered as the studies progress.

The base case used the raised-loop, 205-fuel assembly plant with Mark-BW 17-by-17 fuel assemblies and an initial power level of 3800 MW. An axial power shape with a [] peak at the 9.705-ft elevation was selected for use. The hot channel contained [] assemblies with a peak linear heat rate initialized at 16.5 kW/ft.

The plant design selected for these studies was a representation of the 205-FA RL design. Although the 205-FA RL design was selected, the trends and conclusions reached in the applications are applicable to all classes of B&W-designed plants. Trip setpoints, delay times, and lengths of the phases are different between the plants, but these differences do not affect the conclusions drawn about the compliance or convergence of the methods.

Previous SBLOCA analyses performed on B&W-designed plants have not predicted core uncovering and cladding temperature excursions. However, demonstration of converged cladding temperature predictions during temperature excursions should be included in the SBLOCA EM sensitivity studies. To assure cladding heatup, the nominal CFT fill pressure of 615 psia was artificially reduced by 100 psia to 515 psia. This reduction delayed CFT injection and allowed the core boiling and flashing terms to decrease the core liquid inventory beyond the point where cladding temperature excursions occurred.

The input model for the raised-loop plant was developed based on the requirements identified in Section 4. Individual cases were performed with variations on user-requested time step size, pressurizer location, core crossflow resistance, and core noding.

For these studies, general comparison plots are provided for the primary system pressure, break mass flow rate, RV mixture level, RV collapsed level, and hot channel cladding temperatures.

Following completion of these comparison studies, the full cold leg pump discharge (CLPD) break spectrum, core flood line resistance study, break discharge study, core flood line break, and high pressure injection line break cases were performed. After completion of the spectrum analyses and sensitivity studies, a final, most-severe break case was performed with slight changes in the base case modeling. For these cases, plots of the system pressure, vessel collapsed levels, break and ECCS mass flow rates, break-node void fraction, RCS loop collapsed levels, CLPS liquid volumes, RVVV and hot leg filtered mass flow rates, core mixture levels, and upper core hot and average channel cladding and steam temperatures are provided. The timing of key events during the transient such as reactor trip, ESFAS, AFW actuation, reverse heat transfer, CFT actuation, peak clad temperature, and core refill are also summarized in tables.

This page is intentionally left blank.

A.2. SBLOCA Time Step Study and Base Case Results

The first study performed was the time step sensitivity study. In RELAP5/MOD2-B&W, the user specifies a maximum time step that is modified by the RELAP5/MOD2-B&W internal time step control in the event of convergence or Courant limitations. However, neither the RELAP5/MOD2-B&W convergence criteria nor the Courant limitation, both being large break-oriented, necessarily assure converged results for small break LOCAs. Therefore, to demonstrate the convergence of the SBLOCA calculations, several cases were analyzed with varied time step requests.

Time step sizes of 10, 20, and 25 milliseconds were used in this sensitivity study. The time step size of 10 milliseconds for the first case was chosen based on the allowable size used for previous SBLOCA analyses performed on recirculating steam generator plants (Ref. A-3). This time step was much smaller than the values used for previous MIST benchmarks (Ref. A-4), therefore, increases in the allowable time step were investigated.

The time step was increased to 20 and 25 milliseconds for cases two and three, respectively, to establish an optimum time step that would minimize the RELAP5/MOD2-B&W code run-time for the SBLOCA transient, while demonstrating adequate convergence of results. Comparison results for this study are presented in Figures A-1 through A-6 and in Table A-1.

The comparison plots show slight variations in RCS pressure and pump suction liquid volumes between the first two cases. For the 20-millisecond time step, more liquid flowed into the downcomer and reactor vessel from the pump suction regions. Consequently, the core collapsed level was slightly higher resulting in later cladding heatup. The cladding heatup profile, however, was almost identical to the 10-millisecond case after accounting for the time shift due to the collapsed liquid level differences. The variations of the peak clad temperature predictions were within 10

F, demonstrating well-converged results. This convergence allows the base time step to be increased to 20 milliseconds.

The system response for the 25-millisecond case was similar to that of the 20-millisecond case. The system pressure, reactor vessel collapsed liquid levels, core mixture levels, and cladding heat-up predictions followed each other closely until the CFT fill pressure was reached. Following the initiation of CFT, the 20-millisecond case had a sustained increase in break flow that the 25-millisecond case did not. As a result, the core mixture level recovery was slower, and the peak cladding temperature was approximately 60 F higher. Had the HPI fluid not been continuously carried out the break in this case, the mixture levels and the cladding temperature profiles would have been almost identical to those predicted for the 25-millisecond case.

The results of the time step sensitivity study indicate that a time step of 25 milliseconds begins to produce divergent results during the later portion of the SBLOCA transient. Smaller requested time steps of 20 and 10 milliseconds produce converged results with a peak cladding temperature variation of less than 10 F. Since the results of smaller time step cases were effectively the same, the larger time step of 20 milliseconds will be used for all future studies to improve code run time.

The 0.1-ft² CLPD break with a 20-millisecond time step was selected as the base case for subsequent studies. The overall results of this analysis are shown in Figures A-7 through A-20 and are summarized in Table A-1. The following paragraphs present the progression of the base case transient in detail.

Following the break opening, the RCS depressurized to the low pressure reactor trip setpoint of 1885 psia by 12.3 seconds. An 0.65-second delay time was used for control rod scram and turbine trip. Turbine trip caused a main feedwater (MFW) pump trip, and after a 12-second delay, the MFW flow was terminated. A loss-of-

offsite-power (LOOP) was assumed to be coincident with reactor trip. The RC pumps were tripped on the 1615 psia ESFAS trip at 19.8 seconds. A conservative 60-second delay time was assumed for ECCS activation. A level-rate-dependent AFW flow controller, which initiated on ESFAS with a 40-second delay time, was used to fill the secondary level from 3 ft to 11.5 ft above the upper face of the lower tube sheet (UFLTS). The UFLTS is also the datum for the RCS system elevation plots.

During the subcooled depressurization and the loop flow coastdown phases, the RCS pressure dipped to 1475 psia. Hot leg U-bend voiding decreased the natural circulation loop flows causing a reduction in the primary-to-secondary heat transfer. The decrease in steam generator heat removal and the core boiling caused the subsequent repressurization of the RCS to 1600 psia. At approximately 100 seconds, AFW flow began. By this time, the primary levels had descended into both steam generators, resulting in high-elevation BCM cooling. As a result, the RCS pressure declined steadily during the loop draining phase due to the combined leak-HPI and BCM cooling. The AFW terminated at 490 seconds as the secondary levels reached the maximum control level of 11.5 ft. The RCS depressurization slowed after the BCM cooling was lost. The loop draindown maintained lower quality at the break that limited the volumetric discharge out of the break. Loop draining was completed by 1000 seconds. Without the RCP liquid spillover from the loop draining, both the leak quality and volumetric discharge increased. This improved leak-HPI cooling increased the RCS depressurization rate and marked the beginning of the boiling-pot phase.

The reactor vessel mixture level descended into the heated core region by 2050 seconds, resulting in a cladding temperature excursion in the upper-most heated segment. Two additional segments were uncovered before the RCS pressure reached the CFT fill pressure at 2280 seconds. The CFT flow initiated a slow core refill which eventually halted the cladding temperature increase.

A peak cladding temperature (PCT) of 1057 F occurred in Segment 20 at 2523 seconds. The core refill was slow but steady when the calculations were stopped at 3000 seconds.

A.3. SBLOCA Pressurizer Location Study

The pressurizer was connected to the intact loop in the base case analysis. In this study, the pressurizer surge line connection was moved from Control Volume 105 to Control Volume 205 in the broken loop. Comparison results are presented in Figures A-21 through A-26 and in Table A-2.

The revised pressurizer location produced results almost identical to those of the base case up to the time of CFT injection. Following the initiation of CFT, the base case had a sustained increase in break flow that the revised pressurizer location case did not obtain. In both cases, a portion of the intact loop HPI liquid was carried out the break when CFT injection began. The carryout was sustained in the base case, but not in the revised pressurizer location case. (Refer to discussion in Section A.4 regarding this phenomenon.) This occurrence caused a lower core mixture level in the base case than that predicted in the revised pressurizer location case. Consequently, the peak cladding temperature in the base case was 18 F higher and occurred approximately 100 seconds later in the transient. Had the HPI fluid not been continuously carried out the break in the base case, the mixture levels and the cladding temperature profiles in both cases would have been nearly identical. Since the variation between these cases was small, the pressurizer will remain connected to the intact loop for all future analyses.

This page is intentionally left blank.

A.4. SBLOCA Core Crossflow Resistance Study

The approach used to develop the crossflow areas and form loss factors was established by considering the thermal-hydraulics of channels that have significantly different radial power factors. In the hot channel, additional boiling produces higher void fractions, which tend to create more mixture level swell. The void gradient in the pool region is sustained only if the cross flow is relatively small. Once the core-average mixture level is reached, the hot channel level swell increase is restricted as the elevation head quickly disperses the welling up of the frothy mixture. Modeling of this behavior in RELAP5/MOD2-B&W is achieved through a segmented crossflow form loss method that uses higher resistances in the pool region and lower resistances from the hot-to-average channel near or above the mixture level interface. Additionally, the average-to-hot resistance near or above the mixture level is set to a higher value to minimize the potential effect of mixing with cooler average channel fluid with that of the hot channel. Table A-3 shows the recommended form loss coefficients. The fluid behavior in each channel is observed during this study to assure that reasonable thermal-hydraulic effects are produced by this modeling technique. A sensitivity study is also performed to confirm that the results produced by this technique are appropriate and converged.

Table A-3 presents the various core crossflow form loss factors and the case parametrics for this sensitivity study. The results of the core crossflow study are presented graphically in Figures

A-27 through A-44. A short description of the various crossflow-related results is provided for the base case as well as the other three sensitivity study cases. In addition, Table A-4 gives a summary of the key SBLOCA parameters for the four cases.

The base case results for the 0.1-ft² break are given in Figures A-7 through A-20. Figure A-16 shows that the hot and average channel mixture levels are in agreement for the majority of the transient. The level variations noted when the mixture level is within the heated core region show that the hot channel swell slightly exceeds the average channel swell, as expected.

Note: The base case core crossflow modeling was selected as the method to be applied in the EM calculations based on the studies described in this section. The demonstration case used a fixed resistance based on the Base Case inputs from Table A-3. Subsequent SBLOCA applications revealed that the user selection of where the form loss transition was modeled resulted in some variation in the predicted PCTs. In Revision 4 of RELAP5/MOD2-B&W code (Reference A-1), a model was created to automatically adjust the location of where the break point is between the high and low resistances based on the adjoining control volume void fractions. This void-dependent core crossflow model, which was developed after the EM was submitted, was approved for use in B&W plant SBLOCA analyses as stated in the RELAP5 SER on Revision 4.

A.4.1. High Crossflow Resistance Study: Case A

The crossflow resistances used in the base case were replaced with the Case A values given in Table A-3. In this case the higher resistances tended to separate the fluid channels and allow larger asymmetries to be established. The results of this analysis are summarized in Table A-4 and plotted in Figures A-27 through A-40.

Figure A-32 shows the mixture levels for the Case A results. The hot channel level was consistently six to eight inches above the

average channel level. The higher hot channel level swell was expected, but a difference of more than several inches was considered excessive. The additional hot channel level swell reduced the peak cladding temperature by 246 F as shown in Figure A-36. This large variation was produced by a combination of the reduced length of the dry steam region and the shorter duration of the uncovering. In Case A, only two heat structure segments underwent a dryout and heatup, whereas the base case resulted in the dryout and heatup of three segments.

A.4.2. Low Crossflow Resistance Study: Case B

Case B used the base case model with the low crossflow resistances listed in Table A-3. In this case, the communication between the two channels was improved by reducing the crossflow form loss coefficients. The results of the analysis are shown in Figures A-27 through A-40. Figure A-33 shows the close agreement between the two mixture levels. The peak cladding temperature in this case, shown in Figure A-36, was 123 F below that of the base case.

Three segments uncovered briefly in both analyses. The hot channel void distribution, shown in Figure A-43, was observed to be wavy as cross flows circulated to balance the manometric differences between the channels. These rapid fluctuations of the hot channel void fraction represent a potential problem in that they can lead to inconsistent, and possibly un-reproducible results. In the cases using higher resistances, stable void distributions were established in which the additional hot channel boiling created a void fraction response that closely followed that of the average channel. Figures A-41, A-42, and A-44 give the void distribution for the base case and the other two crossflow studies.

A.4.3. Reduced Upper Region Crossflow Resistance Study: Case C

[] mixture levels (Figure A-34) for Case C indicates that the hot and average channel mixture levels were in close agreement and match those of the base case until 2400 seconds in the transient. After that time, the mixture level in Case C recovered faster than that of the base case.

A close examination of the two cases indicated that the mixture level recovery was not due to the crossflow form loss changes, but to a variation in liquid discharge out of the break. The leak flow plot for the base case (Figure A-29) had a sustained increase in break flow during the CFT injection period. None of the other cases showed this increase. The cause of the increase was carryout of intact loop HPI liquid to the break. Upon CFT injection, the horizontal stratification model used in the cold leg pump discharge volumes switched from a stratified to non-stratified condition. As a result, each of the intact leg upper cold leg junctions allowed liquid to flow into the downcomer Volume 303 and across to the broken cold leg.

In the base case, the horizontal stratification mode was never regained, therefore, intact loop HPI liquid carryout continued. In Case C, however, the horizontal stratification mode was lost only momentarily. Liquid carryover was not sustained with any of the other crossflow study cases. This behavior was only noted in the base case. It resulted in less water reaching the core for the base case, than for Case C, and thus a lower mixture level. Figures A-30 and A-31 graphically demonstrate this unexpected nonphysical behavior.

In order to compare the base case with Case C it was desirable to equate the amount of HPI carryout into an equivalent mixture

level. Assuming that all of the intact loop HPI reached the vessel, the difference in the break flow rates was integrated from 2300 seconds until the end of the transient. The integrated liquid would have entered the downcomer in the base case and contributed to the vessel inventory. A mixture level advancement rate of 0.00187 ft/sec was calculated for the base case. Thus, by 3000 seconds the mixture level would have been at the top of the core, and there would have been virtually no difference in the mixture level between the base case and Case C.

By using the base case mixture level adjustment, it was concluded that the form loss factors used in the base case and Case C are equally acceptable. The form loss factors for the base case are

This page is intentionally left blank.

A.5. SBLOCA Core Channel Modeling Study



AREVA NP, INC.

BAW-10192NP-02

This page is intentionally left blank.

A.6. CLPD Break Spectrum

Previous small break LOCA experience (from Ref. A-5) has demonstrated that the most limiting small break location is at the bottom of the cold leg pump discharge piping. A break in the hot leg piping results in earlier saturation at the break site and continuous venting of steam out the break. Also, in a hot leg break all HPI is available for core cooling, whereas in a limiting CLPD break nearly all of HPI flow into the broken leg is lost out of the break and is unavailable for core cooling. The SBLOCA studies therefore, modeled a spectrum of small breaks in the bottom of the cold leg pump discharge piping.

Break sizes ranging from 0.04 ft² to 1.43 ft² were included in the spectrum study. Specifically, break sizes of 0.04, 0.07, 0.1, 0.125, 0.15, 0.175, 0.2, 0.3, 0.5, 0.75, 1.0, and 1.43 ft² were analyzed. The study concentrated on breaks in the 0.1-ft² to 0.2-ft² size to ensure that the most limiting peak cladding temperature (PCT) was determined. For discussion purposes, the breaks were divided into three groups (small, intermediate, and large) based on break size.

Composite results for the spectrum of bottom-of-the-pipe CLPD SBLOCAs are presented in Figures A-205 through A-212, with additional results summarized in Tables A-6 through A-8. These analyses used an artificially low CFT fill pressure to delay CFT injection flow. As a result, the vessel mixture level descended into the core heated region causing a maximum clad temperature excursion that reached 1057 F for the 0.1-ft² CLPD break.

A.6.1. Small CLPD SBLOCAs (0.04, 0.07, 0.1, 0.125 ft²)

The smallest LOCAs challenge the high pressure ECCS systems to provide makeup flow to offset core boiling and maintain continuous core cooling. Breaks of 0.04, 0.07, 0.1, and 0.125 ft² were

considered in this range. The RCS depressurization rates are relatively slow for these breaks. As a result, each of the five phases of the transient were easily identified.

The 0.04-ft² break was the smallest CLPD break performed. The results of the analysis are shown in Figures A-51 through A-64 and summarized in Table A-6. This break size quickly depressurized the RCS until liquid in the hot legs and upper reactor vessel liquid saturated, ending the subcooled blowdown phase within 60 seconds. Flashing in the hot legs formed a steam bubble in the U-bend that displaced the riser mixture levels below the U-bend spillover elevation, interrupting natural circulation.

Intermittent hot leg spillovers occurred between 300 and 700 seconds. The spillovers reactivated primary-to-secondary heat removal and caused alternating periods of RCS depressurization and repressurization. As the steam spaces grew, the levels were forced into the steam generator tube regions, initiating high elevation BCM heat removal.

The loop draindown period began at the cessation of the last hot leg spillover. An orderly cooldown commenced once operator action was taken at 2700 seconds after ESFAS to depressurize the secondary-side at a rate of 100 F per hour. Continual depressurization of the secondary side resulted in flashing and heat transfer that reduced the inventory below the control level. AFW, actuated to maintain the control level, reactivated a continuous BCM heat removal process. HPI and SG condensate matched the core decay heat, wall heat, and flashing contributions prior to CFT injection.

The boiling pot phase was never reached for this break size. The hot legs were not completely emptied, therefore the core remained covered throughout the transient. The peak cladding temperature for this transient was the initial steady-state value.

The 0.07-ft² break results are shown in Figures A-65 through A-78 and summarized in Table A-6. This break size caused more rapid liquid loss that ended the flow coastdown phase by 200 seconds. After the break flow saturated, the increased volumetric discharge allowed leak-HPI cooling to continuously depressurize the RCS. At approximately 400 seconds, a high-elevation BCM occurred, and AFW terminated shortly thereafter as the secondary control level was reached.

The slow RCS depressurization continued during the loop draining phase due to leak-HPI cooling. At 1620 seconds, both hot legs emptied. This draining marked the beginning of the boiling pot phase. The reactor vessel collapsed and mixture levels declined until the CFT fill pressure was reached at 4160 seconds. The additional ECCS flow matched the boiloff and flashing rates in the vessel, and initiated the refill phase. The minimum core mixture level remained above the heated core region throughout the event, preventing any clad temperature excursion.

The 0.1-ft² break, shown in Figures A-7 through A-20 (base case), behaved similarly to the 0.07-ft² break. The hot leg risers in both loops emptied, and the pump suction regions cleared before CFT flow began. Loop draining allowed complete voiding at the break site, which increased the leak volumetric flow rate. The system continuously depressurized because of leak-HPI cooling until the CFT fill pressure was reached at 2270 seconds. During this period, the RV mixture levels dropped into the core heated region resulting in a cladding temperature excursion. The calculated hot channel peak clad temperature was 1057 F. Core refill commenced as soon as the CFT flow began.

The 0.125-ft² break results are shown in Figures A-79 through A-92 and summarized in Table A-6. This increased break size behaved similarly to the 0.1-ft² case. A lower PCT of 779 F was predicted for the 0.125-ft² break size, because of the shorter period in which the core was uncovered by the mixture level. The duration

of the uncovering was so short that clad temperatures did not rise to values at which decay heat was matched by steam cooling, as noted in the 0.1-ft² case. Therefore, the PCT observed in this case was lower.

A.6.2. Intermediate CLPD SBLOCAs (0.15, 0.175, 0.2, 0.3 ft²)

Four intermediate CLPD breaks were performed with break areas of 0.15, 0.175, 0.2, 0.3 ft². These break sizes caused the RCS to depressurize faster and to enter the boiling pot phase sooner. Steam generator heat removal became ineffective in assisting the RCS depressurization. The core mixture levels continued to drop into the core heated region. A decreasing minimum core collapsed liquid level with increasing break size trend was observed. However, the level swell from flashing, coupled with shorter uncovering periods, produced cladding temperature excursions that peaked at values similar to those of the initial cladding temperatures.

The 0.15- and 0.175-ft² break analysis results are shown in Figures A-93 through A-106 and Figures A-107 through A-120, respectively. The 0.2- and 0.3-ft² break analysis results are shown in Figures A-121 through A-134 and Figures A-135 through A-148, respectively. The sequences of events for the intermediate CLPD SBLOCAs are summarized in Table A-7. The PCT for 0.3-ft² break was only 20 F higher than the initial cladding temperature. The PCT occurred because the time interval in which the mixture level was below the top of the core was slightly greater than the 0.2-ft² case. This increase allowed the cladding to heat up longer and exceed the initial value.

A.6.3. Large CLPD SBLOCAs (0.5, 0.75, 1.0, 1.43 ft²)

The largest SBLOCAs quickly depressurize the RCS and cause significant core voiding and core flow perturbations. These breaks were not expected to be limiting in PCT since the intermediate breaks produced cladding temperatures generally less than or equal to the initial temperatures. These breaks were analyzed specifically to determine the maximum break size that belongs in the SBLOCA classification. Definition of this break size was determined based on the predicted cladding temperature response. Breaks that cause the cladding to undergo initial DNB belong in the transition break region of the LBLOCA spectrum (See Section 4.3.7.1 of Volume I). In this respect, the maximum SBLOCA break size may vary slightly with the plant design. The DNB response is also somewhat dependent on break location, since the location will influence the core flows.

The 0.5-ft² and 0.75-ft² CLPD break results are summarized in Table A-8 and shown in Figures A-149 through A-162 and Figures A-163 through A-176, respectively. These breaks were large enough to depressurize the RCS through saturation and secondary system equilibrium to pressures below the CFT and--eventually--the low pressure injection (LPI) system actuations. The system inventories were severely depleted, and the core levels dropped into the heated core region. The rapid RCS depressurization, however, led to significant mixture level swell from flashing, decay heat, and primary metal contributions. The 0.5-ft² break showed slight core uncovering and cladding heatup, but the heatup was less than that calculated for the 0.3-ft² case. For the 0.75-ft² case, the level swell was adequate to prevent cladding temperature excursions.

The 1.0-ft² CLPD break was the largest break size analyzed using the SBLOCA methodology that produced results characteristic of an SBLOCA. Although the transient progressed rapidly, the distinct phases of a small break are still discernable in Figures A-177

through A-190 and Table A-8. The level swell predicted in the 1.0-ft² case was adequate to maintain mixture levels above the core heated region throughout the event.

The 1.43-ft² CLPD break analysis was performed to identify the "transition" break range where in the system response was more characteristic of a large break LOCA than that of a small break LOCA. The results of this analysis are summarized in Table A-8 and shown in Figures A-191 through A-204. The occurrence of DNB immediately after break initiation indicated the typical large break behavior and established the SBLOCA "transition" break range between 1.0 and 1.43 ft².

In comparable terms, the 1.43-ft² SBLOCA case, with a $C_d = 0.7$ on the Moody discharge model, was equivalent to the LBLOCA break case of 1.0 ft², with a Moody $C_d = 1.0$. Likewise, the 1.0-ft² SBLOCA case represents an 0.7-ft² LBLOCA case. Therefore, the transition from the small to the large break LOCA methods occurred in the 0.75-ft² range when referenced to the LBLOCA break area. This break size was not determined to be an absolute, but rather a reasonable transition point for the calculational models.

A.7. SBLOCA Core Flood Line Resistance Study

AREVA NP, INC.

BAW-10192NP-02

A.8. CLPD Break Correlation Discharge Coefficient Study

For break volume void fractions greater than seventy percent, the spectrum and sensitivity studies used a Moody discharge coefficient of 0.7. Use of this reduced coefficient was based on previous applications contained in BAW-10168 for recirculating steam generator plants. Confirmation of the appropriateness and conservatism of the reduced discharge coefficient method is provided by reanalyzing two spectrum cases using discharge coefficients of 1.0 for all fluid states. For these two cases, the break area is reduced by 0.7 to preserve the saturated break discharge rate and validate the comparison with the previous spectrum case. The 0.1-ft² and 0.3-ft² breaks were chosen for reanalysis because they had the most significant cladding heatups calculated for the entire spectrum.

A.8.1. Reanalysis of 0.1-ft² Break Using 1.0 for the Moody C_d

The 0.1-ft² case was reanalyzed with a break area of 0.07 ft² and Moody and Murdock-Bauman break flow model discharge coefficients of 1.0. The results of the analysis are shown in Figures A-225 through A-238 and summarized in Table A-10. Six comparison plots are given in Figures A-239 through A-244. The primary differences between the two analyses were most obvious during the flow coastdown and early loop draining phase from 50 to 350 seconds. The source of the differences is the break discharge rate during the subcooled and low void two-phase discharge period. The high void break coefficient method used for the reanalysis reduced the peak discharge rate during this period by approximately 30 percent which resulted in a higher RCS pressure. However, the flow coastdown phase lasted approximately 100 seconds longer. During this period, the integrated mass loss (Figure A-242) out of the break exceeded the integrated value obtained with the larger break simulation. As a result, the minimum core liquid inventory was slightly lower and the PCT was higher by 92 F.

A.8.2. Reanalysis of 0.3-ft² Break Using 1.0 for the Moody C_d

The 0.3-ft² case was reanalyzed with a break area of 0.21 ft² and Moody and Murdock-Bauman break flow model discharge coefficients of 1.0. The results of the analysis are shown in Figures A-245 through A-258 and summarized in Table A-10. Six comparison plots are given in Figures A-259 through A-264. The primary differences between the two analyses were most obvious before the loop draindown ended at approximately 220 seconds. The source of the differences is the break discharge rate during the subcooled and low void two-phase discharge period. The high void break coefficient method used for the reanalysis reduced the break discharge rate which resulted in a higher RCS pressure. A maximum RCS pressure difference of 100 psi developed between 80 and 90 seconds.

The pressure difference decreased in magnitude as the transient progressed. The integrated break flows converged by 240 seconds because of additional pump suction liquid loss out of the break. Both vessel liquid inventories declined together from 250 seconds until the CFT flow was initiated. The cladding temperature excursion began five seconds sooner in the 0.3-ft² break as compared with the 0.21-ft² break. Because of the higher system pressure, the CFT flow was delayed by ten seconds for the smaller break area case. This delay led to continued clad heatup that postponed the recovery time by approximately 17 seconds. During that time, the cladding temperature increased to a peak of 789 F. The larger break peak cladding temperature of 742 F occurred 17 seconds earlier.

A.8.3. Conclusions and Break Discharge Coefficient Method Change

The two most severe CLPD breaks identified in the spectrum analysis were reanalyzed with the break area reduced by a factor of 0.7 and all break discharge coefficients set to 1.0. Contrary to expectations, the reanalysis PCTs were slightly higher than the previous cases. Compensating effects from variations in governing transient phases resulted in lower core mixture levels and higher PCTs.

Investigation of the results began with the development of the break discharge coefficient method from BAW-10168 (Ref. 6). That model was based on comparisons against experimental data (Ref. 6, pp. LA-251 through LA-269). It concluded that the Moody critical flow model overpredicted two-phase leak flows for void fractions greater than twenty to thirty percent while underpredicting the flow for lower void fractions. Preservation of the relative discharge rates in the subcooled, two-phase, superheated region was considered important for providing reasonable leak flows in SBLOCA analyses that confirm the adequacy of the ECCS. Overprediction of the two-phase discharge can lead to accelerated RCS depressurization that can increase the ECCS injection, and may result in nonconservative clad temperature predictions. Therefore, the original discharge coefficient application was selected to best represent the relative discharge relationships.

The subcooled discharge coefficient of 1.0 was used because extended Henry-Fauske correlated well against most test data. The two-phase transition region used the Moody model with a discharge coefficient of 1.0. This region was defined with α_{lower} , set to a one-percent void fraction, and α_{upper} , set to seventy-percent void fraction. The Moody two-phase discharge coefficient was set to 0.7 for void fractions greater than seventy percent. The superheated regime coefficient was maintained at a conservatively low value of 0.7, to provide continuity of the break flow at the saturated-to-superheated boundary.

Investigation of the results for both the original spectrum and revised discharge coefficient analyses revealed that during the majority of the transient, especially the critical boiling pot phase, the break volume void fraction was approximately 98 to 99 percent. The data in Reference 6 indicated that the Moody discharge rates were closer to the experimental rates above 95 percent void fraction. That is, the discharge coefficient of 0.7 should be increasing back to 1.0. Therefore, the 0.7 discharge coefficient is not the best choice for typical EM applications. Use of a Moody discharge coefficient of 1.0 is the best choice for the pumps-tripped CLPD SBLOCA analysis. In addition, the superheated regime discharge coefficient should be set to 1.0 to preserve the discharge at the saturated-to-superheated boundary and provide the best estimate of the superheated discharge.

The discharge coefficient method is henceforth changed. The trends and conclusions drawn from the previous spectrum analyses are not invalidated by this change. The break area used in those cases is effectively 70 percent of the reported area. Therefore, the range of break sizes in which cladding temperature excursions occur shifts. The special breaks analyzed in the next section will use the new break discharge coefficient method with all values set to 1.0.

A.9. Special Breaks

A rupture in either a core flood line or a high pressure injection line between the RCS and the first check valve is categorized as a special break. Special breaks present unique challenges to core cooling because they result in reduced ECC flow reaching the RCS. Since these key safety-feature boundary conditions are altered, these breaks are treated as special cases. For these two breaks, the initial pressurizer liquid volume was specified near the lower end of the nominal range to further reduce the RCS liquid inventory and maximize clad temperature excursions.

The break discharge coefficients were set to 1.0 for all phases and correlations for both of these analyses. It is expected that the break fluid state will rapidly transition from subcooled liquid to saturated or superheated steam in these analyses. Therefore, the high or low break void fraction model described in Section 4.3.2.4 is most appropriate for these analyses.

A.9.1. Core Flood Line Break

The core flood line break is identified as a special small break case because of the treatment of the ECCS injection flows, compared with the normal evaluation model scenarios. During a core flood line break, the break location prevents one CFT and one LPI train from injecting into the reactor vessel. If the LPI piping arrangement does not have cross-connect piping that opens valves in both injection lines, then a single failure of the emergency diesel generator leaves the core protection to one CFT and one HPI pump.

The results of the CFT line break, using one CFT and one HPI pump, are presented in Figures A-265 through A-278 and are summarized in Table A-11. The break was assumed to be at the end of the CFT line RV nozzle. The break area was limited by the cross-sectional

area of the nozzle insert to a size of 0.44 ft². Rapid initial depressurization caused reactor trip at 0.44 seconds and ESFAS actuation at 7.72 seconds. The hot leg liquid saturated and the U-bends and upper plenum began voiding almost immediately after the break opening.

Following RC pump trip at ESFAS, pump and loop flow coastdown began. Loop flow ended around 60 seconds. The RCS continued to depressurize through saturation, but the depressurization rate slowed because of flashing and the onset of significant core steam production. At approximately 75 seconds, the RCS pressure dropped below the secondary SG pressure, and the secondary side became a heat source to the primary.

At 150 seconds, the hot leg risers in both loops were empty, and the pump suction regions were clear. Voiding at the break site increased the leak volumetric flow rate, which allowed more rapid depressurization until the CFT fill pressure of 515 psia was reached at 175 seconds. During this period, the RV mixture levels remained continuously above the core heated region. The RV began refilling upon CFT flow initiation. Long-term cooling was ensured as the HPI flow continued and decay heat diminished.

The RVEVs provided a path for the core steam to reach the break. The break voiding assisted the rapid RCS depressurization to the intact CFT fill pressure. Use of the nominal CFT line resistance emptied the tank quickly. From that time on, the residual RV liquid and the HPI were the only cooling sources for the core. The residual inventory provided sufficient time delay such that the decay heat contribution dropped below the HPI absorption capacity. Therefore, the results of this case demonstrate that one CFT and one train of HPI provide adequate cooling to mitigate the consequences of a core flood line break event.

A.9.2. High Pressure Injection Line Break

The high pressure injection line break is identified as a special small break case because this break results in the loss of one of four injection paths to the RCS. Additionally, preferential feeding of the broken line due to its lower back pressure is an additional challenge to the HPI flow that does not apply to other break sites or sizes. The handling of the break location is important in the evaluation of the ECCS performance. The results of the HPI line break are presented in Figures A-279 through A-292, with additional results summarized in Table A-11.

The break was assumed to occur at the end of the HPI line nozzle joining the line to the cold leg pump discharge piping. The break was modeled at the elevation of the HPI nozzle, which was the top of Volume 275. The break area was limited to the cross-sectional area of the nozzle, with the thermal sleeve insert removed (0.02463 ft^2). Following leak initiation, subcooled RCS depressurization caused reactor trip on low pressure at 45.16 seconds and initiated a low pressure ESFAS signal at 72.82 seconds. The ESFAS signal began RC pump coastdown and terminated MFW flow following a 12-second delay. A delay of 600 seconds was assumed after ESFAS before HPI was initiated, and only 50 percent of the HPI was assumed to enter the RCS. At approximately 100 seconds, the hot legs saturated and system flashing caused void formation in the U-bends and the upper plenum.

Following the subcooled depressurization period, the RCS underwent cycles of repressurization and depressurization caused by intermittent spillovers from the hot legs into the primary SG region. When AFW was flowing, high elevation BCM heat transfer rapidly depressurized the RCS. When AFW flow terminated, however, the RCS began repressurizing. The RVVV flow, break flow, and RV collapsed levels responded accordingly.

At 2773 seconds, operator action was taken to cool the secondary side at a rate of 100 F per hour. The operator-controlled RCS depressurization supported higher HPI flow rates. At approximately 4800 seconds, prior to the end of loop draining, the SG heat removal and HPI flow matched all core boil-off due to core decay heat, wall energy, and flashing contributions. Throughout the transient the upper plenum mixture levels remained slightly above the top of the hot leg nozzle. Long-term cooling was ensured as HPI flow increased, and the RCS pressure decreased to the CFT fill pressure.

The results of the HPI line break demonstrate that 50 percent of one HPI train was adequate to mitigate the consequences of an HPI line break event. This percentage of HPI flow offset core decay heat until operator actions were credited to initiate a secondary side cooldown. The cooldown ensured that the RCS pressure would continue its decrease, thereby increasing the HPI flow injection. It also ensured that the CFT fill pressure would be reached, resulting in increased ECCS injection into the RCS. These actions would maintain continuous core cooling throughout the transient.

A.10. Most Severe SBLOCA Case

The most severe SBLOCA case was determined by the spectrum analysis and break discharge coefficient study. The break spectrum study identified the 0.1-ft² break with a Moody C_d of 0.7 on the bottom of the cold leg pump discharge piping as the worst break size and location. The break discharge coefficient study using a break area of 0.07 ft² with Moody C_d of 1.0 produced the highest peak cladding temperature of 1149 F for any case. The results of this most severe SBLOCA case are given in Figures A-225 through A-238, and summarized in Table A-12 for clarity. The artificially low CFT fill pressure of 515 psia, chosen to delay the initiation of CFT flow and core refill, was directly responsible for the cladding temperature excursions. Had a nominal pressure been used, the CFT flow would have actuated before core uncovering began.

AREVA NP, INC.

BAW-10192NP-02

This page is intentionally left blank.

A.11. Summary and Conclusions

Numerous studies were performed and documented in this appendix to demonstrate the adequacy of the SBLOCA methods for 10CFR50.46 calculations. These studies confirmed convergence and identified the relative sensitivity in the calculated results for several key variations in the SBLOCA methods. The artificial lowering of the nominal CFT fill pressure to 515 psia, chosen to delay the initiation of CFT flow and core refill, was effective in producing the desired cladding temperature excursions. The model demonstrated acceptable behavior during cladding temperature excursions imposed by this input specification. If a nominal pressure of 615 psia was used, the CFT flow would have actuated before the mixture level descended into the heated core region. These extrapolations are consistent with the previous EM results that calculated no cladding heatup for SBLOCAs on B&W-designed plants.

The spectrum of CLPD breaks that were performed with the conservative CFT fill pressure predicted cladding heatup for breaks between 0.1 and 0.5 ft² using a Moody C_d of 0.7. The spectrum indicated that the 1.0-ft² break was the largest break that demonstrated typical SBLOCA behavior. The 1.43-ft² break size was not typical of SBLOCA transients. Initial cladding DNB resulted in significant heatup in the first five seconds of the event. This behavior is typical of LBLOCAs and therefore belongs in the transition region defined in Volume I. In comparable terms, the 1.43-ft² SBLOCA spectrum case, with a C_d = 0.7 on the Moody discharge model, is equivalent to the LBLOCA break case of 1.0 ft², with a Moody C_d = 1.0. Likewise, the 1.0-ft² SBLOCA case represents an 0.7-ft² LBLOCA case. Therefore, the transition from the small to the large break LOCA methods occurs in the 0.75-ft² range when referenced to the LBLOCA break area or the revised SBLOCA break Moody discharge coefficient of 1.0. This range is not an absolute but a reasonable transition point for the calculational models.

The worst fuel pin time in life in the SBLOCA EM was addressed by specification of beginning-of-life (BOL) oxide thicknesses and stored fuel energy, with an end-of-life (EOL) fuel pin pressure. The EOL fuel pin pressure was used to increase the likelihood of fuel pin rupture. Clad rupture was not predicted for any case.

The consistency and continuity of the LOCA results calculated with this EM are best demonstrated by a comparison of the peak cladding temperature as a function of break sizes from 0.02463 ft^2 to a full, double area guillotine break of the largest pipe in the RCS. This representative PCT versus break size, shown in Figure A-293, includes the results from Volume I LBLOCA studies. The Volume II SBLOCA results are reported from the spectrum approach using the Moody C_d of 0.7. This figure demonstrates the continuity of results, calculated with the models and methods defined in this three volume EM report for B&W-designed plants.

In summary, the SBLOCA evaluation model conforms and complies with all of the Appendix K features and criteria. The sensitivity and break spectrum studies included in this appendix demonstrate the convergence and adequacy of the methods described in Volume II of this report. Therefore, this EM is acceptable for use in performing 10CFR50.46 SBLOCA applications for all three classes of B&W-designed plants identified in Table 1-1.

A.12. Appendix A References

Note: These references reflect the revision levels of topical reports used in the sensitivity studies reported in this appendix. The most current revisions of the topicals marked with an "*" are discussed in Section 9 and listed in the Section 10 reference list.

- | A-1. *J. A. Klingenfus, et al., "RELAP5/MOD2-B&W -- An Advanced Computer Program for Light Water Reactor LOCA and Non-LOCA Transient Analysis," BAW-10164 Rev. 3, Babcock & Wilcox, Lynchburg, Virginia, October 1992.
- | A-2. BAW-10102, ECCS Evaluation of B&W's 205FA NSS, Revision 2, B&W Nuclear Technologies, Lynchburg, Virginia, December 1975.
- | A-3. *BAW-10168P, "RSG LOCA - BWNT Loss-of-Coolant Accident Evaluation Model for Recirculating Steam Generator Plants." Revision 2, B&W Nuclear Technologies, Lynchburg, Virginia, October 1992.
- | A-4. J. A. Klingenfus and M. V. Parece, "Multiloop Integral System Test (MIST): Final Report - RELAP5/MOD2 MIST Analysis Comparisons (Vol. 10)," NUREG/CR-5395, EPRI/NP-6480, BAW-2078, December 1989.
- | A-5. BAW-10154PA, "B&W's Small-Break LOCA Evaluation Model," Babcock & Wilcox, Lynchburg, Virginia, July 1985.

This page is intentionally left blank.

Table A-1. SBLOCA Time Step Study Sequence of Events.

Parameter	Maximum Requested Time Step		
	<u>10 msec</u>	<u>20 msec*</u>	<u>25 msec</u>
Break Opens (sec)	0.0	0.0	0.0
LP Reactor Trip (sec)	12.32	12.33	12.34
ESFAS (sec)	19.79	19.78	19.8
Subcooled Blowdown Ends (sec)	~40	~40	~40
HPI On (sec)	79.79	79.78	79.8
AFW On (sec)	~110	~110	~110
AFW Off (sec)	~500	~490	~490
Loop Draining Begins (sec)	~160	~160	~160
Boiling Pot Begins (sec)	~1000	~1000	~1010
CFT Actuation (sec)	~2260	~2270	~2270
Refill Begins (sec)	~2260	~2270	~2270
Calculations Stopped (sec)	3000.0	3000.0	3000.0
HC Peak Clad Temp (F) Segment Time (sec)	1063.5 20 2489.9	1057.2 20 2523.4	996.36 20 2384.5
AC Peak Clad Temp (F) Segment Time (sec)	780.12 19 2347.2	742.53 20 2500.1	732.6 20 2378.2

* Designated as Base Case

Table A-2. SBLOCA Pressurizer Location Study Sequence of Events.

Parameter	<u>Base Case</u>	<u>Pressurizer in Broken Loop</u>
Break Opens (sec)	0.0	0.0
LP Reactor Trip (sec)	12.33	12.22
ESFAS (sec)	19.78	19.68
Subcooled Blowdown Ends (sec)	~40	~40
HPI On (sec)	79.78	79.68
AFW On (sec)	~110	~110
AFW Off (sec)	~490	~490
Loop Draining Begins (sec)	~160	~160
Boiling Pot Begins (sec)	~1000	~1000
CFT Actuation (sec)	~2270	~2265
RV Refill Begins (sec)	~2270	~2265
Calculations Stopped (sec)	3000.0	3000.0
HC Peak Clad Temp (F) Segment Time (sec)	1057.2 20 2523.4	1039.4 20 2427.6
AC Peak Clad Temp (F) Segment Time (sec)	742.53 20 2500.1	738.3 20 2420.6

AREVA NP, INC.

BAW-10192NP-02

Table A-3. SBLOCA Core Crossflow Form Loss Factors.

Table A-4. SBLOCA Core Crossflow Study Sequence of Events.

<u>Parameter</u>	<u>Base Case Variable</u>	<u>Case A High Resist</u>	<u>Case B Low Resist</u>	<u>Case C Upper Adj</u>
Break Opens (sec)	0.0	0.0	0.0	0.0
LP Reactor Trip (sec)	12.33	11.88	12.5	12.32
ESFAS (sec)	19.78	19.30	19.98	19.78
Subcooled Blowdown Ends (sec)	~40	~40	~40	~40
HPI On (sec)	79.78	79.30	79.98	79.78
AFW On (sec)	~110	~110	~110	~110
AFW Off (sec)	~490	~490	~490	~490
Loop Draining Begins (sec)	~160	~160	~160	~160
Boiling Pot Begins (sec)	~1000	~1000	~1000	~1000
CFT Actuation (sec)	~2270	~2275	~2275	~2275
Refill Begins (sec)	~2270	~2275	~2275	~2275
Calculations Stopped (sec)	3000.0	3200.0	3200.0	3200.0
HC Peak Clad Temp (F) Segment Time (sec)	1057.2 20 2523.4	811.47 20 2377.7	934.25 20 2403.4	989.37 20 2392.3
AC Peak Clad Temp (F) Segment Time (sec)	742.53 20 2500.1	733.63 20 2385.9	737.46 20 2391.3	735.58 20 2386.6

Table A-5. SBLOCA Core Noding Study Sequence of Events.

<u>Parameter</u>	<u>Base Case</u>	<u>Hot Channel</u>
Break Opens (sec)	0.0	0.0
LP Reactor Trip (sec)	12.33	12.60
ESFAS (sec)	19.78	19.82
Subcooled Blowdown Ends (sec)	~40	~40
HPI On (sec)	79.78	79.82
AFW On (sec)	~110	~110
AFW Off (sec)	~490	~490
Loop Draining Begins (sec)	~160	~160
Boiling Pot Begins (sec)	~1000	~1000
CFT Actuation (sec)	~2270	~2275
RV Refill Begins (sec)	~2270	~2275
Calculations Stopped (sec)	3000.0	3200.0
HC Peak Clad Temp (F) Segment Time (sec)	1057.2 20 2523.4	1068.0 20 2529.7
AC Peak Clad Temp (F) Segment Time (sec)	742.53 20 2500.1	724.67 20 2282.0

Table A-6. Small CLPD SBLOCA Spectrum Sequence of Events.

Parameter	<u>0.04 ft²</u>	<u>0.07 ft²</u>	<u>0.10 ft²</u>	<u>0.125 ft²</u>
Break Opens (sec)	0.0	0.0	0.0	0.0
LP Reactor Trip (sec)	33.1	17.88	12.33	9.54
ESFAS (sec)	41.06	25.6	19.78	16.88
Subcooled Blowdown Ends (sec)	~60	~50	~40	~30
HPI On (sec)	101.08	85.6	79.78	76.88
AFW On (sec)	~130	~120	~110	~110
AFW Off (sec)	~540	~520	~490	~470
Loop Draining Begins (sec)	~320	~180	~160	~140
Boiling Pot Begins (sec)	NA	~1620	~1000	~720
CFT Actuation (sec)	NA	~4160	~2270	~1580
Refill Begins (sec)	NA	~4160	~2270	~1580
Calculations Stopped (sec)	5600.0	4800.0	3000.0	2500.0
HC Peak Clad Temp (F) Segment Time (sec)	722.26 17 0.0	722.26 17 0.0	1057.2 20 2523.4	770.14 20 1658.8
AC Peak Clad Temp (F) Segment Time (sec)	695.46 17 0.0	695.46 17 0.0	742.53 20 2500.1	695.46 17 0.0

Table A-7. Intermediate CLPD SBLOCA Spectrum Sequence of Events.

<u>Parameter</u>	<u>0.15 ft²</u>	<u>0.175 ft²</u>	<u>0.2 ft²</u>	<u>0.3 ft²</u>
Break Opens (sec)	0.0	0.0	0.0	0.0
LP Reactor Trip (sec)	7.62	6.30	5.36	3.44
ESFAS (sec)	14.86	13.4	12.32	9.80
Subcooled Blowdown Ends (sec)	~30	~30	~30	~20
HPI On (sec)	74.86	73.4	72.23	69.82
AFW On (sec)	~110	~115	~120	~130
AFW Off (sec)	~430	~400	~390	~310
Loop Draining Begins (sec)	~110	~110	~100	~60
Boiling Pot Begins (sec)	~530	~400	~340	~220
CFT Actuation (sec)	~1150	~895	~720	~425
Refill Begins (sec)	~1150	~895	~720	~425
Calculations Stopped (sec)	1600.0	1400.0	1000.0	500.0
HC Peak Clad Temp (F) Segment Time (sec)	722.26 17 0.0	722.26 17 0.0	722.26 17 0.0	742.28 20 443.84
AC Peak Clad Temp (F) Segment Time (sec)	695.46 17 0.0	695.46 17 0.0	695.46 17 0.0	695.46 17 0.0

Table A-8. Large CLPD SBLOCA Spectrum Sequence of Events.

<u>Parameter</u>	<u>0.5 ft²</u>	<u>0.75 ft²</u>	<u>1.0 ft²</u>	<u>1.43 ft²</u>
Break Opens (sec)	0.0	0.0	0.0	0.0
LP Reactor Trip (sec)	0.36	0.20	0.16	0.11
ESFAS (sec)	6.50	5.60	5.07	4.44
Subcooled Blowdown Ends (sec)	~20	~15	~10	~10
HPI On (sec)	66.52	65.62	65.08	64.46
AFW On (sec)	NA	NA	NA	NA
AFW Off (sec)	NA	NA	NA	NA
Loop Draining Begins (sec)	~45	~40	~30	~25
Boiling Pot Begins (sec)	~120	~70	~55	NA
CFT Actuation (sec)	~210	~130	~95	~60
Refill Begins (sec)	~210	~130	~95	~60
Calculations Stopped (sec)	435.0	160.0	160.0	160.0
HC Peak Clad Temp (F) Segment Time (sec)	722.25 17 0.0	722.28 17 0.0	750.35 18 1.181	1147.2 18 2.18
AC Peak Clad Temp (F) Segment Time (sec)	695.46 17 0.0	695.49 17 0.0	695.46 17 0.0	845.02 17 93.32

Table A-9. Core Flood Line Resistance Study Sequence of Events.

<u>Parameter</u>	<u>0.1-ft² CLPD Break</u>		<u>1.0-ft² CLPD Break</u>	
	<u>Nominal Resistance</u>	<u>Increased Resistance</u>	<u>Nominal Resistance</u>	<u>Increased Resistance</u>
Break Opens (sec)	0.0	0.0	0.0	0.0
LP Reactor Trip (sec)	12.32	12.33	0.16	0.16
ESFAS (sec)	19.78	19.78	5.07	5.07
Subcooled Blowdown Ends (sec)	~40	~40	~10	~10
HPI On (sec)	79.78	79.78	65.08	65.08
AFW On (sec)	~110	~110	NA	NA
AFW Off (sec)	~490	~490	NA	NA
Loop Draining Begins (sec)	~160	~160	~30	~30
Boiling Pot Begins (sec)	~1000	~1000	~55	~55
CFT Actuation (sec)	~2270	~2270	~94	~94
Refill Begins (sec)	~2270	~2270	~94	~94
Calculations Stopped (sec)	3200.0	3000.0	160.0	160.0
HC Peak Clad Temp (F) Segment Time (sec)	1032.7 20 2620.5	1057.2 20 2523.4	750.35 18 1.181	750.35 18 1.181
AC Peak Clad Temp (F) Segment Time (sec)	745.94 20 2417.1	742.53 20 2500.1	695.46 17 0.0	695.46 17 0.0

Table A-10. CLPD Break Discharge Coefficient Study Sequence of Events.

Parameter	Break Area Moody Cd	0.07-ft ² CLPD Break		0.21-ft ² CLPD Break	
		0.07 ft ² 1.0	0.10 ft ² 0.7	0.21 ft ² 1.0	0.30 ft ² 0.7
Break Opens (sec)		0.0	0.0	0.0	0.0
LP Reactor Trip (sec)		17.89	12.33	5.06	3.44
ESFAS (sec)		25.6	19.78	11.96	9.8
Subcooled Blowdown Ends (sec)		~50	~40	~20	~20
HPI On (sec)		85.6	79.78	71.96	69.82
AFW On (sec)		~115	~110	~125	~130
AFW Off (sec)		~480	~490	~350	~310
Loop Draining Begins (sec)		~250	~160	~90	~60
Boiling Pot Begins (sec)		~990	~1000	~220	~220
CFT Actuation (sec)		~2260	~2270	~430	~420
Refill Begins (sec)		~2260	~2270	~430	~440
Calculations Stopped (sec)		3200.0	3000.0	500.0	500.0
HC Peak Clad Temp (F) Segment Time (sec)		1148.8 19 2550.2	1057.2 20 2523.4	788.65 20 461.1	742.28 20 443.8
AC Peak Clad Temp (F) Segment Time (sec)		818.24 19 2406.7	742.53 20 2500.1	695.46 17 0.0	695.46 17 0.0

Table A-11. Special SBLOCA Sequence of Events.

Parameter	CFT Line Break	HPI Line Break
Break Opens (sec)	0.0	0.0
LP Reactor Trip (sec)	0.44	45.16
ESFAS (sec)	7.72	72.82
Subcooled Blowdown Ends (sec)	~20	~100
HPI On (sec)	67.72	672.8
AFW On (sec)	NA	~140
AFW Off (sec)	NA	~600
Loop Draining Begins (sec)	~60	~400
Boiling Pot Begins (sec)	~150	NA
CFT Actuation (sec)	~175	NA
RV Refill Begins (sec)	~175	NA
Calculations Stopped (sec)	300.0	6400.0
HC Peak Clad Temp (F) Segment Time (sec)	722.25 17 0.0	722.27 17 0.0
AC Peak Clad Temp (F) Segment Time (sec)	695.45 17 0.0	695.47 17 0.0

Table A-12. Most Severe SBLOCA Sequence of Events.

Parameter	Most Severe SBLOCA
Break Area (ft ²)	0.07
Moody Discharge Coefficient	1.0
Break Opens (sec)	0.0
LP Reactor Trip (sec)	17.89
ESFAS (sec)	25.6
Subcooled Blowdown Ends (sec)	~50
HPI On (sec)	85.6
AFW On (sec)	~115
AFW Off (sec)	~480
Loop Draining Begins (sec)	~150
Boiling Pot Begins (sec)	~990
CFT Actuation (sec)	~2260
RV Refill Begins (sec)	~2260
Calculations Stopped (sec)	3200.0
HC Peak Clad Temp (F) Segment Time (sec)	1148.8 19 2550.2
AC Peak Clad Temp (F) Segment Time (sec)	818.24 19 2406.7

FIGURE A-1. SBLOCA TIME STEP STUDY FOR 0.1-FT² CLPD BREAK - RCS PRESSURE.

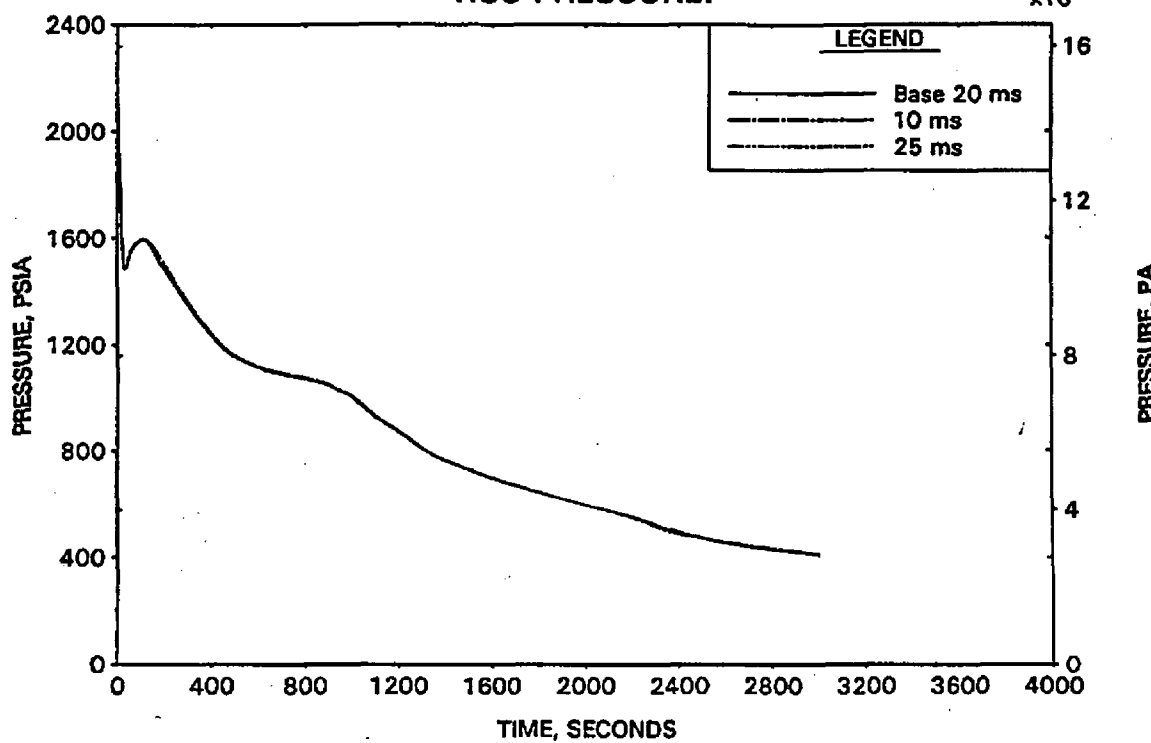


FIGURE A-2. SBLOCA TIME STEP STUDY FOR 0.1-FT² CLPD BREAK - BREAK FLOW RATES.

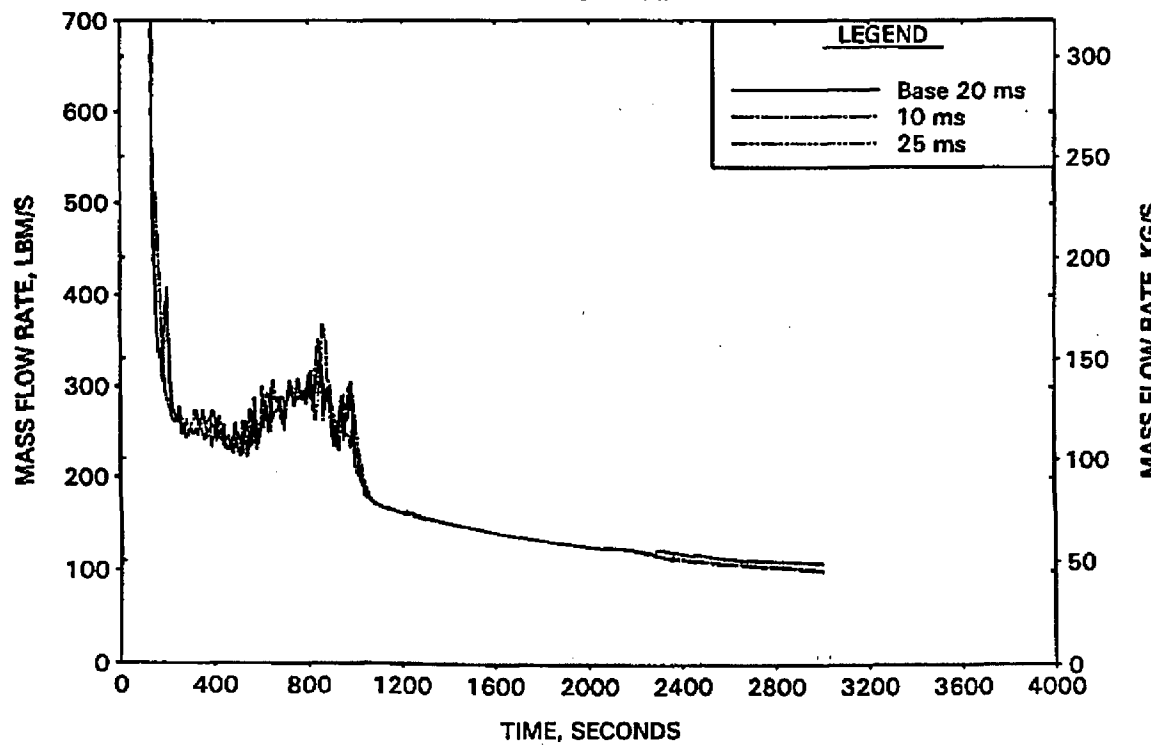


FIGURE A-3. SBLOCA TIME STEP STUDY FOR 0.1-FT² CLPD BREAK - REACTOR VESSEL COLLAPSED LEVEL.

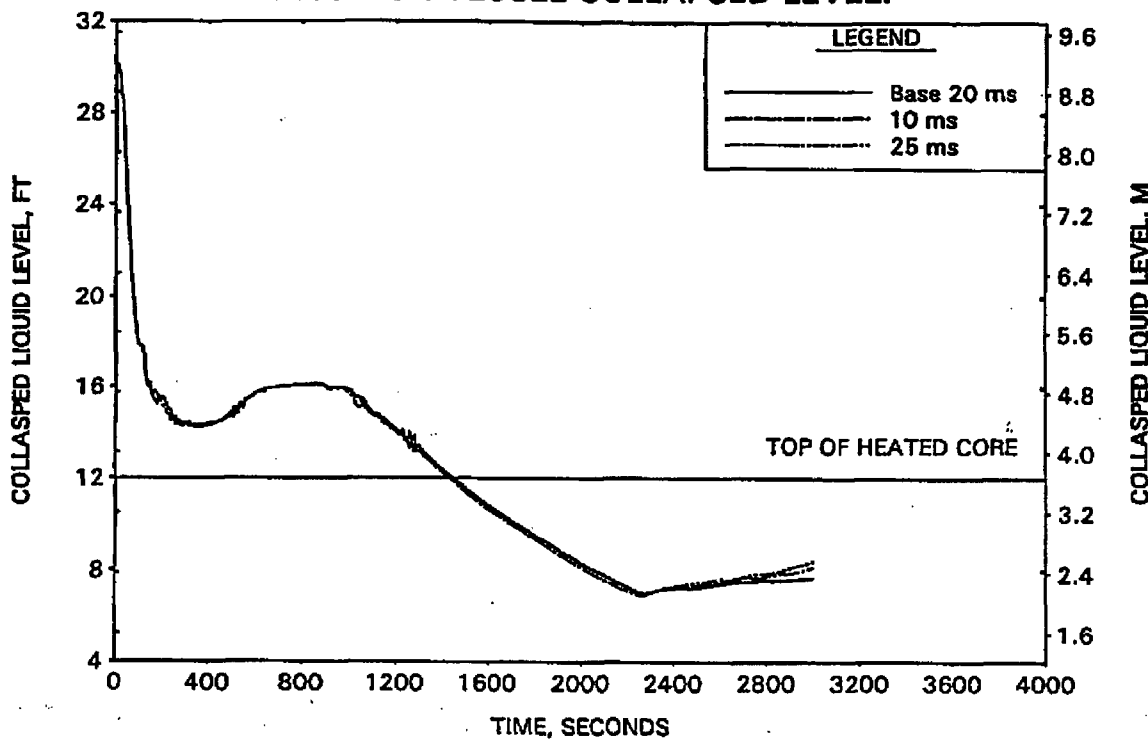


FIGURE A-4. SBLOCA TIME STEP STUDY FOR 0.1-FT² CLPD BREAK - CLPS LIQUID VOLUME.

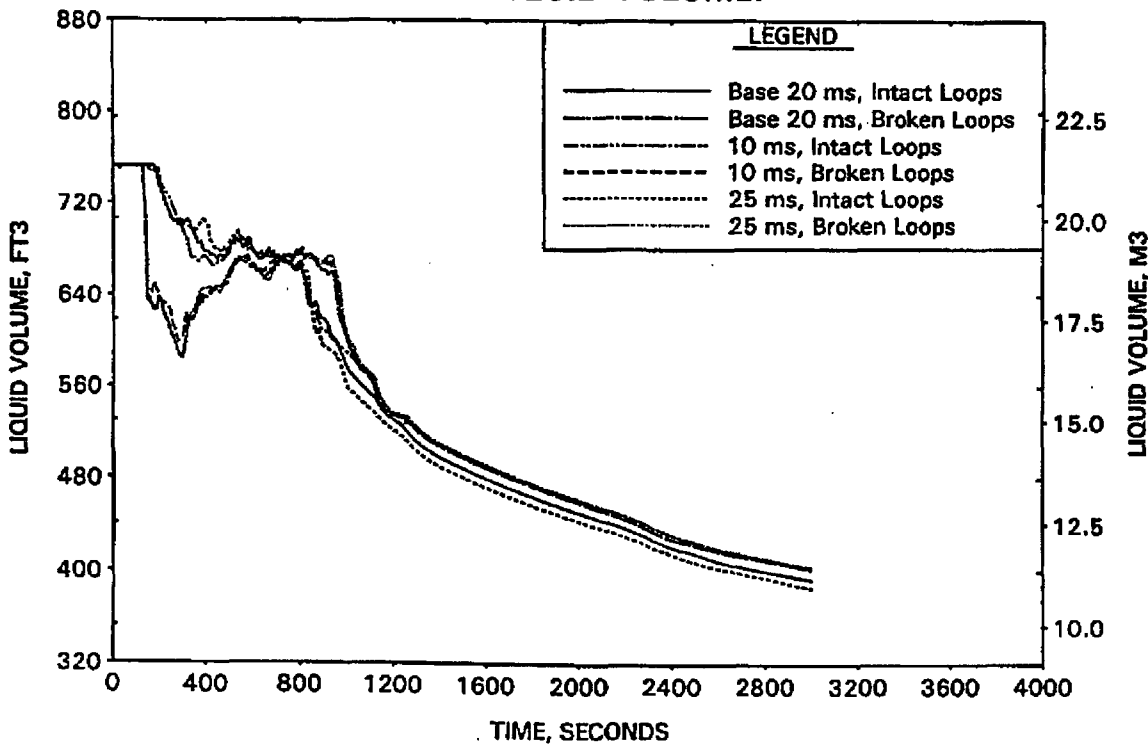


FIGURE A-5. SBLOCA TIME STEP STUDY FOR 0.1-FT2 CLPD BREAK -
CORE HOT CHANNEL MIXTURE LEVEL.

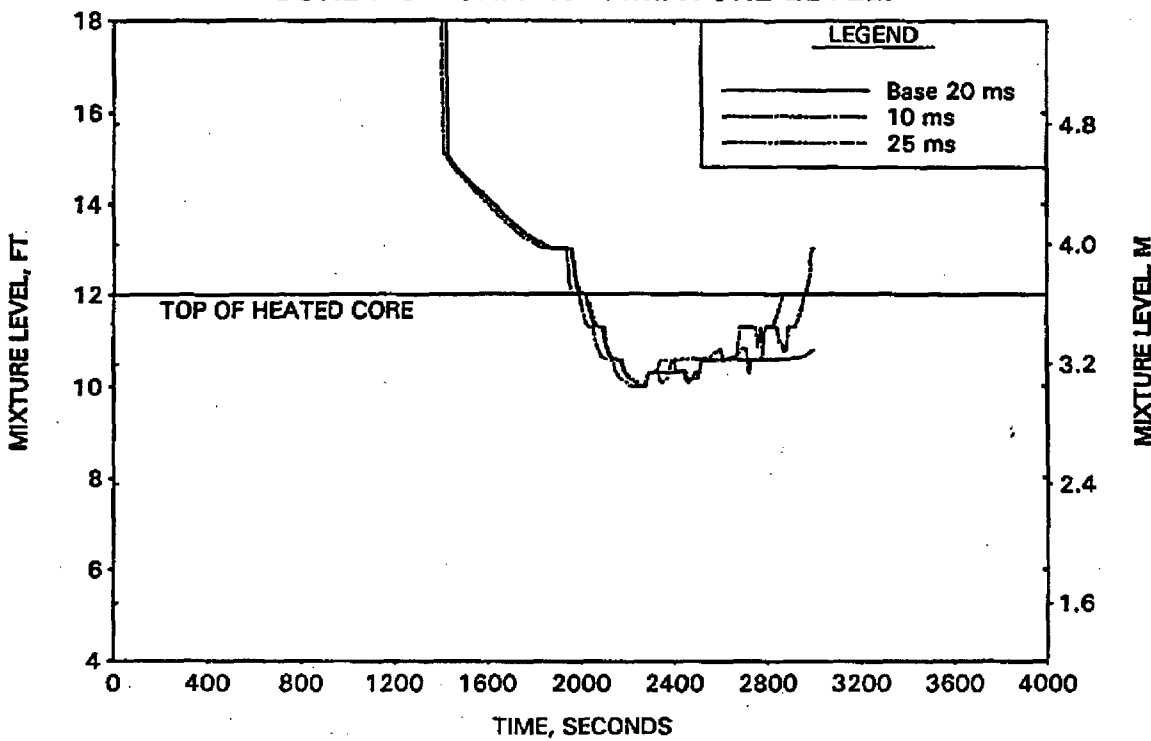


FIGURE A-6. SBLOCA TIME STEP STUDY FOR 0.1-FT2 CLPD BREAK -
PEAK CLADDING TEMPERATURE.

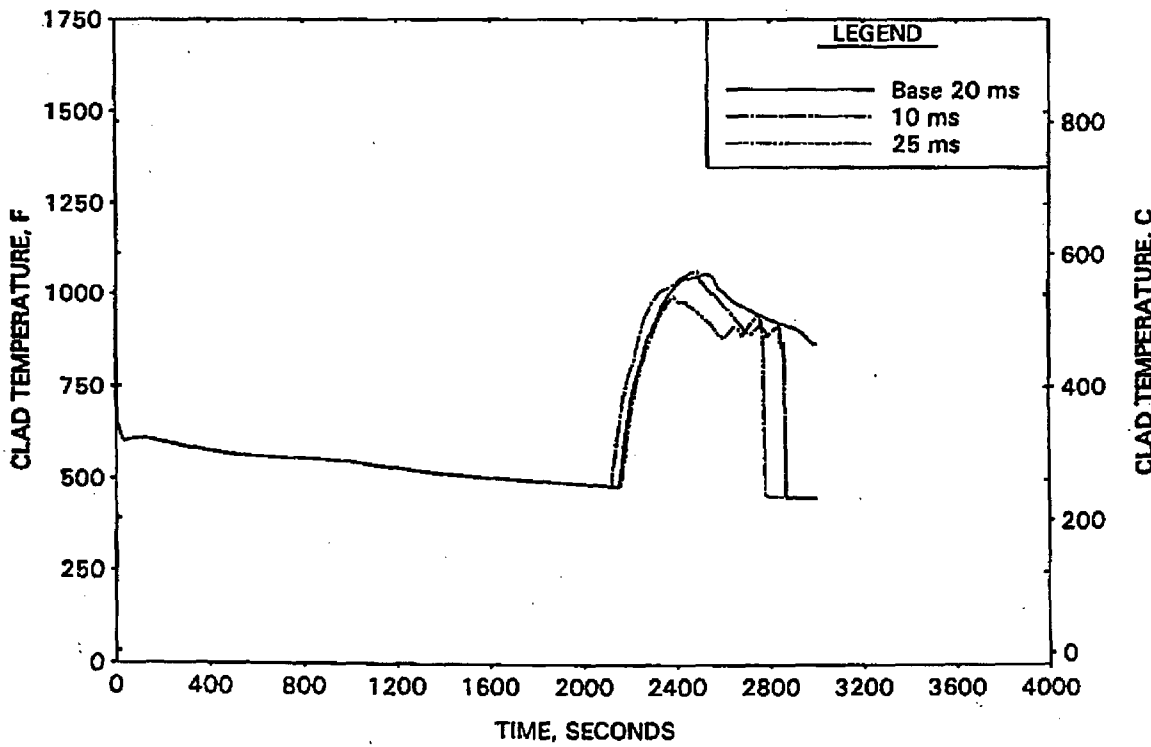


FIGURE A-7. BASE 0.1-FT2 CLPD BREAK RESULTS - RCS PRESSURES.

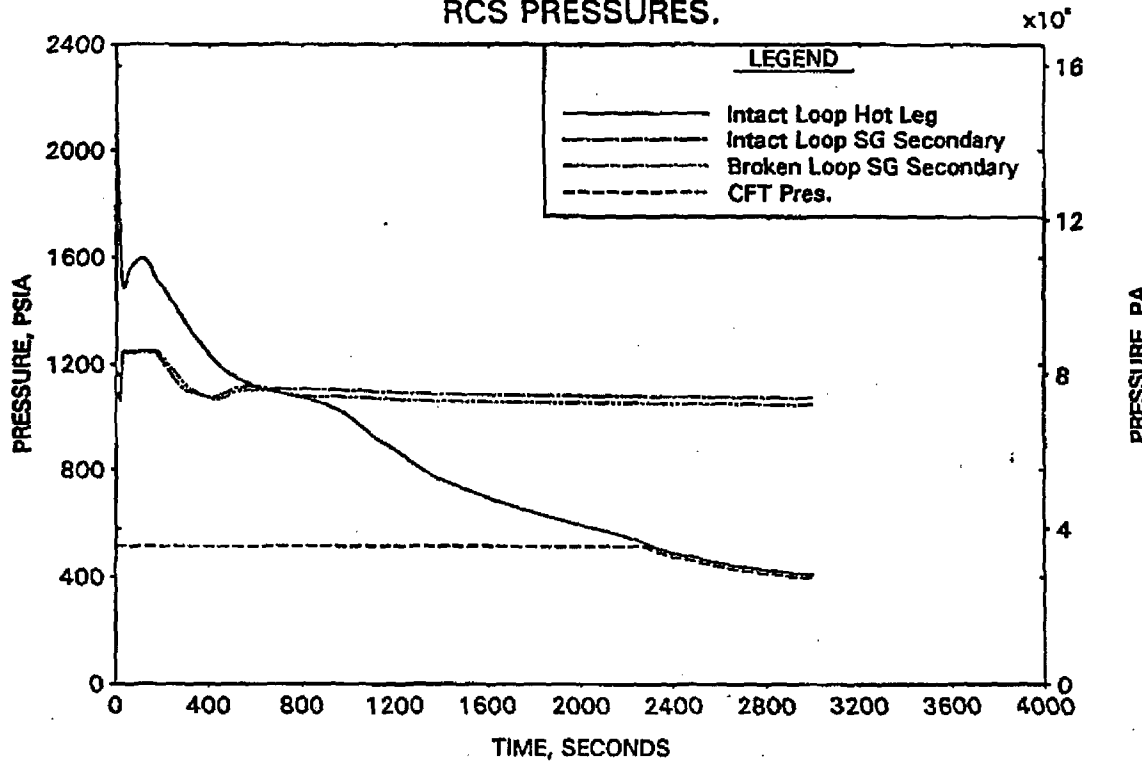


FIGURE A-8. BASE 0.1-FT2 CLPD BREAK RESULTS - DC, RV, AND CORE COLLAPSED LEVELS.

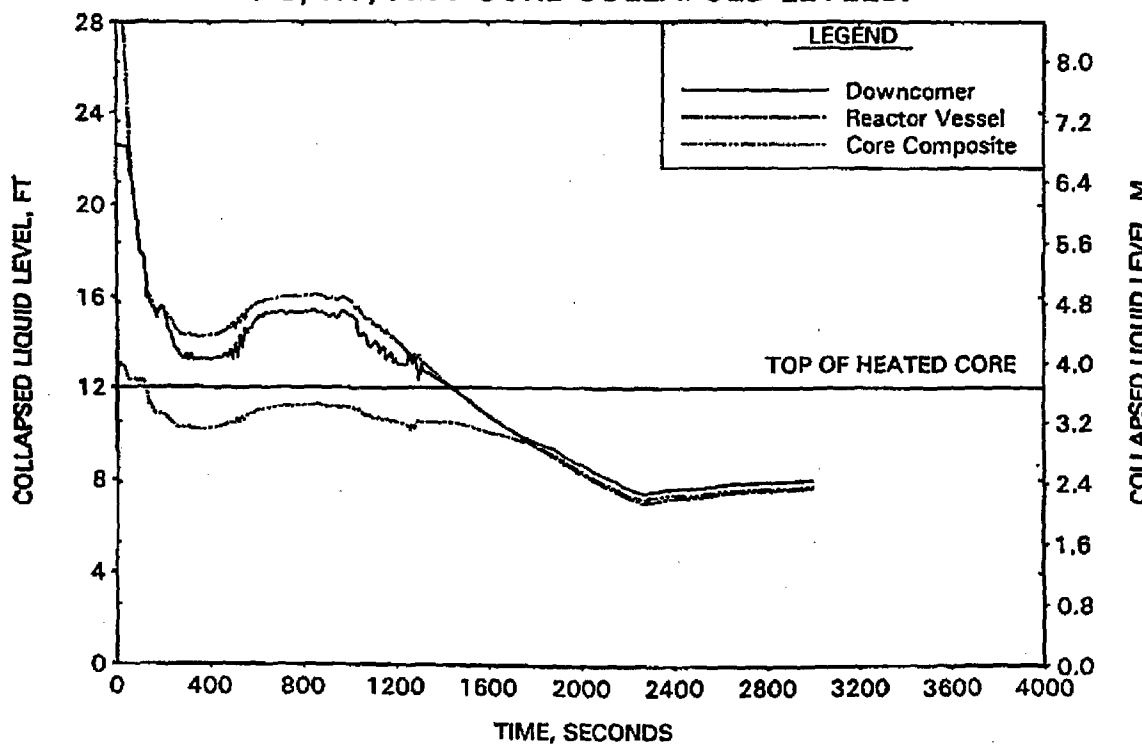


FIGURE A-9. BASE 0.1-FT² CLPD BREAK RESULTS -
BREAK AND TOTAL ECCS FLOWS.

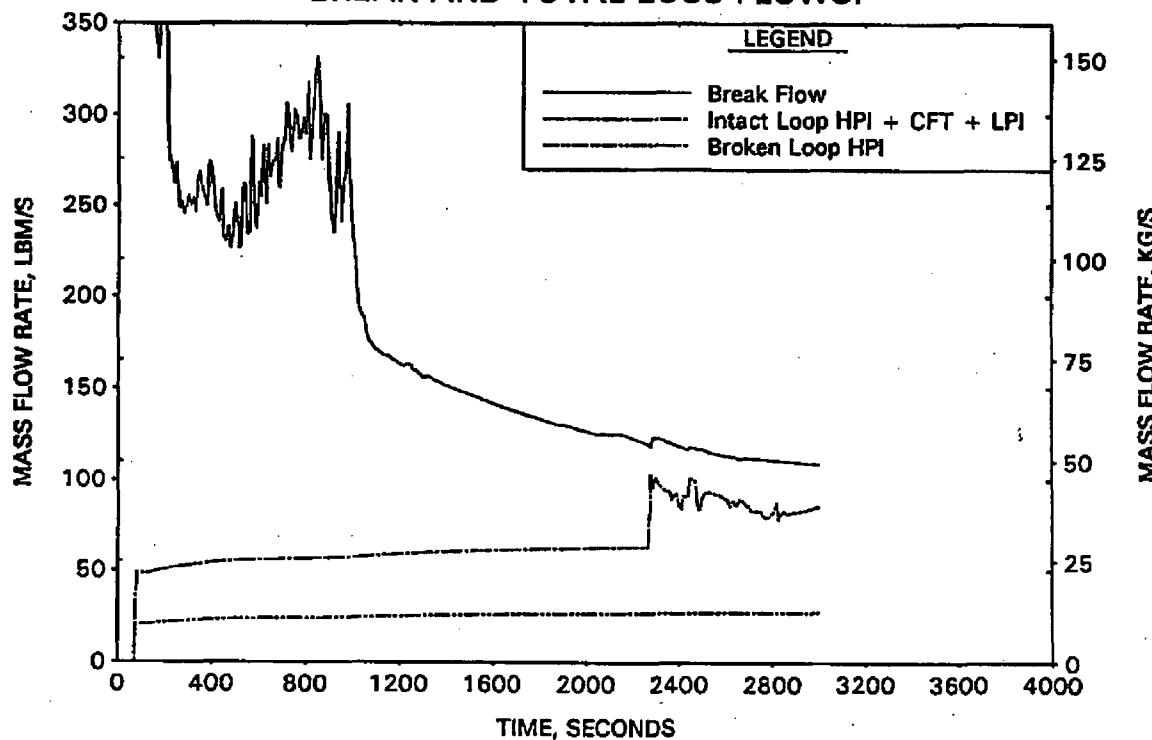


FIGURE A-10. BASE 0.1-FT² CLPD BREAK RESULTS -
BREAK VOLUME VOID FRACTION.

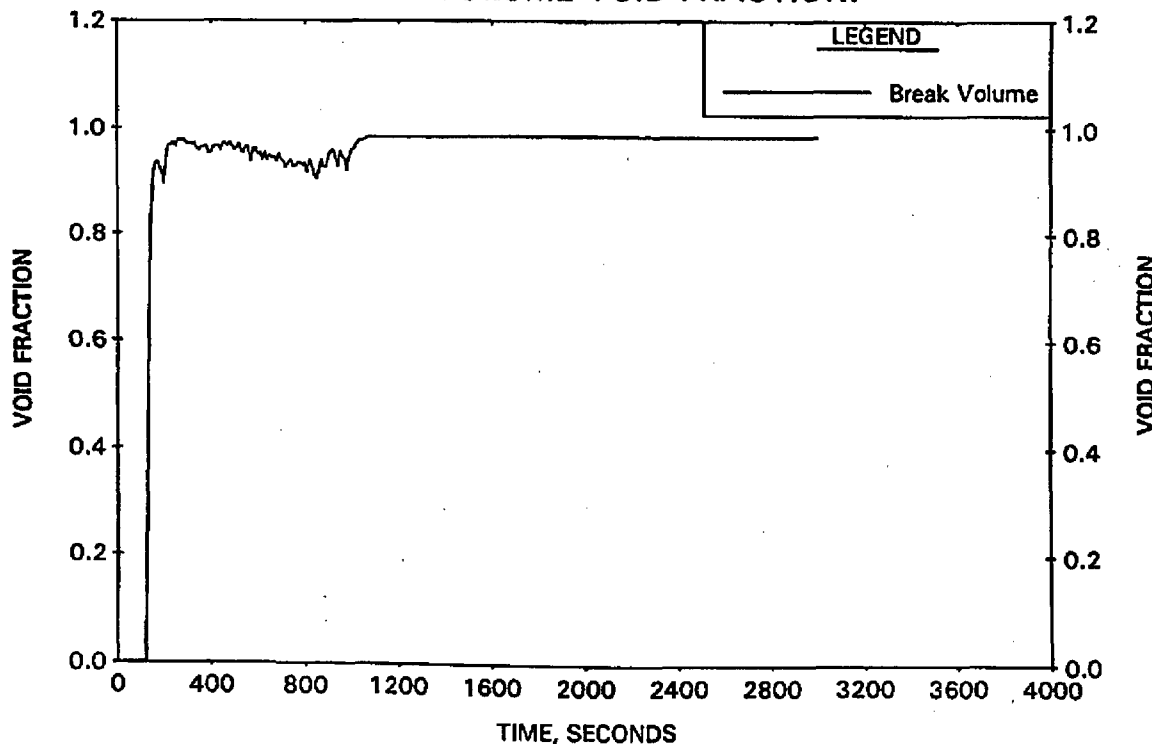


FIGURE A-11. BASE 0.1-FT2 CLPD BREAK RESULTS -
BROKEN LOOP COLLAPSED LEVELS.

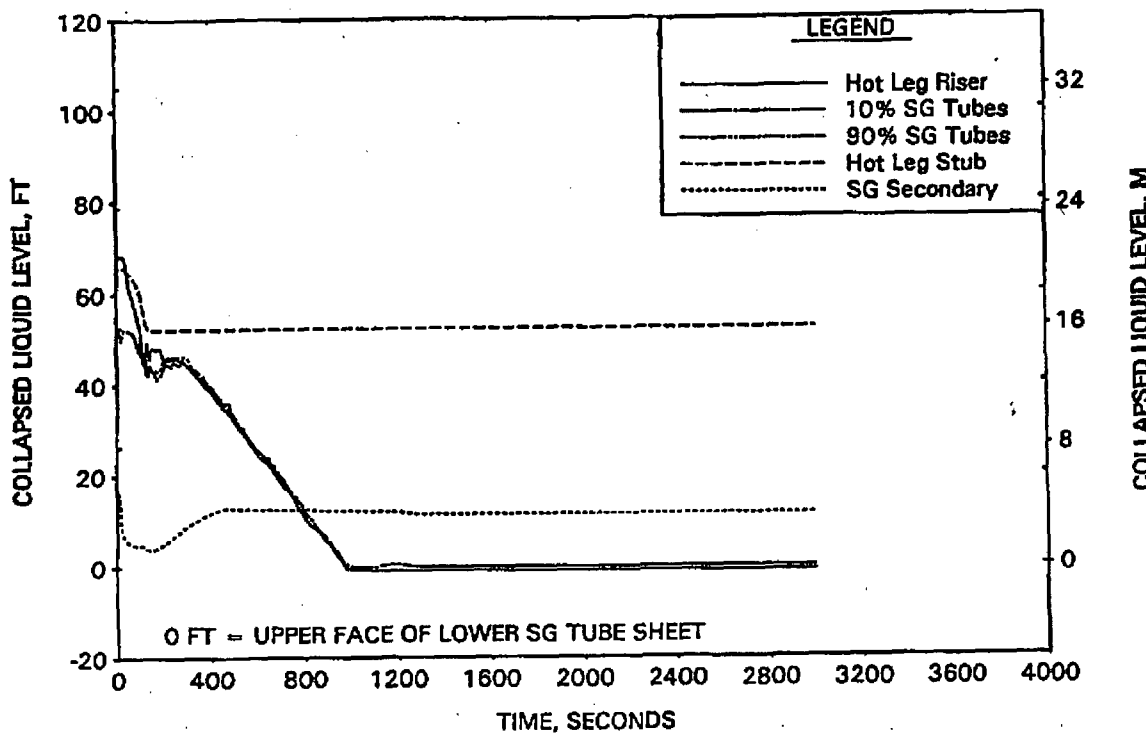


FIGURE A-12. BASE 0.1-FT2 CLPD BREAK RESULTS -
INTACT LOOP COLLAPSED LEVELS.

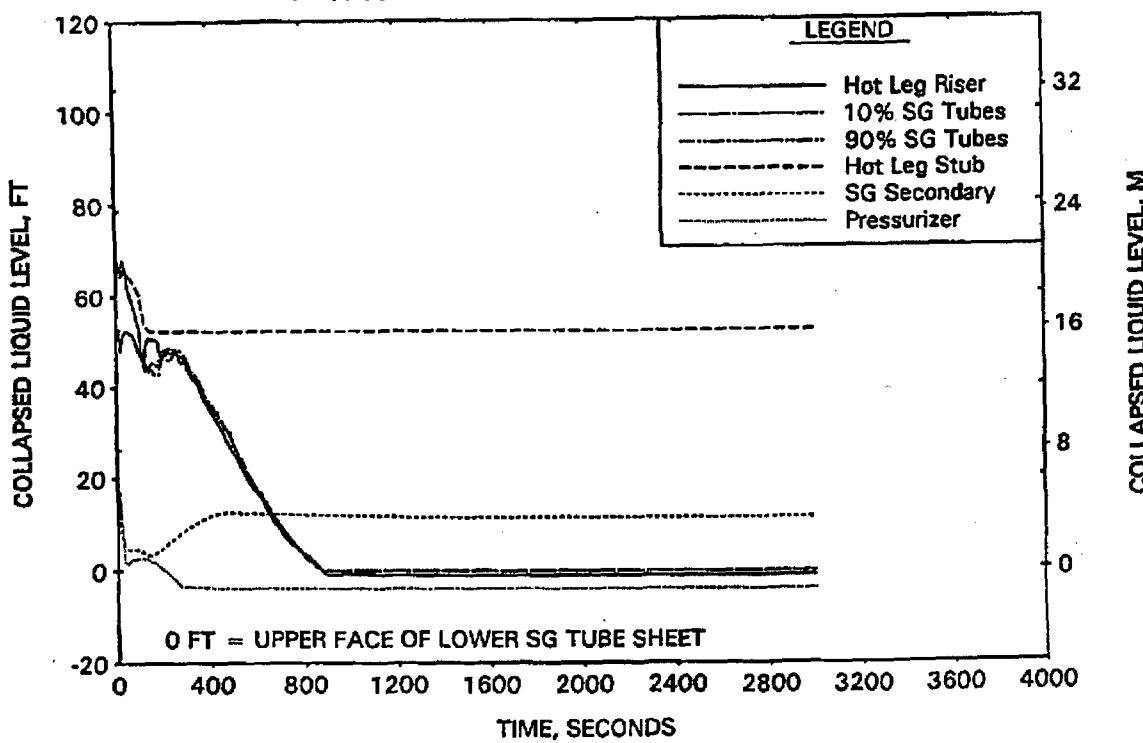


FIGURE A-13. BASE 0.1-FT² CLPD BREAK RESULTS -
CLPD COLLAPSED LEVELS.

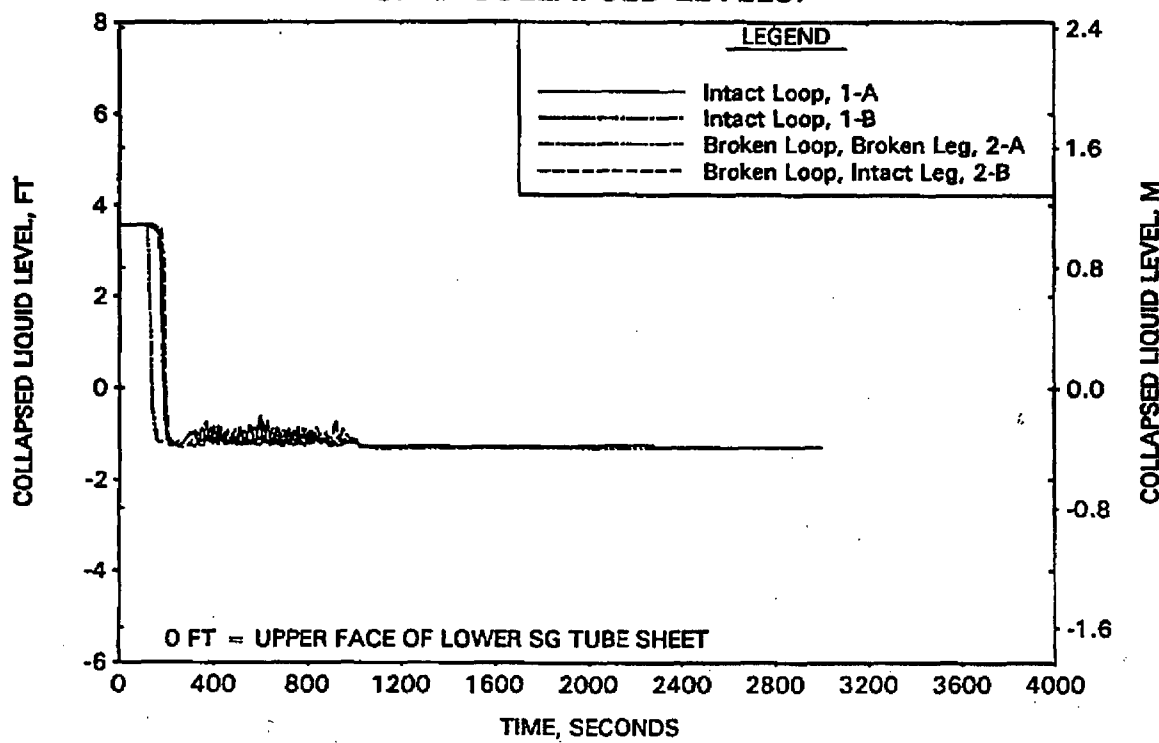


FIGURE A-14. BASE 0.1-FT² CLPD BREAK RESULTS -
CLPS LIQUID VOLUME.

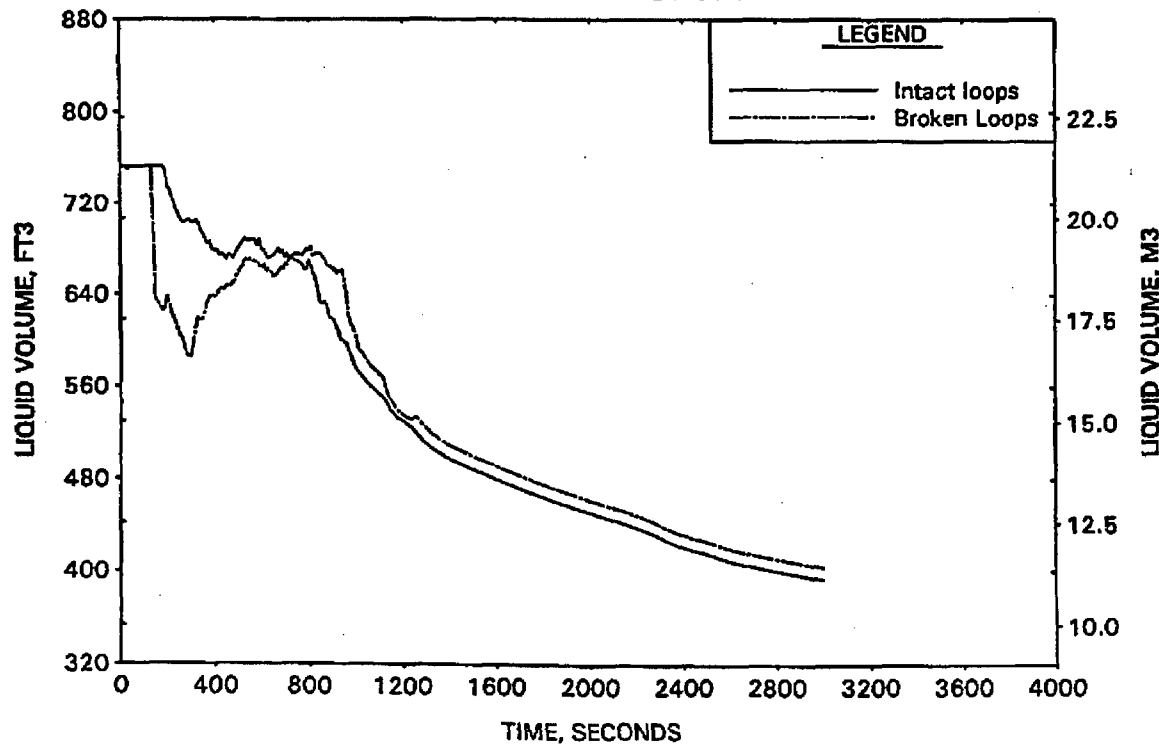


FIGURE A-15. BASE 0.1-FT2 CLPD BREAK RESULTS -
HOT LEG AND RVVV FLOWS.

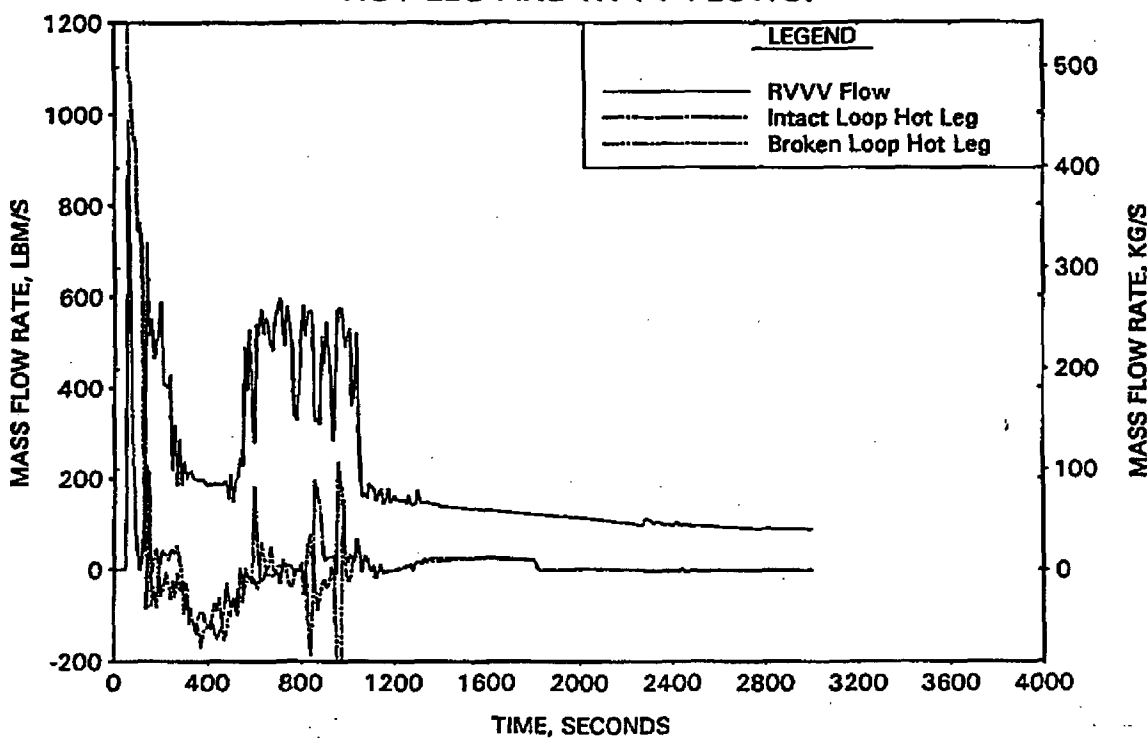


FIGURE A-16. BASE 0.1-FT2 CLPD BREAK RESULTS -
CORE MIXTURE LEVELS.

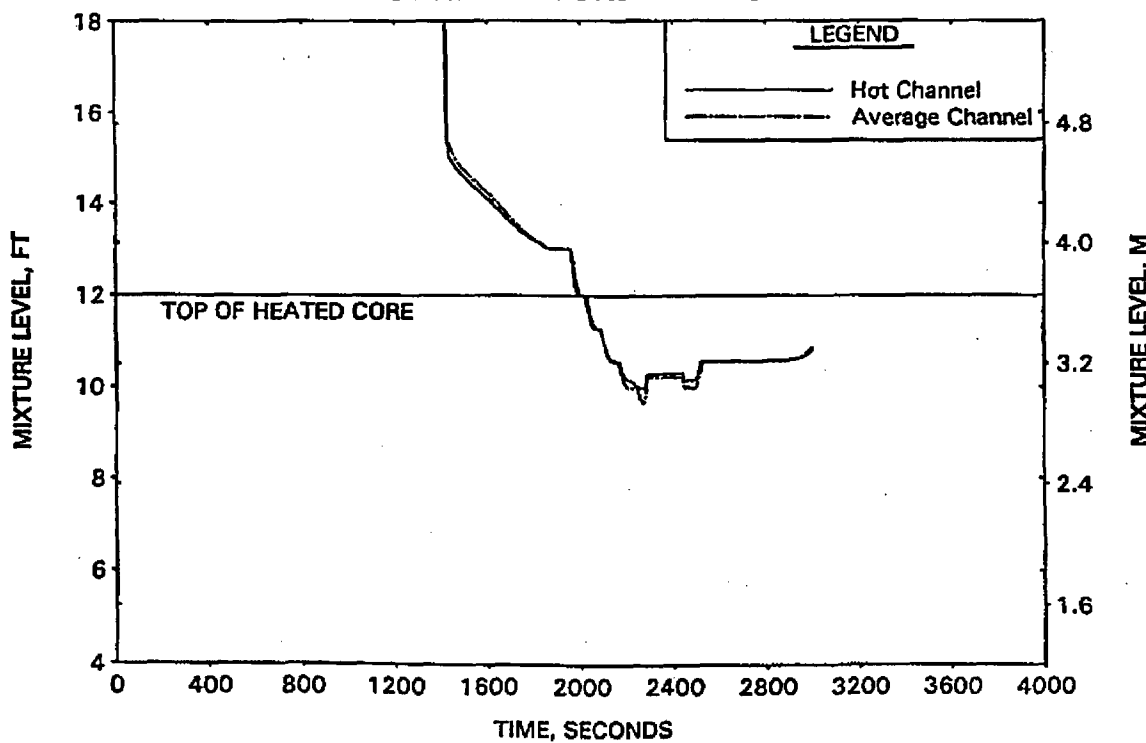


FIGURE A-17. BASE 0.1-FT² CLPD BREAK RESULTS -
HOT CHANNEL CLAD TEMPERATURES.

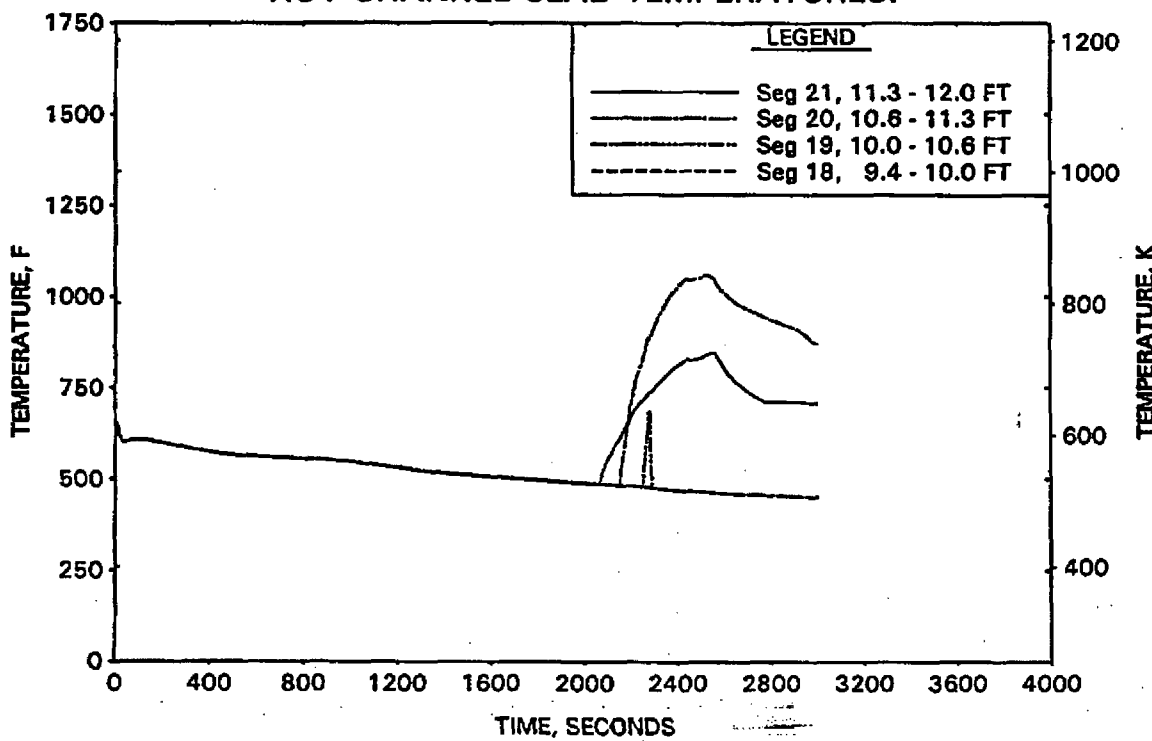


FIGURE A-18. BASE 0.1-FT² CLPD BREAK RESULTS -
HOT CHANNEL STEAM TEMPERATURES.

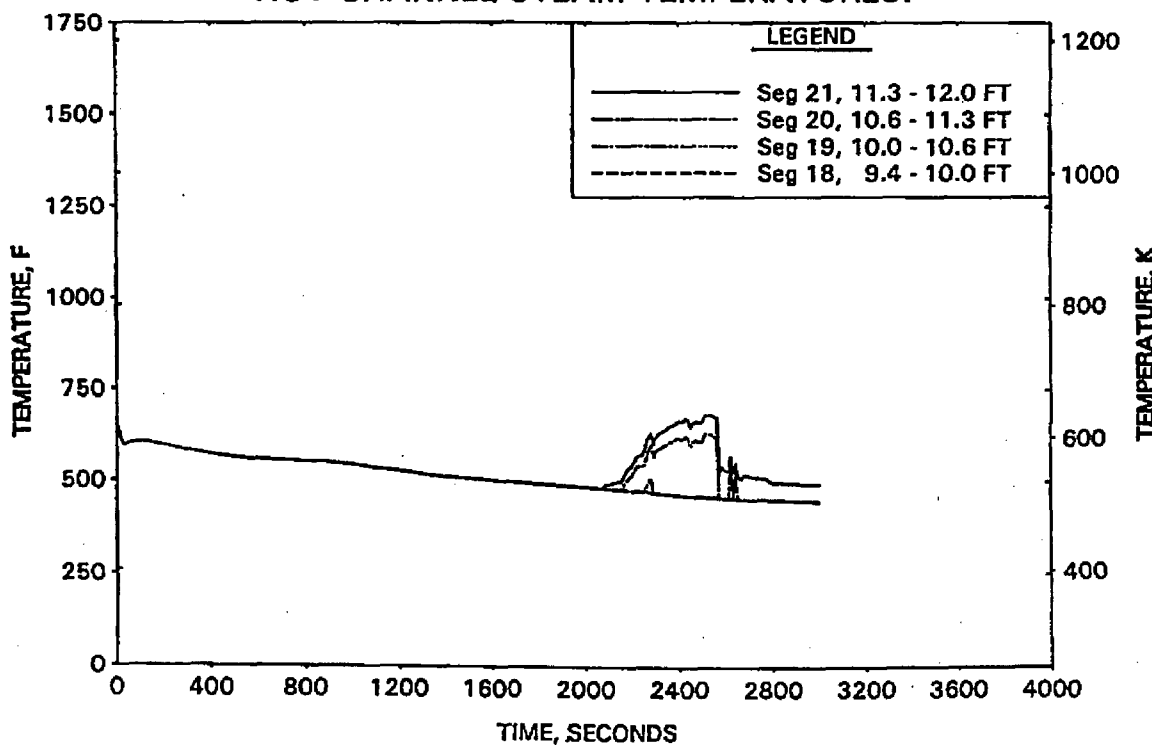


FIGURE A-19. BASE 0.1-FT2 CLPD BREAK RESULTS -
UPPER ELEVATION AVE CHANNEL CLAD TEMPERATURES.

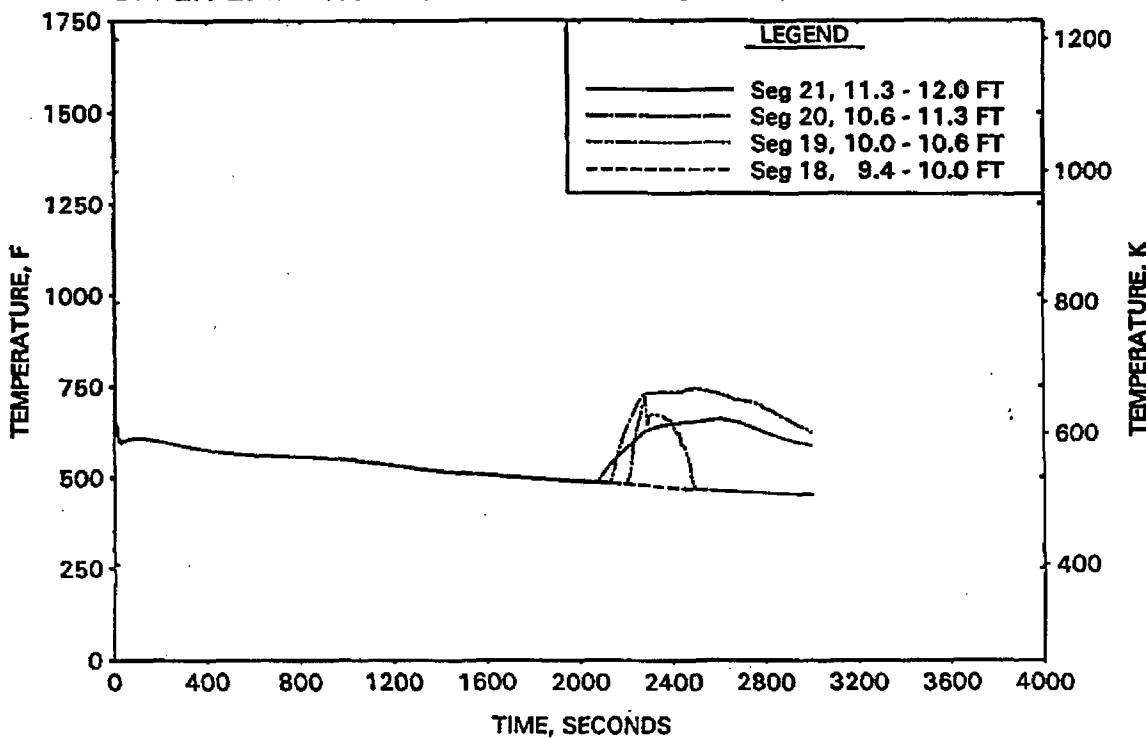


FIGURE A-20. BASE 0.1-FT2 CLPD BREAK RESULTS -
UPPER ELEVATION AVE CHANNEL STEAM TEMPERATURES.

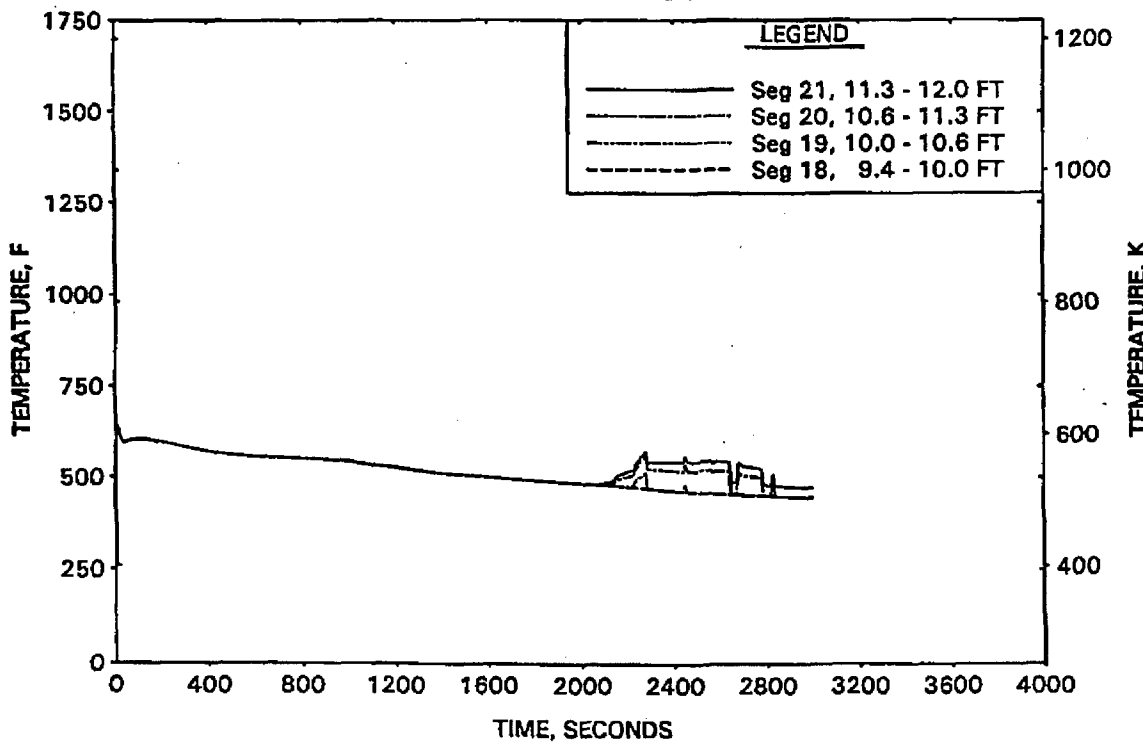


FIGURE A-21. PRESSURIZER LOCATION STUDY FOR 0.1-FT² CLPD BREAK - RCS PRESSURE.

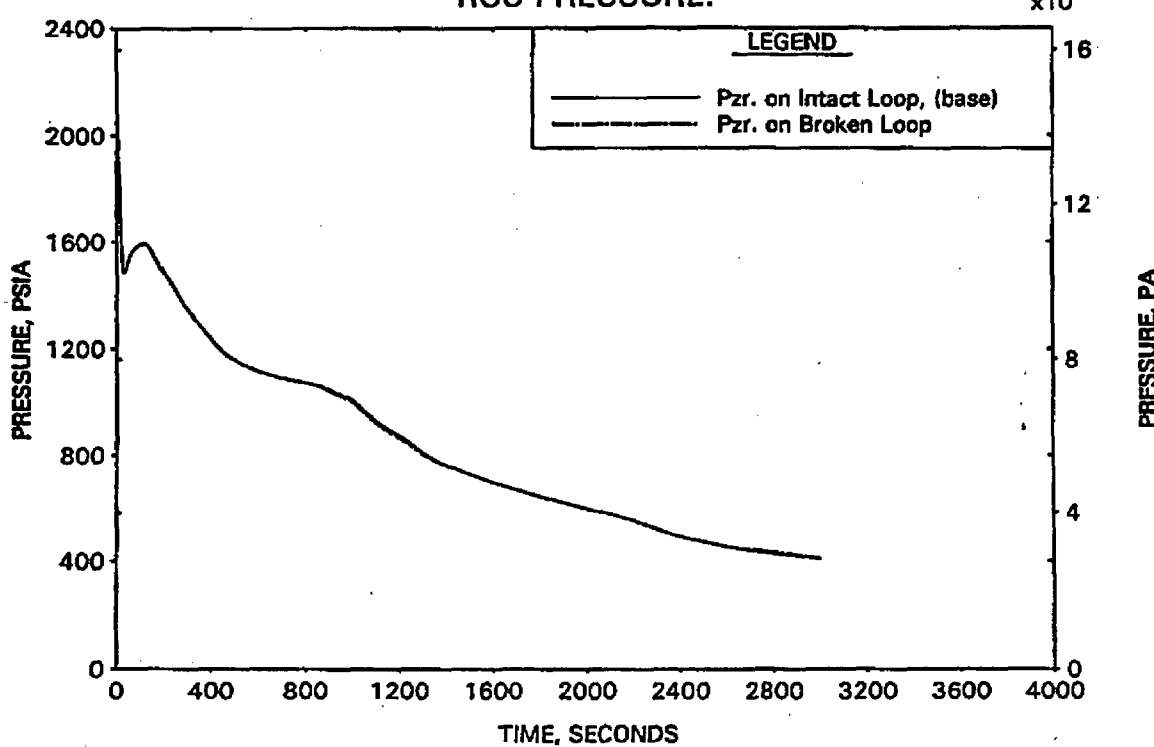


FIGURE A-22. PRESSURIZER LOCATION STUDY FOR 0.1-FT² CLPD BREAK - BREAK FLOW RATES.

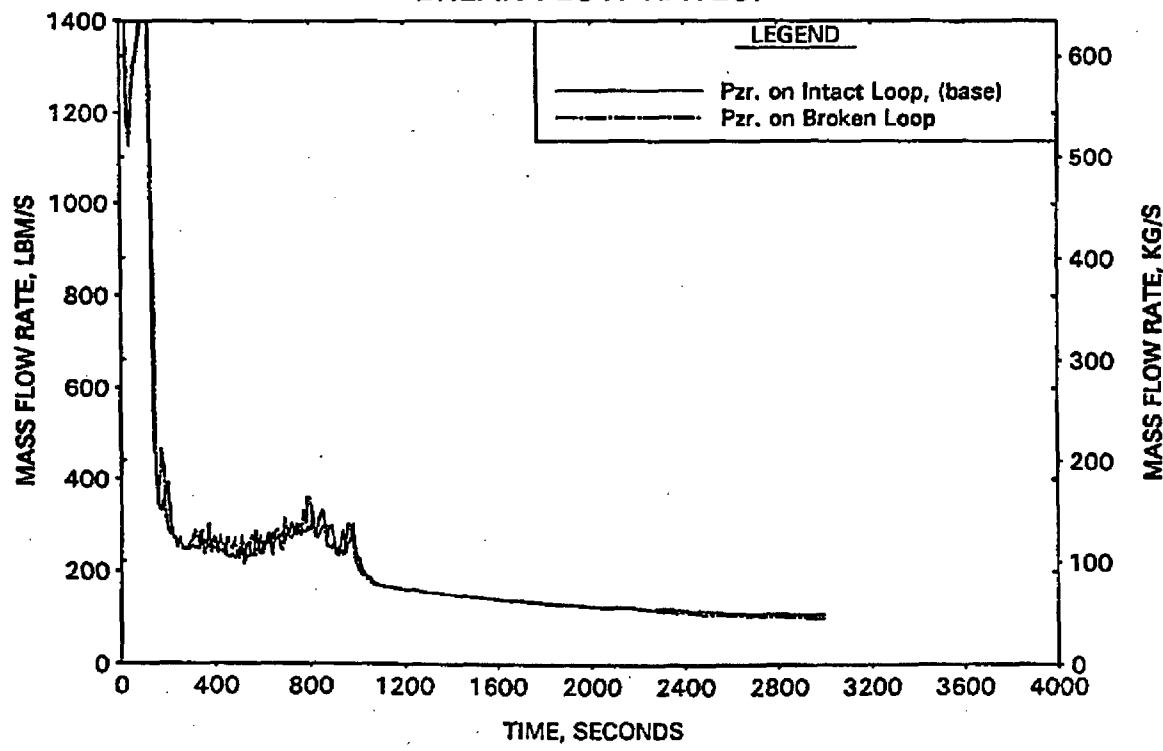


FIGURE A-23. PRESSURIZER LOCATION STUDY FOR 0.1-FT2 CLPD BREAK - REACTOR VESSEL COLLAPSED LEVEL.

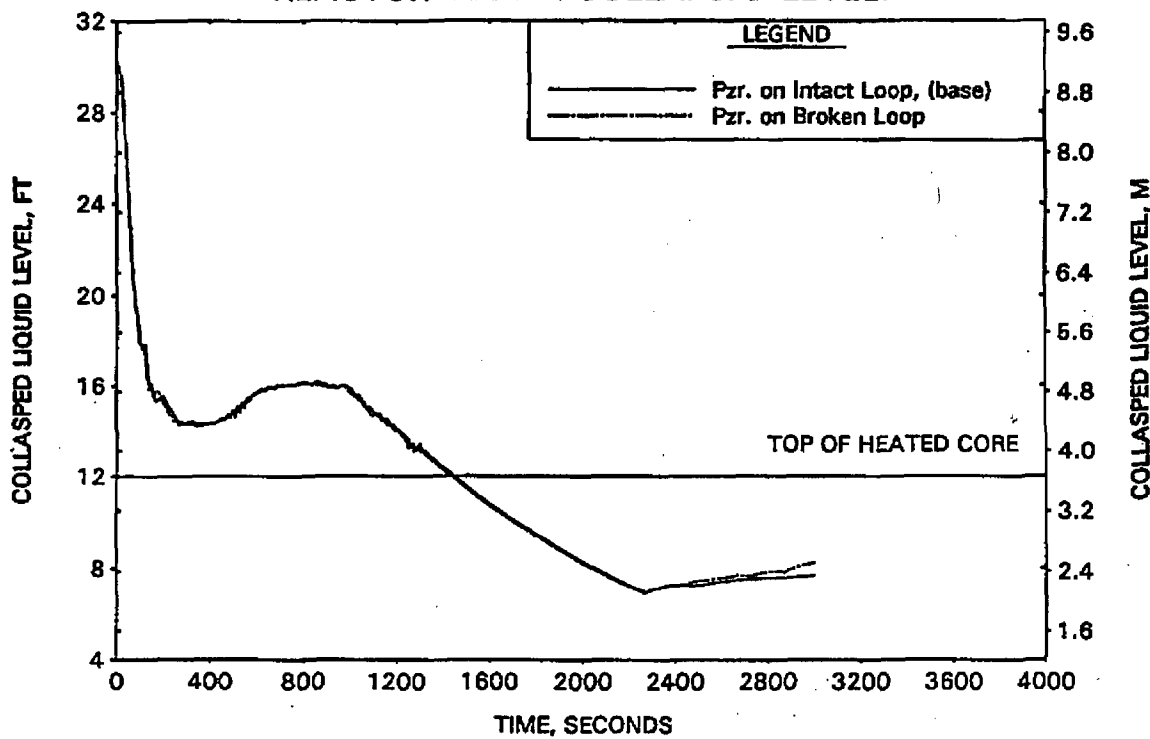


FIGURE A-24. PRESSURIZER LOCATION STUDY FOR 0.1-FT2 CLPD BREAK - CLPS LIQUID VOLUME.

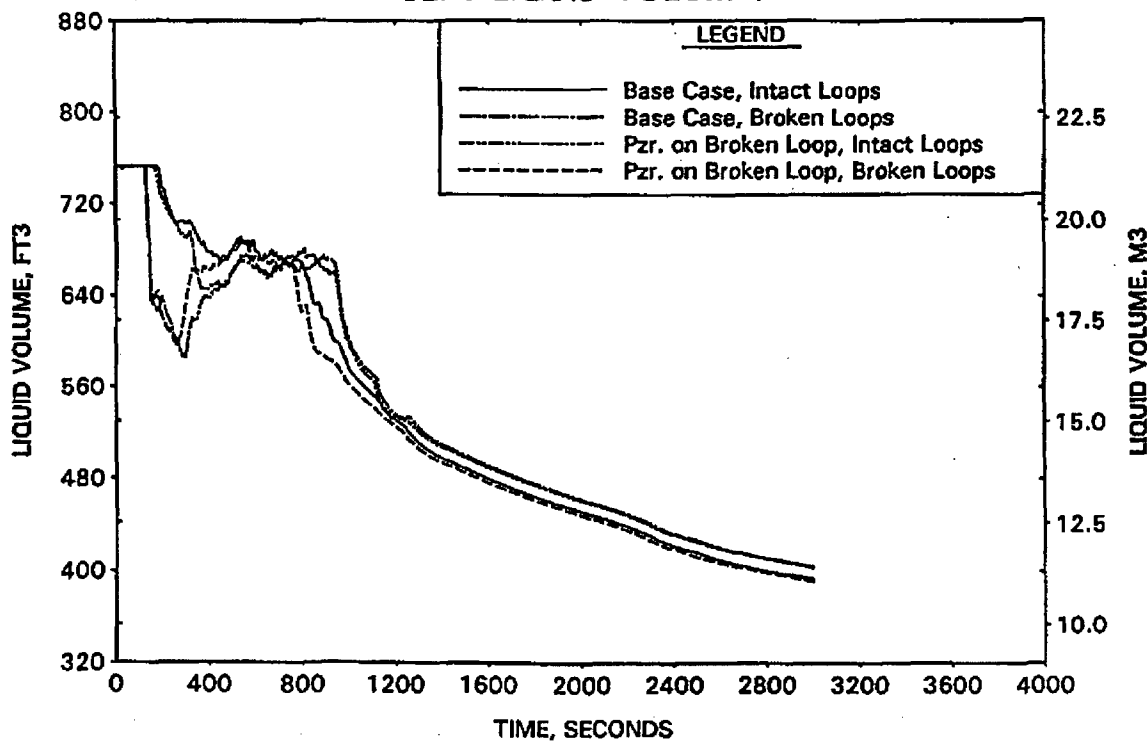


FIGURE A-25. PRESSURIZER LOCATION STUDY FOR 0.1-FT2 CLPD BREAK - CORE HOT CHANNEL MIXTURE LEVEL.

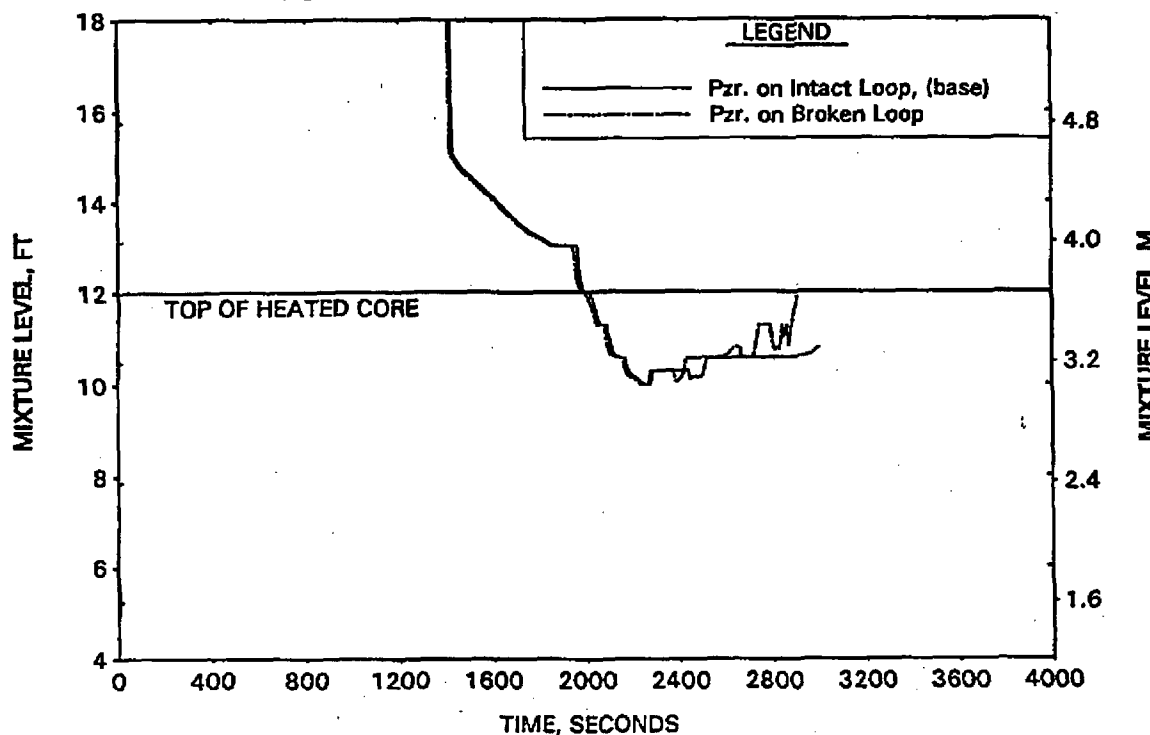


FIGURE A-26. PRESSURIZER LOCATION STUDY FOR 0.1-FT2 CLPD BREAK - PEAK CLADDING TEMPERATURE.

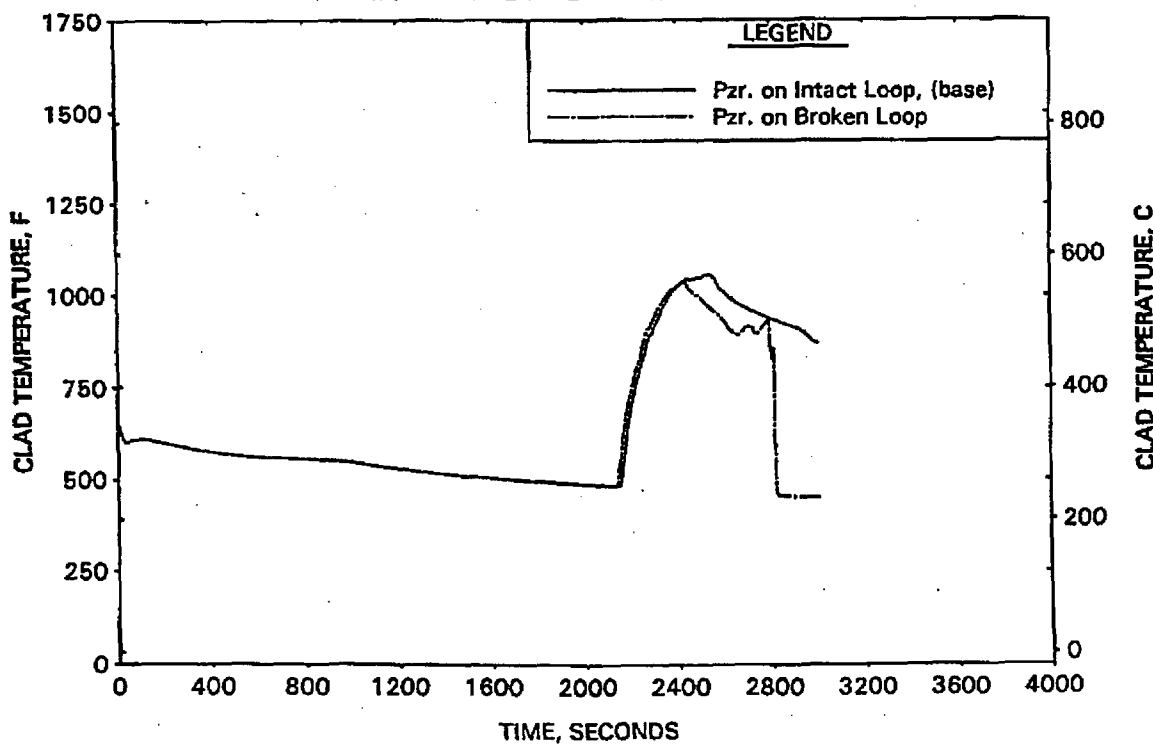


FIGURE A-27. CORE CROSSFLOW STUDY FOR 0.1-FT² CLPD BREAK - RCS PRESSURES.

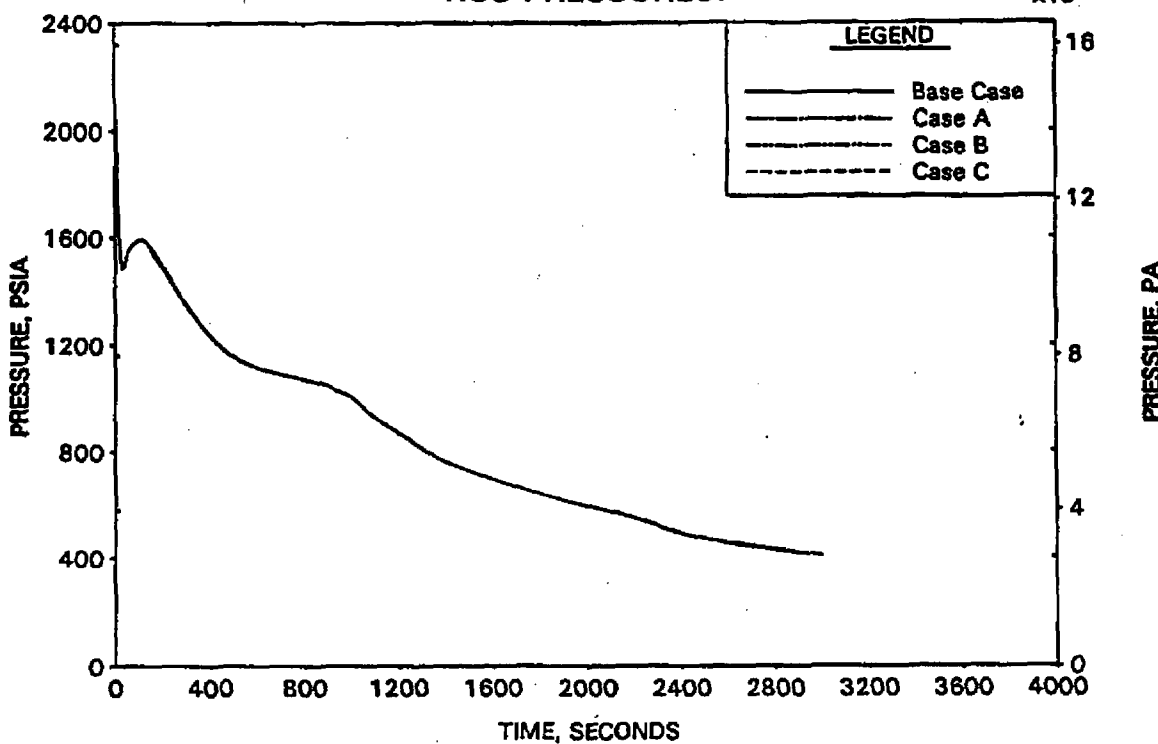


FIGURE A-28. CORE CROSSFLOW STUDY FOR 0.1-FT² CLPD BREAK - REACTOR VESSEL COLLAPSED LEVELS.

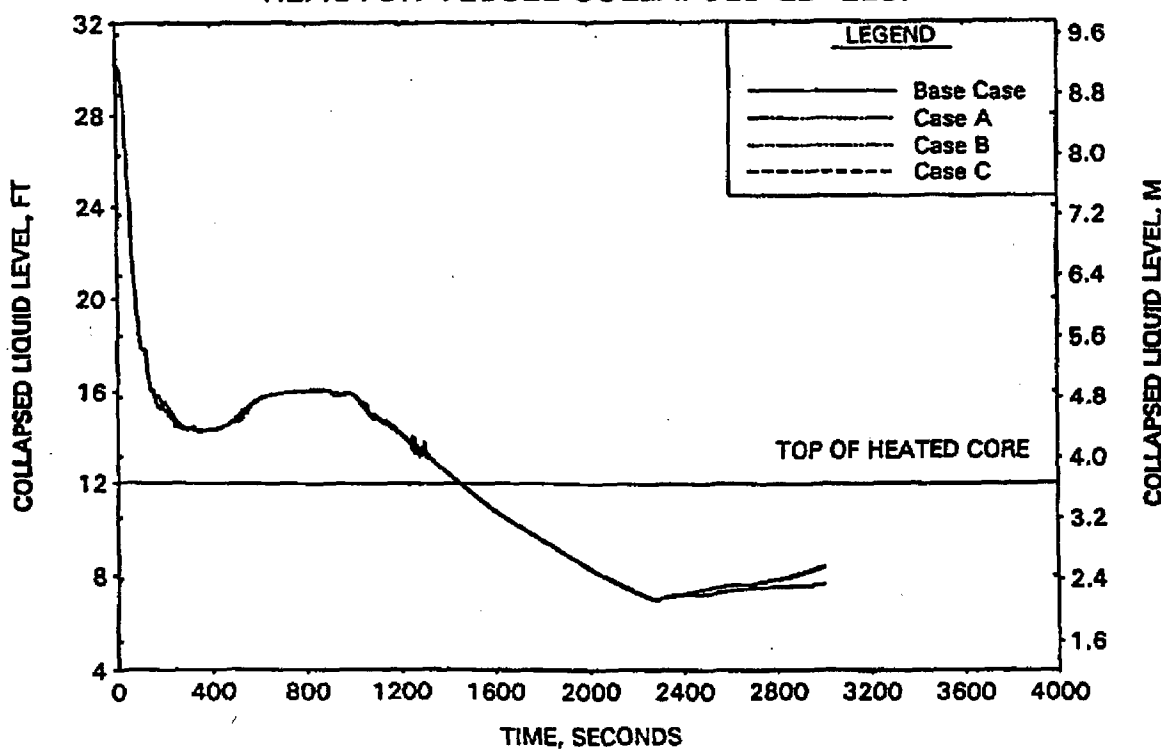


FIGURE A-29. CORE CROSSFLOW STUDY FOR 0.1-FT² CLPD BREAK -
BREAK FLOW RATES

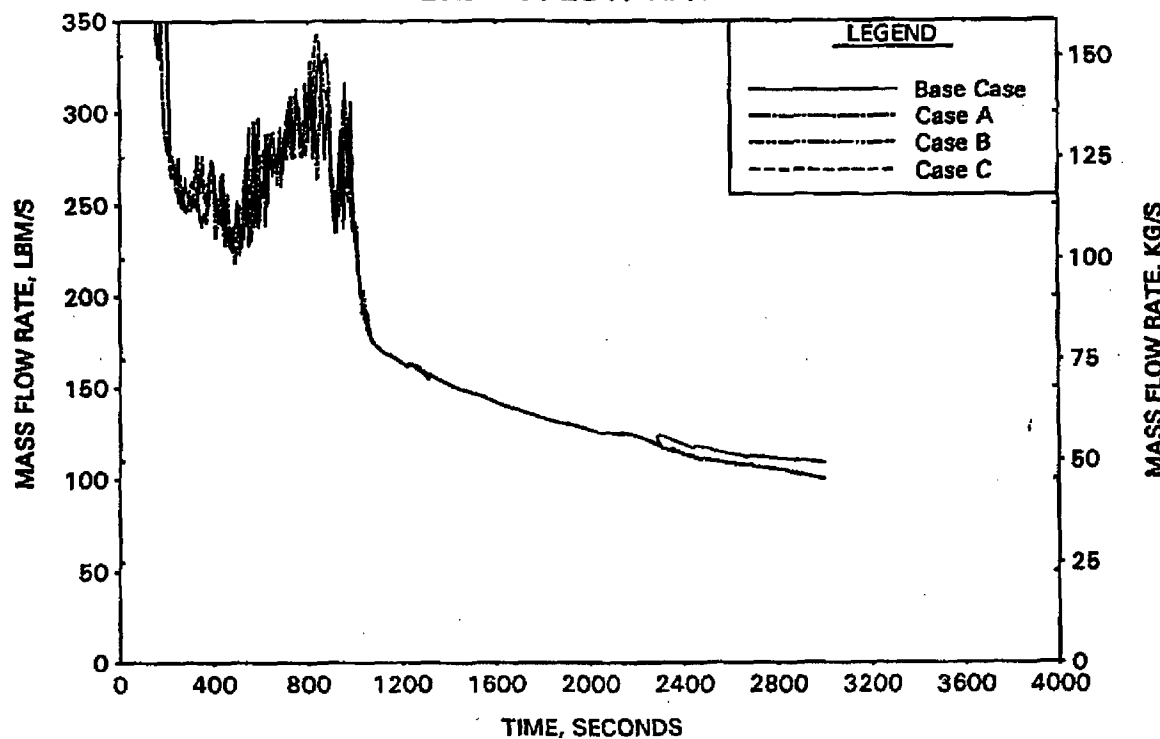


FIGURE A-30. CORE CROSSFLOW STUDY FOR 0.1-FT² CLPD BREAK -
HOT CHANNEL MIXTURE LEVELS.

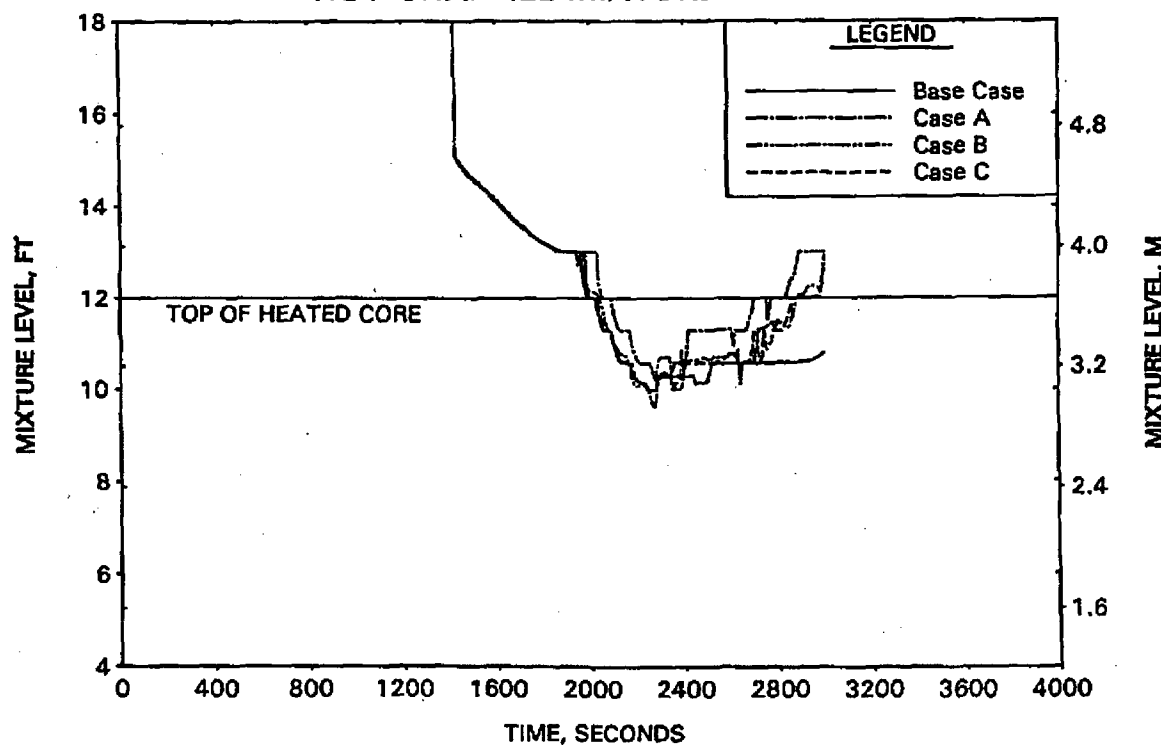


FIGURE A-31. CORE CROSSFLOW STUDY FOR 0.1-FT² CLPD BREAK - AVERAGE CHANNEL MIXTURE LEVELS.

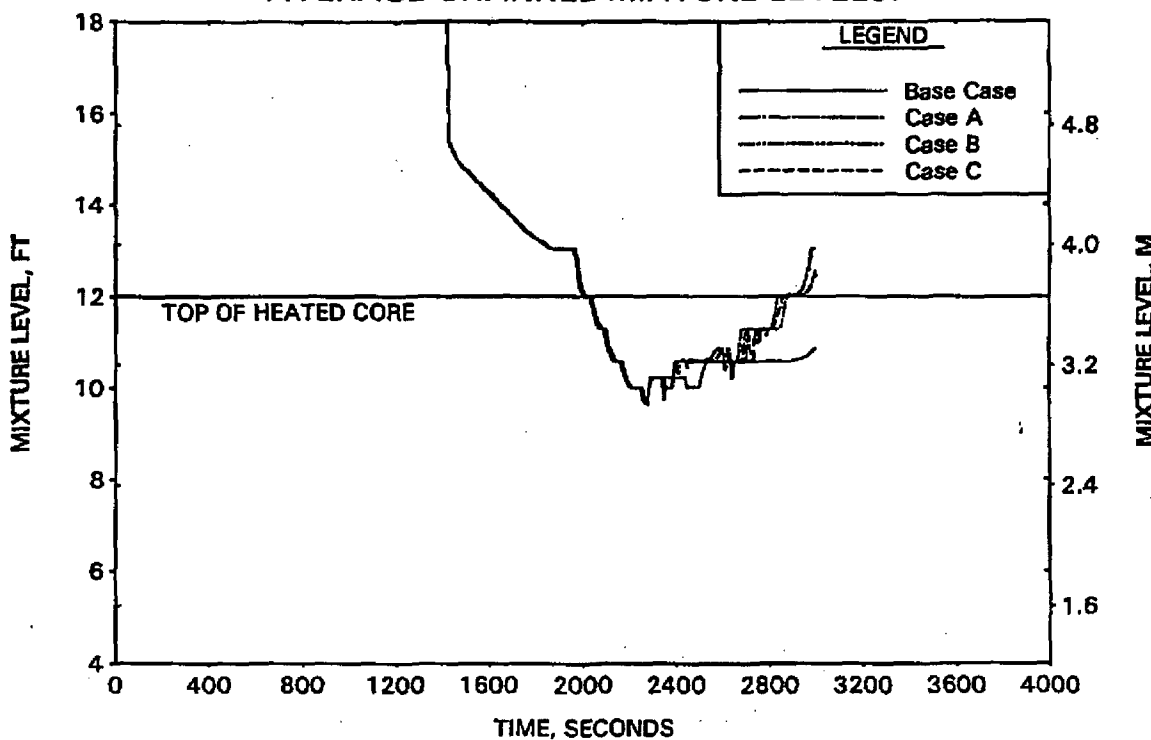


FIGURE A-32. CORE CROSSFLOW STUDY FOR 0.1-FT² CLPD BREAK - HOT AND AVE. CHANNEL MIXTURE LEVELS - CASE A.

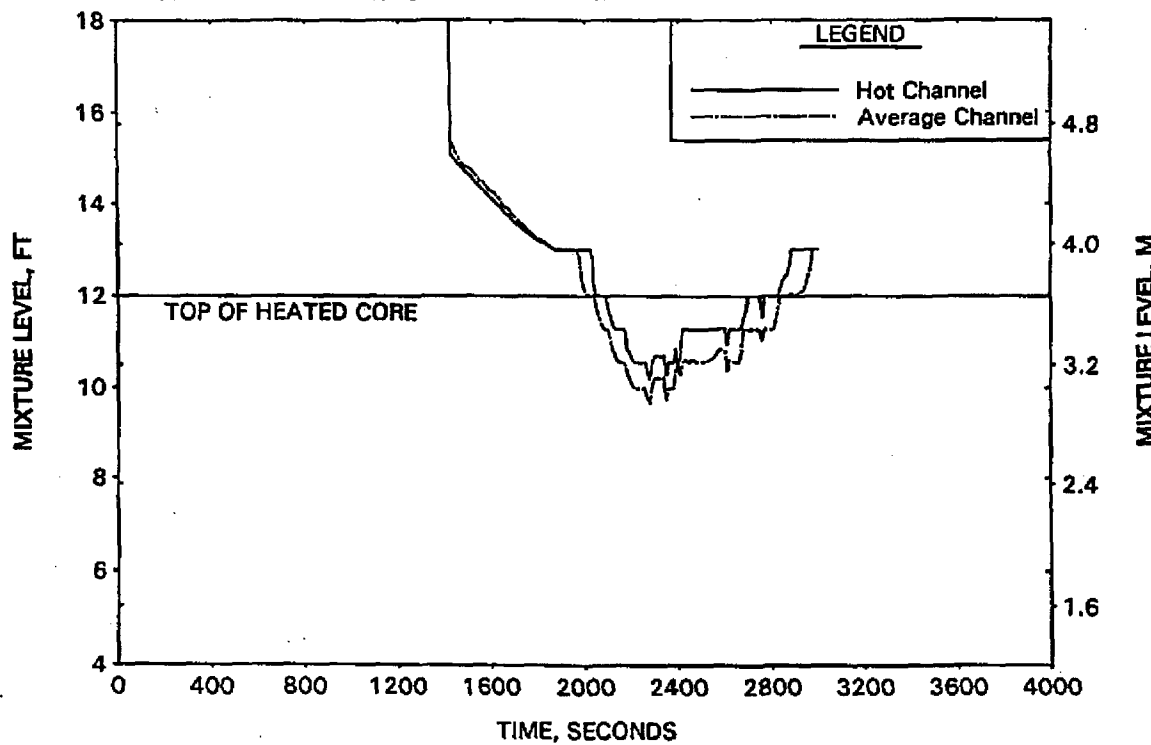


FIGURE A-33. CORE CROSSFLOW STUDY FOR 0.1-FT² CLPD BREAK - HOT AND AVE. CHANNEL MIXTURE LEVELS - CASE B.

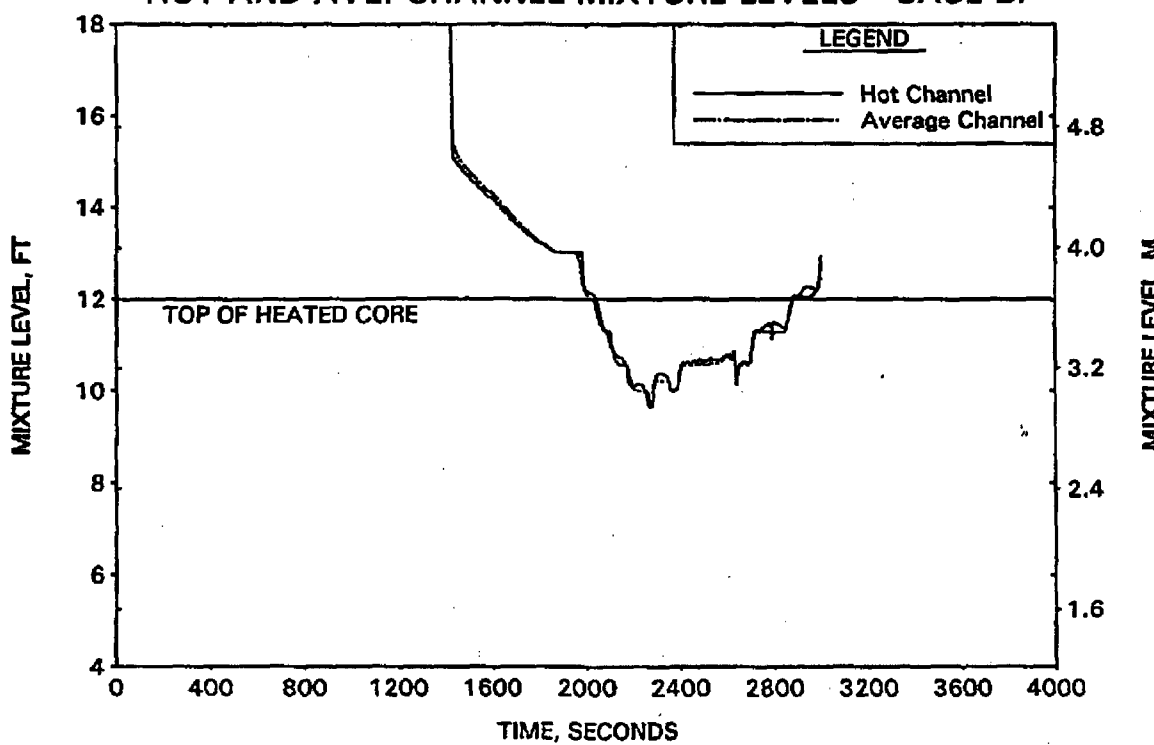


FIGURE A-34. CORE CROSSFLOW STUDY FOR 0.1-FT² CLPD BREAK - HOT AND AVE. CHANNEL MIXTURE LEVELS - CASE C.

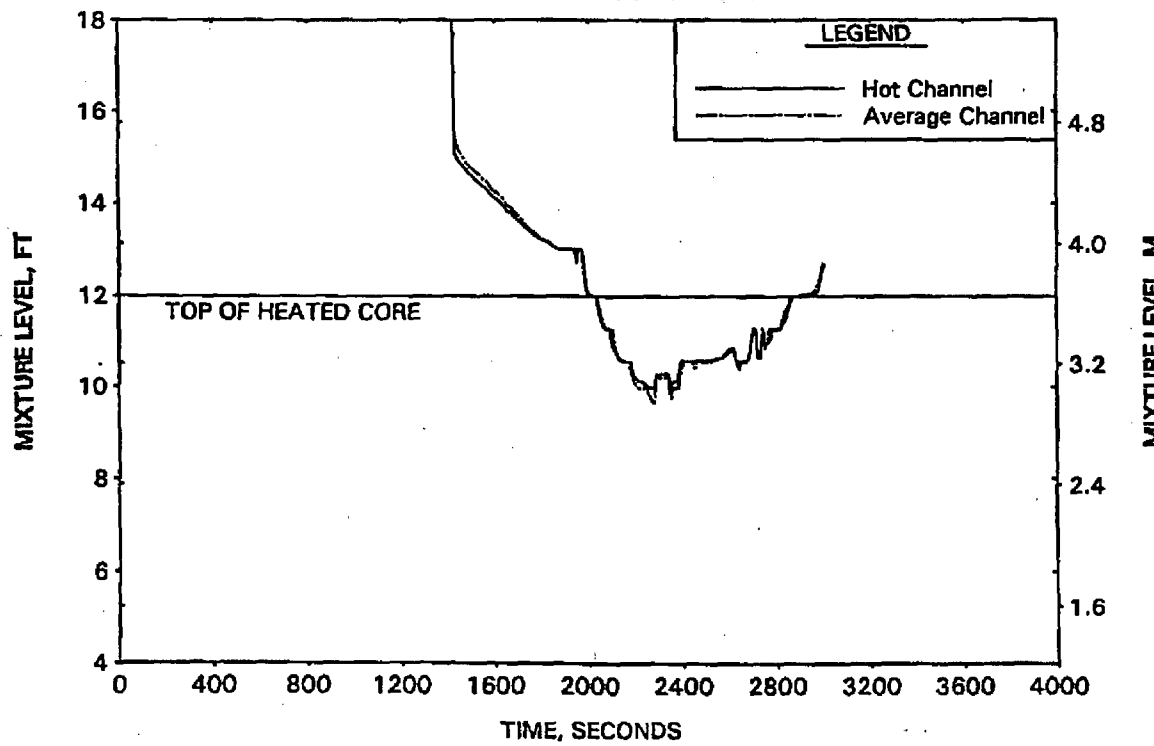


FIGURE A-35. CORE CROSSFLOW STUDY FOR 0.1-FT² CLPD BREAK - HOT CHANNEL SEGMENT 19 CLAD TEMPERATURES.

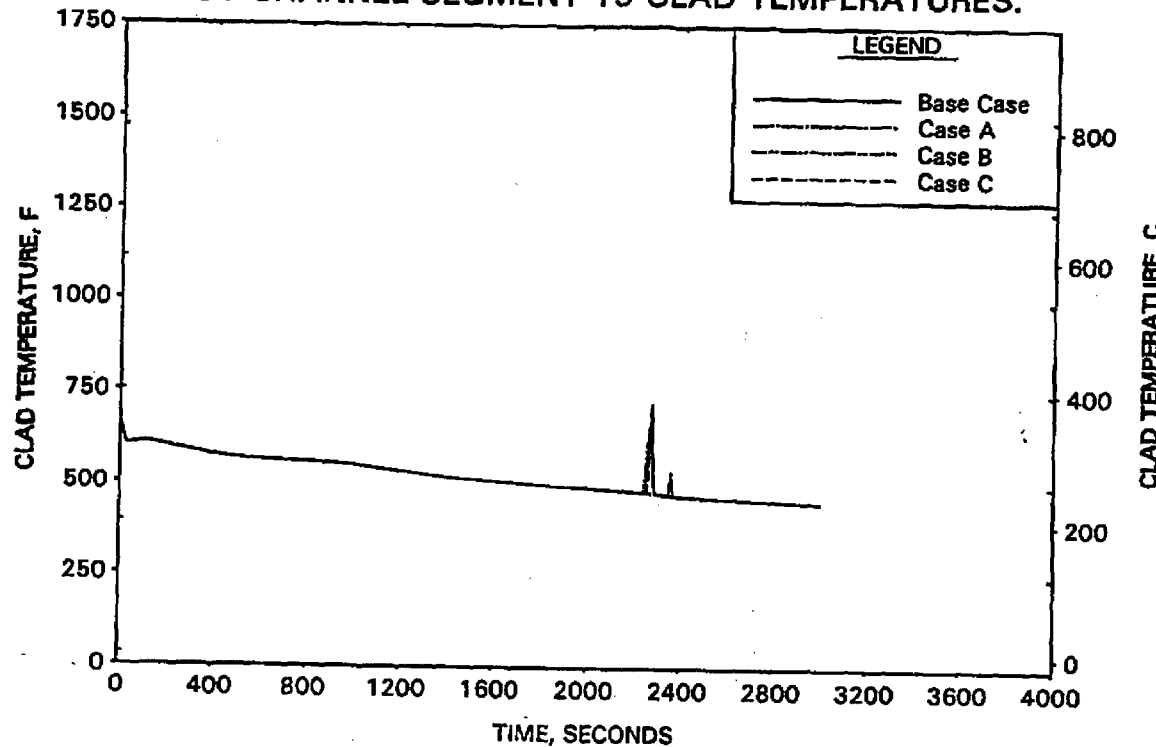


FIGURE A-36. CORE CROSSFLOW STUDY FOR 0.1-FT² CLPD BREAK - HOT CHANNEL SEGMENT 20 CLAD TEMPERATURES.

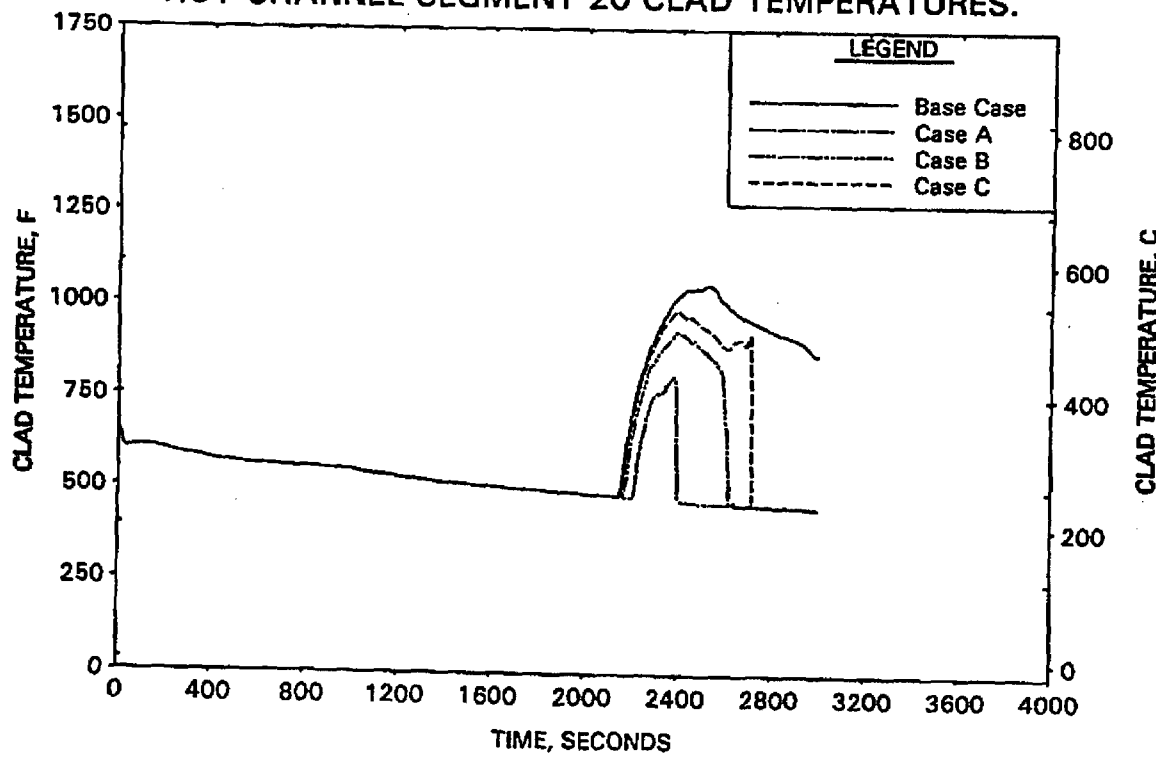


FIGURE A-37. CORE CROSSFLOW STUDY FOR 0.1-FT² CLPD BREAK - HOT CHANNEL SEGMENT 21 CLAD TEMPERATURES.

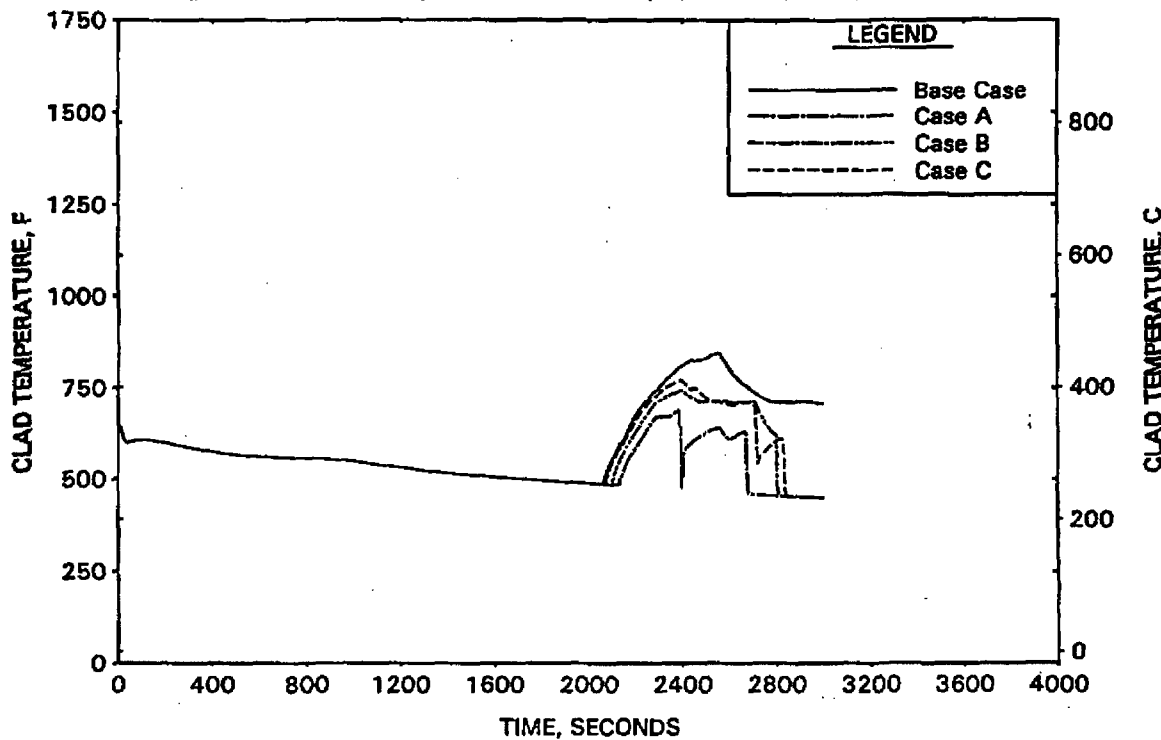


FIGURE A-38. CORE CROSSFLOW STUDY FOR 0.1-FT² CLPD BREAK - AVE CHANNEL SEGMENT 19 CLAD TEMPERATURES.

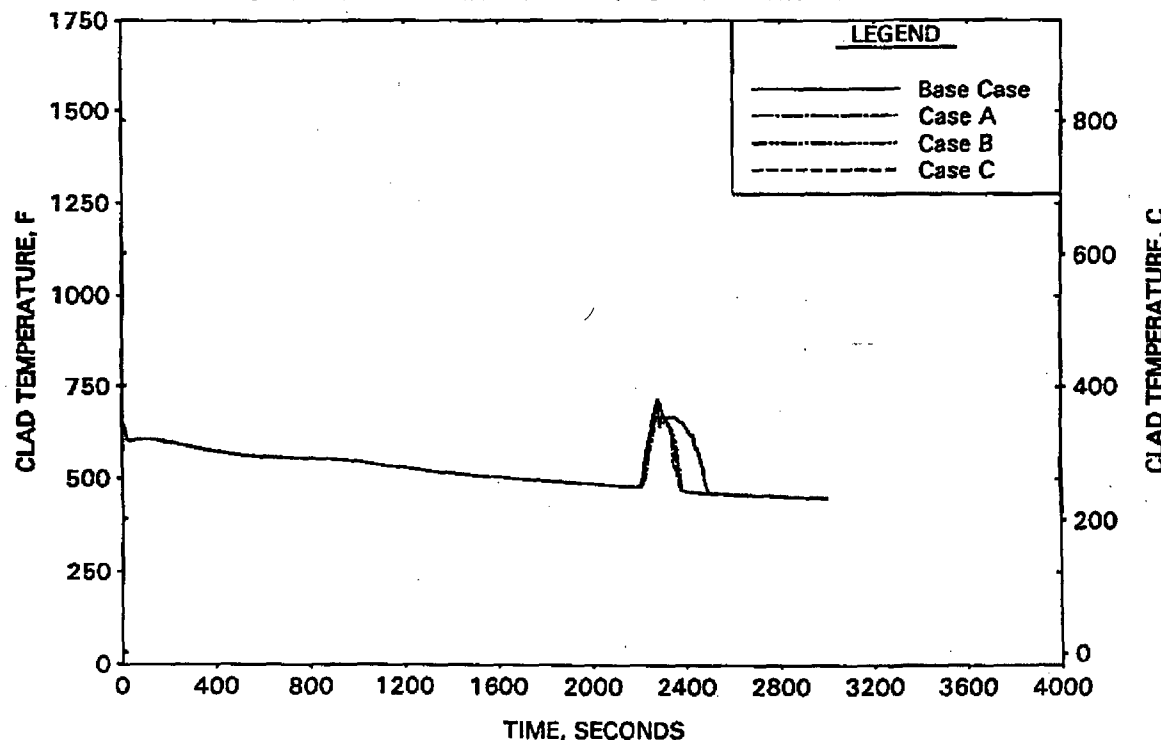


FIGURE A-39. CORE CROSSFLOW STUDY FOR 0.1-FT² CLPD BREAK -
AVE CHANNEL SEGMENT 20 CLAD TEMPERATURES.

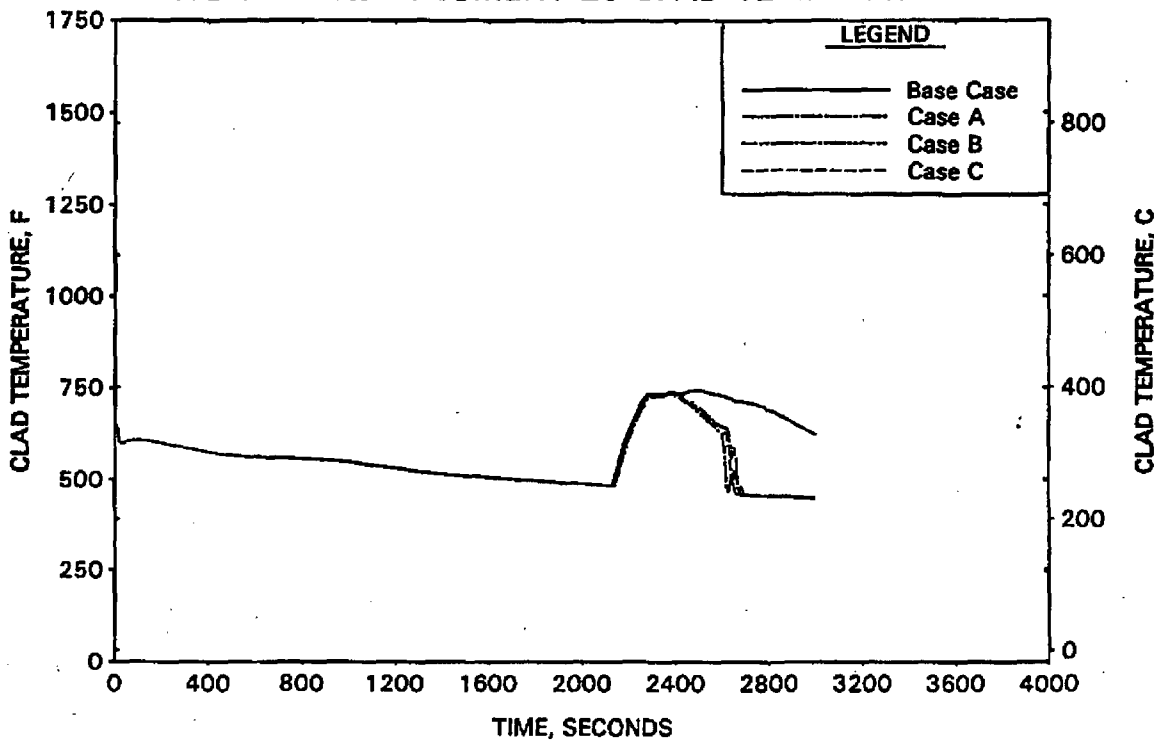


FIGURE A-40. CORE CROSSFLOW STUDY FOR 0.1-FT² CLPD BREAK -
AVE CHANNEL SEGMENT 21 CLAD TEMPERATURES.

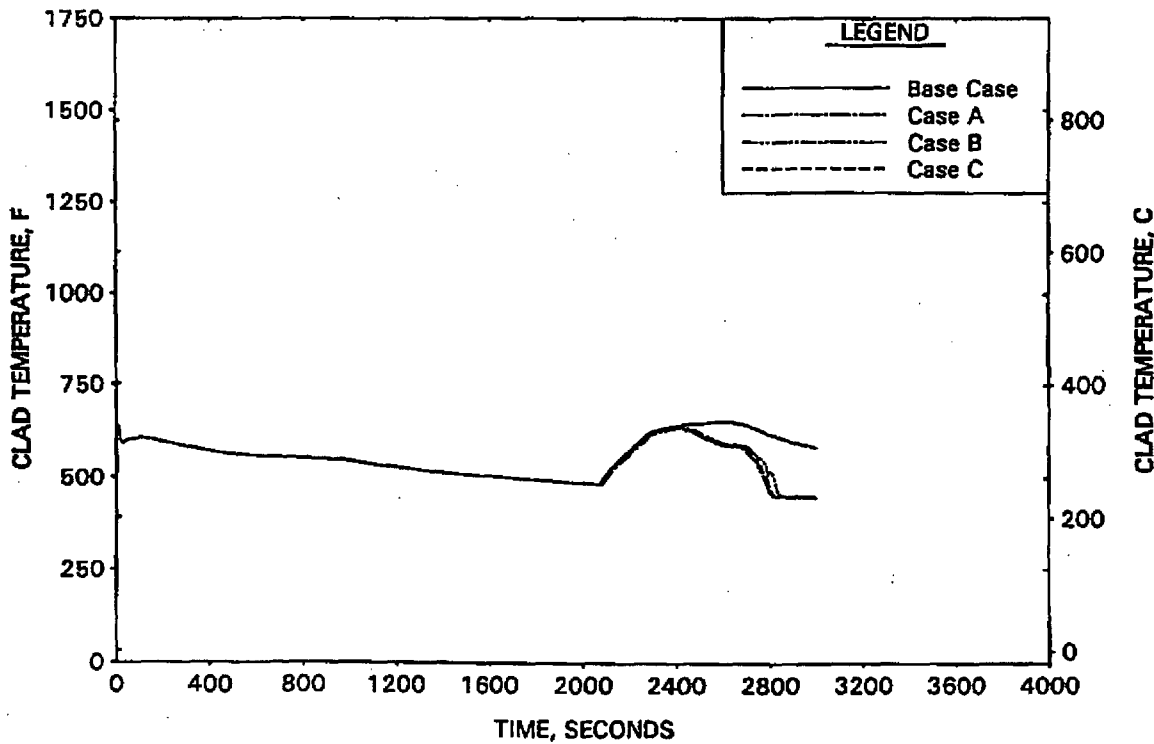


FIGURE A-41. CORE CROSSFLOW STUDY FOR 0.1-FT² CLPD BREAK -
BASE CASE CORE VOID FRACTIONS AT 2350 SECONDS.

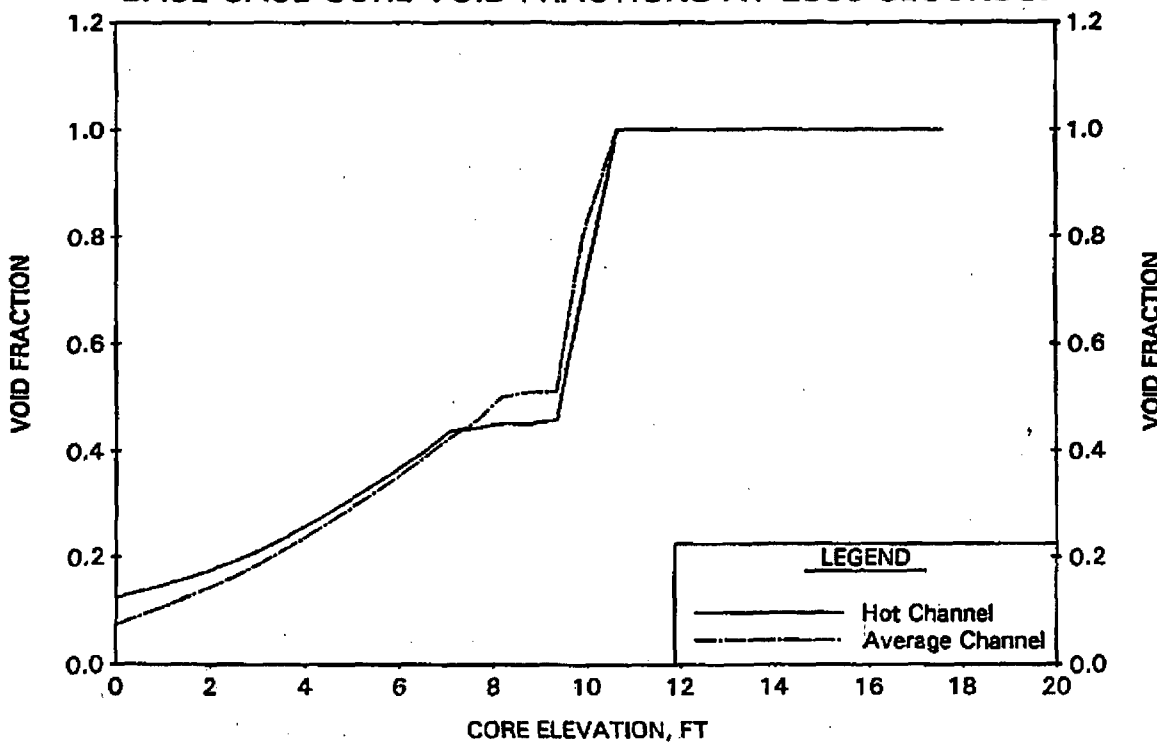


FIGURE A-42. CORE CROSSFLOW STUDY FOR 0.1-FT² CLPD BREAK -
CASE A CORE VOID FRACTIONS AT 2350 SECONDS.

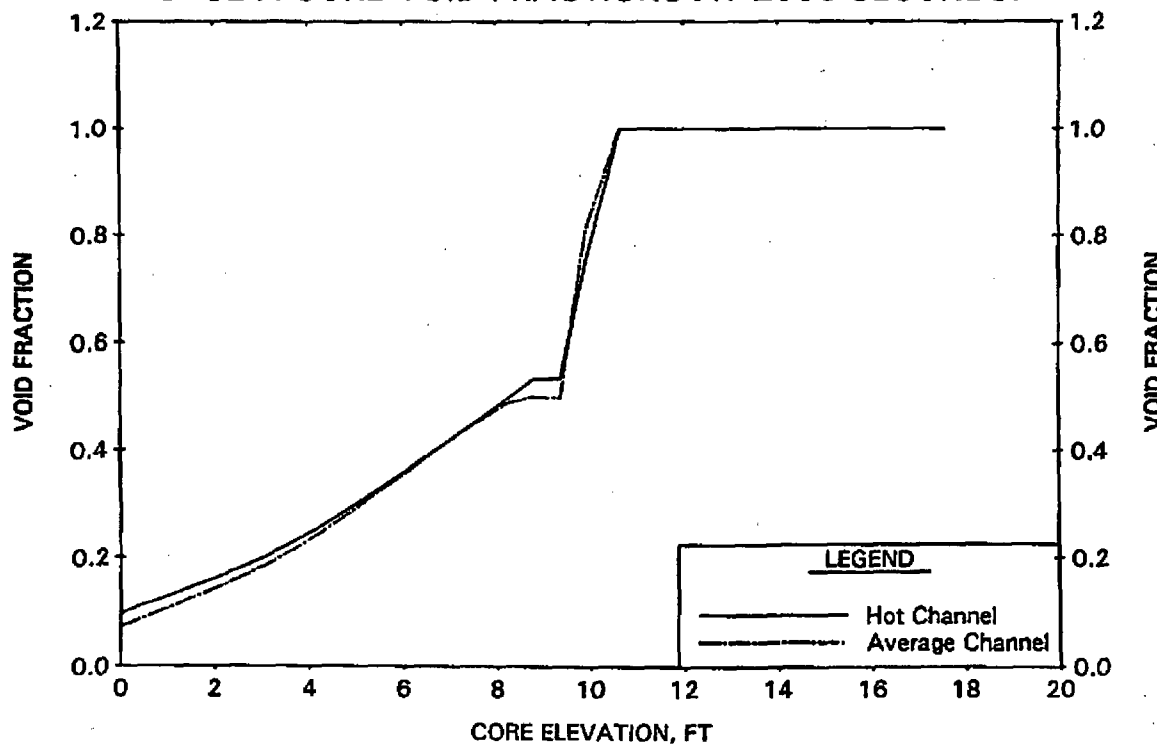


FIGURE A-43. CORE CROSSFLOW STUDY FOR 0.1-FT² CLPD BREAK -
CASE B CORE VOID FRACTIONS AT 2350 SECONDS.

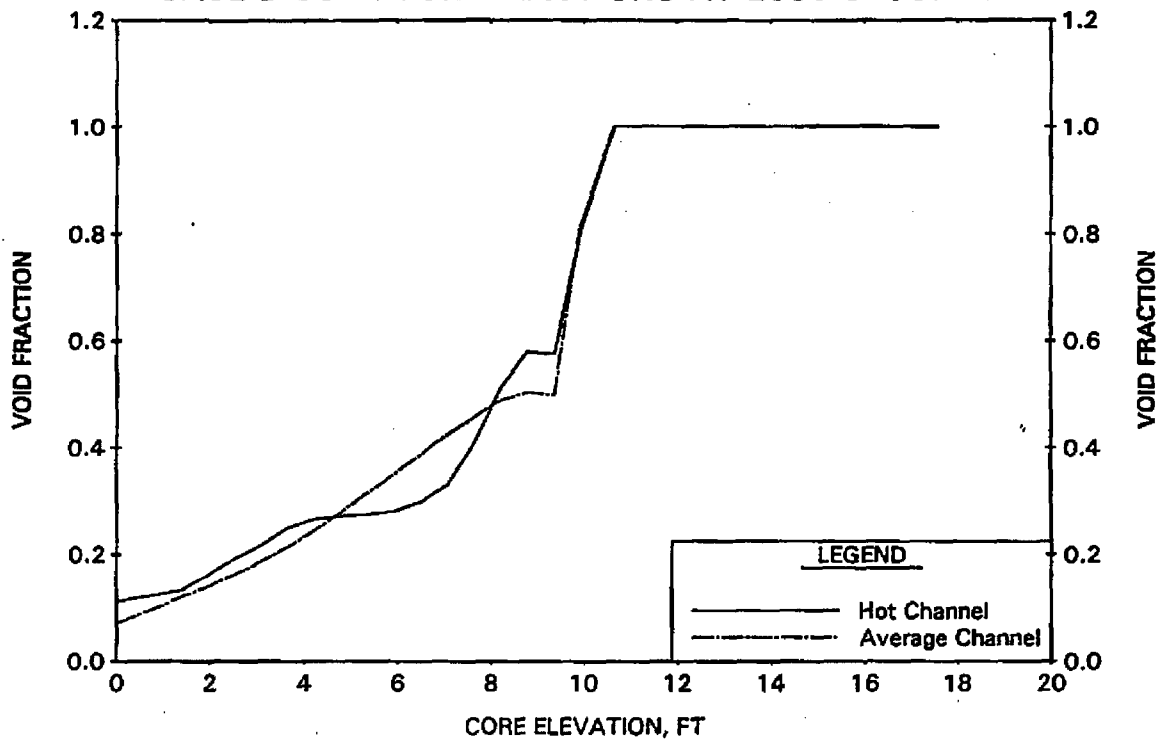


FIGURE A-44. CORE CROSSFLOW STUDY FOR 0.1-FT² CLPD BREAK -
CASE C CORE VOID FRACTIONS AT 2350 SECONDS.

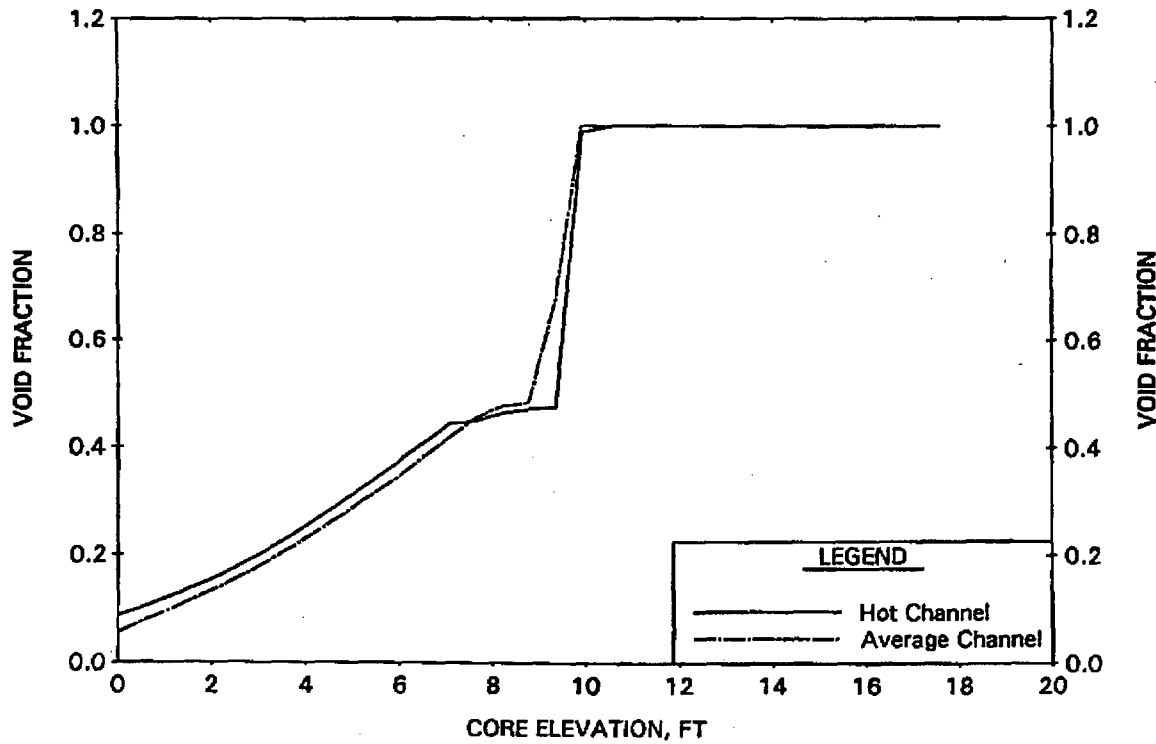


FIGURE A-45. CORE NODING STUDY FOR 0.1-FT² CLPD BREAK - RCS PRESSURE.

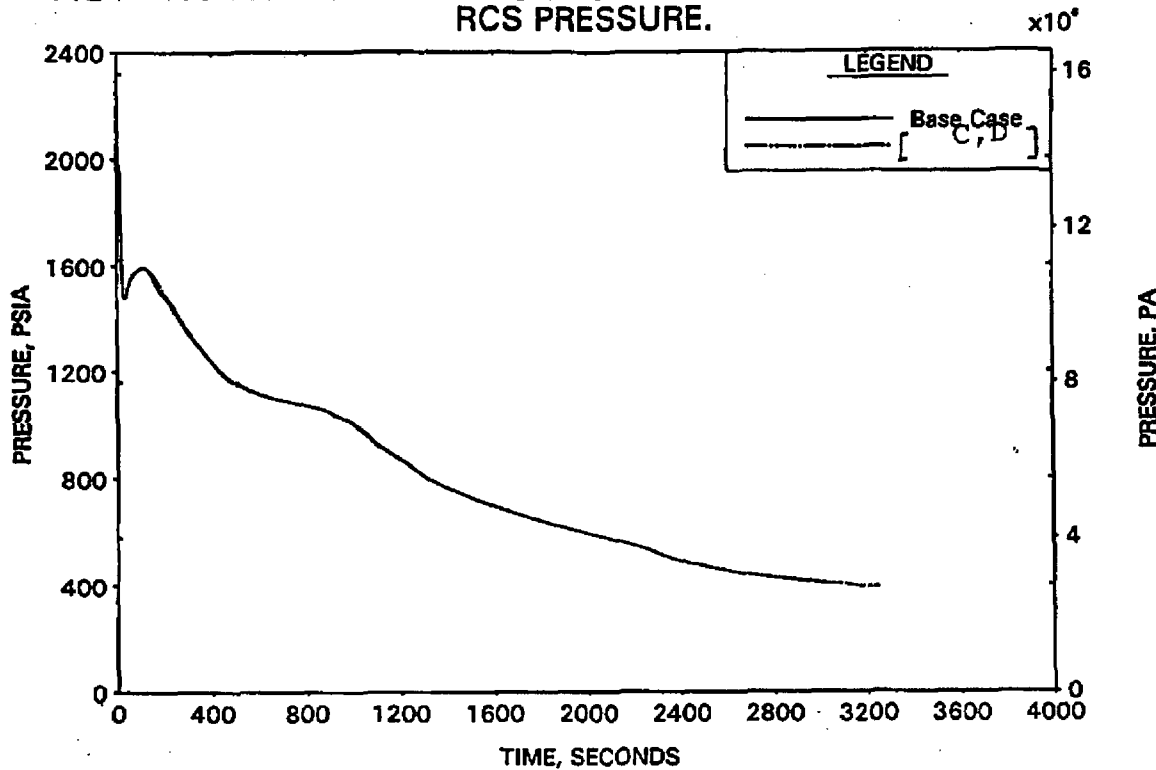


FIGURE A-46. CORE NODING STUDY FOR 0.1-FT² CLPD BREAK - REACTOR VESSEL COLLAPSED LEVEL.

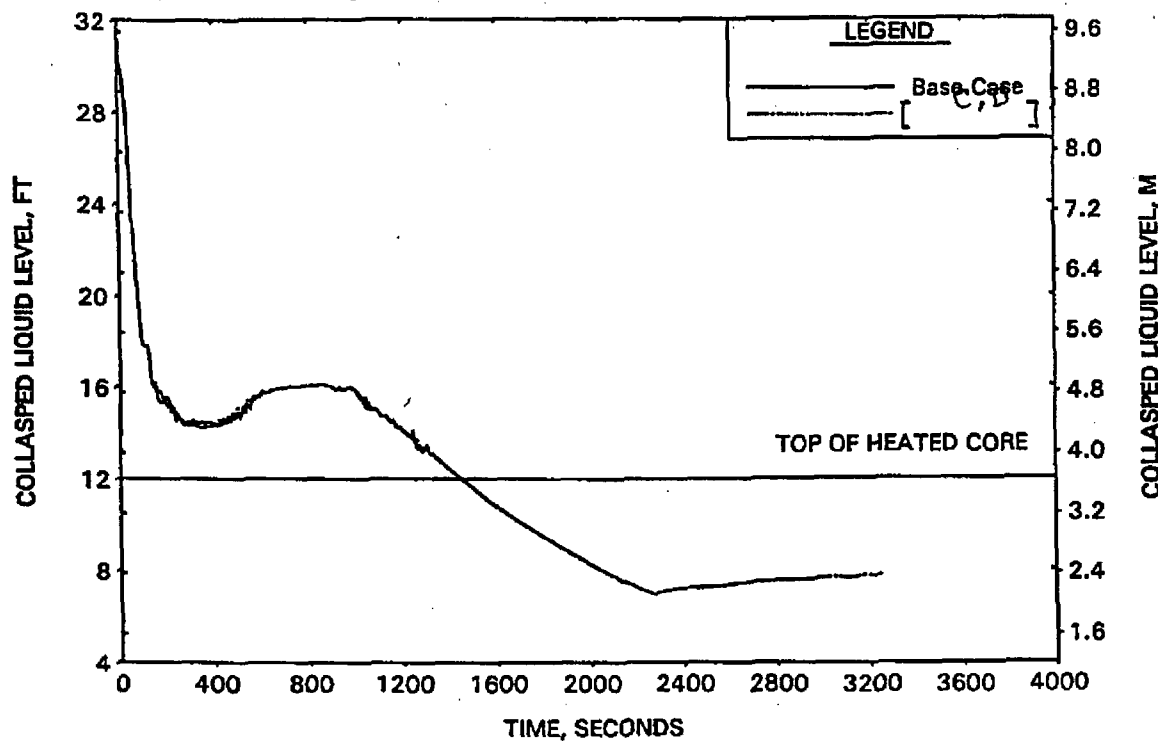


FIGURE A-47. CORE NODING STUDY FOR 0.1-FT² CLPD BREAK - HOT CHANNEL MIXTURE LEVEL.

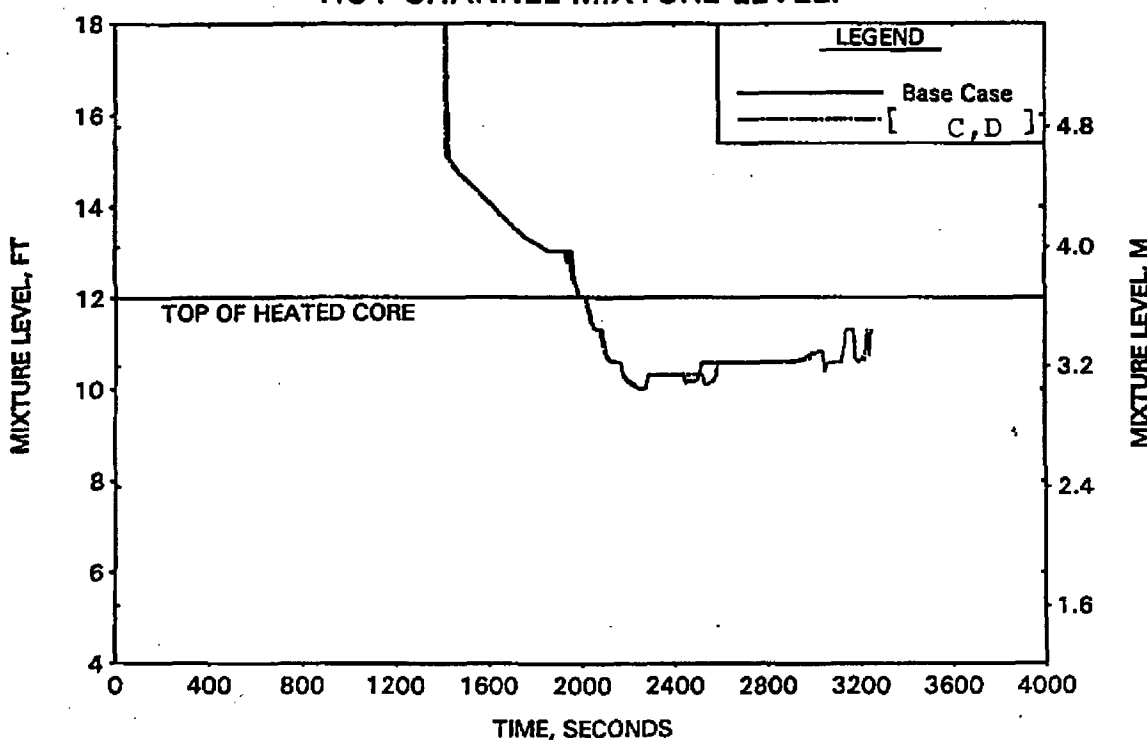


FIGURE A-48. CORE NODING STUDY FOR 0.1-FT² CLPD BREAK AVERAGE CHANNEL MIXTURE LEVELS.

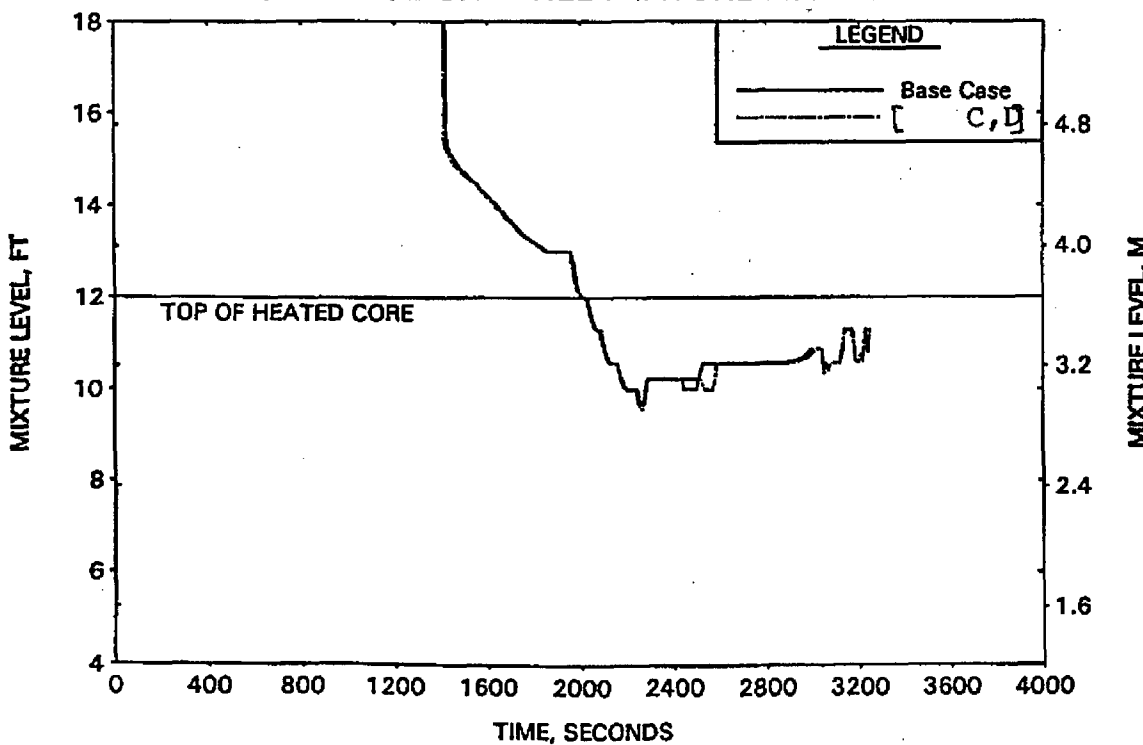


FIGURE A-49. CORE NODING STUDY FOR 0.1-FT² CLPD BREAK
HOT CHANNEL PEAK CLAD TEMPERATURES.

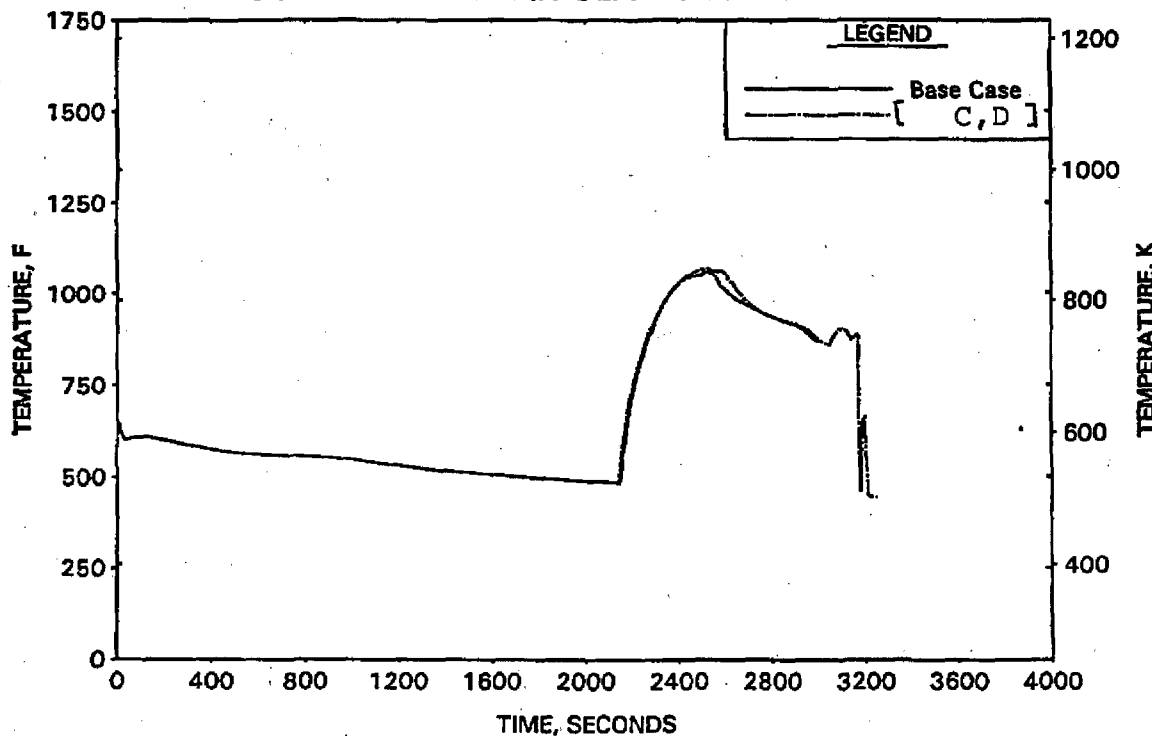


FIGURE A-50. CORE NODING STUDY FOR 0.1-FT² CLPD BREAK
AVERAGE CHANNEL PEAK CLAD TEMPERATURES.

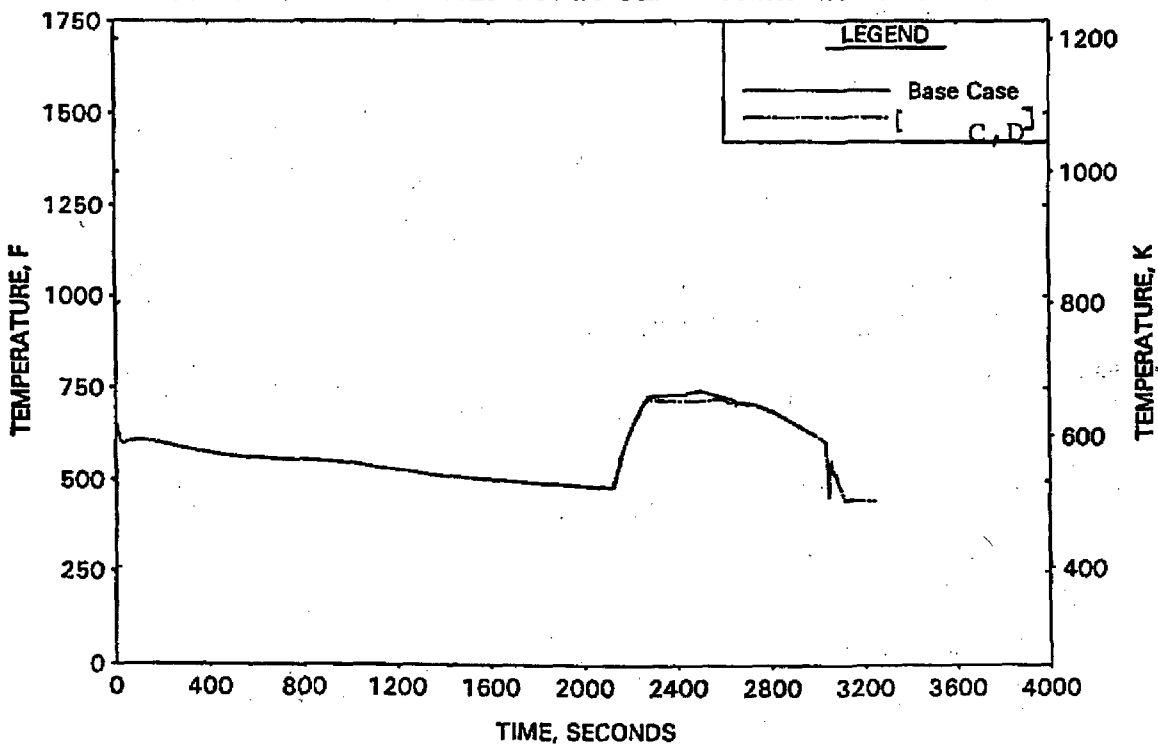


FIGURE A-51. CLPD BREAK SPECTRUM STUDY FOR 0.04-FT² BREAK - RCS PRESSURES.

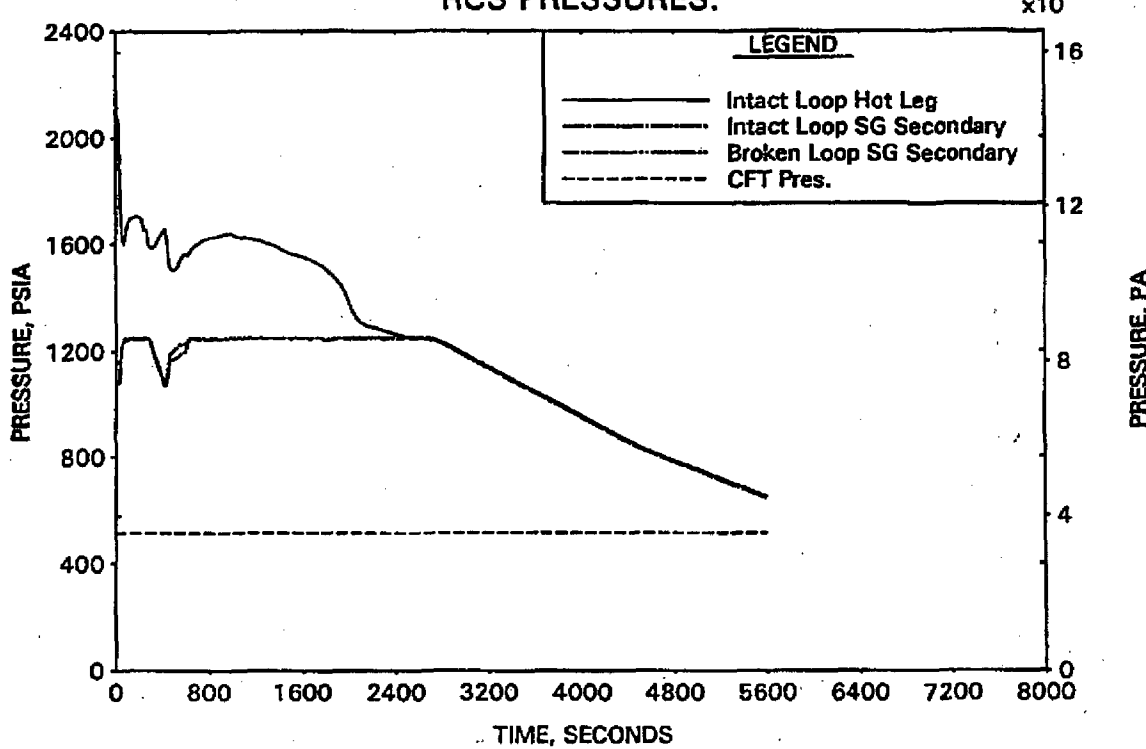


FIGURE A-52. CLPD BREAK SPECTRUM STUDY FOR 0.04-FT² BREAK - DC, RV, AND CORE COLLAPSED LEVELS.

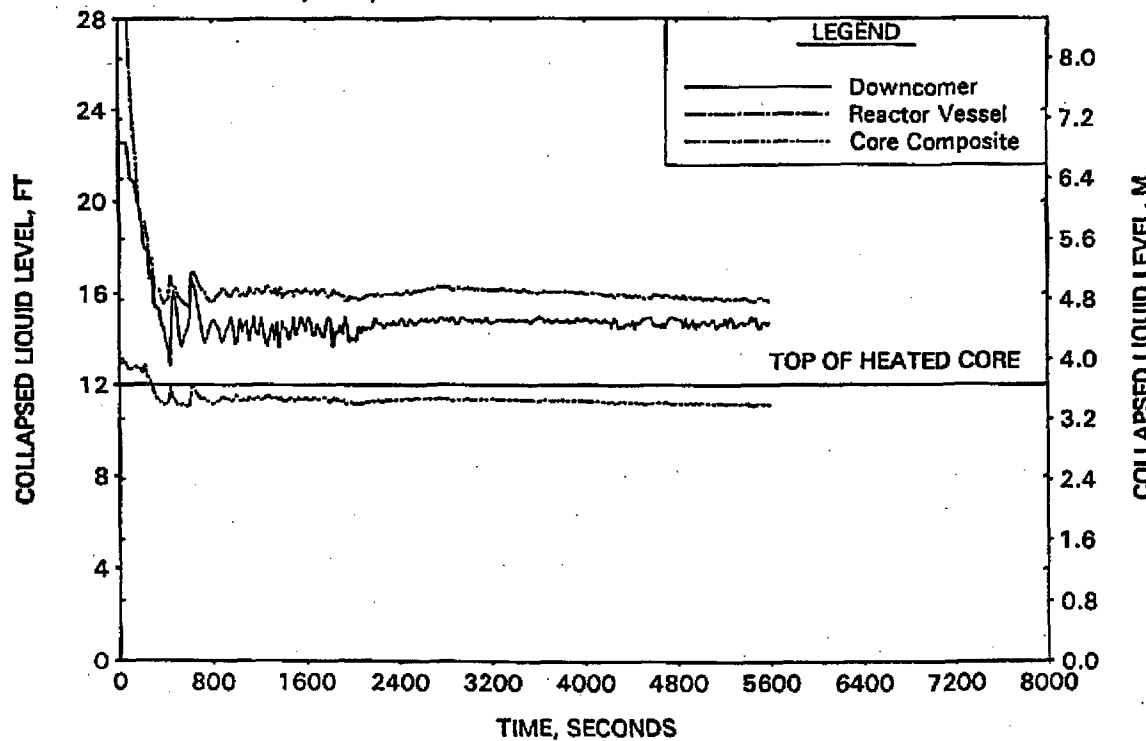


FIGURE A-53. CLPD BREAK SPECTRUM STUDY FOR 0.04-FT² BREAK -
BREAK AND TOTAL ECCS FLOWS.

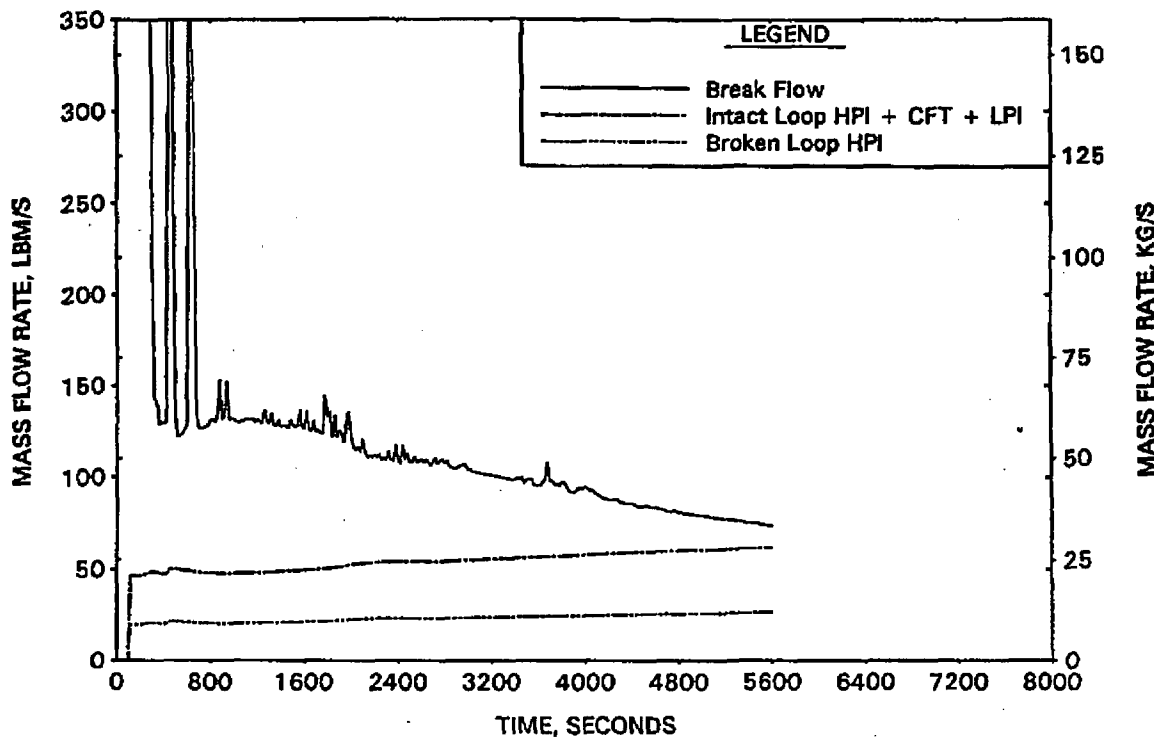


FIGURE A-54. CLPD BREAK SPECTRUM STUDY FOR 0.04-FT² BREAK -
BREAK VOLUME VOID FRACTION.

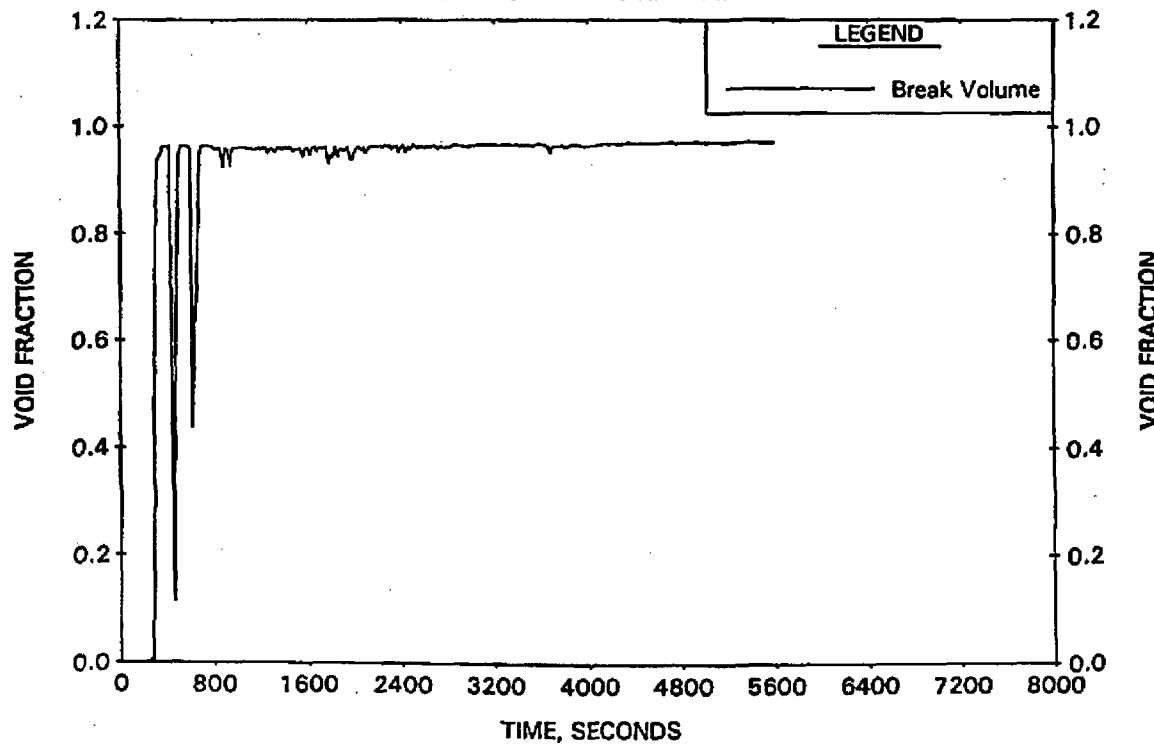


FIGURE A-55. CLPD BREAK SPECTRUM STUDY FOR 0.04-FT² BREAK - BROKEN LOOP COLLAPSED LEVELS.

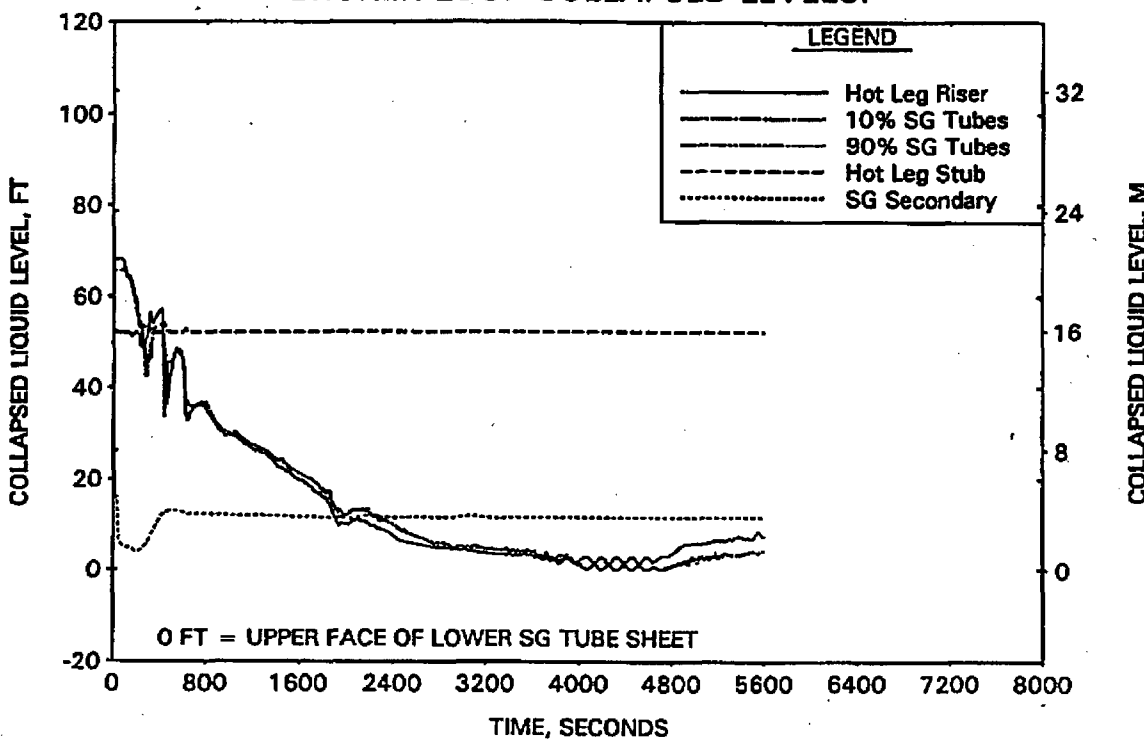


FIGURE A-56. CLPD BREAK SPECTRUM STUDY FOR 0.04-FT² BREAK - INTACT LOOP COLLAPSED LEVELS.

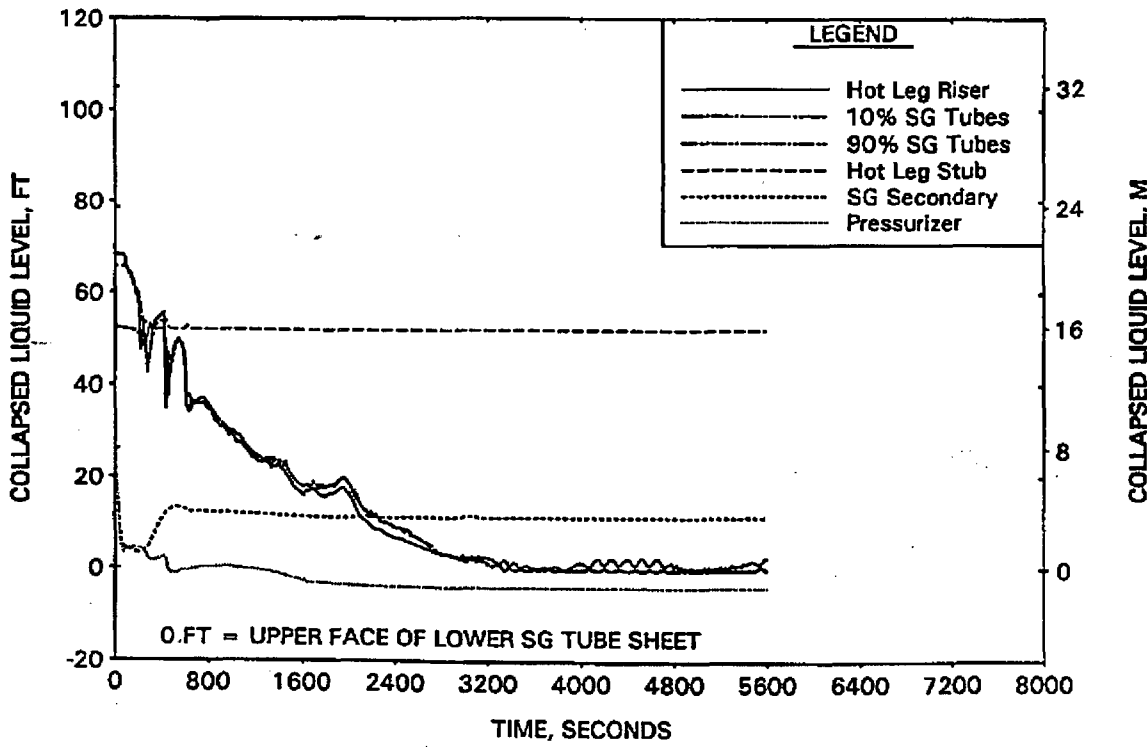


FIGURE A-57. CLPD BREAK SPECTRUM STUDY FOR 0.04-FT² BREAK - CLPD COLLAPSED LEVELS.

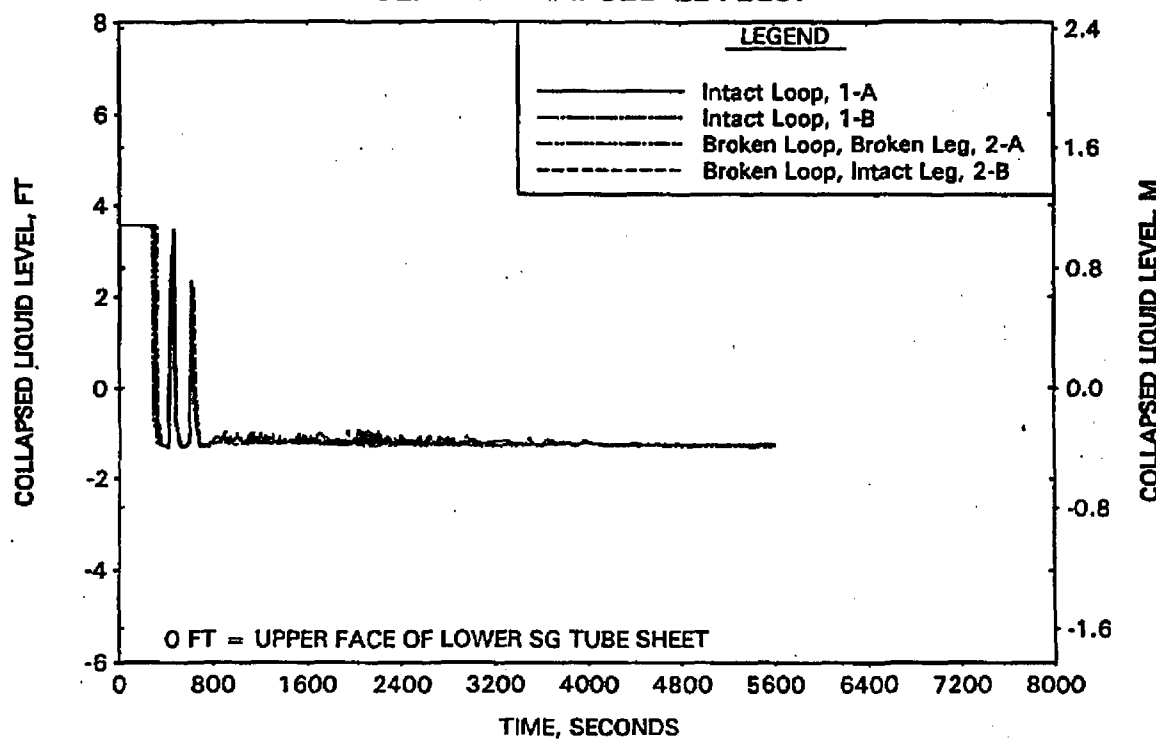


FIGURE A-58. CLPD BREAK SPECTRUM STUDY FOR 0.04-FT² BREAK - CLPS LIQUID VOLUME.

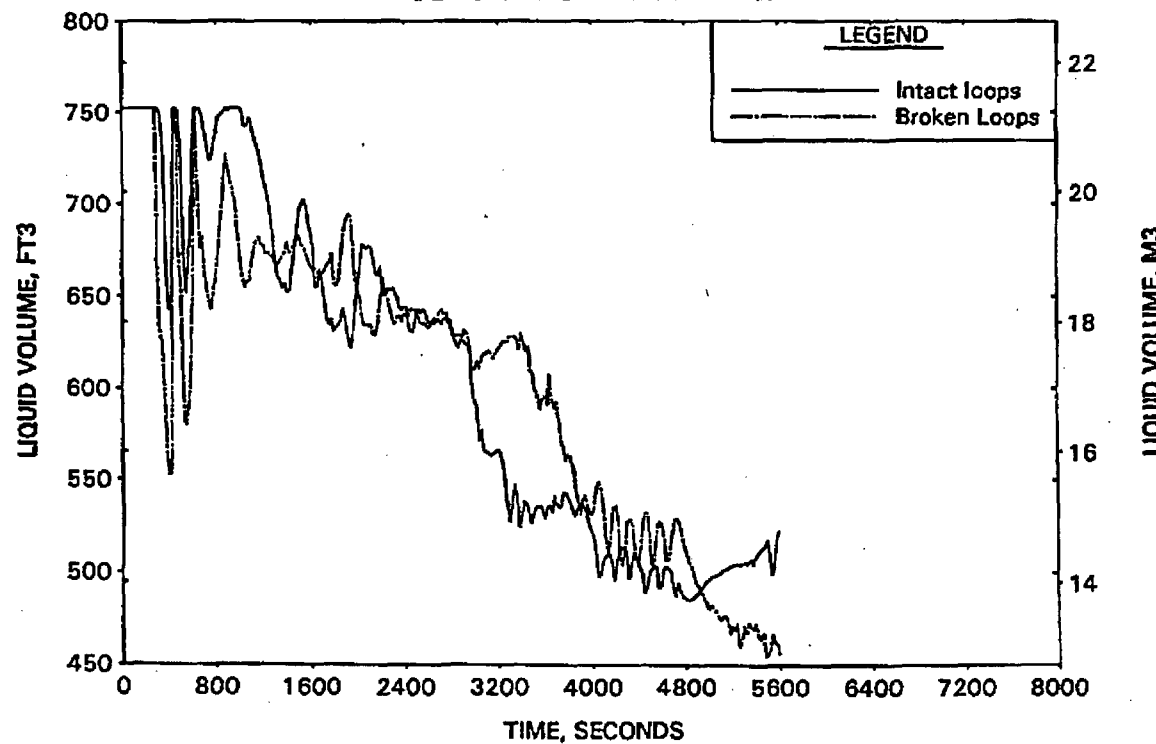


FIGURE A-59. CLPD BREAK SPECTRUM STUDY FOR 0.04-FT² BREAK - FILTERED HOT LEG AND RVVV FLOWS.

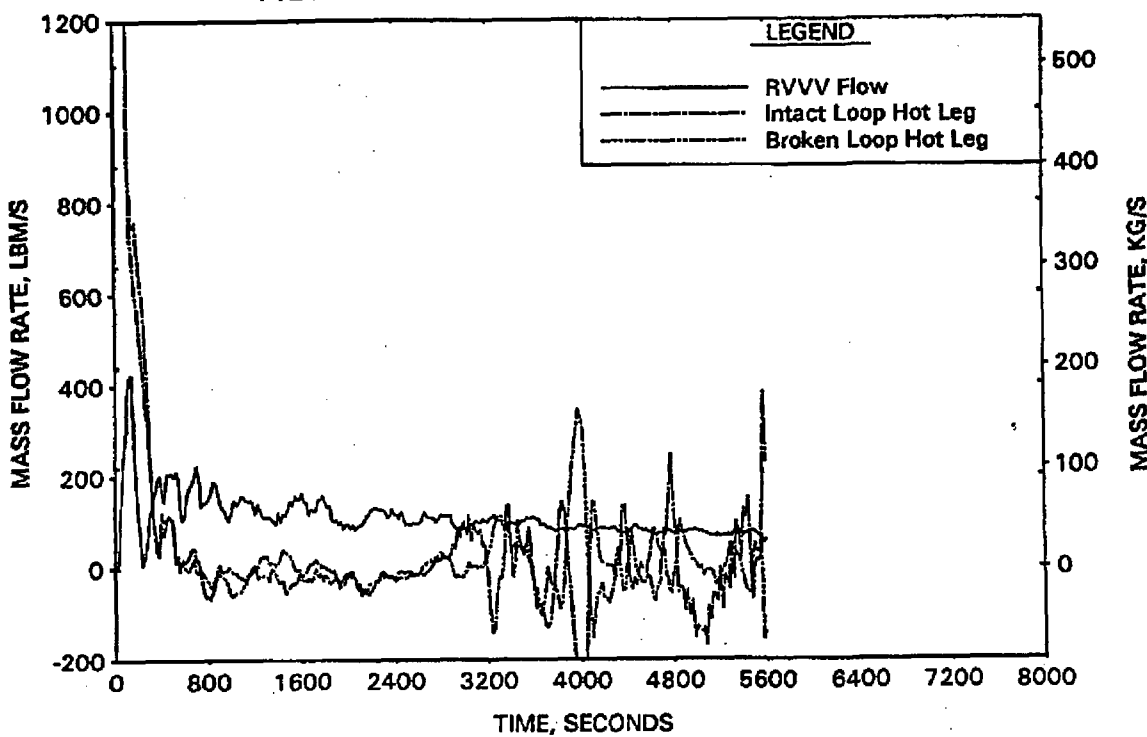


FIGURE A-60. CLPD BREAK SPECTRUM STUDY FOR 0.04-FT² BREAK - CORE MIXTURE LEVELS.

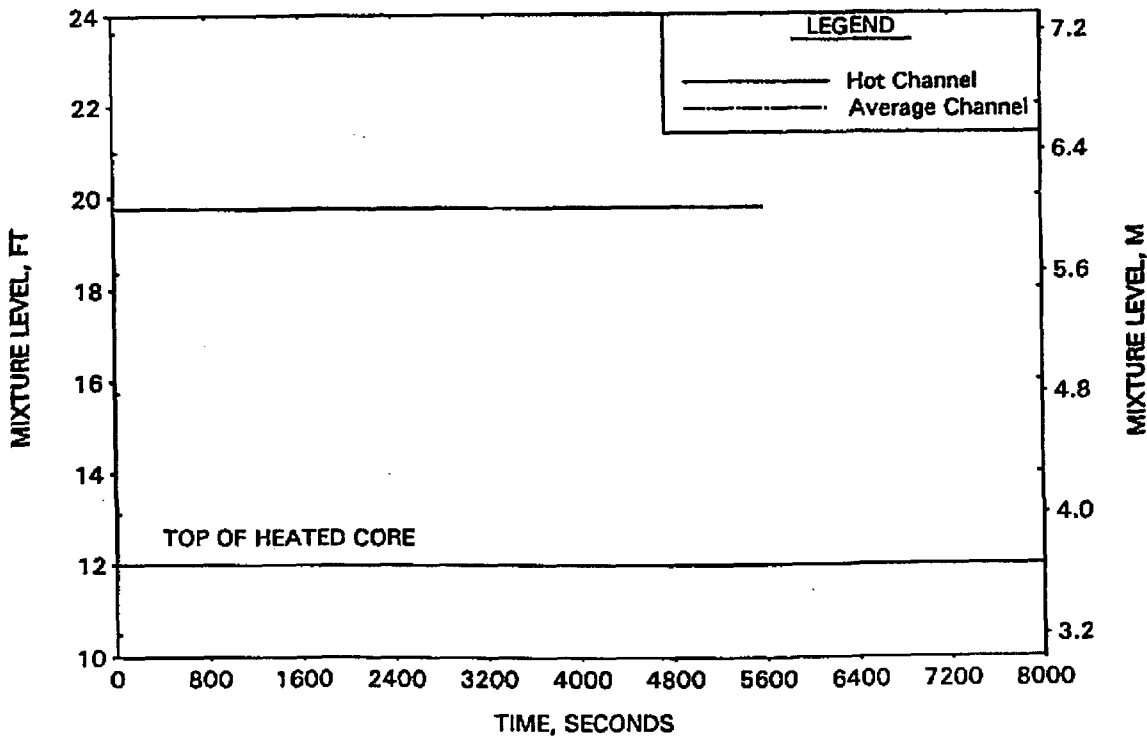


FIGURE A-61. CLPD BREAK SPECTRUM STUDY FOR 0.04-FT² BREAK - HOT CHANNEL CLAD TEMPERATURES.

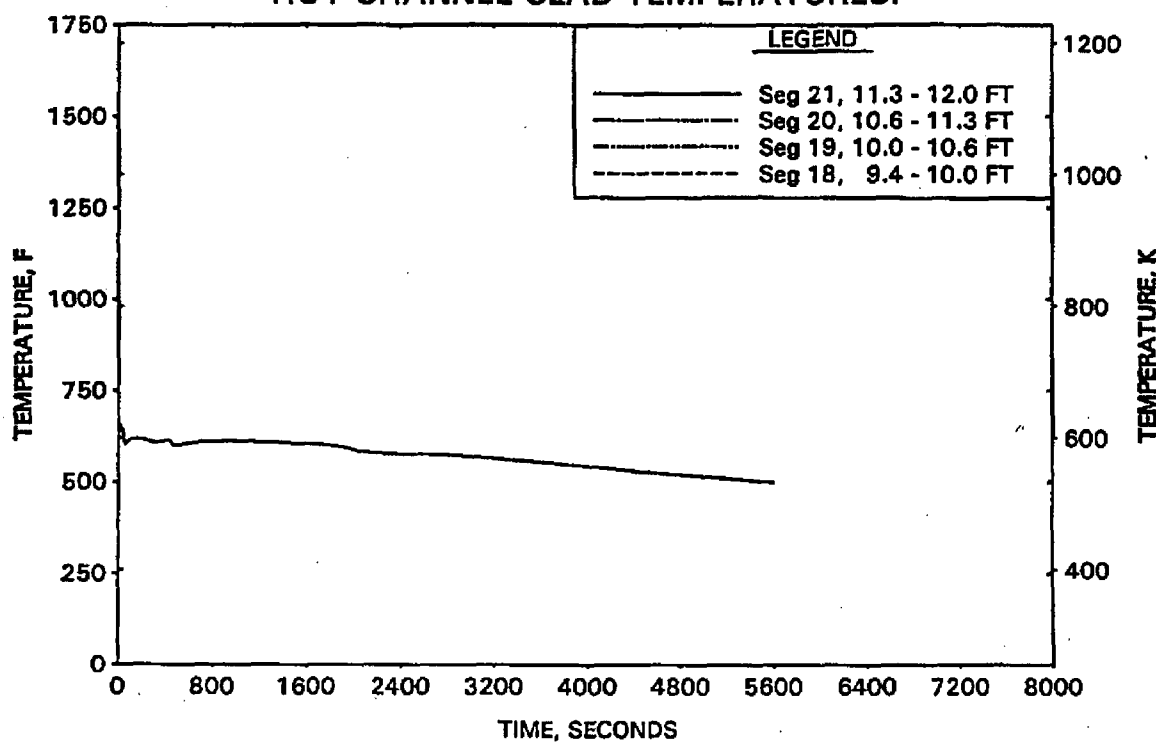


FIGURE A-62. CLPD BREAK SPECTRUM STUDY FOR 0.04-FT² BREAK - HOT CHANNEL STEAM TEMPERATURES.

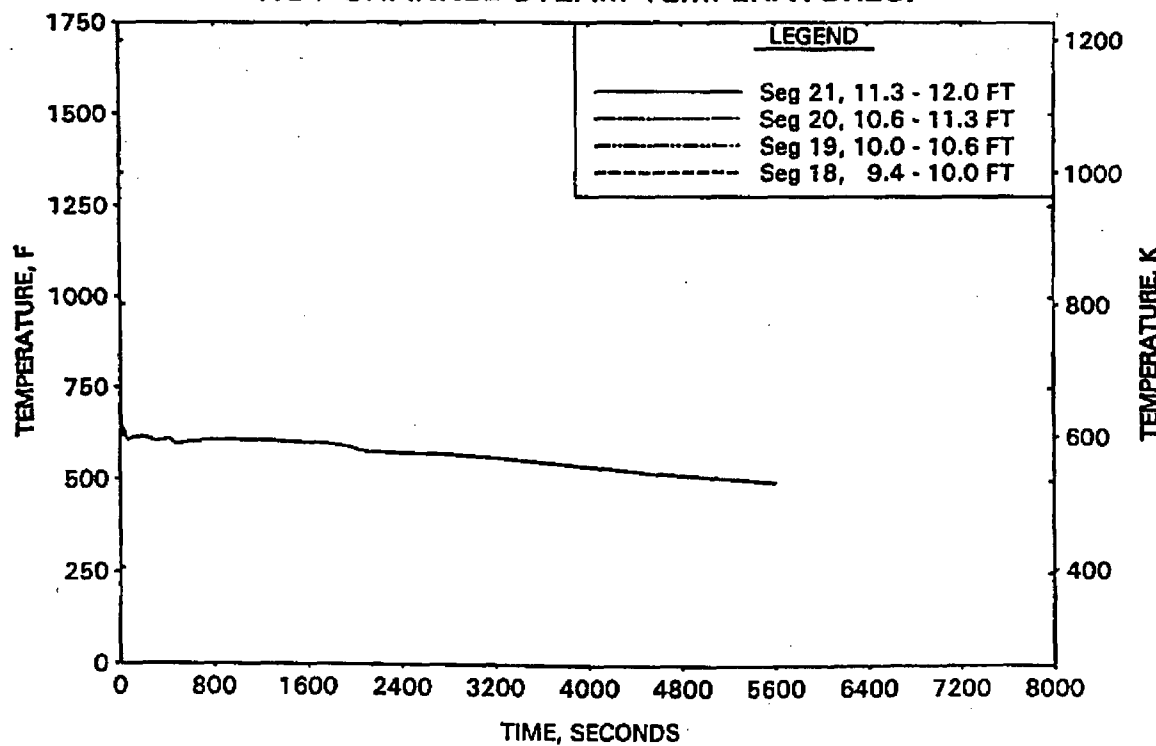


FIGURE A-63. CLPD BREAK SPECTRUM STUDY FOR 0.04-FT2 BREAK -
UPPER ELEVATION AVE CHANNEL CLAD TEMPERATURES.

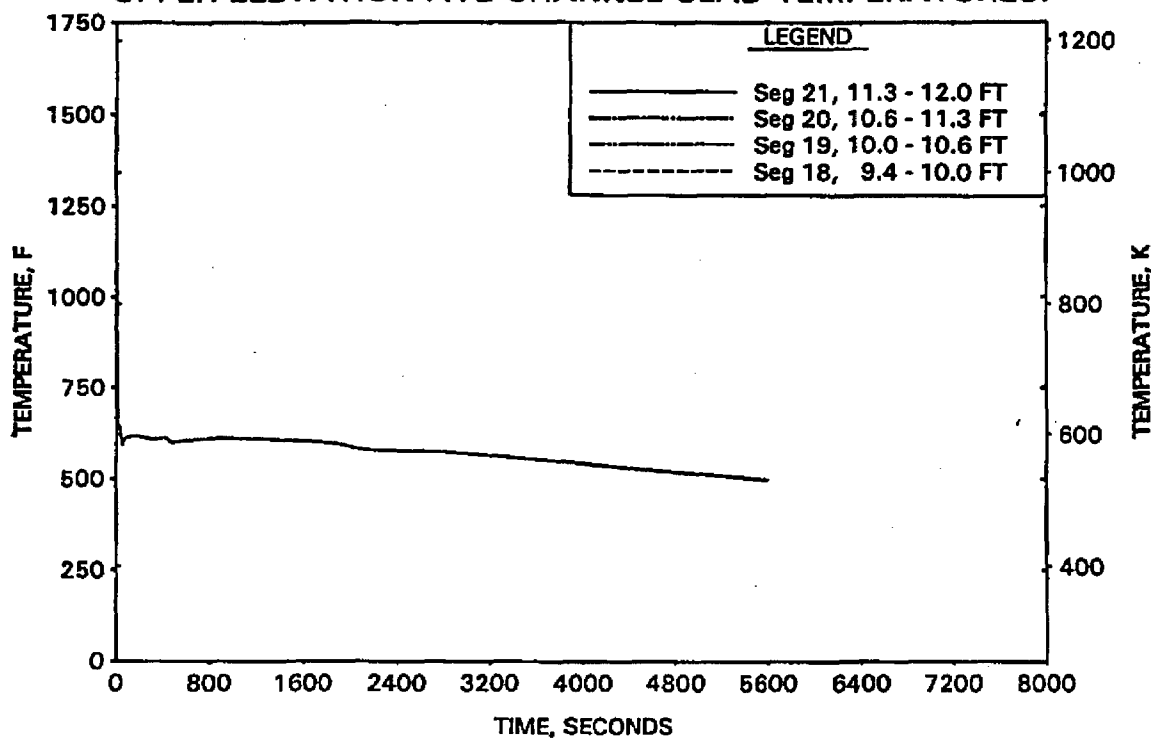


FIGURE A-64. CLPD BREAK SPECTRUM STUDY FOR 0.04-FT2 BREAK -
UPPER ELEVATION AVE CHANNEL STEAM TEMPERATURES.

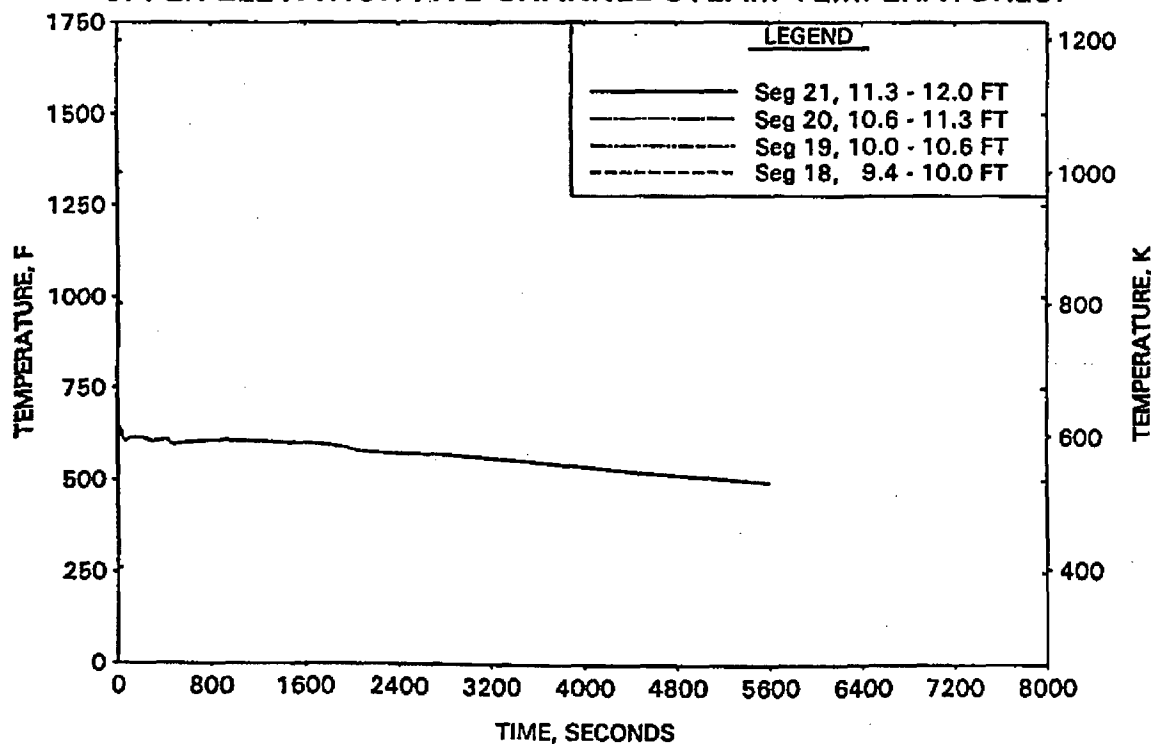


FIGURE A-65. CLPD BREAK SPECTRUM STUDY FOR 0.07-FT² BREAK - RCS PRESSURES.

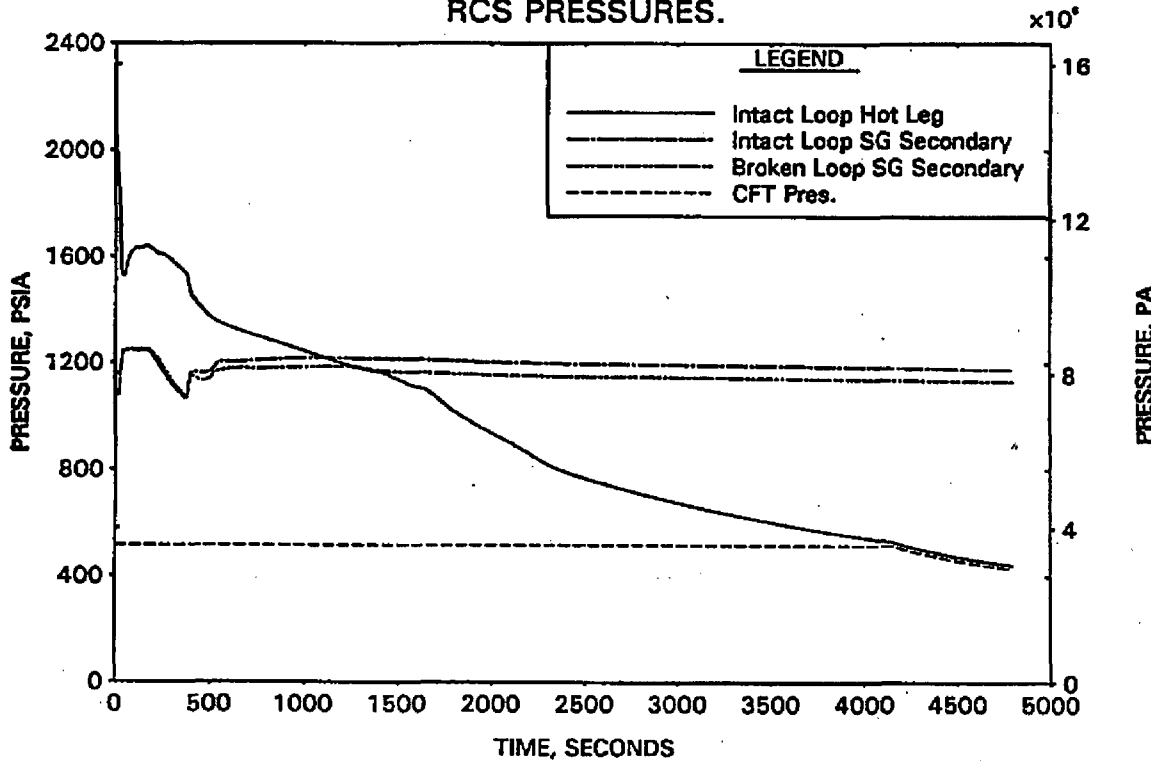


FIGURE A-66. CLPD BREAK SPECTRUM STUDY FOR 0.07-FT² BREAK - DC, RV, AND CORE COLLAPSED LEVELS.

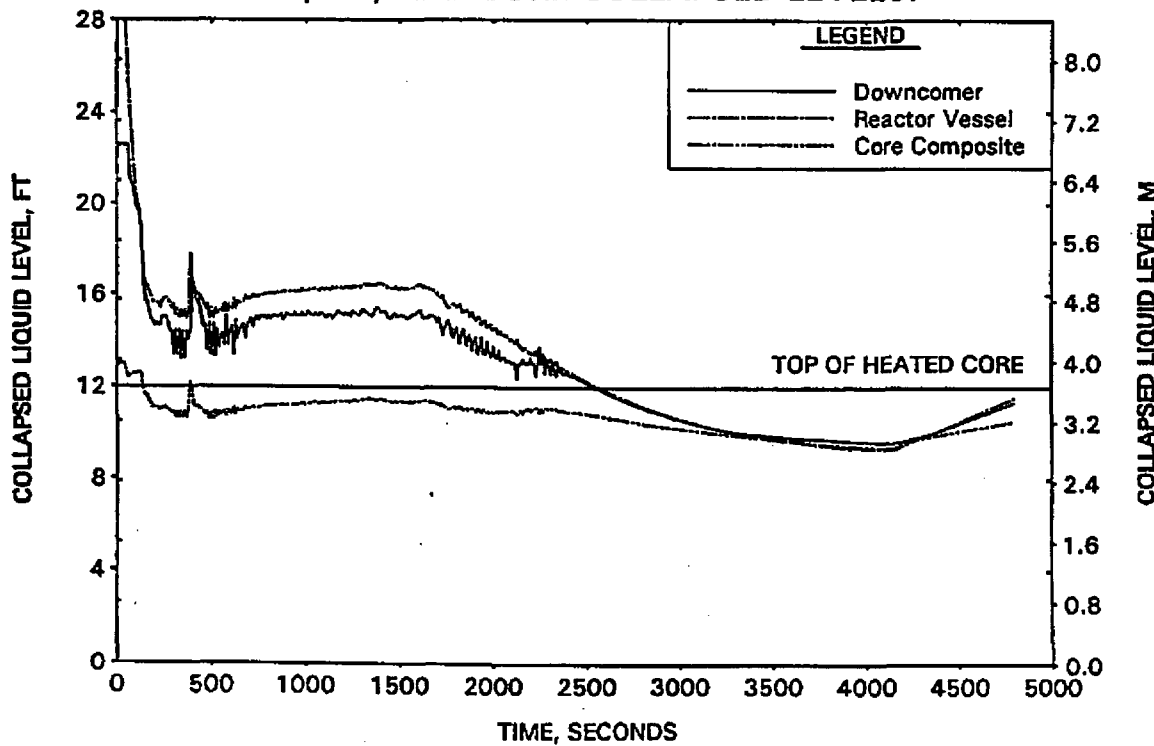


FIGURE A-67. CLPD BREAK SPECTRUM STUDY FOR 0.07-FT² BREAK -
BREAK AND TOTAL ECCS FLOWS.

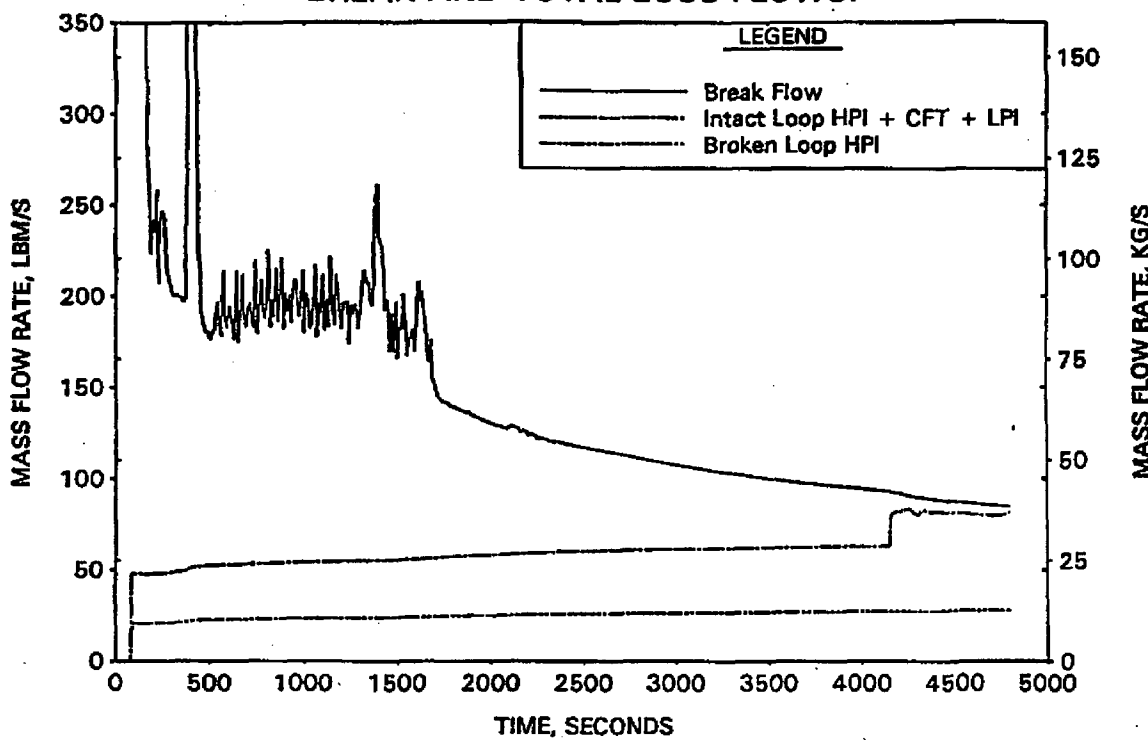


FIGURE A-68. CLPD BREAK SPECTRUM STUDY FOR 0.07-FT² BREAK -
BREAK VOLUME VOID FRACTION.

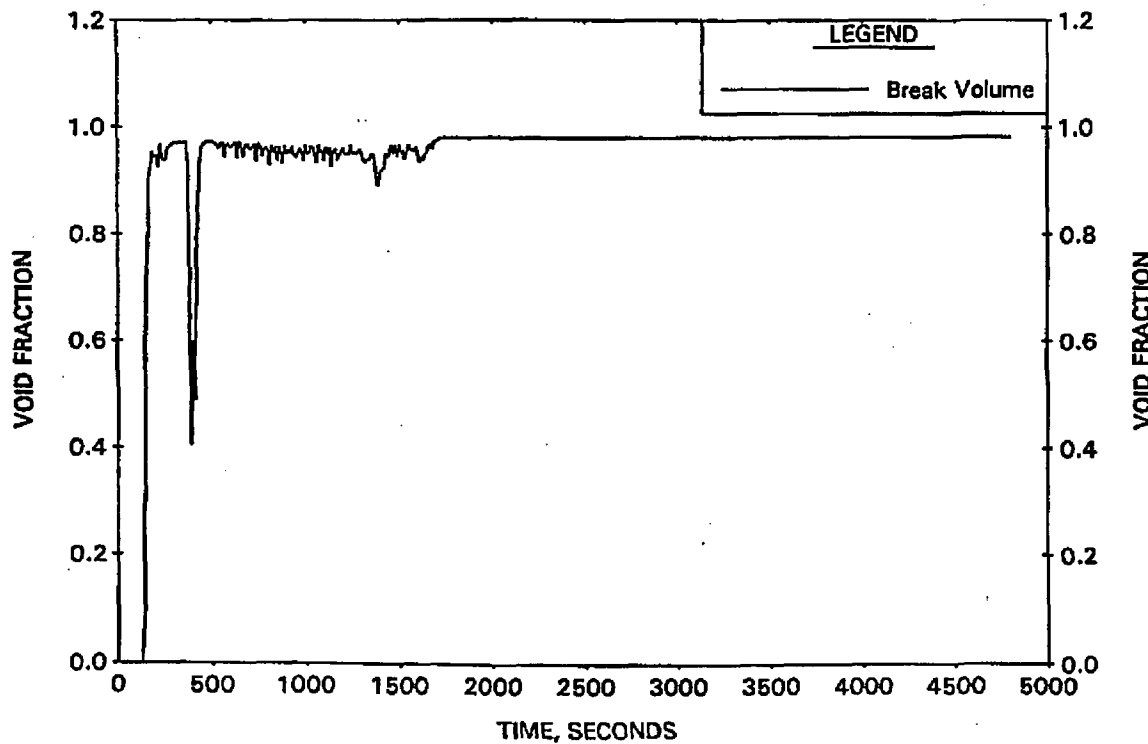


FIGURE A-69. CLPD BREAK SPECTRUM STUDY FOR 0.07-FT² BREAK - BROKEN LOOP COLLAPSED LEVELS.

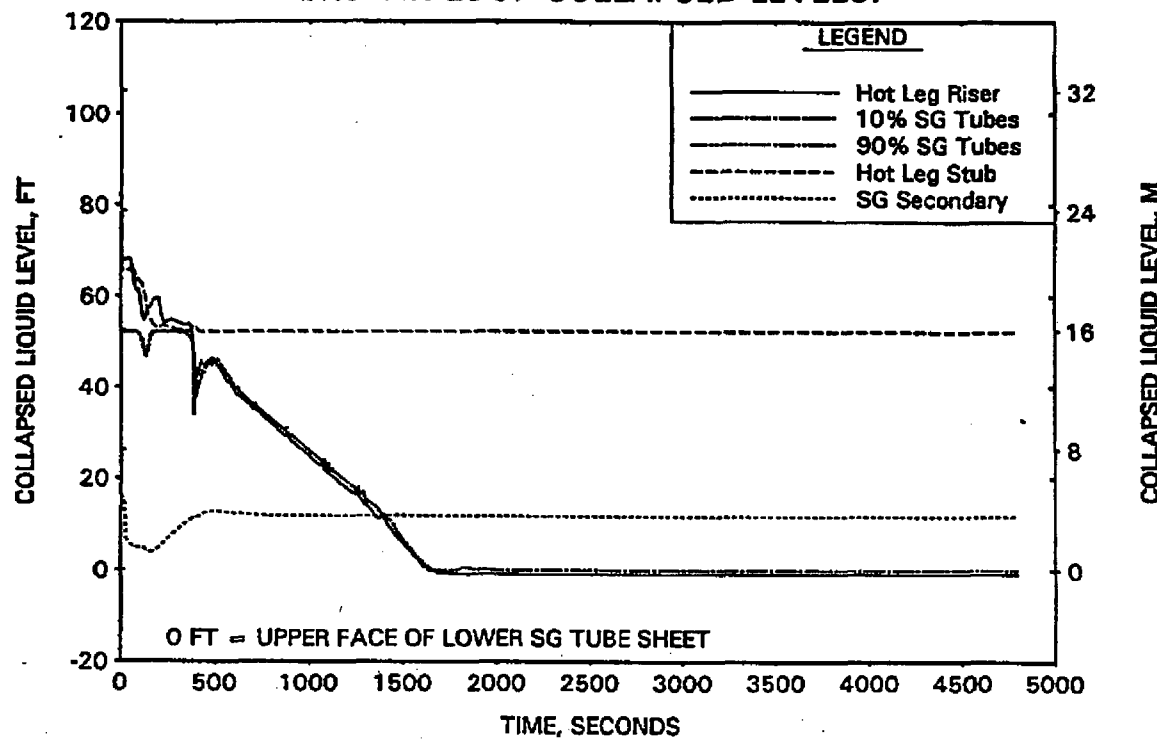


FIGURE A-70. CLPD BREAK SPECTRUM STUDY FOR 0.07-FT² BREAK - INTACT LOOP COLLAPSED LEVELS.

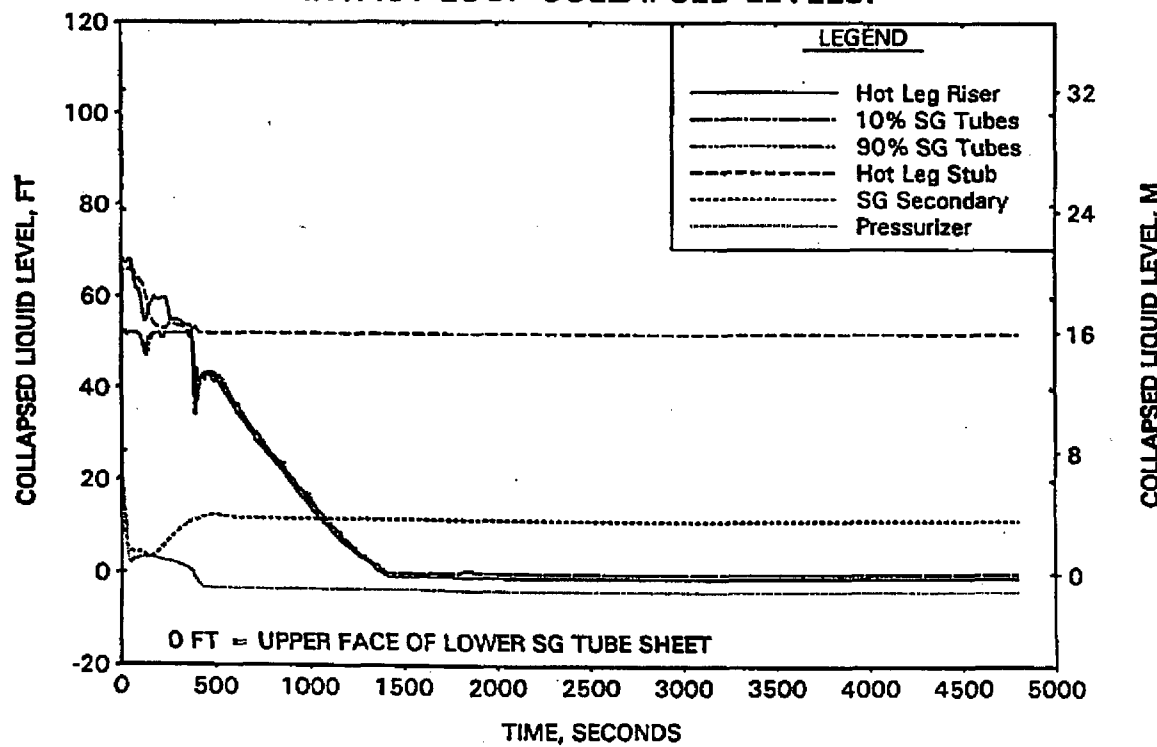


FIGURE A-71. CLPD BREAK SPECTRUM STUDY FOR 0.07-FT² BREAK - CLPD COLLAPSED LEVELS.

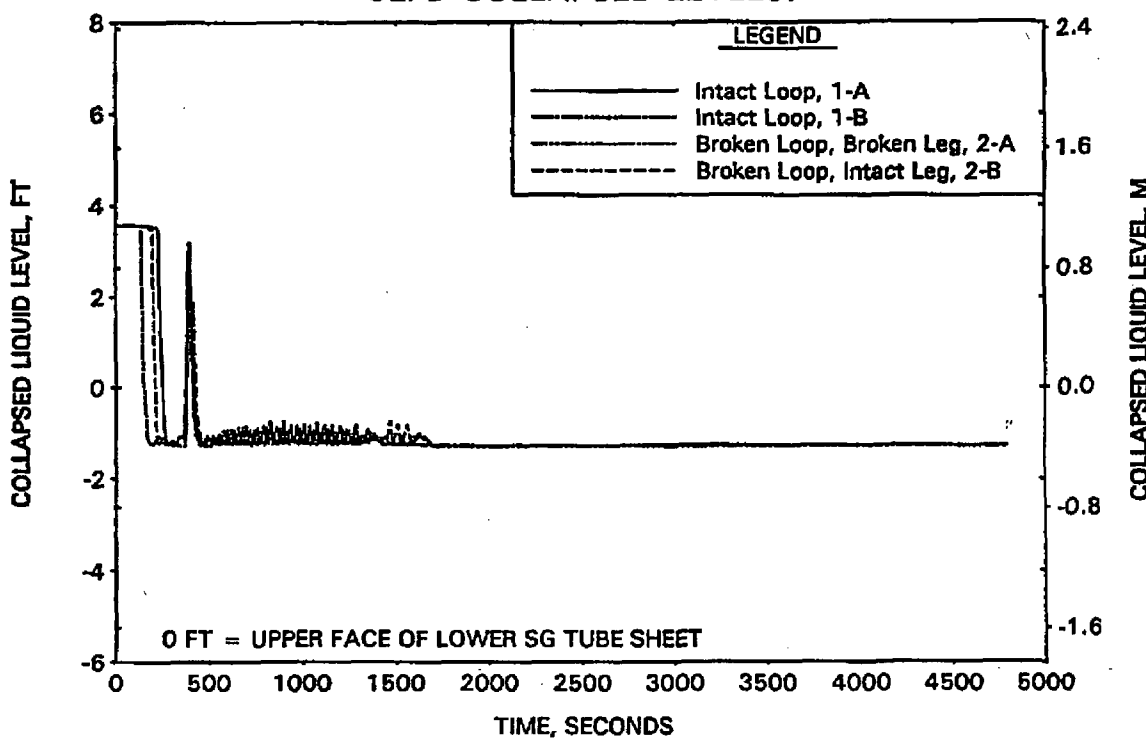


FIGURE A-72. CLPD BREAK SPECTRUM STUDY FOR 0.07-FT² BREAK - CLPS LIQUID VOLUME.

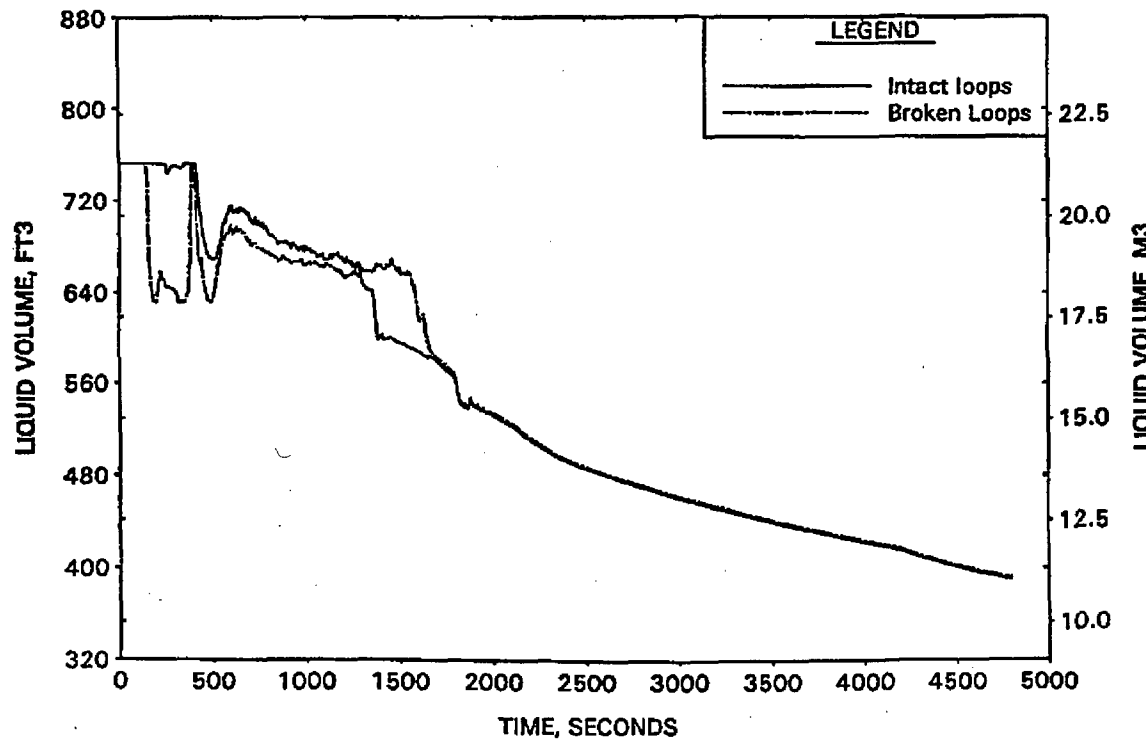


FIGURE A-73. CLPD BREAK SPECTRUM STUDY FOR 0.07-FT² BREAK - FILTERED HOT LEG AND RVVV FLOWS.

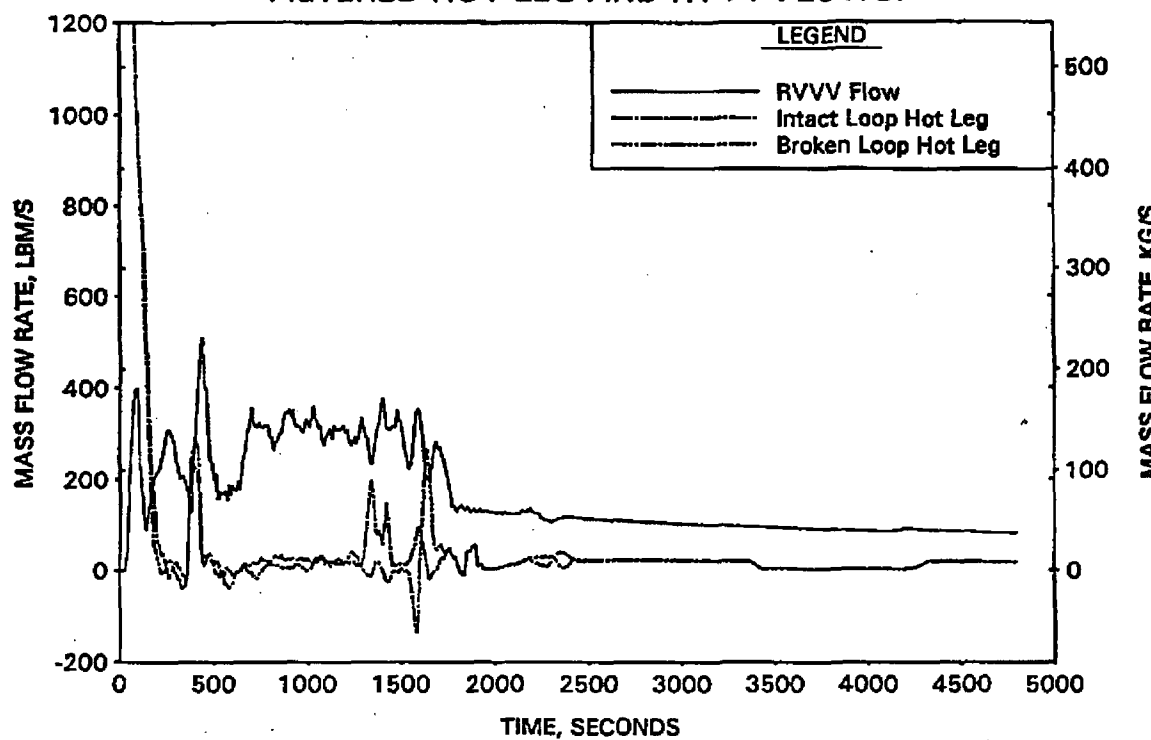


FIGURE A-74. CLPD BREAK SPECTRUM STUDY FOR 0.07-FT² BREAK - CORE MIXTURE LEVELS.

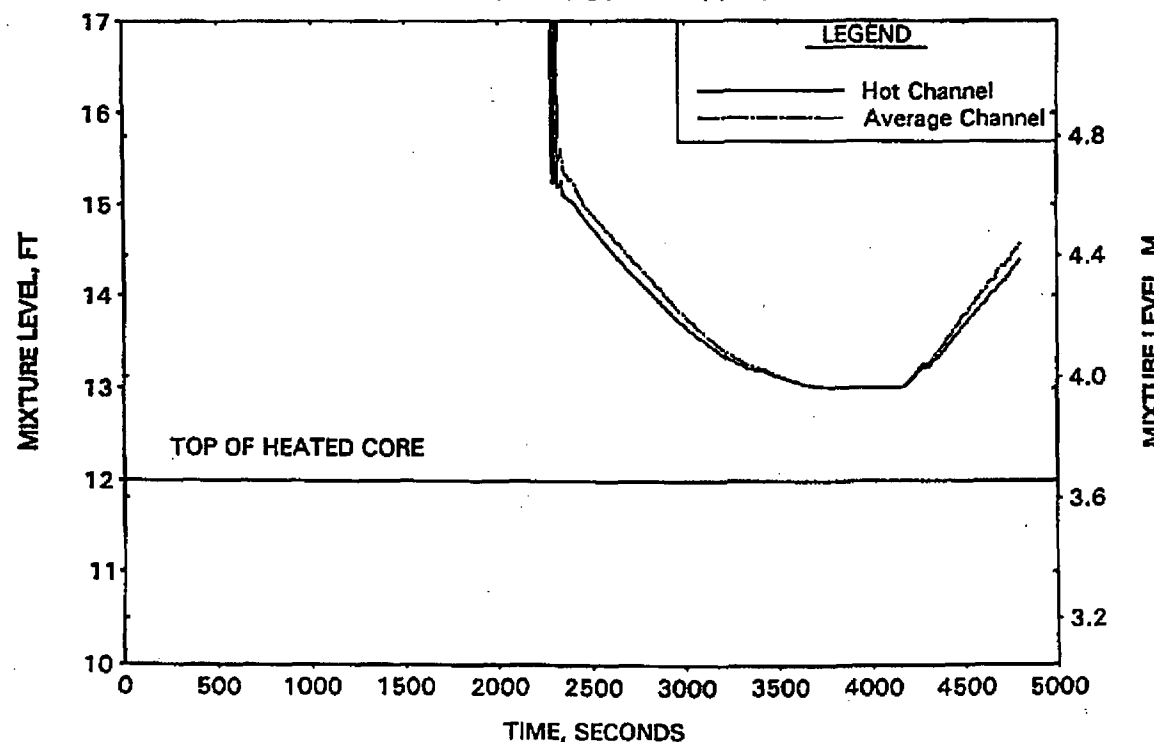


FIGURE A-75. CLPD BREAK SPECTRUM STUDY FOR 0.07-FT² BREAK - HOT CHANNEL CLAD TEMPERATURES.

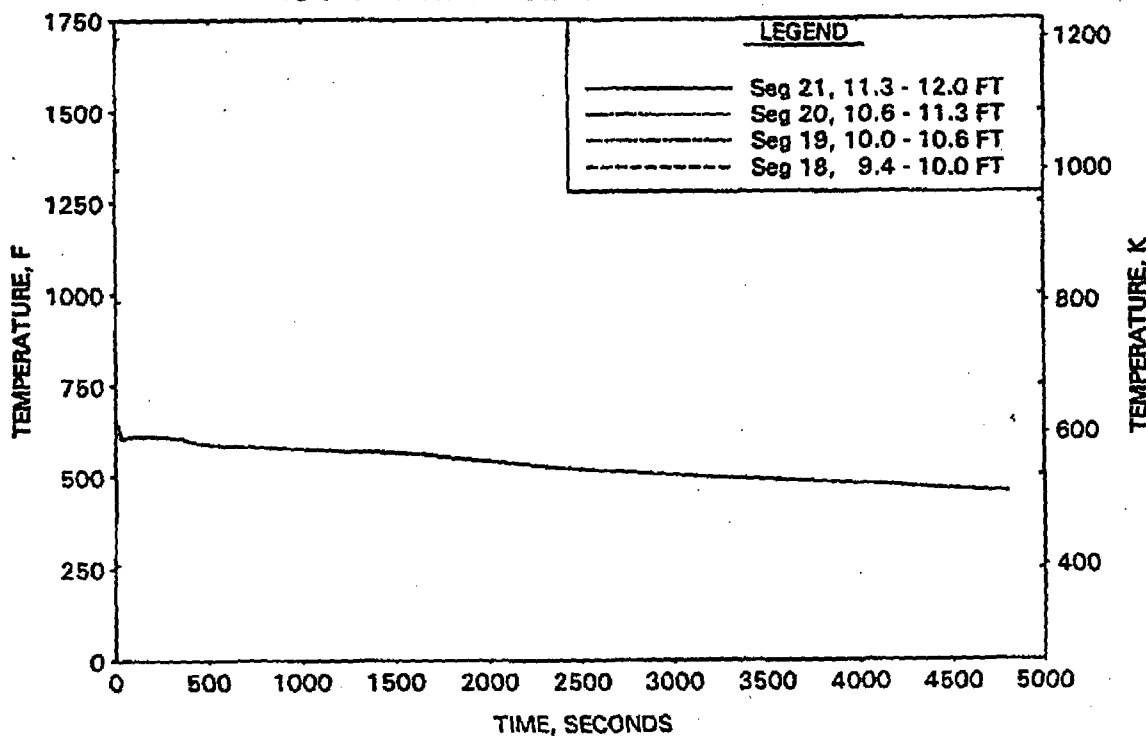


FIGURE A-76. CLPD BREAK SPECTRUM STUDY FOR 0.07-FT² BREAK - HOT CHANNEL STEAM TEMPERATURES.

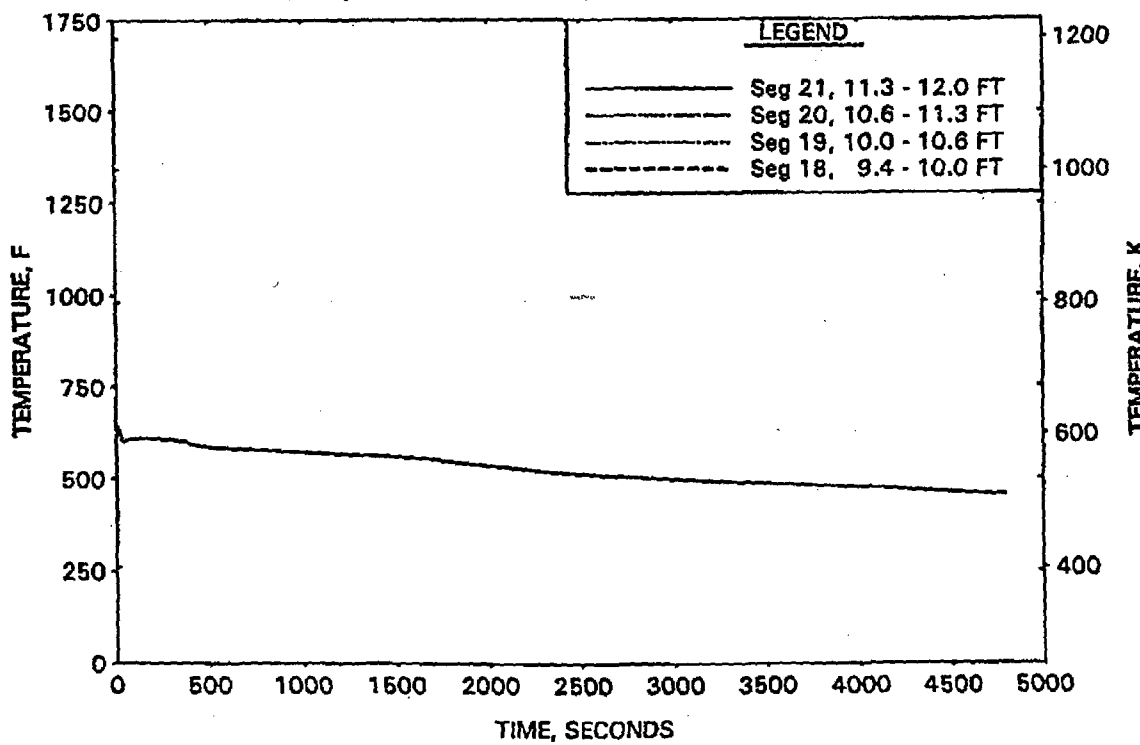


FIGURE A-77. CLPD BREAK SPECTRUM STUDY FOR 0.07-FT² BREAK -
UPPER ELEVATION AVE CHANNEL CLAD TEMPERATURES.

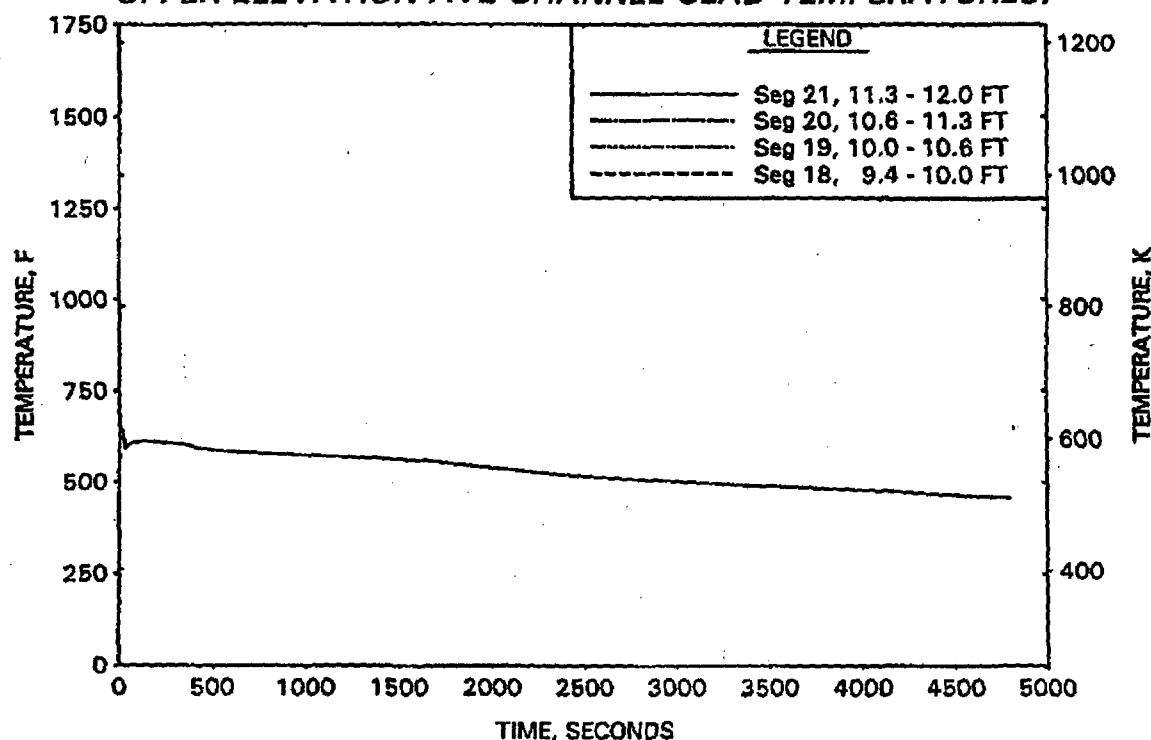


FIGURE A-78. CLPD BREAK SPECTRUM STUDY FOR 0.07-FT² BREAK -
UPPER ELEVATION AVE CHANNEL STEAM TEMPERATURES.

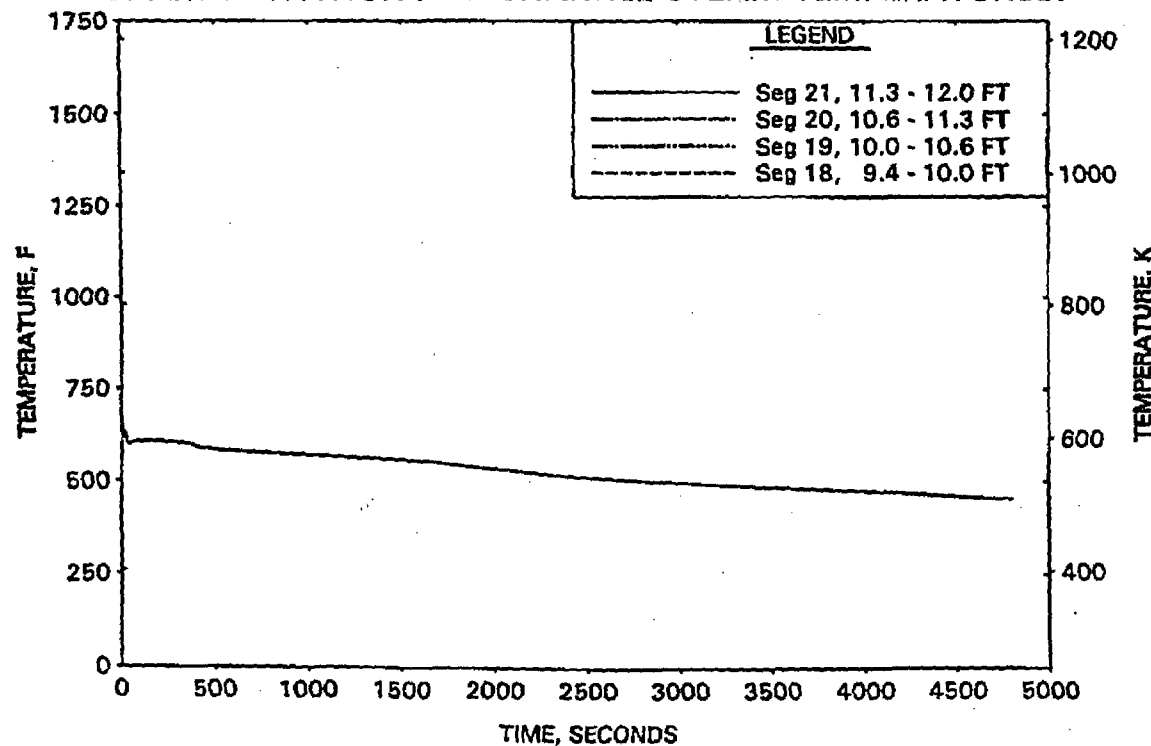


FIGURE A-79. CLPD BREAK SPECTRUM STUDY FOR 0.125-FT² BREAK - RCS PRESSURES.

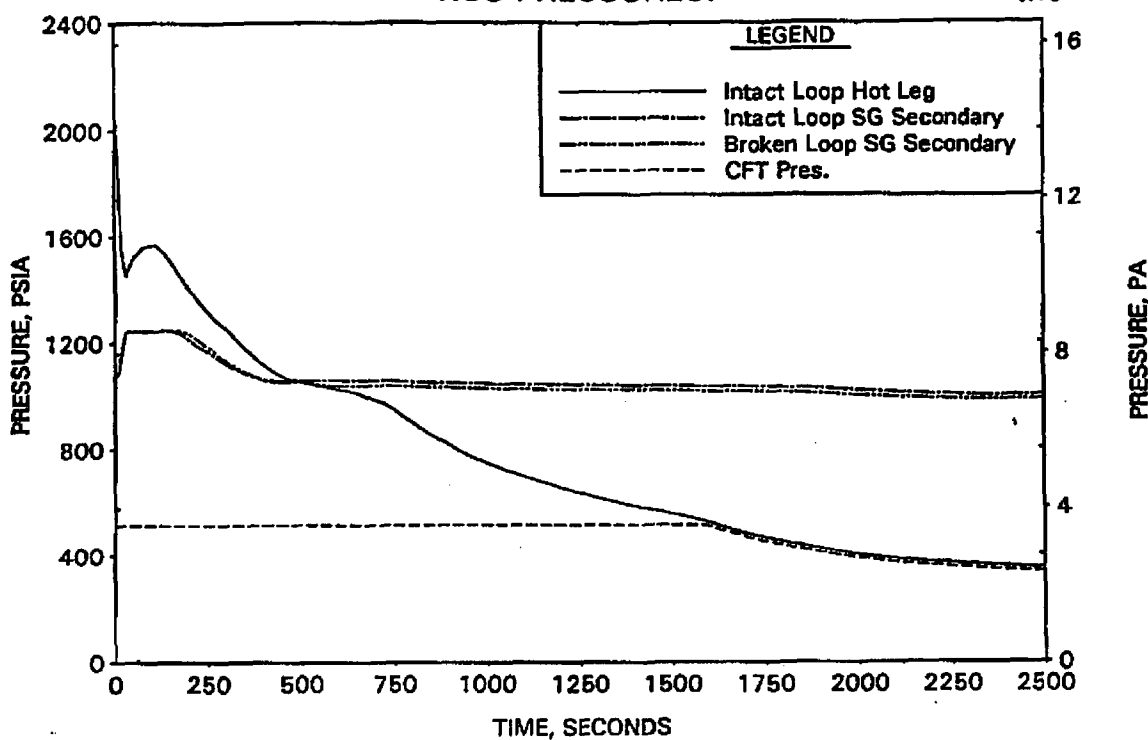


FIGURE A-80. CLPD BREAK SPECTRUM STUDY FOR 0.125-FT² BREAK - DC, RV, AND CORE COLLAPSED LEVELS.

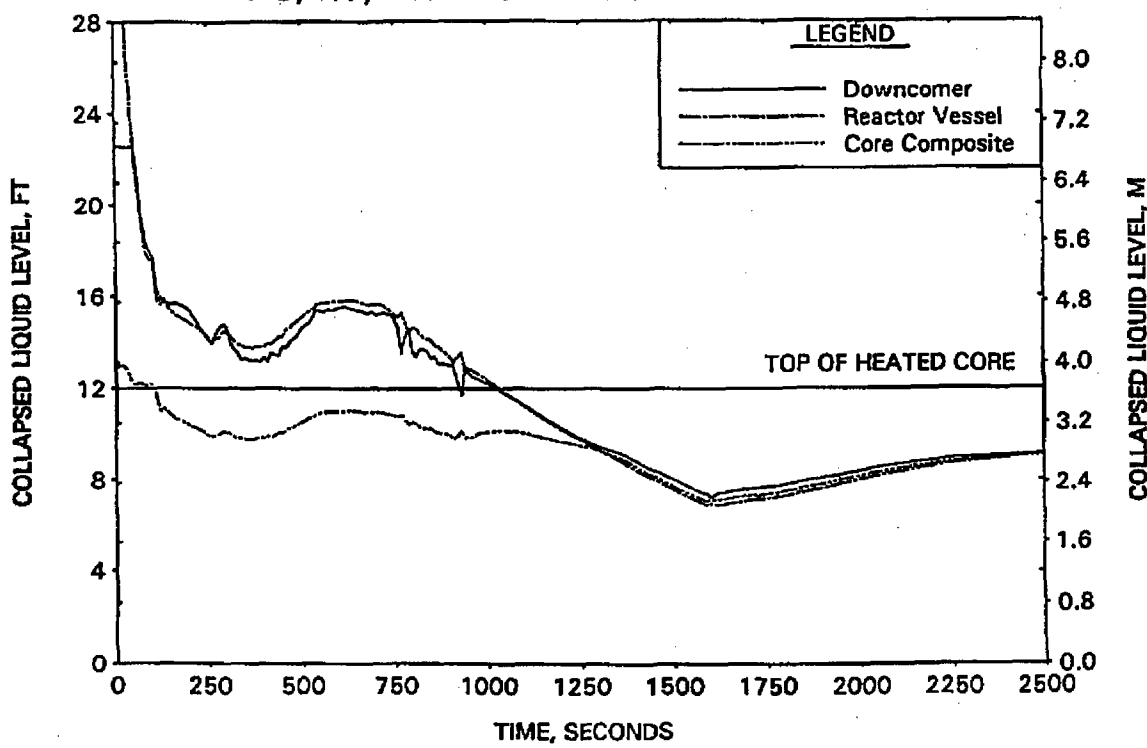


FIGURE A-81. CLPD BREAK SPECTRUM STUDY FOR 0.125-FT² BREAK -
BREAK AND TOTAL ECCS FLOWS.

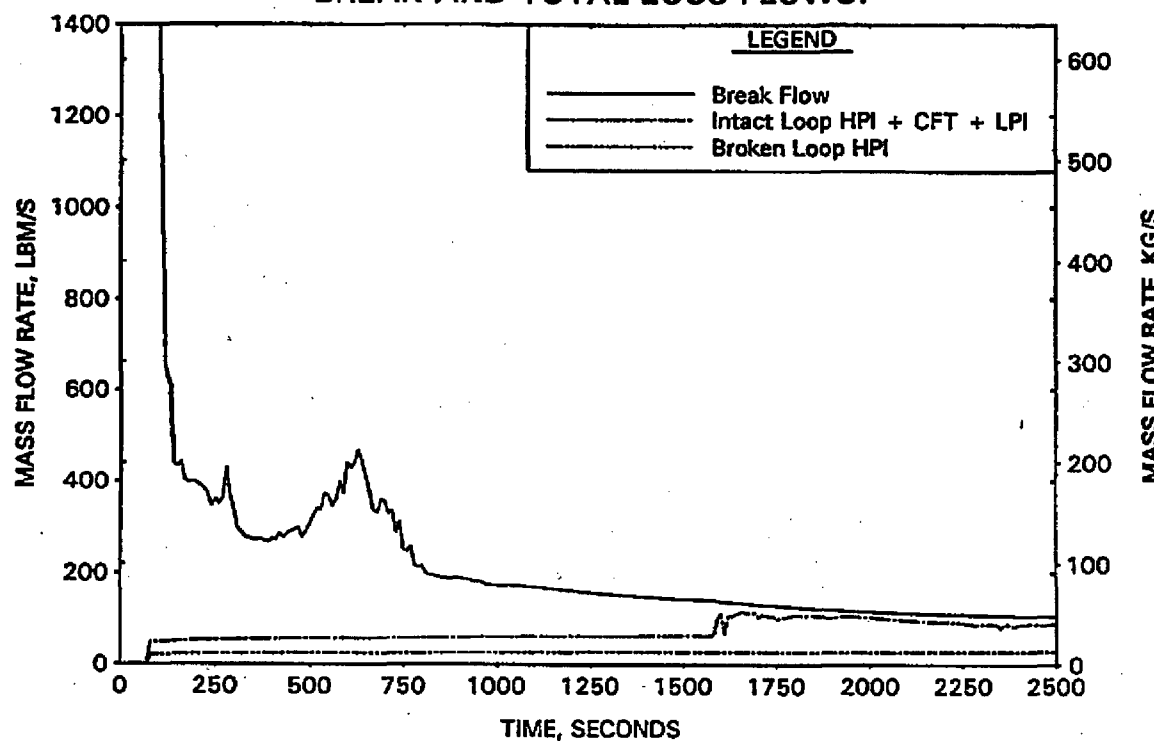


FIGURE A-82. CLPD BREAK SPECTRUM STUDY FOR 0.125-FT² BREAK -
BREAK VOLUME VOID FRACTION.

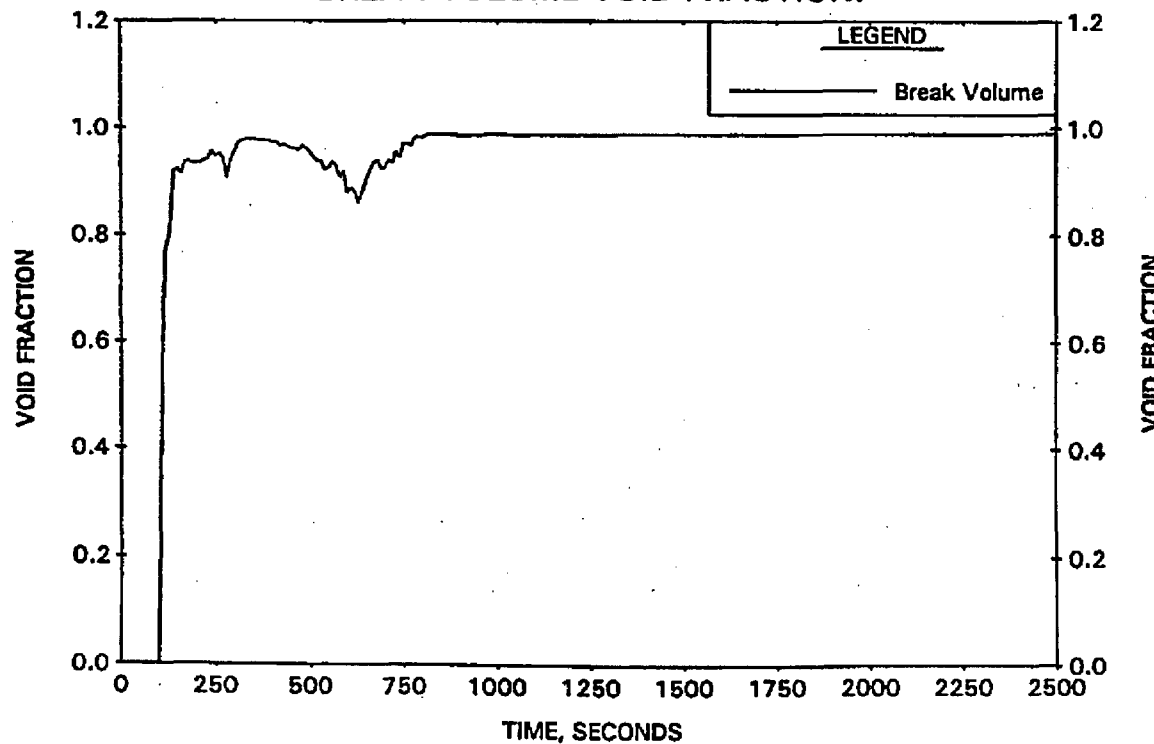


FIGURE A-83. CLPD BREAK SPECTRUM STUDY FOR 0.125-FT2 BREAK - BROKEN LOOP COLLAPSED LEVELS.

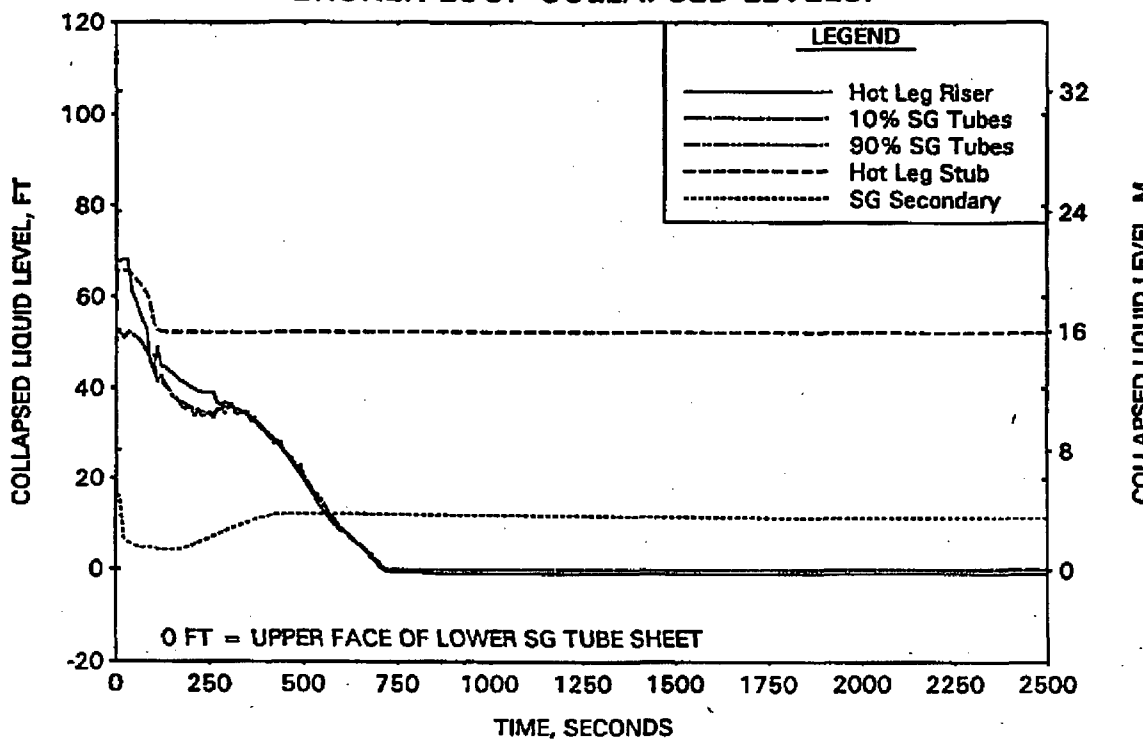


FIGURE A-84. CLPD BREAK SPECTRUM STUDY FOR 0.125-FT2 BREAK - INTACT LOOP COLLAPSED LEVELS.

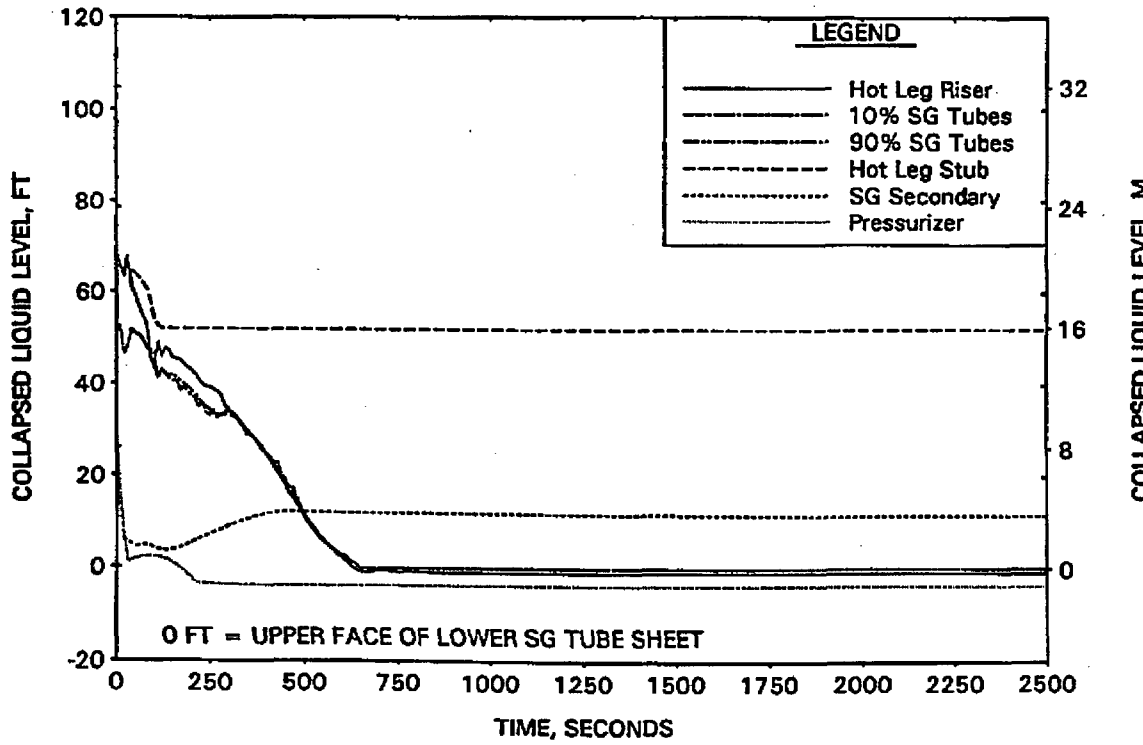


FIGURE A-85. CLPD BREAK SPECTRUM STUDY FOR 0.125-FT² BREAK - CLPD COLLAPSED LEVELS.

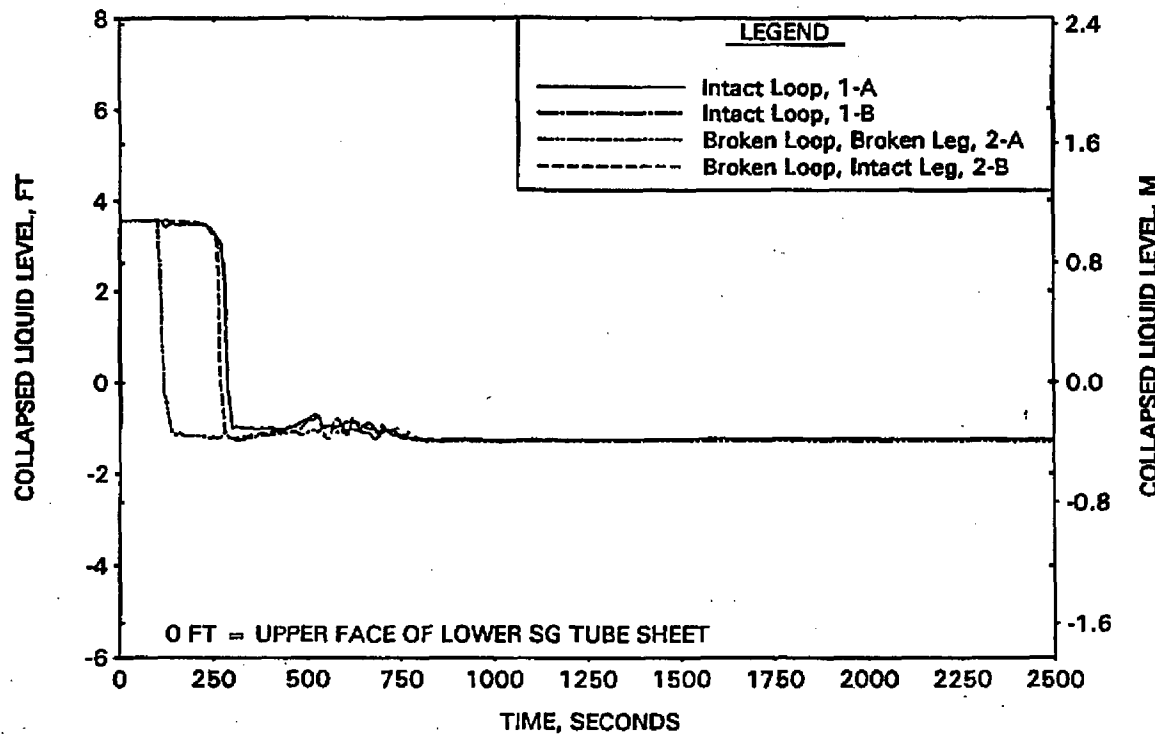


FIGURE A-86. CLPD BREAK SPECTRUM STUDY FOR 0.125-FT² BREAK - CLPS LIQUID VOLUME.

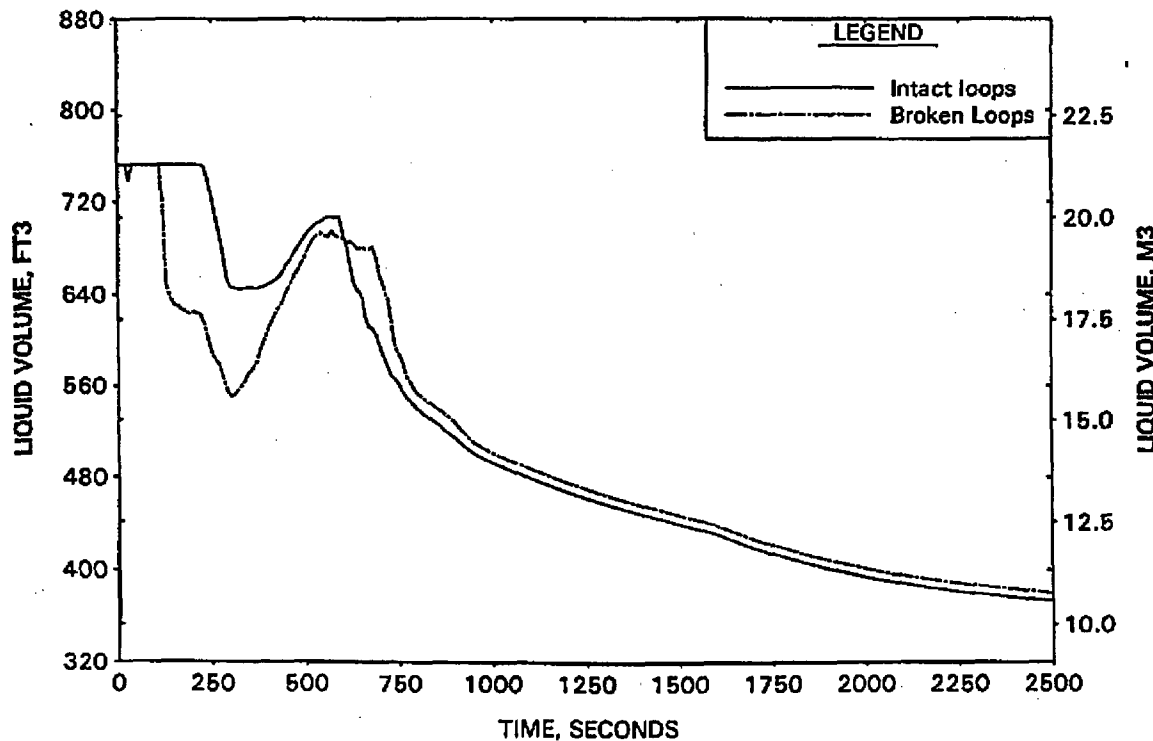


FIGURE A-87. CLPD BREAK SPECTRUM STUDY FOR 0.125-FT² BREAK - HOT LEG AND RVVV FLOWS.

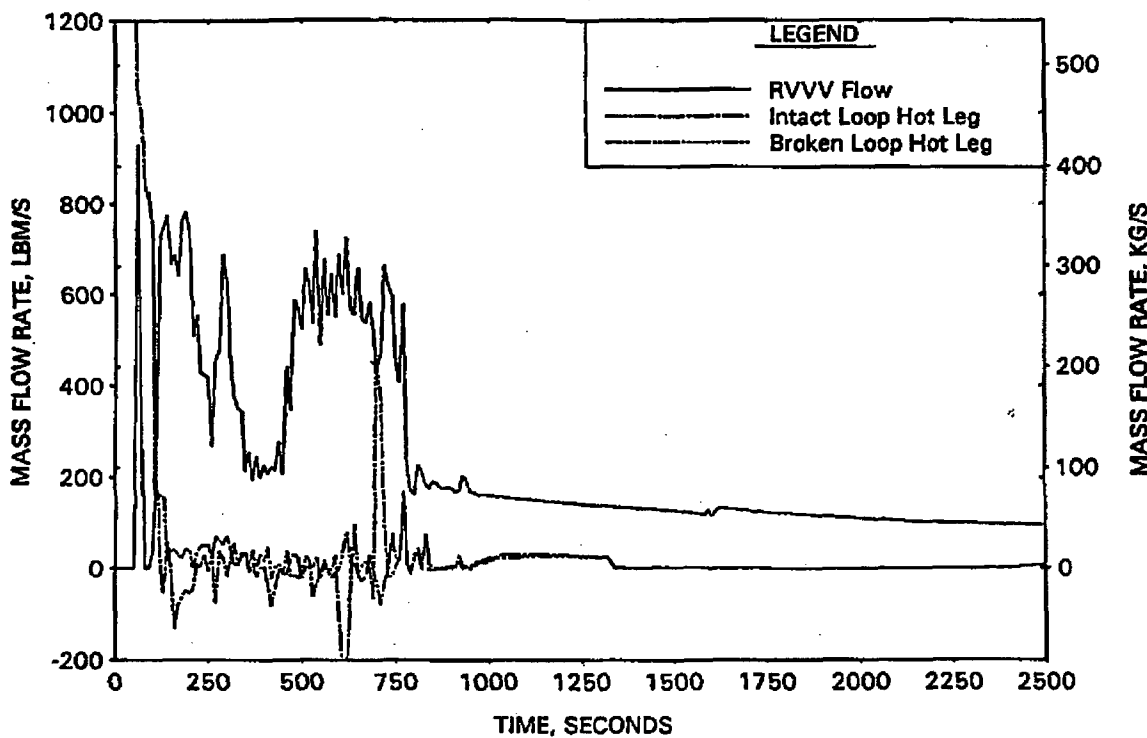


FIGURE A-88. CLPD BREAK SPECTRUM STUDY FOR 0.125-FT² BREAK - CORE MIXTURE LEVELS.

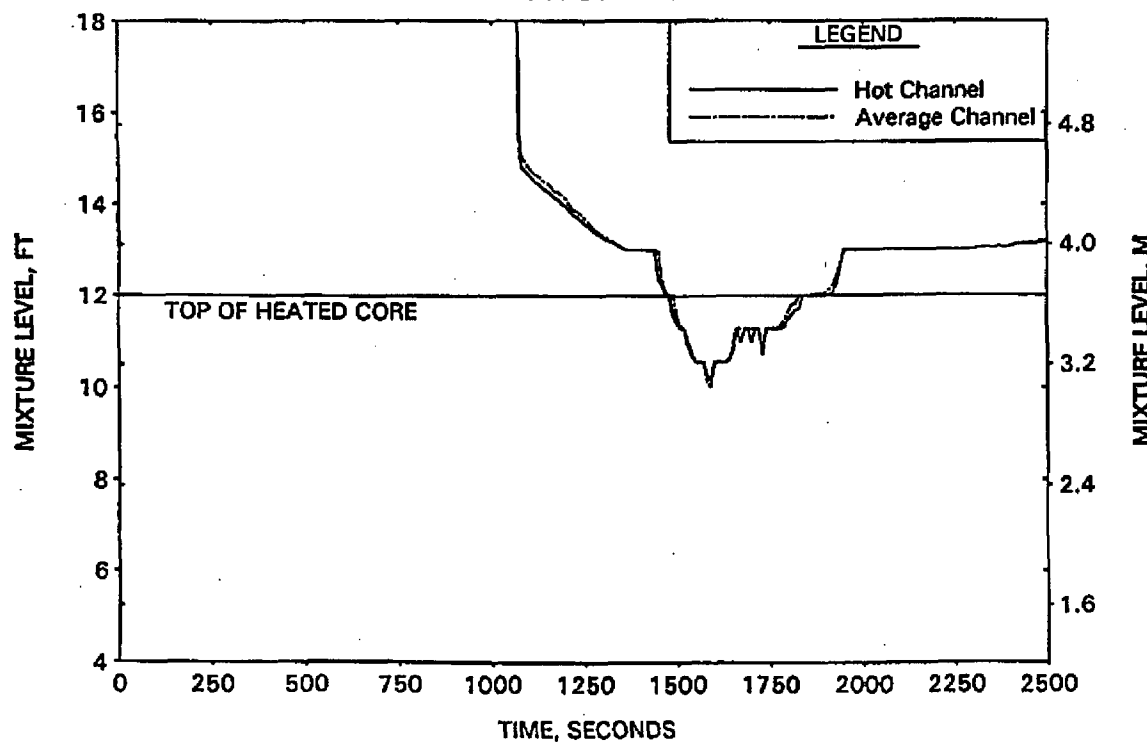


FIGURE A-89. CLPD BREAK SPECTRUM STUDY FOR 0.125-FT2 BREAK - HOT CHANNEL CLAD TEMPERATURES.

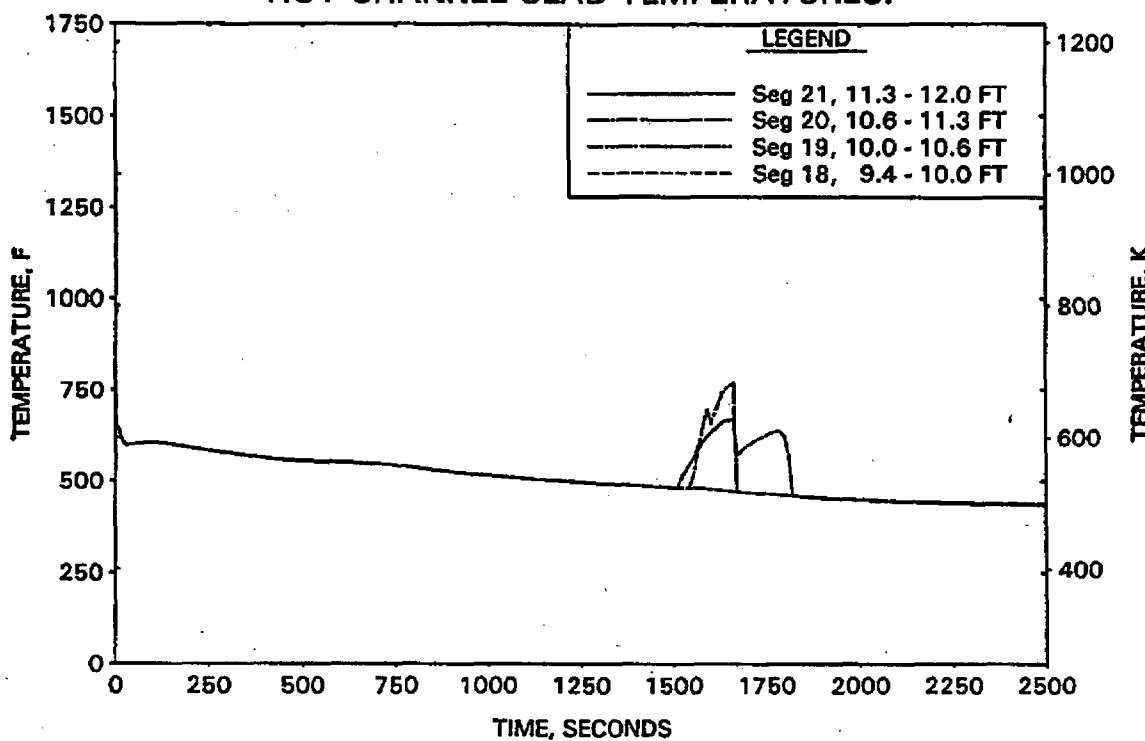


FIGURE A-90. CLPD BREAK SPECTRUM STUDY FOR 0.125-FT2 BREAK - HOT CHANNEL STEAM TEMPERATURES.

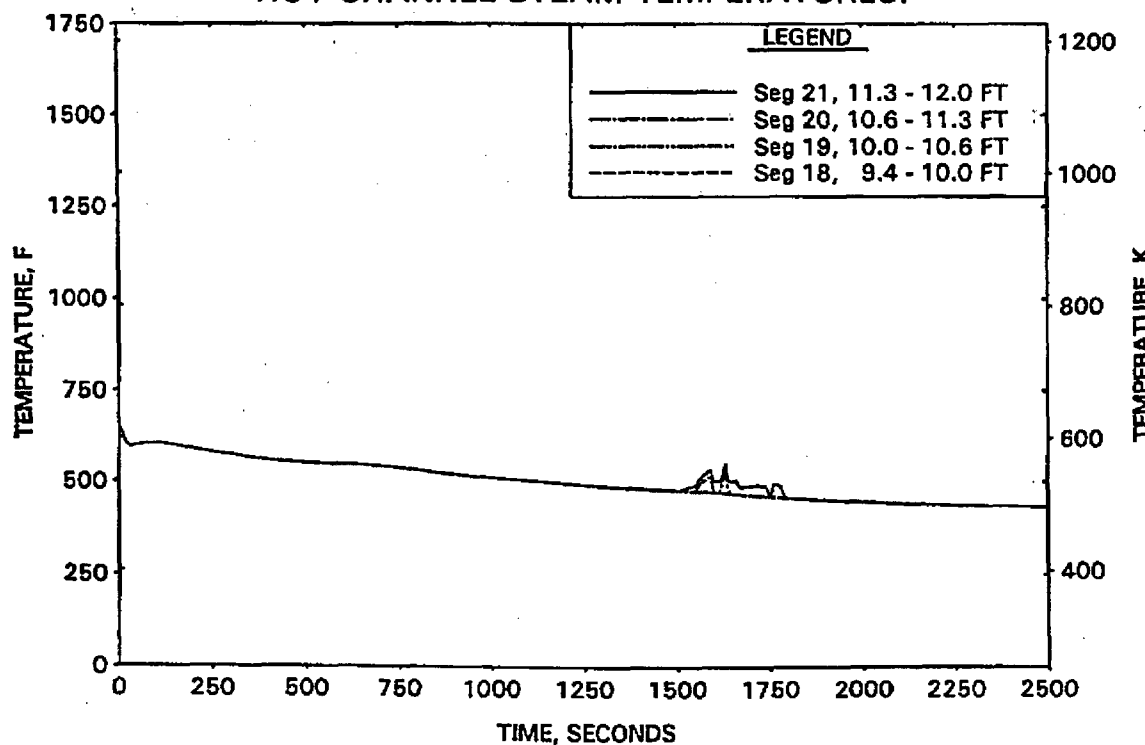


FIGURE A-91. CLPD BREAK SPECTRUM STUDY FOR 0.125-FT² BREAK -
UPPER ELEVATION AVE CHANNEL CLAD TEMPERATURES.

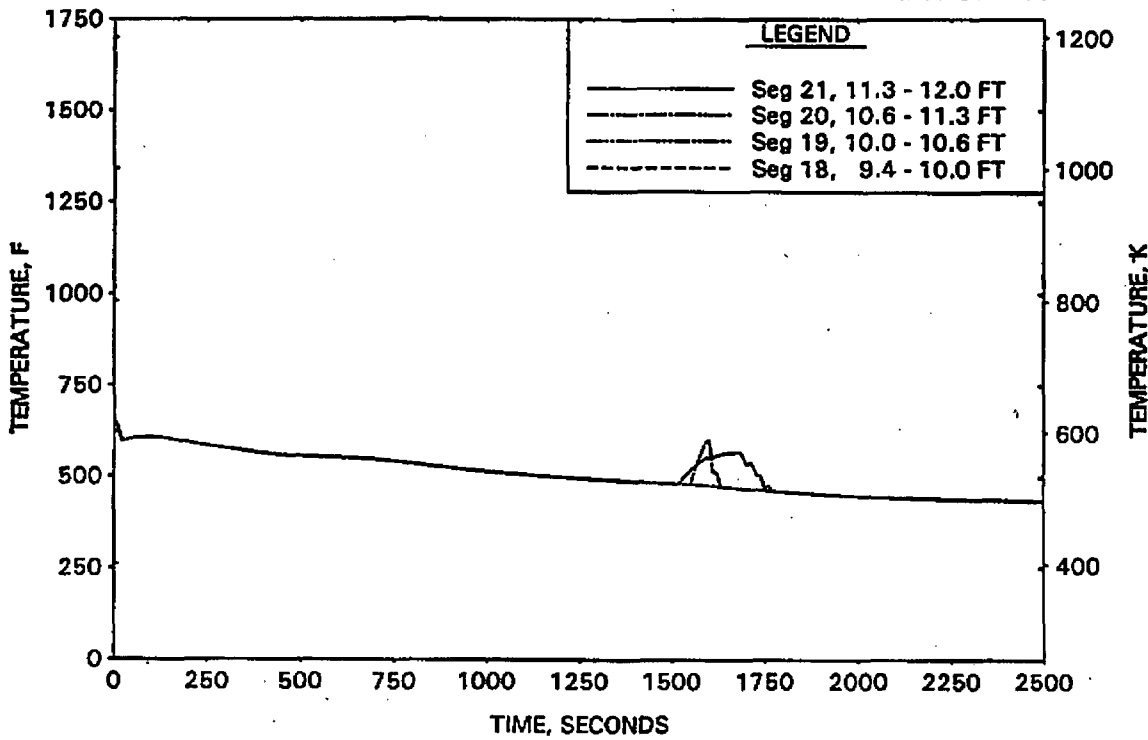


FIGURE A-92. CLPD BREAK SPECTRUM STUDY FOR 0.125-FT² BREAK -
UPPER ELEVATION AVE CHANNEL STEAM TEMPERATURES.

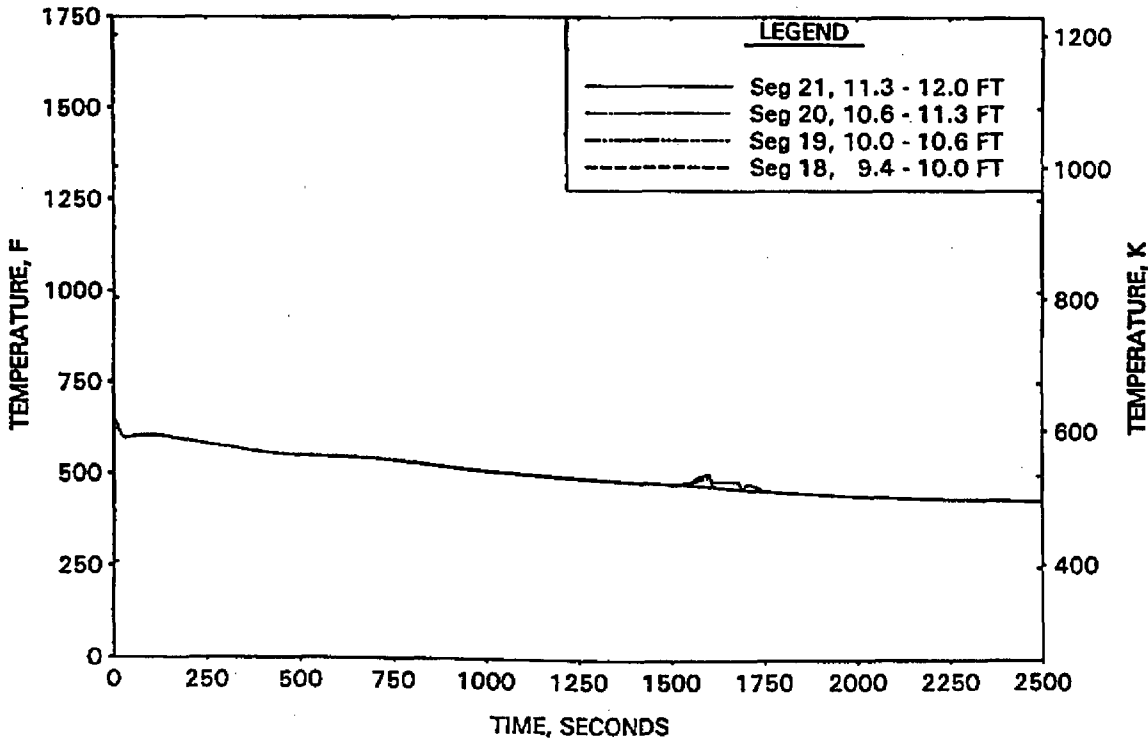


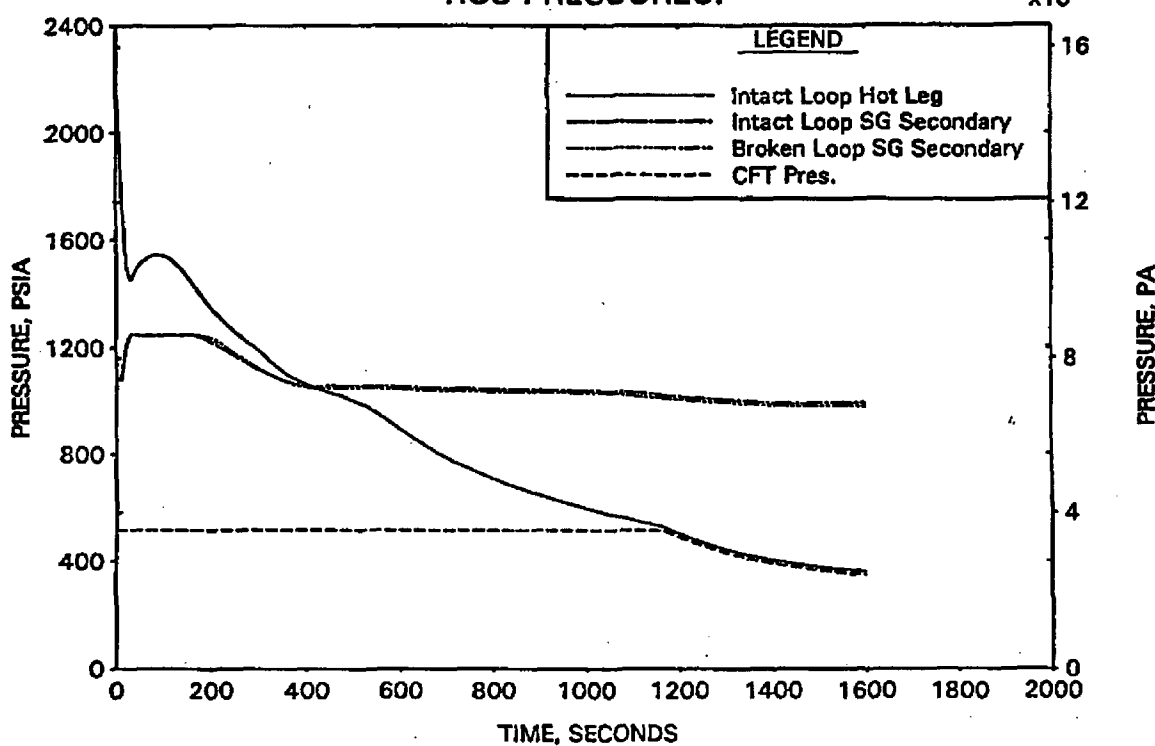
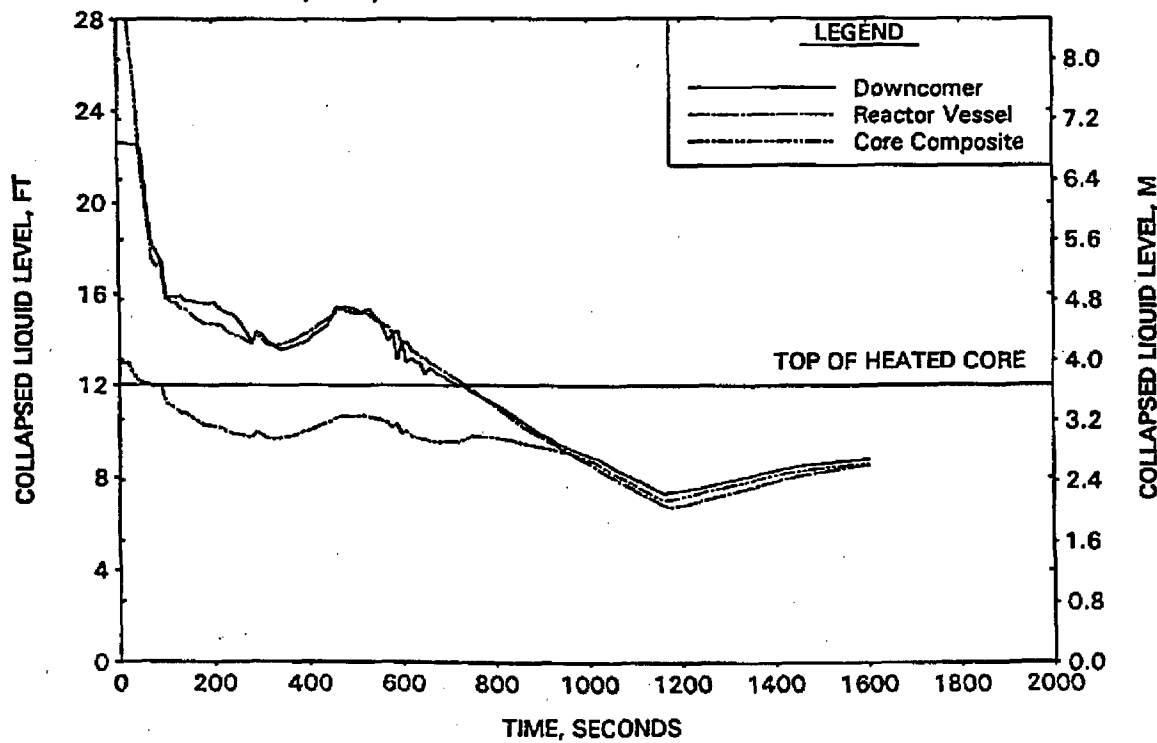
FIGURE A-93. CLPD BREAK SPECTRUM STUDY FOR 0.15-FT² BREAK - RCS PRESSURES.FIGURE A-94. CLPD BREAK SPECTRUM STUDY FOR 0.15-FT² BREAK - DC, RV, AND CORE COLLAPSED LEVELS.

FIGURE A-95. CLPD BREAK SPECTRUM STUDY FOR 0.15-FT² BREAK -
BREAK AND TOTAL ECCS FLOWS.

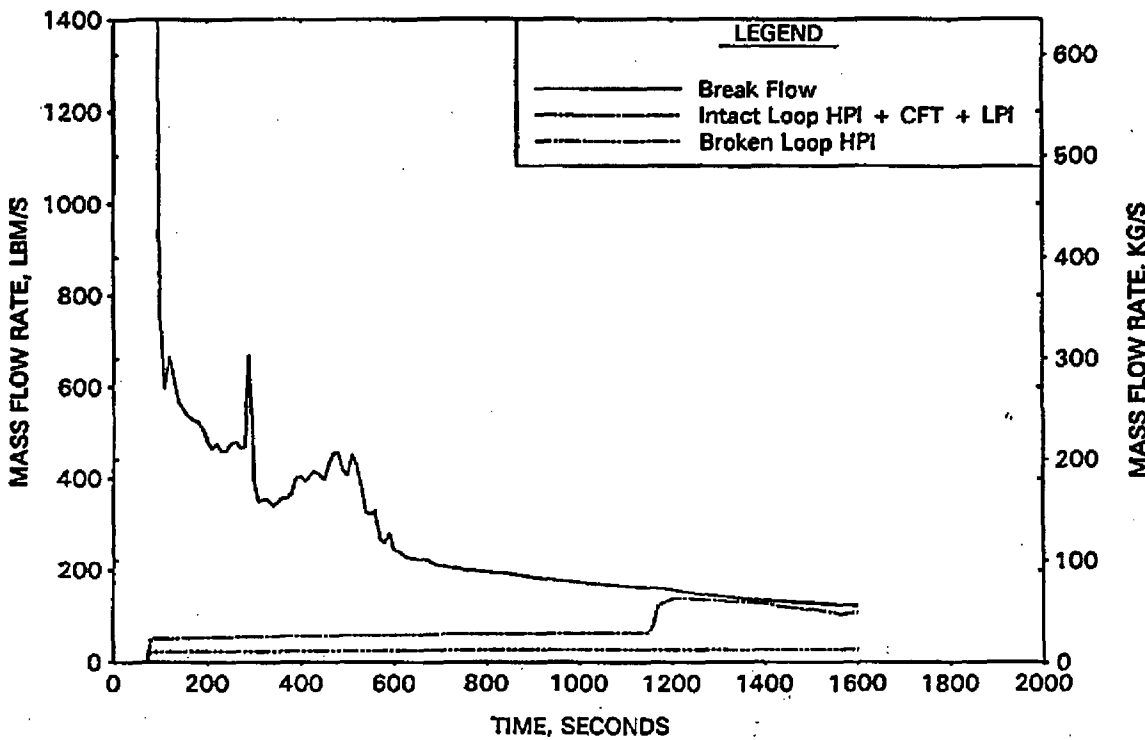


FIGURE A-96. CLPD BREAK SPECTRUM STUDY FOR 0.15-FT² BREAK -
BREAK VOLUME VOID FRACTION.

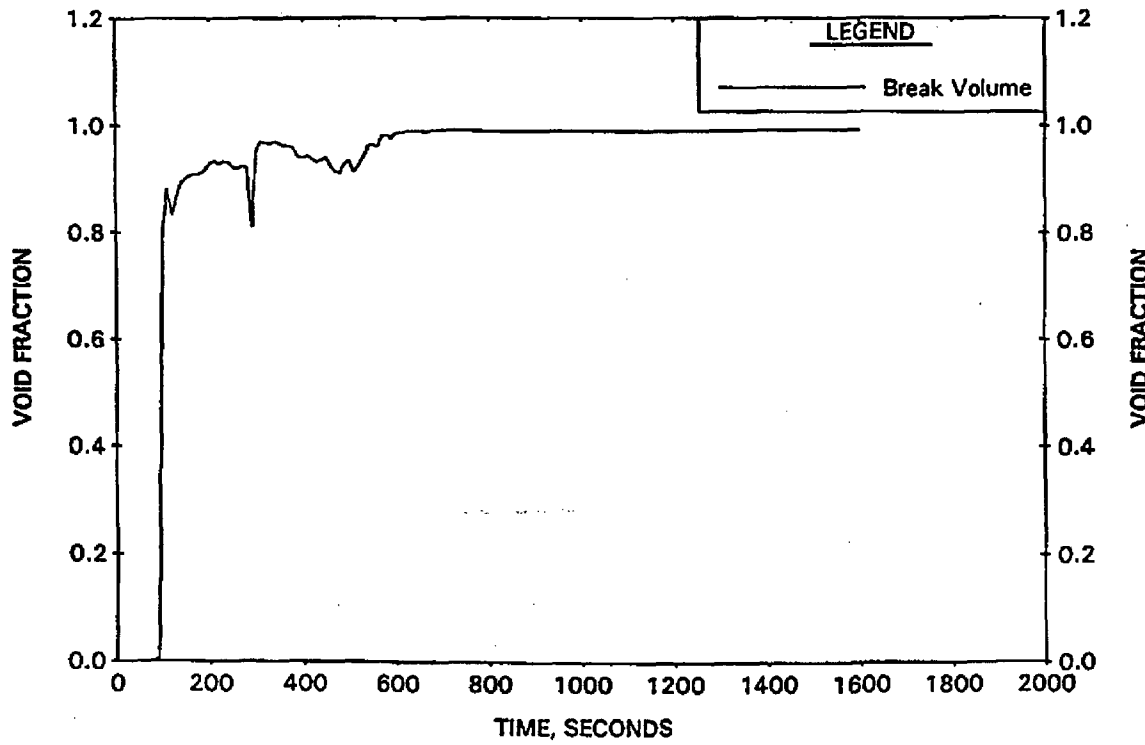


FIGURE A-97. CLPD BREAK SPECTRUM STUDY FOR 0.15-FT² BREAK - BROKEN LOOP COLLAPSED LEVELS.

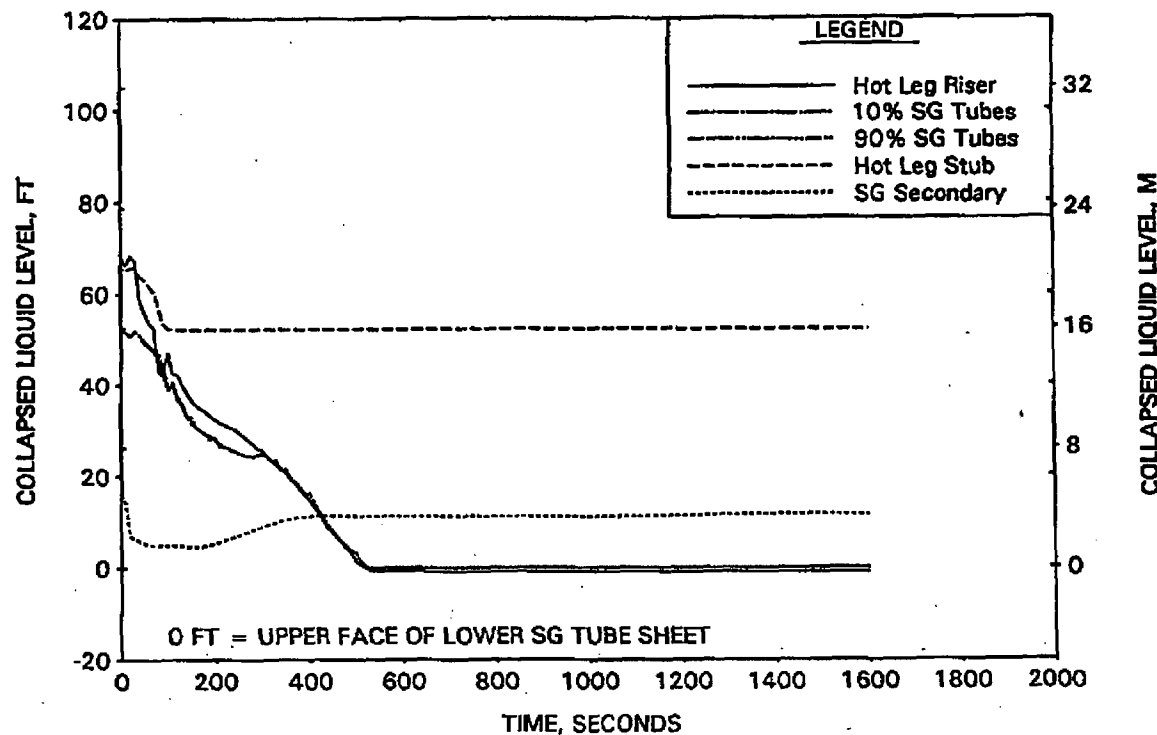


FIGURE A-98. CLPD BREAK SPECTRUM STUDY FOR 0.15-FT² BREAK - INTACT LOOP COLLAPSED LEVELS.

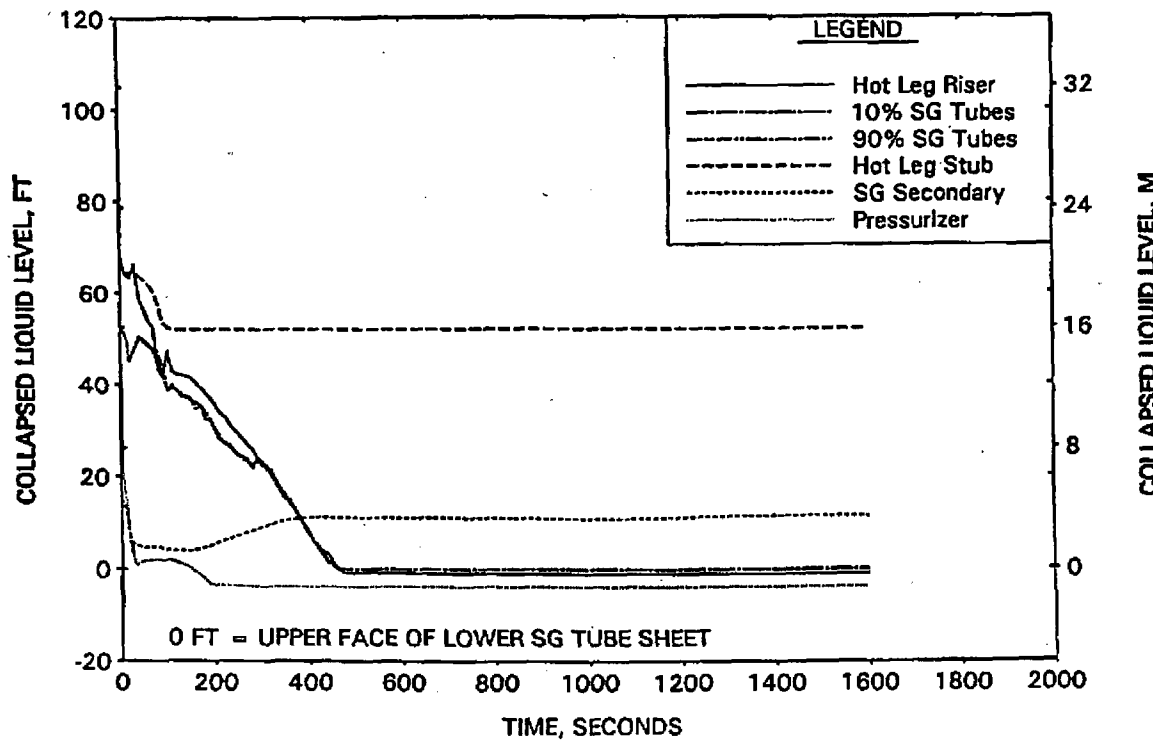


FIGURE A-99. CLPD BREAK SPECTRUM STUDY FOR 0.15-FT² BREAK - CLPD COLLAPSED LEVELS.

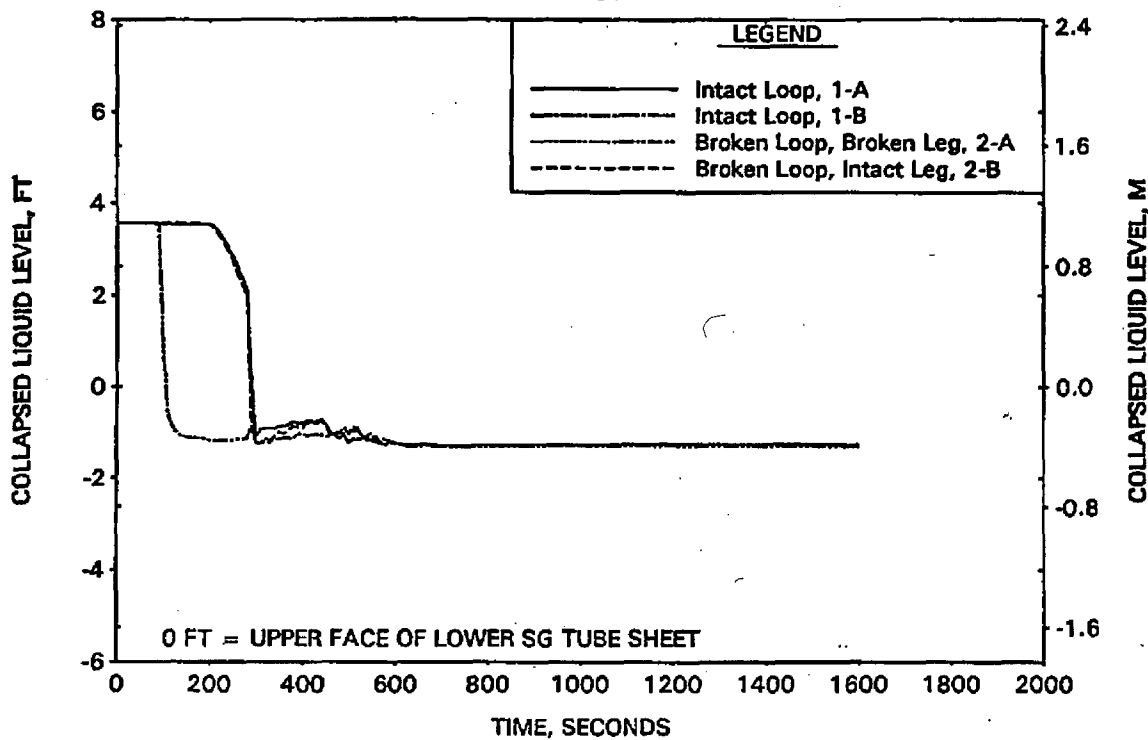


FIGURE A-100. CLPD BREAK SPECTRUM STUDY FOR 0.15-FT² BREAK - CLPS LIQUID VOLUME.

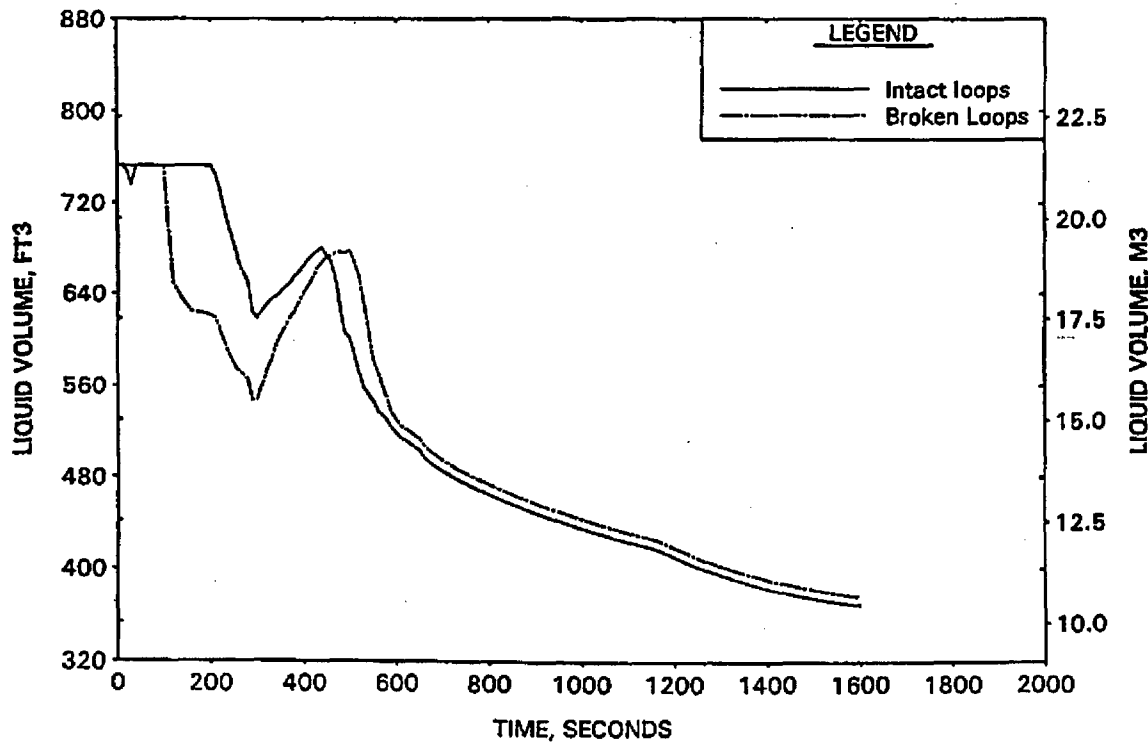


FIGURE A-101. CLPD BREAK SPECTRUM STUDY FOR 0.15-FT² BREAK - HOT LEG AND RVVV FLOWS.

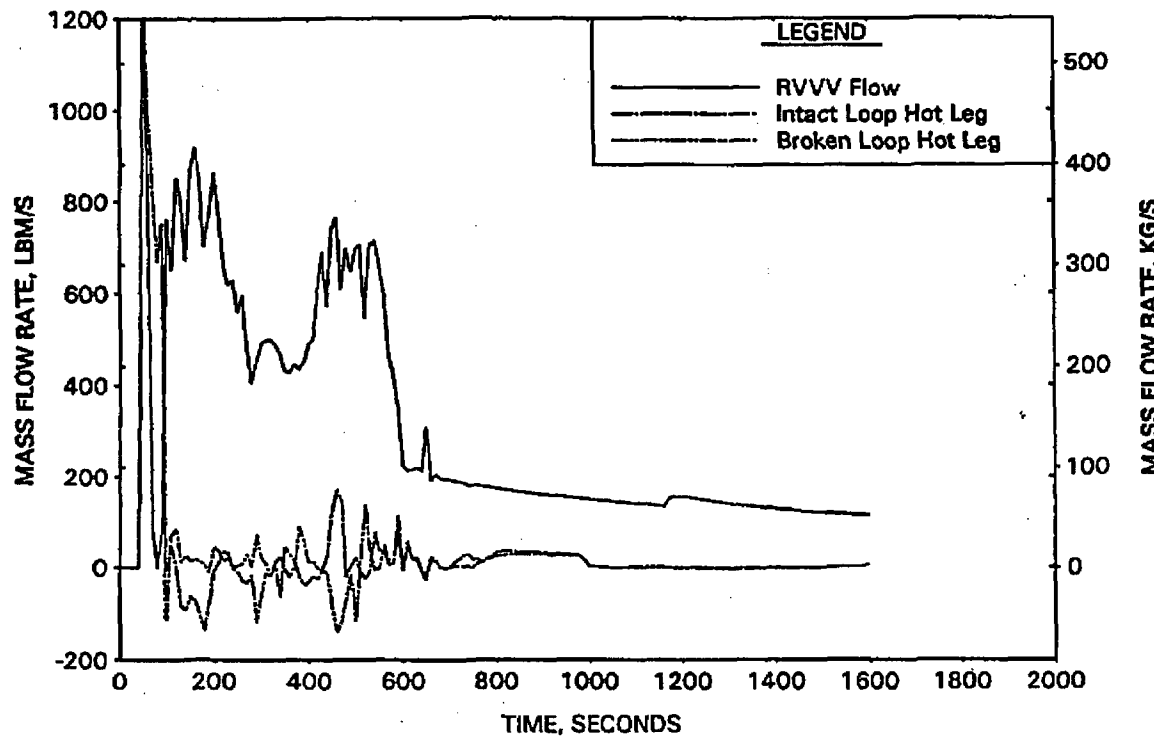


FIGURE A-102. CLPD BREAK SPECTRUM STUDY FOR 0.15-FT² BREAK - CORE MIXTURE LEVELS.

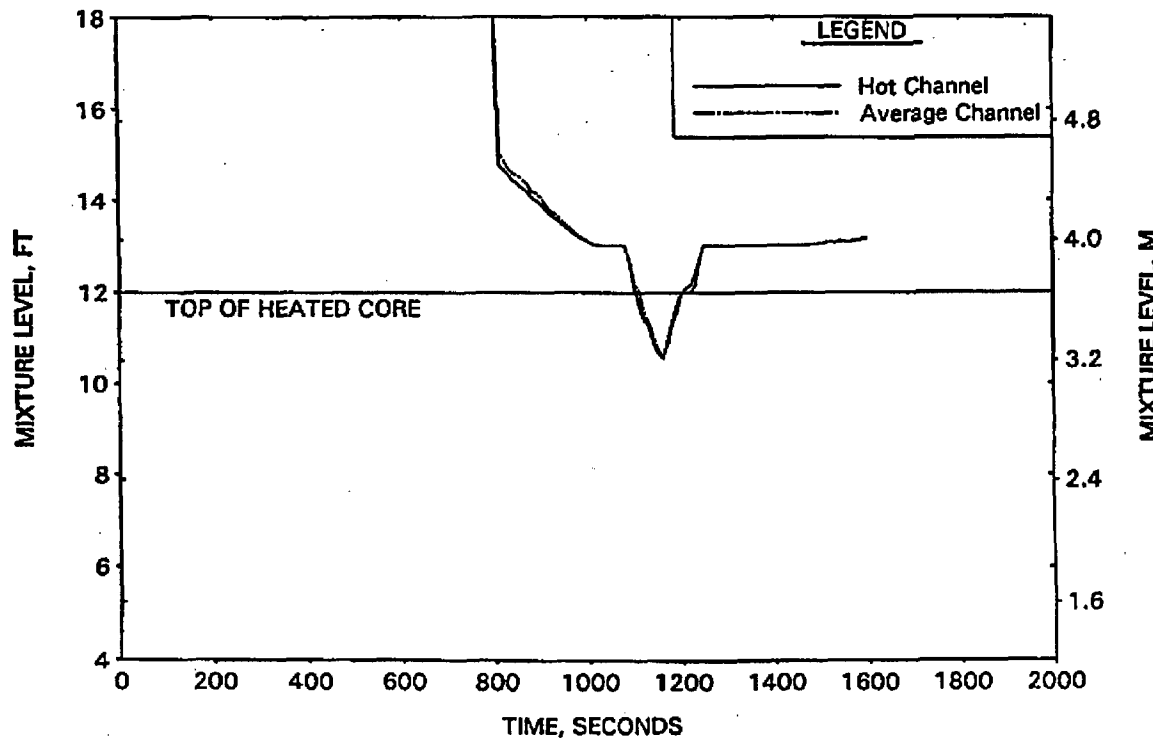


FIGURE A-103. CLPD BREAK SPECTRUM STUDY FOR 0.15-FT² BREAK - HOT CHANNEL CLAD TEMPERATURES.

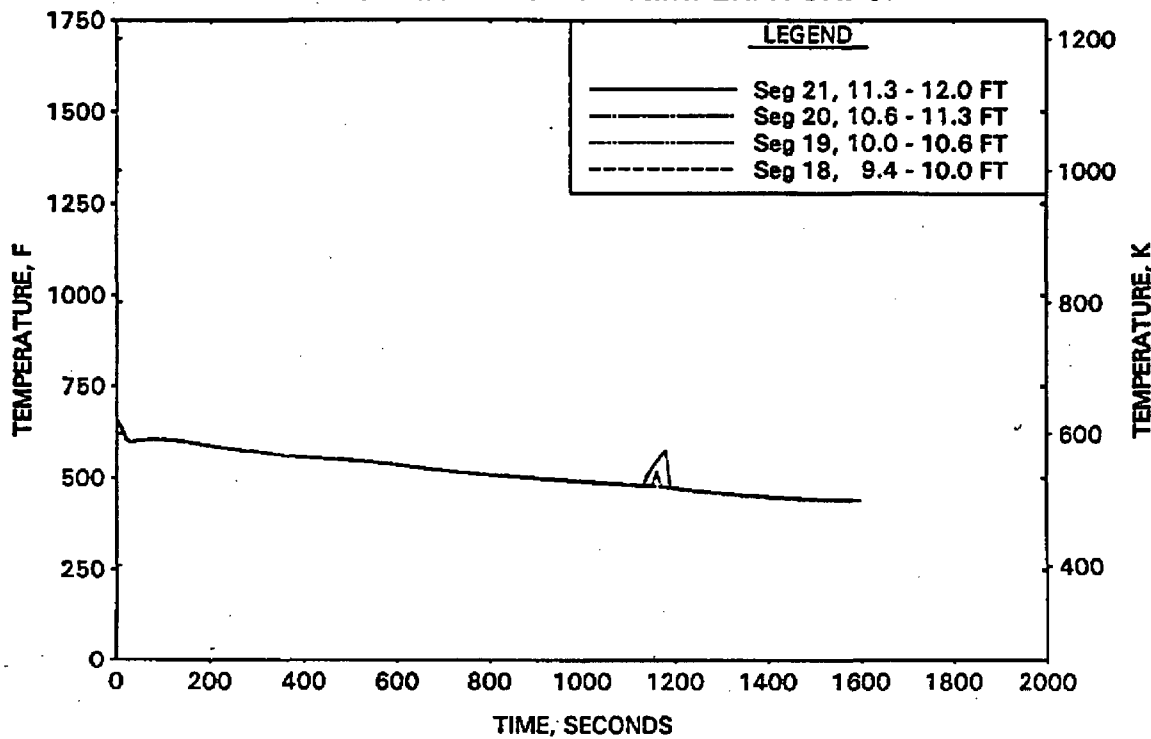


FIGURE A-104. CLPD BREAK SPECTRUM STUDY FOR 0.15-FT² BREAK - HOT CHANNEL STEAM TEMPERATURES.

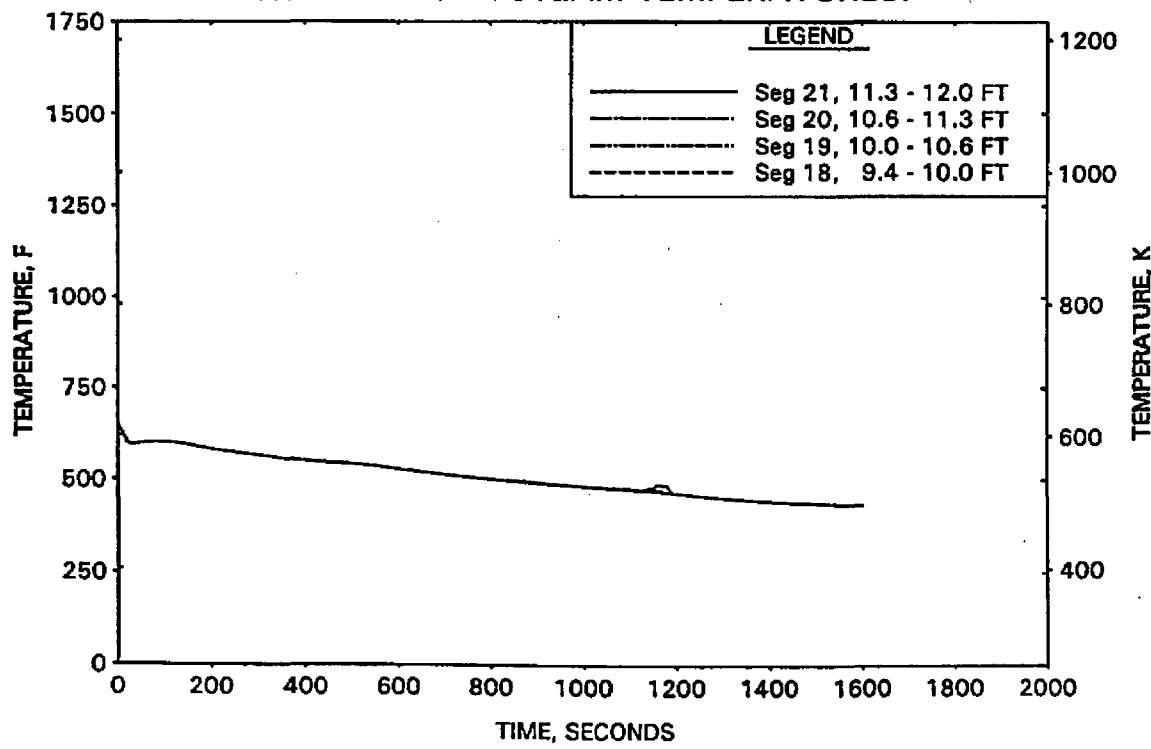


FIGURE A-105. CLPD BREAK SPECTRUM STUDY FOR 0.15-FT2 BREAK -
UPPER ELEVATION AVE CHANNEL CLAD TEMPERATURES.

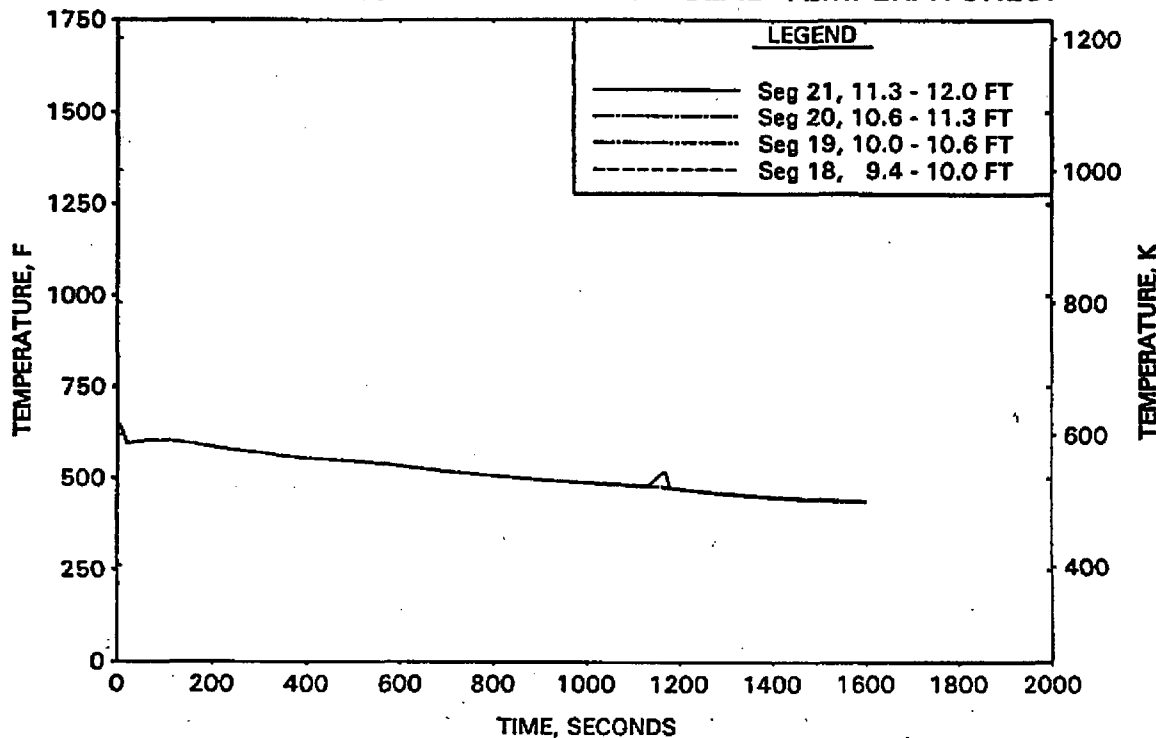


FIGURE A-106. CLPD BREAK SPECTRUM STUDY FOR 0.15-FT2 BREAK -
UPPER ELEVATION AVE CHANNEL STEAM TEMPERATURES.

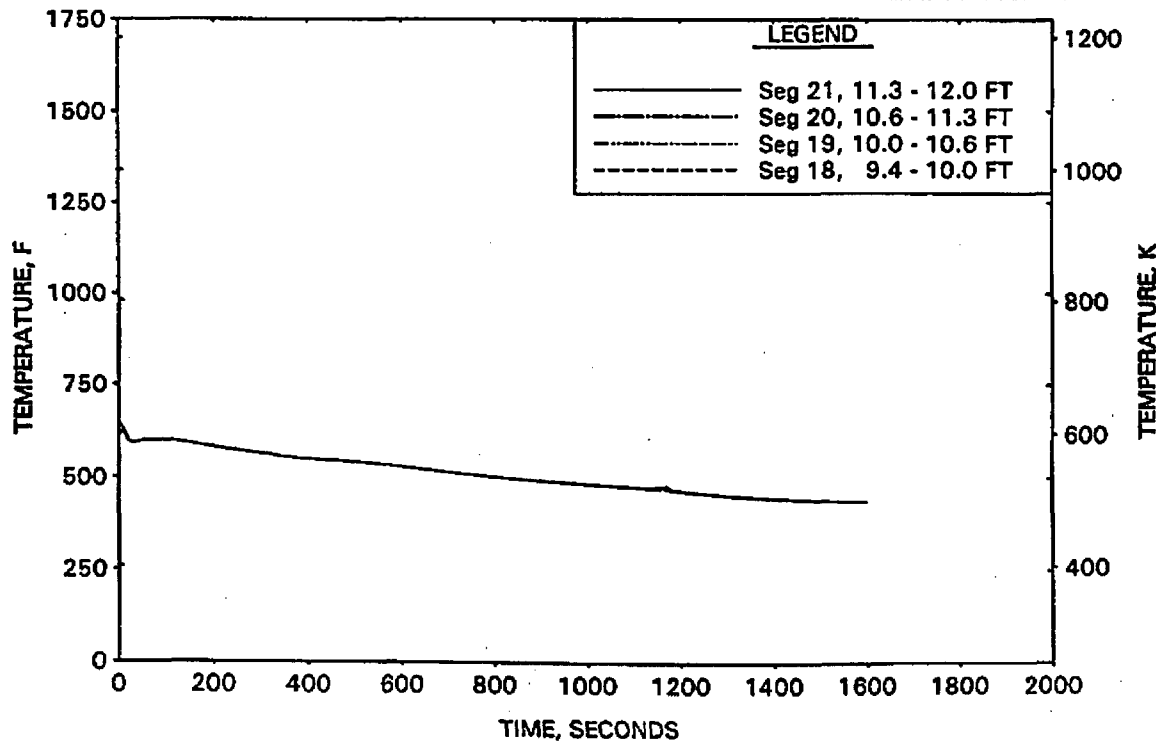


FIGURE A-107. CLPD BREAK SPECTRUM STUDY FOR 0.175-FT² BREAK - RCS PRESSURES.

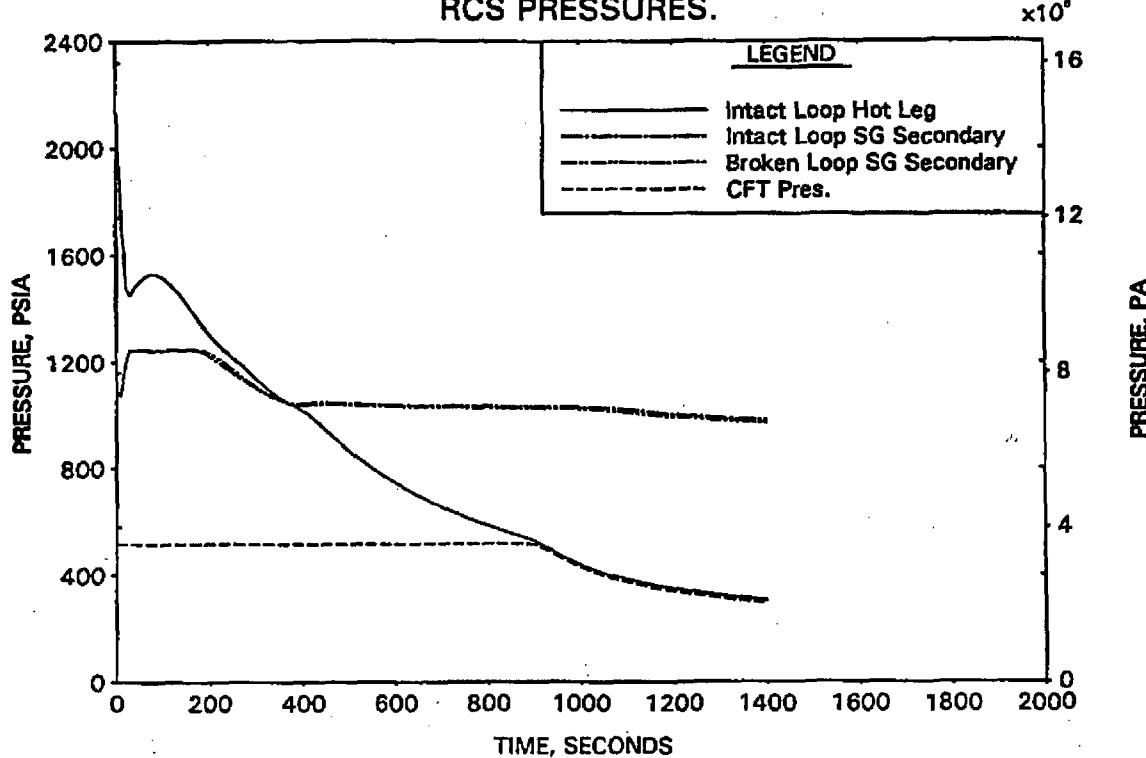


FIGURE A-108. CLPD BREAK SPECTRUM STUDY FOR 0.175-FT² BREAK - DC, RV, AND CORE COLLAPSED LEVELS.

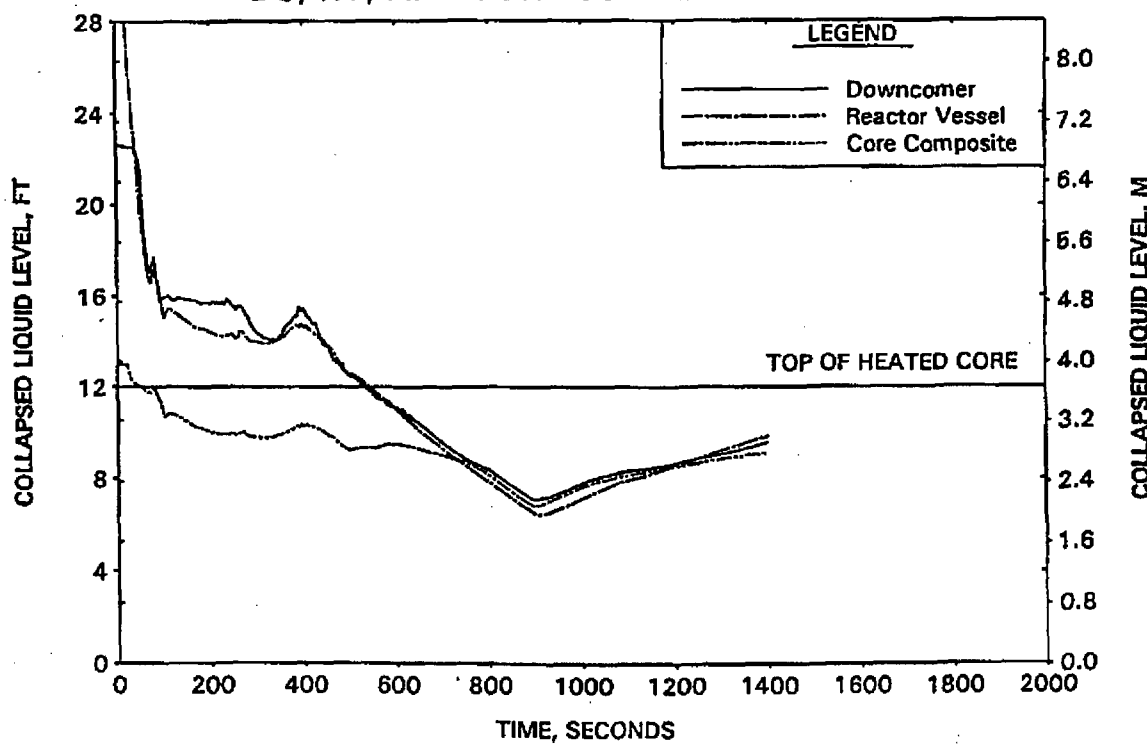


FIGURE A-109. CLPD BREAK SPECTRUM STUDY FOR 0.175-FT² BREAK - BREAK AND TOTAL ECCS FLOWS.

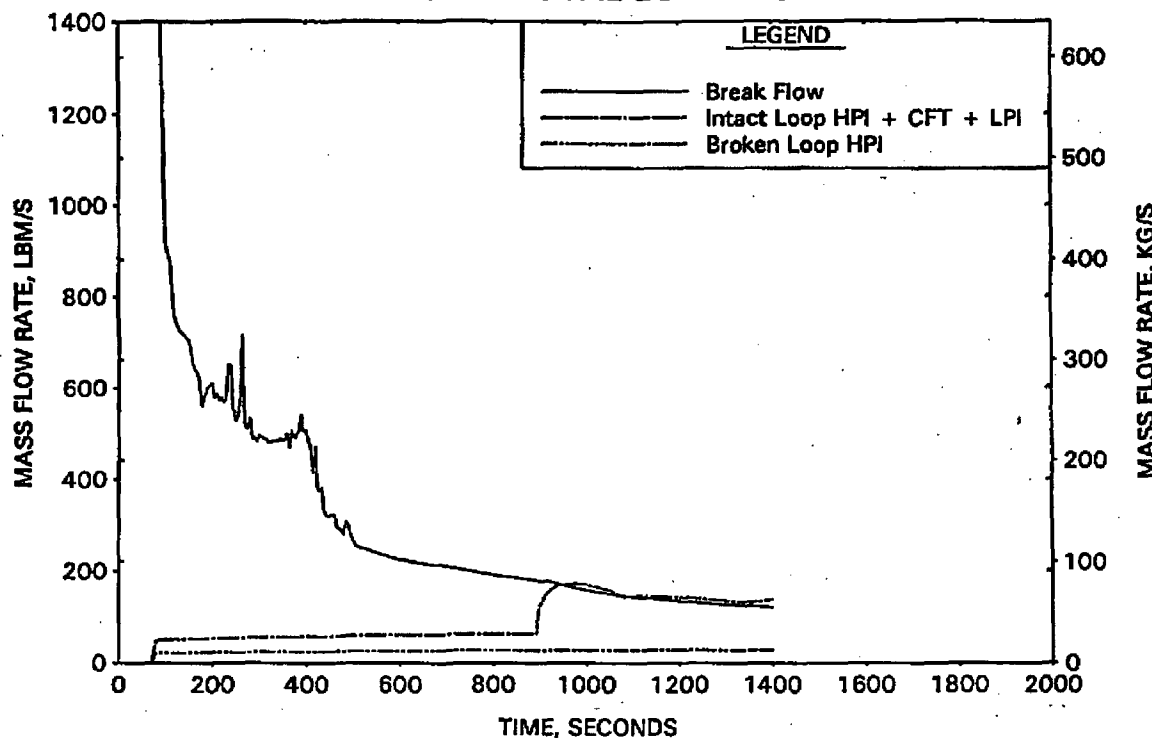


FIGURE A-110. CLPD BREAK SPECTRUM STUDY FOR 0.175-FT² BREAK - BREAK VOLUME VOID FRACTION.

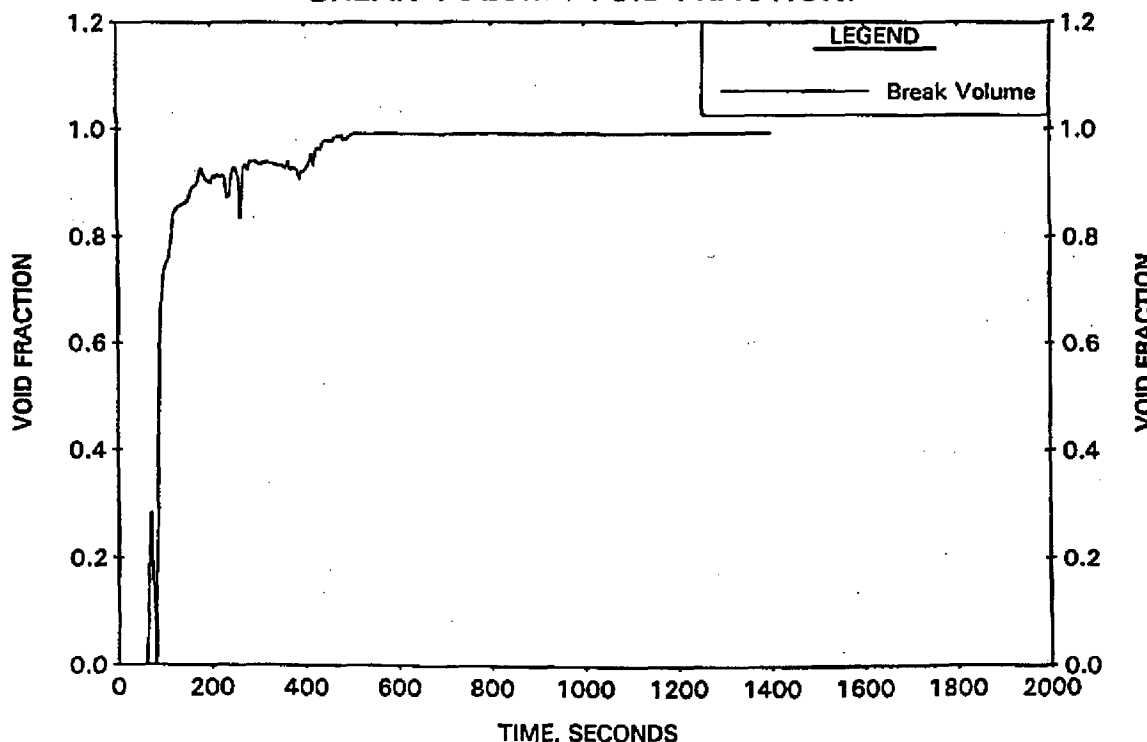


FIGURE A-111. CLPD BREAK SPECTRUM STUDY FOR 0.175-FT² BREAK - BROKEN LOOP COLLAPSED LEVELS.

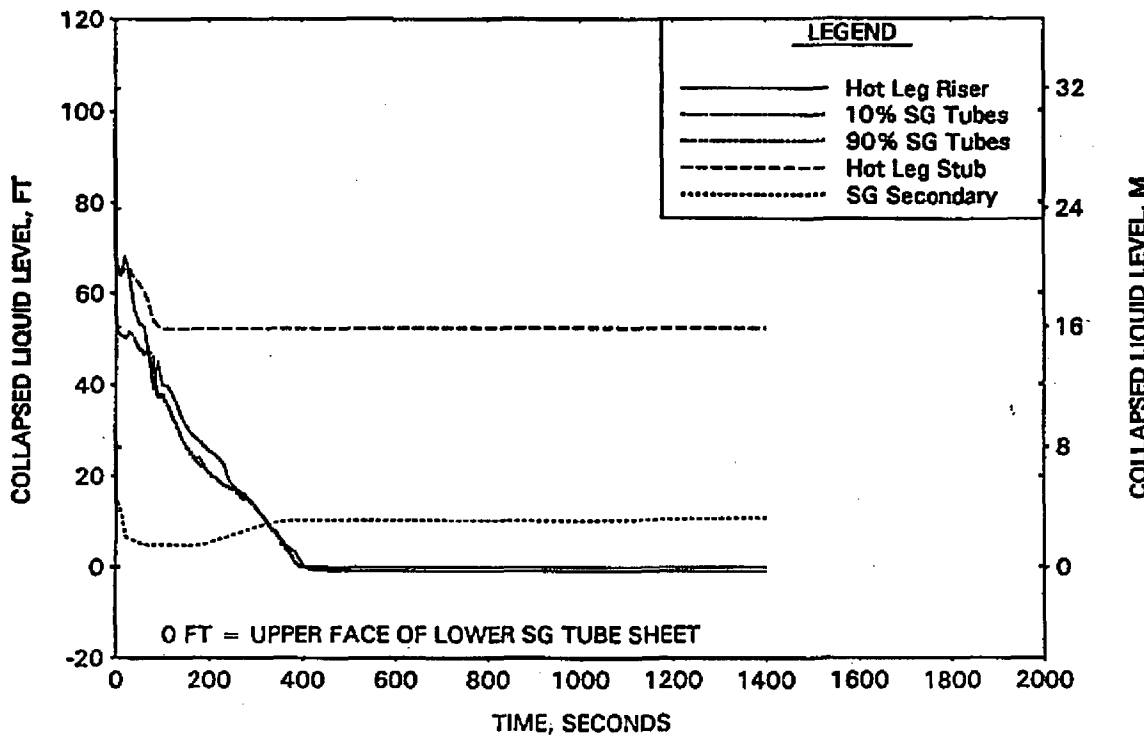


FIGURE A-112. CLPD BREAK SPECTRUM STUDY FOR 0.175-FT² BREAK - INTACT LOOP COLLAPSED LEVELS.

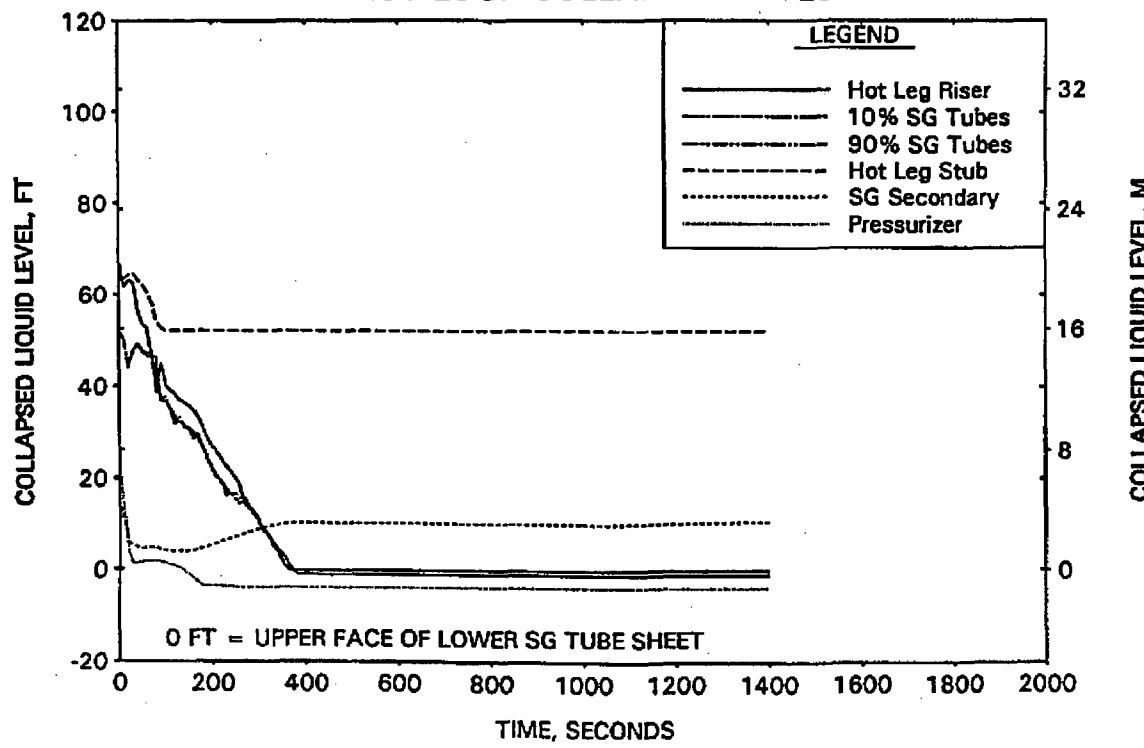


FIGURE A-113. CLPD BREAK SPECTRUM STUDY FOR 0.175-FT² BREAK - CLPD COLLAPSED LEVELS.

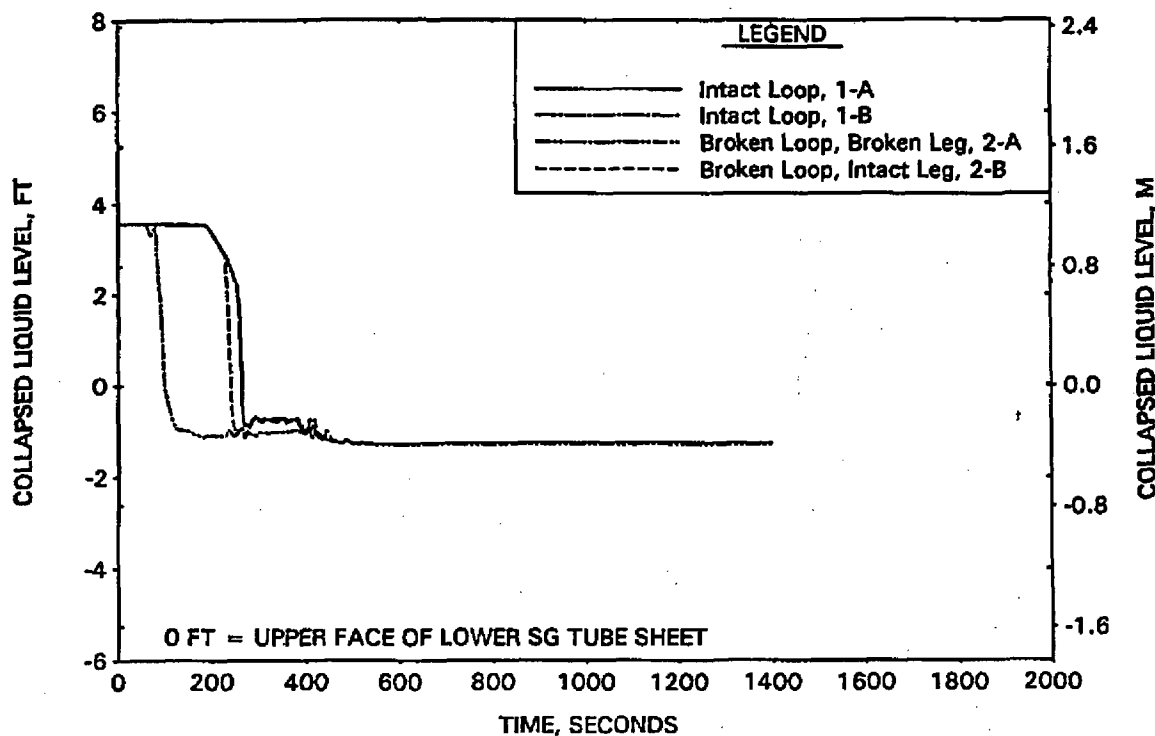


FIGURE A-114. CLPD BREAK SPECTRUM STUDY FOR 0.175-FT² BREAK - CLPS LIQUID VOLUME.

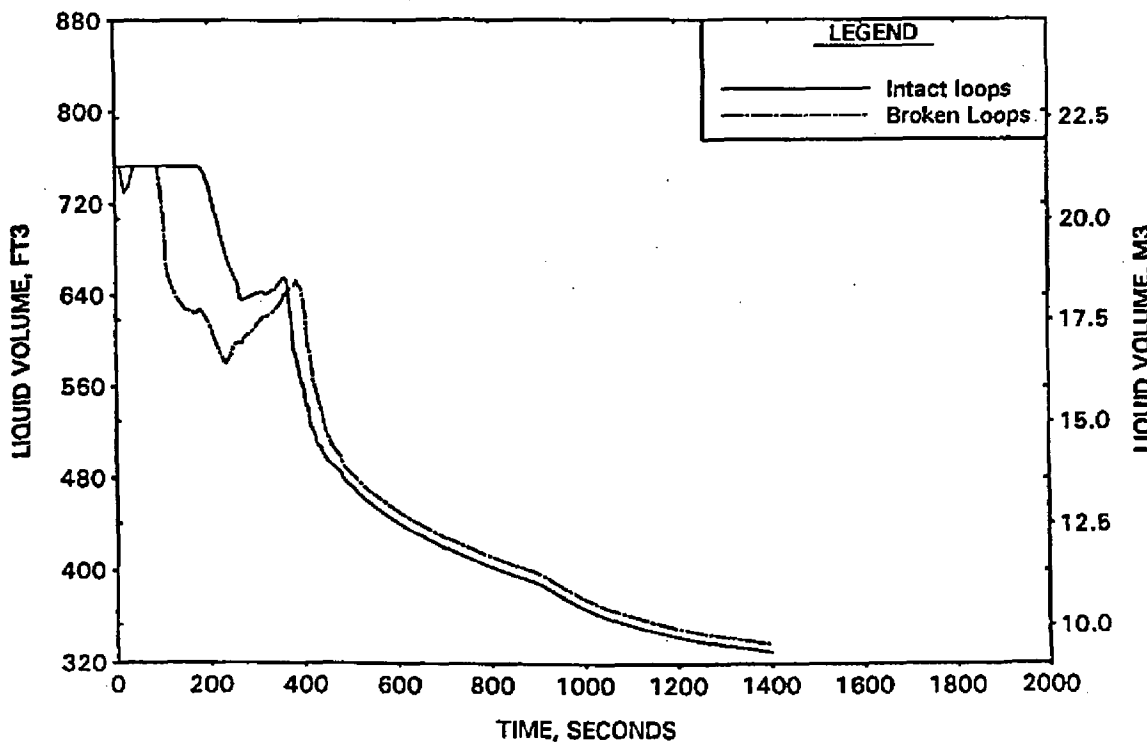


FIGURE A-115. CLPD BREAK SPECTRUM STUDY FOR 0.175-FT² BREAK - HOT LEG AND RVVV FLOWS.

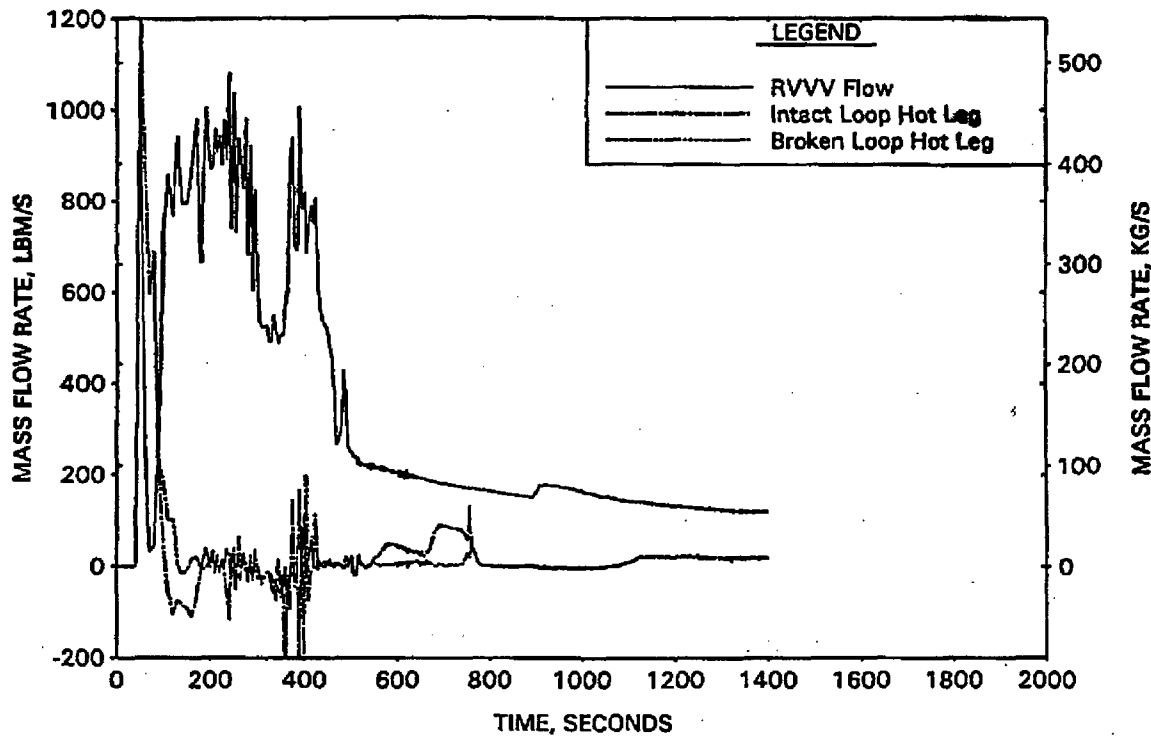


FIGURE A-116. CLPD BREAK SPECTRUM STUDY FOR 0.175-FT² BREAK - CORE MIXTURE LEVELS.

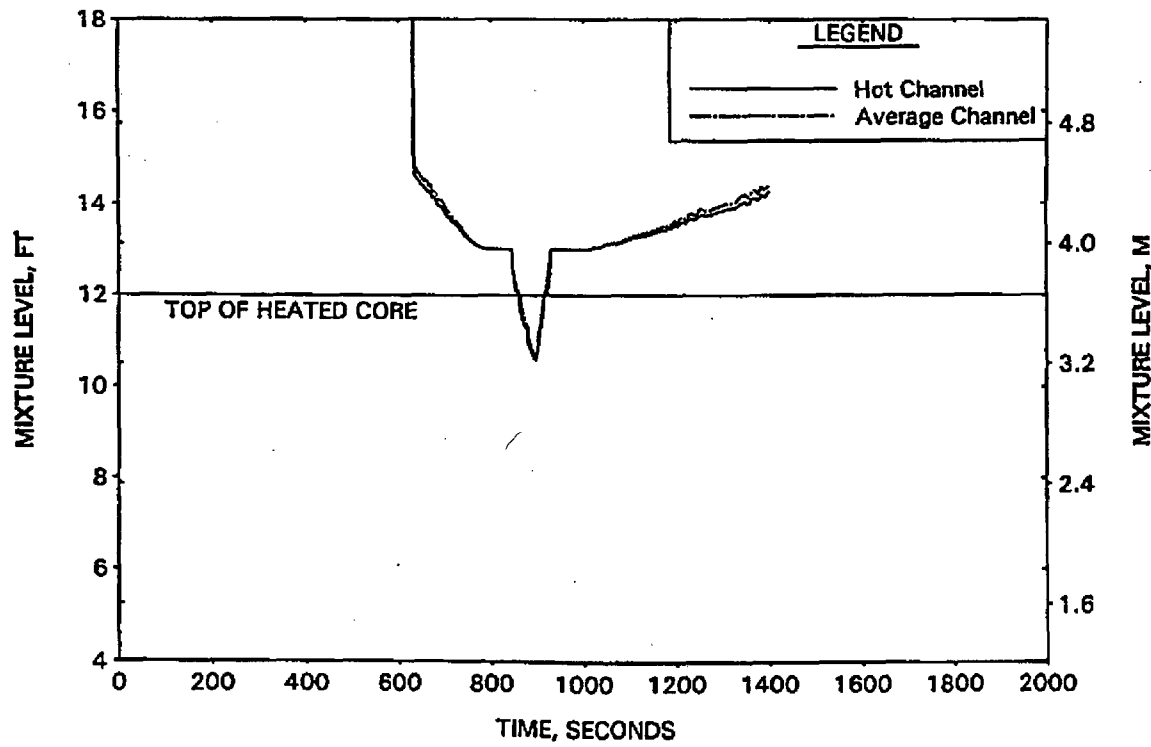


FIGURE A-117. CLPD BREAK SPECTRUM STUDY FOR 0.175-FT2 BREAK - HOT CHANNEL CLAD TEMPERATURES.

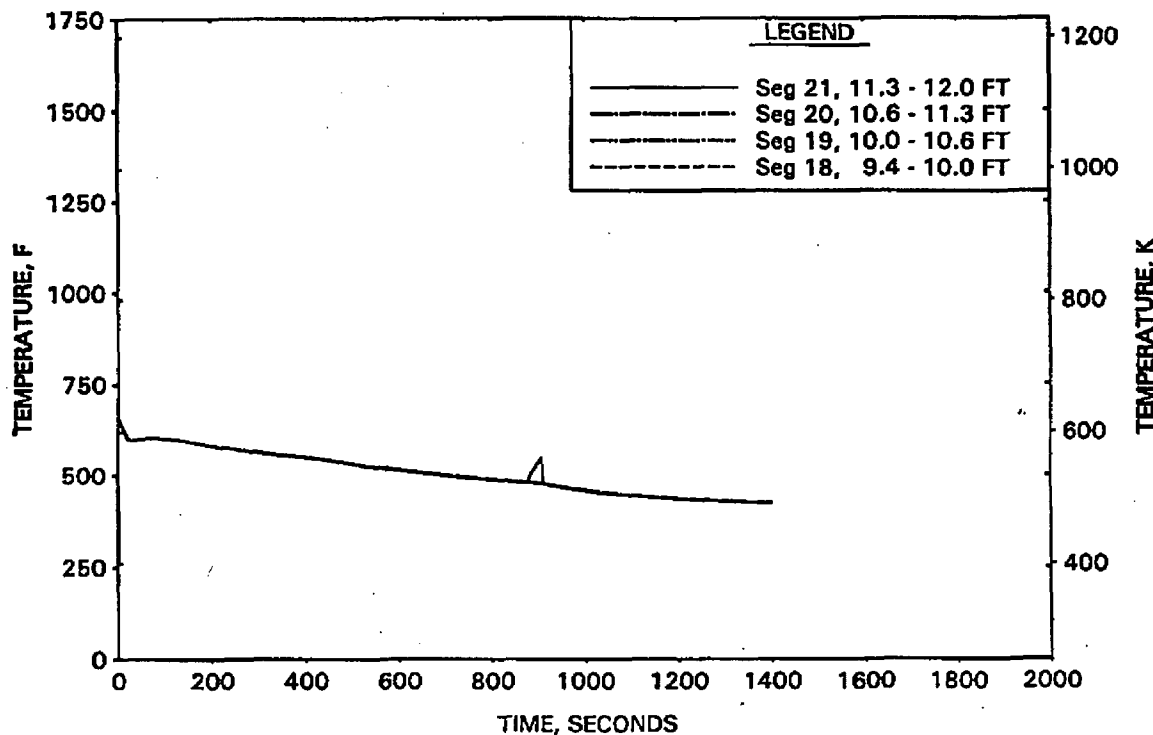


FIGURE A-118. CLPD BREAK SPECTRUM STUDY FOR 0.175-FT2 BREAK - HOT CHANNEL STEAM TEMPERATURES.

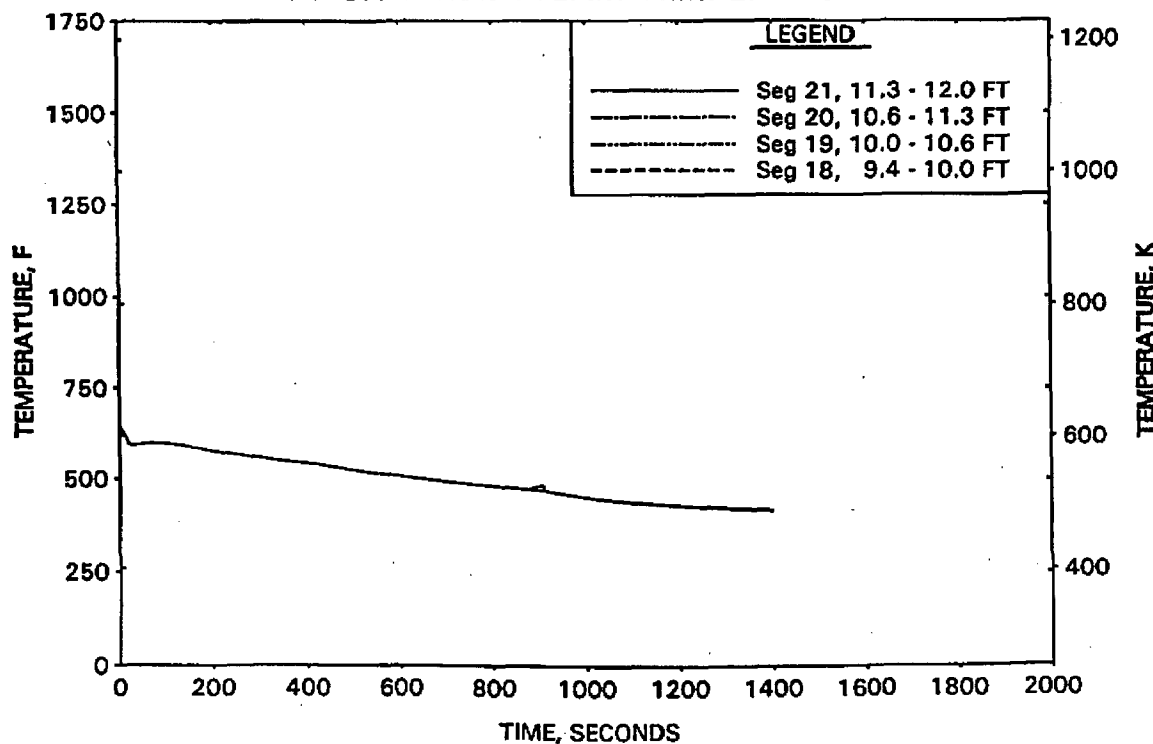


FIGURE A-119. CLPD BREAK SPECTRUM STUDY FOR 0.175-FT2 BREAK -
UPPER ELEVATION AVE CHANNEL CLAD TEMPERATURES.

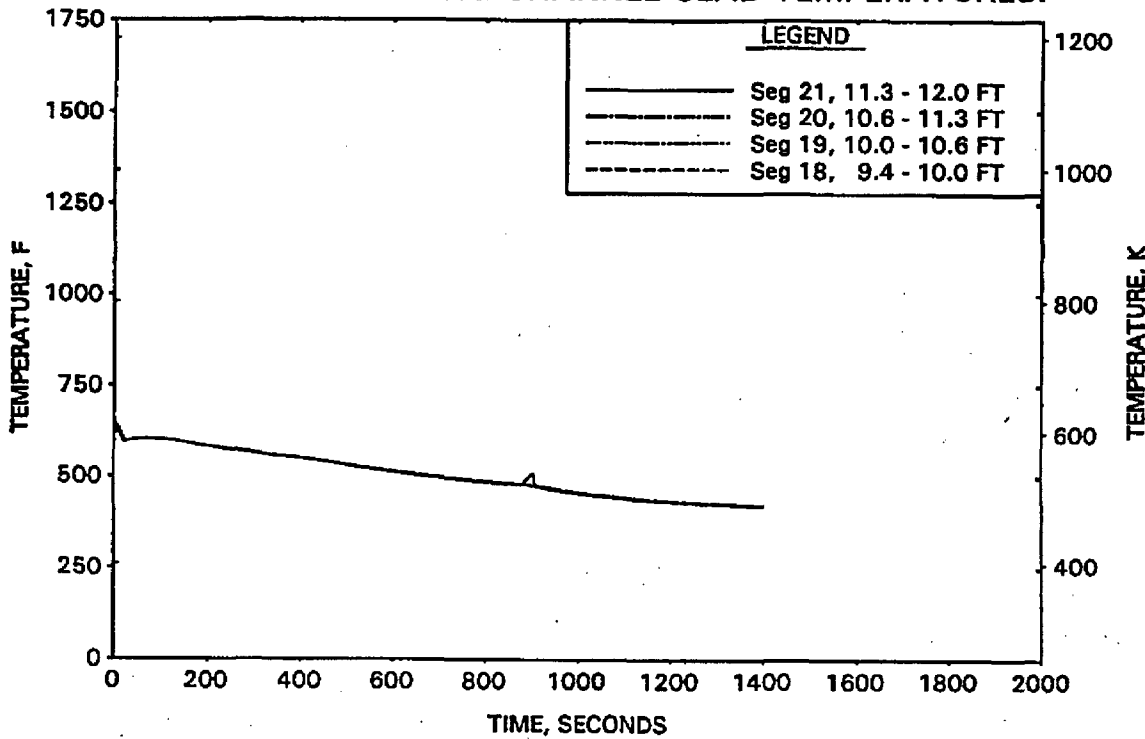


FIGURE A-120. CLPD BREAK SPECTRUM STUDY FOR 0.175-FT2 BREAK -
UPPER ELEVATION AVE CHANNEL STEAM TEMPERATURES.

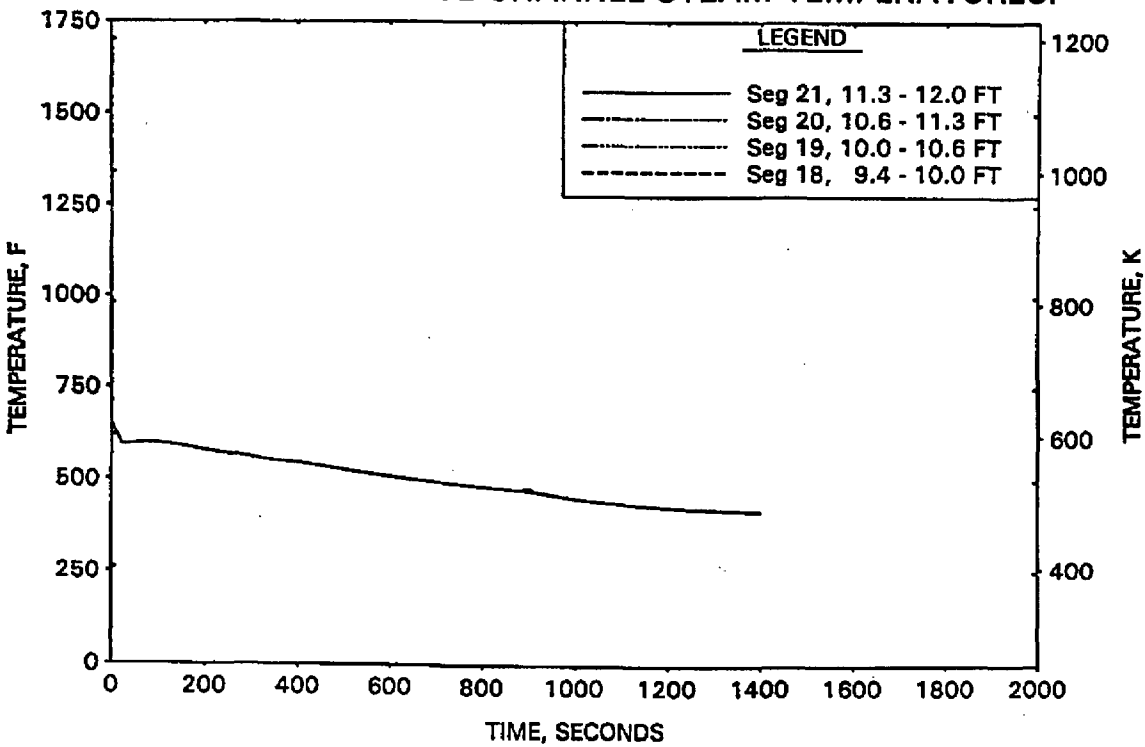


FIGURE A-121. CLPD BREAK SPECTRUM STUDY FOR 0.2-FT² BREAK - RCS PRESSURES.

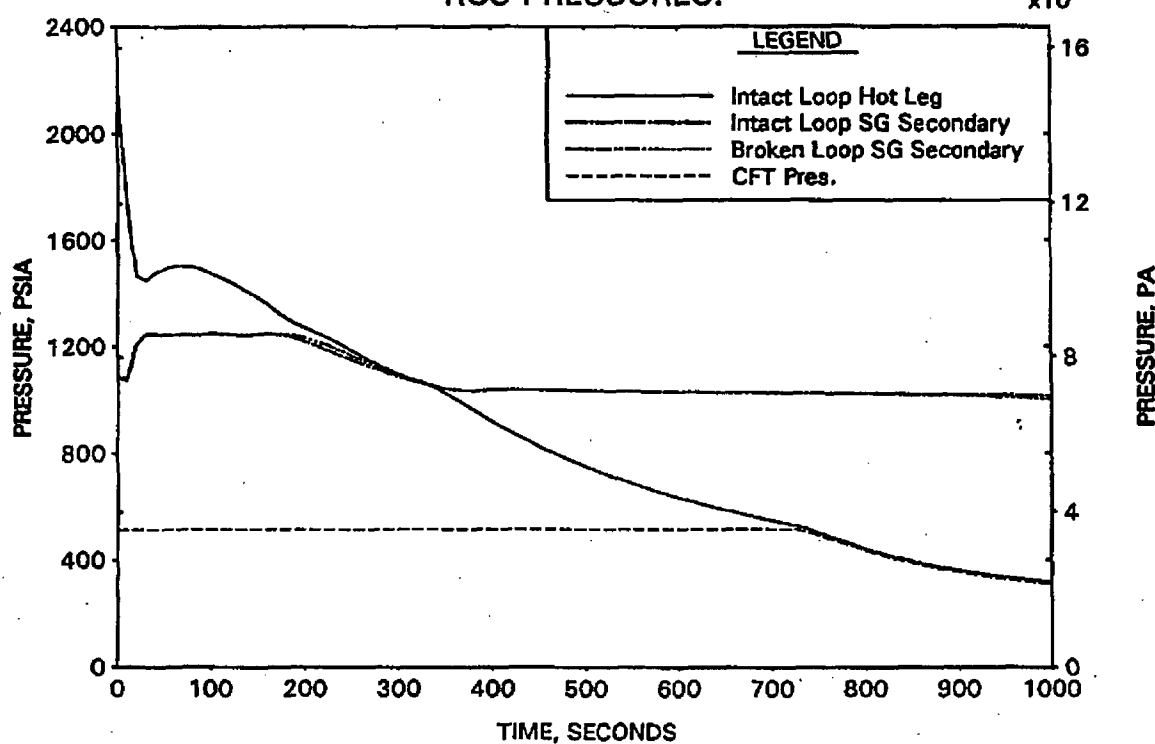


FIGURE A-122. CLPD BREAK SPECTRUM STUDY FOR 0.2-FT² BREAK - DC, RV, AND CORE COLLAPSED LEVELS.

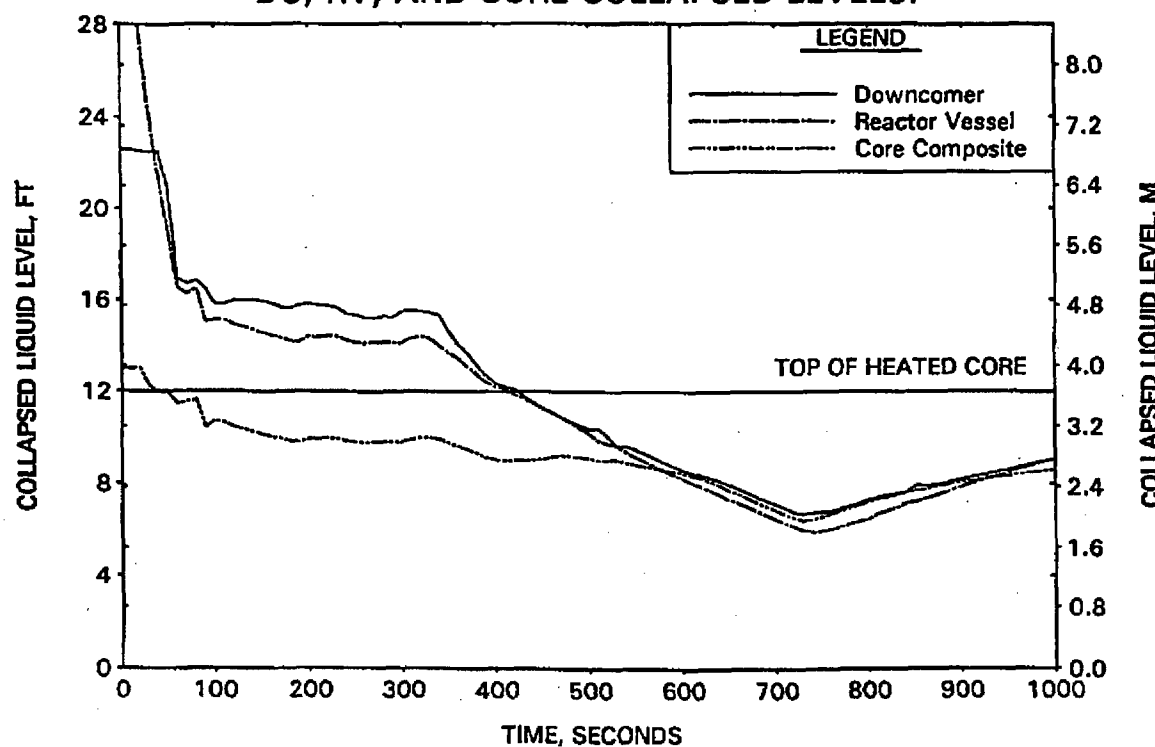


FIGURE A-123. CLPD BREAK SPECTRUM STUDY FOR 0.2-FT² BREAK -
BREAK AND TOTAL ECCS FLOWS.

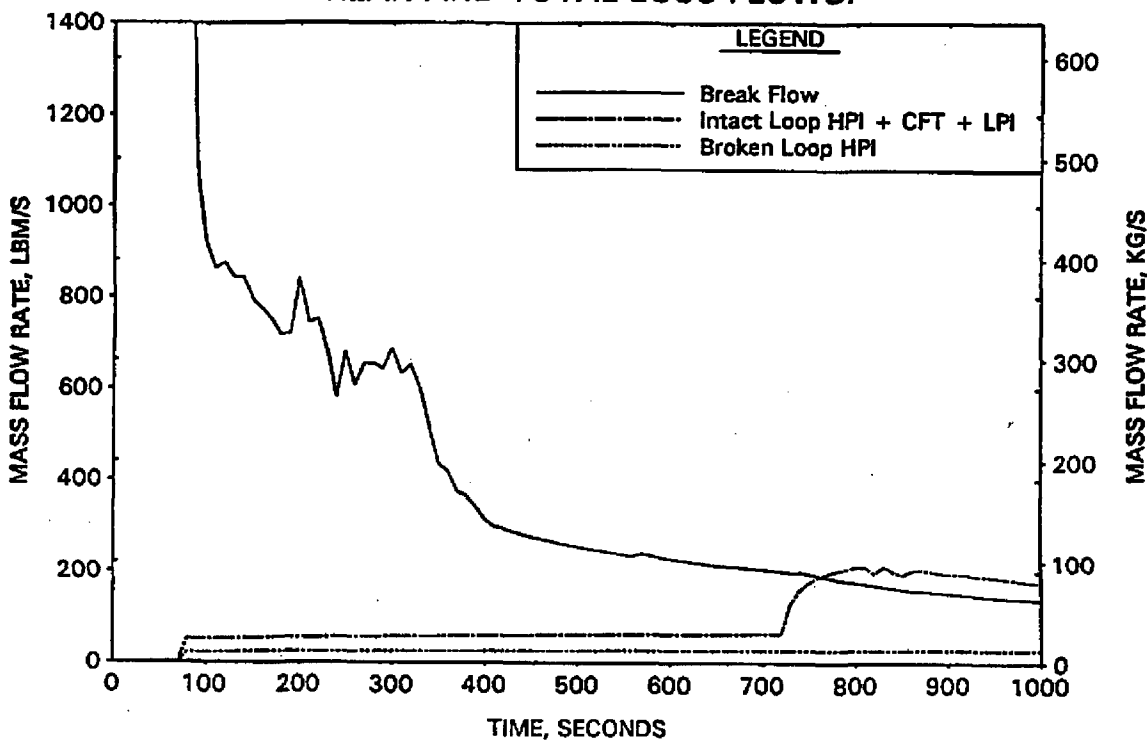


FIGURE A-124. CLPD BREAK SPECTRUM STUDY FOR 0.2-FT² BREAK -
BREAK VOLUME VOID FRACTION.

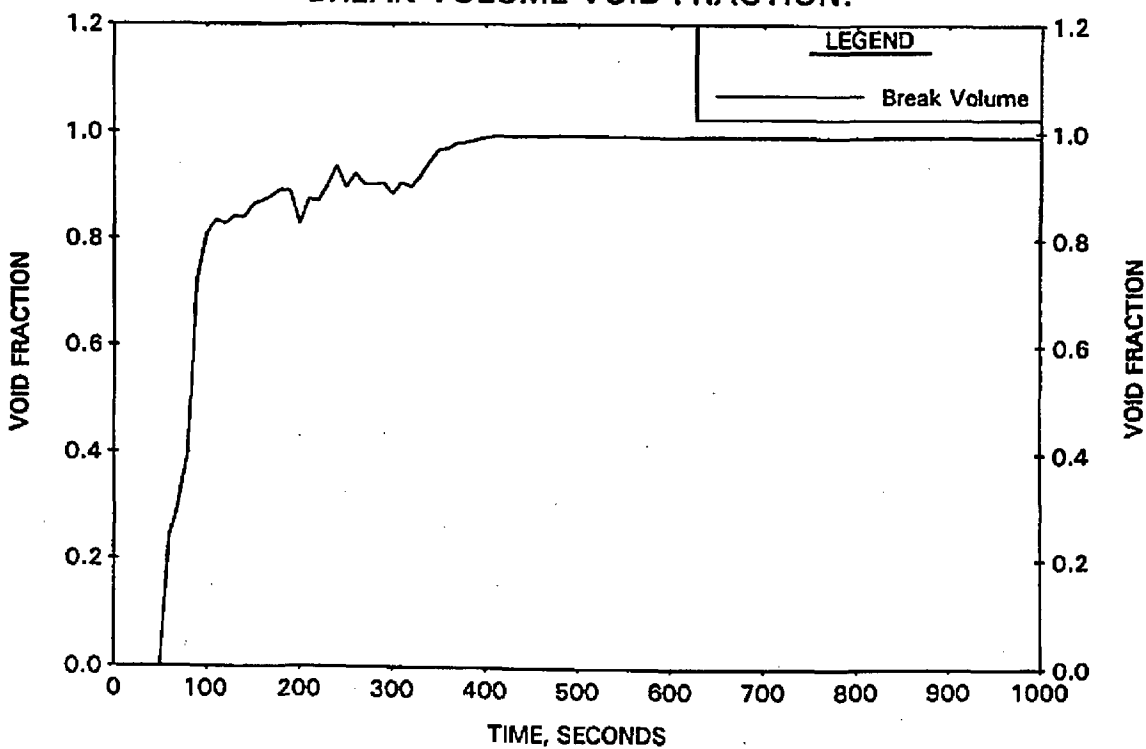


FIGURE A-125. CLPD BREAK SPECTRUM STUDY FOR 0.2-FT² BREAK - BROKEN LOOP COLLAPSED LEVELS.

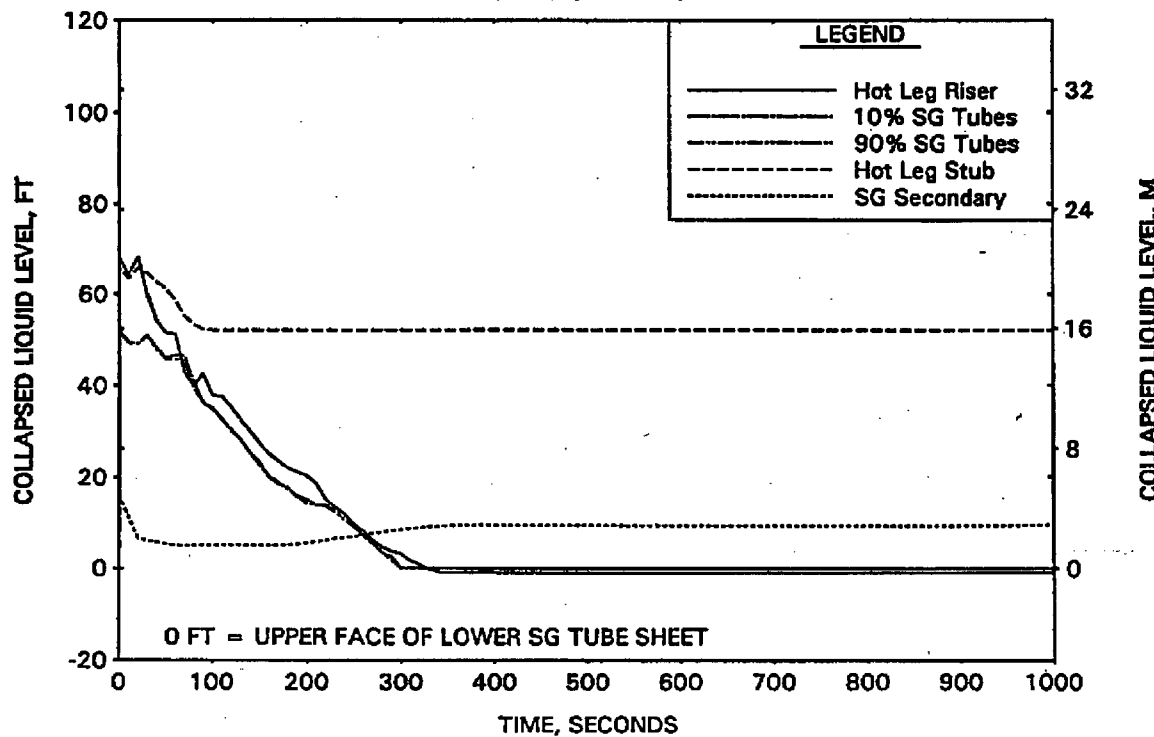


FIGURE A-126. CLPD BREAK SPECTRUM STUDY FOR 0.2-FT² BREAK - INTACT LOOP COLLAPSED LEVELS.

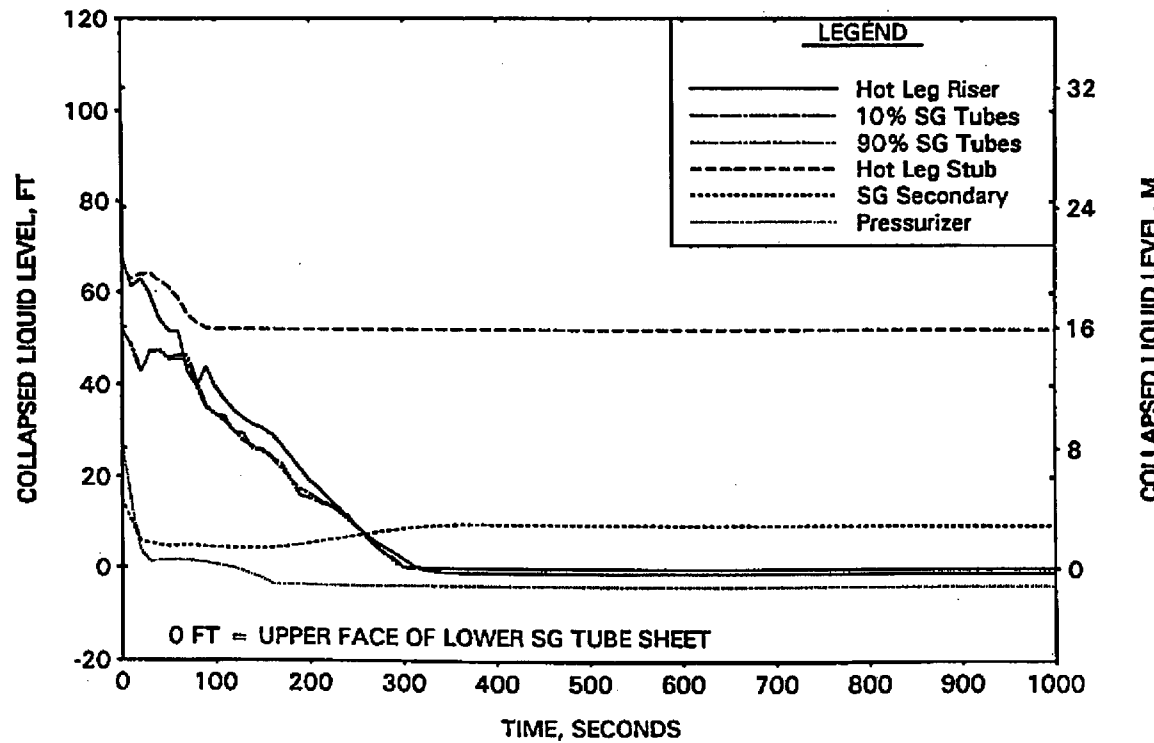


FIGURE A-127. CLPD BREAK SPECTRUM STUDY FOR 0.2-FT² BREAK - CLPD COLLAPSED LEVELS.

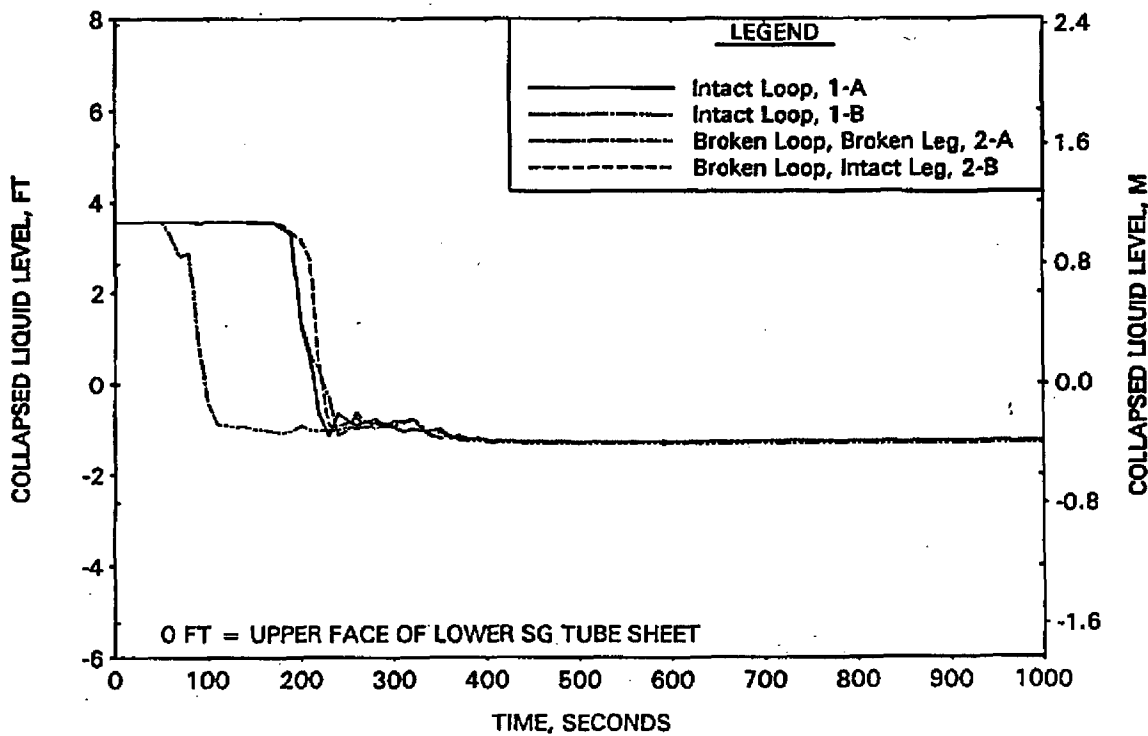


FIGURE A-128. CLPD BREAK SPECTRUM STUDY FOR 0.2-FT² BREAK - CLPS LIQUID VOLUME.

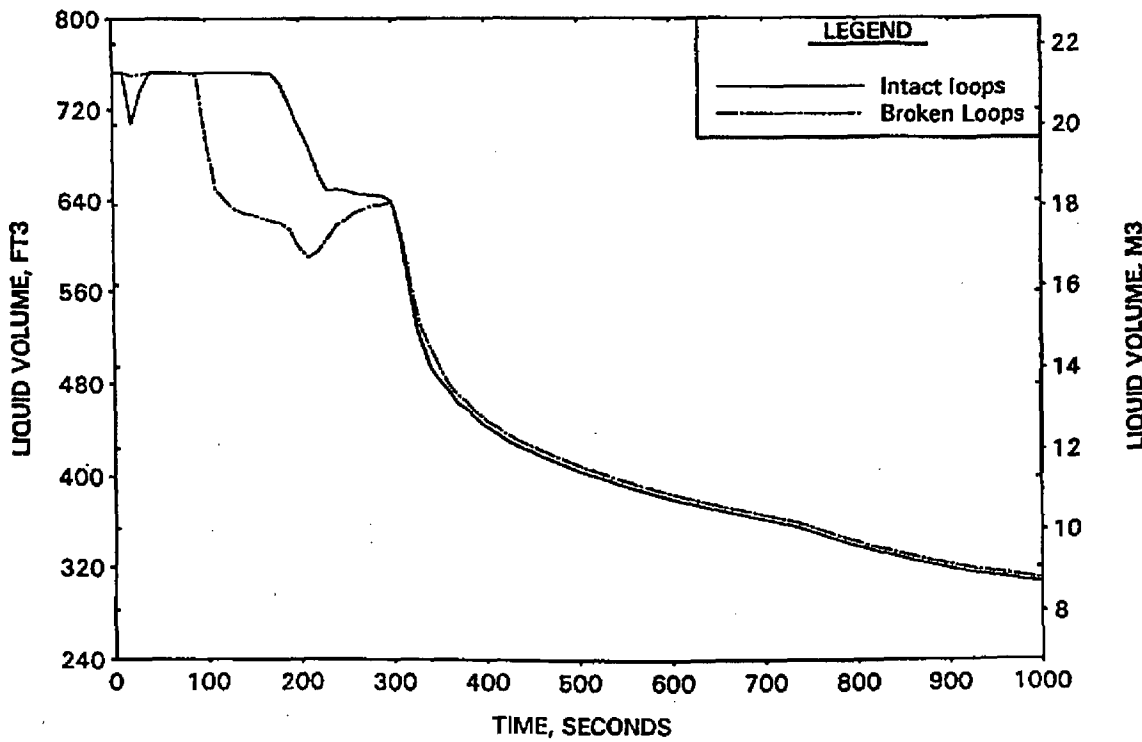


FIGURE A-129. CLPD BREAK SPECTRUM STUDY FOR 0.2-FT² BREAK - HOT LEG AND RVVV FLOWS.

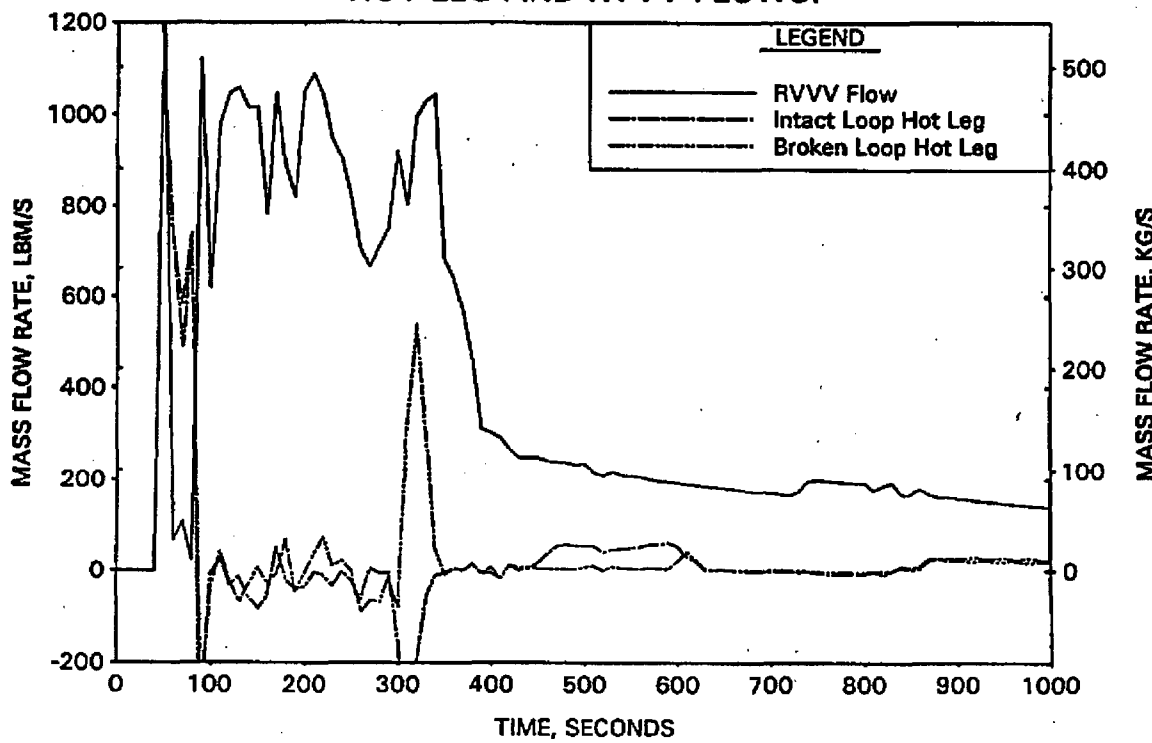


FIGURE A-130. CLPD BREAK SPECTRUM STUDY FOR 0.2-FT² BREAK - CORE MIXTURE LEVELS.

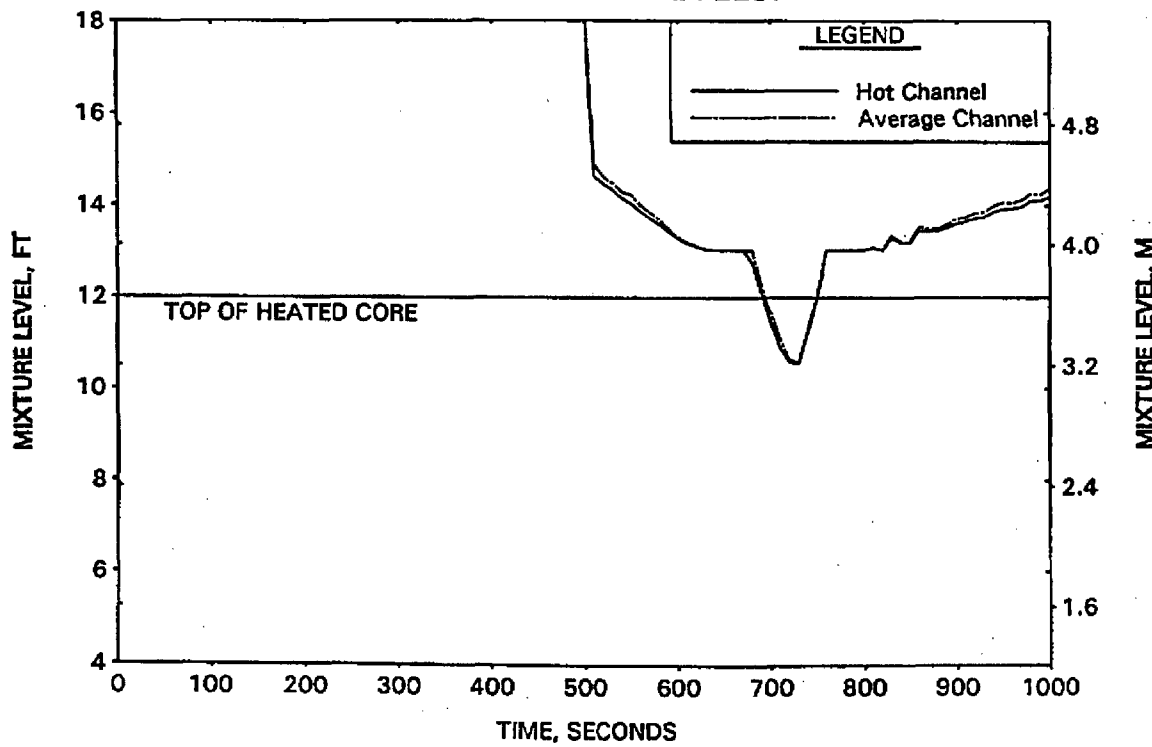


FIGURE A-131. CLPD BREAK SPECTRUM STUDY FOR 0.2-FT2 BREAK - HOT CHANNEL CLAD TEMPERATURES.

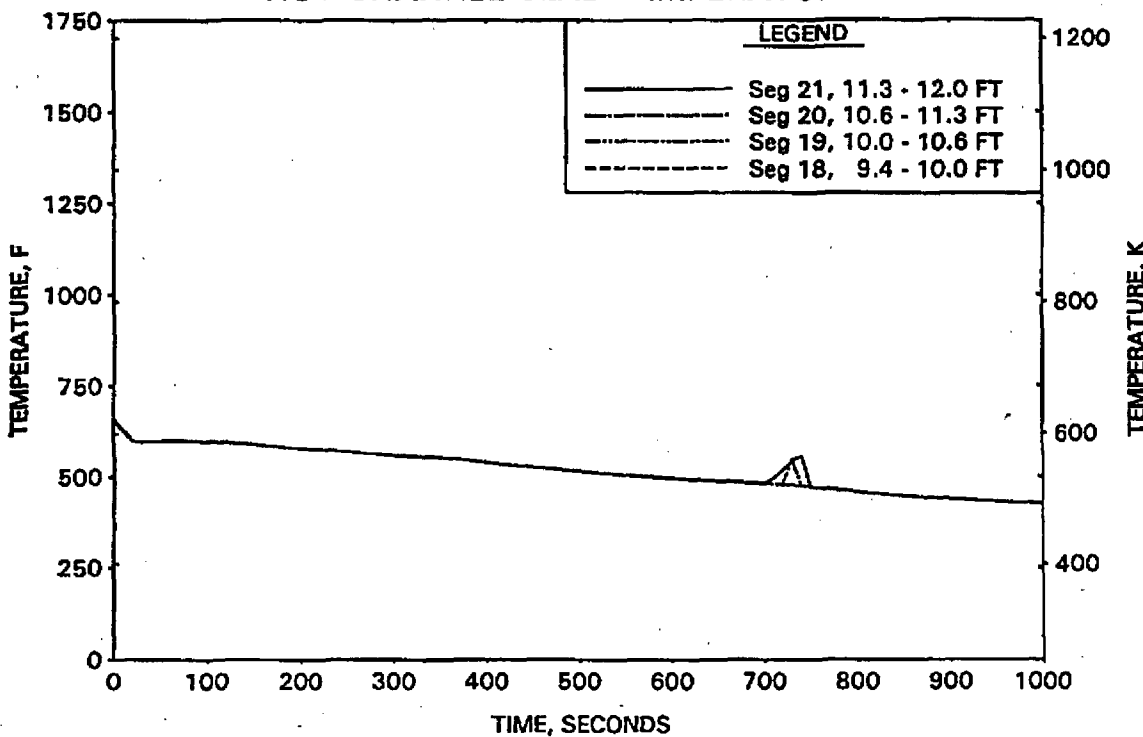


FIGURE A-132. CLPD BREAK SPECTRUM STUDY FOR 0.2-FT2 BREAK - HOT CHANNEL STEAM TEMPERATURES.

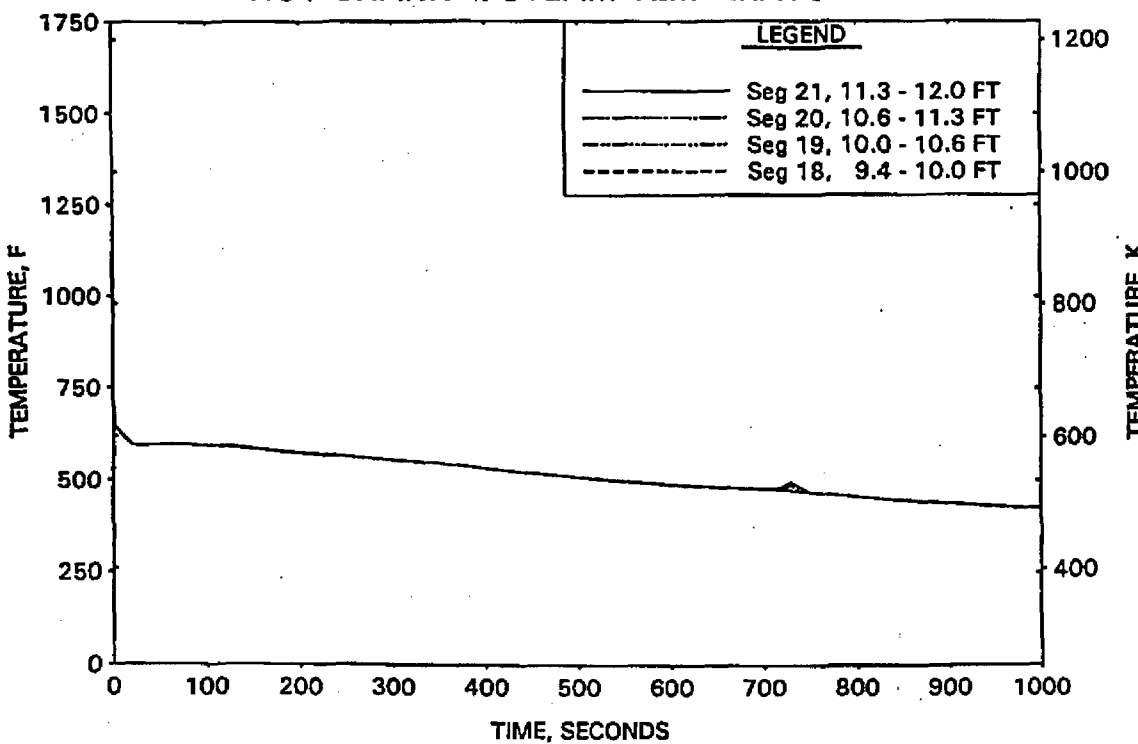


FIGURE A-133. CLPD BREAK SPECTRUM STUDY FOR 0.2-FT2 BREAK -
UPPER ELEVATION AVE CHANNEL CLAD TEMPERATURES.

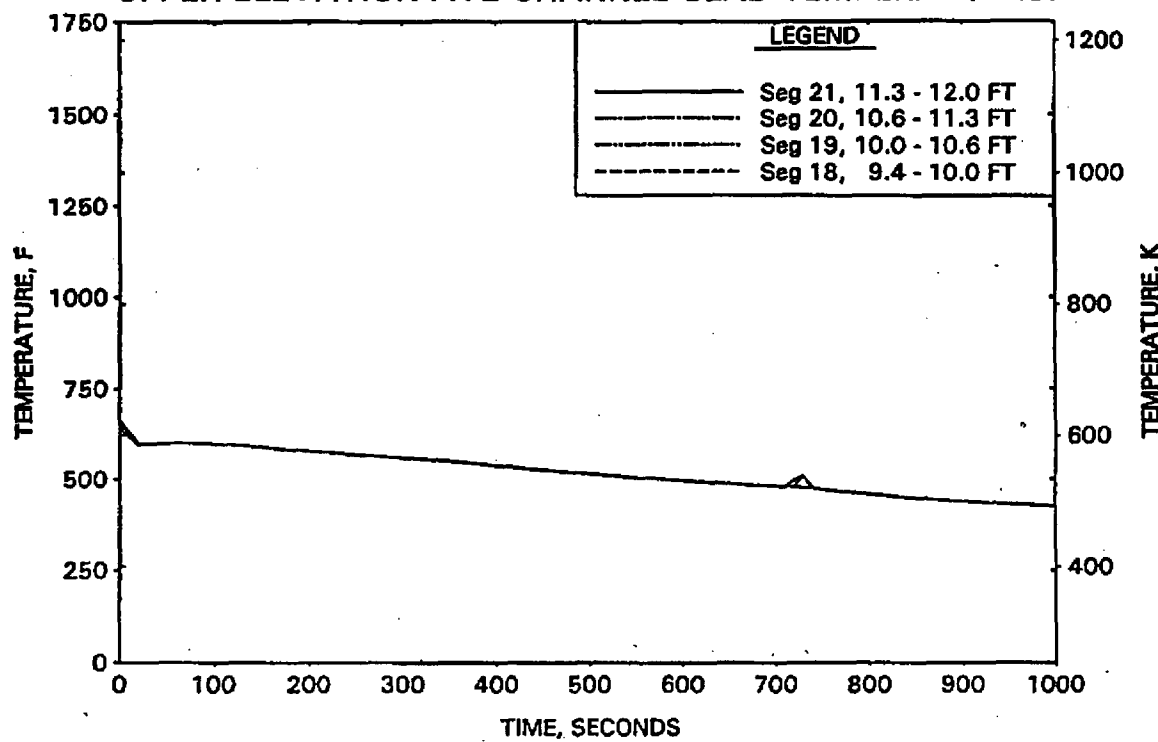


FIGURE A-134. CLPD BREAK SPECTRUM STUDY FOR 0.2-FT2 BREAK -
UPPER ELEVATION AVE CHANNEL STEAM TEMPERATURES.

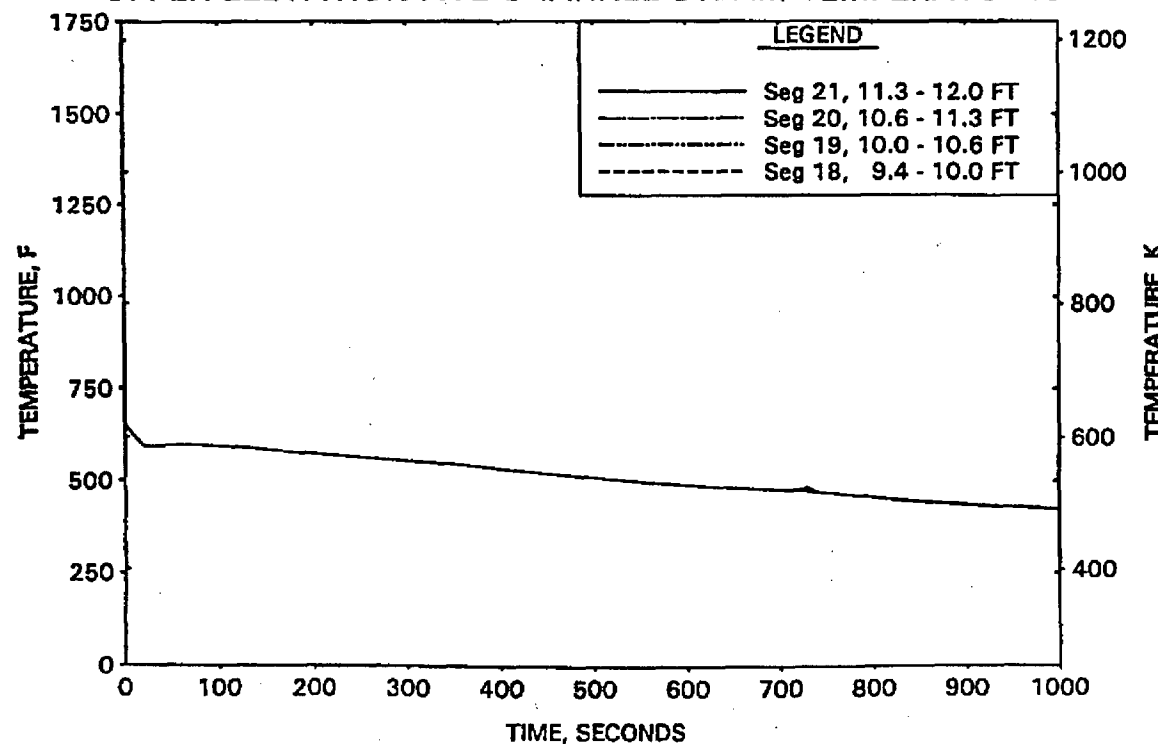


FIGURE A-135. CLPD BREAK SPECTRUM STUDY FOR 0.3-FT2 BREAK - RCS PRESSURES.

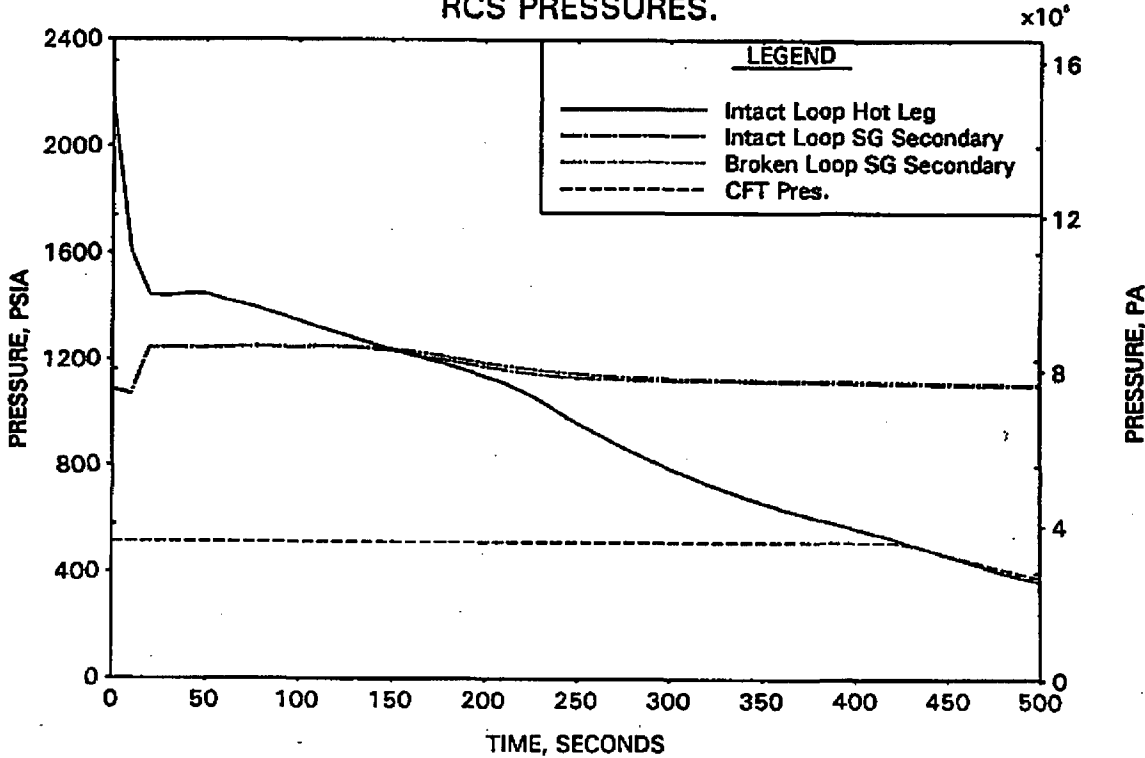


FIGURE A-136. CLPD BREAK SPECTRUM STUDY FOR 0.3-FT2 BREAK - DC, RV, AND CORE COLLAPSED LEVELS.

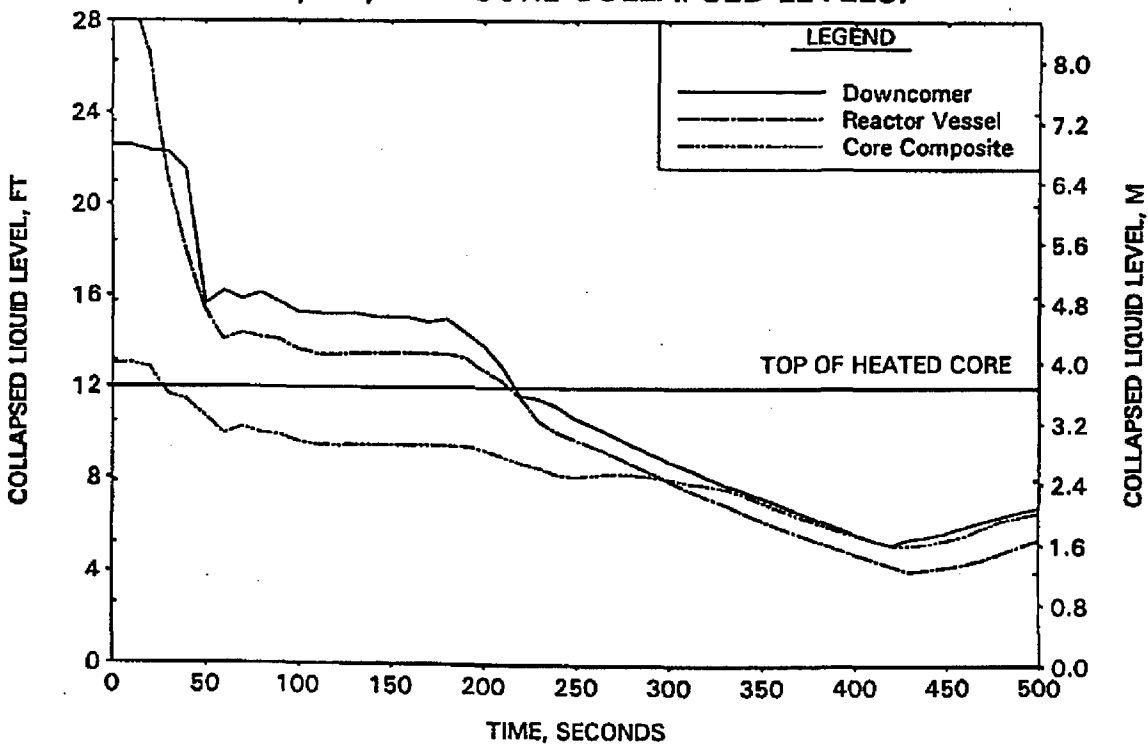


FIGURE A-137. CLPD BREAK SPECTRUM STUDY FOR 0.3-FT² BREAK -
BREAK AND TOTAL ECCS FLOWS.

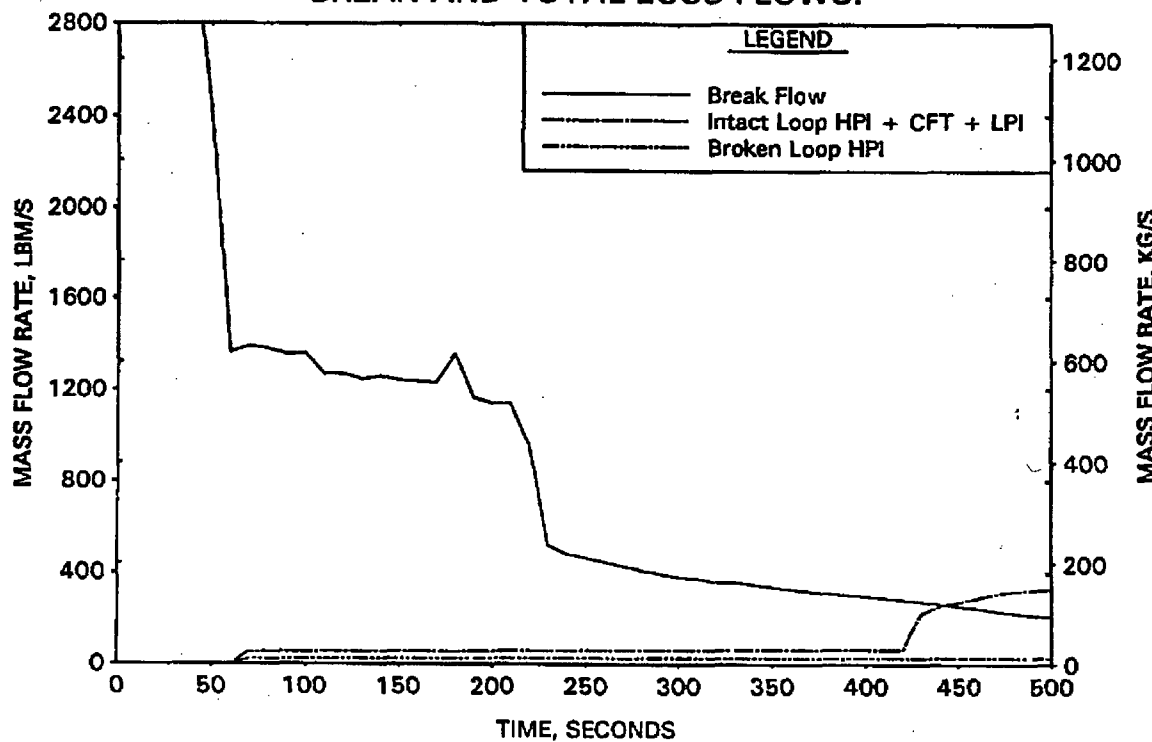


FIGURE A-138. CLPD BREAK SPECTRUM STUDY FOR 0.3-FT² BREAK -
BREAK VOLUME VOID FRACTION.

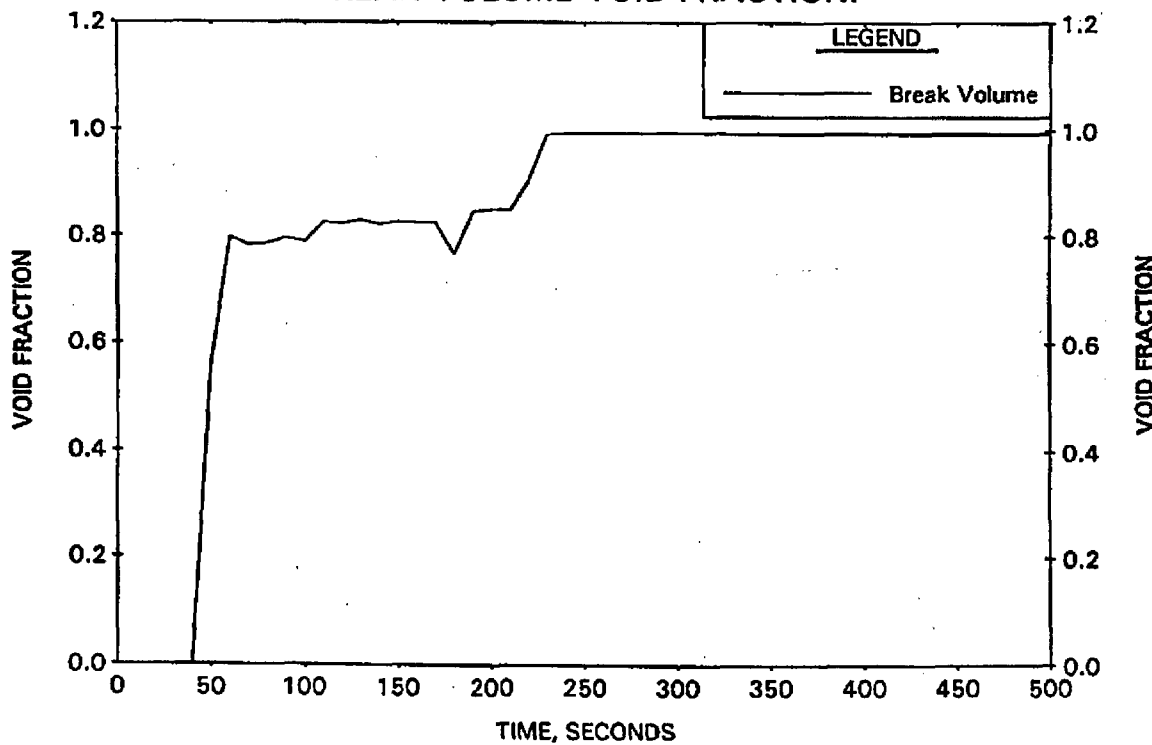


FIGURE A-139. CLPD BREAK SPECTRUM STUDY FOR 0.3-FT² BREAK - BROKEN LOOP COLLAPSED LEVELS.

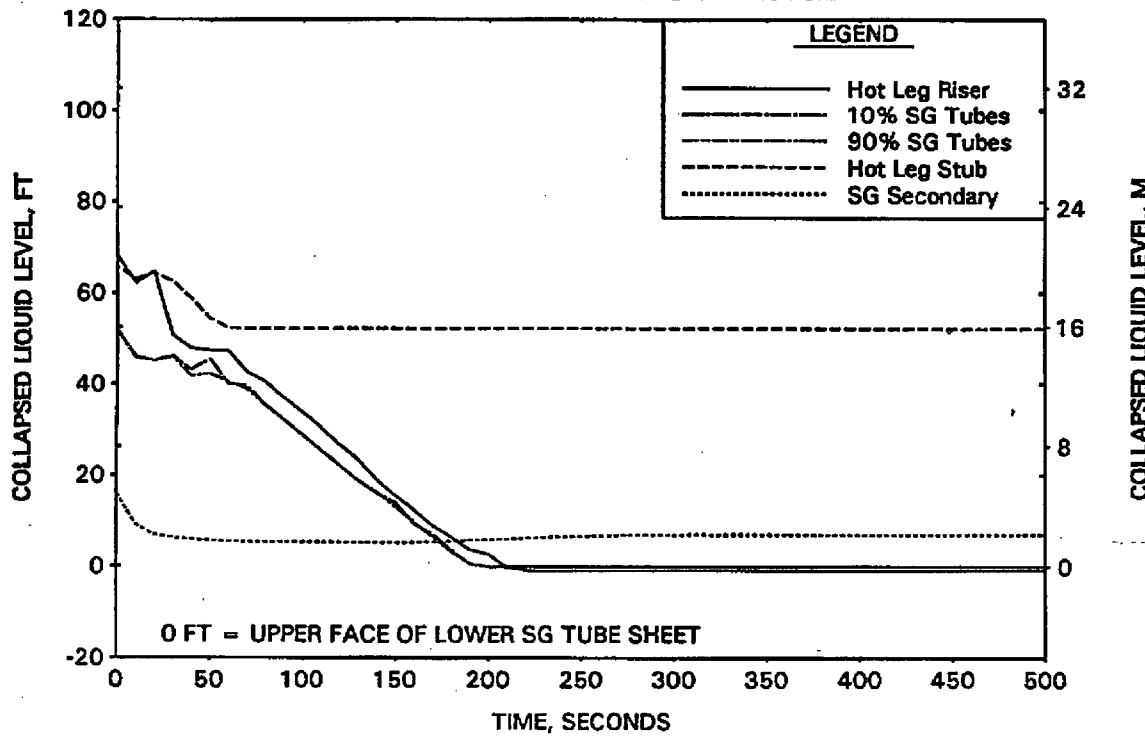


FIGURE A-140. CLPD BREAK SPECTRUM STUDY FOR 0.3-FT² BREAK - INTACT LOOP COLLAPSED LEVELS.

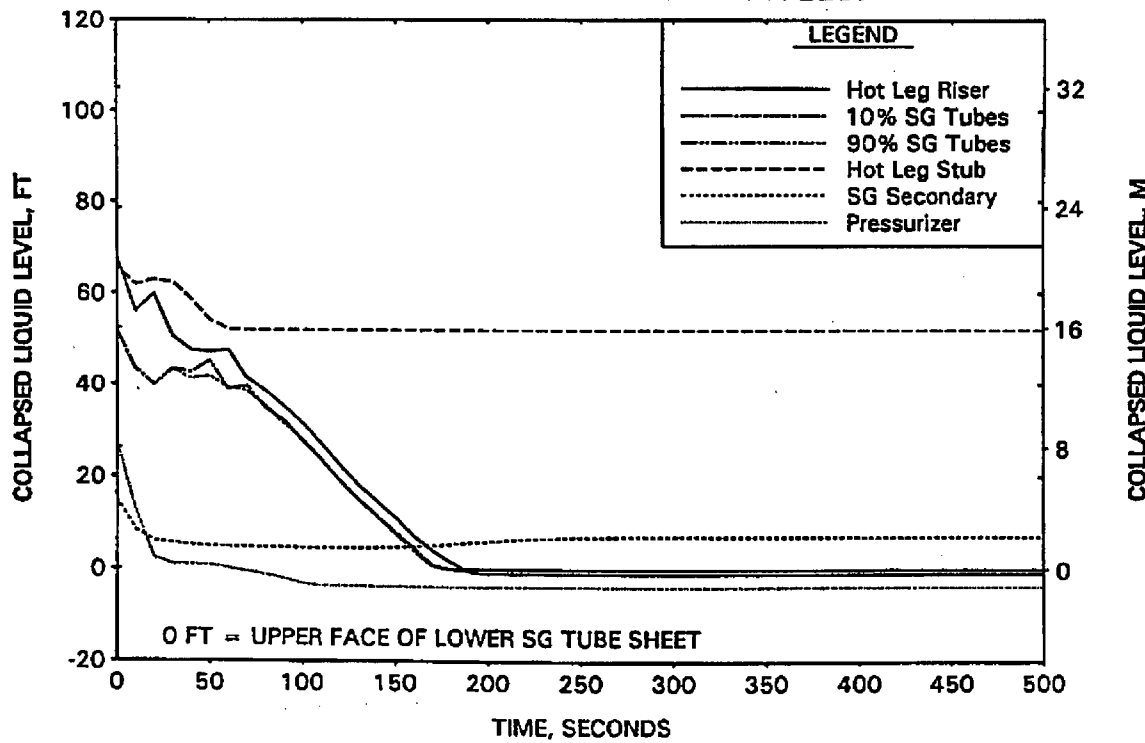


FIGURE A-141. CLPD BREAK SPECTRUM STUDY FOR 0.3-FT² BREAK - CLPD COLLAPSED LEVELS.

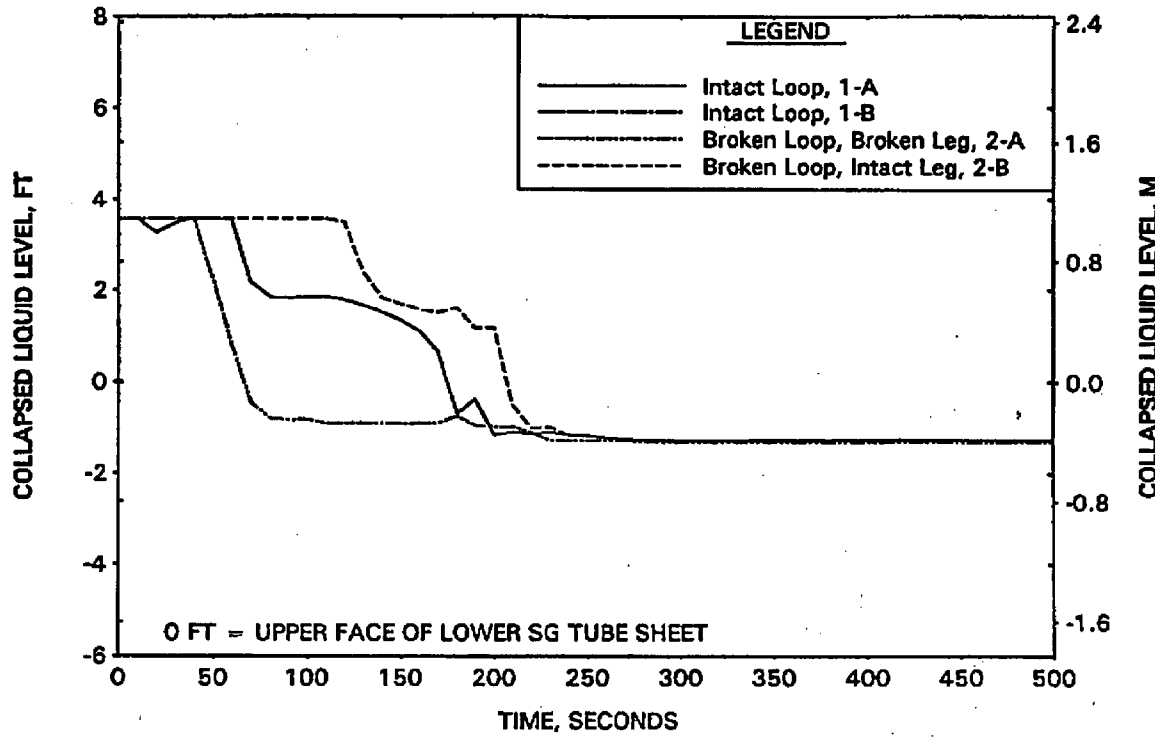


FIGURE A-142. CLPD BREAK SPECTRUM STUDY FOR 0.3-FT² BREAK - CLPS LIQUID VOLUME.

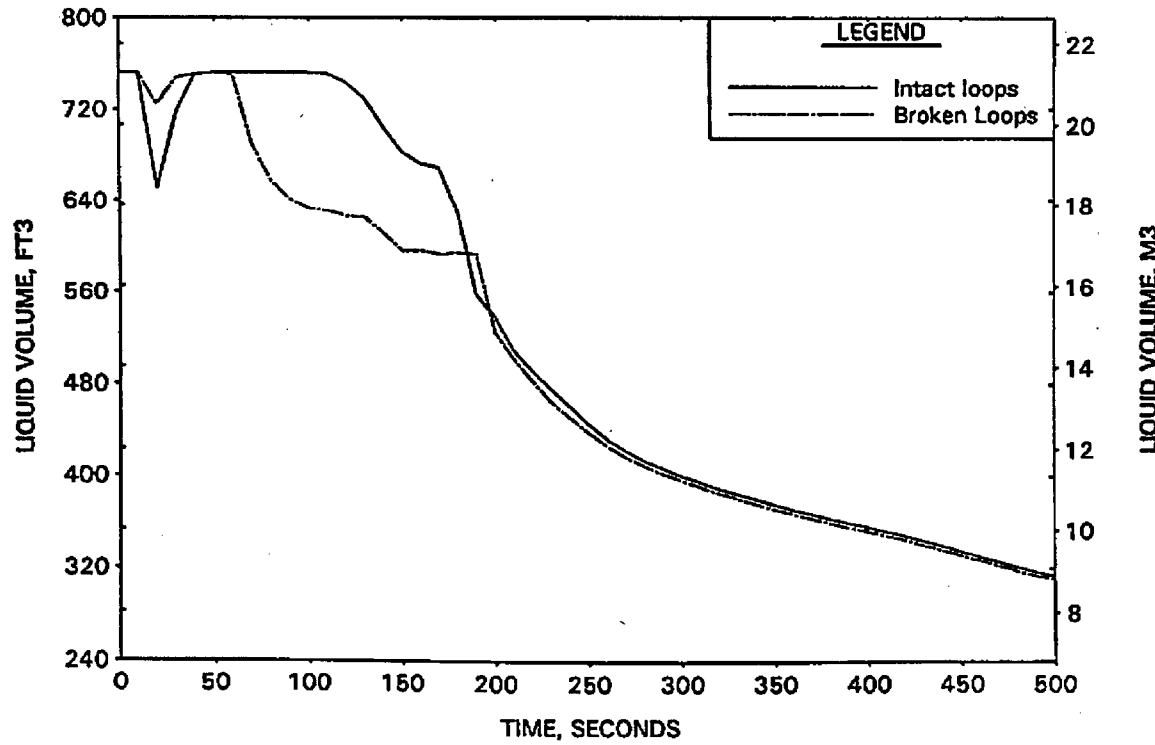


FIGURE A-143. CLPD BREAK SPECTRUM STUDY FOR 0.3-FT² BREAK - HOT LEG AND RVVV FLOWS.

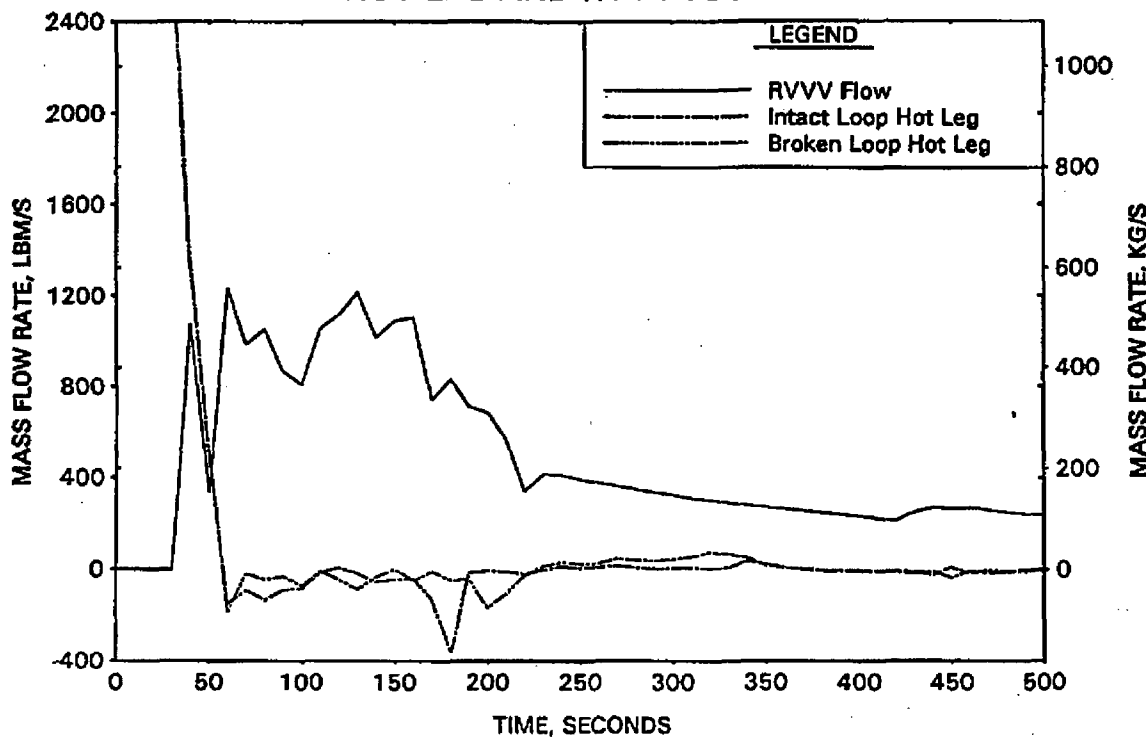


FIGURE A-144. CLPD BREAK SPECTRUM STUDY FOR 0.3-FT² BREAK - CORE MIXTURE LEVELS.

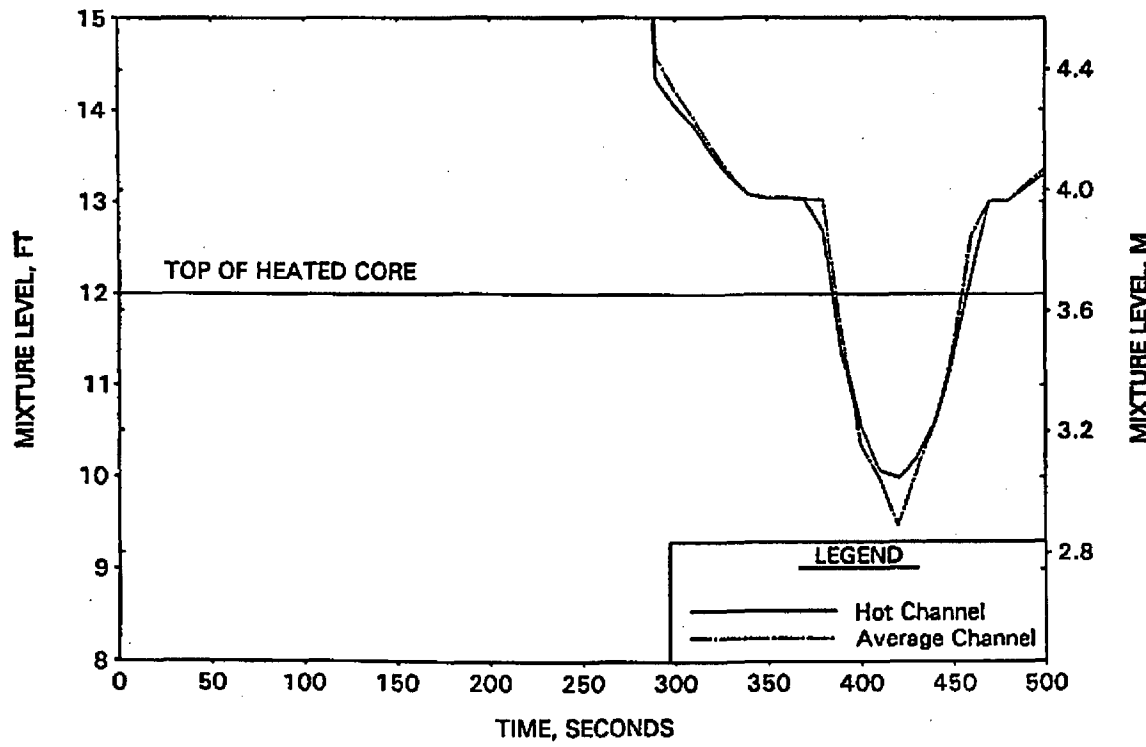


FIGURE A-145. CLPD BREAK SPECTRUM STUDY FOR 0.3-FT2 BREAK - HOT CHANNEL CLAD TEMPERATURES.

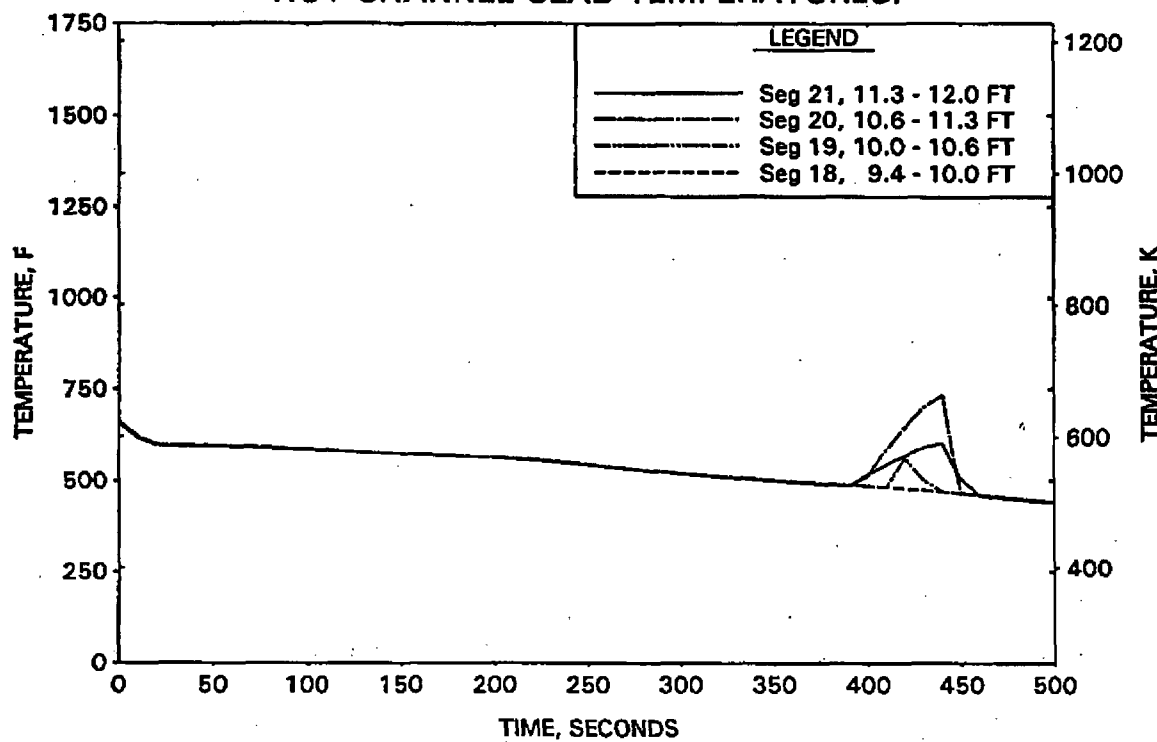


FIGURE A-146. CLPD BREAK SPECTRUM STUDY FOR 0.3-FT2 BREAK - HOT CHANNEL STEAM TEMPERATURES.

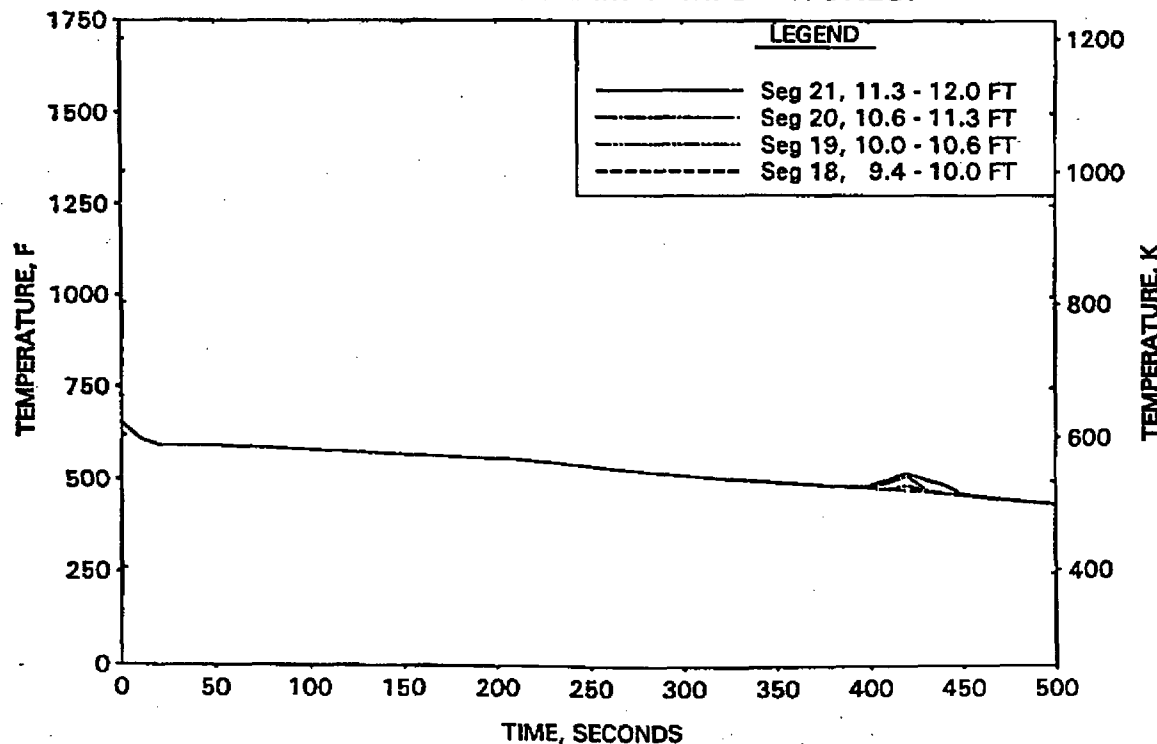


FIGURE A-147. CLPD BREAK SPECTRUM STUDY FOR 0.3-FT2 BREAK -
UPPER ELEVATION AVE CHANNEL CLAD TEMPERATURES.

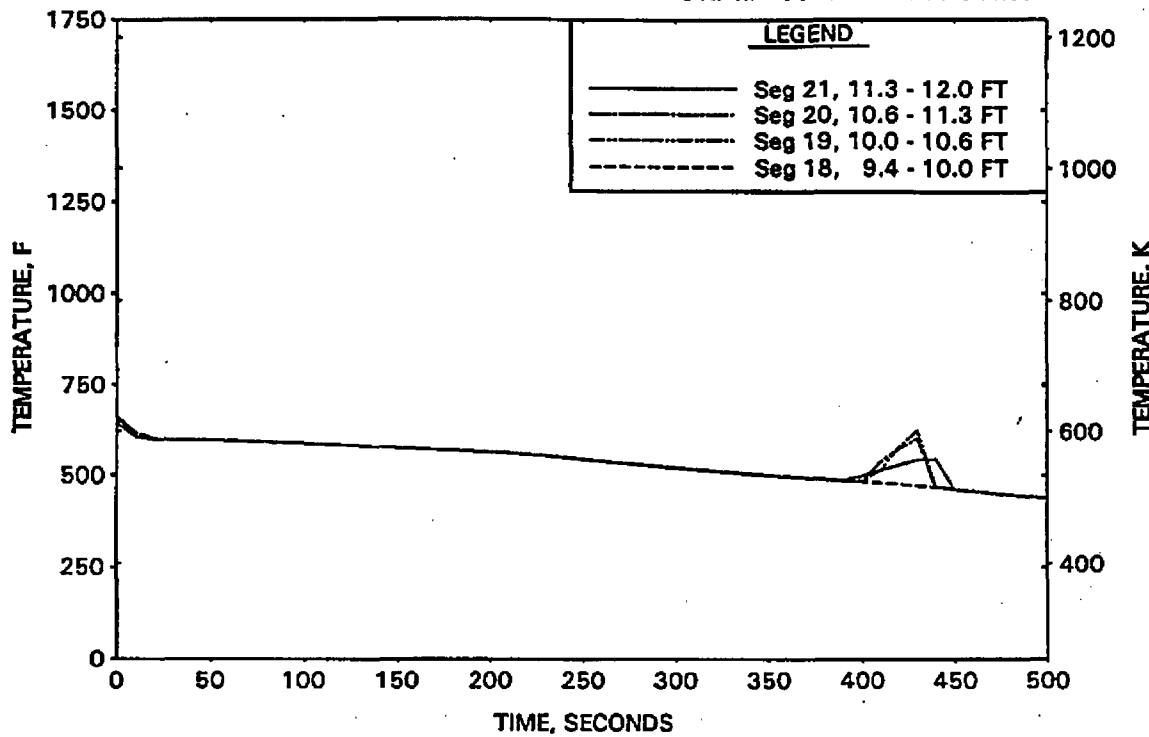


FIGURE A-148. CLPD BREAK SPECTRUM STUDY FOR 0.3-FT2 BREAK -
UPPER ELEVATION AVE CHANNEL STEAM TEMPERATURES.

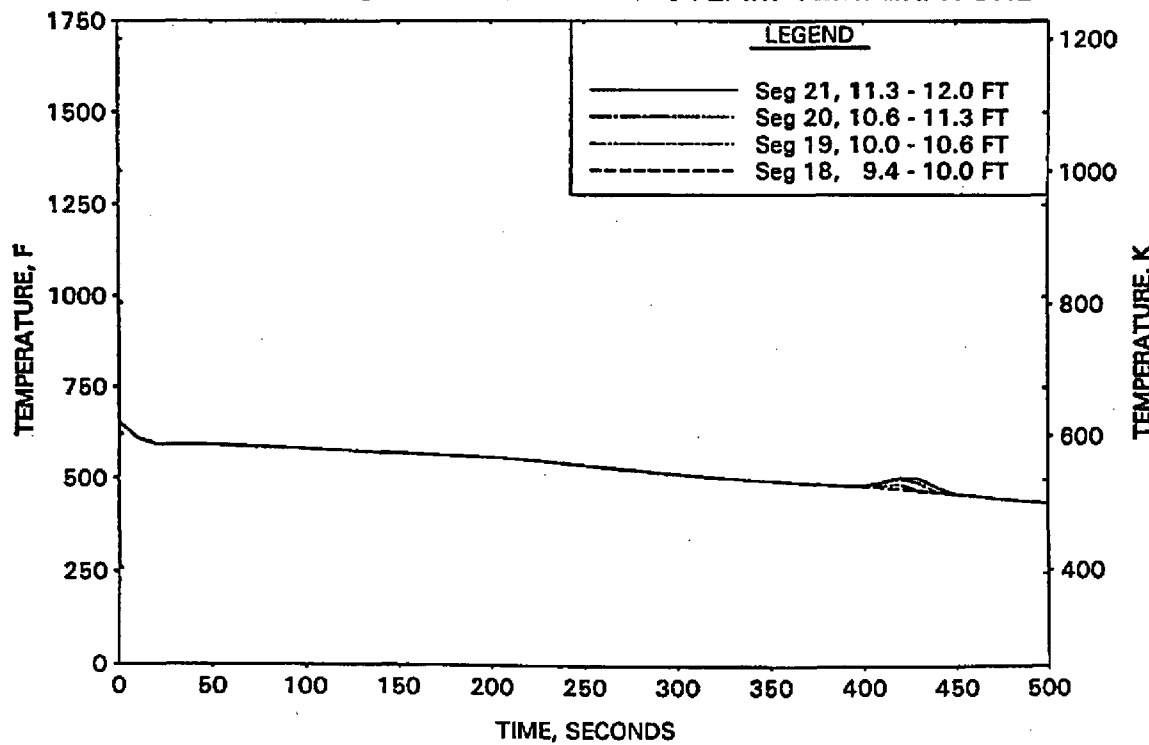


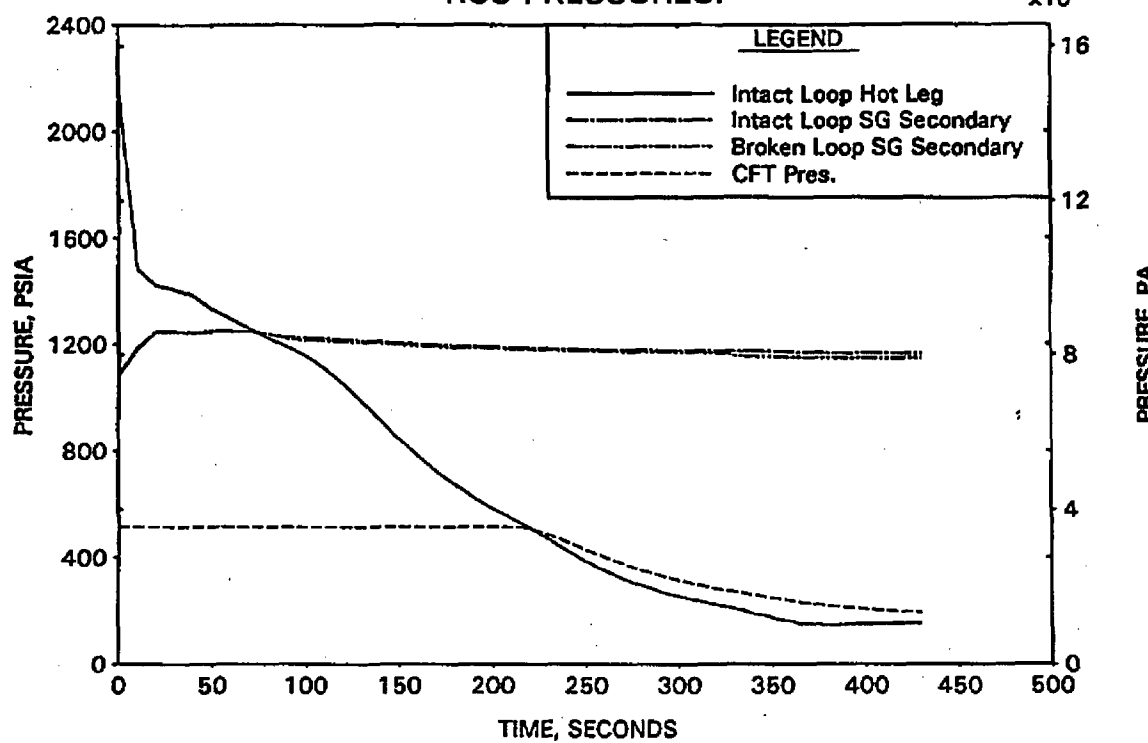
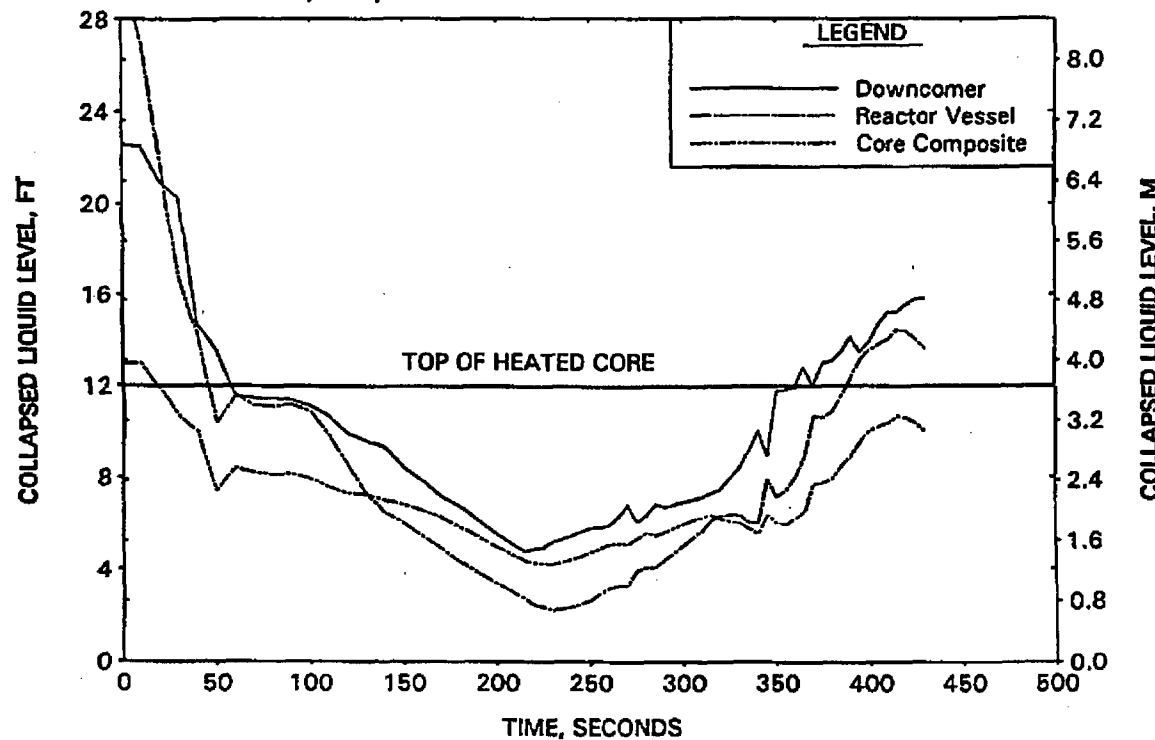
FIGURE A-149. CLPD BREAK SPECTRUM STUDY FOR 0.5-FT² BREAK - RCS PRESSURES.FIGURE A-150. CLPD BREAK SPECTRUM STUDY FOR 0.5-FT² BREAK - DC, RV, AND CORE COLLAPSED LEVELS.

FIGURE A-151. CLPD BREAK SPECTRUM STUDY FOR 0.5-FT² BREAK -
BREAK AND TOTAL ECCS FLOWS.

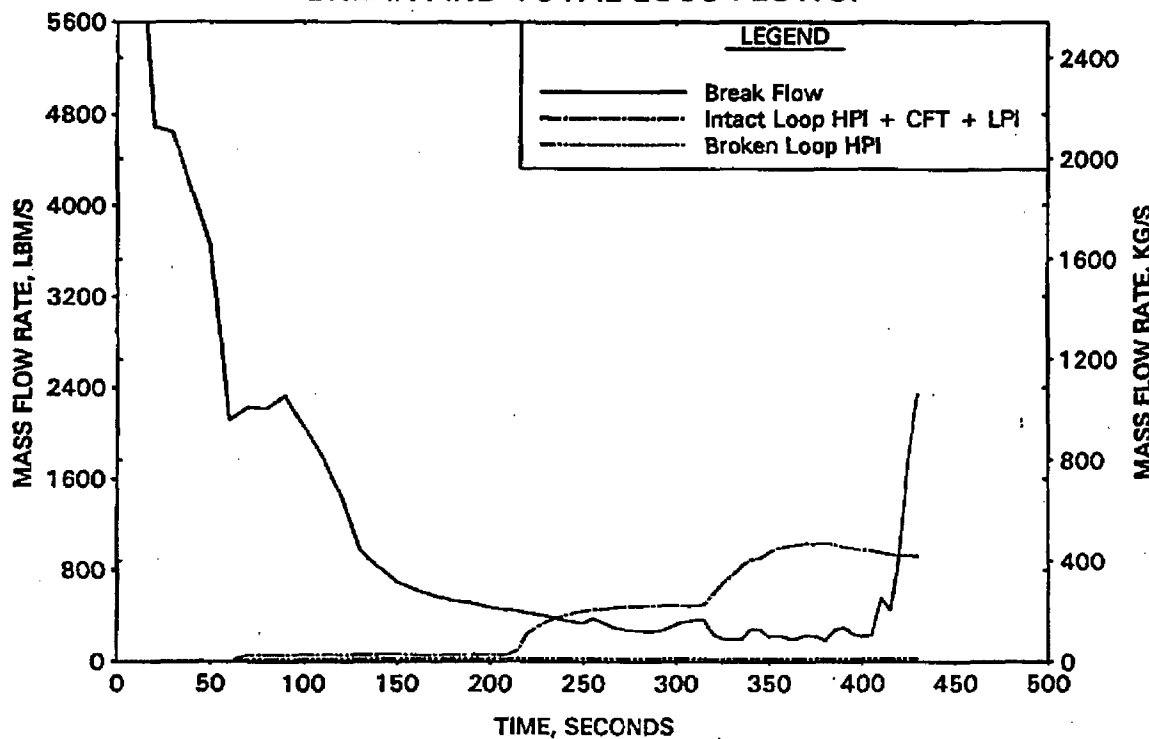


FIGURE A-152. CLPD BREAK SPECTRUM STUDY FOR 0.5-FT² BREAK -
BREAK VOLUME VOID FRACTION.

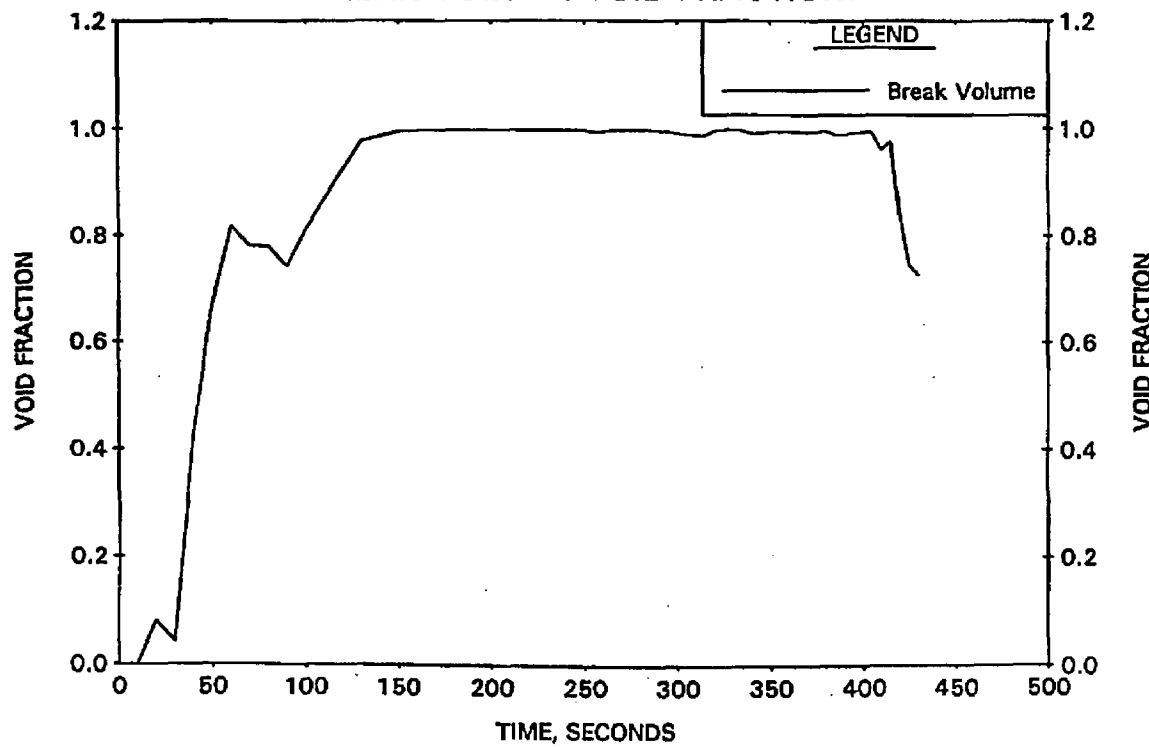


FIGURE A-153. CLPD BREAK SPECTRUM STUDY FOR 0.5-FT² BREAK - BROKEN LOOP COLLAPSED LEVELS.

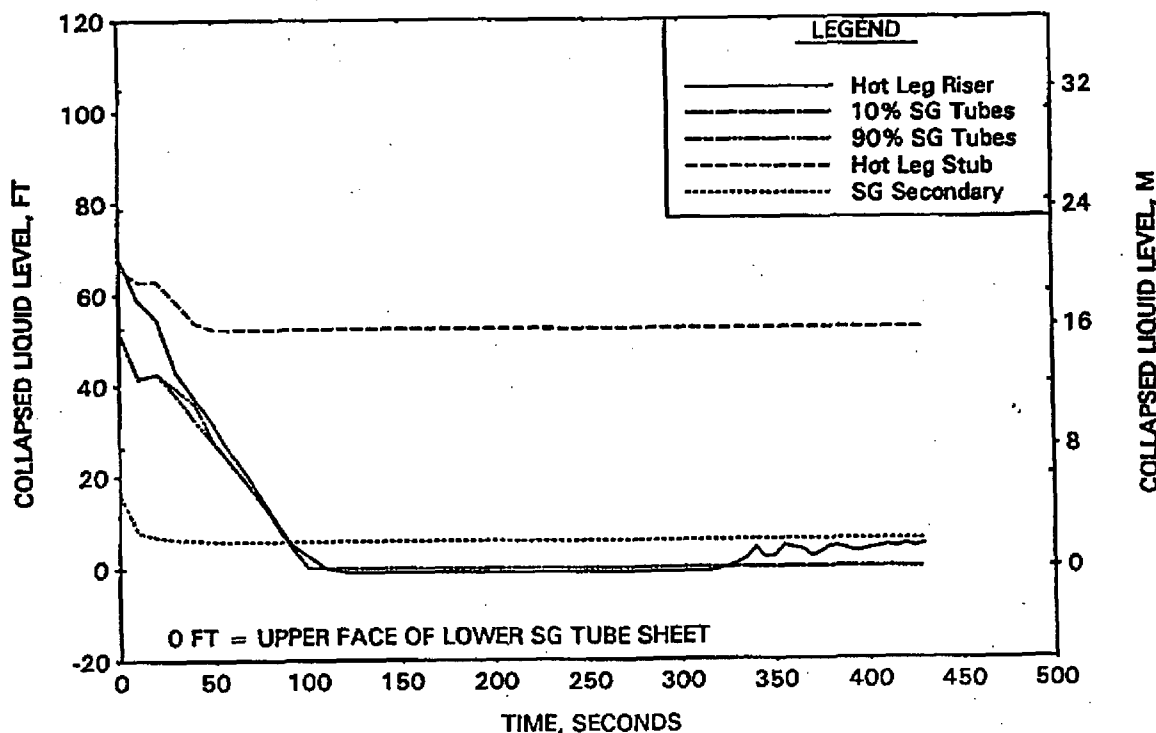


FIGURE A-154. CLPD BREAK SPECTRUM STUDY FOR 0.5-FT² BREAK - INTACT LOOP COLLAPSED LEVELS.

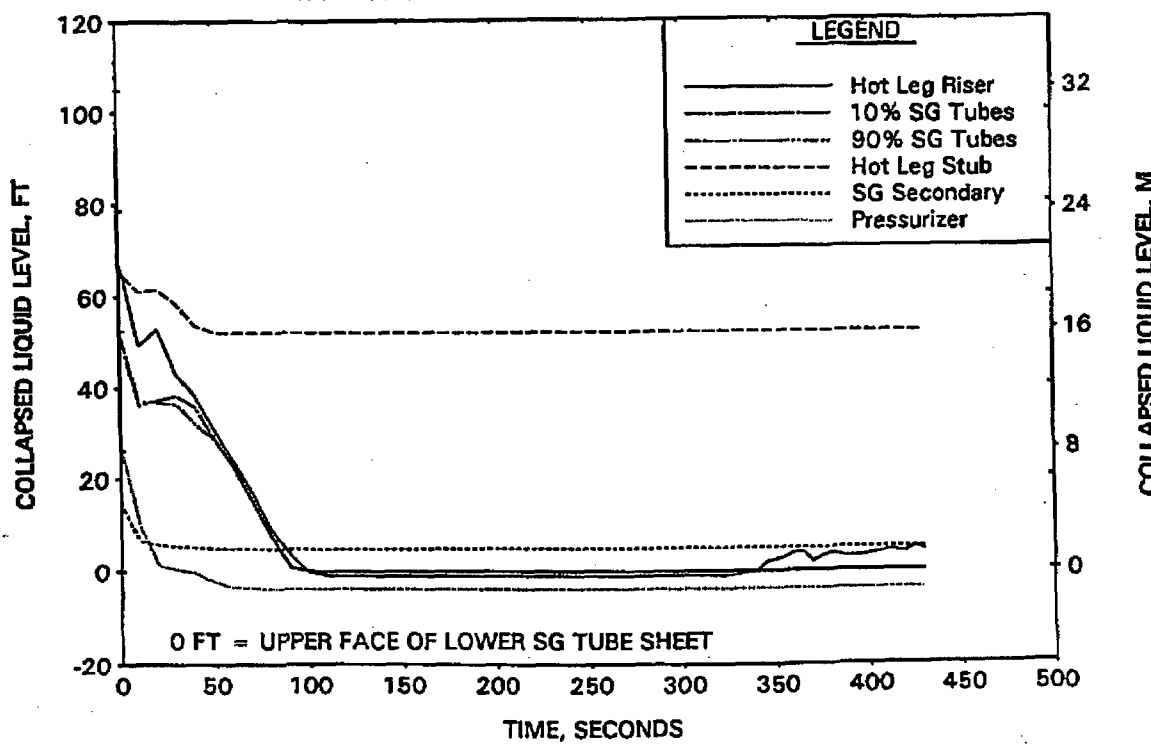


FIGURE A-155. CLPD BREAK SPECTRUM STUDY FOR 0.5-FT² BREAK - CLPD COLLAPSED LEVELS.

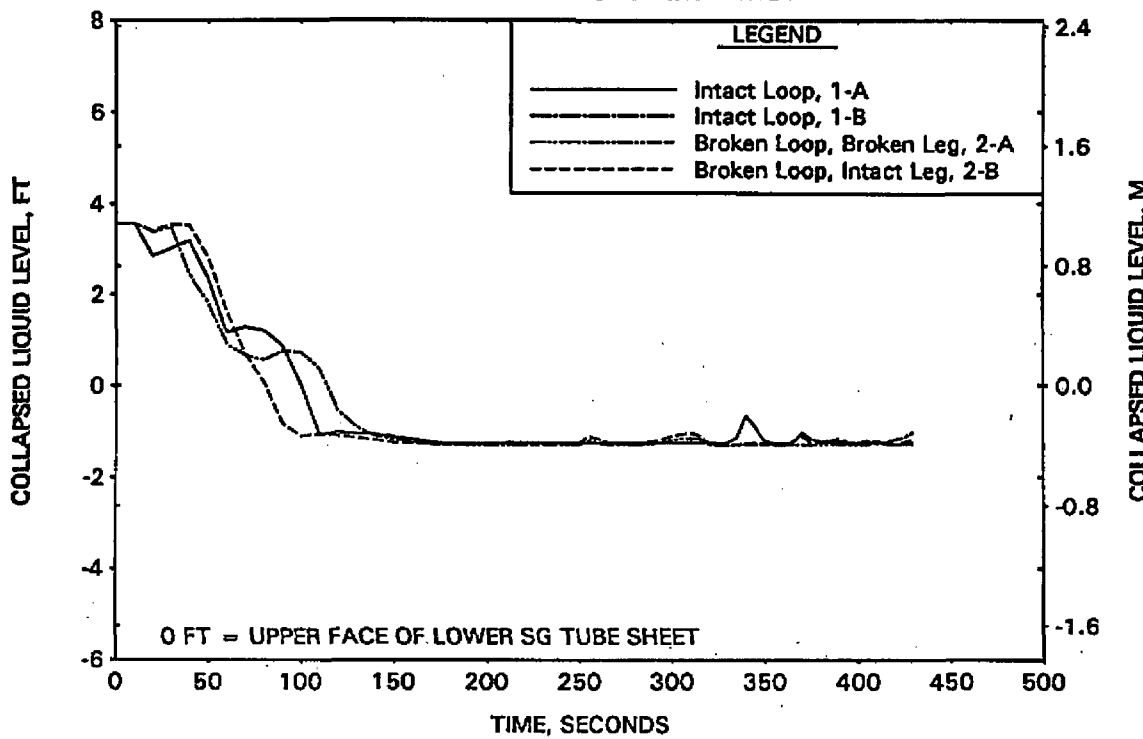


FIGURE A-156. CLPD BREAK SPECTRUM STUDY FOR 0.5-FT² BREAK - CLPS LIQUID VOLUME.

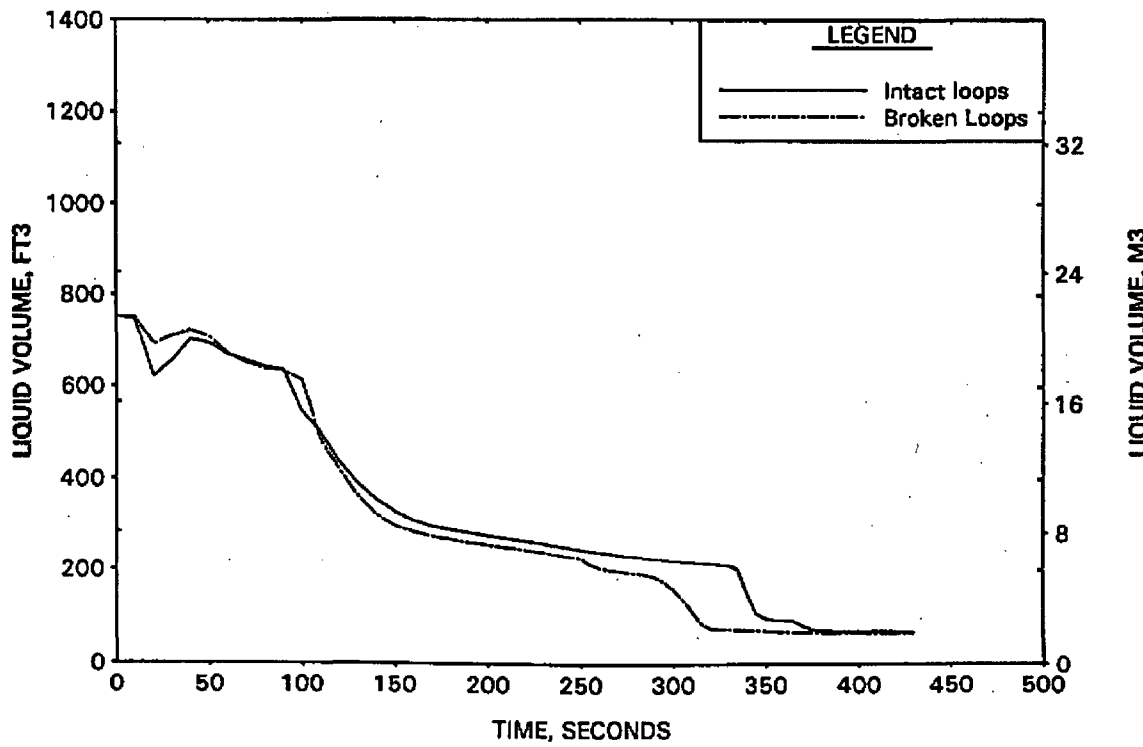


FIGURE A-157. CLPD BREAK SPECTRUM STUDY FOR 0.5-FT² BREAK - HOT LEG AND RVVV FLOWS.

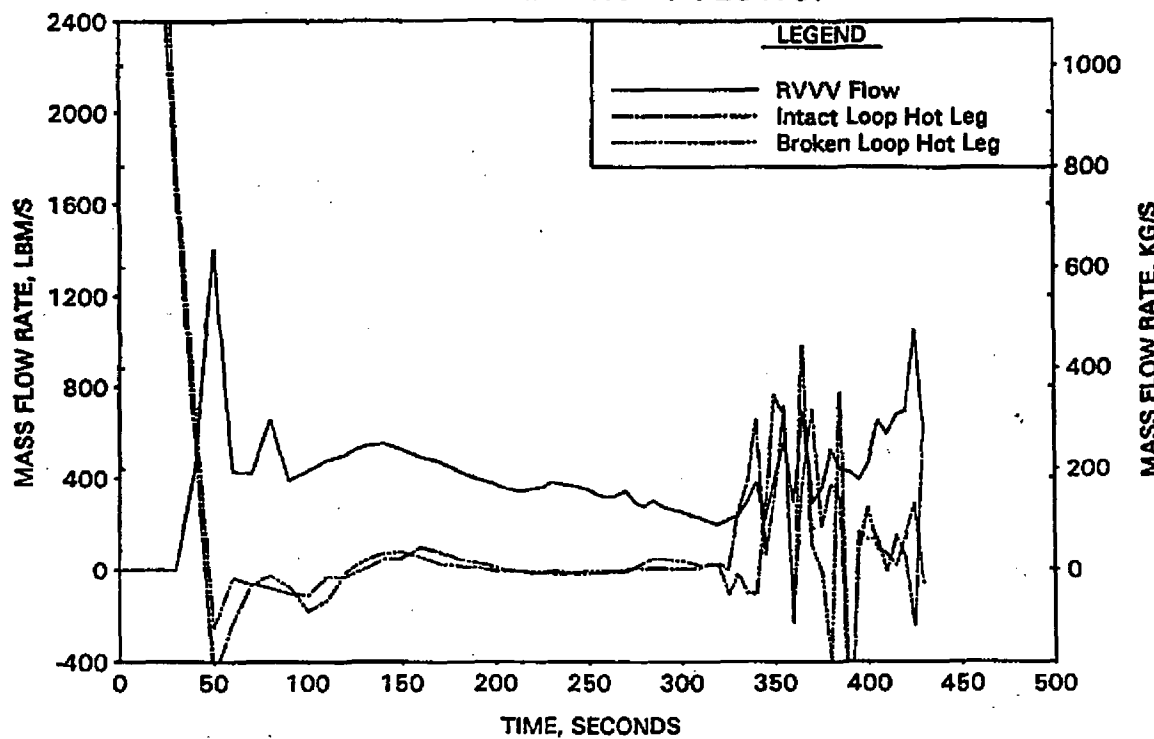


FIGURE A-158. CLPD BREAK SPECTRUM STUDY FOR 0.5-FT² BREAK - CORE MIXTURE LEVELS.

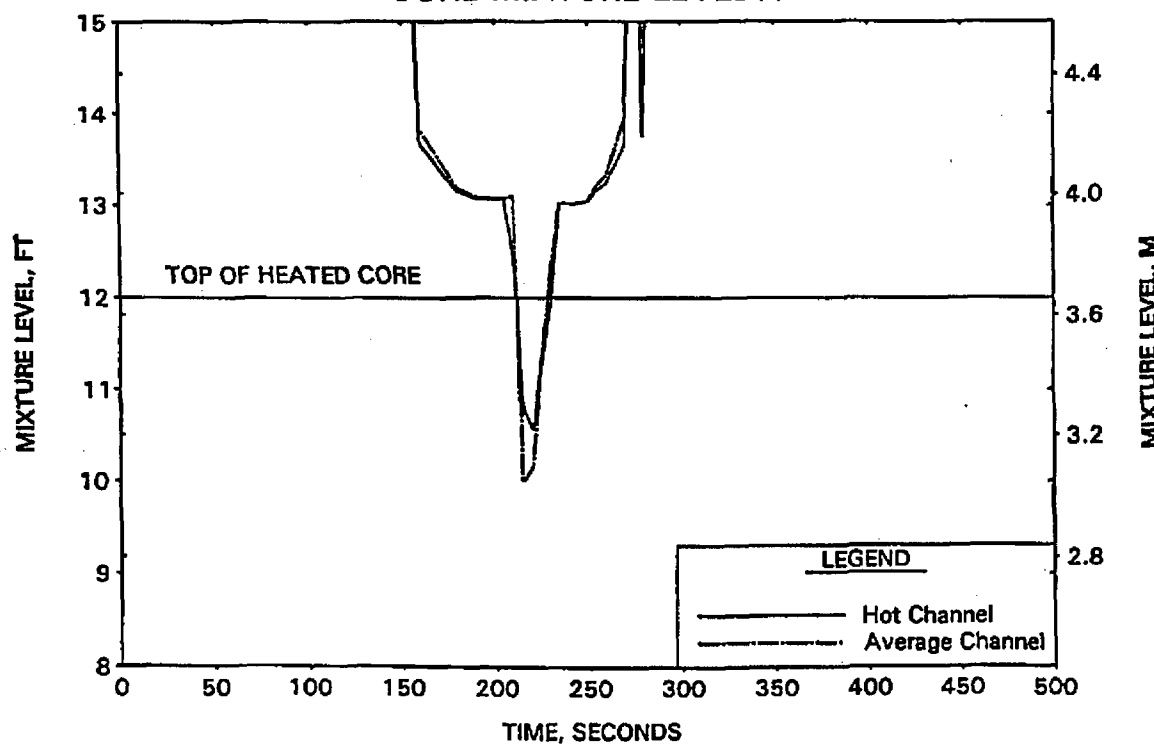


FIGURE A-159. CLPD BREAK SPECTRUM STUDY FOR 0.5-FT2 BREAK - HOT CHANNEL CLAD TEMPERATURES.

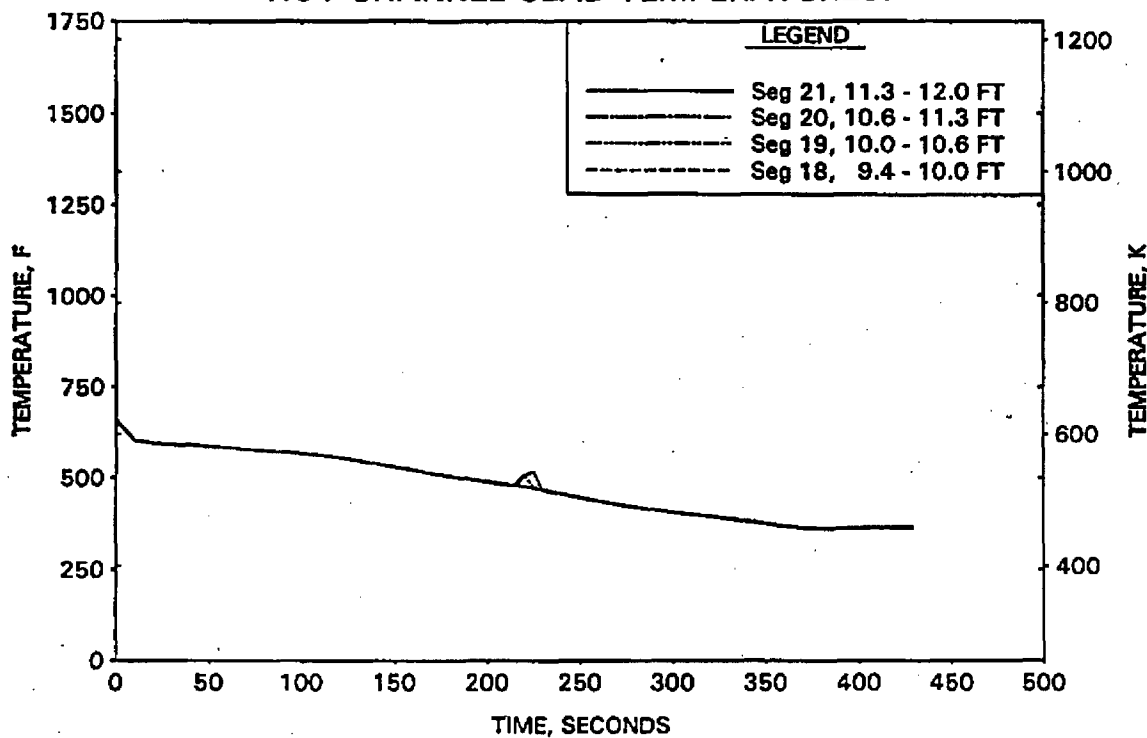


FIGURE A-160. CLPD BREAK SPECTRUM STUDY FOR 0.5-FT2 BREAK - HOT CHANNEL STEAM TEMPERATURES.

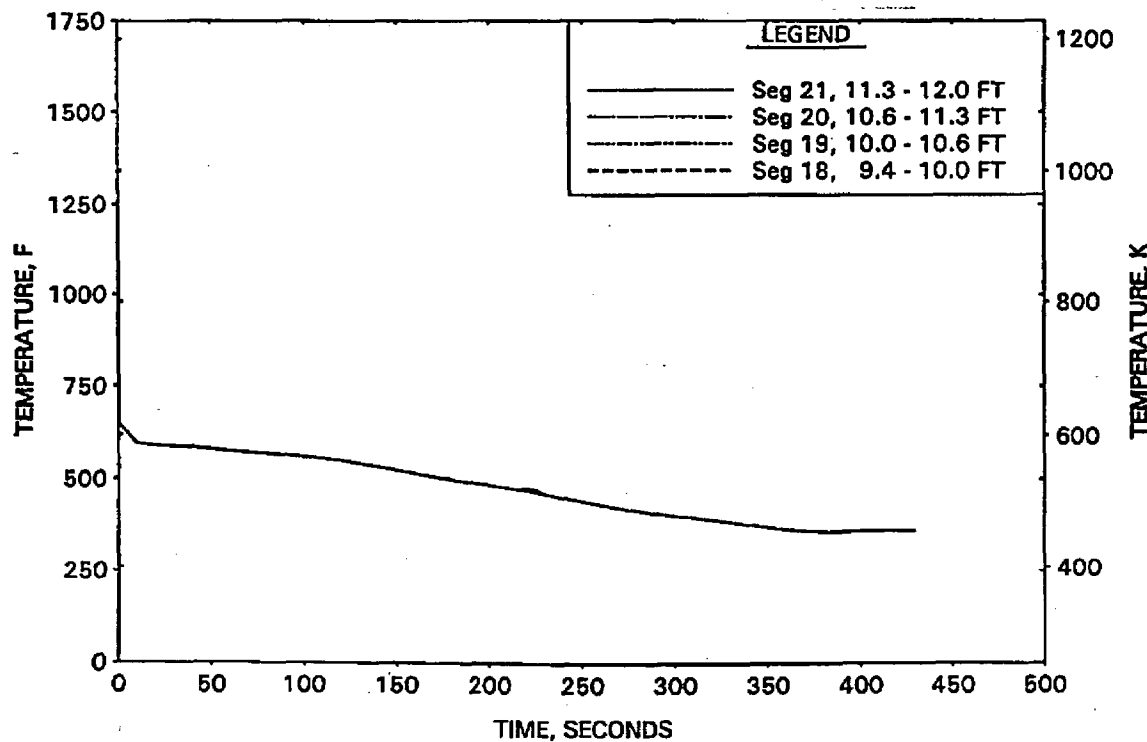


FIGURE A-161. CLPD BREAK SPECTRUM STUDY FOR 0.5-FT² BREAK -
UPPER ELEVATION AVE CHANNEL CLAD TEMPERATURES.

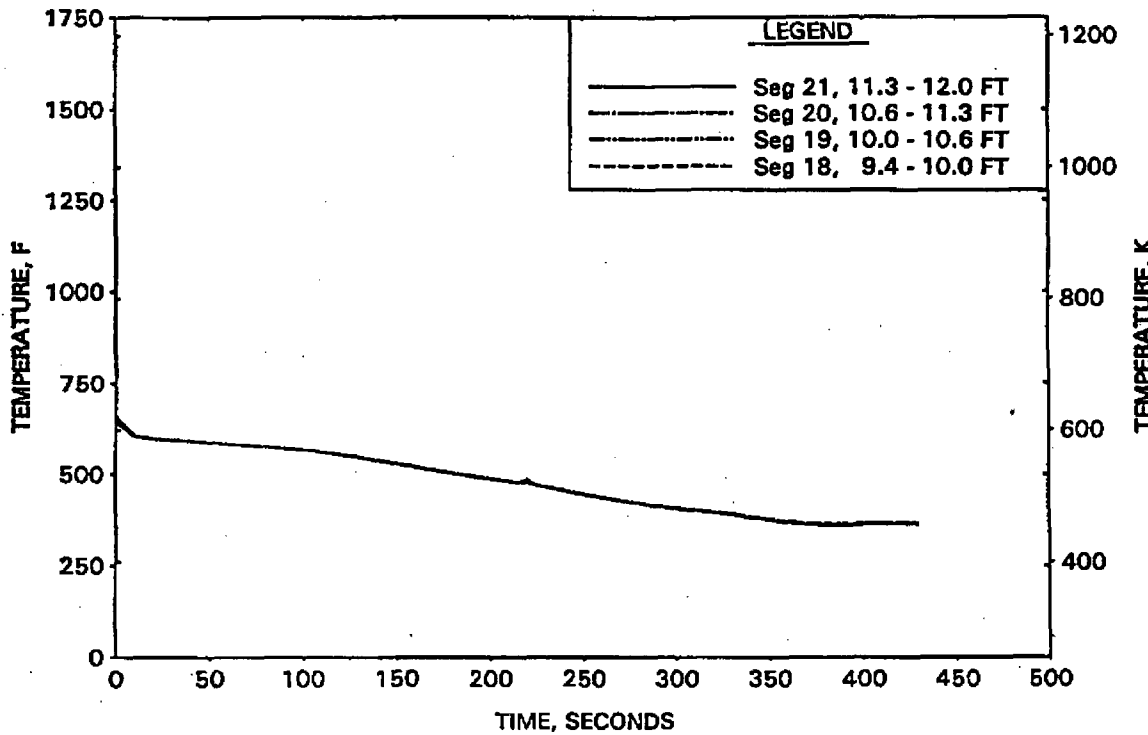


FIGURE A-162. CLPD BREAK SPECTRUM STUDY FOR 0.5-FT² BREAK -
UPPER ELEVATION AVE CHANNEL STEAM TEMPERATURES.

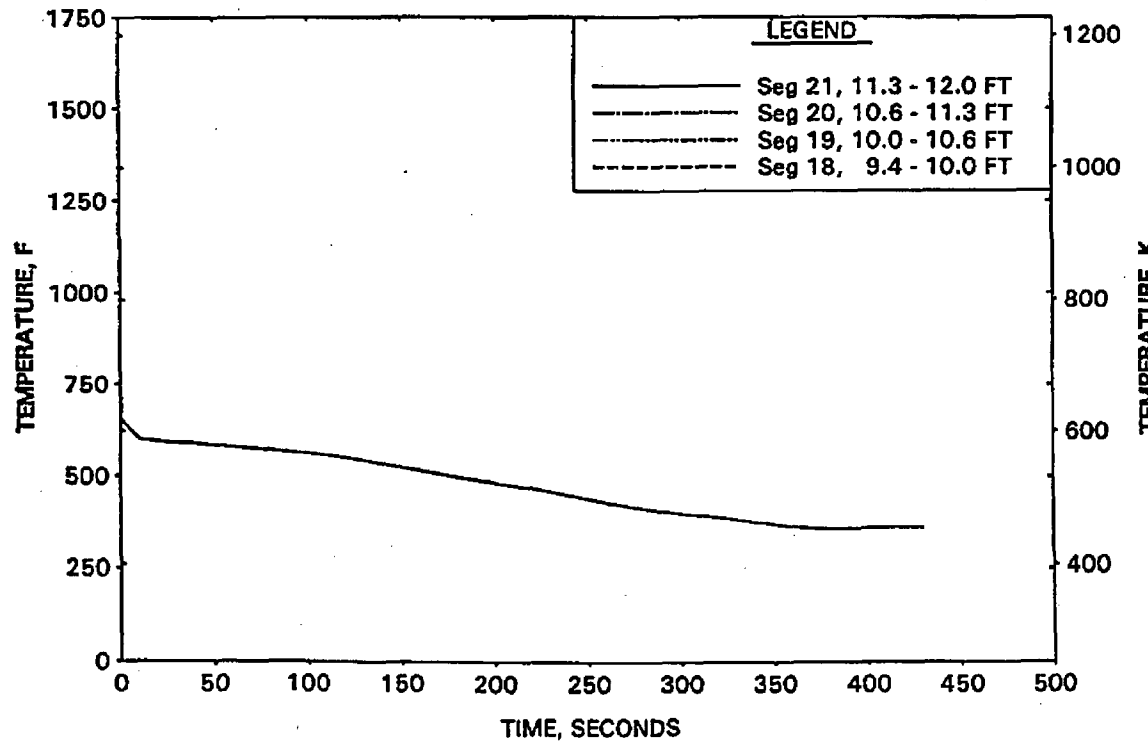


FIGURE A-163. CLPD BREAK SPECTRUM STUDY FOR 0.75-FT² BREAK - RCS PRESSURES.

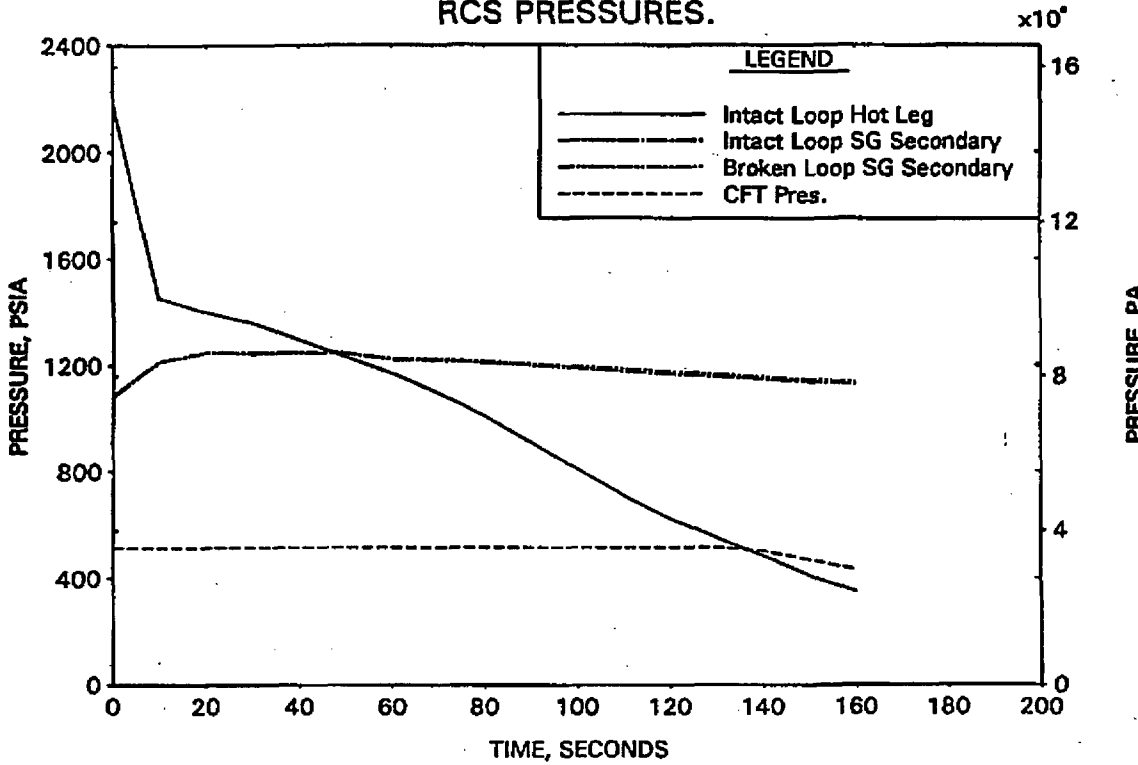


FIGURE A-164. CLPD BREAK SPECTRUM STUDY FOR 0.75-FT² BREAK - DC, RV, AND CORE COLLAPSED LEVELS.

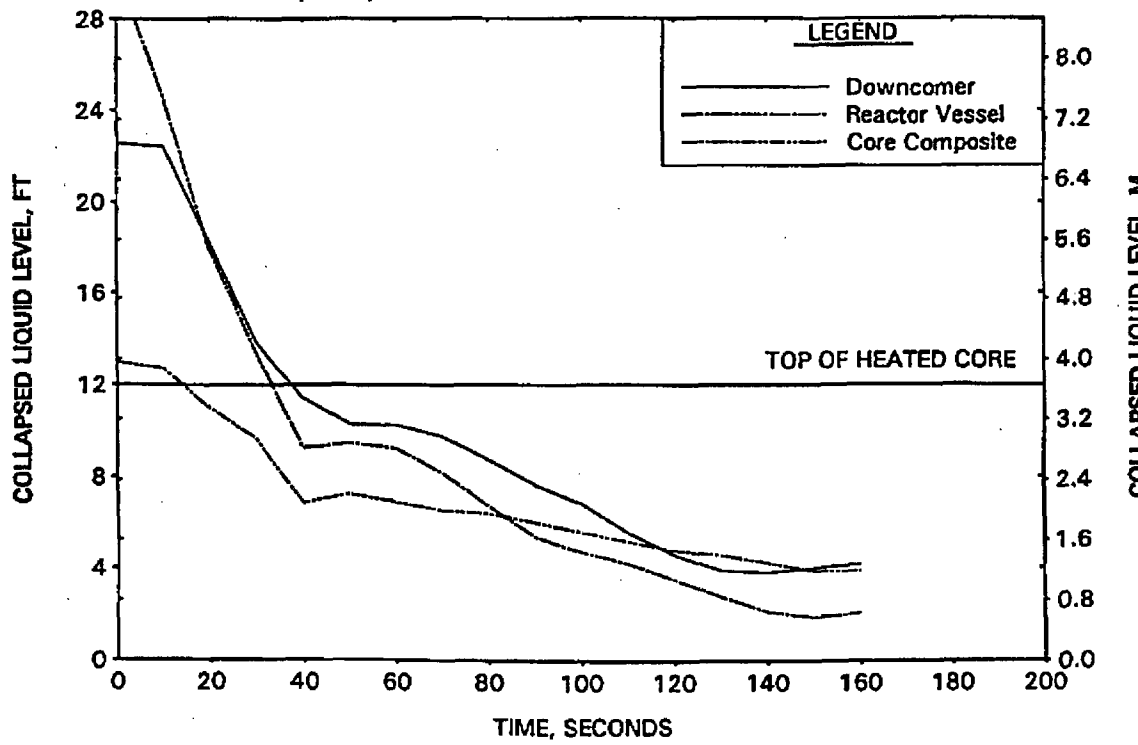


FIGURE A-165. CLPD BREAK SPECTRUM STUDY FOR 0.75-FT² BREAK - BREAK AND TOTAL ECCS FLOWS.

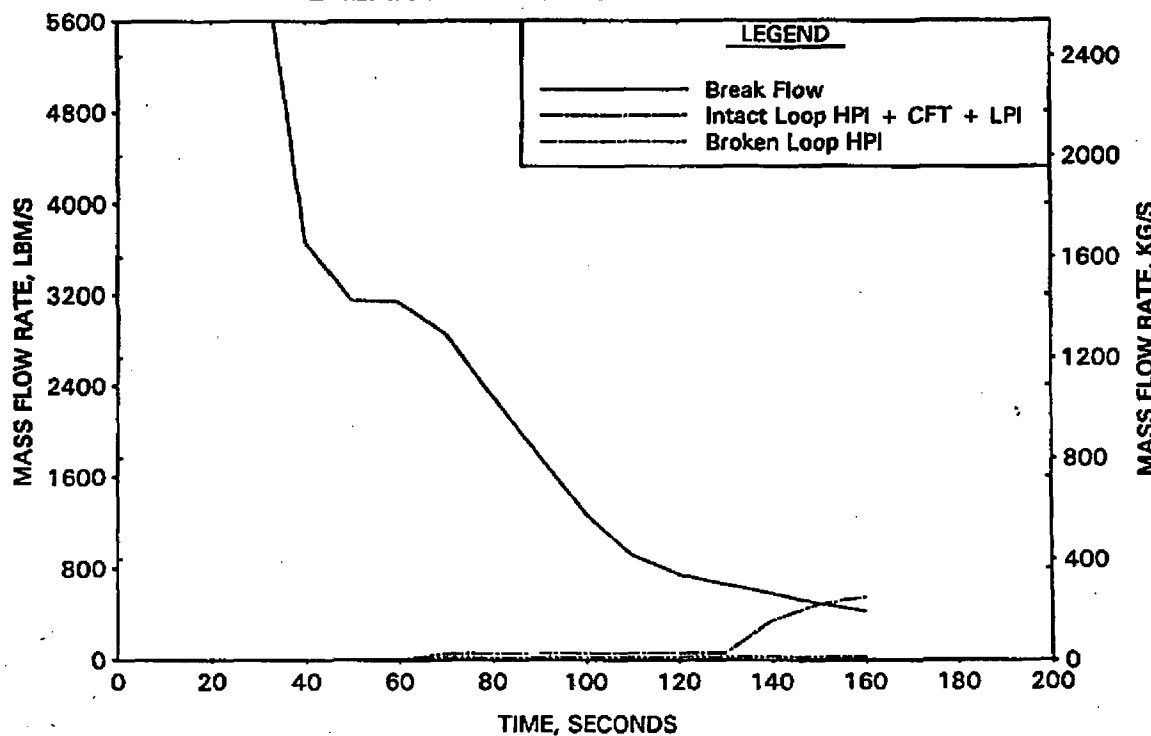


FIGURE A-166. CLPD BREAK SPECTRUM STUDY FOR 0.75-FT² BREAK - BREAK VOLUME VOID FRACTION.

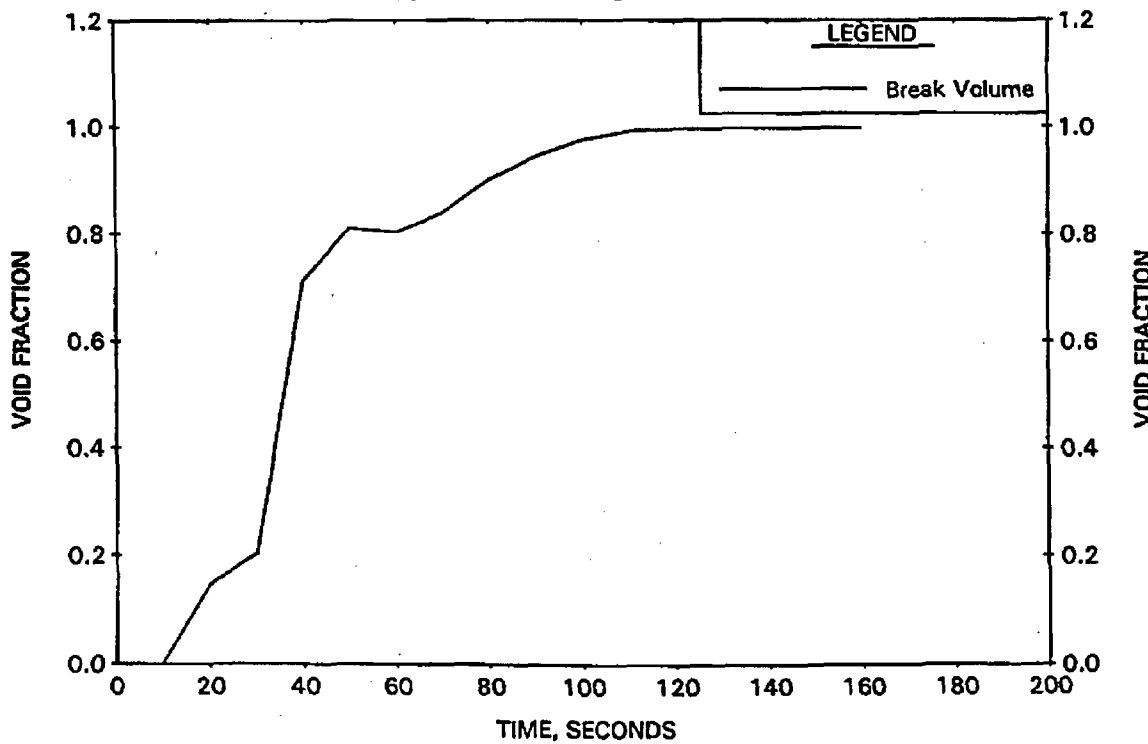


FIGURE A-167. CLPD BREAK SPECTRUM STUDY FOR 0.75-FT² BREAK - BROKEN LOOP COLLAPSED LEVELS.

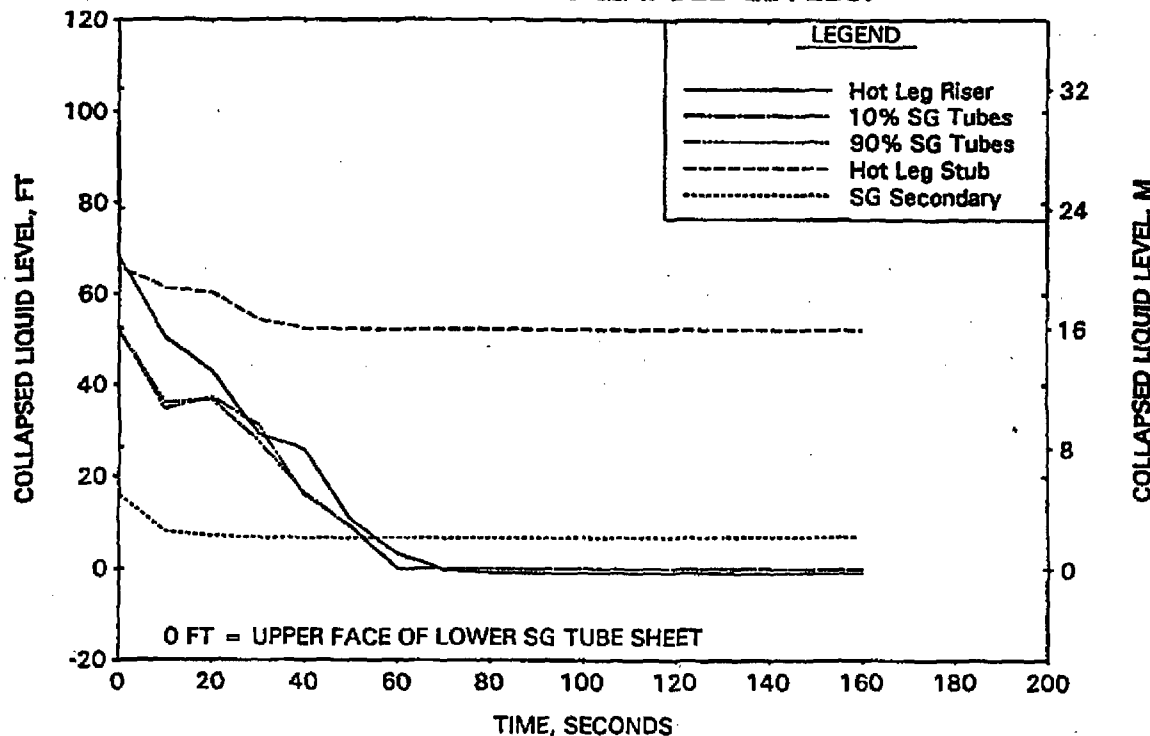


FIGURE A-168. CLPD BREAK SPECTRUM STUDY FOR 0.75-FT² BREAK - INTACT LOOP COLLAPSED LEVELS.

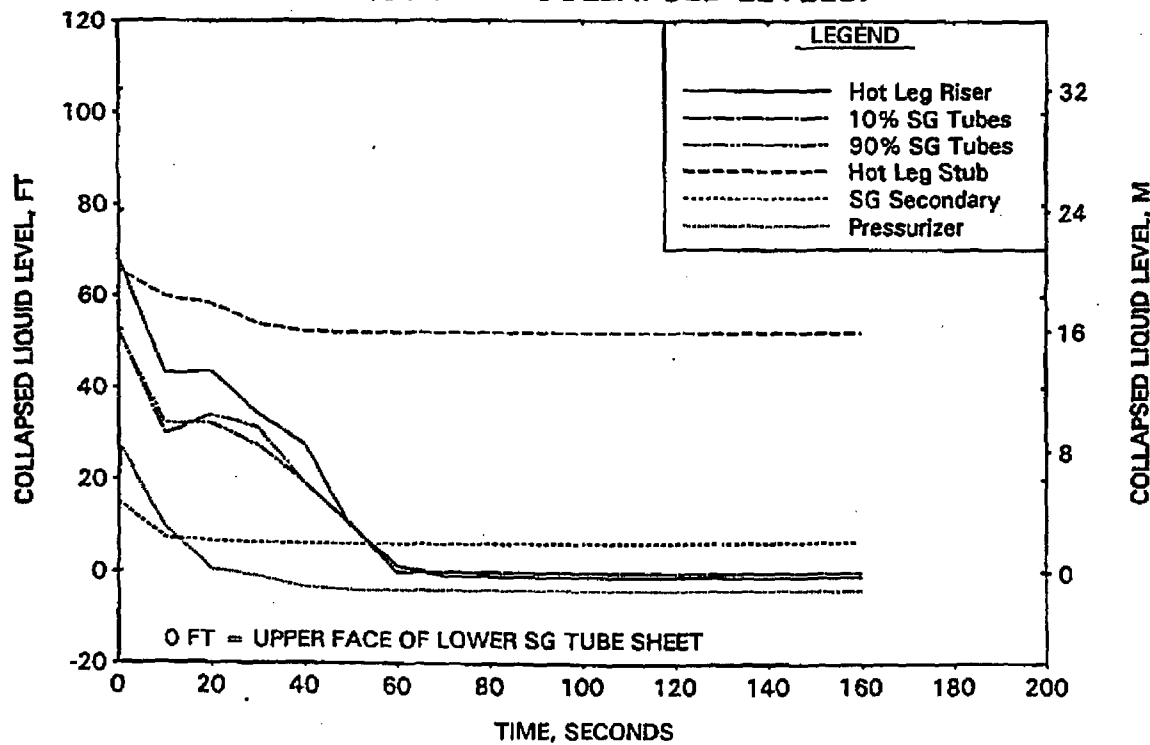


FIGURE A-169. CLPD BREAK SPECTRUM STUDY FOR 0.75-FT² BREAK - CLPD COLLAPSED LEVELS.

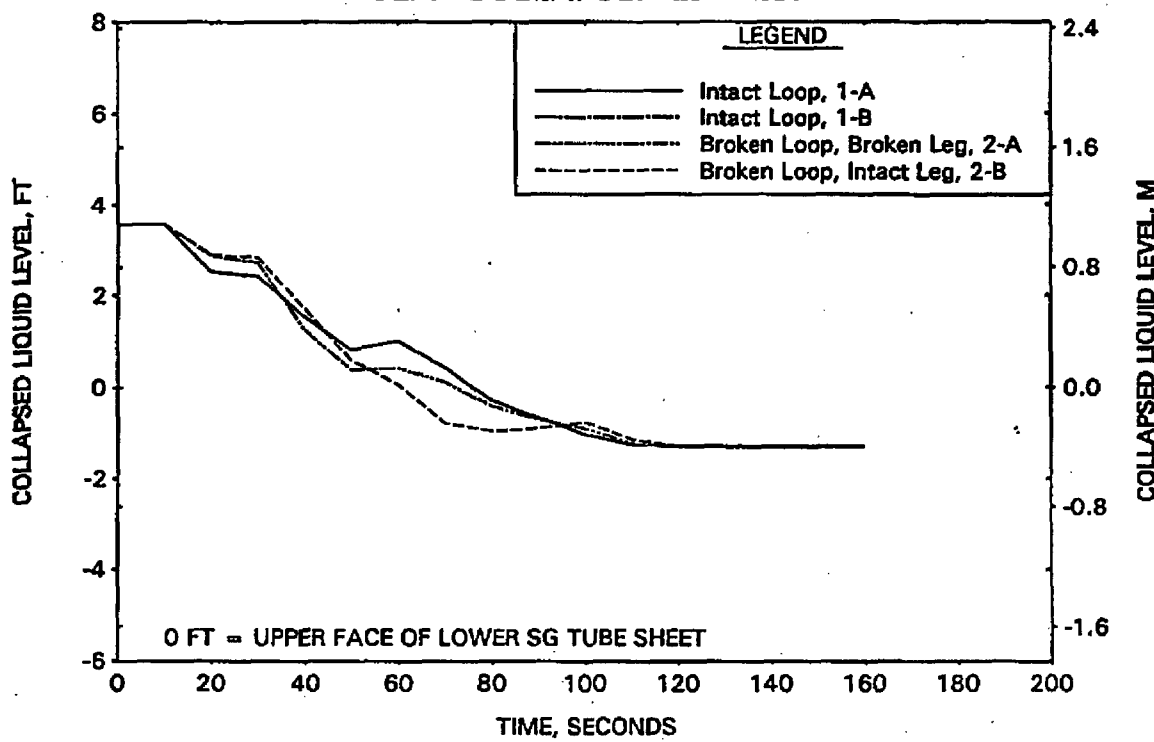


FIGURE A-170. CLPD BREAK SPECTRUM STUDY FOR 0.75-FT² BREAK - CLPS LIQUID VOLUME.

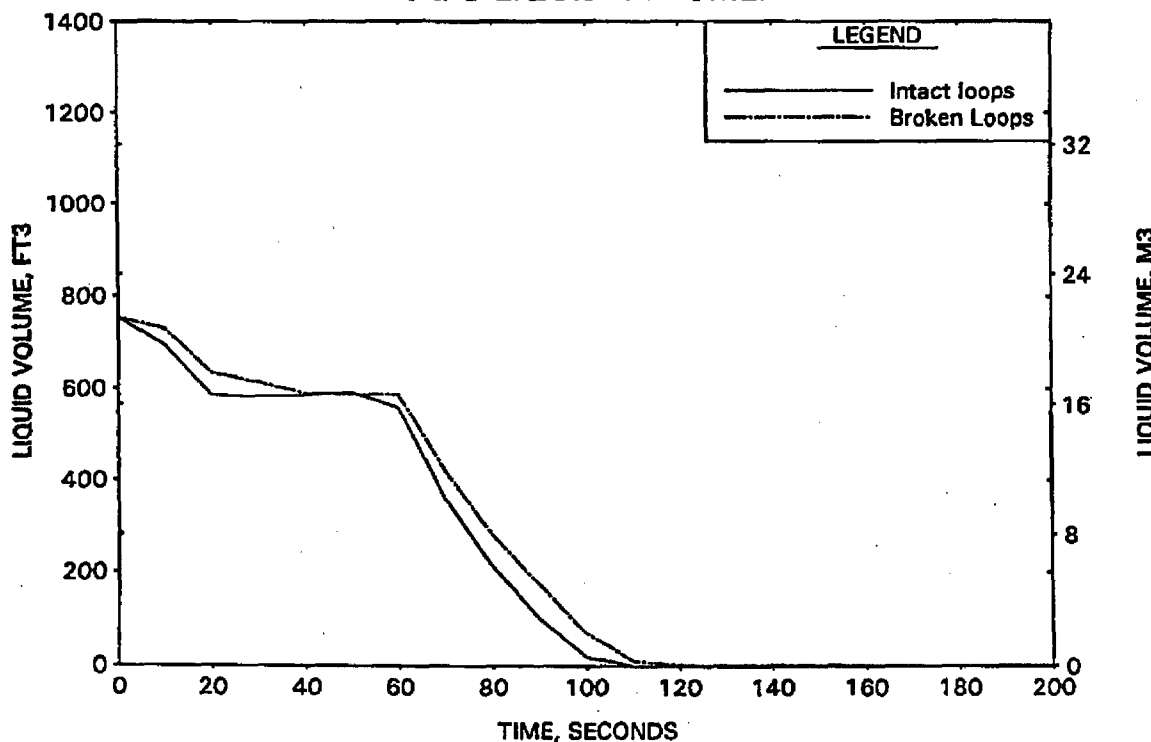


FIGURE A-171. CLPD BREAK SPECTRUM STUDY FOR 0.75-FT² BREAK - HOT LEG AND RVVV FLOWS.

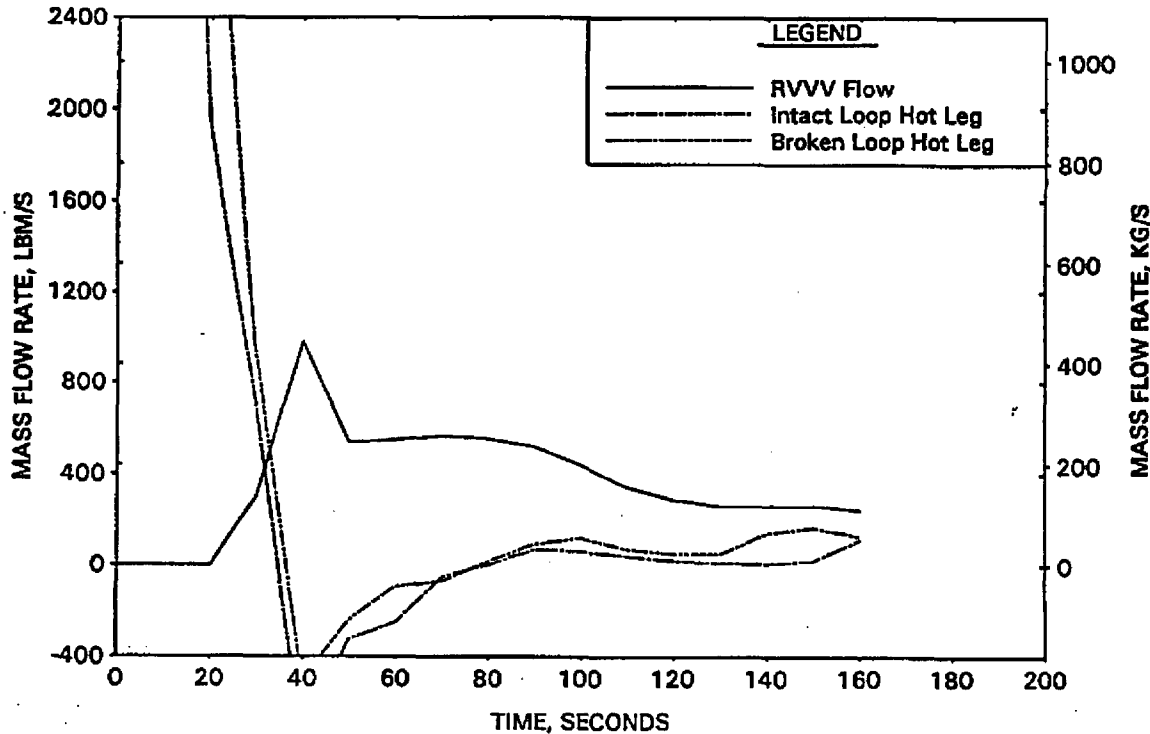


FIGURE A-172. CLPD BREAK SPECTRUM STUDY FOR 0.75-FT² BREAK - CORE MIXTURE LEVELS.

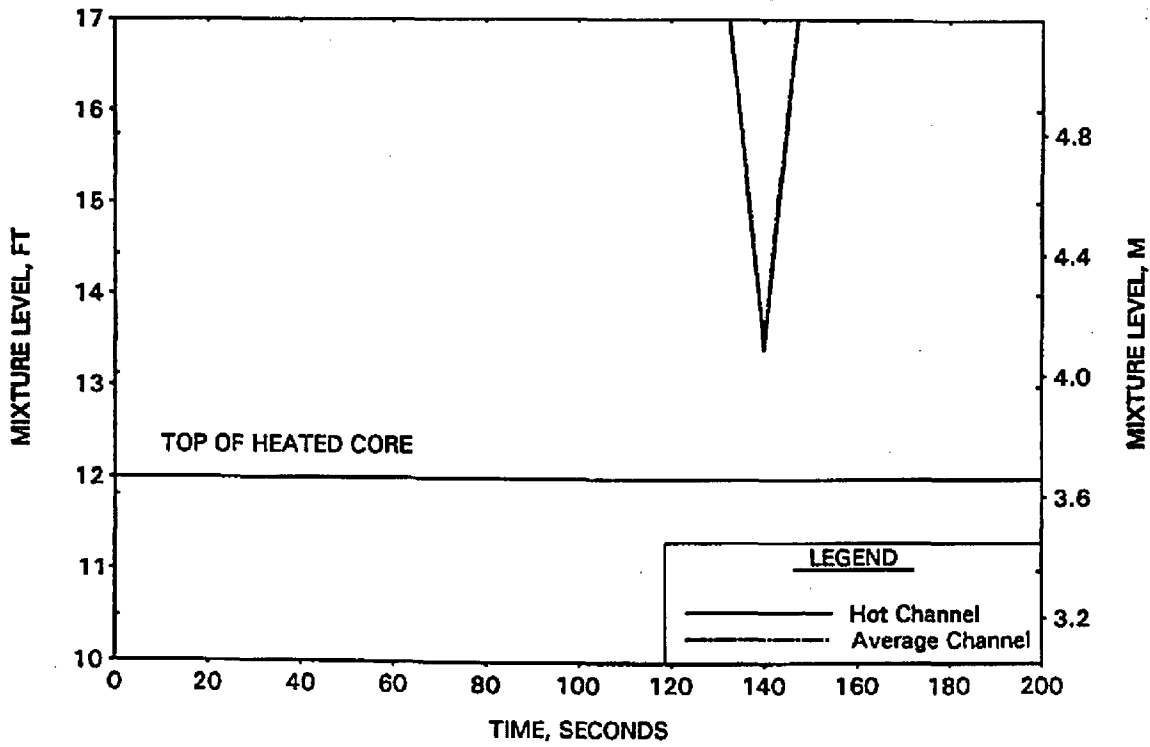


FIGURE A-173. CLPD BREAK SPECTRUM STUDY FOR 0.75-FT2 BREAK - HOT CHANNEL CLAD TEMPERATURES.

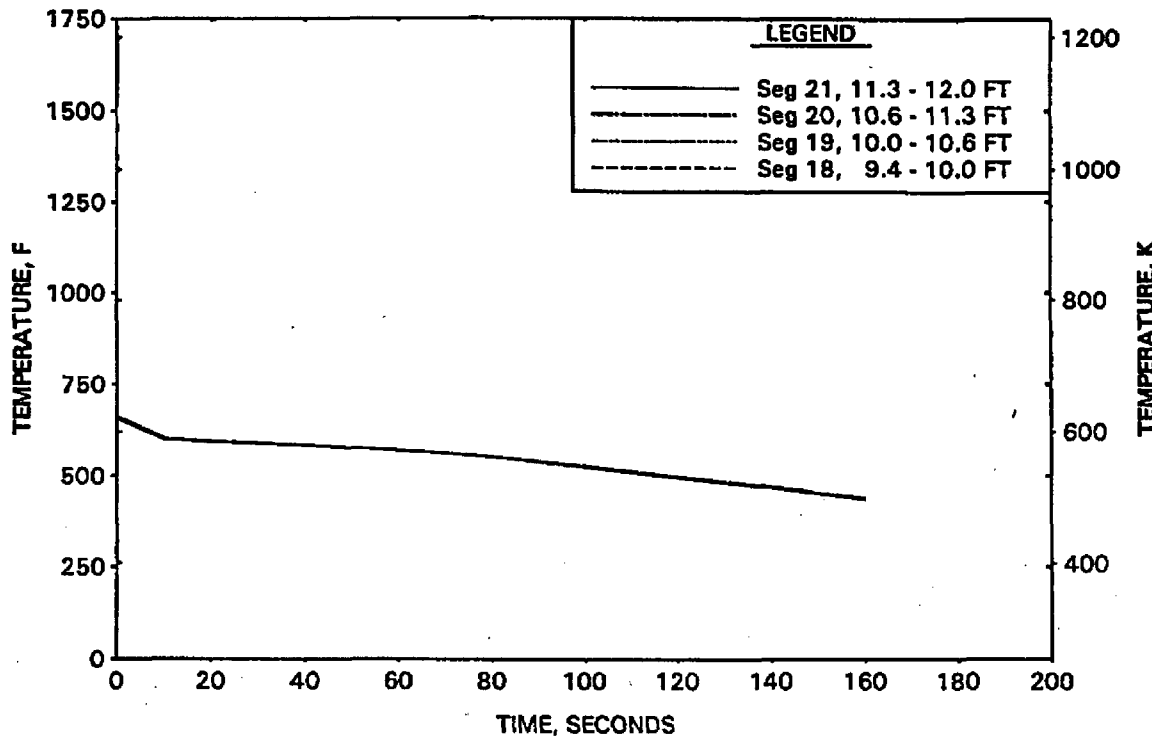


FIGURE A-174. CLPD BREAK SPECTRUM STUDY FOR 0.75-FT2 BREAK - HOT CHANNEL STEAM TEMPERATURES.

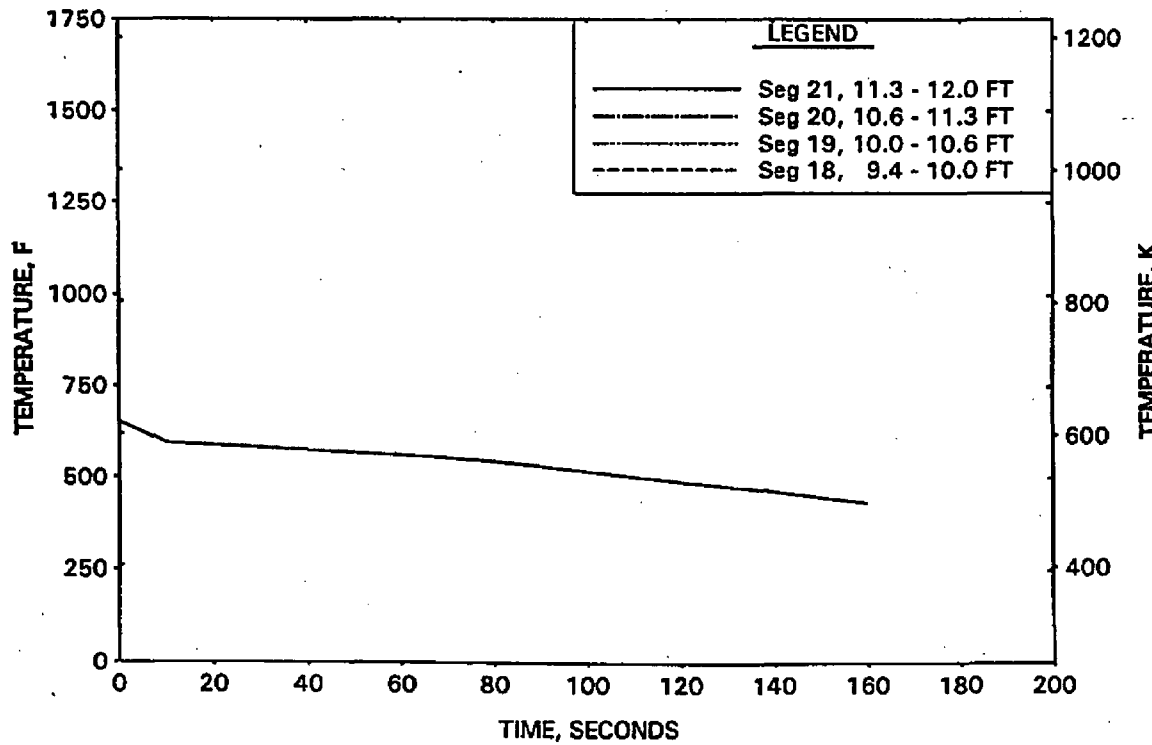


FIGURE A-175. CLPD BREAK SPECTRUM STUDY FOR 0.75-FT2 BREAK -
UPPER ELEVATION AVE CHANNEL CLAD TEMPERATURES.

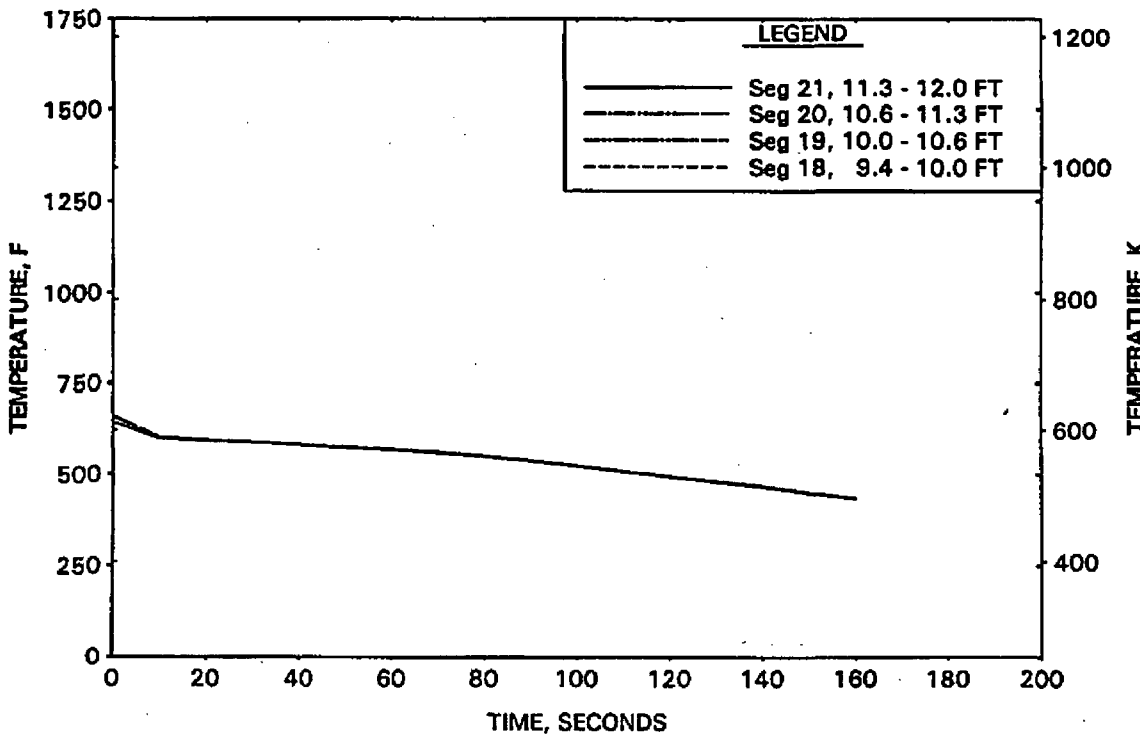


FIGURE A-176. CLPD BREAK SPECTRUM STUDY FOR 0.75-FT2 BREAK -
UPPER ELEVATION AVE CHANNEL STEAM TEMPERATURES.

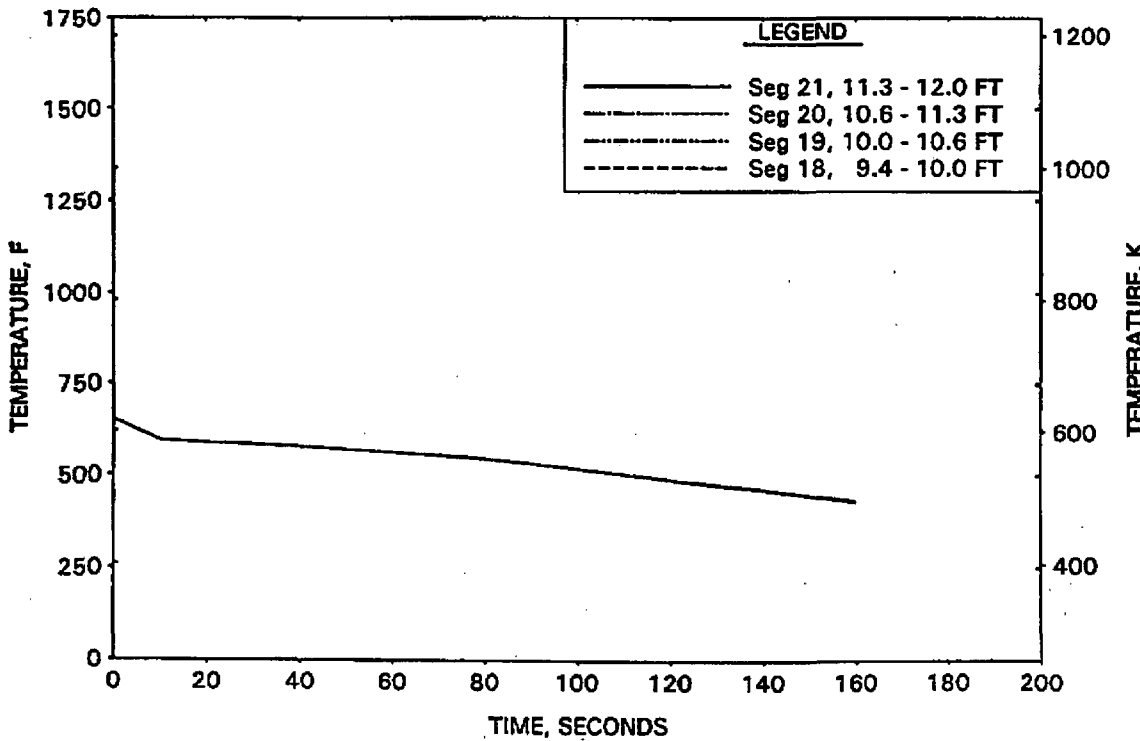


FIGURE A-177. CLPD BREAK SPECTRUM STUDY FOR 1.0-FT² BREAK - RCS PRESSURES.

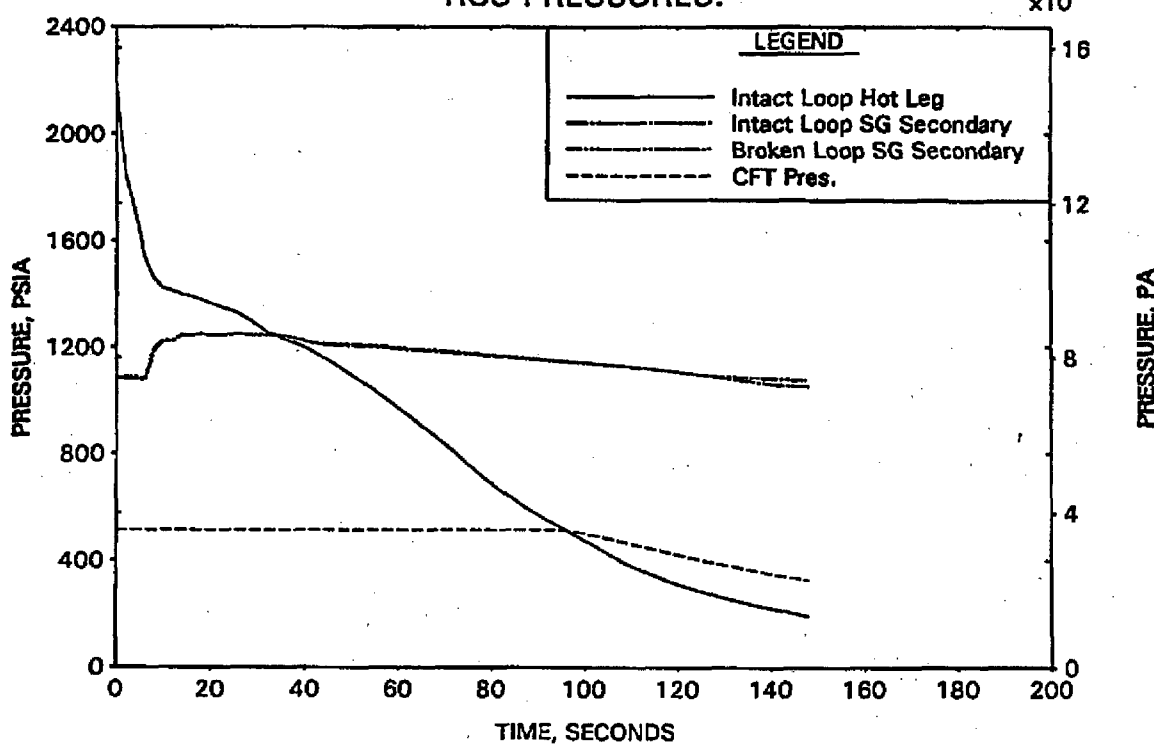


FIGURE A-178. CLPD BREAK SPECTRUM STUDY FOR 1.0-FT² BREAK - DC, RV, AND CORE COLLAPSED LEVELS.

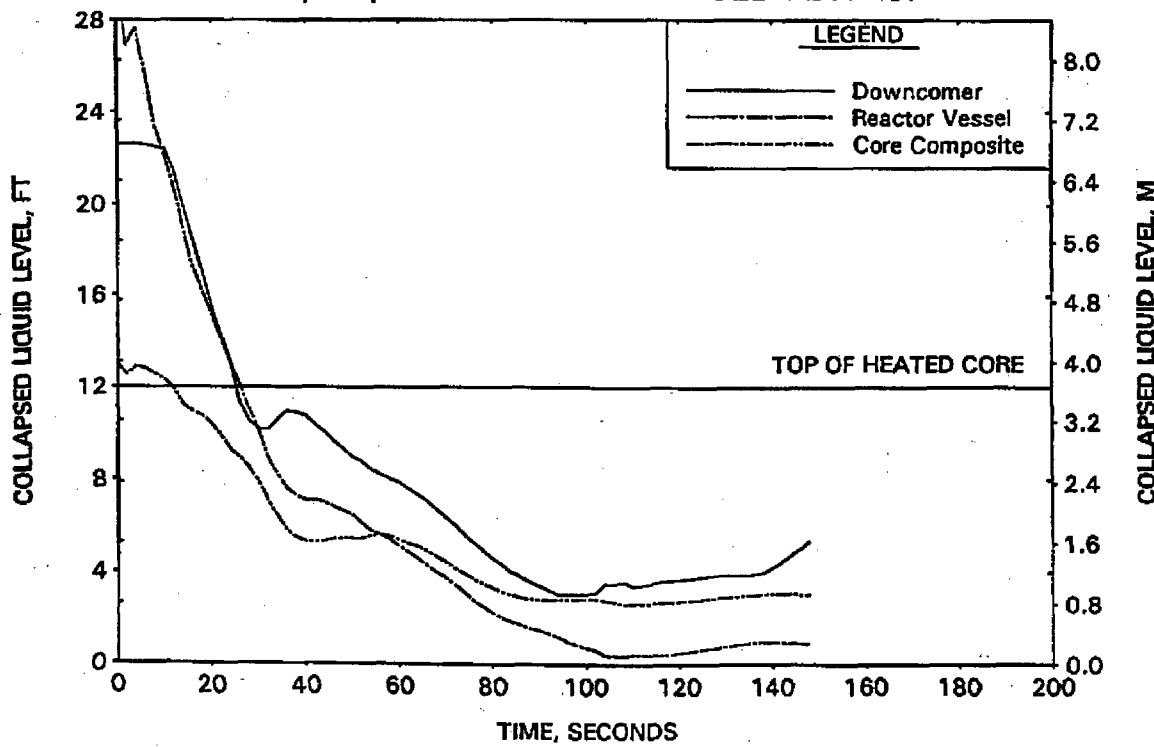


FIGURE A-179. CLPD BREAK SPECTRUM STUDY FOR 1.0-FT² BREAK -
BREAK AND TOTAL ECCS FLOWS.

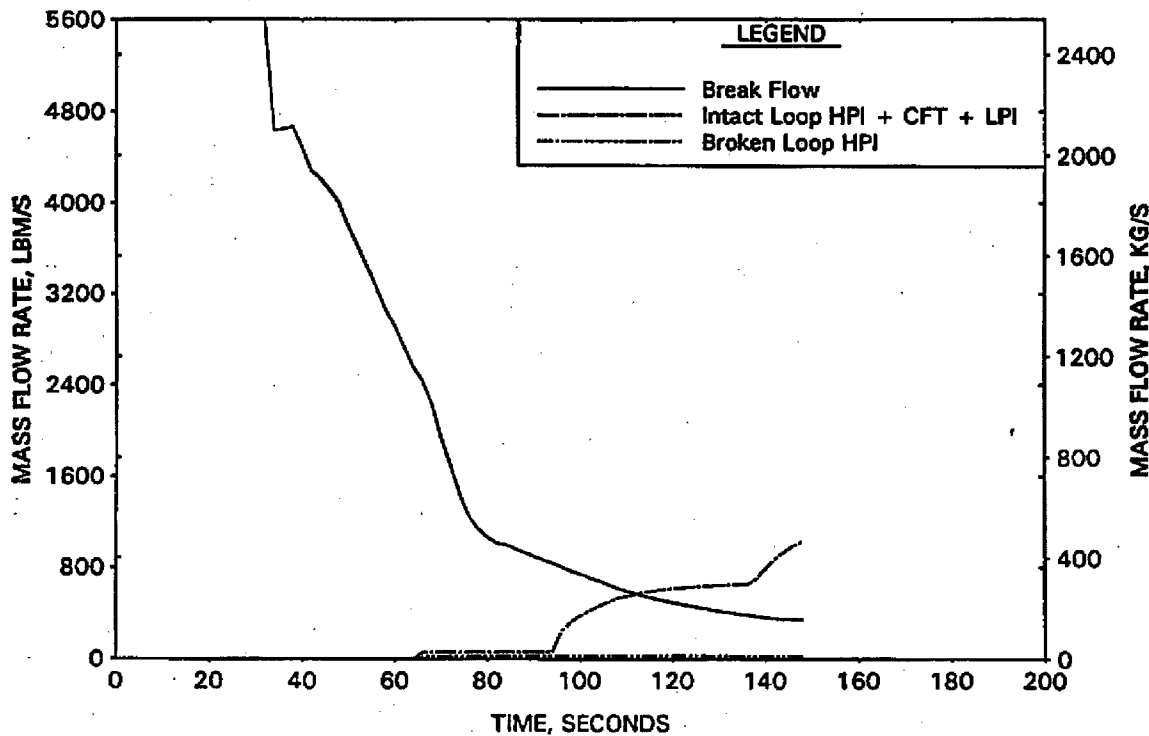


FIGURE A-180. CLPD BREAK SPECTRUM STUDY FOR 1.0-FT² BREAK -
BREAK VOLUME VOID FRACTION.

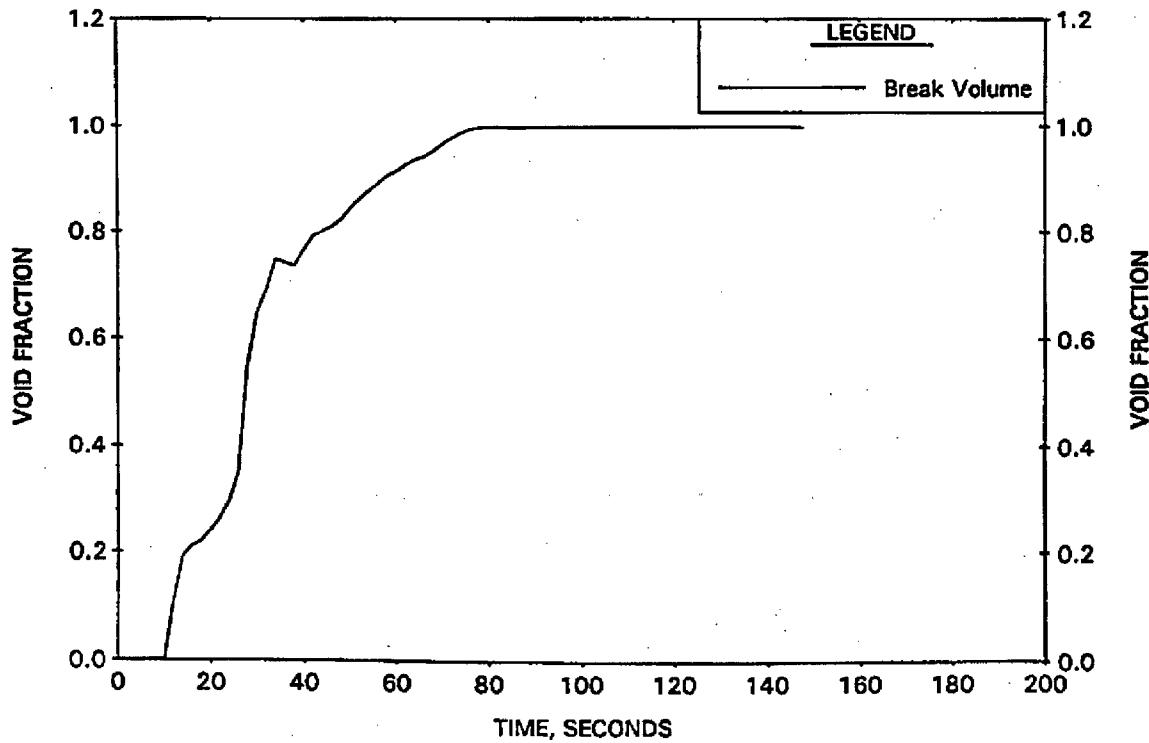


FIGURE A-181. CLPD BREAK SPECTRUM STUDY FOR 1.0-FT² BREAK - BROKEN LOOP COLLAPSED LEVELS.

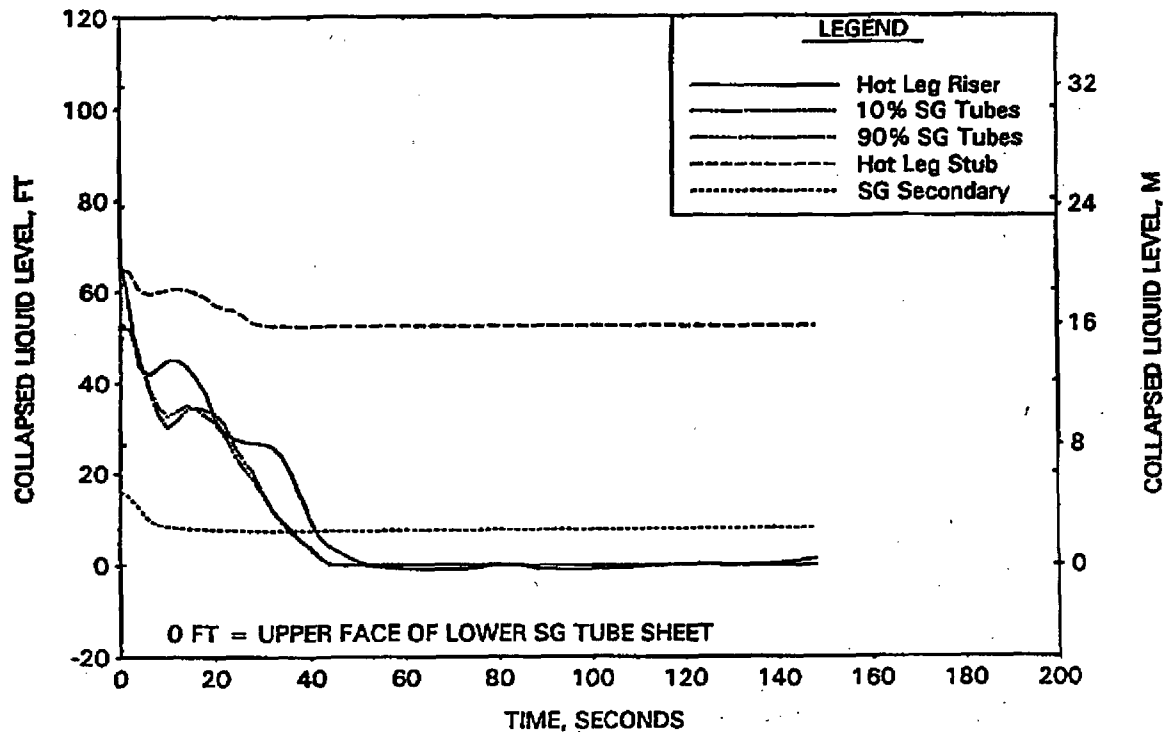


FIGURE A-182. CLPD BREAK SPECTRUM STUDY FOR 1.0-FT² BREAK - INTACT LOOP COLLAPSED LEVELS.

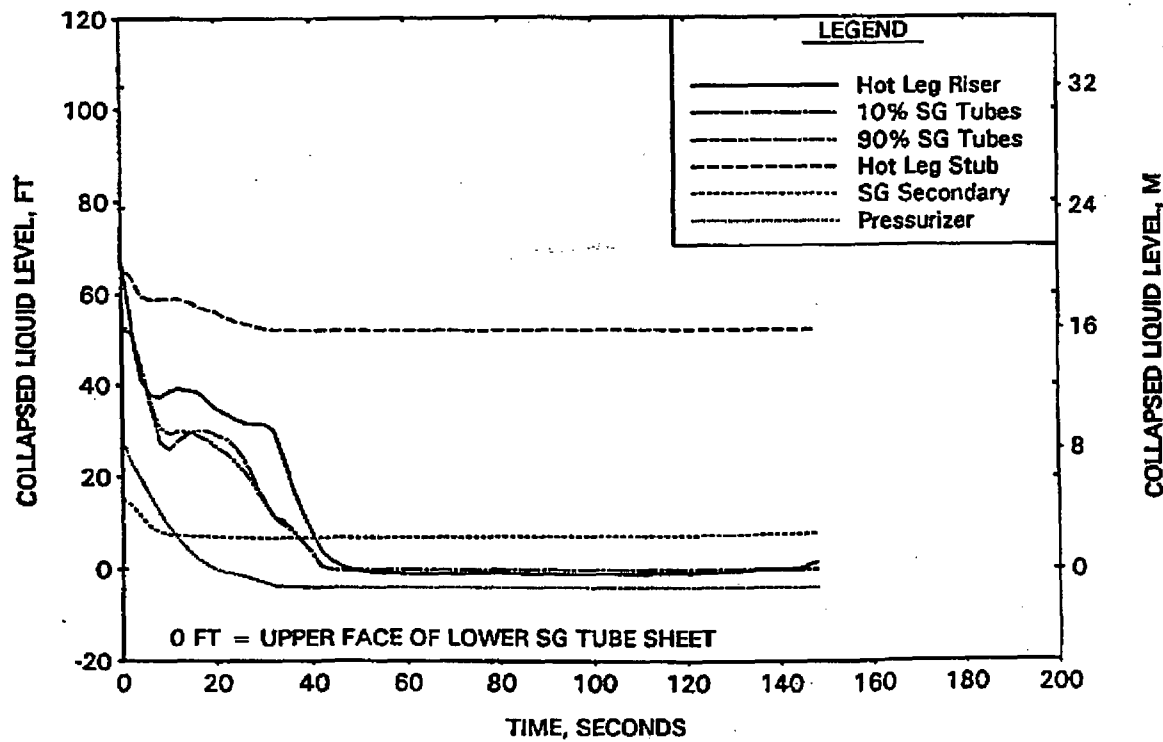


FIGURE A-183. CLPD BREAK SPECTRUM STUDY FOR 1.0-FT² BREAK - CLPD COLLAPSED LEVELS.

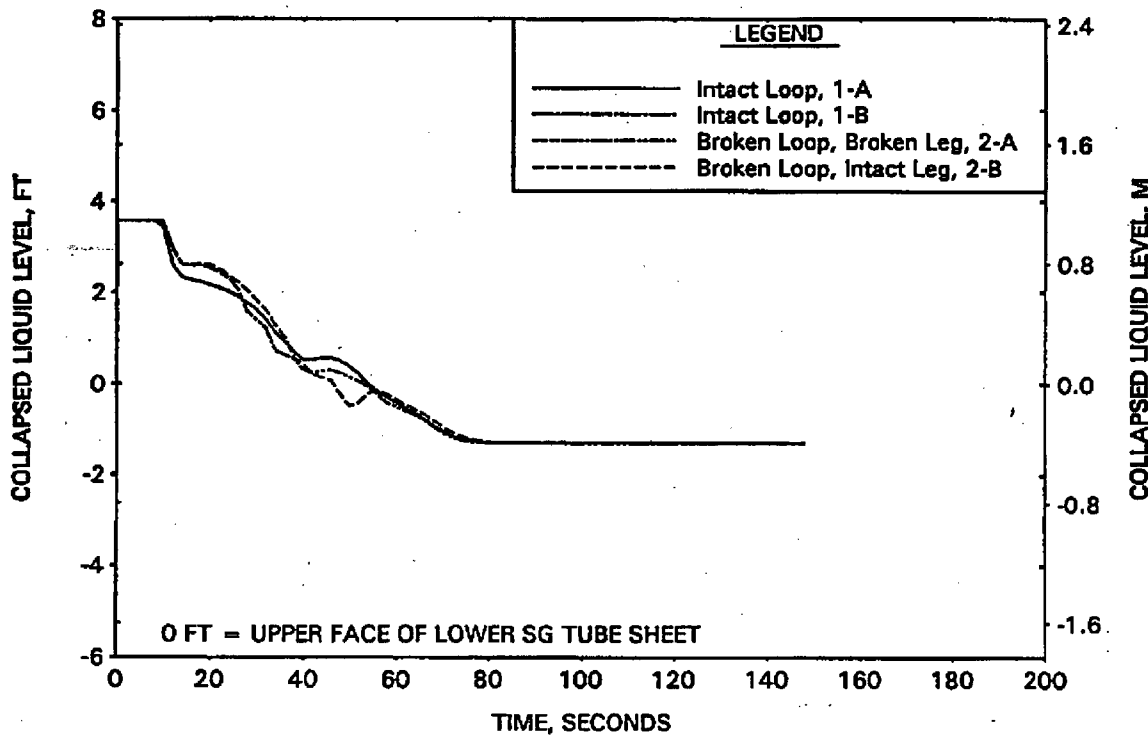


FIGURE A-184. CLPD BREAK SPECTRUM STUDY FOR 1.0-FT² BREAK - CLPS LIQUID VOLUME.

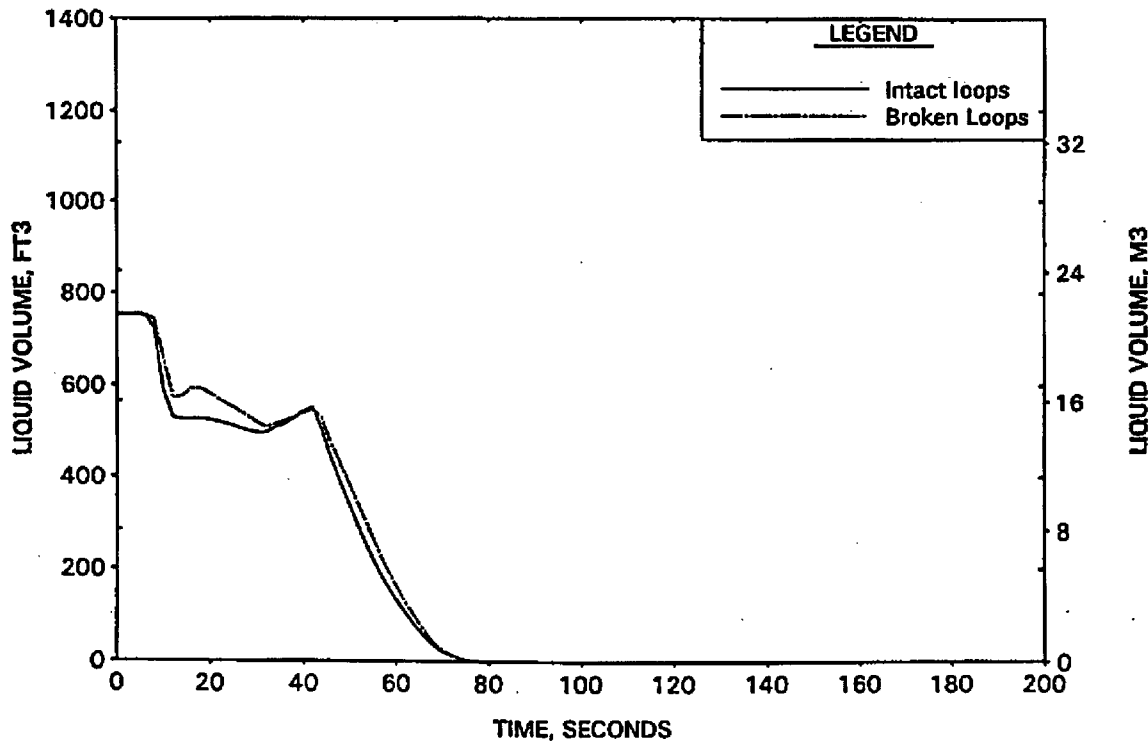


FIGURE A-185. CLPD BREAK SPECTRUM STUDY FOR 1.0-FT² BREAK - HOT LEG AND RVVV FLOWS.

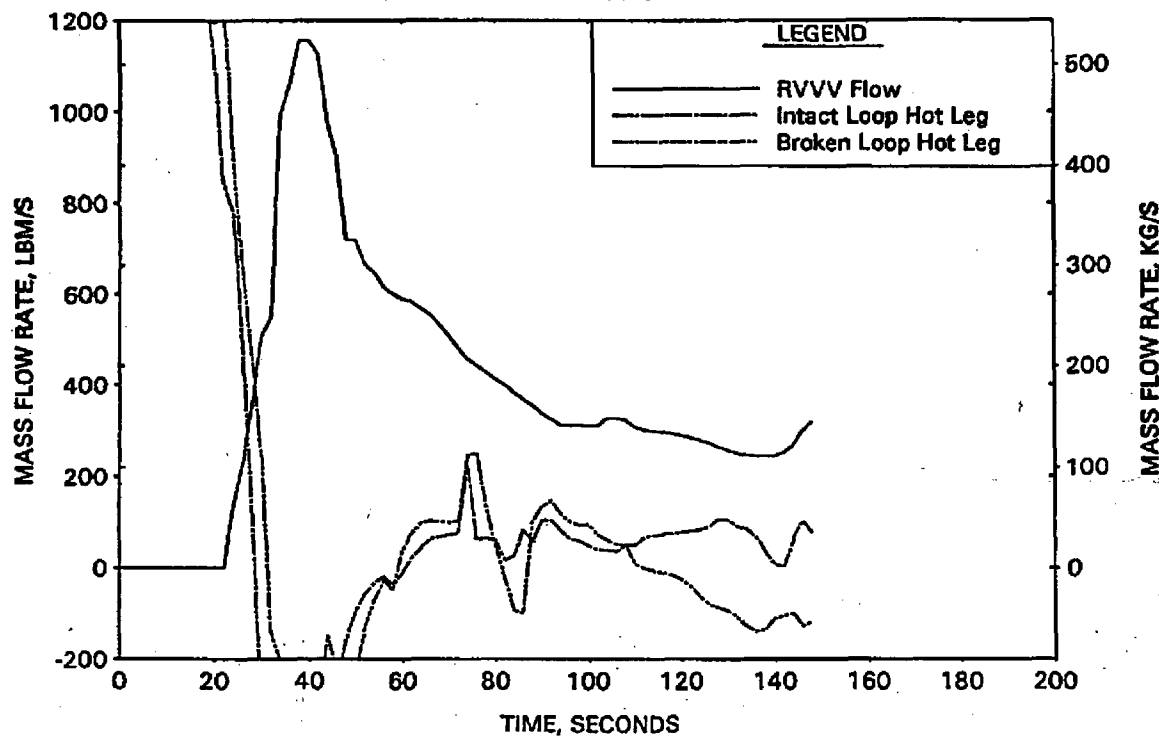


FIGURE A-186. CLPD BREAK SPECTRUM STUDY FOR 1.0-FT² BREAK - CORE MIXTURE LEVELS.

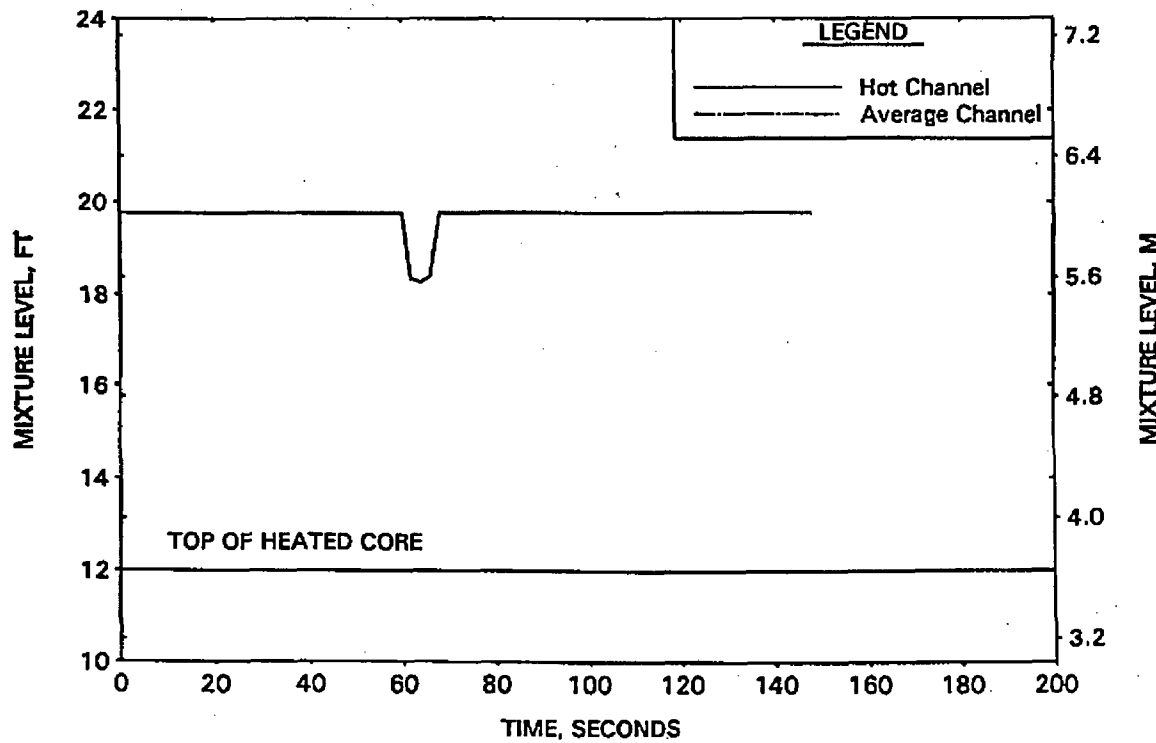


FIGURE A-187. CLPD BREAK SPECTRUM STUDY FOR 1.0-FT2 BREAK - HOT CHANNEL CLAD TEMPERATURES.

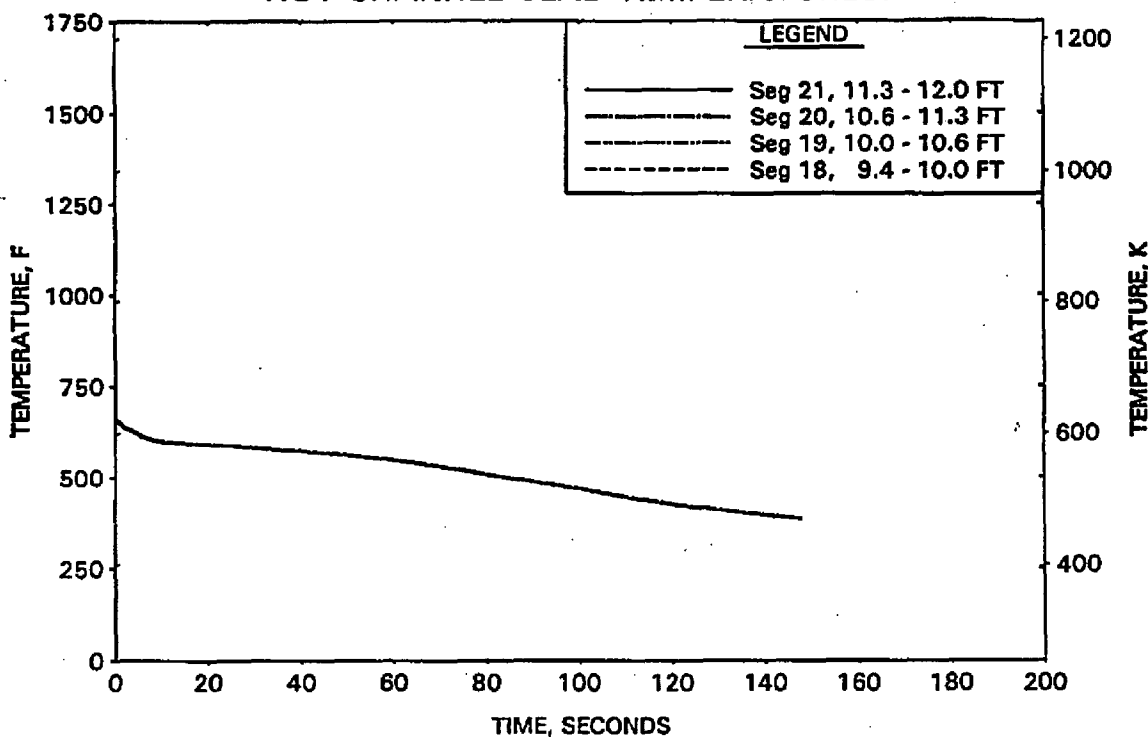


FIGURE A-188. CLPD BREAK SPECTRUM STUDY FOR 1.0-FT2 BREAK - HOT CHANNEL STEAM TEMPERATURES.

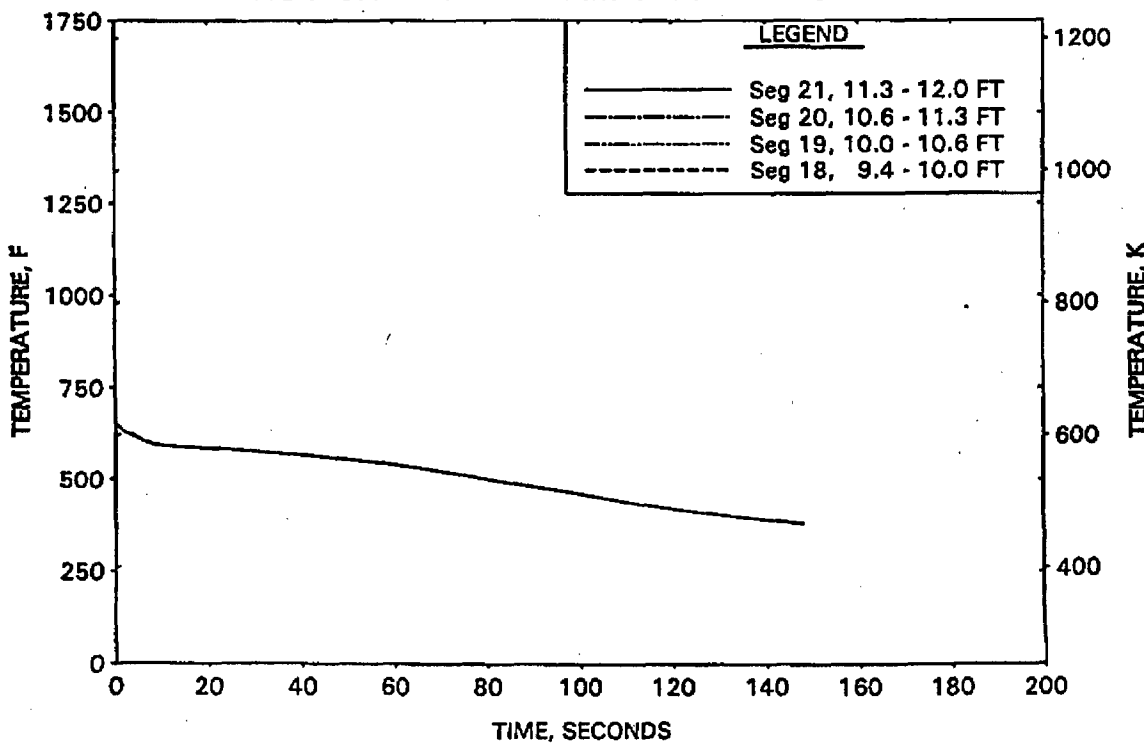


FIGURE A-189. CLPD BREAK SPECTRUM STUDY FOR 1.0-FT2 BREAK -
UPPER ELEVATION AVE CHANNEL CLAD TEMPERATURES.

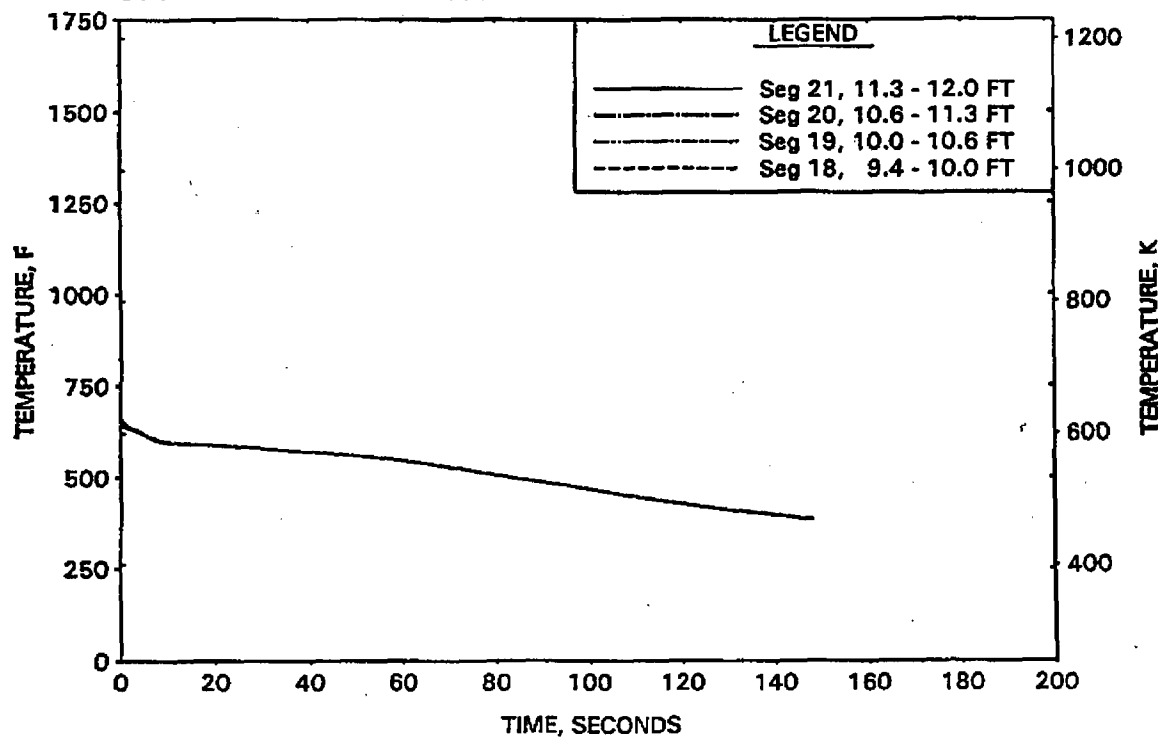


FIGURE A-190. CLPD BREAK SPECTRUM STUDY FOR 1.0-FT2 BREAK -
UPPER ELEVATION AVE CHANNEL STEAM TEMPERATURES.

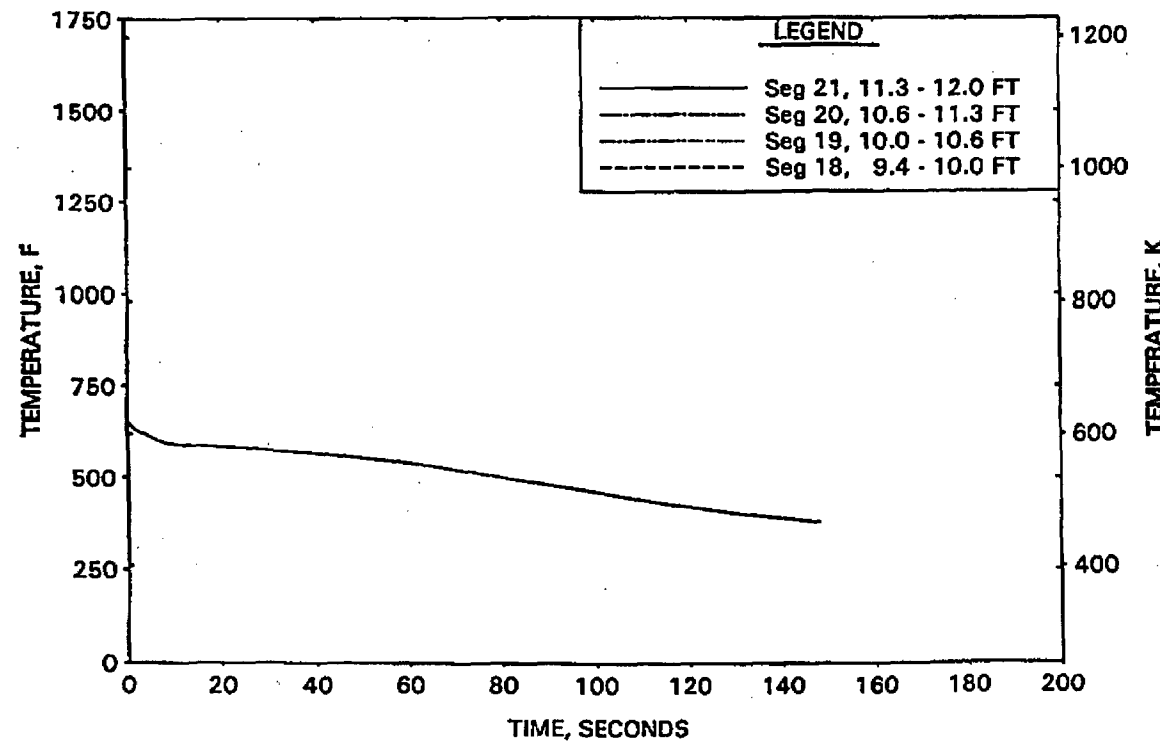


FIGURE A-191. CLPD BREAK SPECTRUM STUDY FOR 1.43-FT² BREAK - RCS PRESSURES.

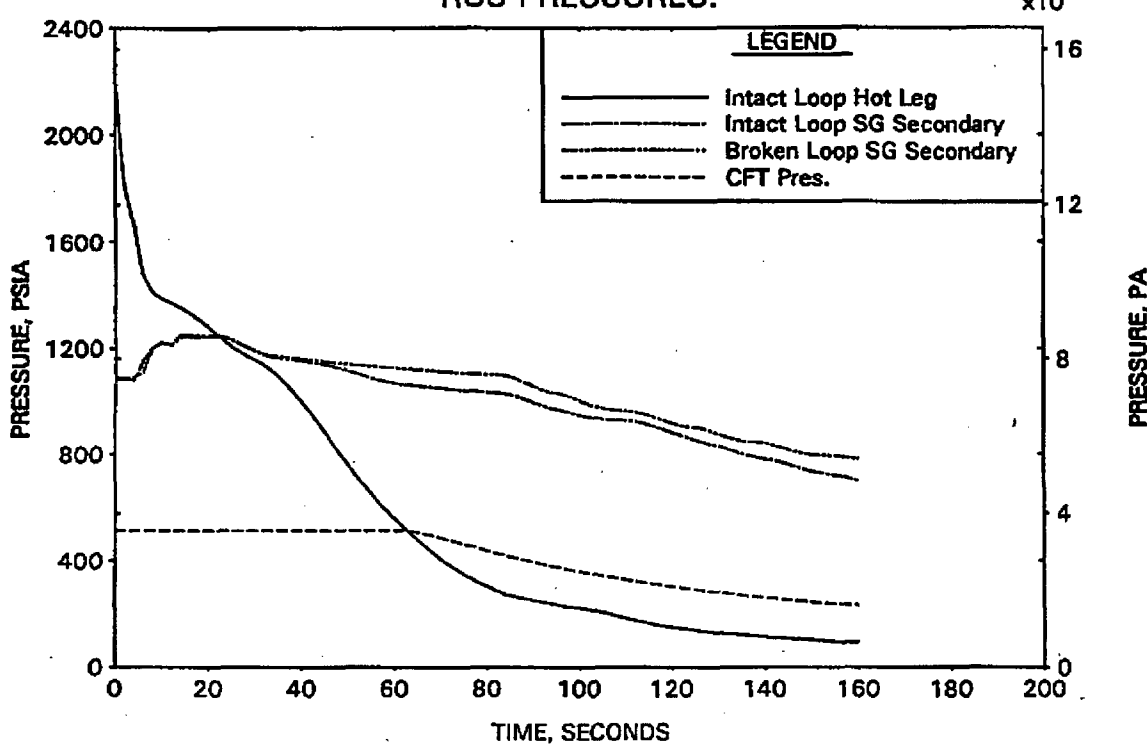


FIGURE A-192. CLPD BREAK SPECTRUM STUDY FOR 1.43-FT² BREAK - DC, RV, AND CORE COLLAPSED LEVELS.

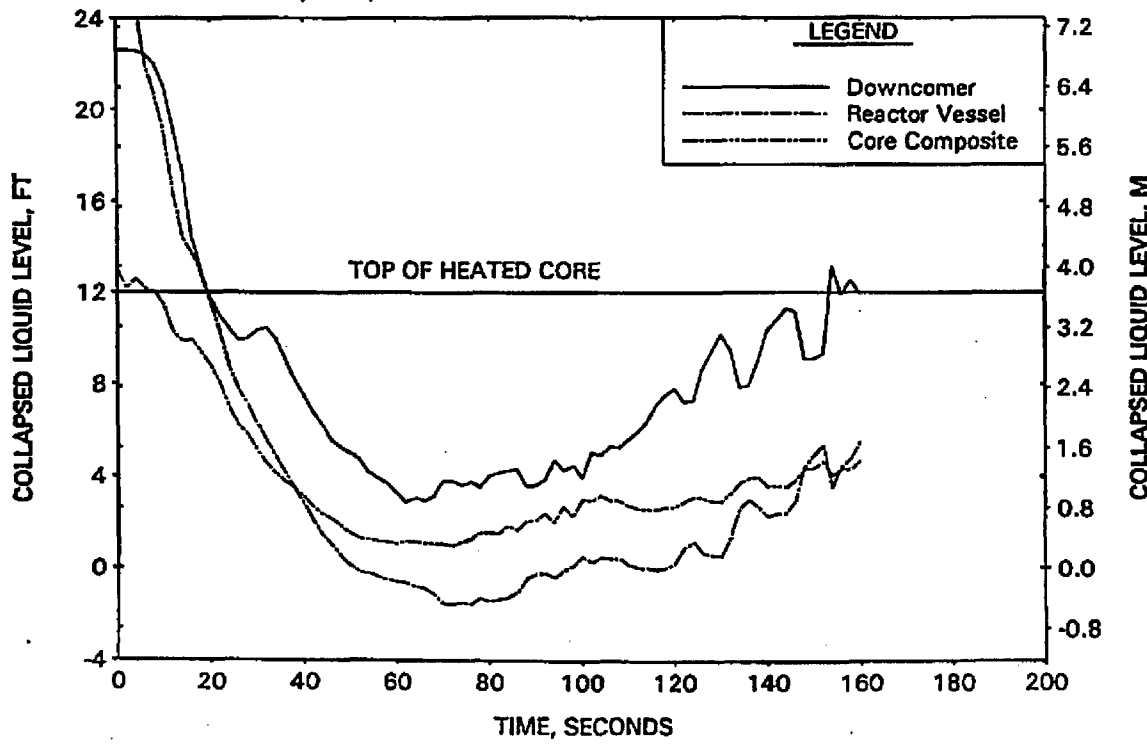


FIGURE A-193. CLPD BREAK SPECTRUM STUDY FOR 1.43-FT² BREAK - BREAK AND TOTAL ECCS FLOWS.

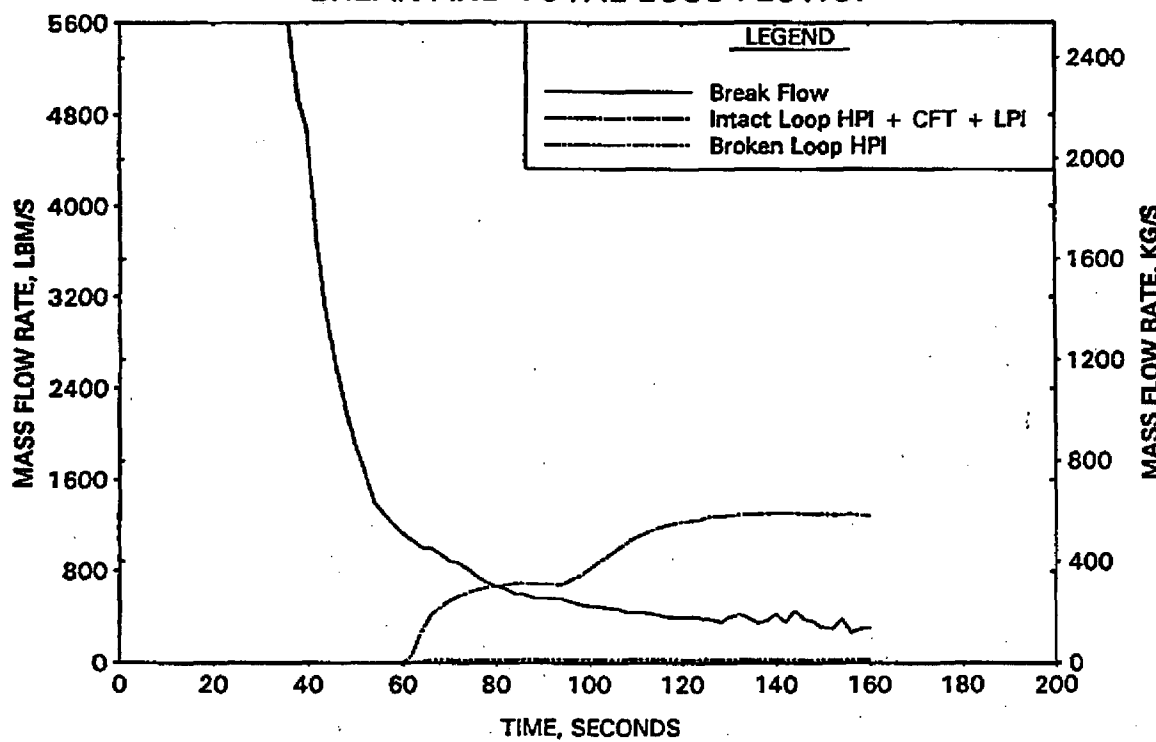


FIGURE A-194. CLPD BREAK SPECTRUM STUDY FOR 1.43-FT² BREAK - BREAK VOLUME VOID FRACTION.

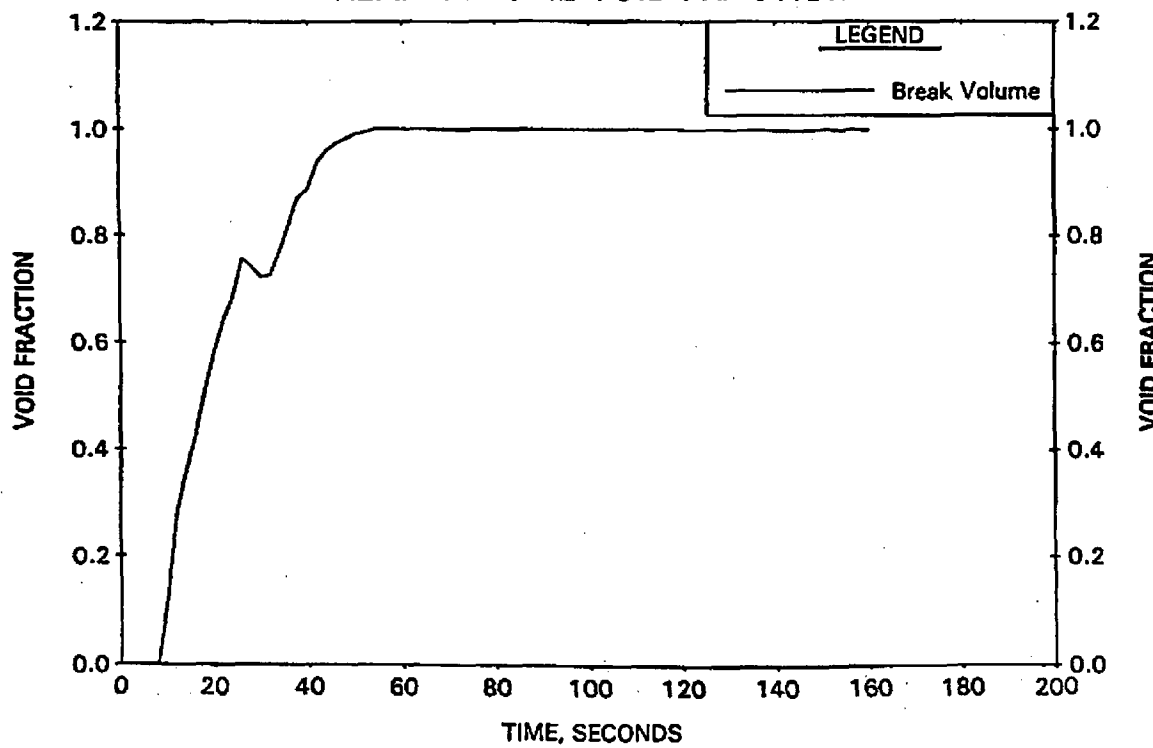


FIGURE A-195. CLPD BREAK SPECTRUM STUDY FOR 1.43-FT2 BREAK - BROKEN LOOP COLLAPSED LEVELS.

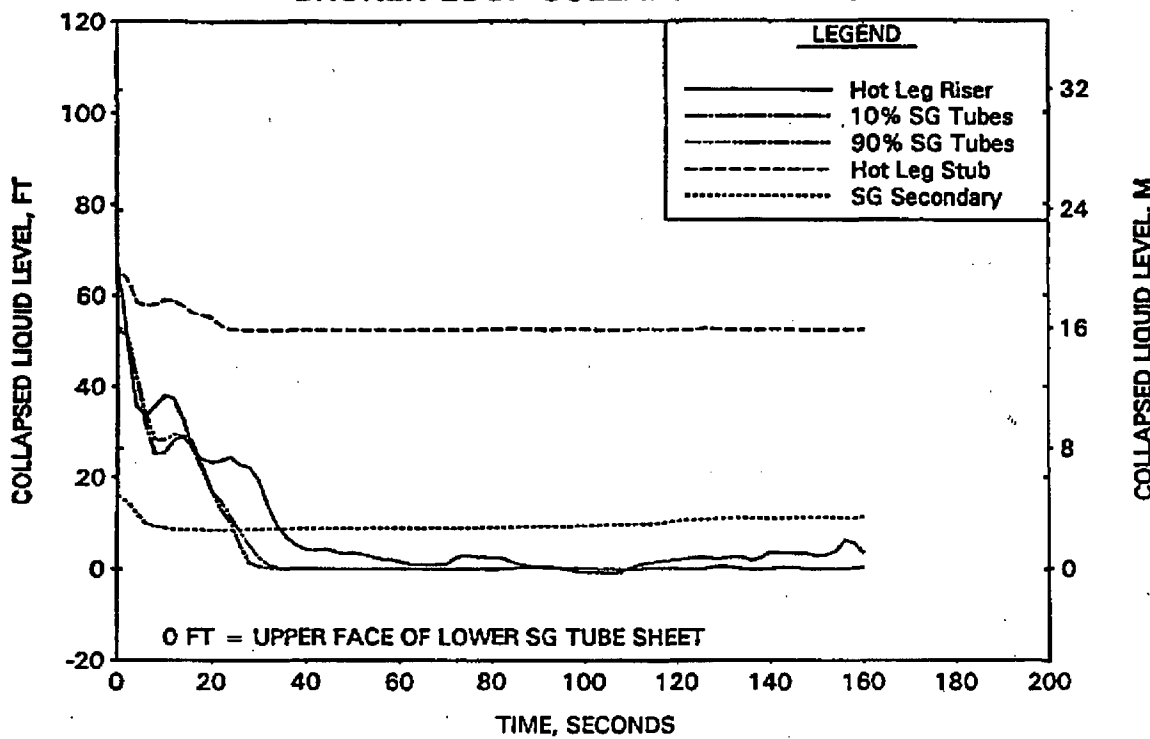


FIGURE A-196. CLPD BREAK SPECTRUM STUDY FOR 1.43-FT2 BREAK - INTACT LOOP COLLAPSED LEVELS.

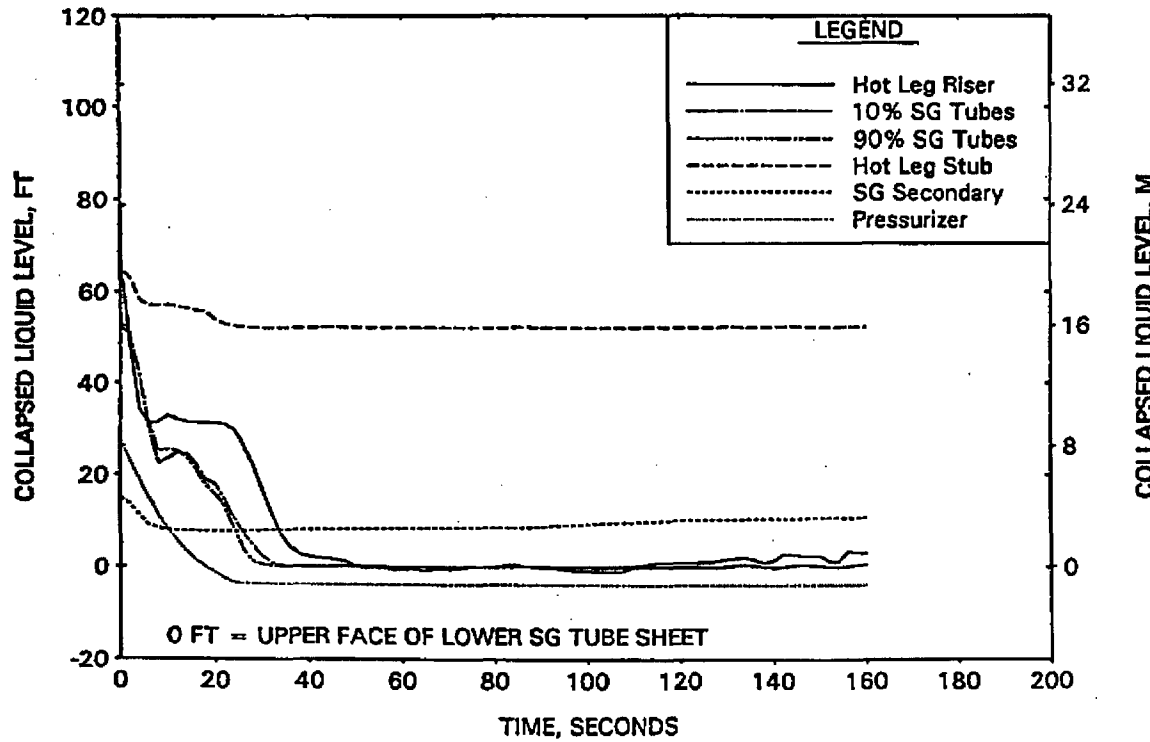


FIGURE A-197. CLPD BREAK SPECTRUM STUDY FOR 1.43-FT² BREAK - CLPD COLLAPSED LEVELS.

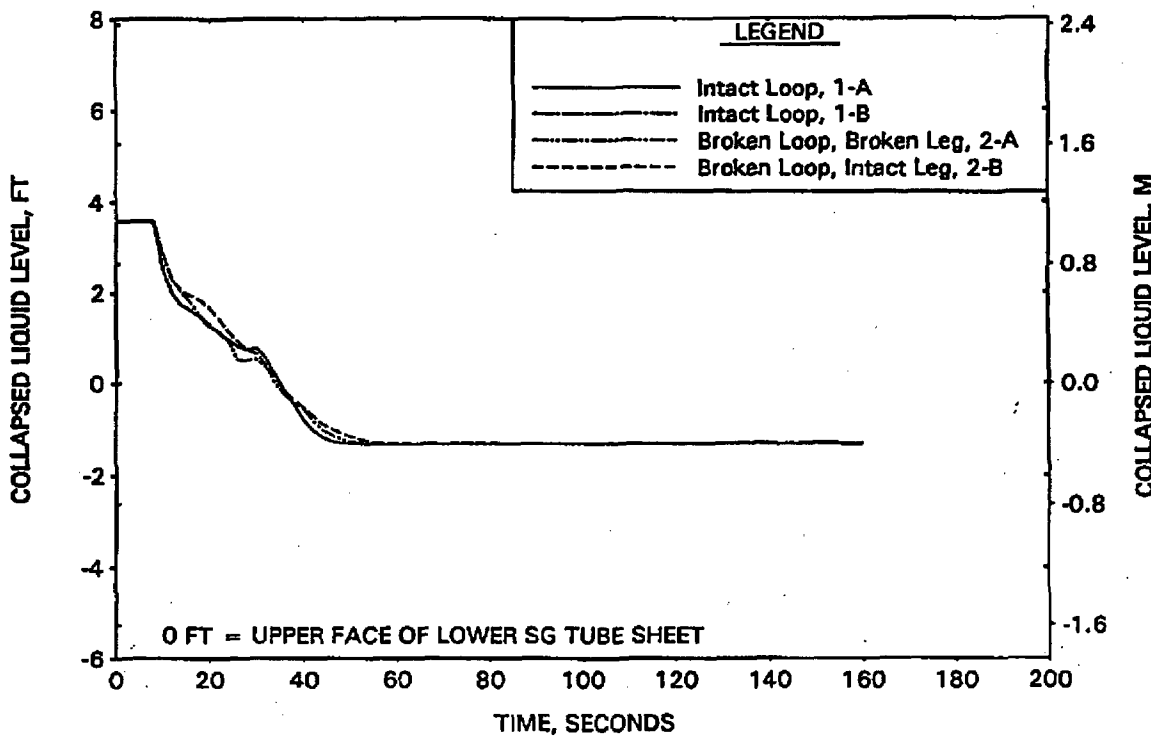


FIGURE A-198. CLPD BREAK SPECTRUM STUDY FOR 1.43-FT² BREAK - CLPS LIQUID VOLUME.

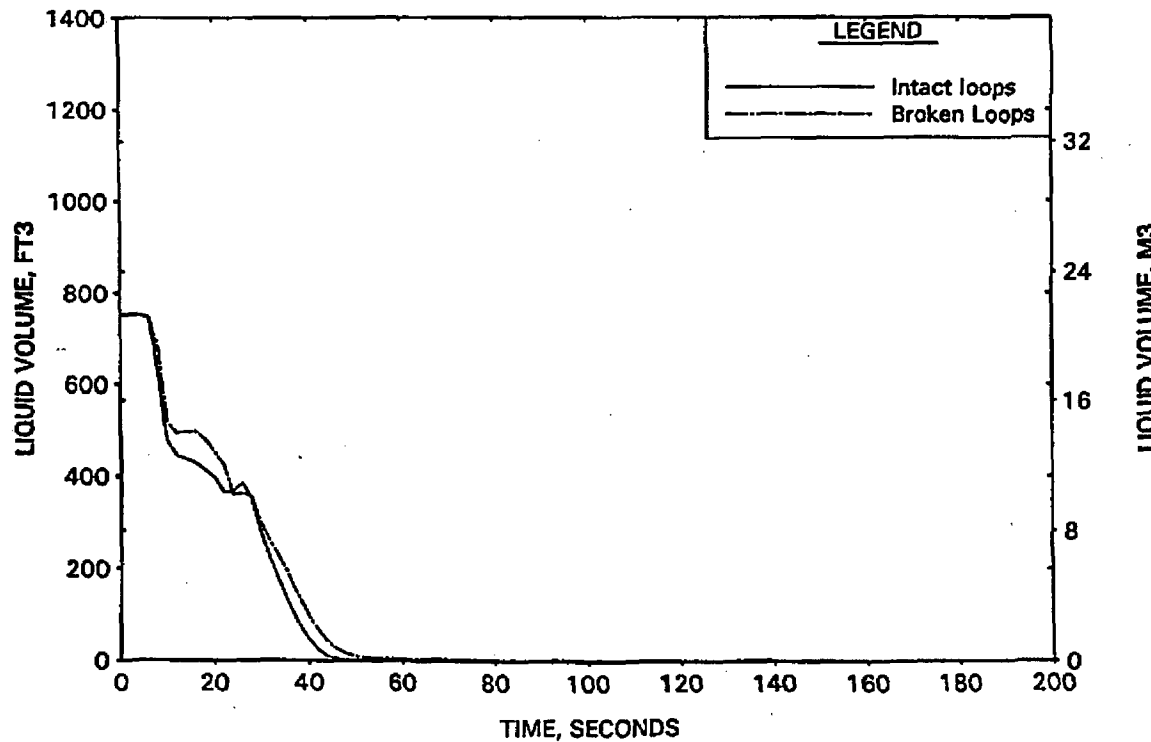


FIGURE A-199. CLPD BREAK SPECTRUM STUDY FOR 1.43-FT² BREAK - HOT LEG AND RVVV FLOWS.

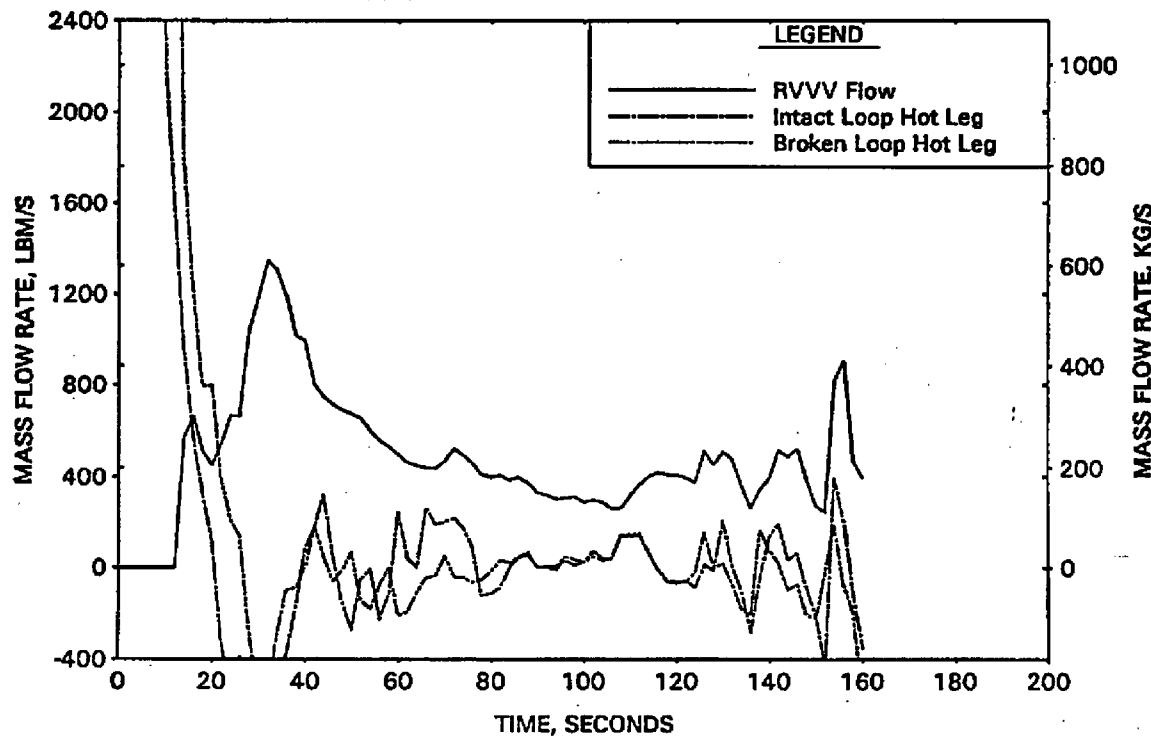


FIGURE A-200. CLPD BREAK SPECTRUM STUDY FOR 1.43-FT² BREAK - CORE MIXTURE LEVELS.

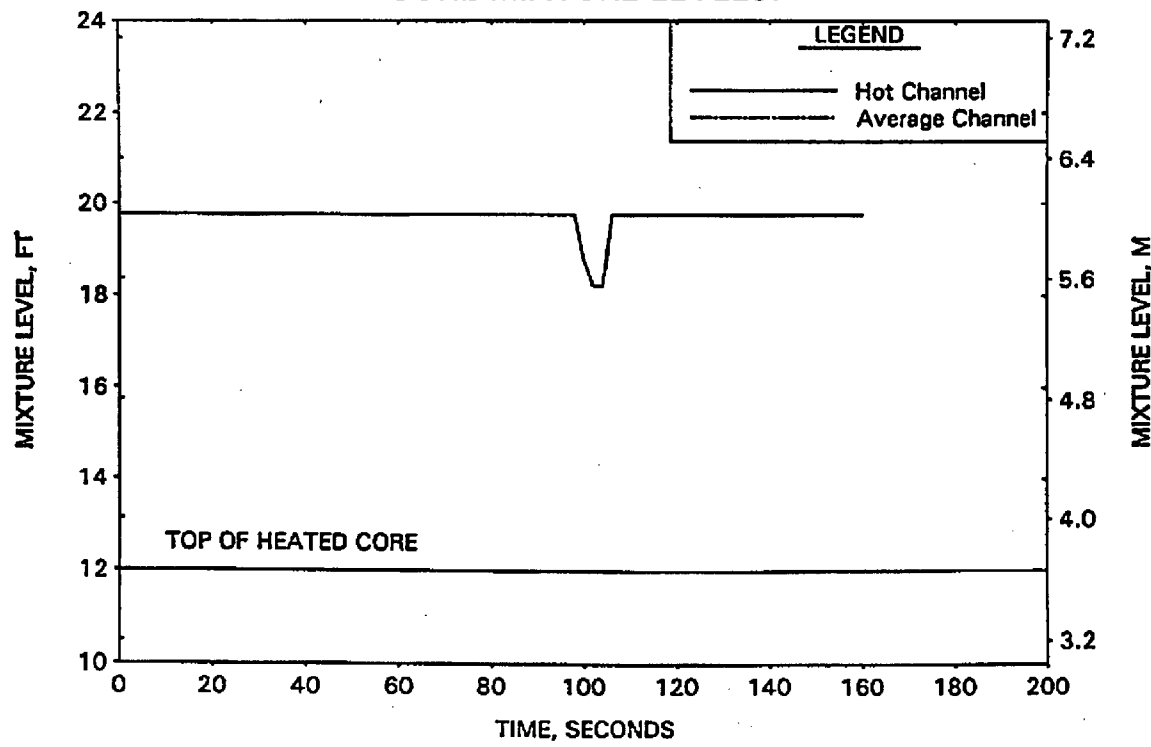


FIGURE A-201. CLPD BREAK SPECTRUM STUDY FOR 1.43-FT2 BREAK - HOT CHANNEL CLAD TEMPERATURES.

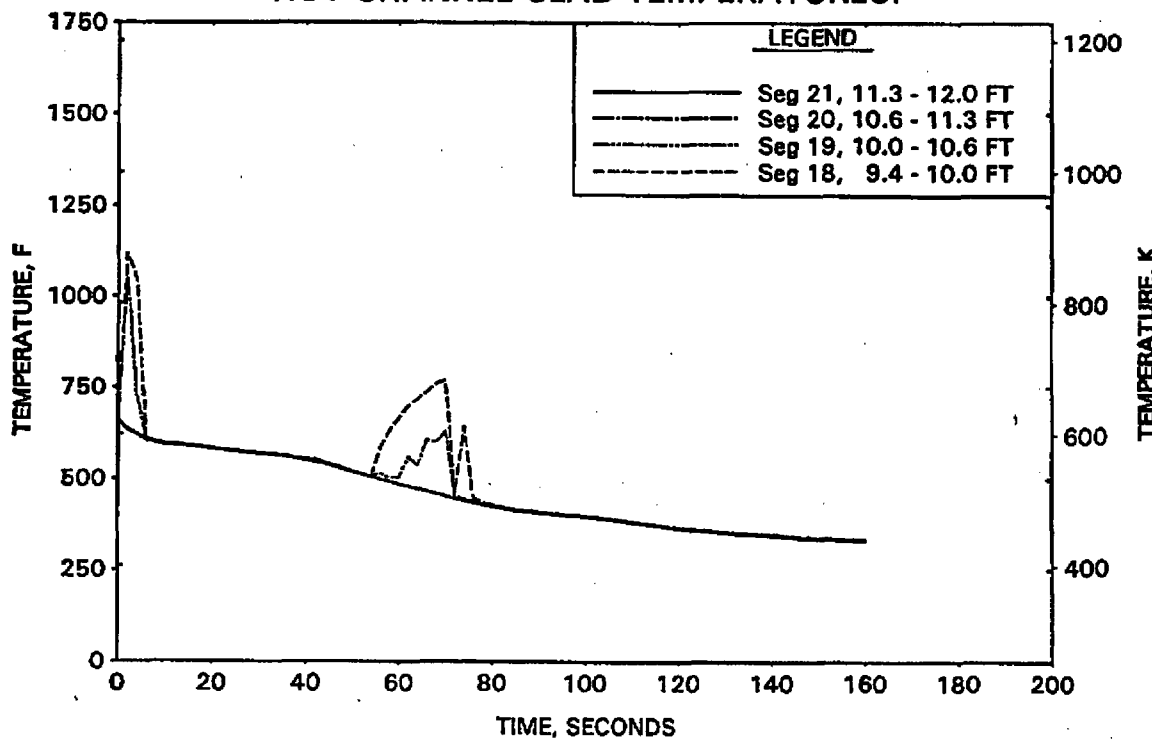


FIGURE A-202. CLPD BREAK SPECTRUM STUDY FOR 1.43-FT2 BREAK - HOT CHANNEL STEAM TEMPERATURES.

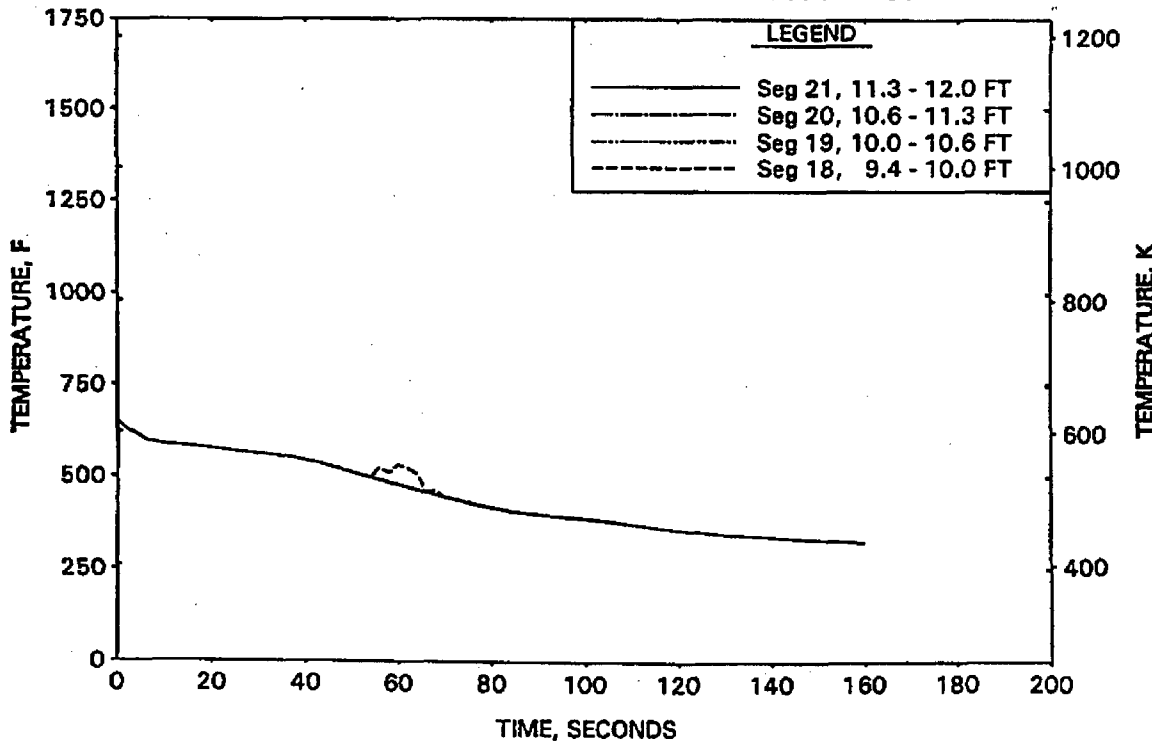


FIGURE A-203. CLPD BREAK SPECTRUM STUDY FOR 1.43-FT2 BREAK -
UPPER ELEVATION AVE CHANNEL CLAD TEMPERATURES.

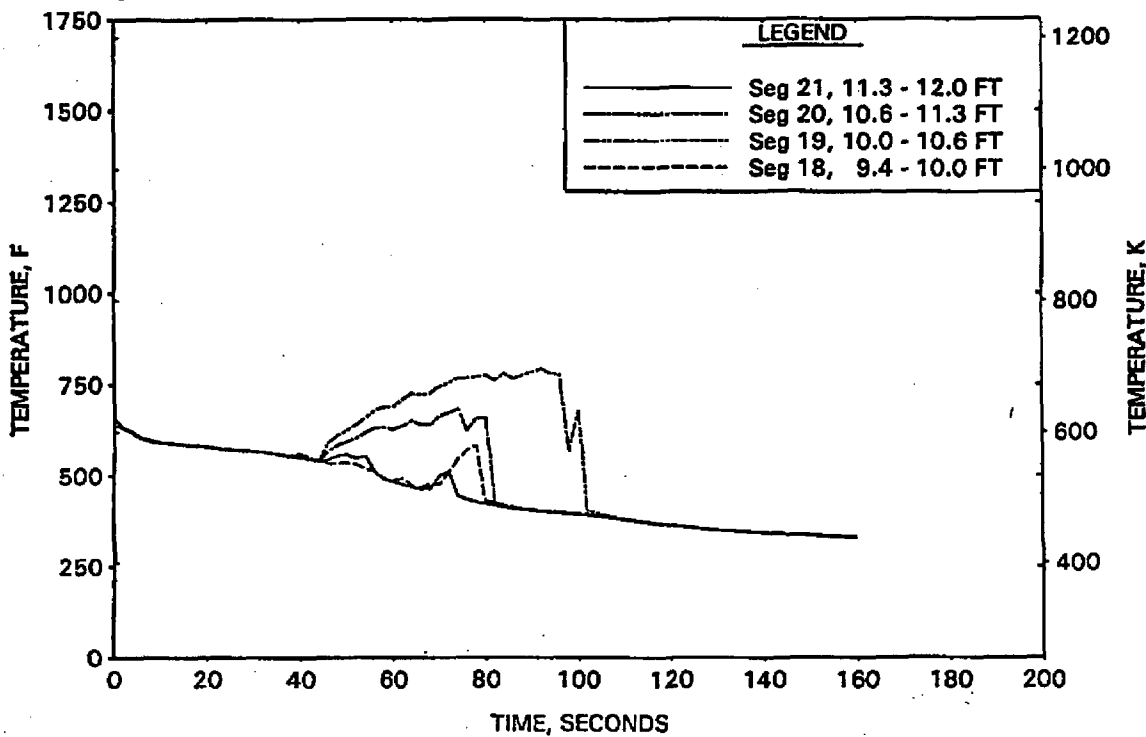


FIGURE A-204. CLPD BREAK SPECTRUM STUDY FOR 1.43-FT2 BREAK -
UPPER ELEVATION AVE CHANNEL STEAM TEMPERATURES.

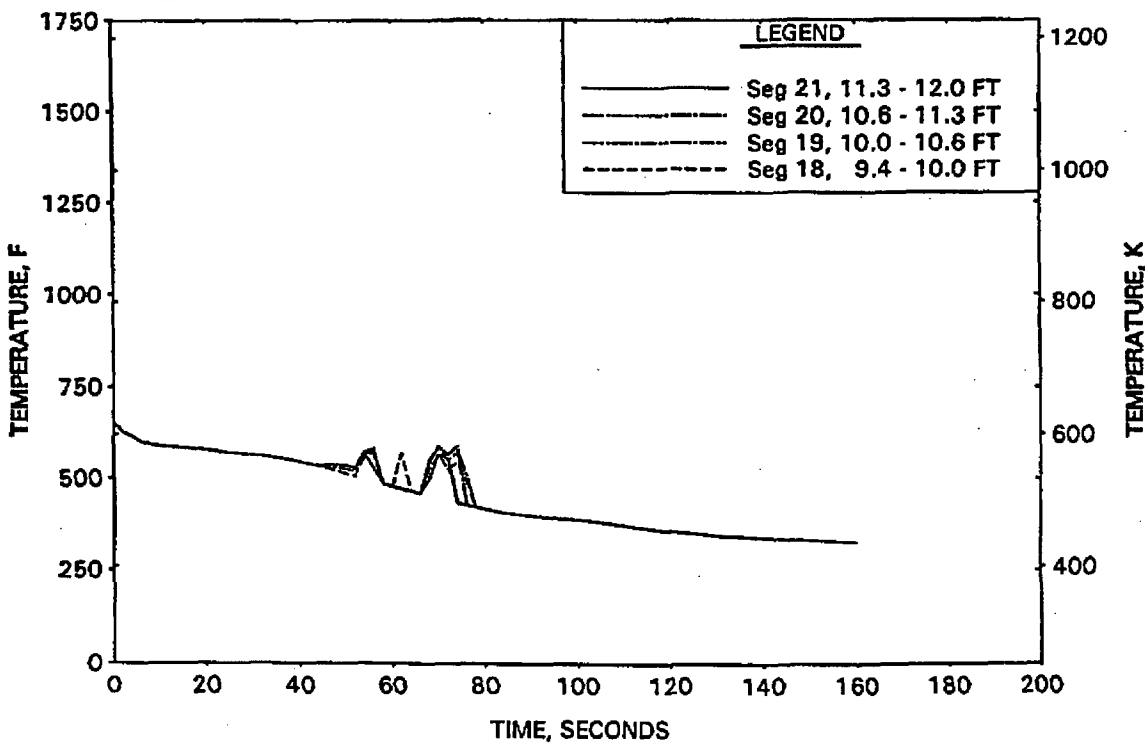


FIGURE A-205. SMALL SBLOCA CLPD BREAK SPECTRUM STUDY -
COMPARISON OF PRIMARY PRESSURES.

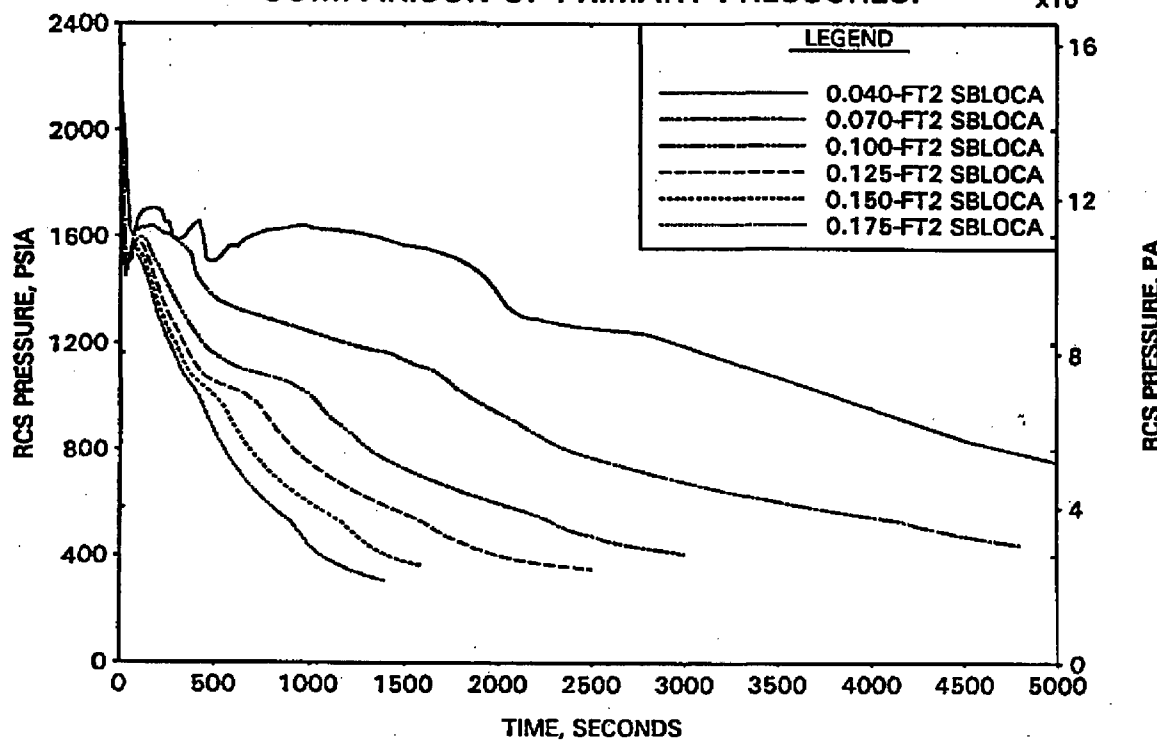


FIGURE A-206. SMALL SBLOCA CLPD BREAK SPECTRUM STUDY -
COMPARISON OF REACTOR VESSEL COLLAPSED LEVELS.

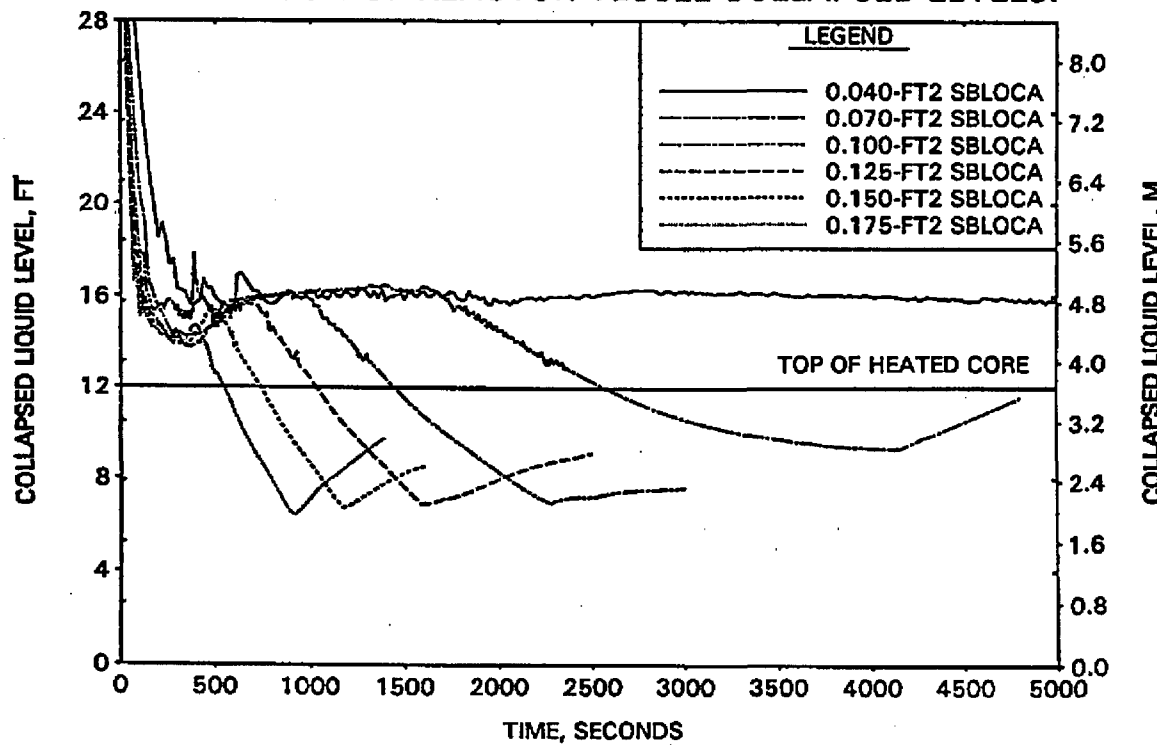


FIGURE A-207. SMALL SBLOCA CLPD BREAK SPECTRUM STUDY -
COMPARISON OF PEAK CLADDING TEMPERATURES.

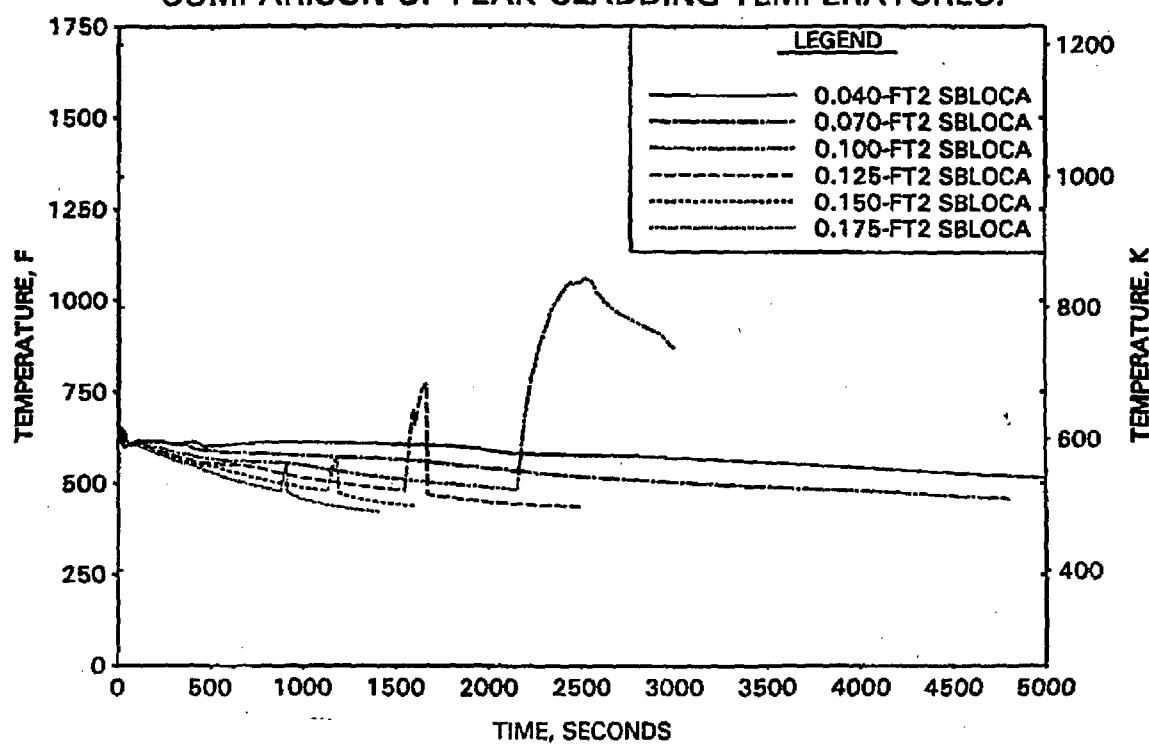


FIGURE A-208. SMALL SBLOCA CLPD BREAK SPECTRUM STUDY -
COMPARISON OF INTACT LOOP HPI + CFT + LPI FLOW RATES.

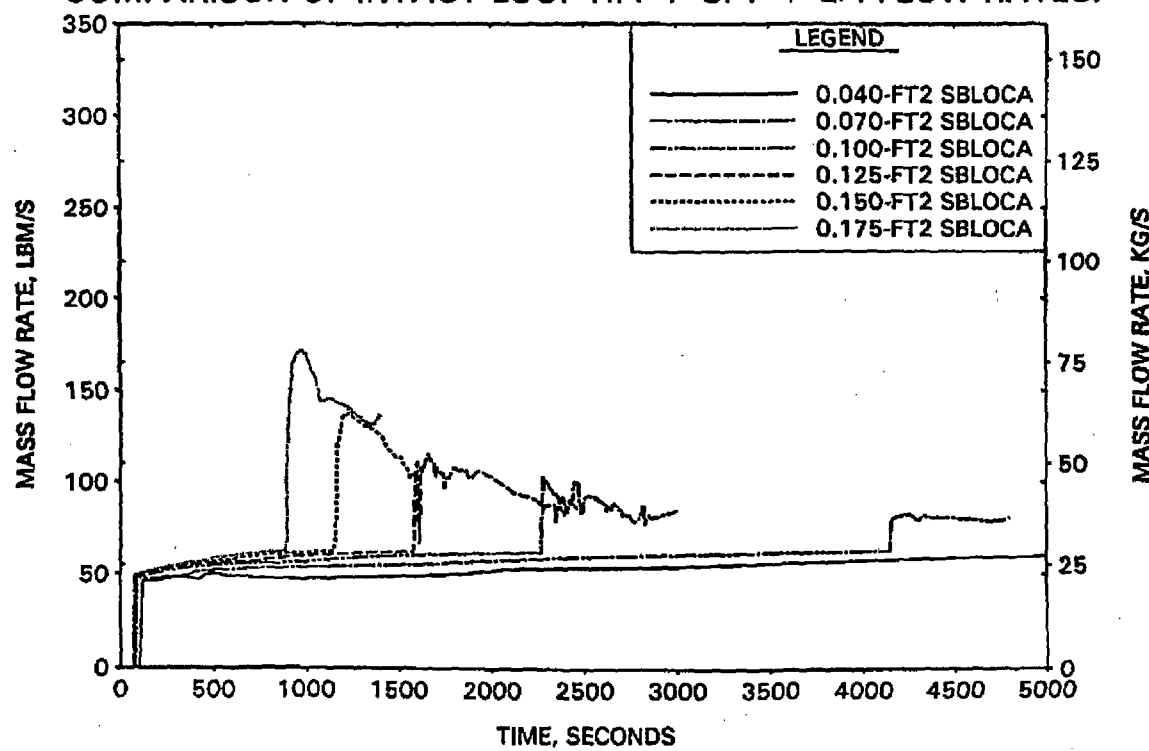


FIGURE A-209. LARGE SBLOCA CLPD BREAK SPECTRUM STUDY -
COMPARISON OF PRIMARY PRESSURES.

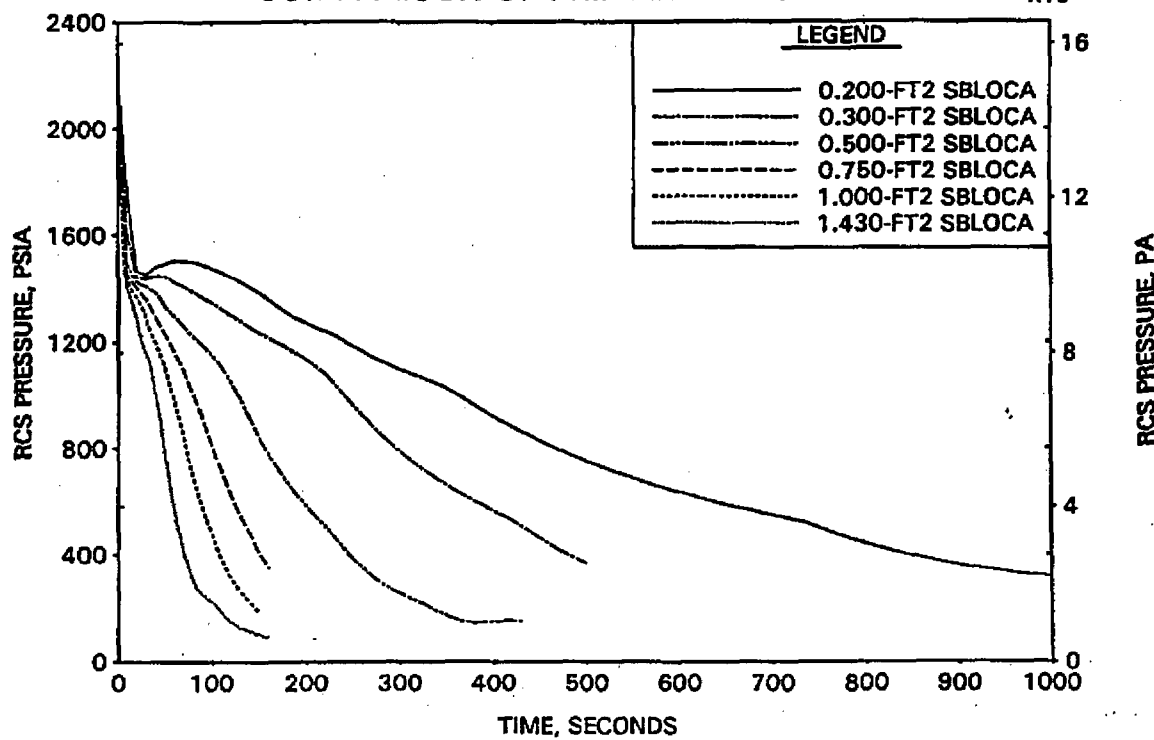


FIGURE A-210. LARGE SBLOCA CLPD BREAK SPECTRUM STUDY -
COMPARISON OF REACTOR VESSEL COLLAPSED LEVELS.

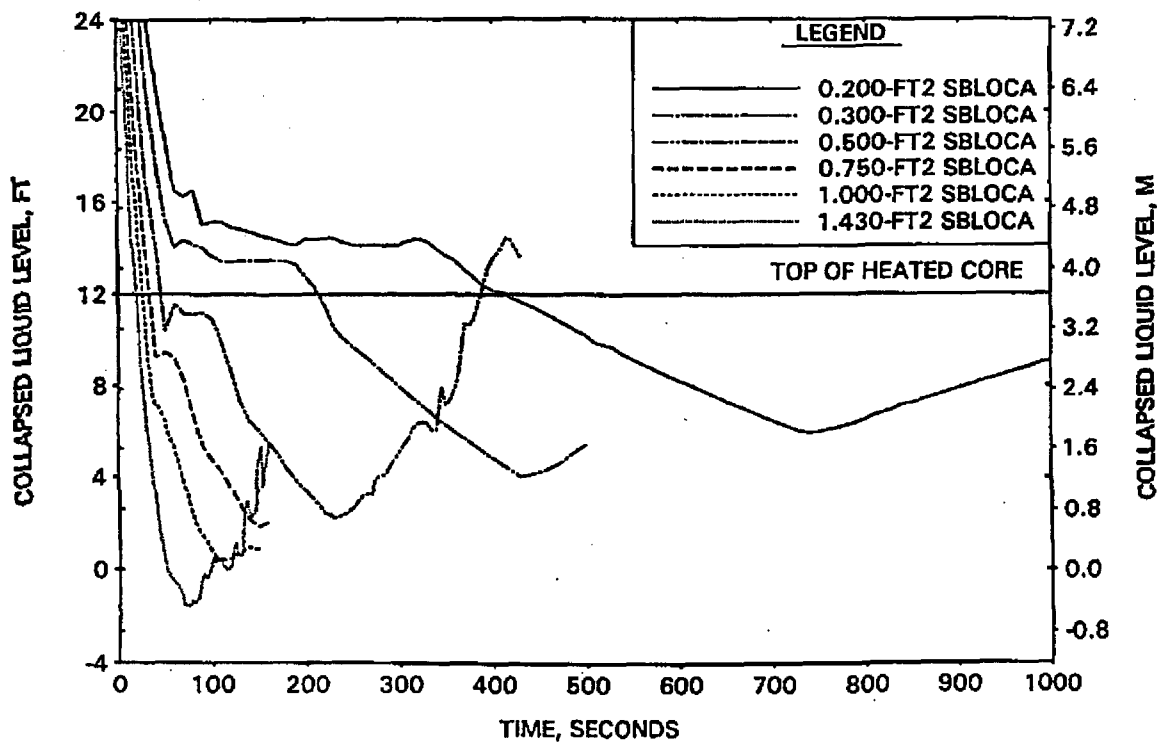


FIGURE A-211. LARGE SBLOCA CLPD BREAK SPECTRUM STUDY - COMPARISON OF PEAK CLADDING TEMPERATURES.

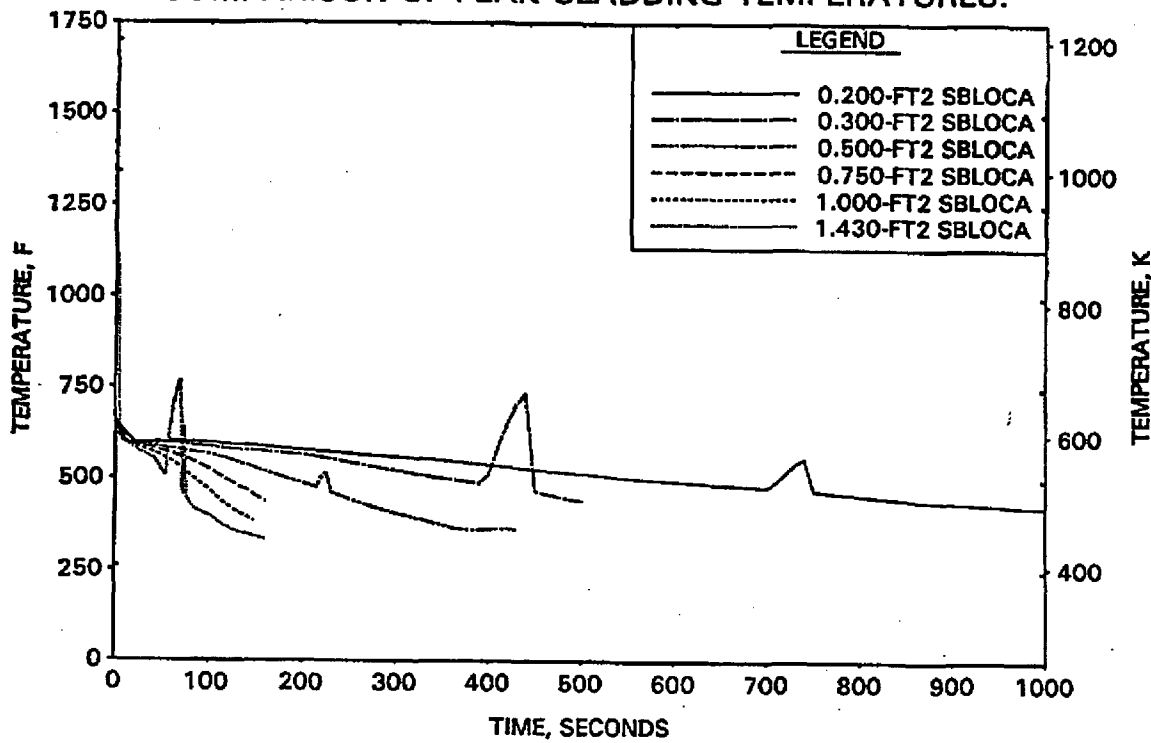


FIGURE A-212. LARGE SBLOCA CLPD BREAK SPECTRUM STUDY - COMPARISON OF INTACT LOOP HPI + CFT + LPI FLOW RATES.

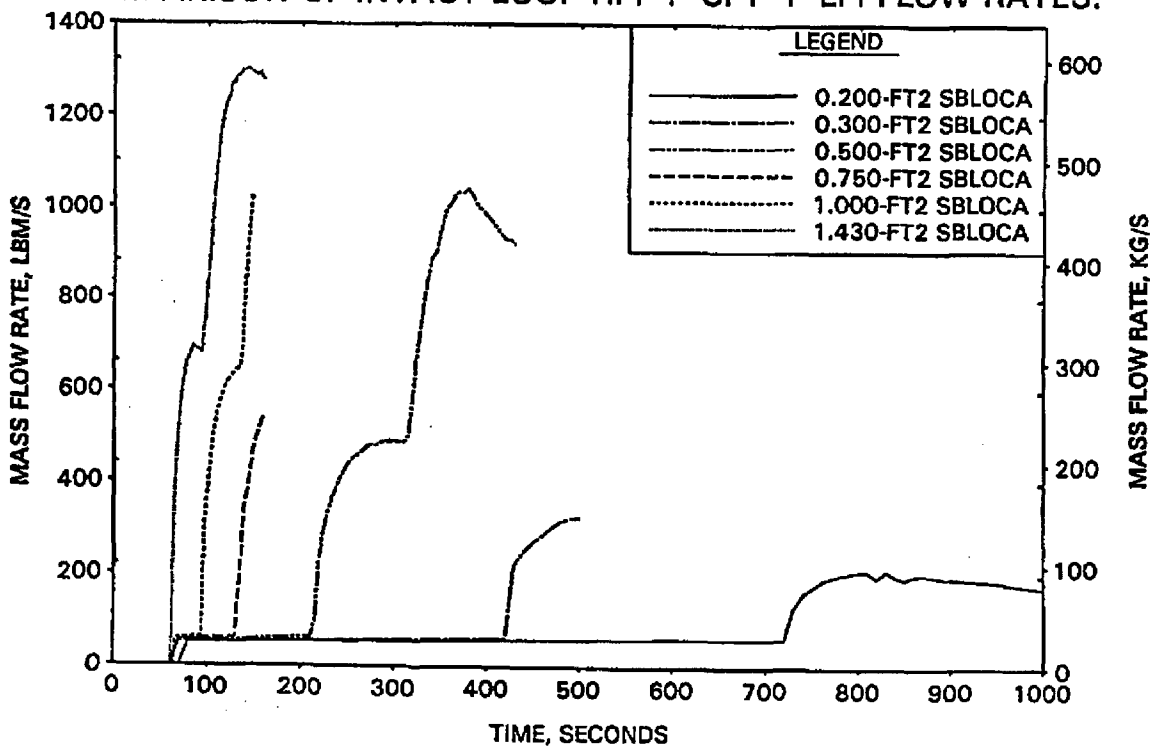


FIGURE A-213. CFT LINE RESISTANCE STUDY FOR 0.1-FT2 CLPD BREAK - RCS PRESSURE.

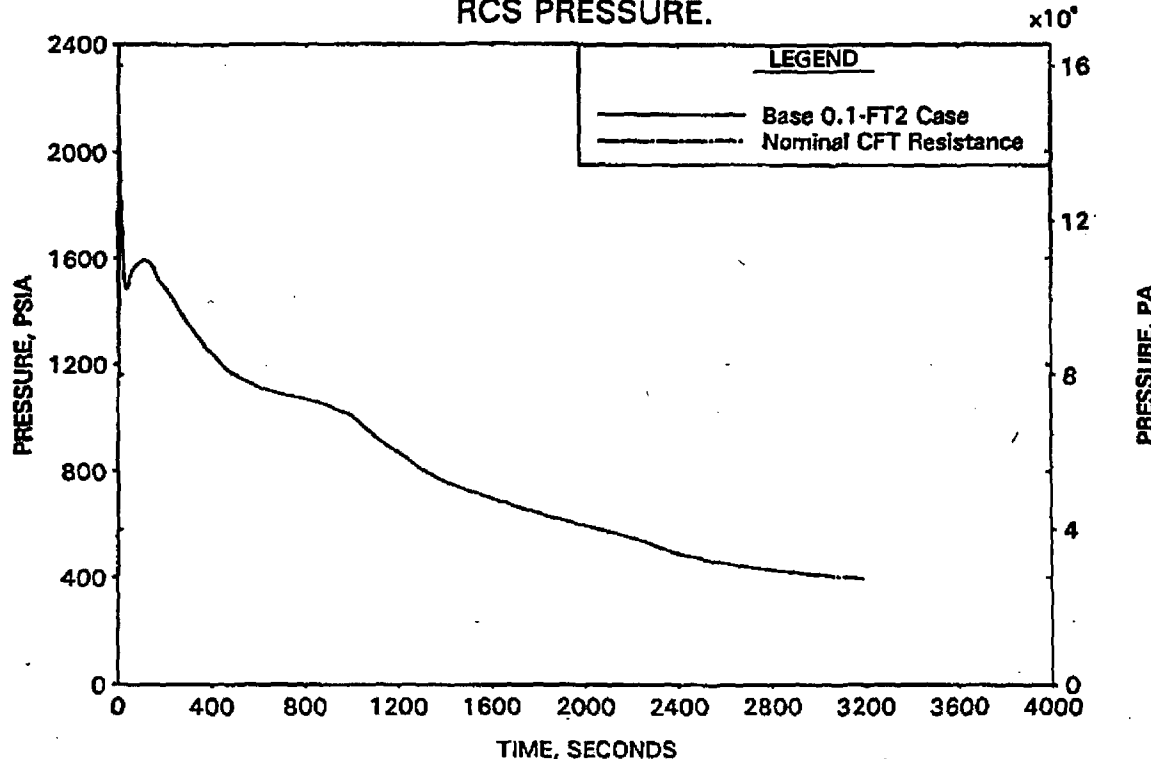


FIGURE A-214. CFT LINE RESISTANCE STUDY FOR 0.1-FT2 CLPD BREAK - BREAK AND TOTAL ECCS FLOWS.

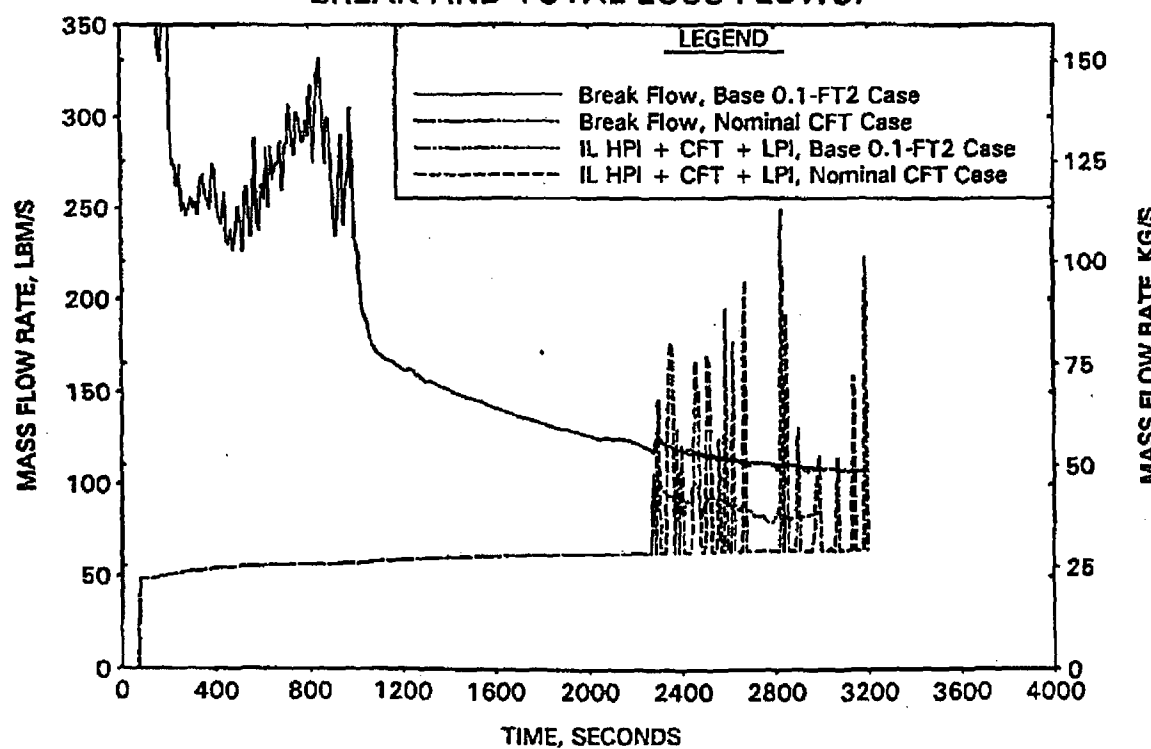


FIGURE A-215. CFT LINE RESISTANCE STUDY FOR 0.1-FT2 CLPD BREAK - REACTOR VESSEL COLLAPSED LEVEL.

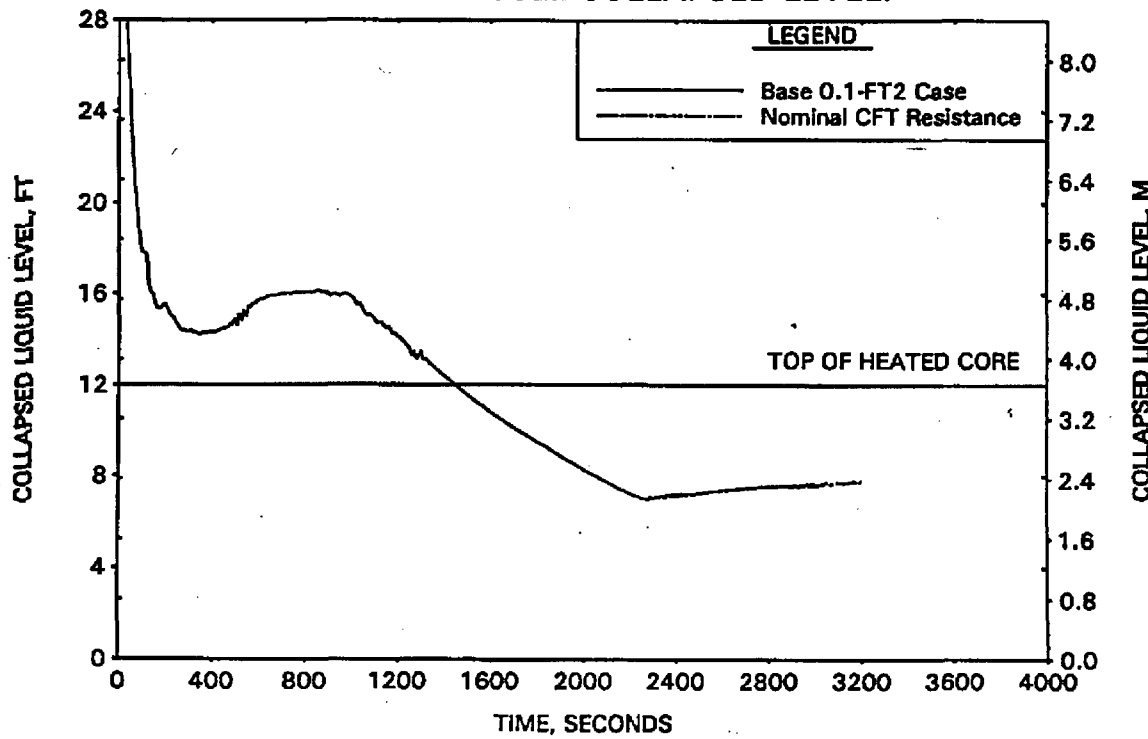


FIGURE A-216. CFT LINE RESISTANCE STUDY FOR 0.1-FT2 CLPD BREAK - CLPS LIQUID VOLUME.

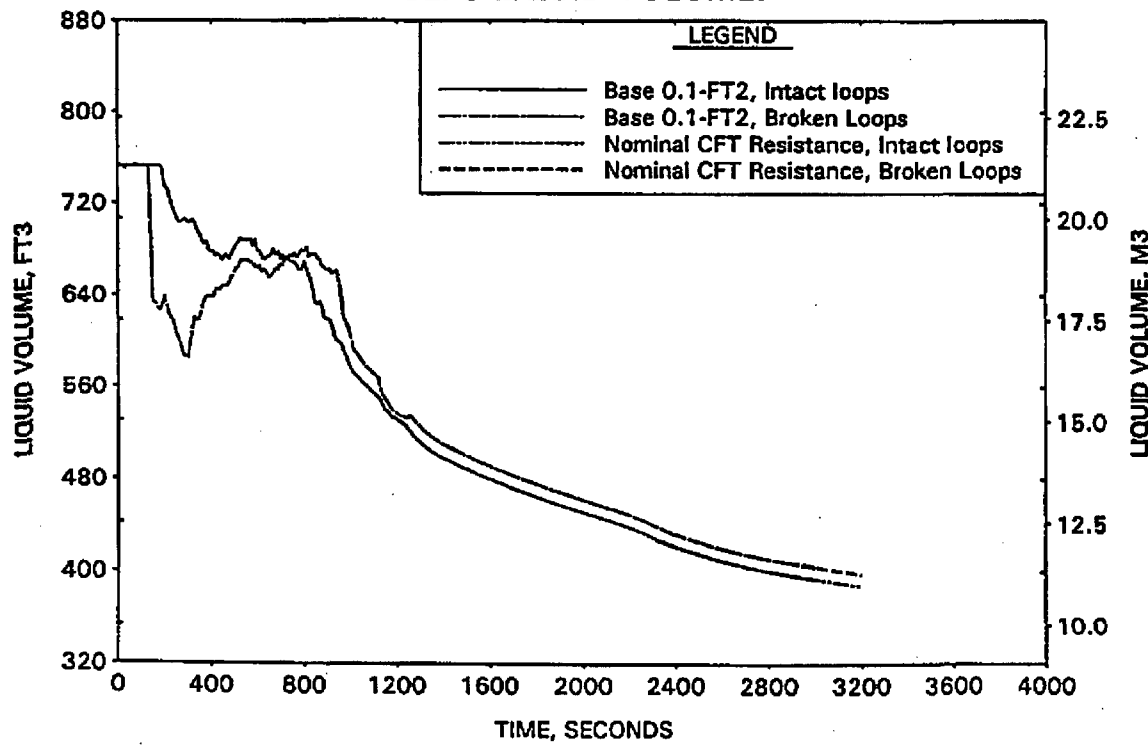


FIGURE A-217. CFT LINE RESISTANCE STUDY FOR 0.1-FT² CLPD BREAK - CORE HOT CHANNEL MIXTURE LEVELS.

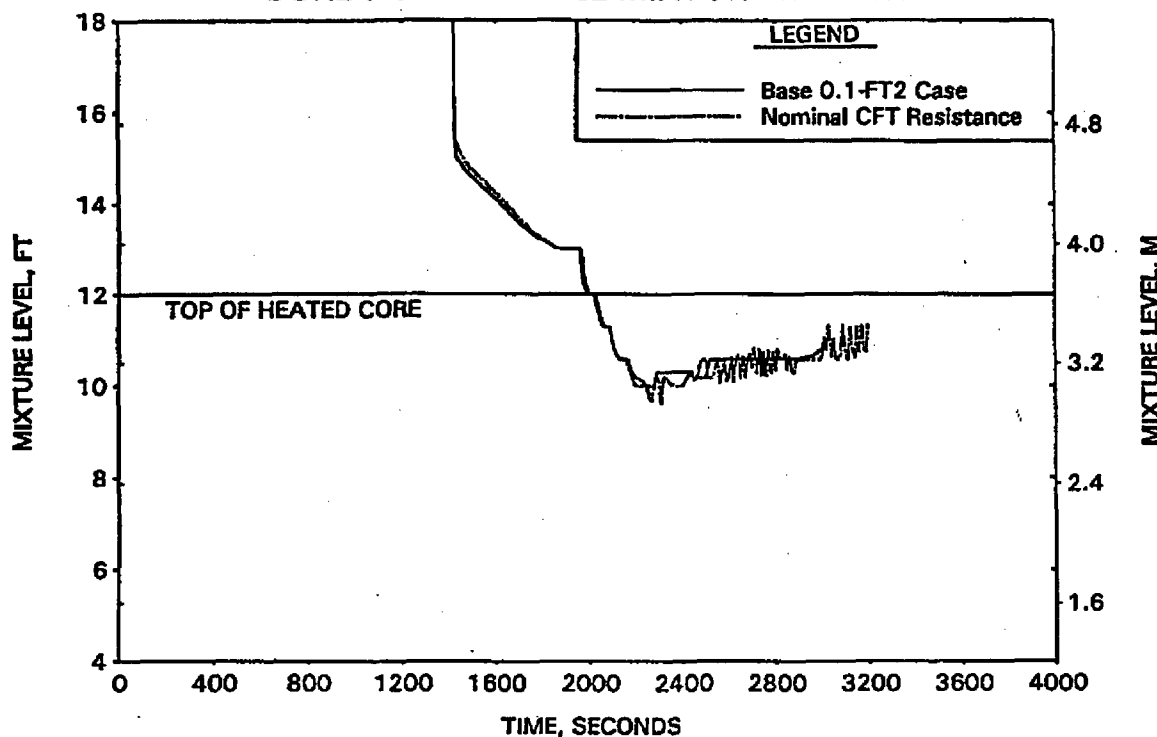


FIGURE A-218. CFT LINE RESISTANCE STUDY FOR 0.1-FT² CLPD BREAK - PEAK CLADDING TEMPERATURE.

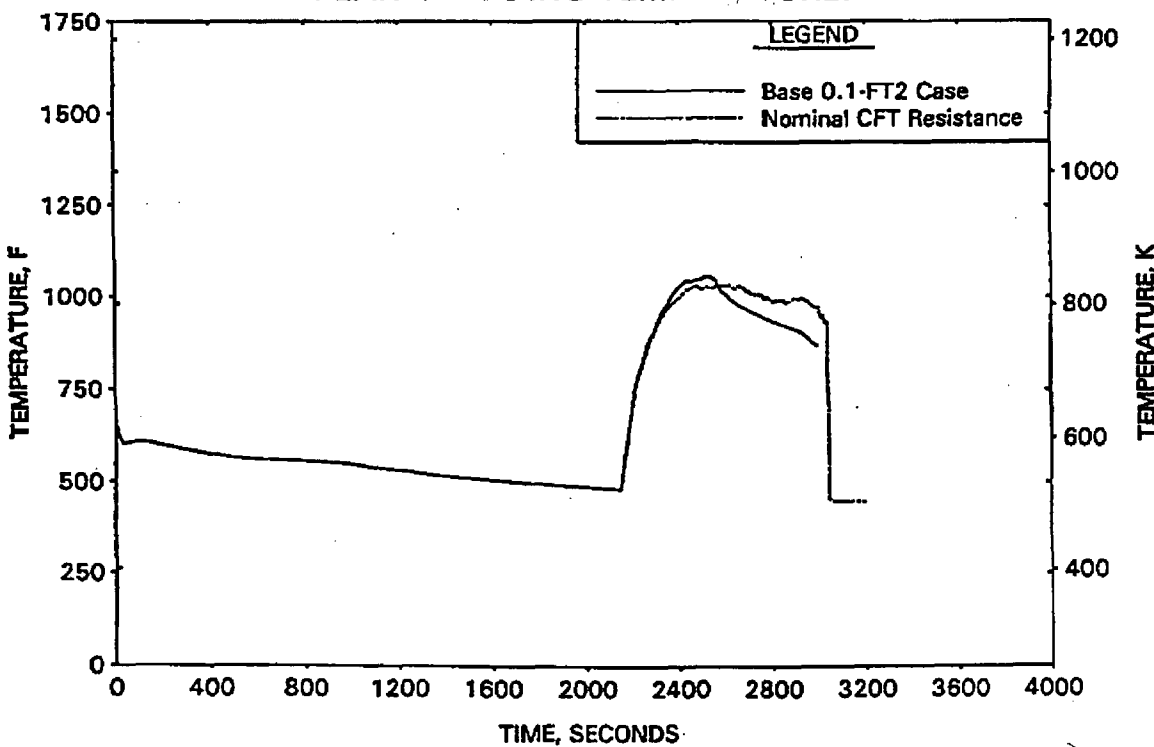


FIGURE A-219. CFT LINE RESISTANCE STUDY FOR 1.0-FT2 CLPD BREAK - RCS PRESSURE.

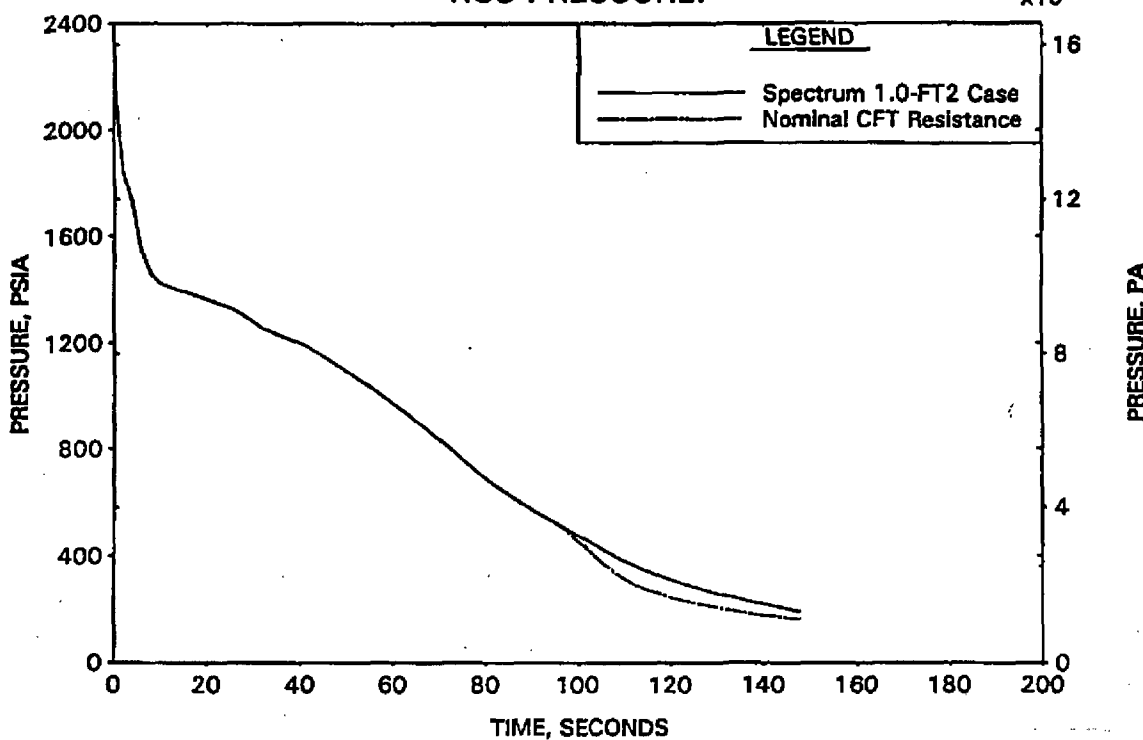


FIGURE A-220. CFT LINE RESISTANCE STUDY FOR 1.0-FT2 CLPD BREAK - BREAK AND TOTAL ECCS FLOWS.

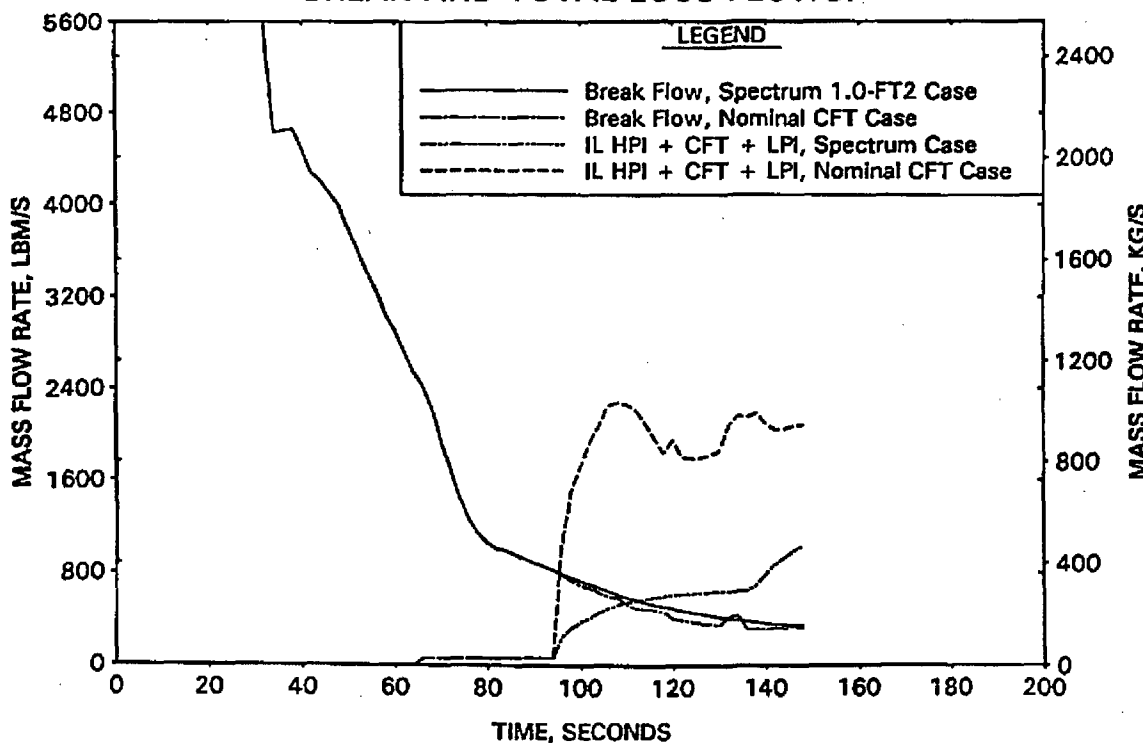


FIGURE A-221. CFT LINE RESISTANCE STUDY FOR 1.0-FT2 CLPD BREAK - REACTOR VESSEL COLLAPSED LEVEL.

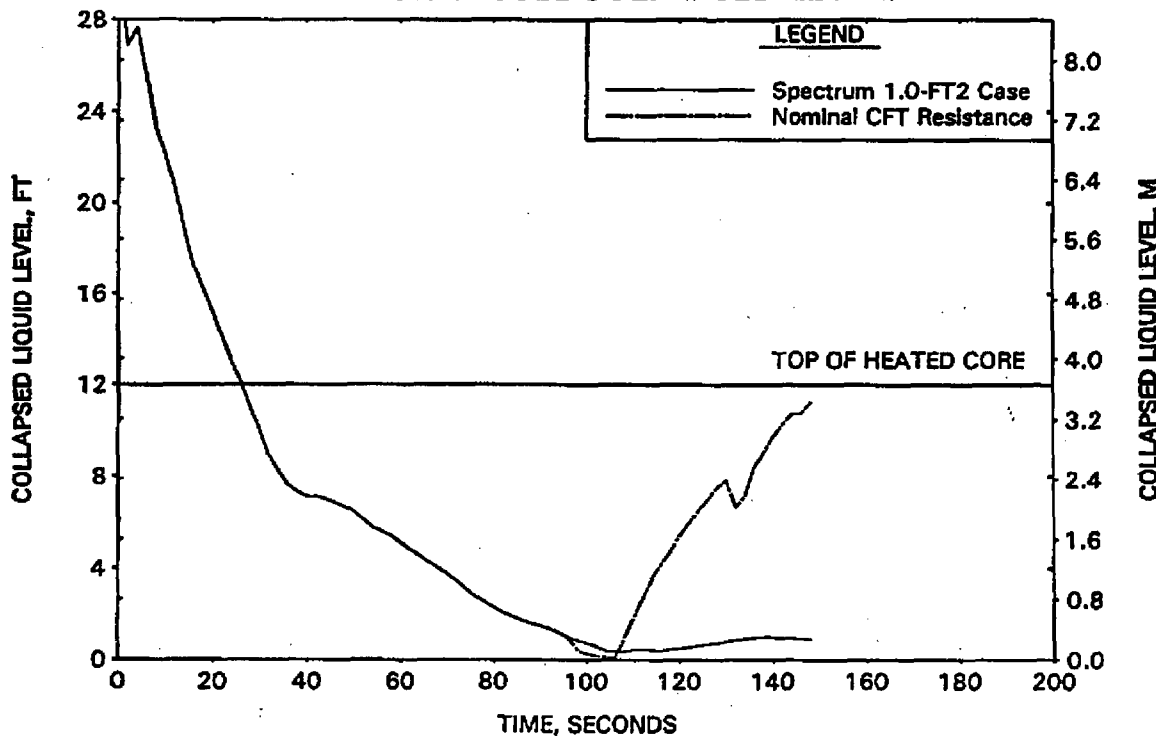


FIGURE A-222. CFT LINE RESISTANCE STUDY FOR 1.0-FT2 CLPD BREAK - CLPS LIQUID VOLUME.

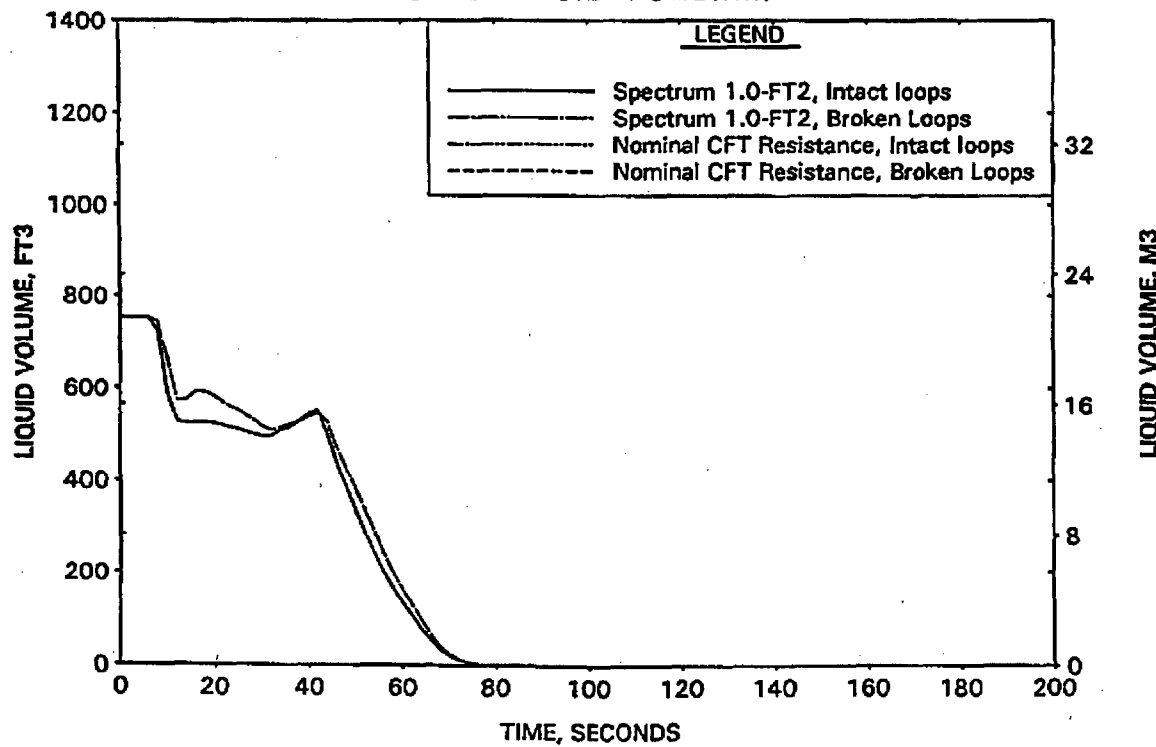


FIGURE A-223. CFT LINE RESISTANCE STUDY FOR 1.0-FT2 CLPD BREAK -
CORE HOT CHANNEL MIXTURE LEVELS.

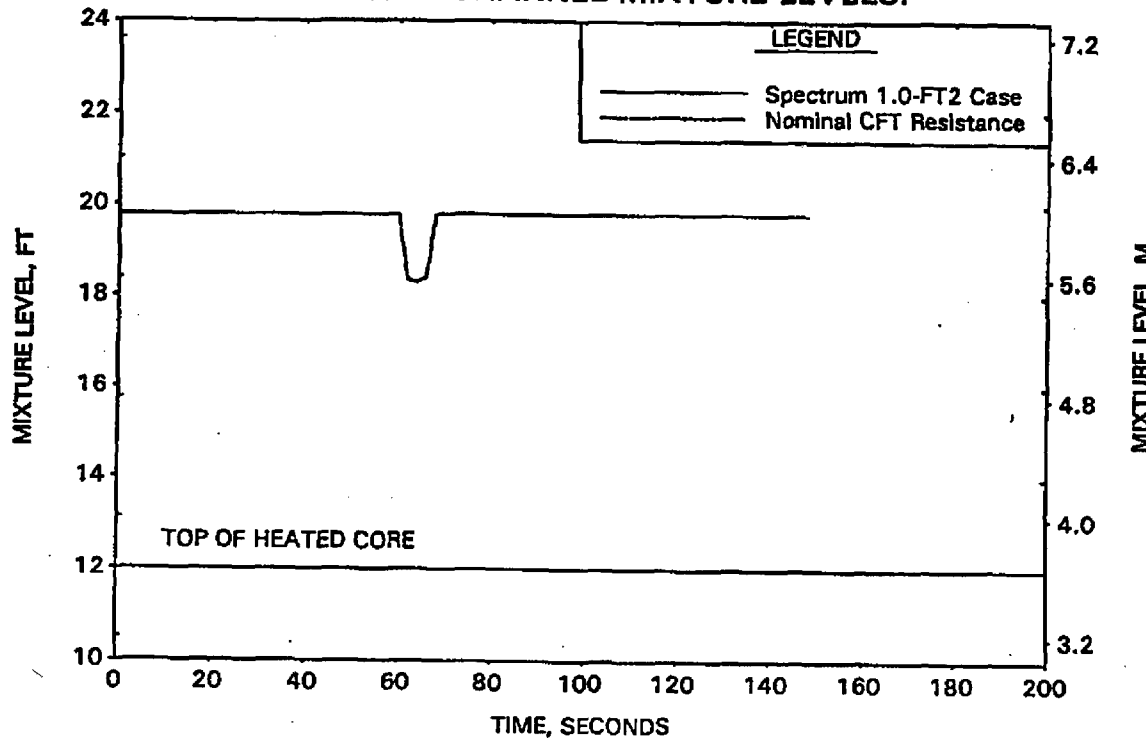


FIGURE A-224. CFT LINE RESISTANCE STUDY FOR 1.0-FT2 CLPD BREAK -
PEAK CLADDING TEMPERATURE.

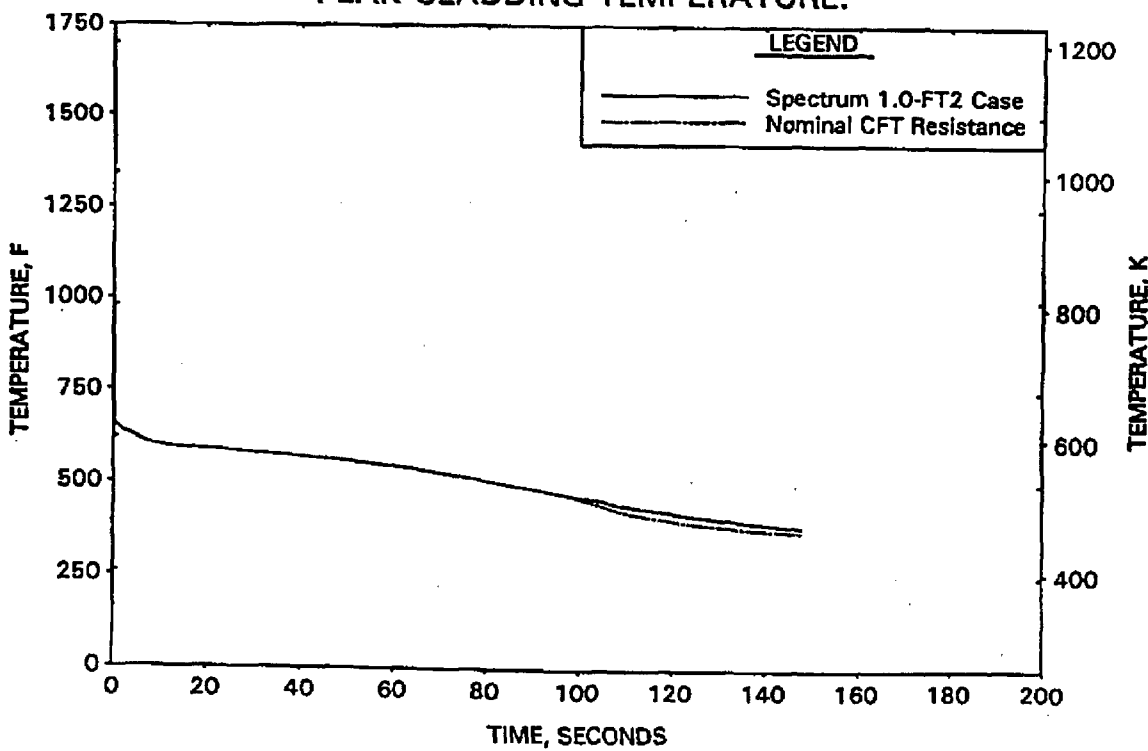


FIGURE A-225. CLPD 0.07-FT2 BREAK DISCHARGE COEFFICIENT STUDY - RCS PRESSURES.

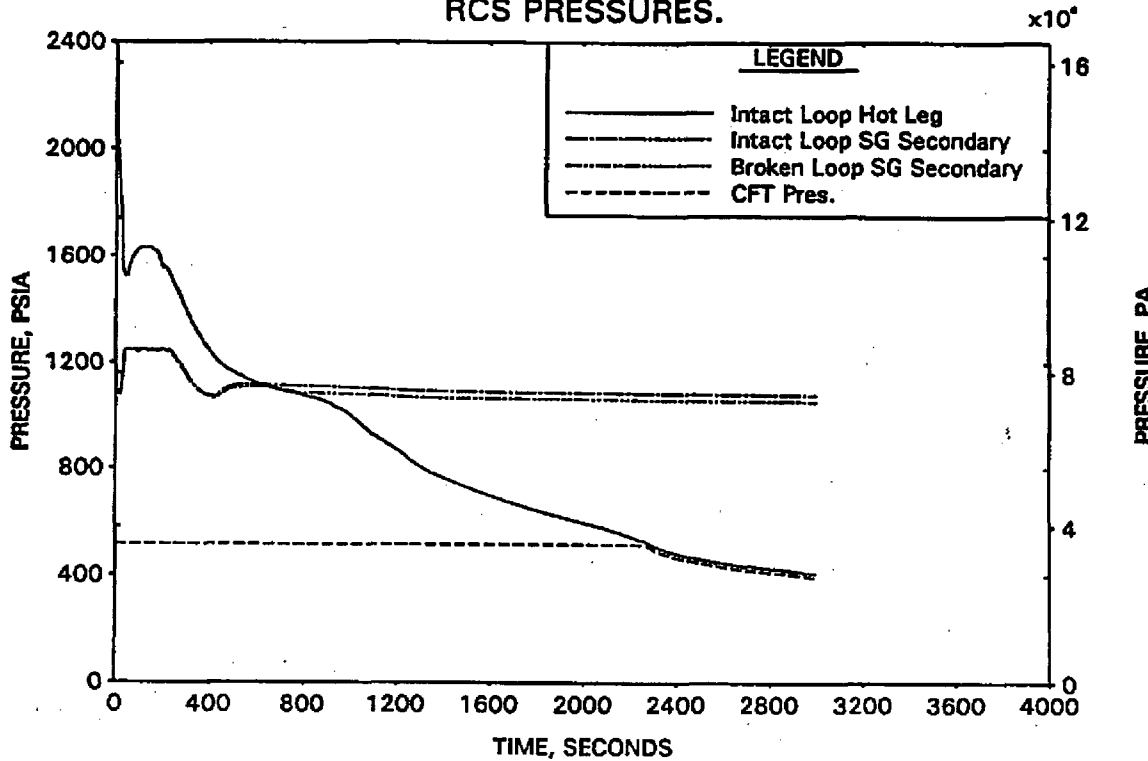


FIGURE A-226. CLPD 0.07-FT2 BREAK DISCHARGE COEFFICIENT STUDY - DC, RV, AND CORE COLLAPSED LEVELS.

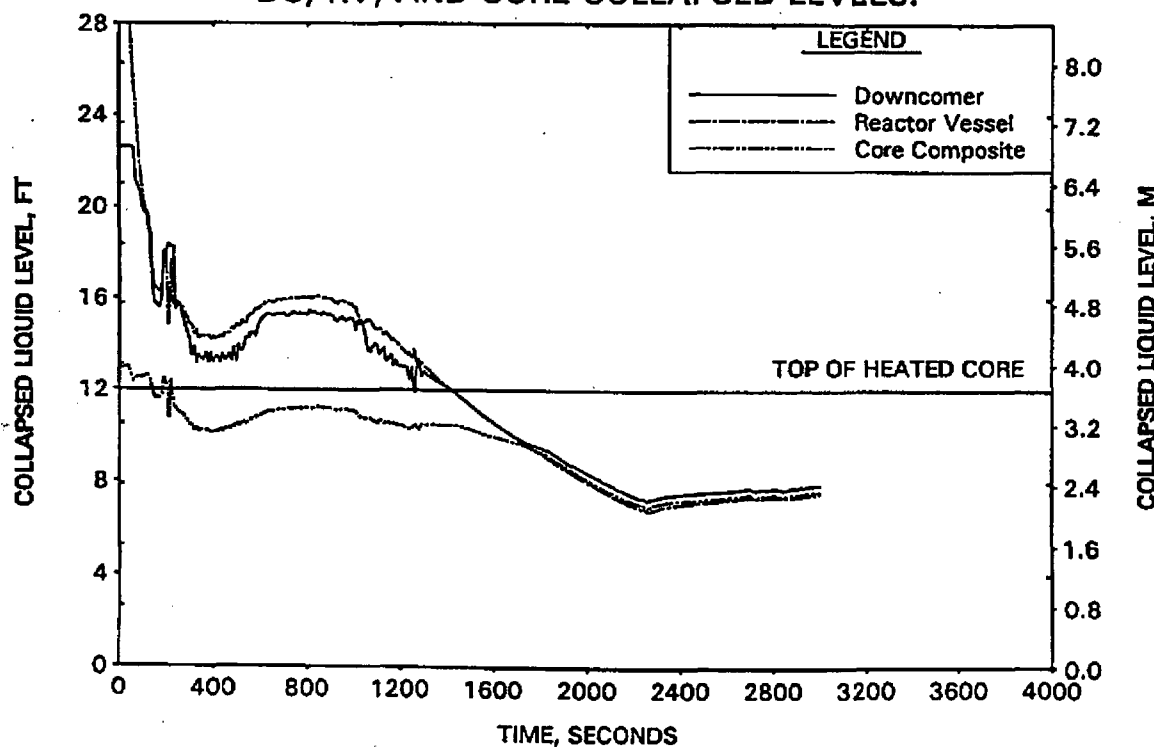


FIGURE A-227. CLPD 0.07-FT2 BREAK DISCHARGE COEFFICIENT STUDY -
BREAK AND TOTAL ECCS FLOWS.

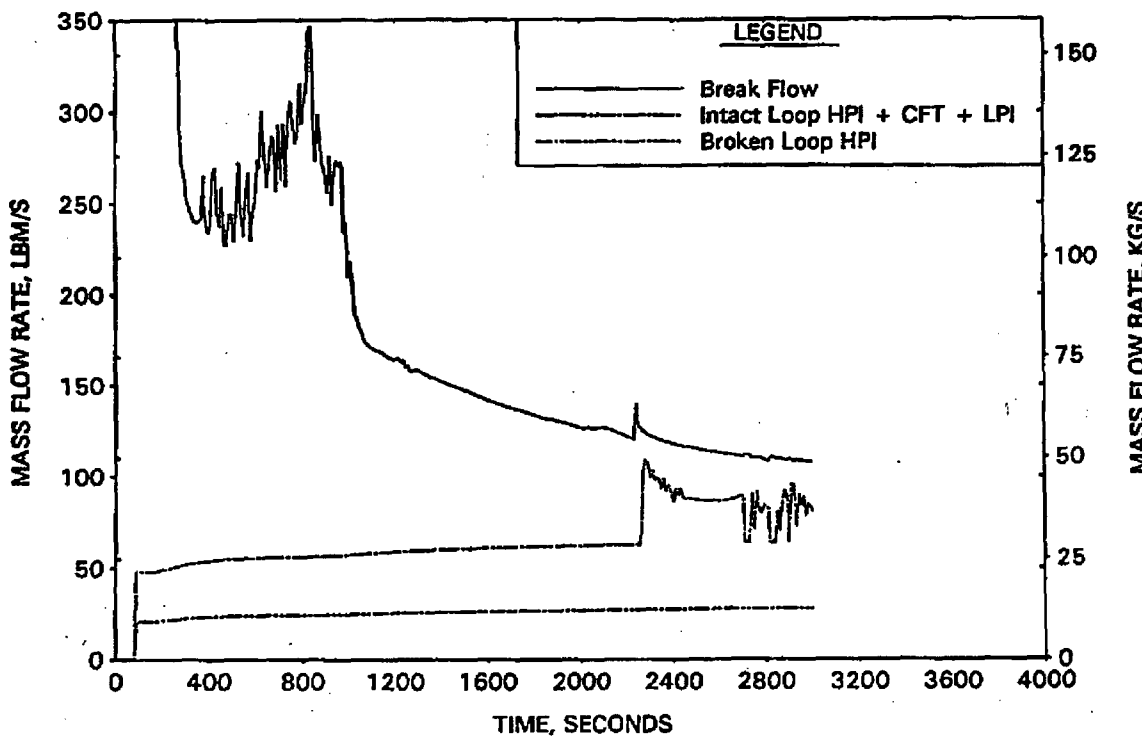


FIGURE A-228. CLPD 0.07-FT2 BREAK DISCHARGE COEFFICIENT STUDY -
BREAK VOLUME VOID FRACTION.

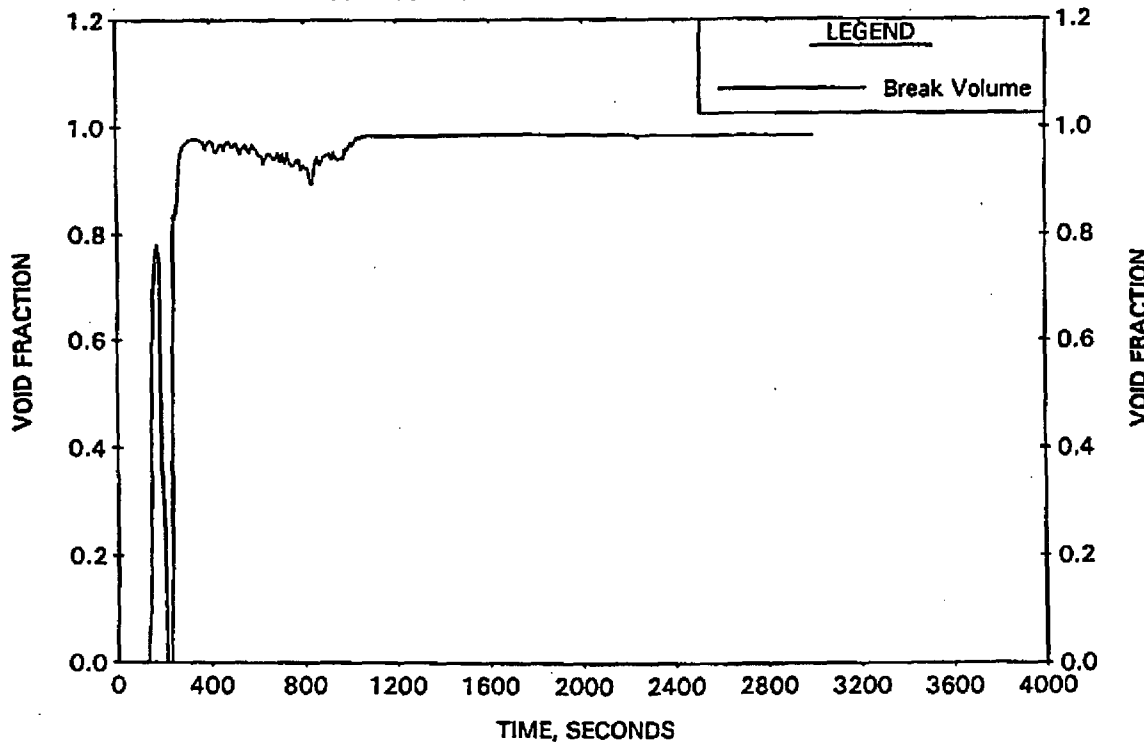


FIGURE A-229. CLPD 0.07-FT2 BREAK DISCHARGE COEFFICIENT STUDY - BROKEN LOOP COLLAPSED LEVELS.

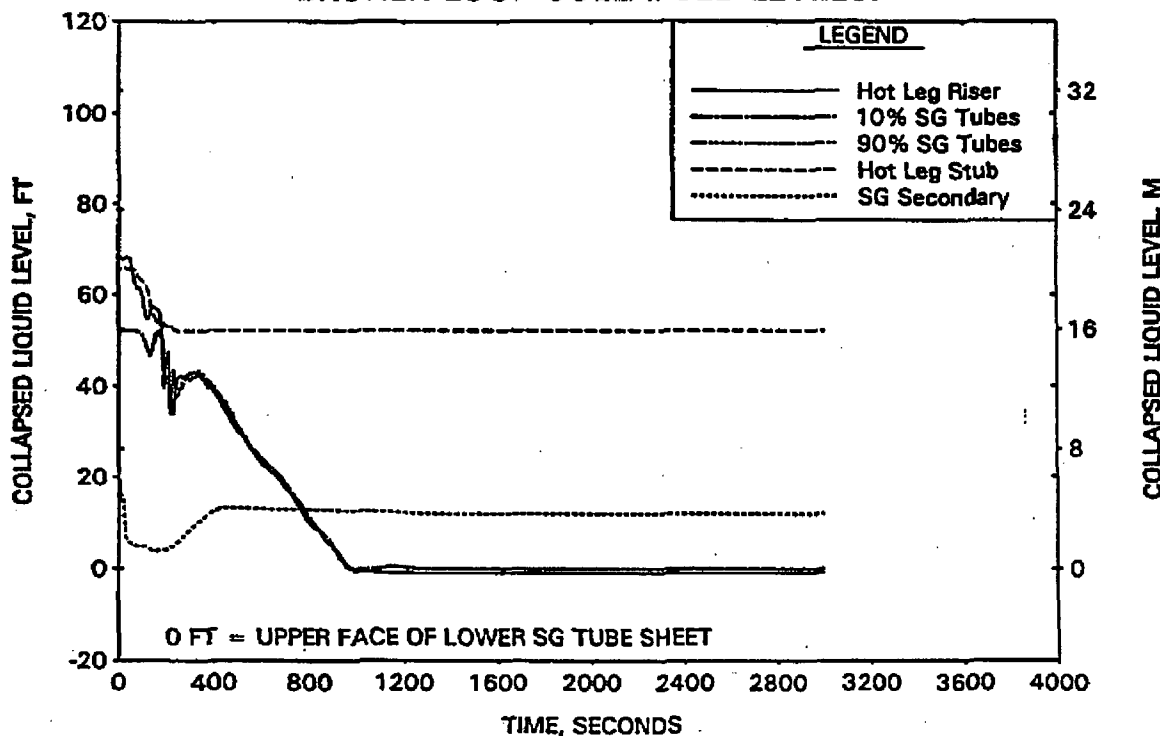


FIGURE A-230. CLPD 0.07-FT2 BREAK DISCHARGE COEFFICIENT STUDY - INTACT LOOP COLLAPSED LEVELS.

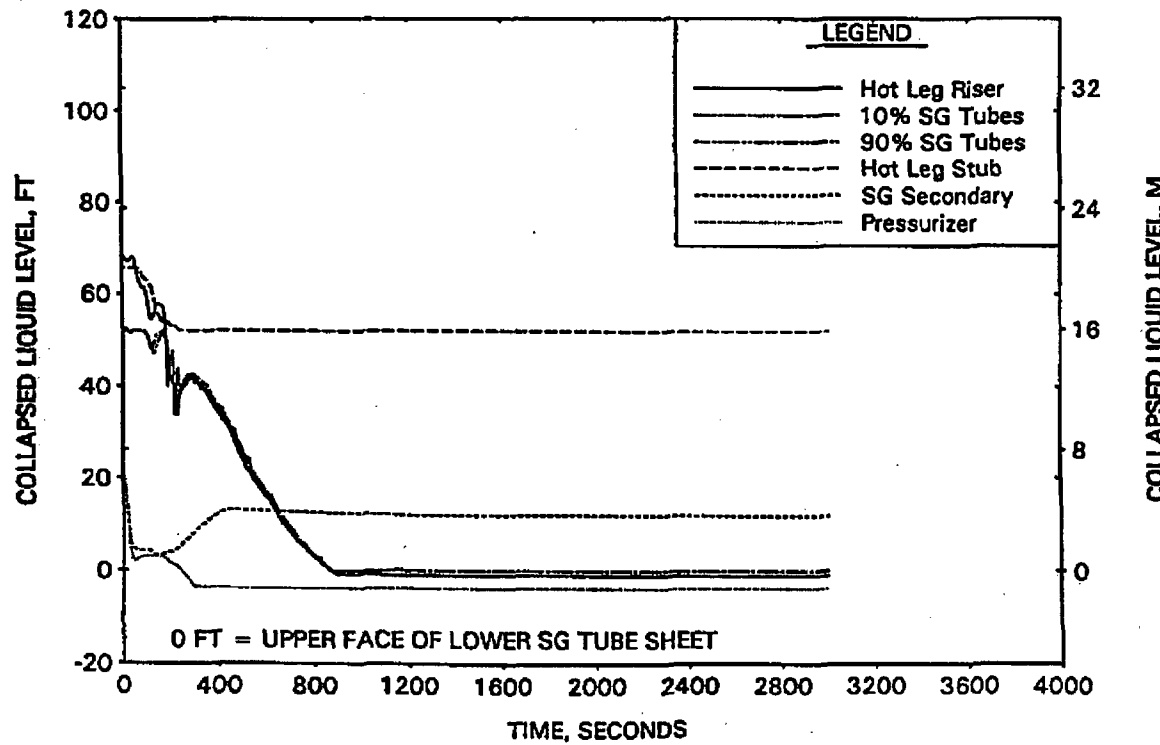


FIGURE A-231. CLPD 0.07-FT² BREAK DISCHARGE COEFFICIENT STUDY - CLPD COLLAPSED LEVELS.

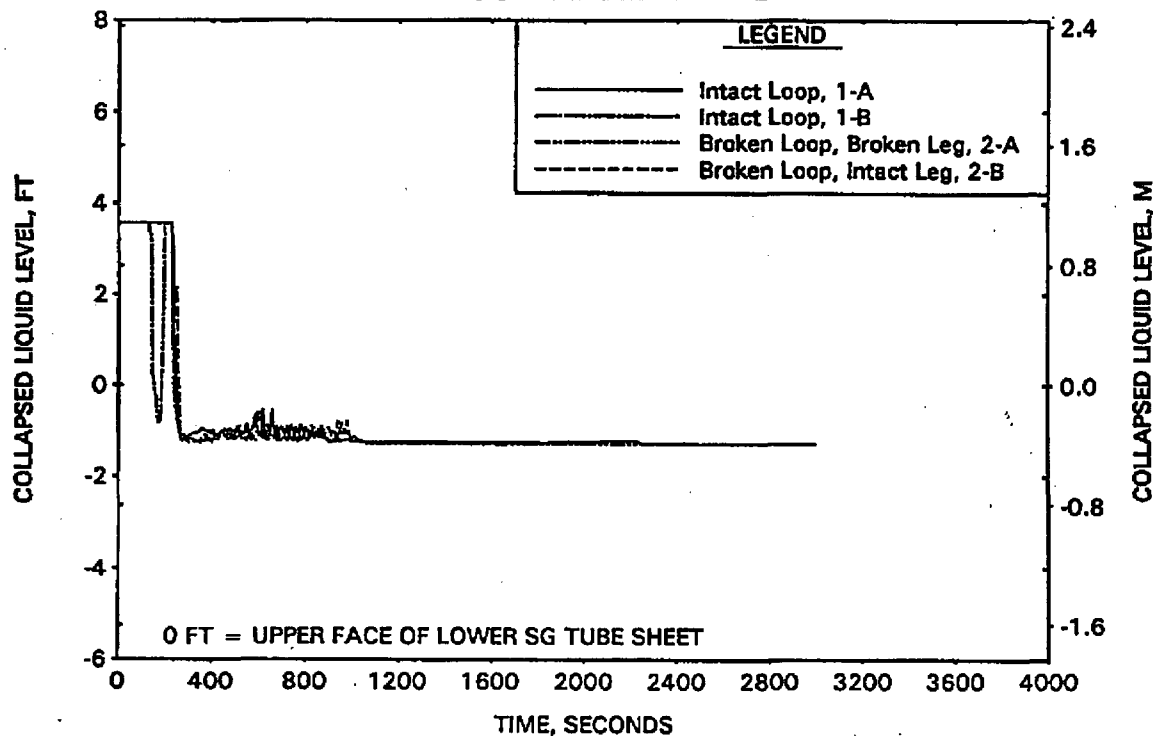


FIGURE A-232. CLPD 0.07-FT² BREAK DISCHARGE COEFFICIENT STUDY - CLPS LIQUID VOLUME.

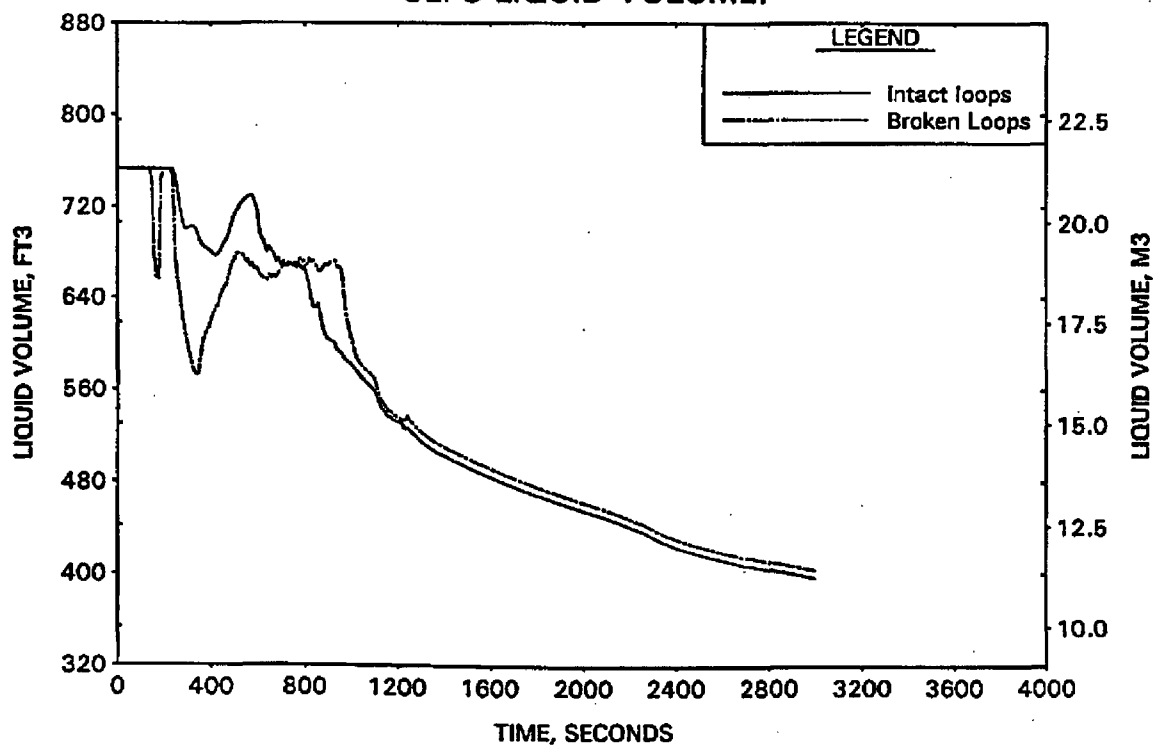


FIGURE A-233. CLPD 0.07-FT2 BREAK DISCHARGE COEFFICIENT STUDY - HOT LEG AND RVVV FLOWS.

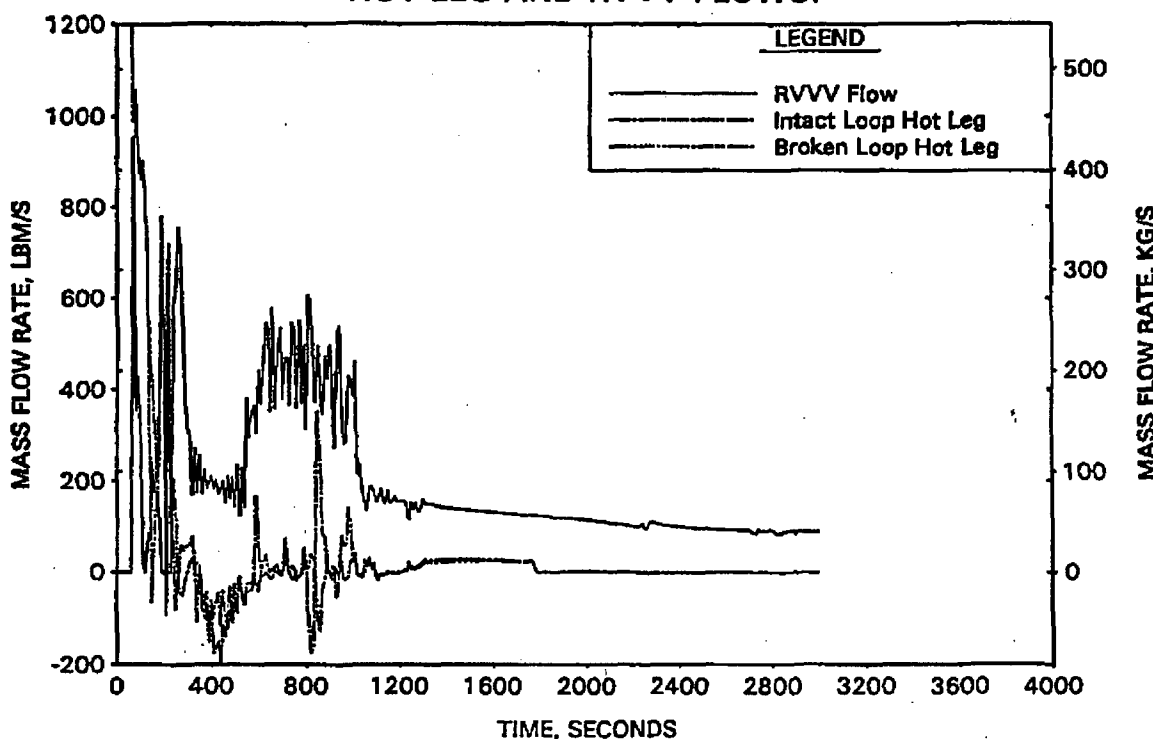


FIGURE A-234. CLPD 0.07-FT2 BREAK DISCHARGE COEFFICIENT STUDY - CORE MIXTURE LEVELS.

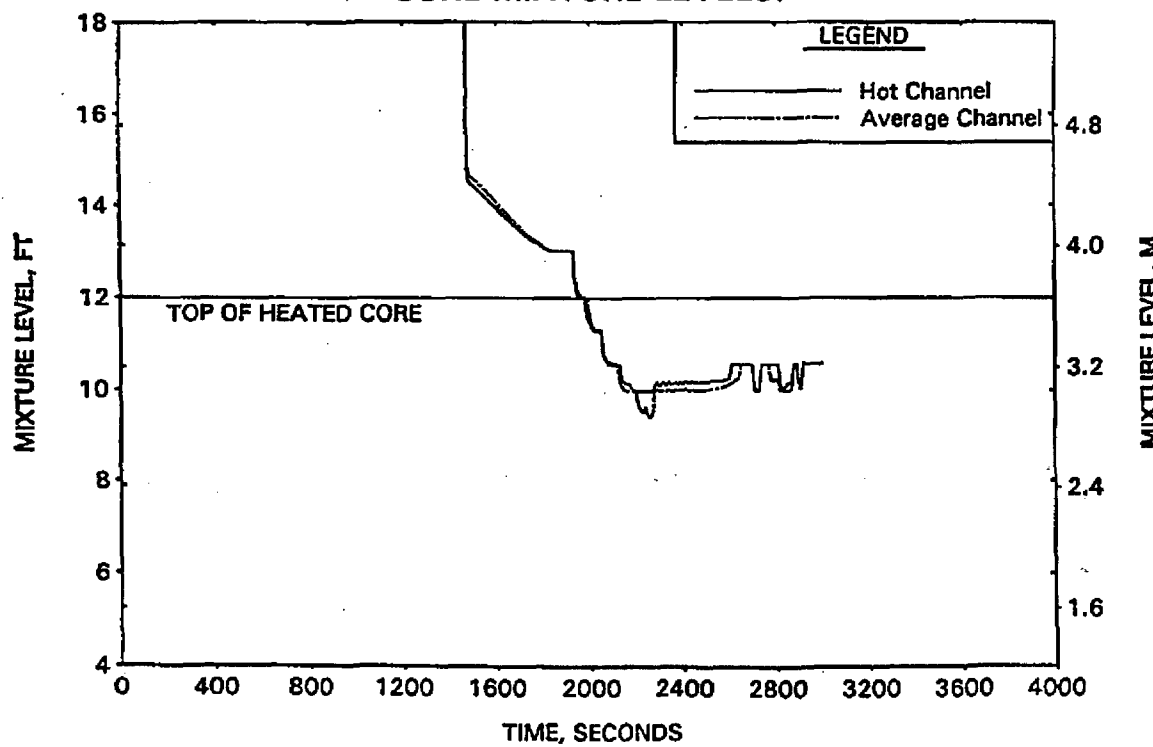


FIGURE A-235. CLPD 0.07-FT² BREAK DISCHARGE COEFFICIENT STUDY - HOT CHANNEL CLAD TEMPERATURES.

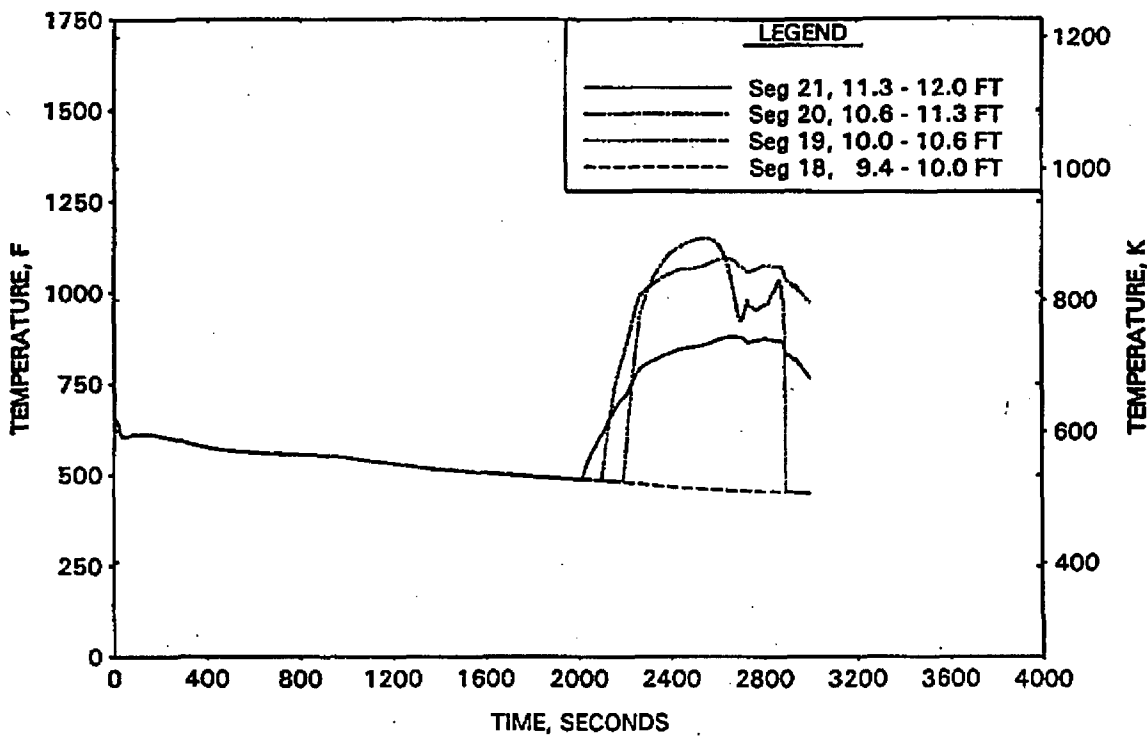


FIGURE A-236. CLPD 0.07-FT² BREAK DISCHARGE COEFFICIENT STUDY - HOT CHANNEL STEAM TEMPERATURES.

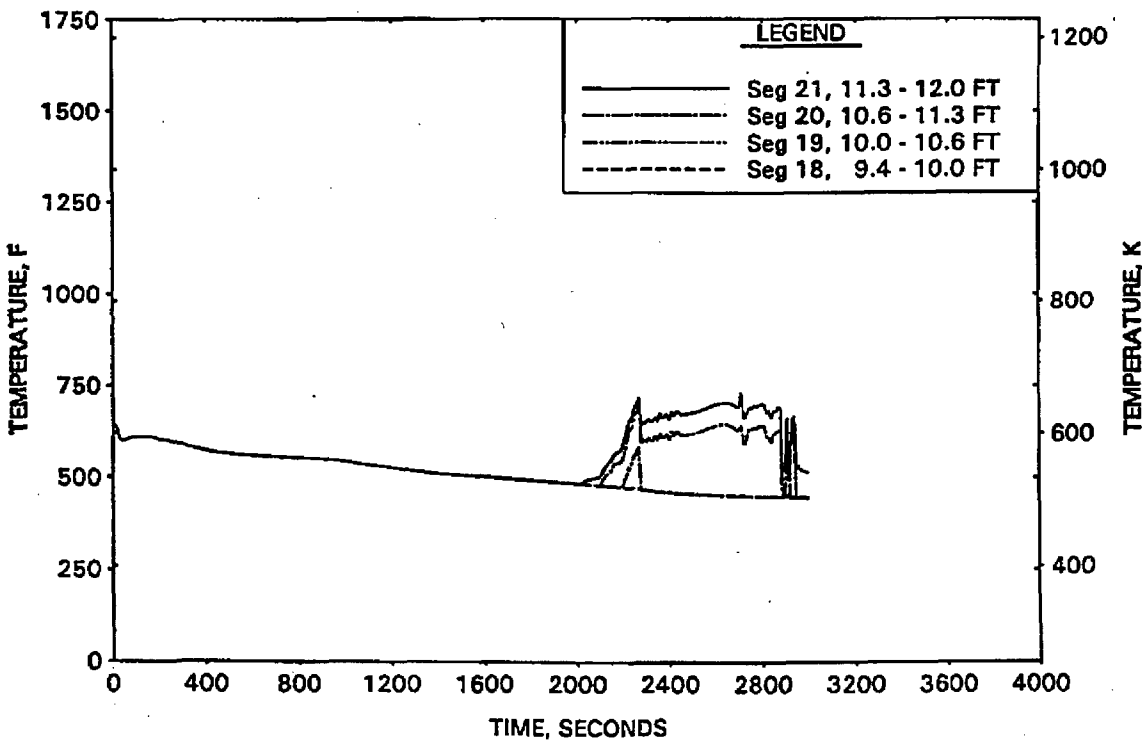


FIGURE A-237. CLPD 0.07-FT2 BREAK DISCHARGE COEFFICIENT STUDY -
UPPER ELEVATION AVE CHANNEL CLAD TEMPERATURES.

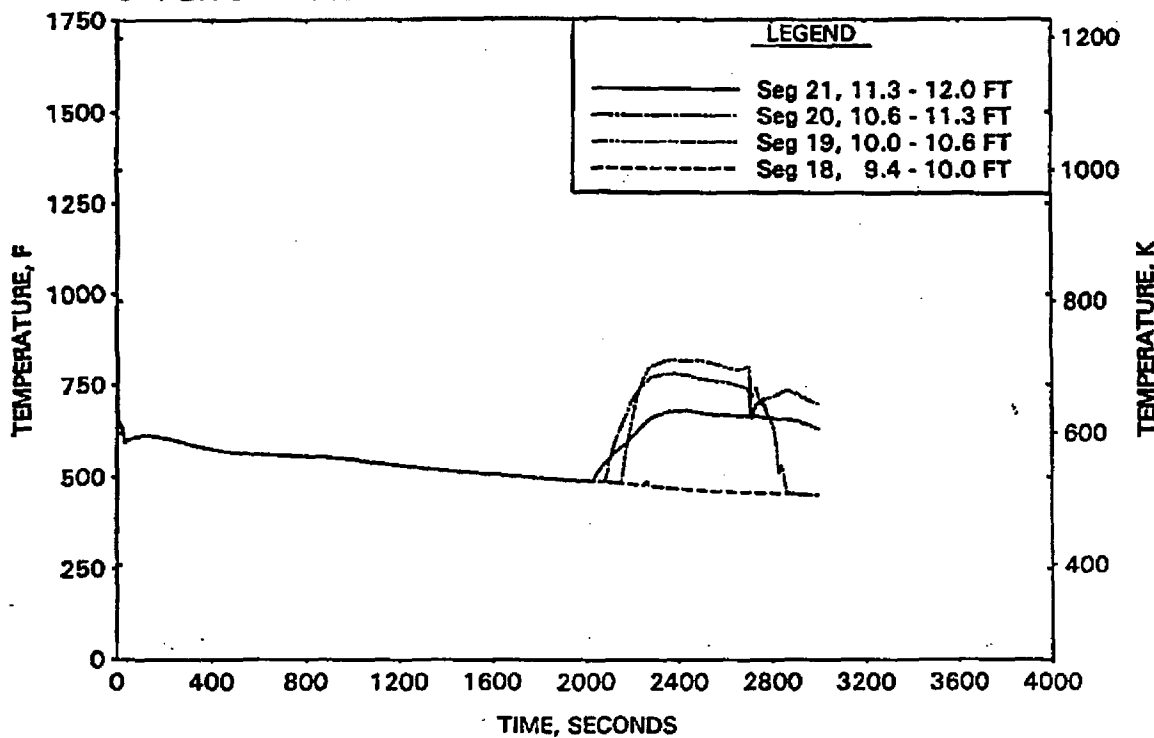


FIGURE A-238. CLPD 0.07-FT2 BREAK DISCHARGE COEFFICIENT STUDY -
UPPER ELEVATION AVE CHANNEL STEAM TEMPERATURES.

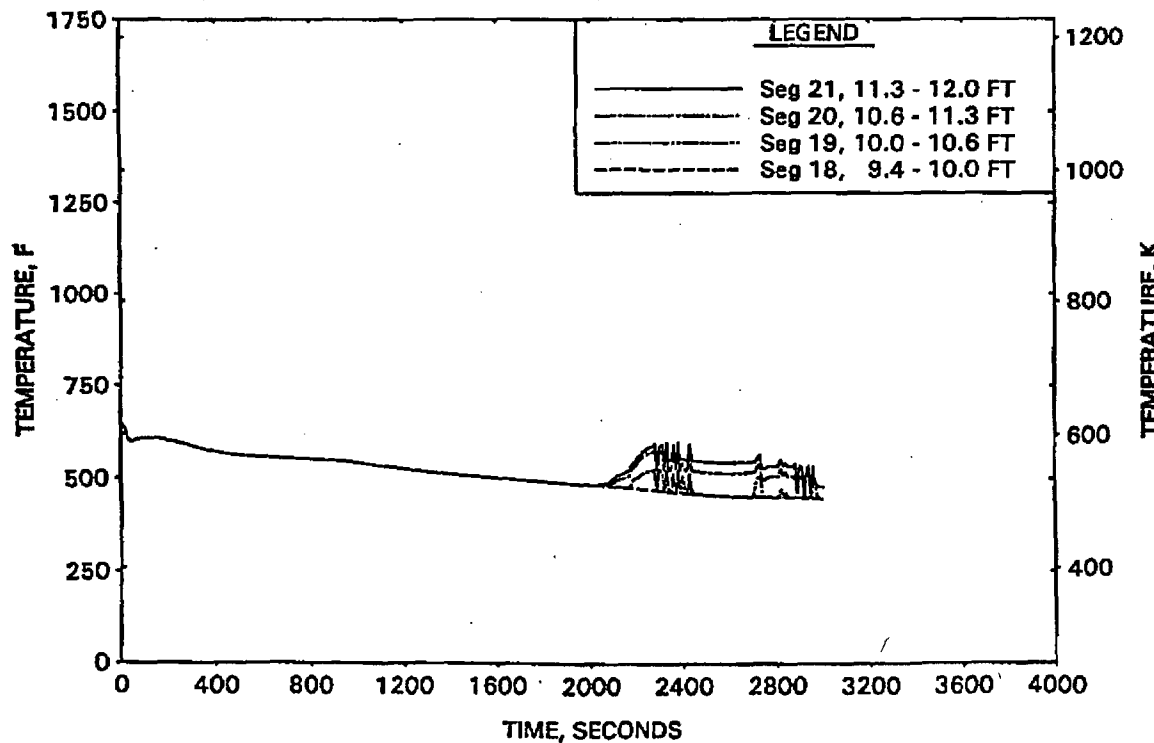


FIGURE A-239. 0.1- AND 0.07-FT² CLPD BREAK DISCHARGE STUDY -
COMPARISON OF RCS PRESSURES.

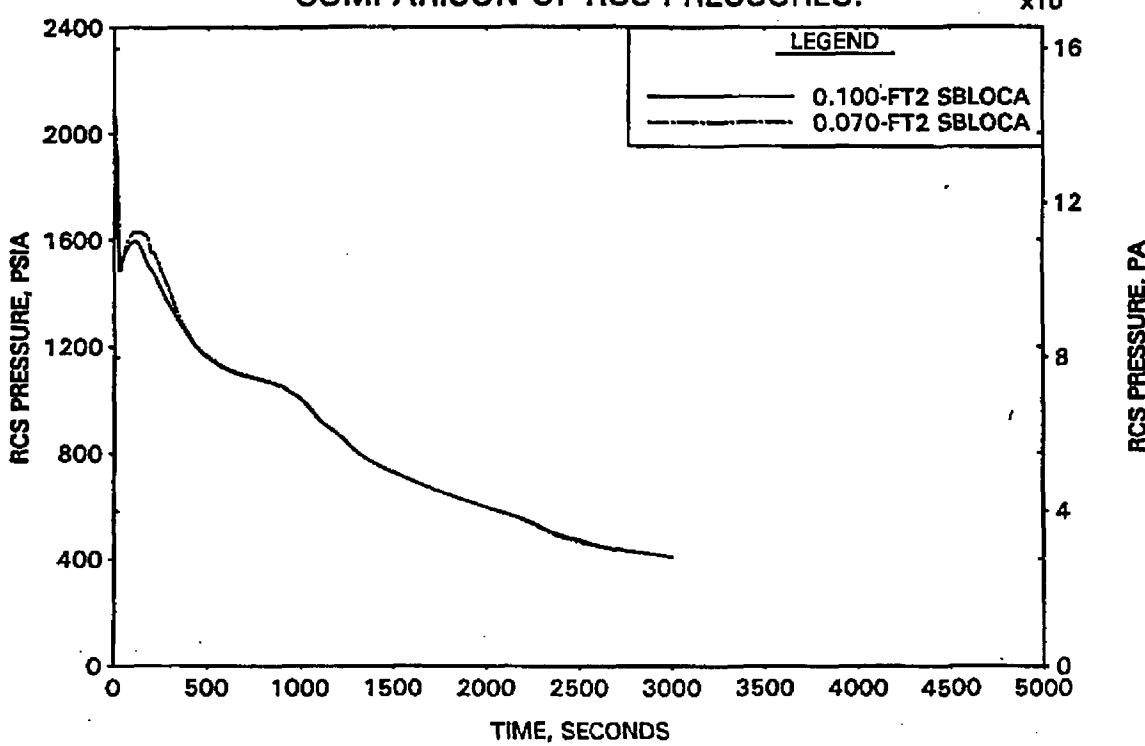


FIGURE A-240. 0.1- AND 0.07-FT² CLPD BREAK DISCHARGE STUDY -
COMPARISON OF BREAK FLOW RATES.

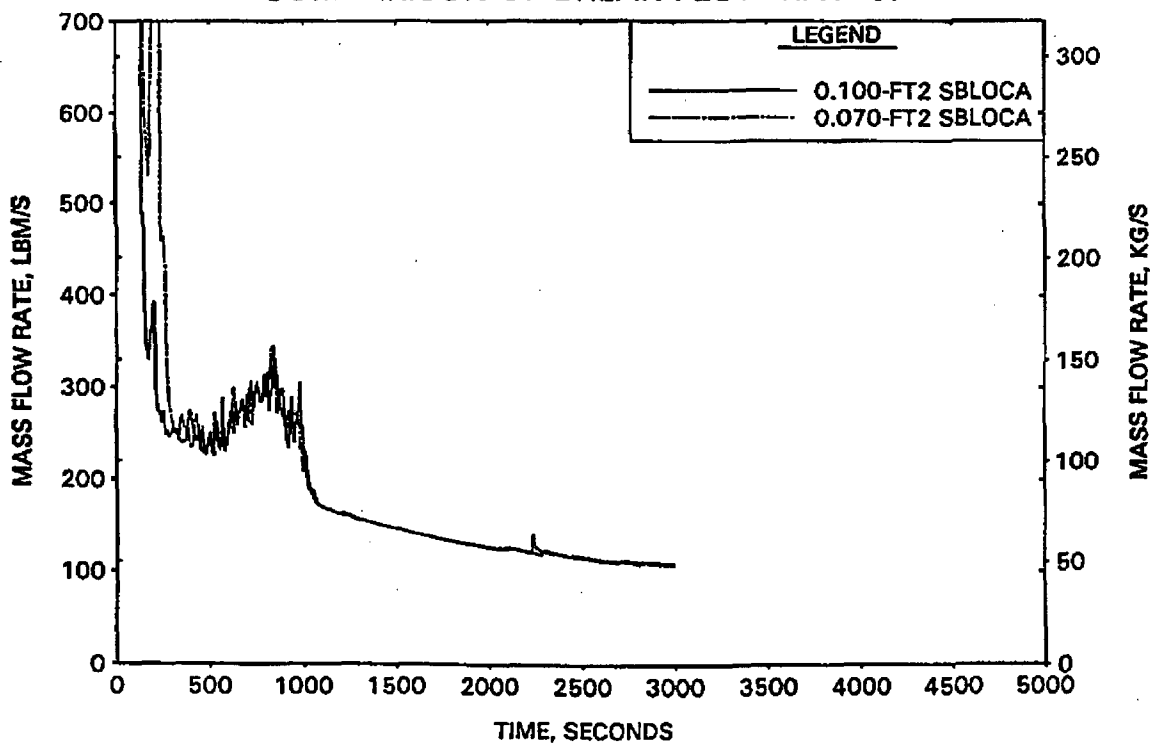


FIGURE A-241. 0.1- AND 0.07-FT2 CLPD BREAK DISCHARGE STUDY - COMPARISON OF REACTOR VESSEL COLLAPSED LEVELS.

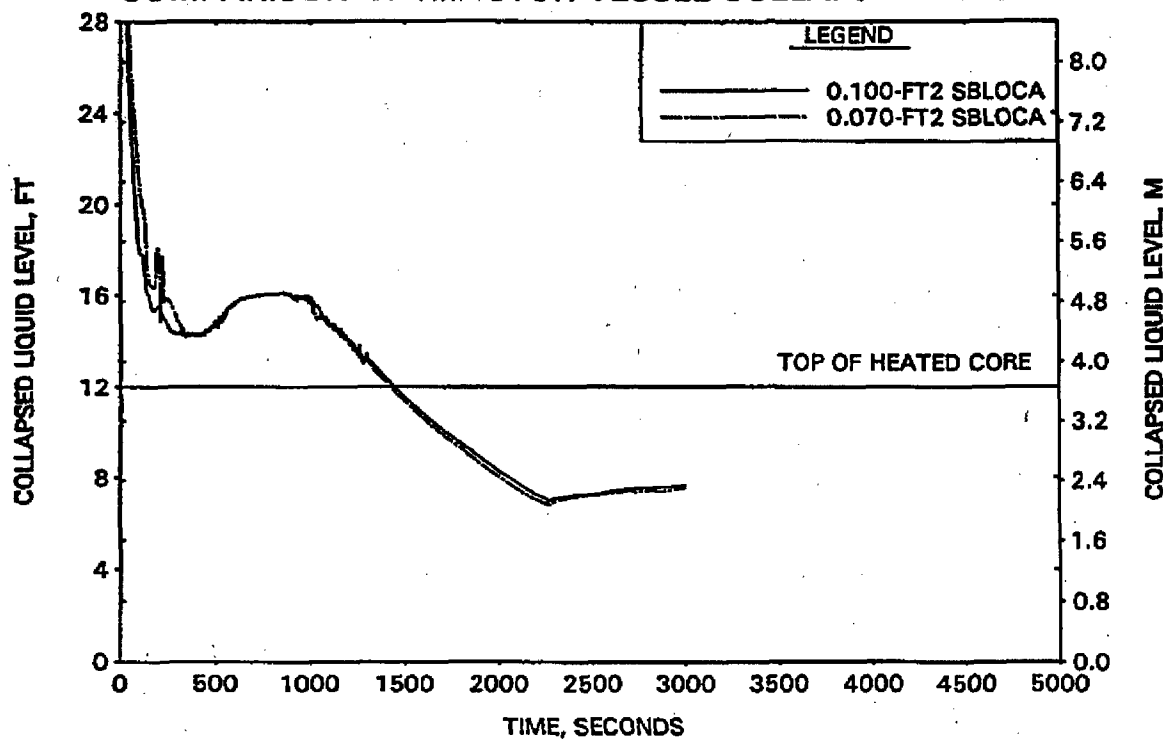


FIGURE A-242. 0.1- AND 0.07-FT2 CLPD BREAK DISCHARGE STUDY - COMPARISON OF INTEGRATED BREAK FLOWS. $\times 10^3$

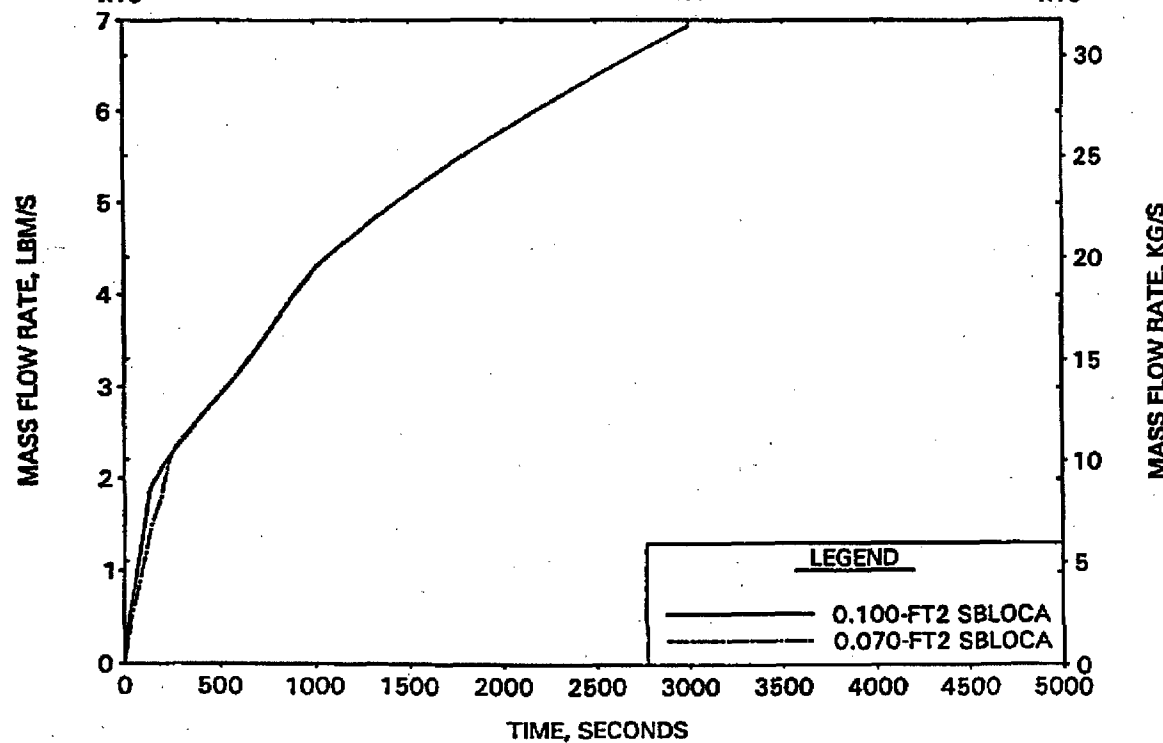


FIGURE A-243. 0.1- AND 0.07-FT2 CLPD BREAK DISCHARGE STUDY - COMPARISON OF HOT CHANNEL MIXTURE LEVELS.

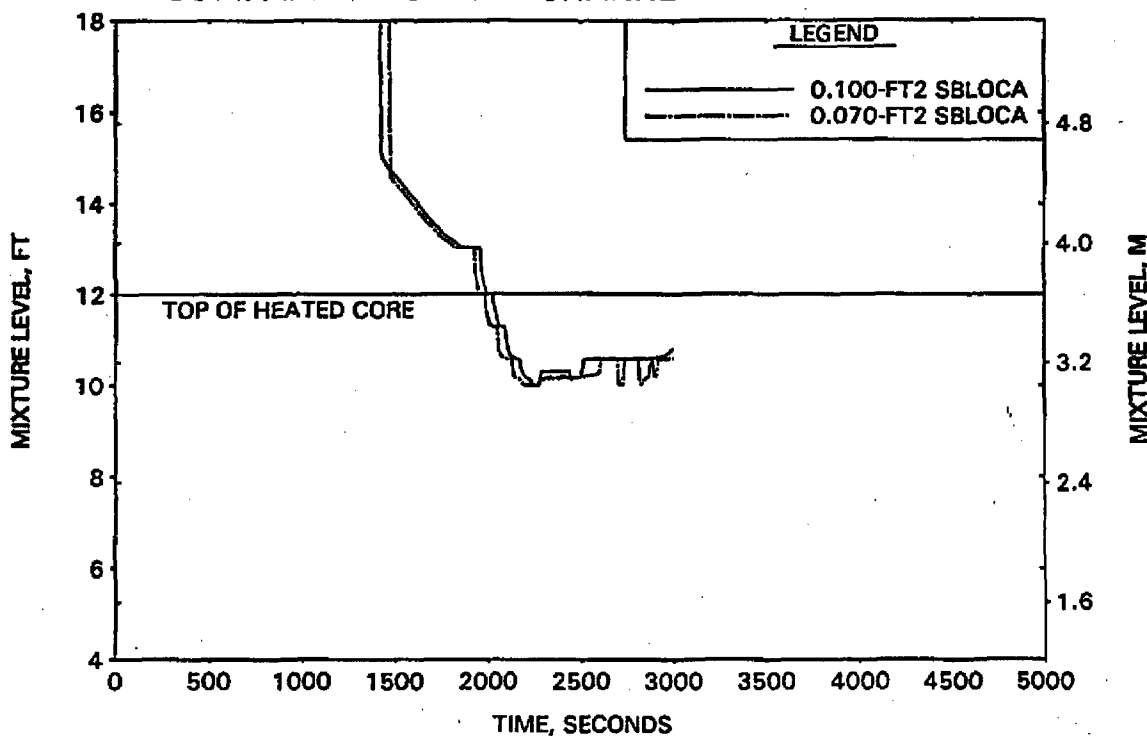


FIGURE A-244. 0.1- AND 0.07-FT2 CLPD BREAK DISCHARGE STUDY - COMPARISON OF PEAK CLADDING TEMPERATURES.

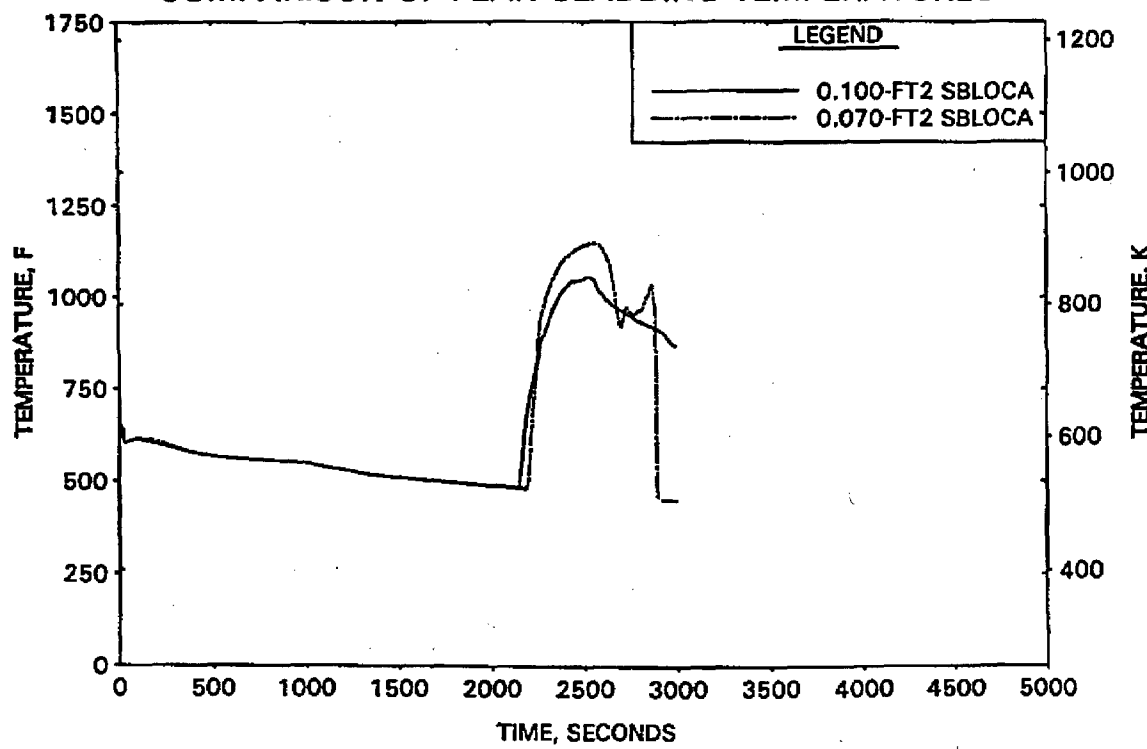


FIGURE A-245. CLPD 0.21-FT2 BREAK DISCHARGE COEFFICIENT STUDY - RCS PRESSURES.

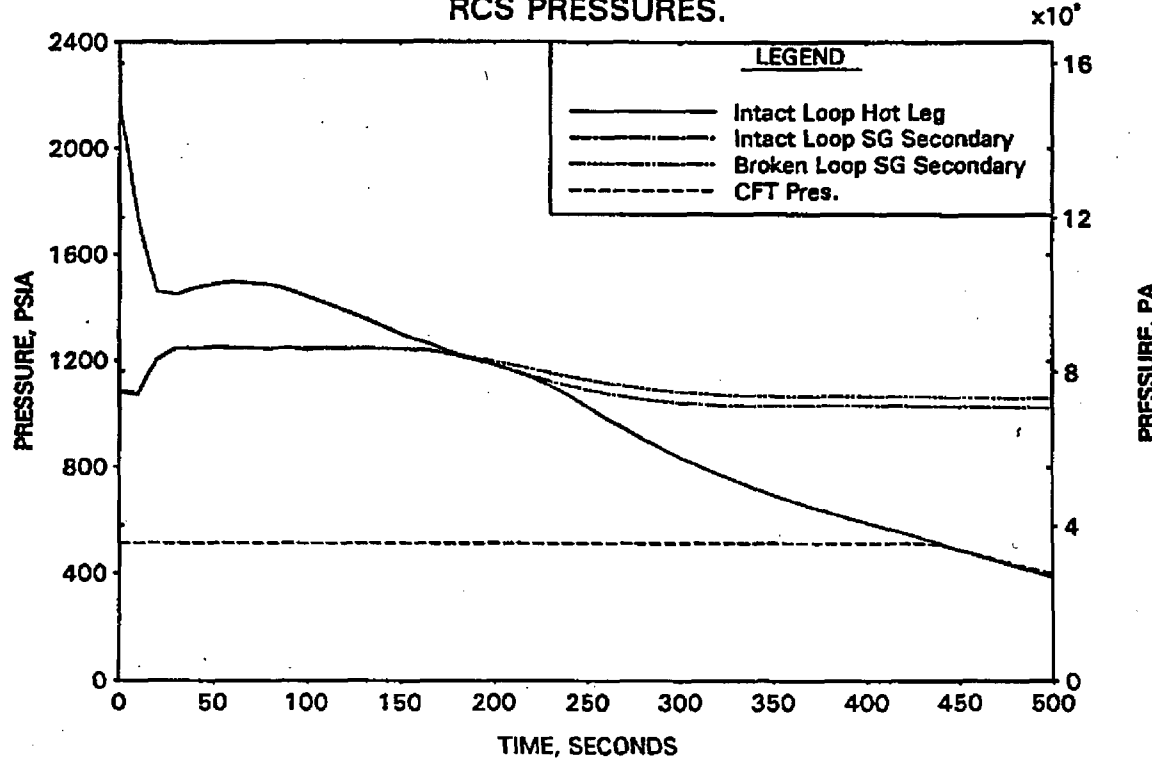


FIGURE A-246. CLPD 0.21-FT2 BREAK DISCHARGE COEFFICIENT STUDY - DC, RV, AND CORE COLLAPSED LEVELS.

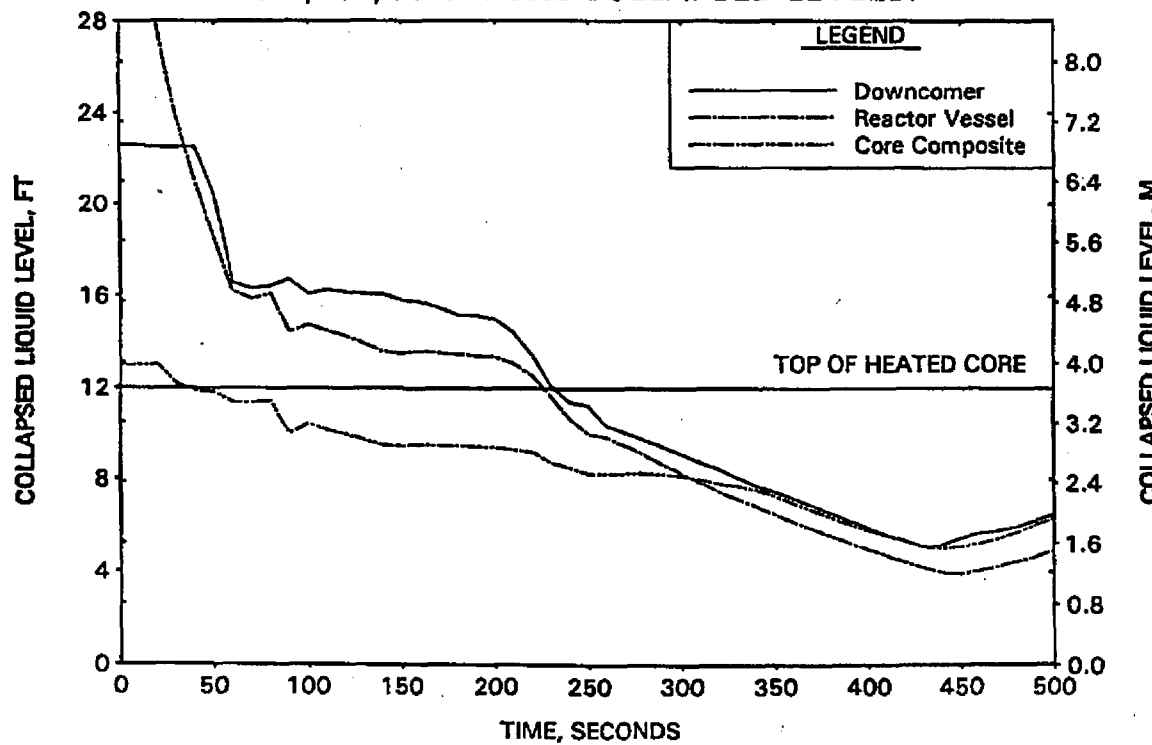


FIGURE A-247. CLPD 0.21-FT² BREAK DISCHARGE COEFFICIENT STUDY -
BREAK AND TOTAL ECCS FLOWS.

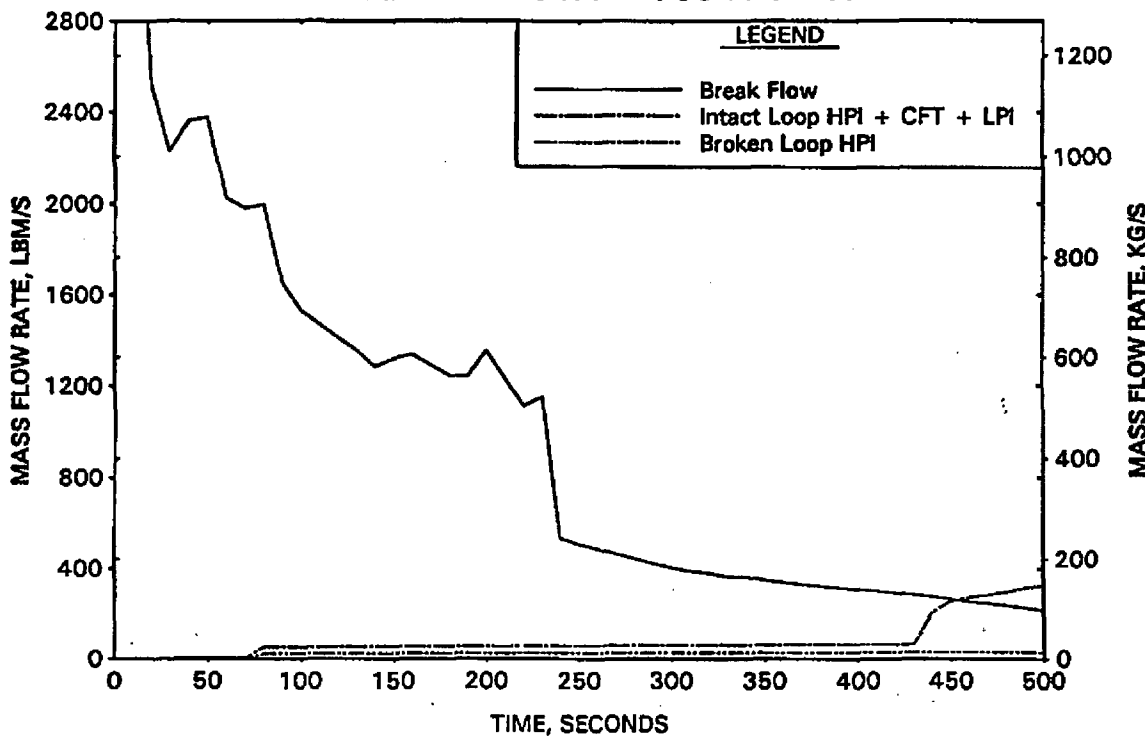


FIGURE A-248. CLPD 0.21-FT² BREAK DISCHARGE COEFFICIENT STUDY -
BREAK VOLUME VOID FRACTION.

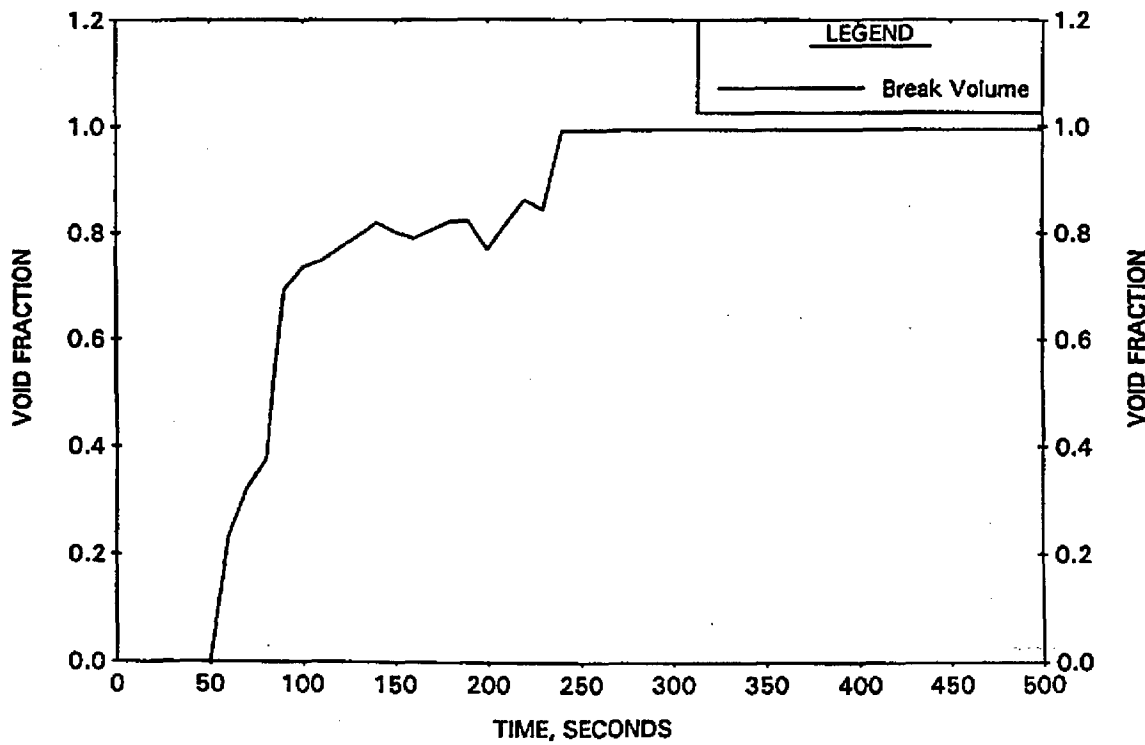


FIGURE A-249. CLPD 0.21-FT2 BREAK DISCHARGE COEFFICIENT STUDY - BROKEN LOOP COLLAPSED LEVELS.

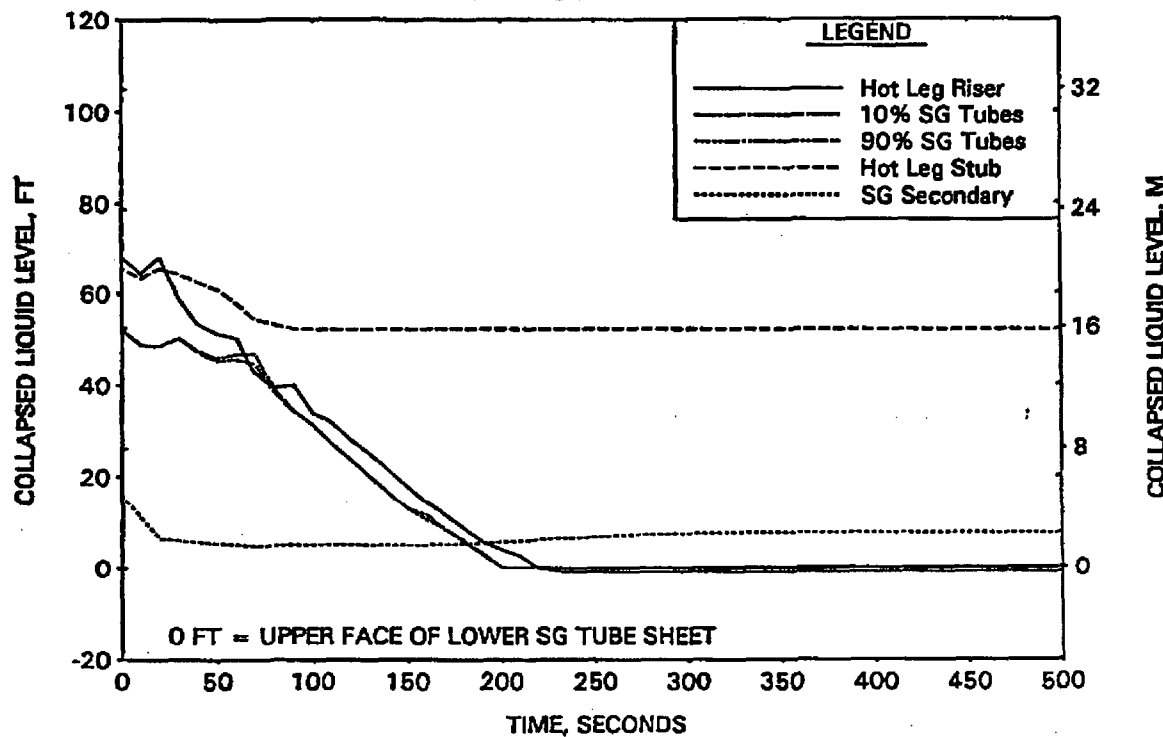


FIGURE A-250. CLPD 0.21-FT2 BREAK DISCHARGE COEFFICIENT STUDY - INTACT LOOP COLLAPSED LEVELS.

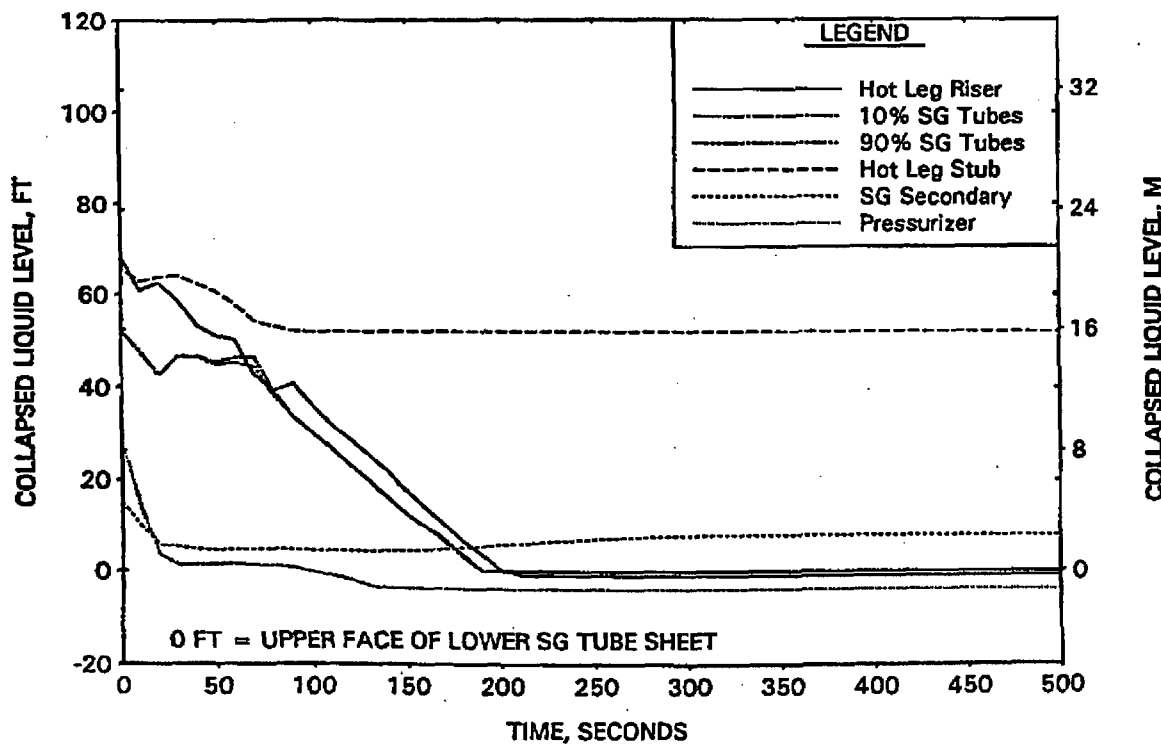


FIGURE A-251. CLPD 0.21-FT² BREAK DISCHARGE COEFFICIENT STUDY - CLPD COLLAPSED LEVELS.

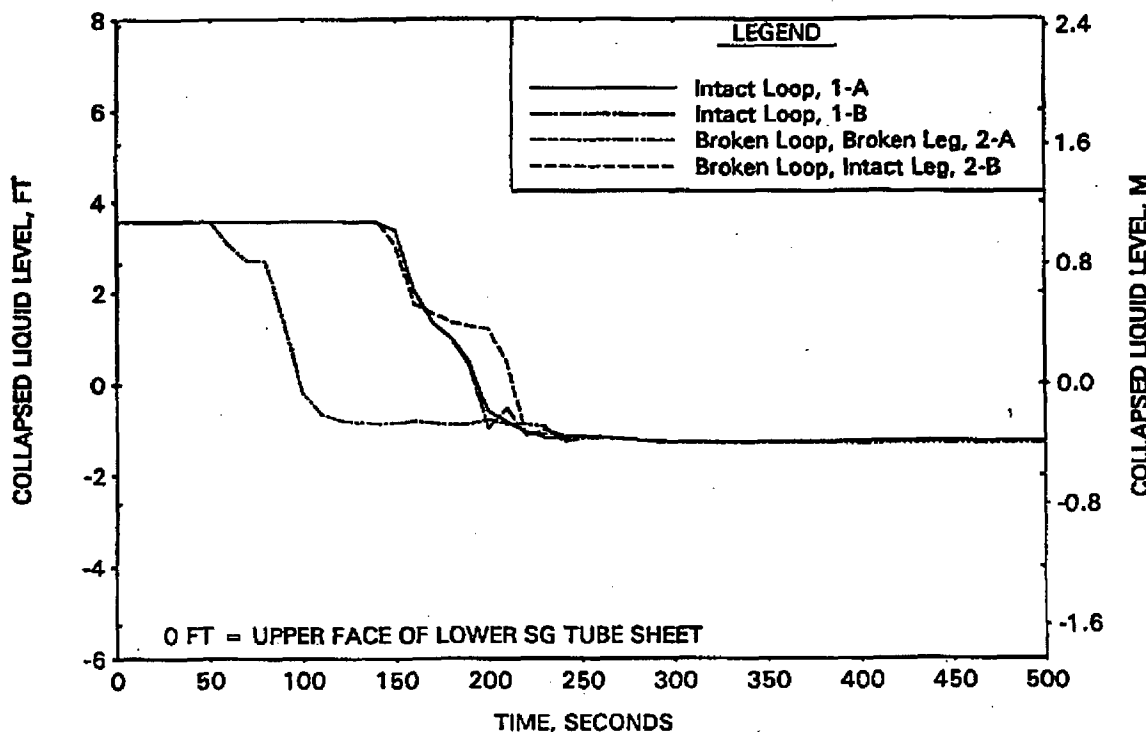


FIGURE A-252. CLPD 0.21-FT² BREAK DISCHARGE COEFFICIENT STUDY - CLPS LIQUID VOLUME.

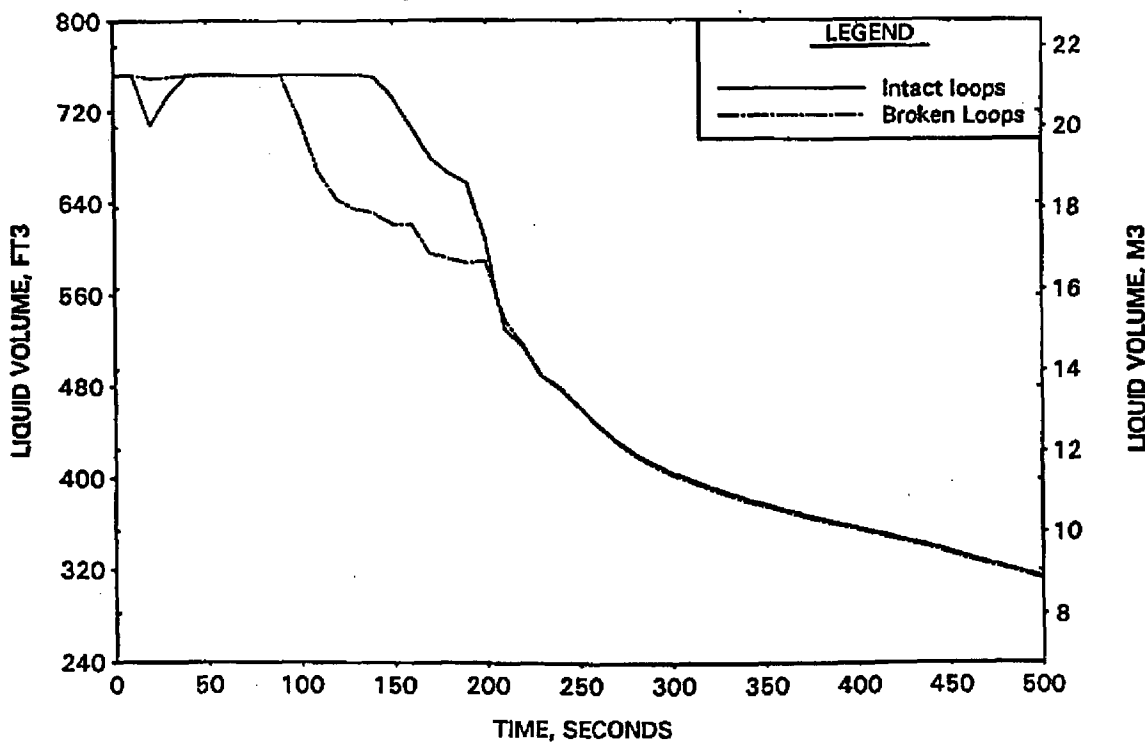


FIGURE A-253. CLPD 0.21-FT² BREAK DISCHARGE COEFFICIENT STUDY - HOT LEG AND RVVV FLOWS.

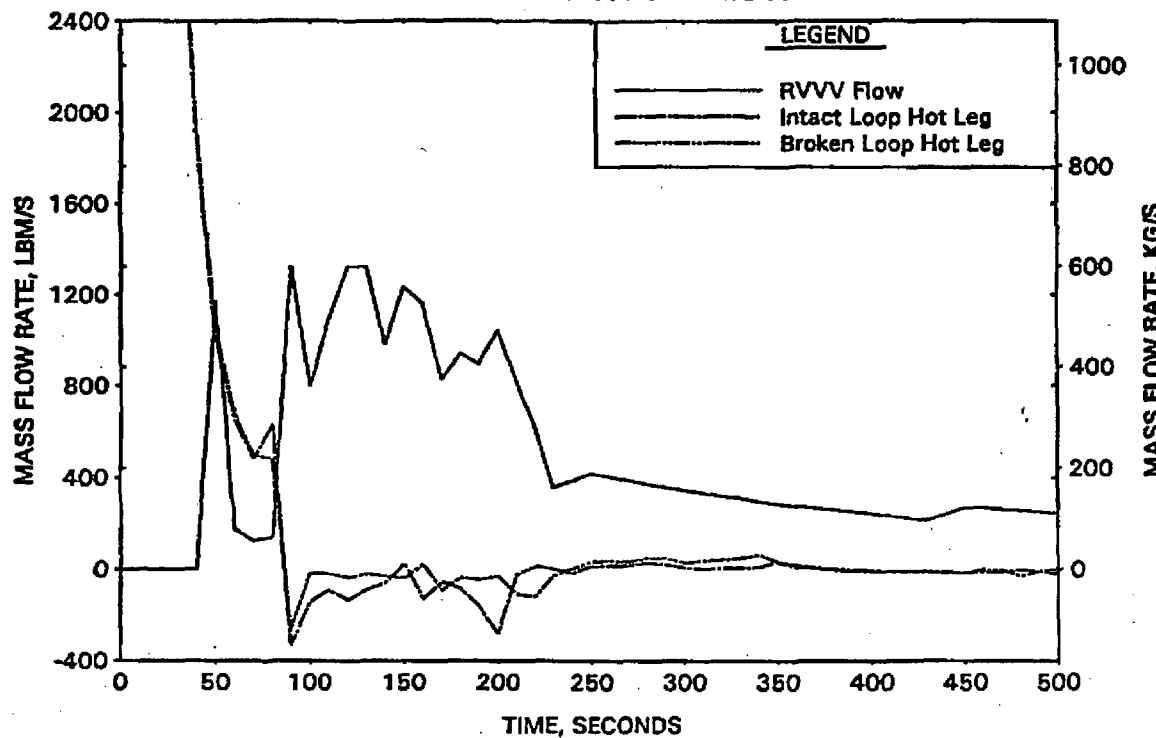


FIGURE A-254. CLPD 0.21-FT² BREAK DISCHARGE COEFFICIENT STUDY - CORE MIXTURE LEVELS.

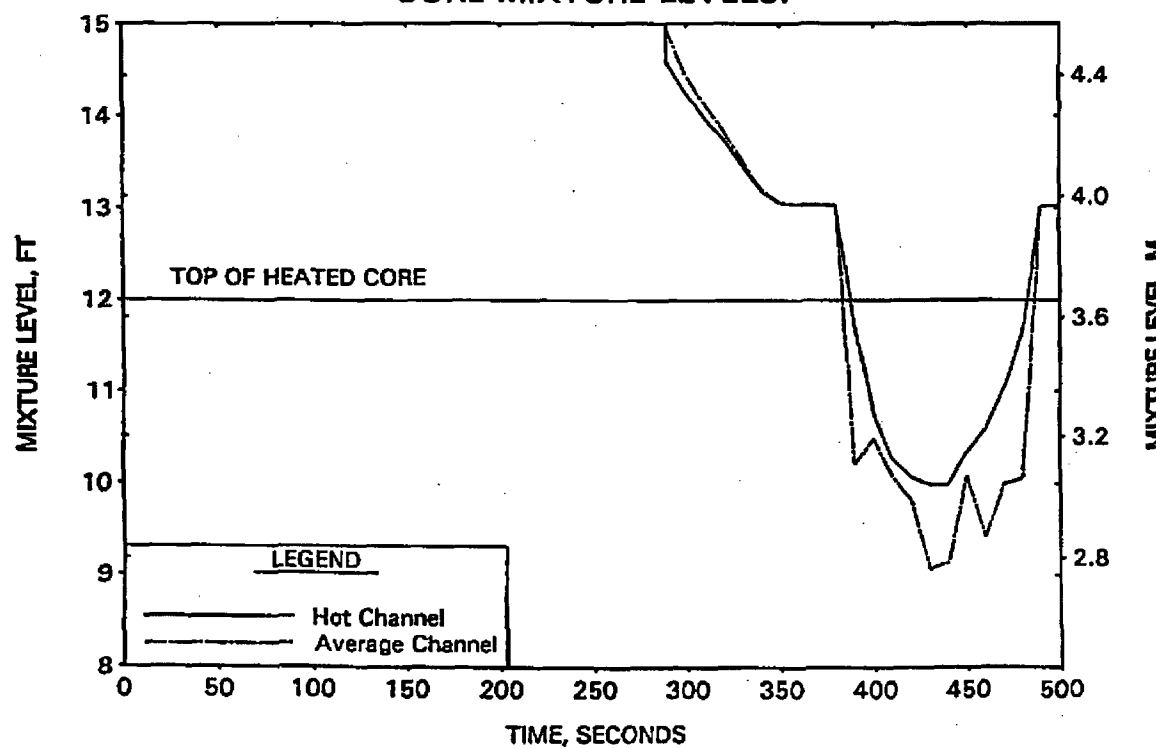


FIGURE A-255. CLPD 0.21-FT² BREAK DISCHARGE COEFFICIENT STUDY - HOT CHANNEL CLAD TEMPERATURES.

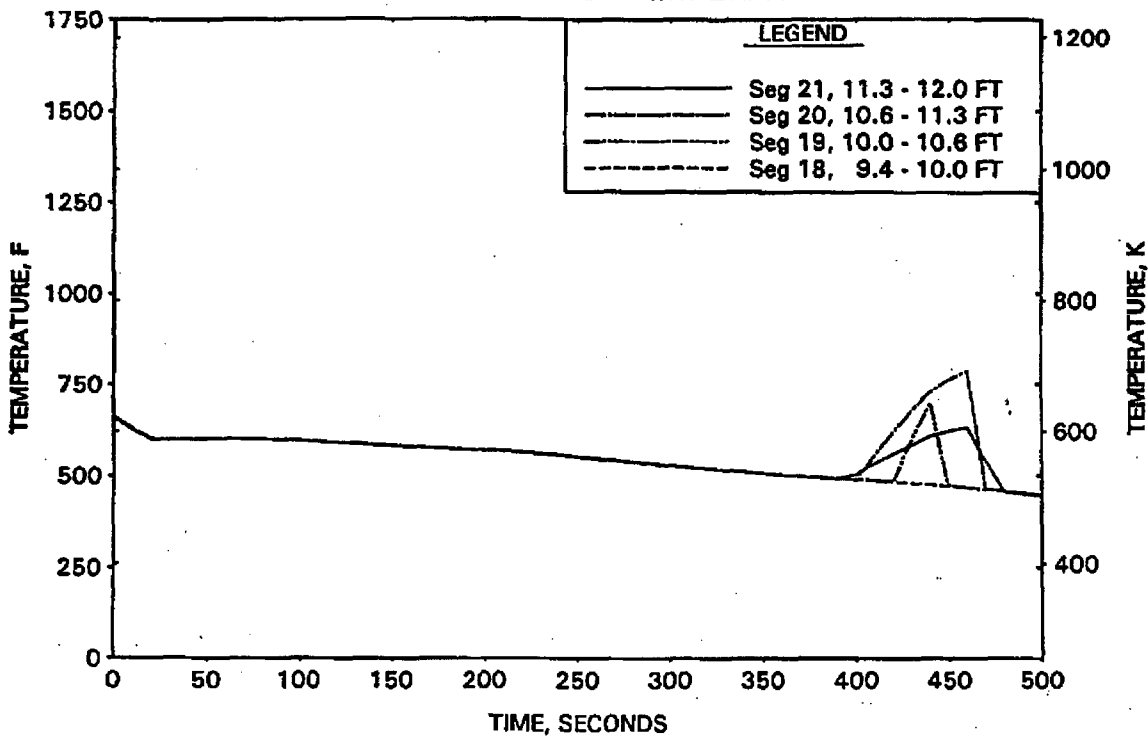


FIGURE A-256. CLPD 0.21-FT² BREAK DISCHARGE COEFFICIENT STUDY - HOT CHANNEL STEAM TEMPERATURES.

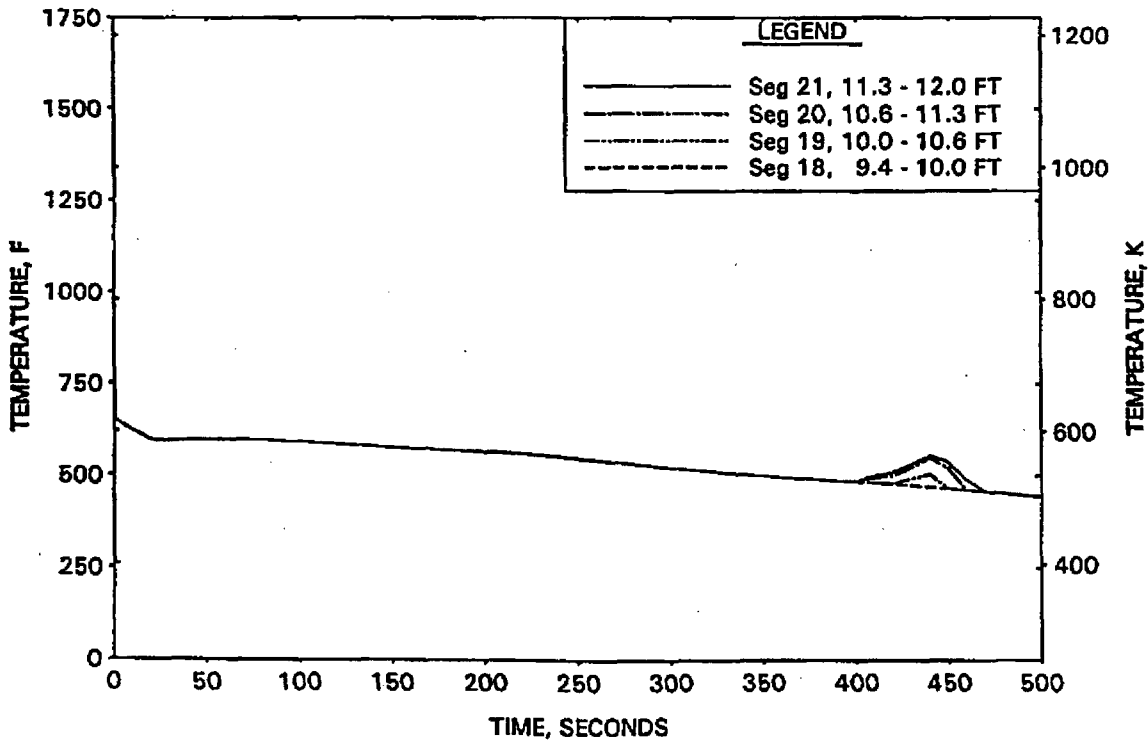


FIGURE A-257. CLPD 0.21-FT2 BREAK DISCHARGE COEFFICIENT STUDY -
UPPER ELEVATION AVE CHANNEL CLAD TEMPERATURES.

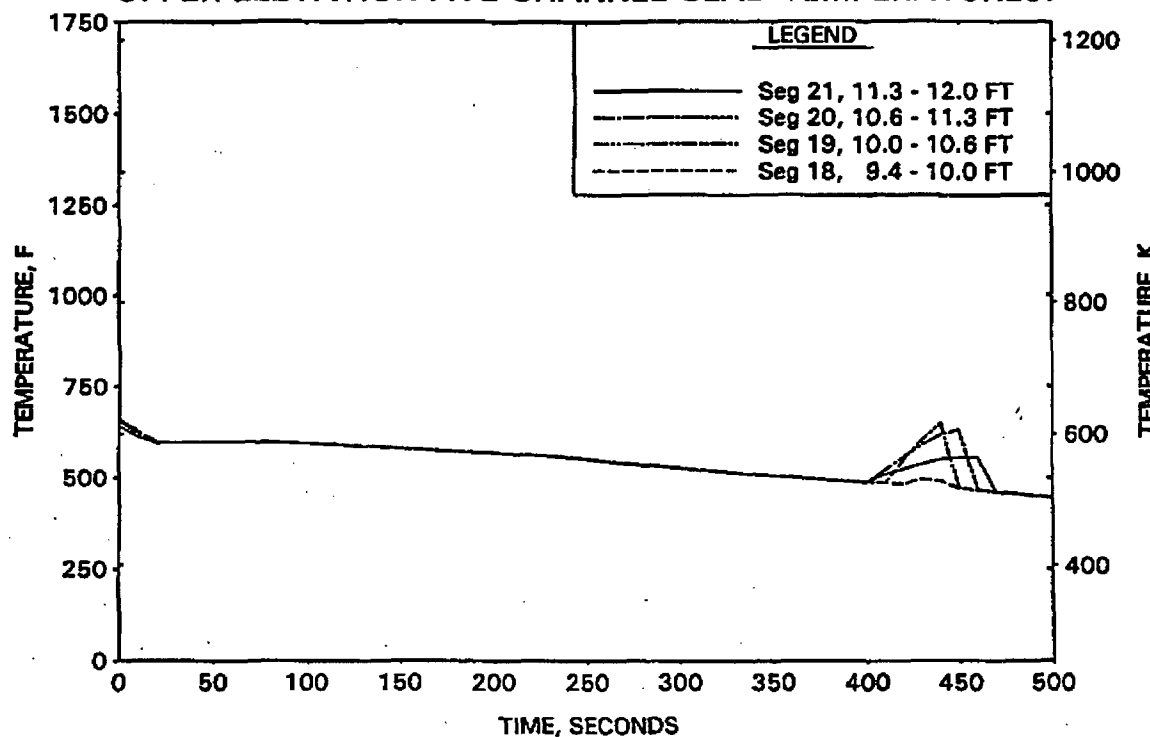


FIGURE A-258. CLPD 0.21-FT2 BREAK DISCHARGE COEFFICIENT STUDY -
UPPER ELEVATION AVE CHANNEL STEAM TEMPERATURES.

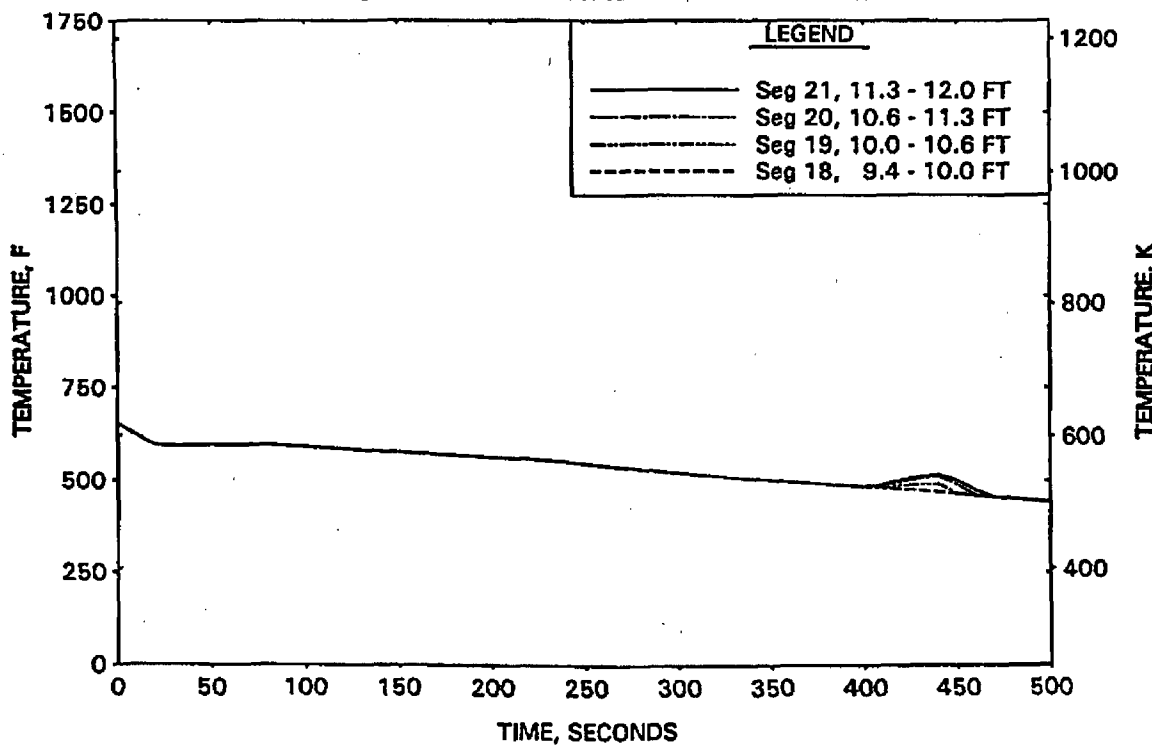


FIGURE A-259. 0.3- AND 0.21-FT² CLPD BREAK DISCHARGE STUDY - COMPARISON OF RCS PRESSURES.

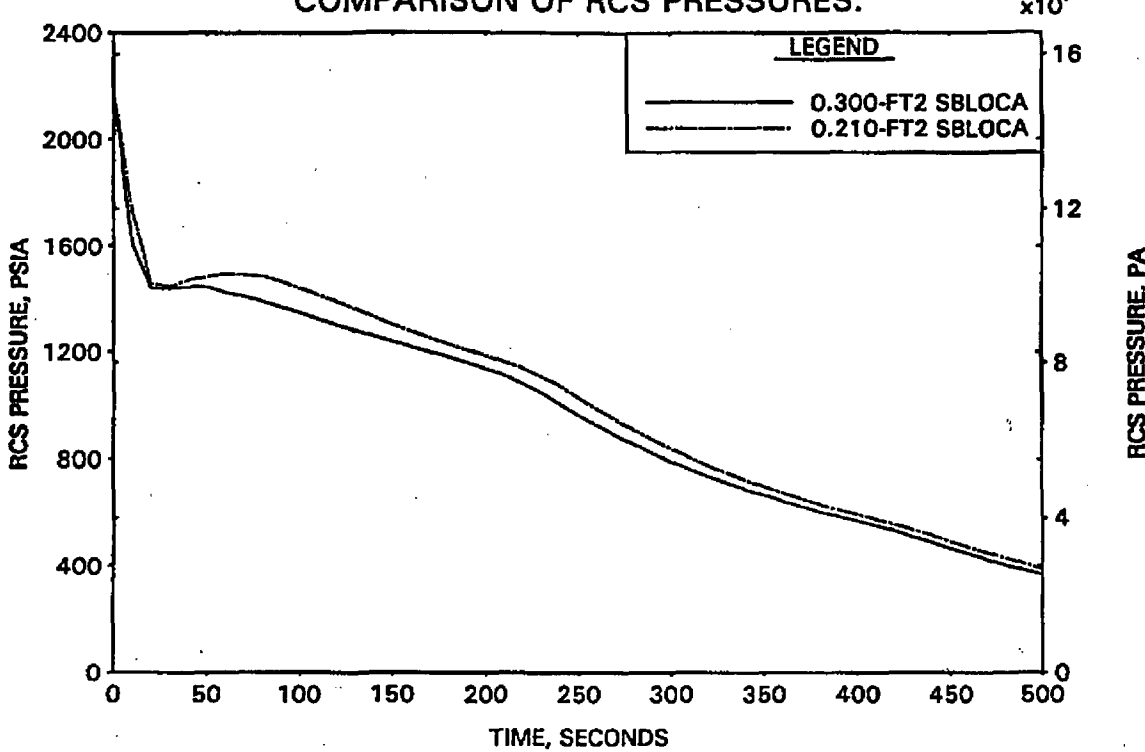


FIGURE A-260. 0.3- AND 0.21-FT² CLPD BREAK DISCHARGE STUDY - COMPARISON OF BREAK FLOW RATES.

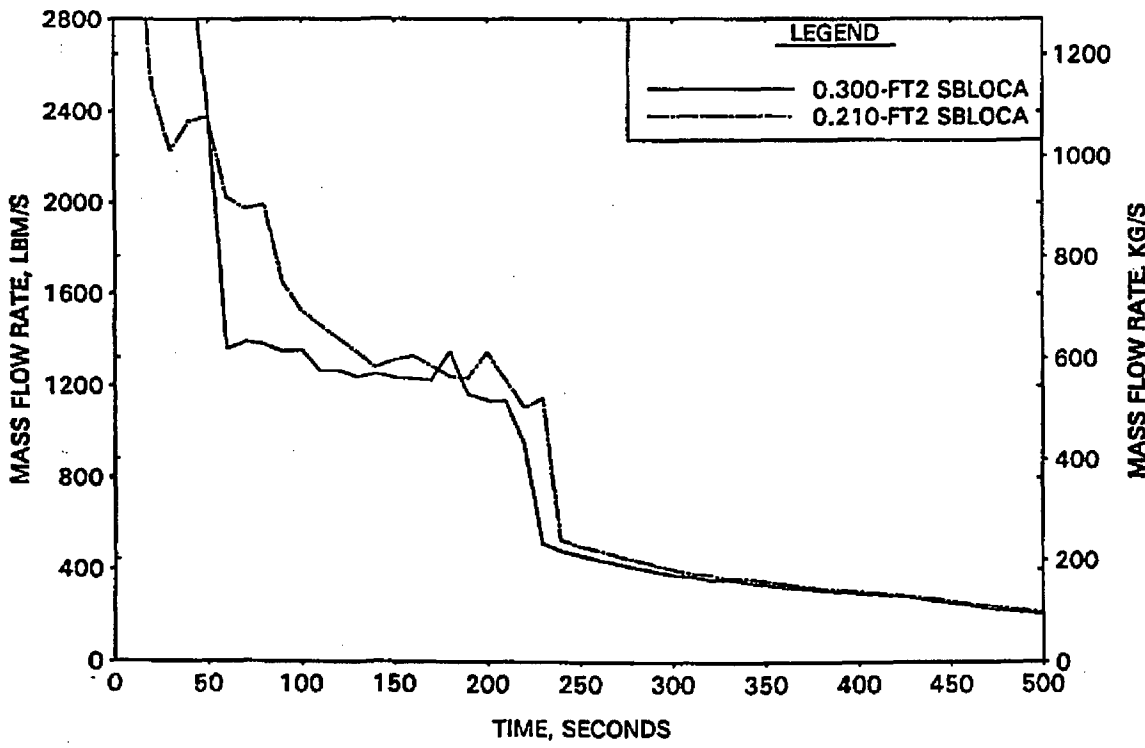


FIGURE A-261. 0.3- AND 0.21-FT² CLPD BREAK DISCHARGE STUDY - COMPARISON OF REACTOR VESSEL COLLAPSED LEVELS.

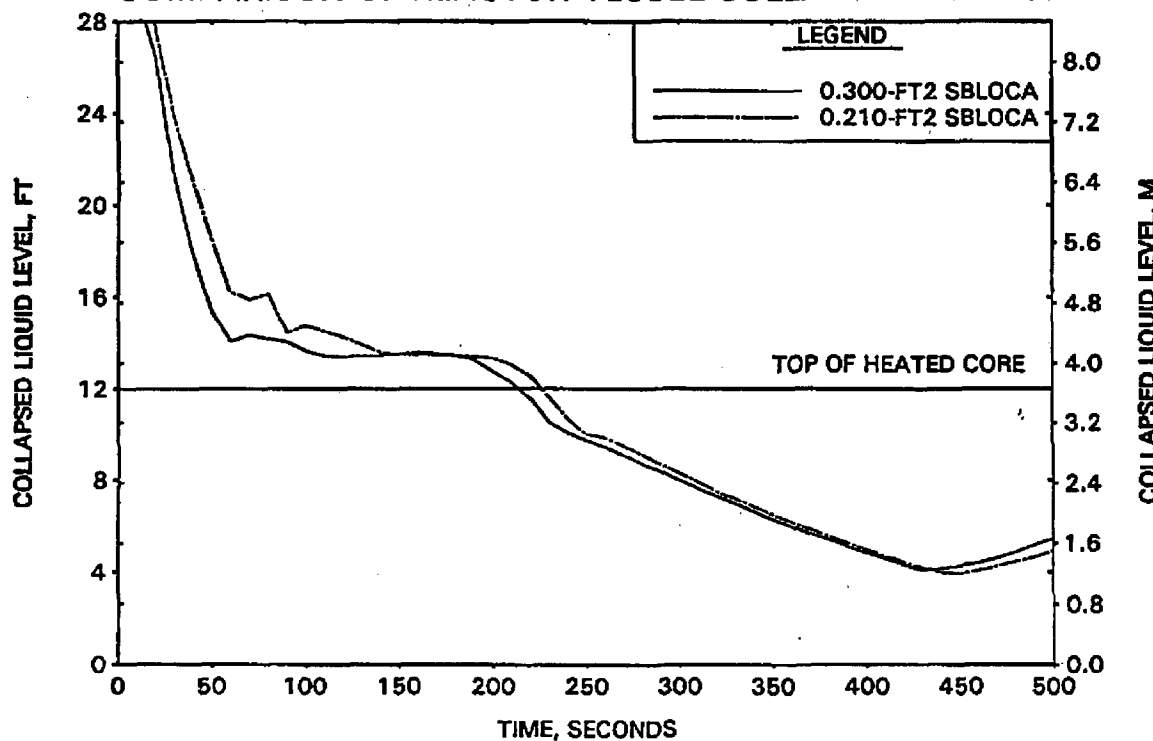


FIGURE A-262. 0.3- AND 0.21-FT² CLPD BREAK DISCHARGE STUDY - COMPARISON OF INTEGRATED BREAK FLOWS.

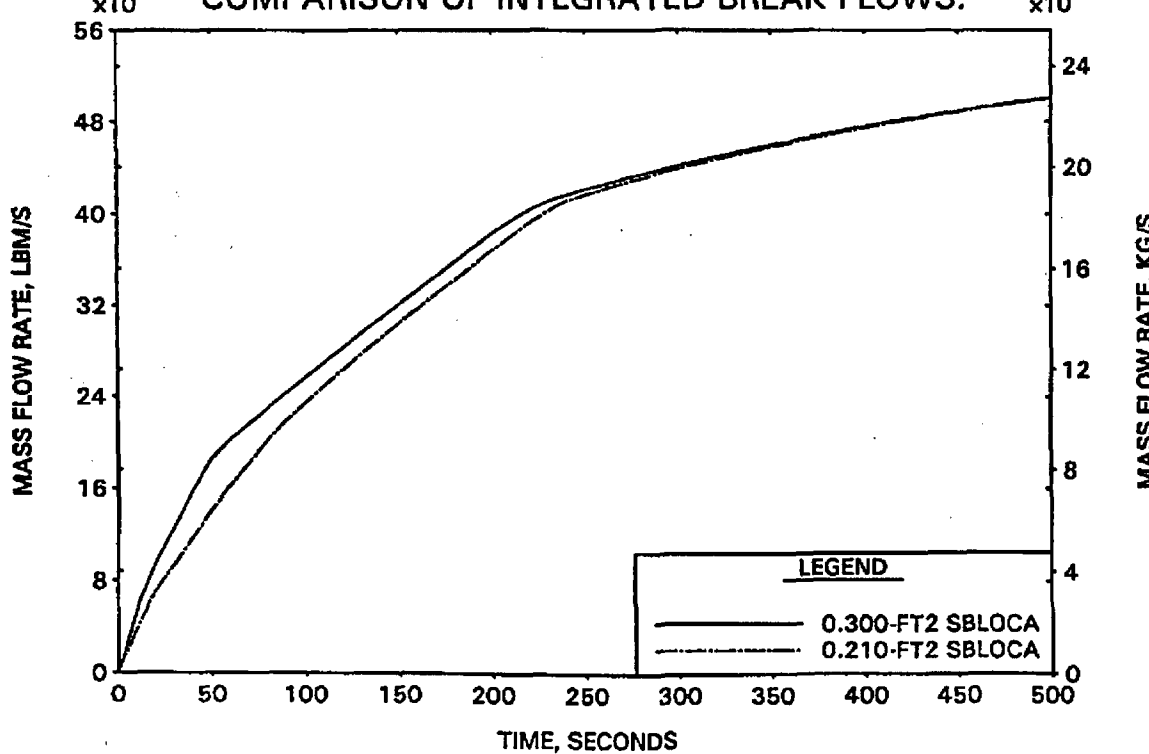


FIGURE A-263. 0.3- AND 0.21-FT2 CLPD BREAK DISCHARGE STUDY -
COMPARISON OF HOT CHANNEL MIXTURE LEVELS.

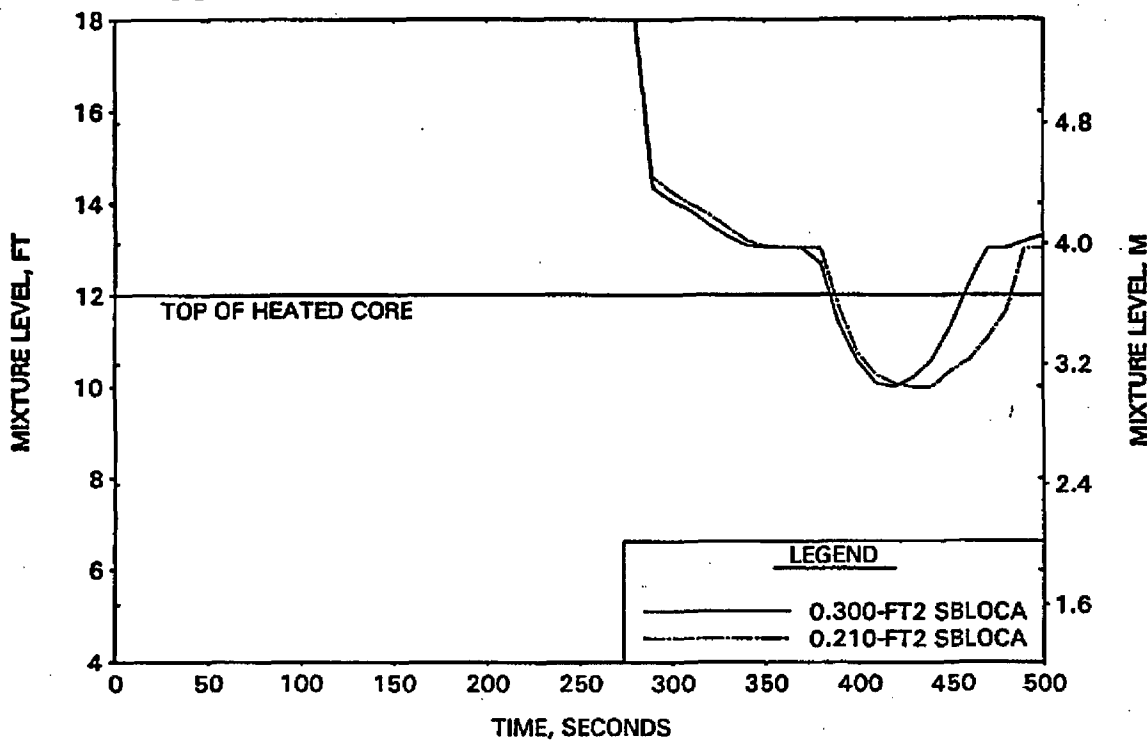


FIGURE A-264. 0.3- AND 0.21-FT2 CLPD BREAK DISCHARGE STUDY -
COMPARISON OF PEAK CLADDING TEMPERATURES.

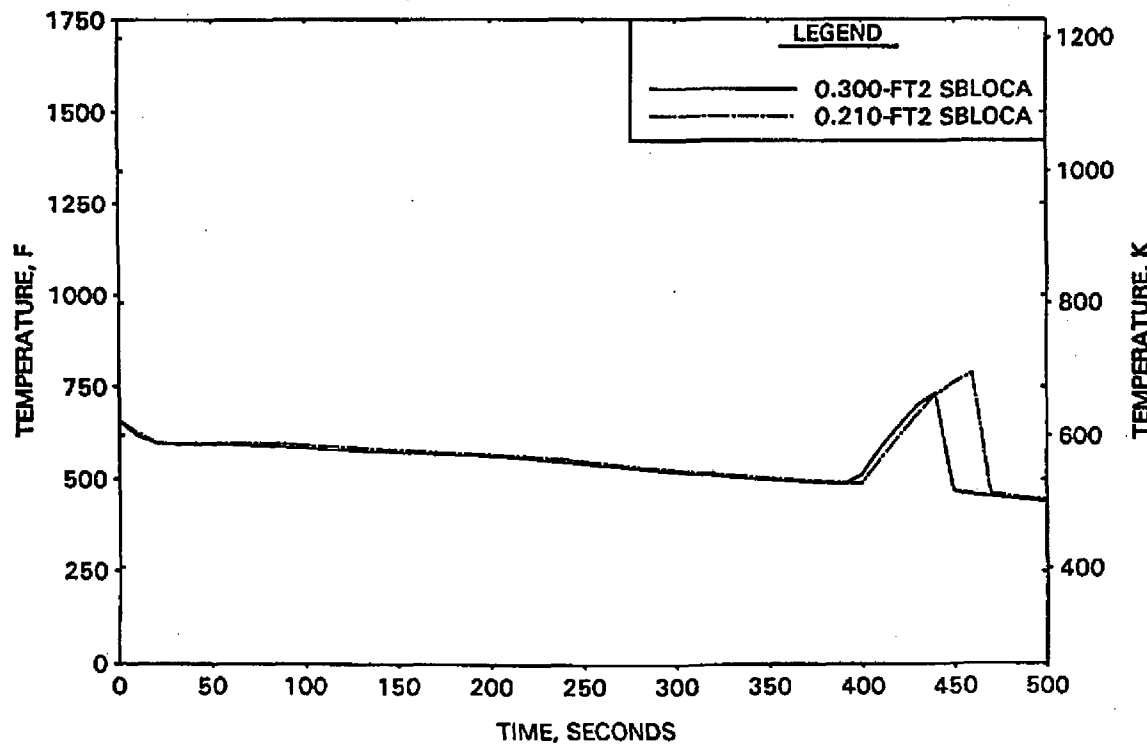


FIGURE A-265. CORE FLOOD LINE BREAK - RCS PRESSURES.

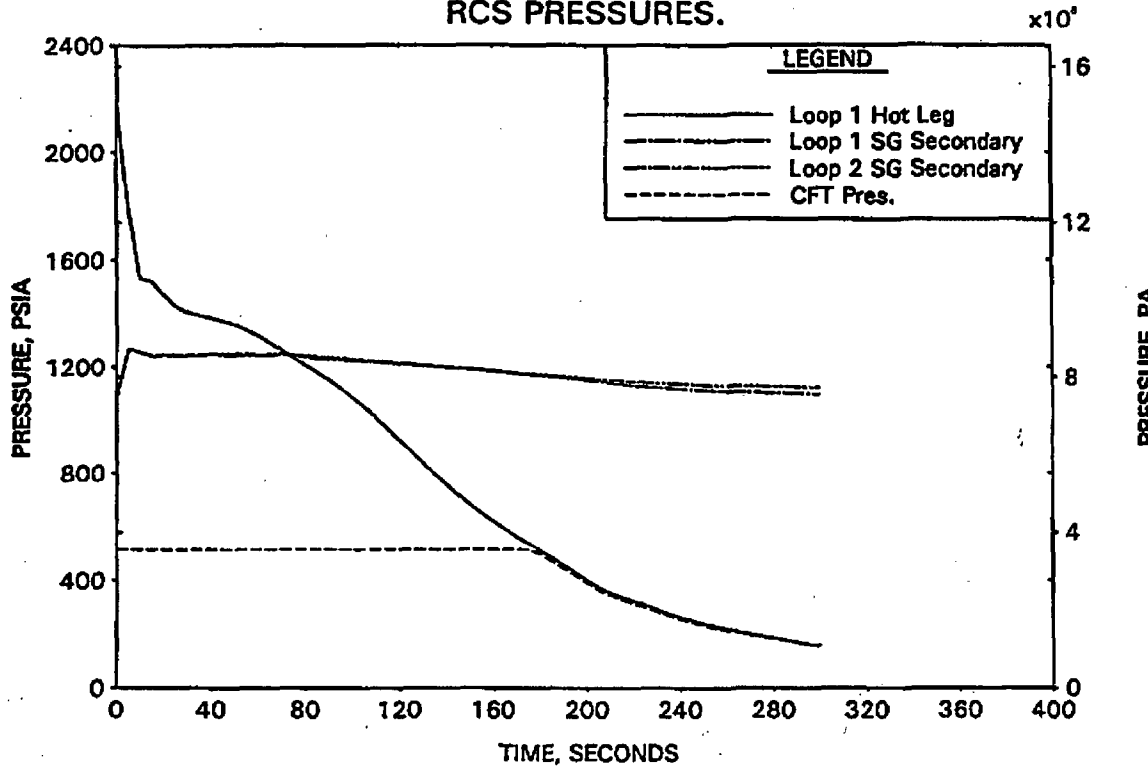


FIGURE A-266. CORE FLOOD LINE BREAK - DC, RV, AND CORE COLLAPSED LEVELS.

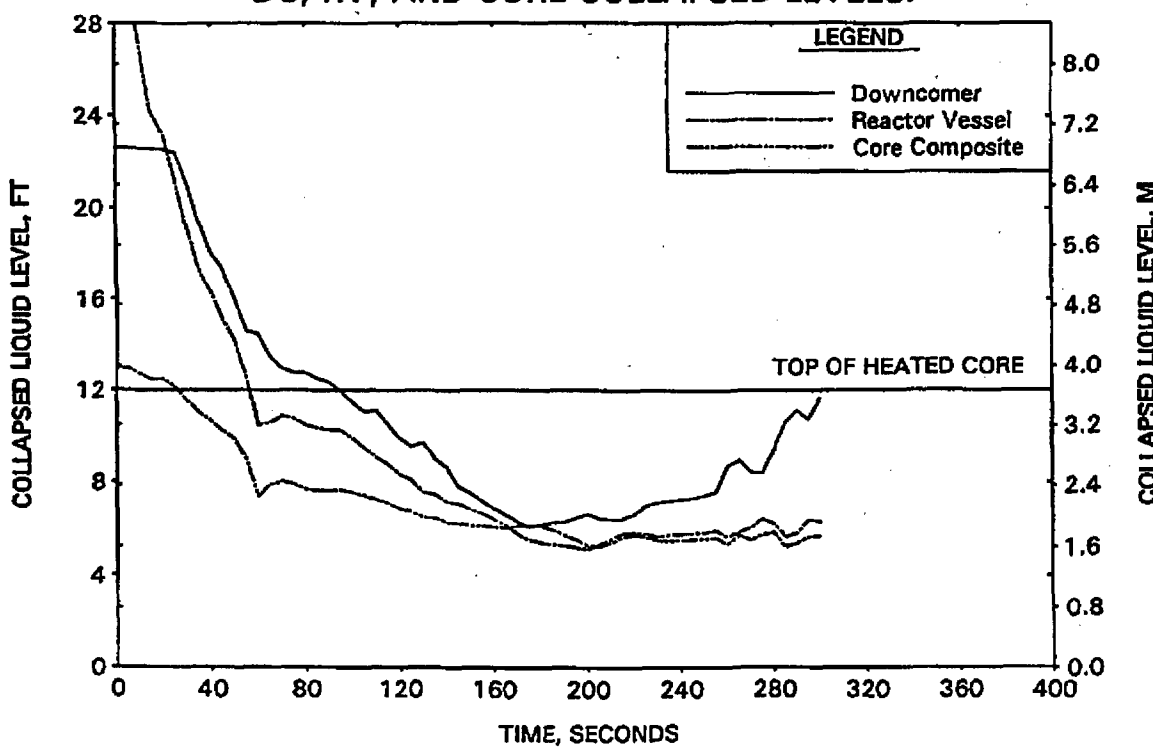


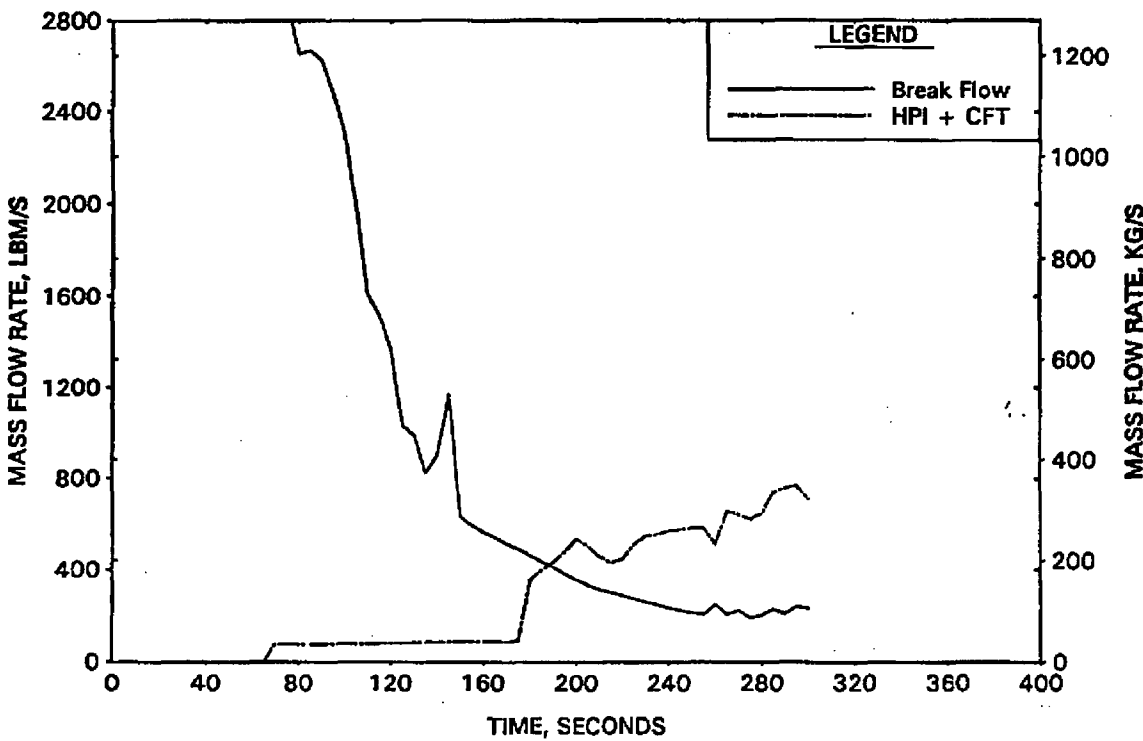
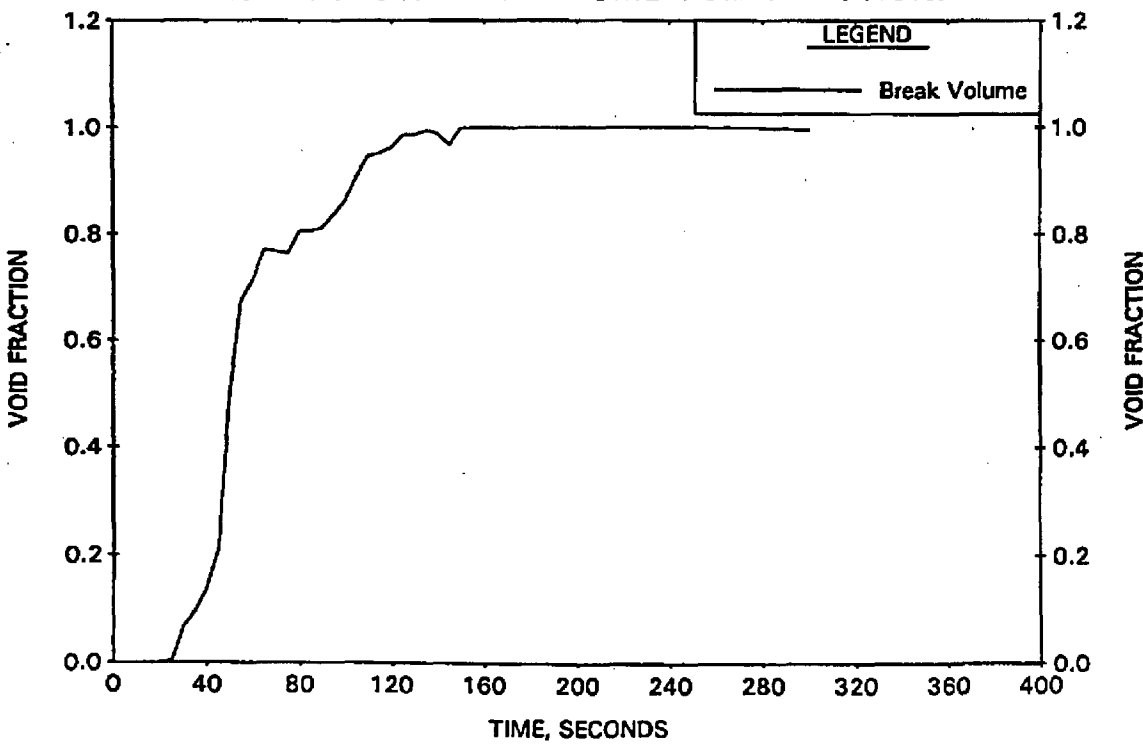
FIGURE A-267. CORE FLOOD LINE BREAK -
BREAK AND TOTAL ECCS FLOWS.FIGURE A-268. CORE FLOOD LINE BREAK -
BREAK UPSTREAM VOLUME VOID FRACTION.

FIGURE A-269. CORE FLOOD LINE BREAK -
LOOP 2 COLLAPSED LEVELS.

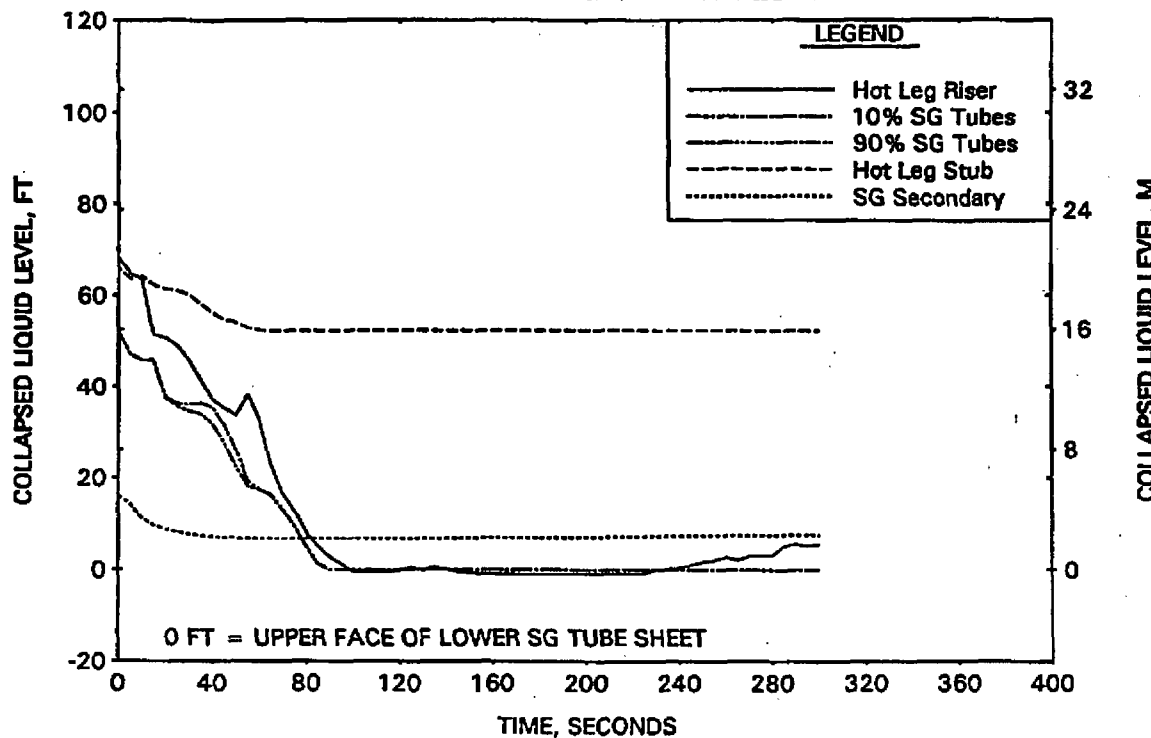


FIGURE A-270. CORE FLOOD LINE BREAK -
LOOP 1 COLLAPSED LEVELS.

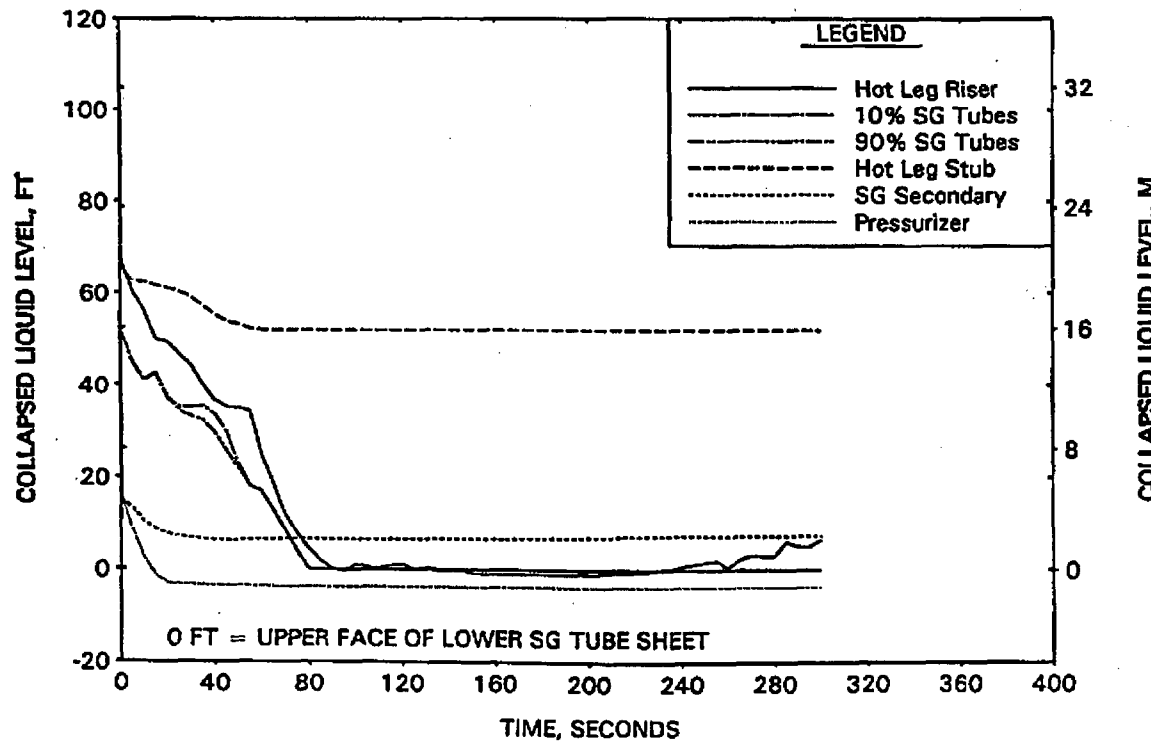


FIGURE A-271. CORE FLOOD LINE BREAK - CLPD COLLAPSED LEVELS.

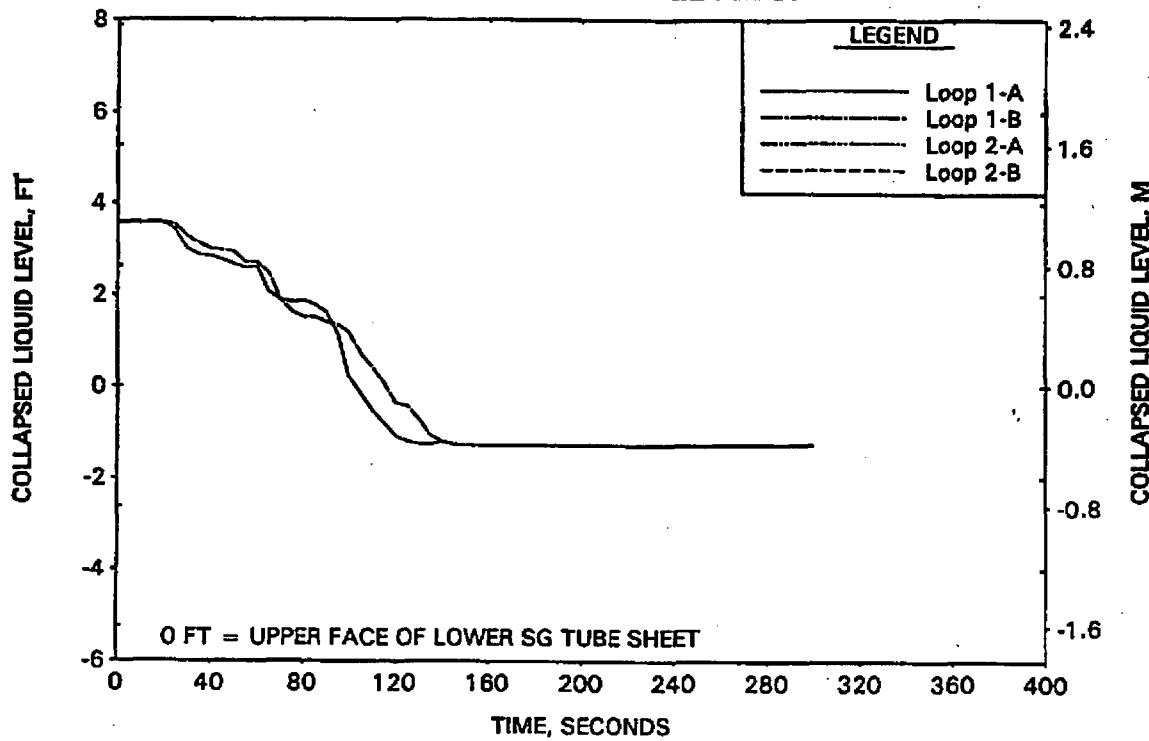


FIGURE A-272. CORE FLOOD LINE BREAK - CLPS LIQUID VOLUME.

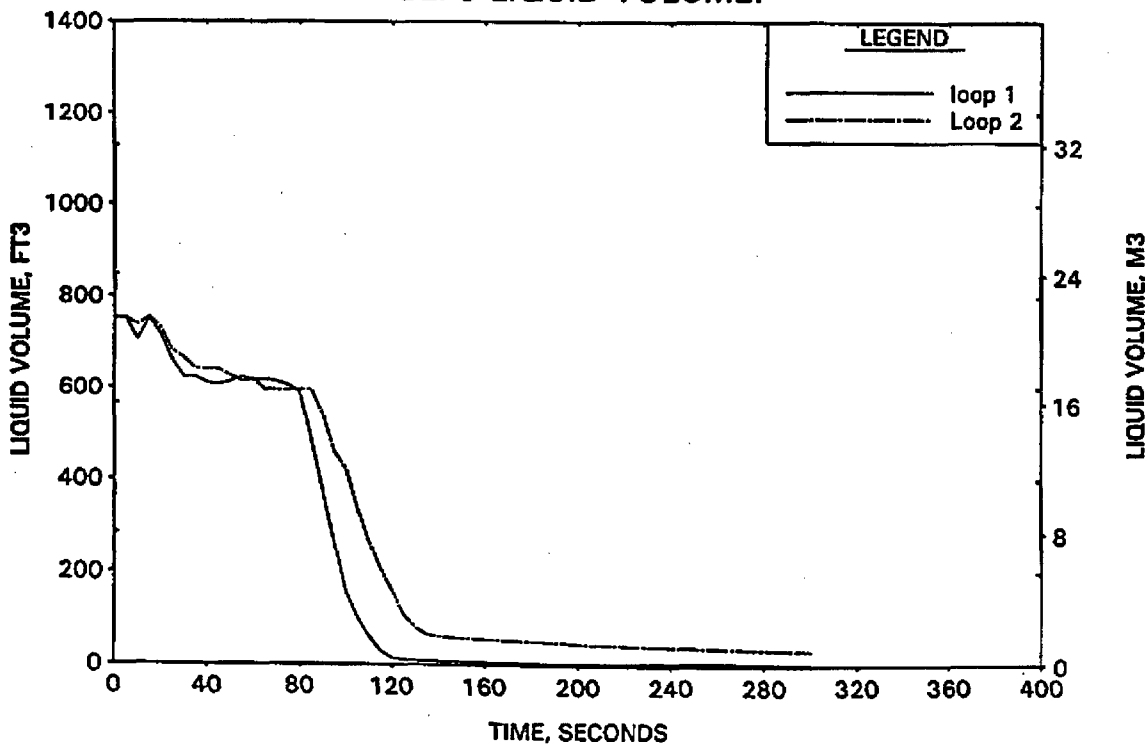


FIGURE A-273. CORE FLOOD LINE BREAK -
FILTERED HOT LEG AND RVVV FLOWS.

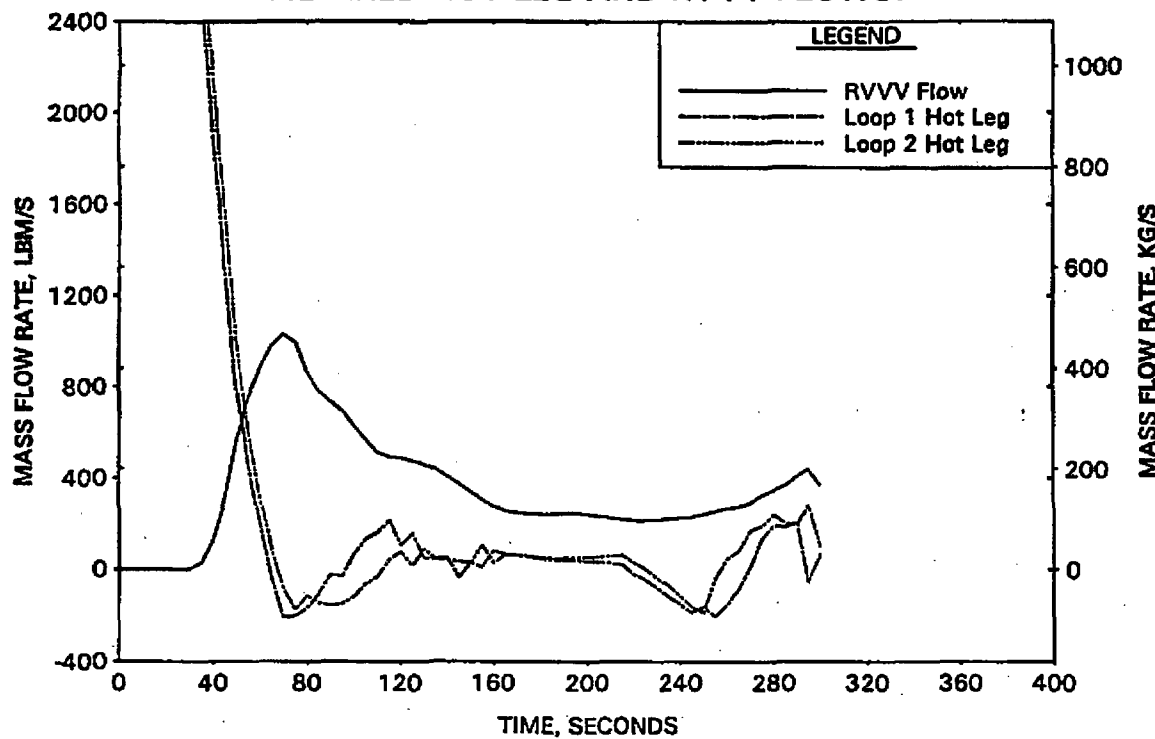


FIGURE A-274. CORE FLOOD LINE BREAK -
CORE MIXTURE LEVELS.

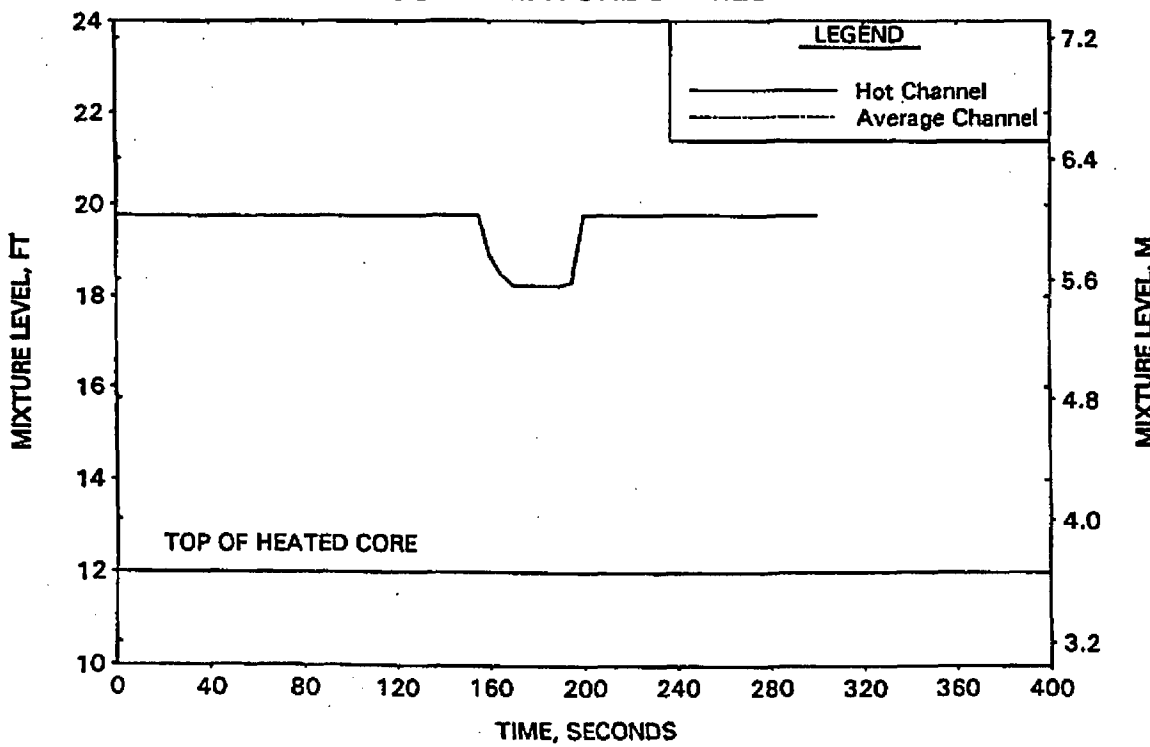


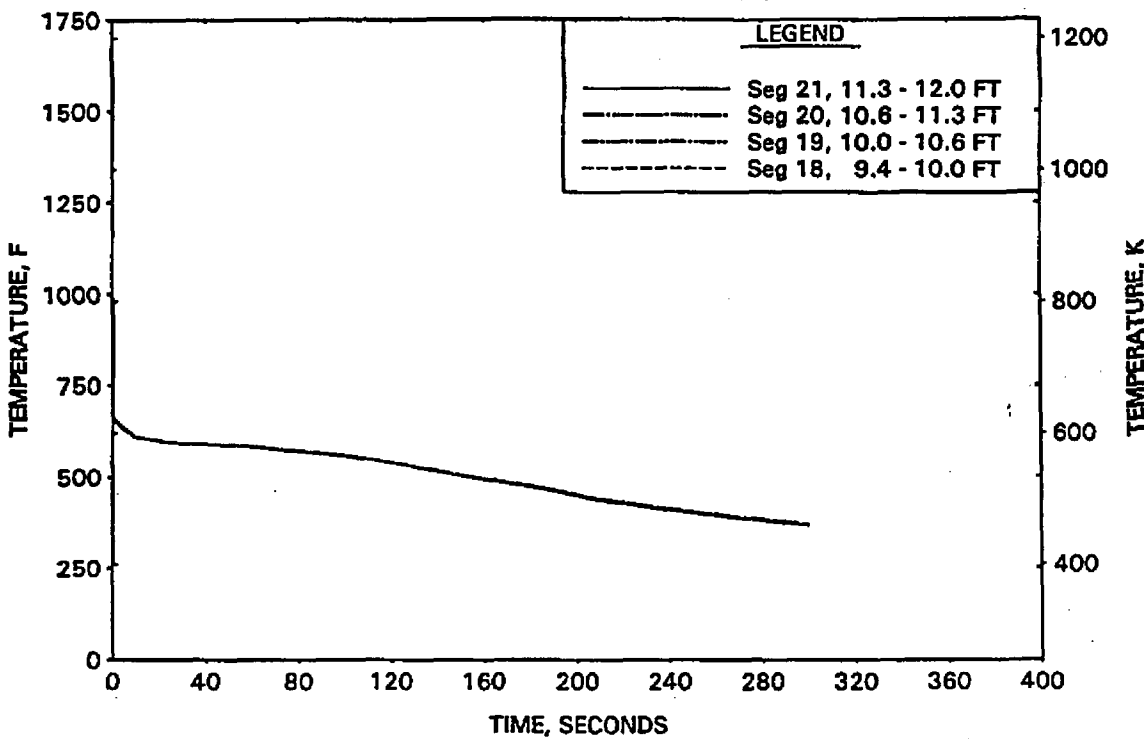
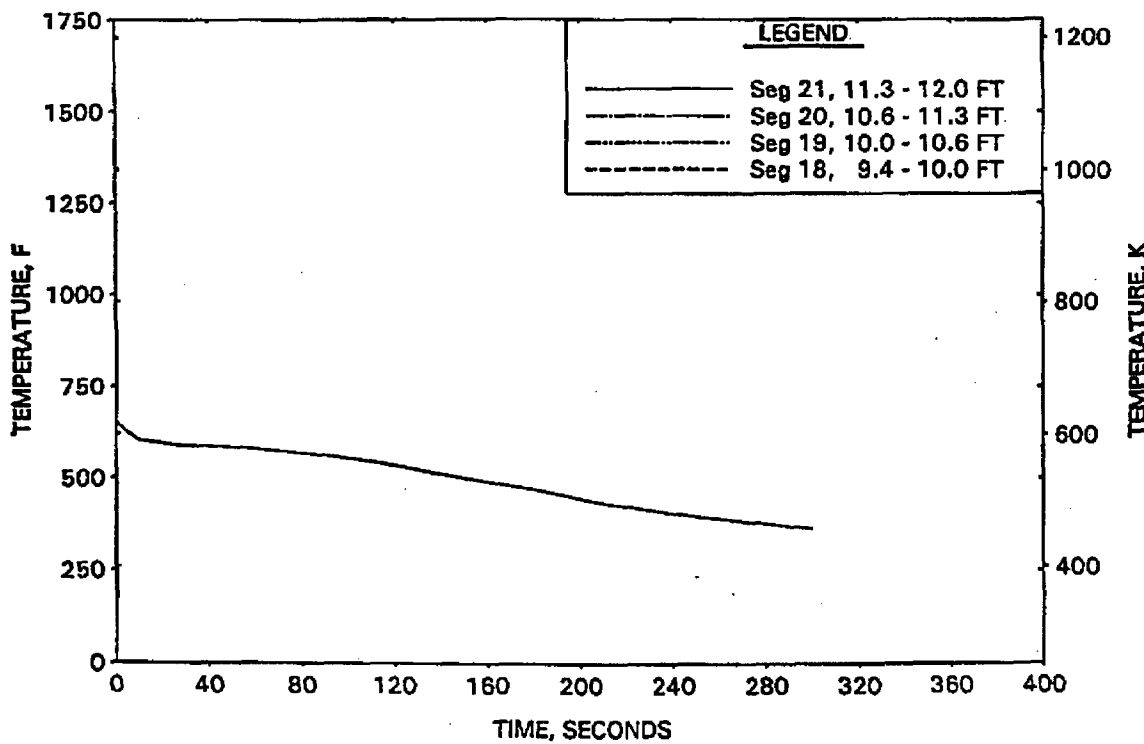
FIGURE A-275. CORE FLOOD LINE BREAK -
HOT CHANNEL CLAD TEMPERATURES.FIGURE A-276. CORE FLOOD LINE BREAK -
HOT CHANNEL STEAM TEMPERATURES.

FIGURE A-277. CORE FLOOD LINE BREAK -
UPPER ELEVATION AVE CHANNEL CLAD TEMPERATURES.

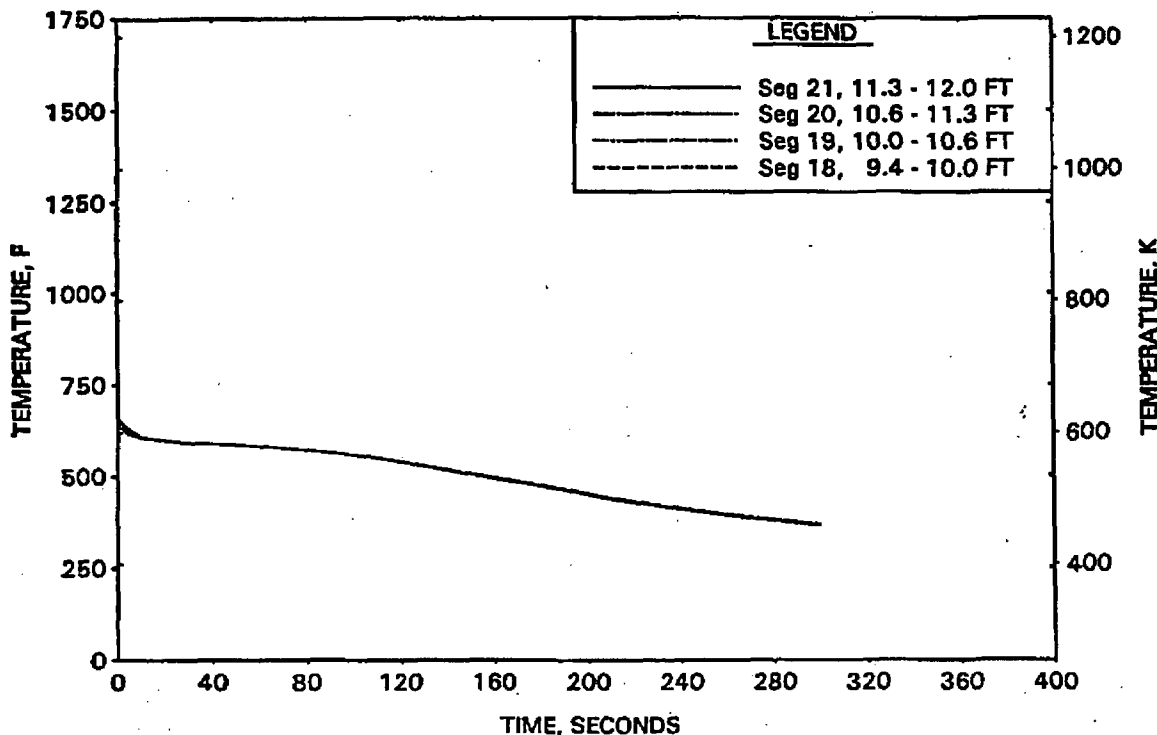


FIGURE A-278. CORE FLOOD LINE BREAK -
UPPER ELEVATION AVE CHANNEL STEAM TEMPERATURES.

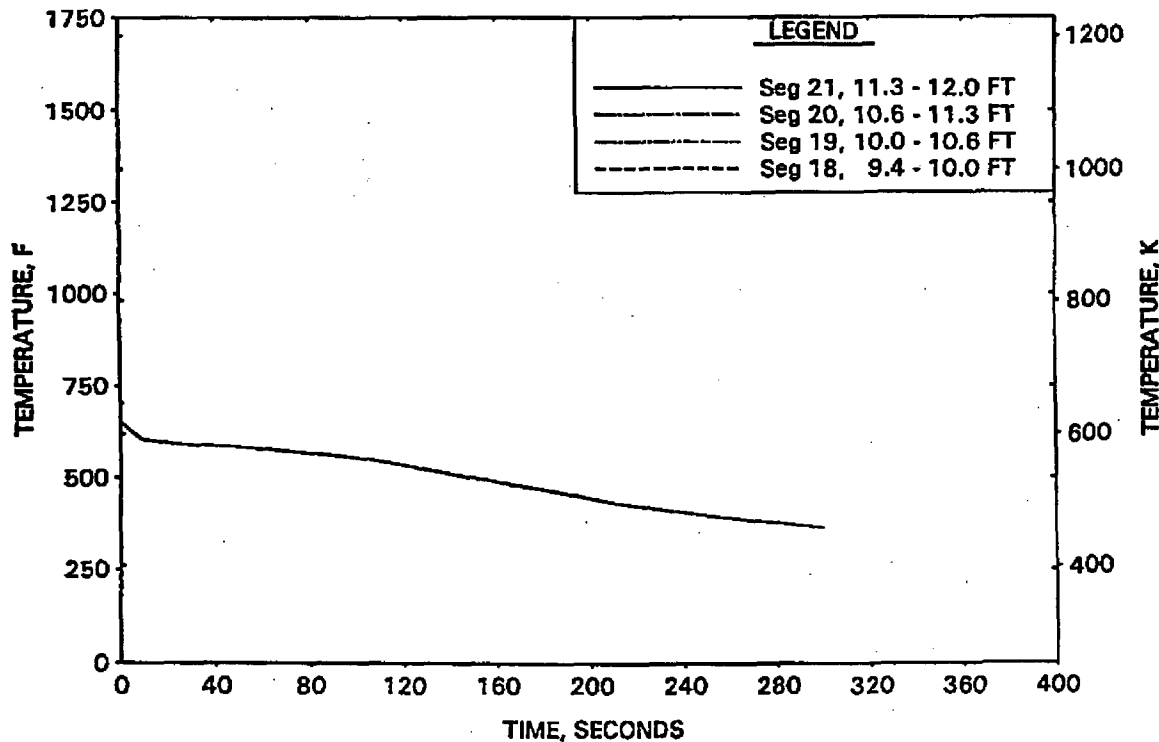


FIGURE A-279. HPI LINE BREAK - RCS PRESSURES.

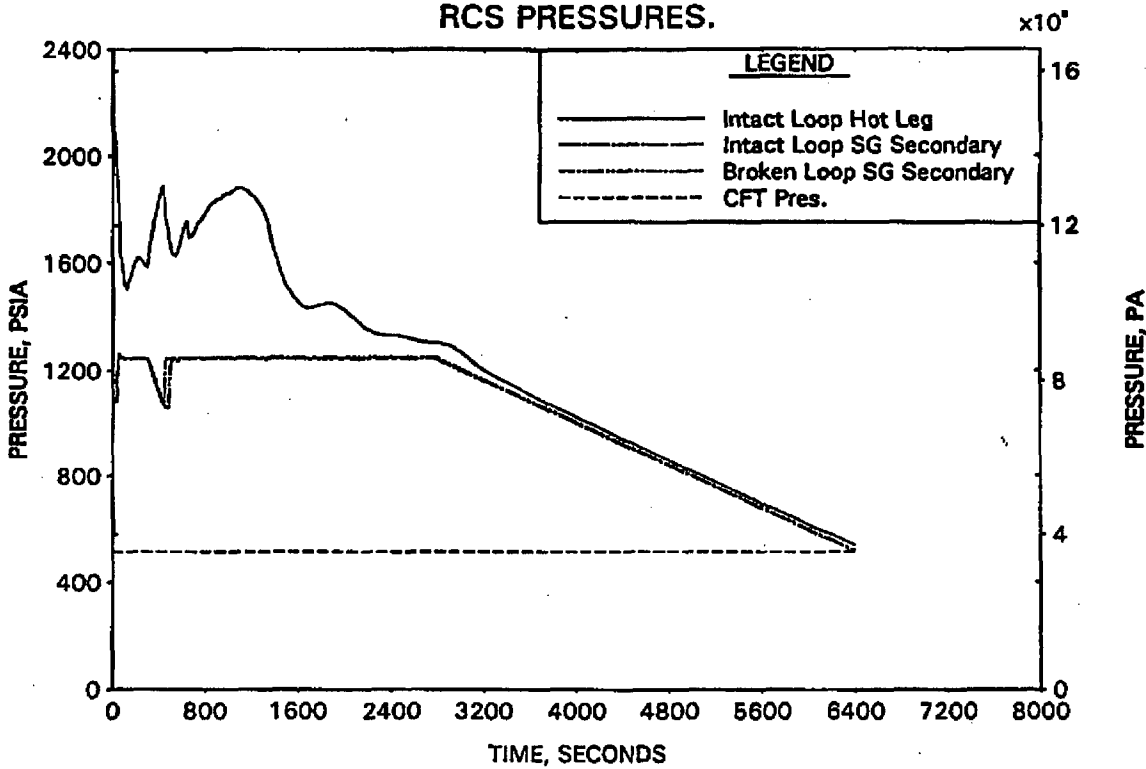


FIGURE A-280. HPI LINE BREAK - DC, RV, AND CORE COLLAPSED LEVELS.

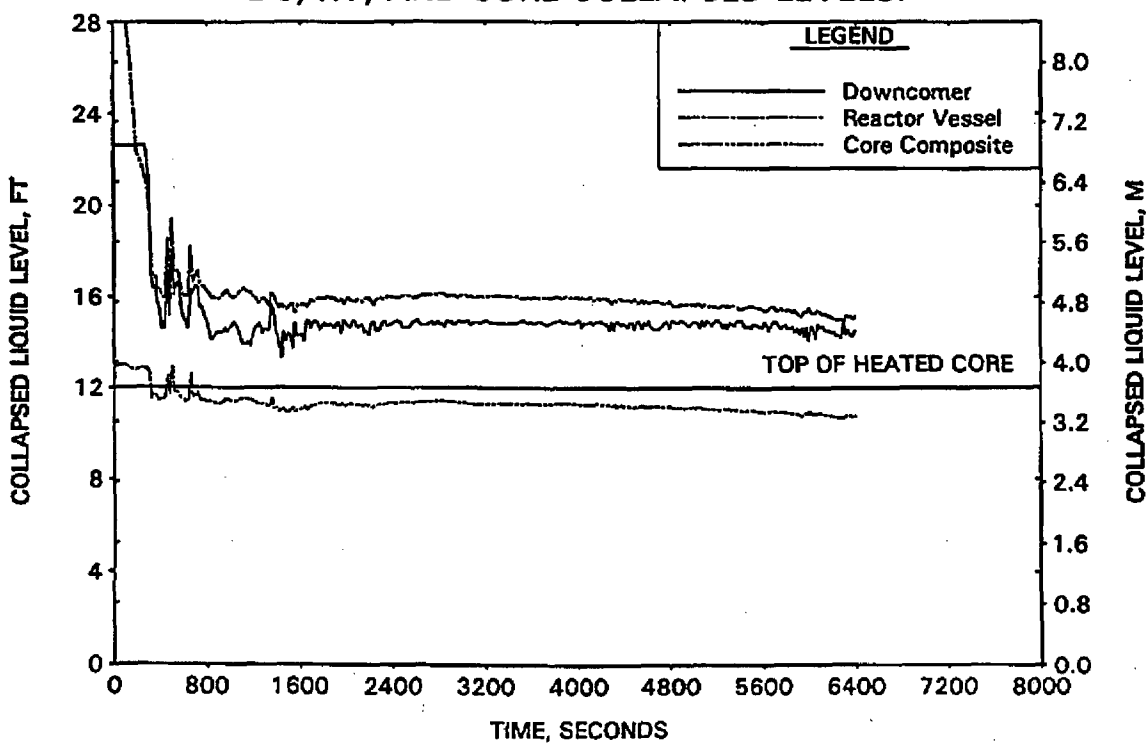


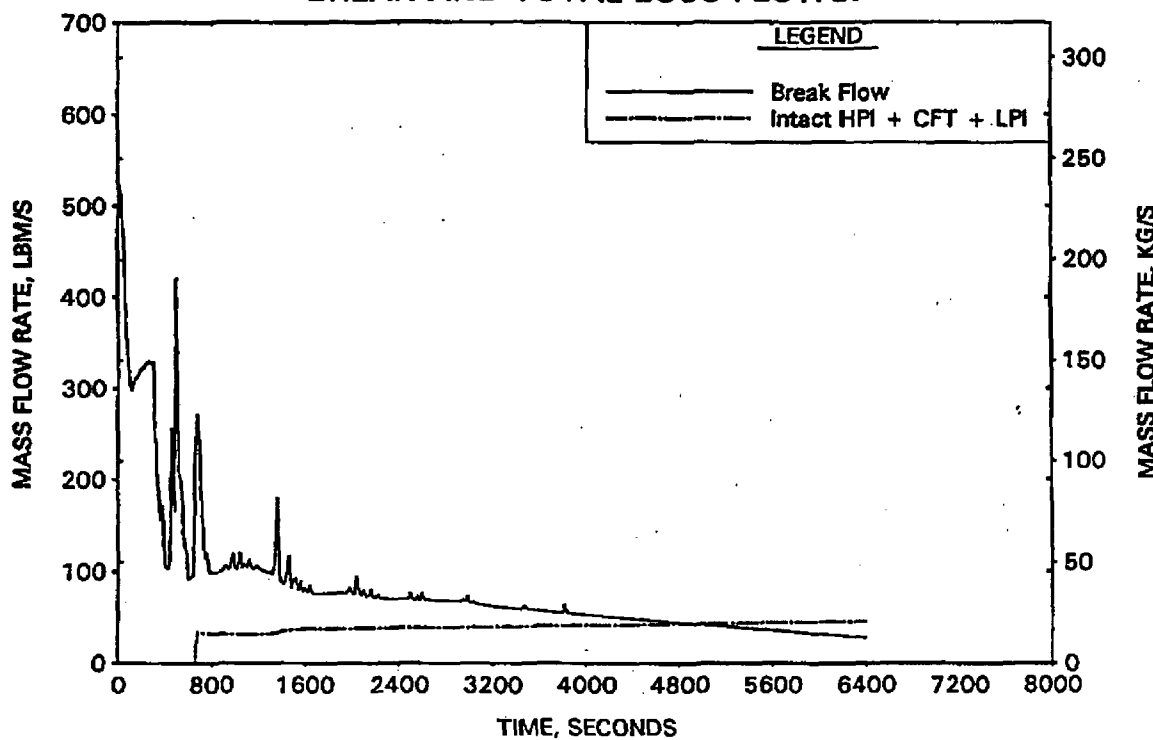
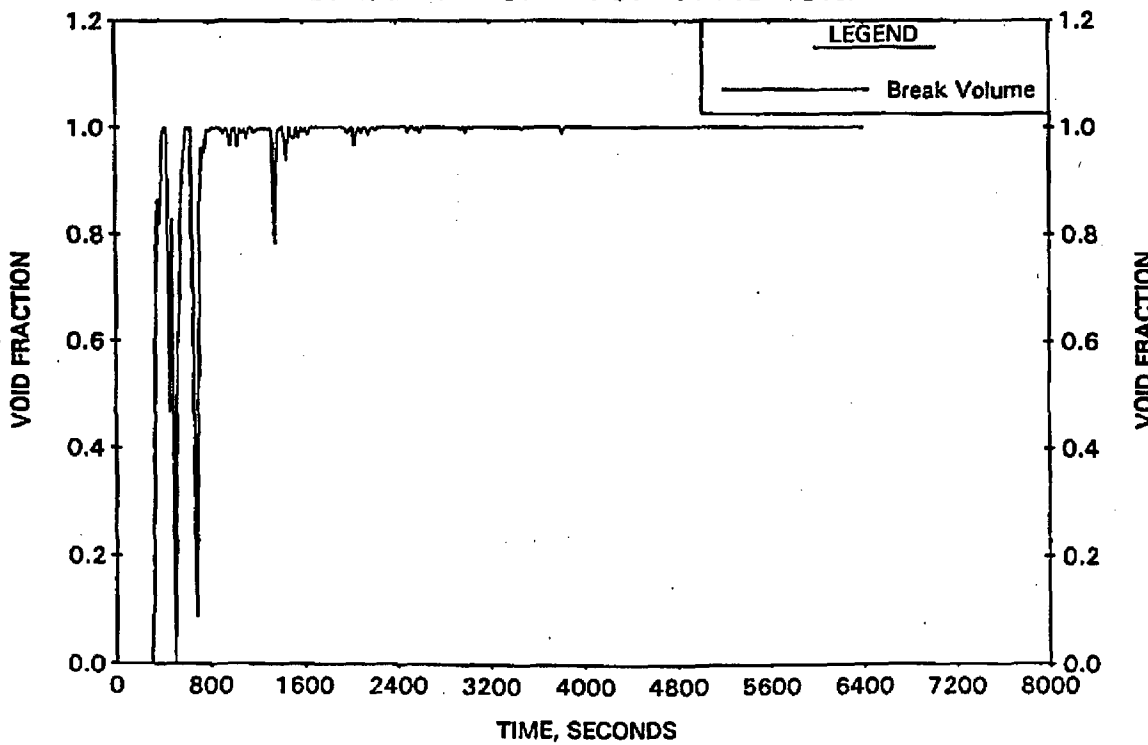
FIGURE A-281. HPI LINE BREAK -
BREAK AND TOTAL ECCS FLOWS.FIGURE A-282. HPI LINE BREAK -
BREAK VOLUME VOID FRACTION.

FIGURE A-283. HPI LINE BREAK -
BROKEN LOOP COLLAPSED LEVELS.

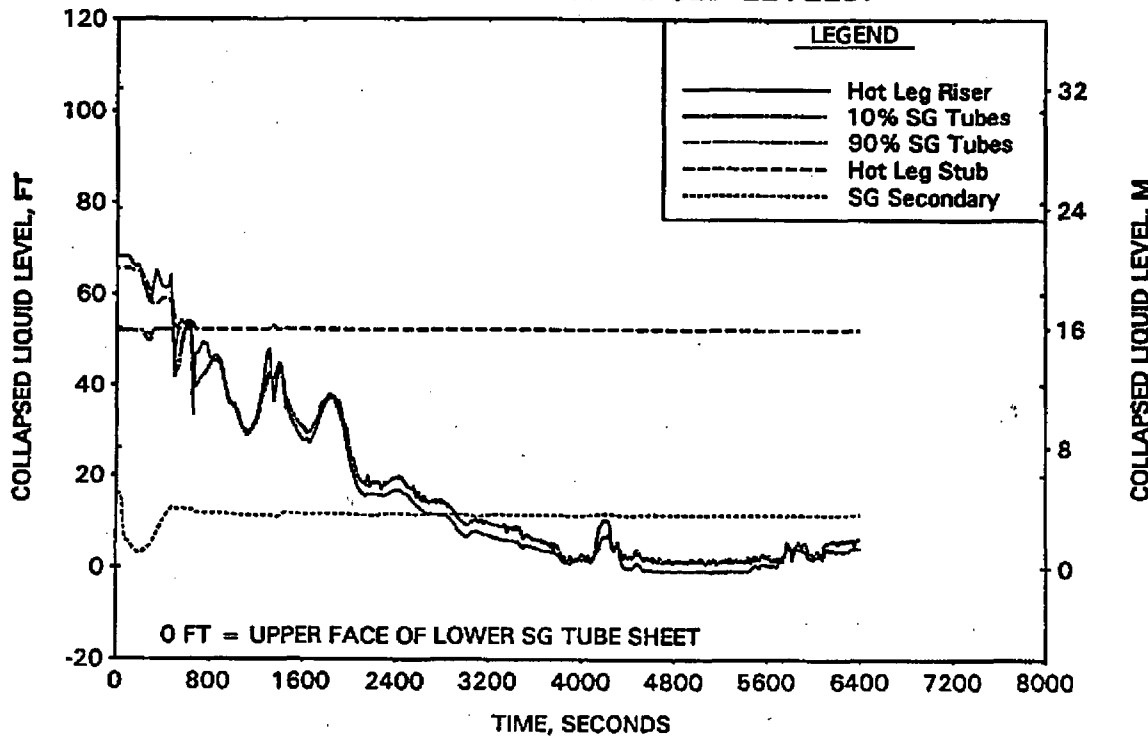


FIGURE A-284. HPI LINE BREAK -
INTACT LOOP COLLAPSED LEVELS.

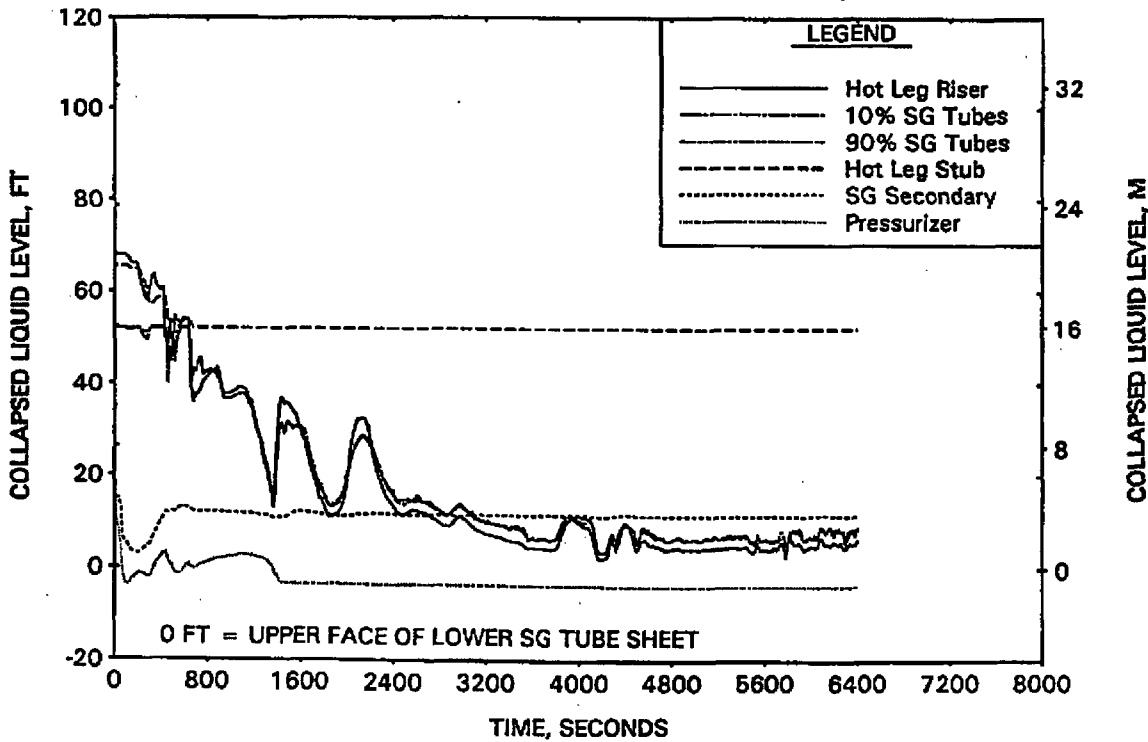


FIGURE A-285. HPI LINE BREAK -
CLPD COLLAPSED LEVELS.

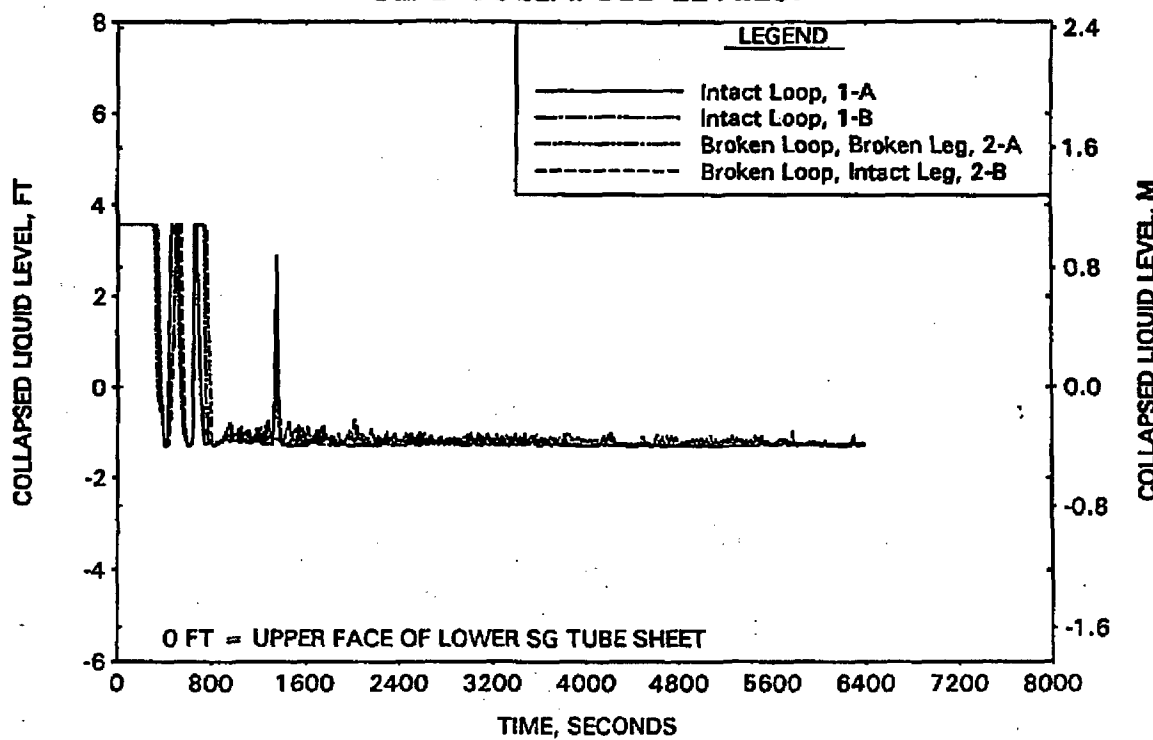


FIGURE A-286. HPI LINE BREAK -
CLPS LIQUID VOLUME.

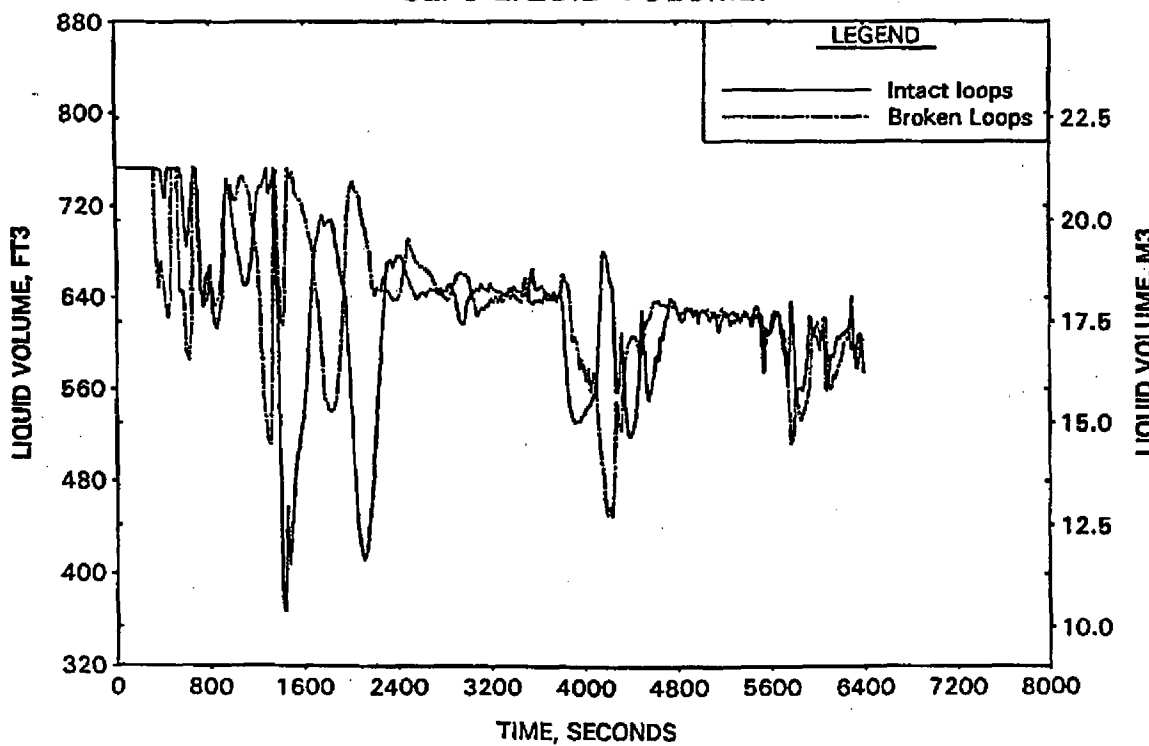


FIGURE A-287. HPI LINE BREAK -
HOT LEG AND RVVV FLOWS.

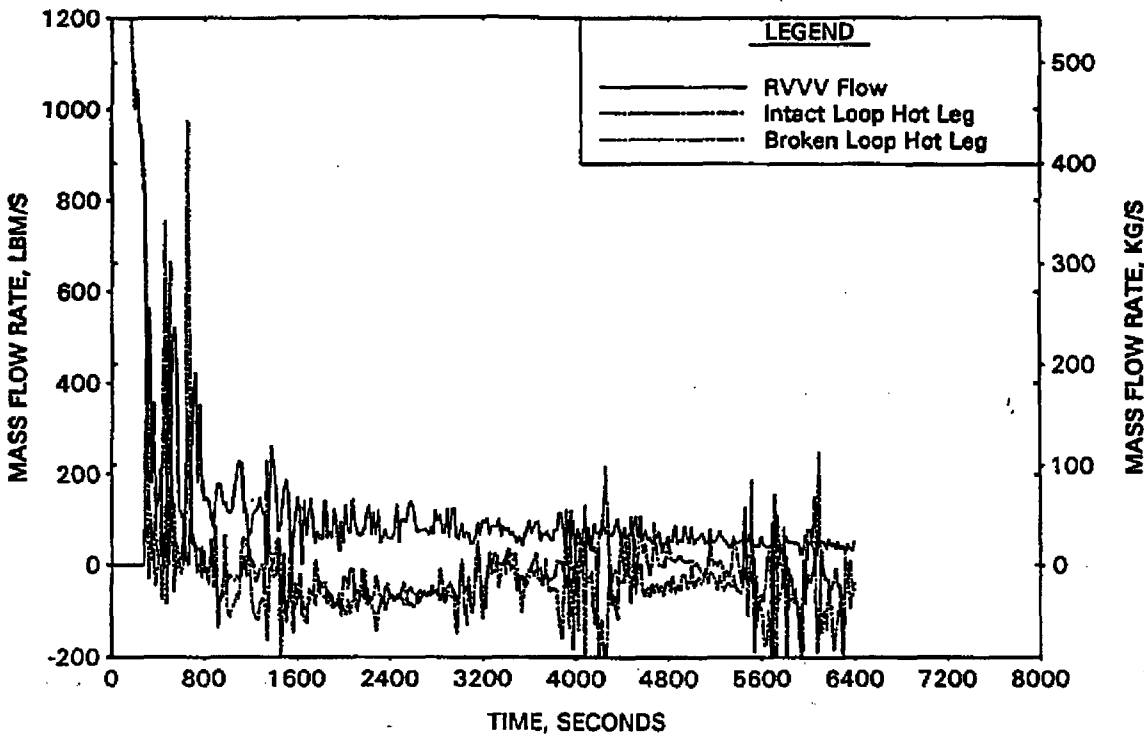


FIGURE A-288. HPI LINE BREAK -
CORE MIXTURE LEVELS.

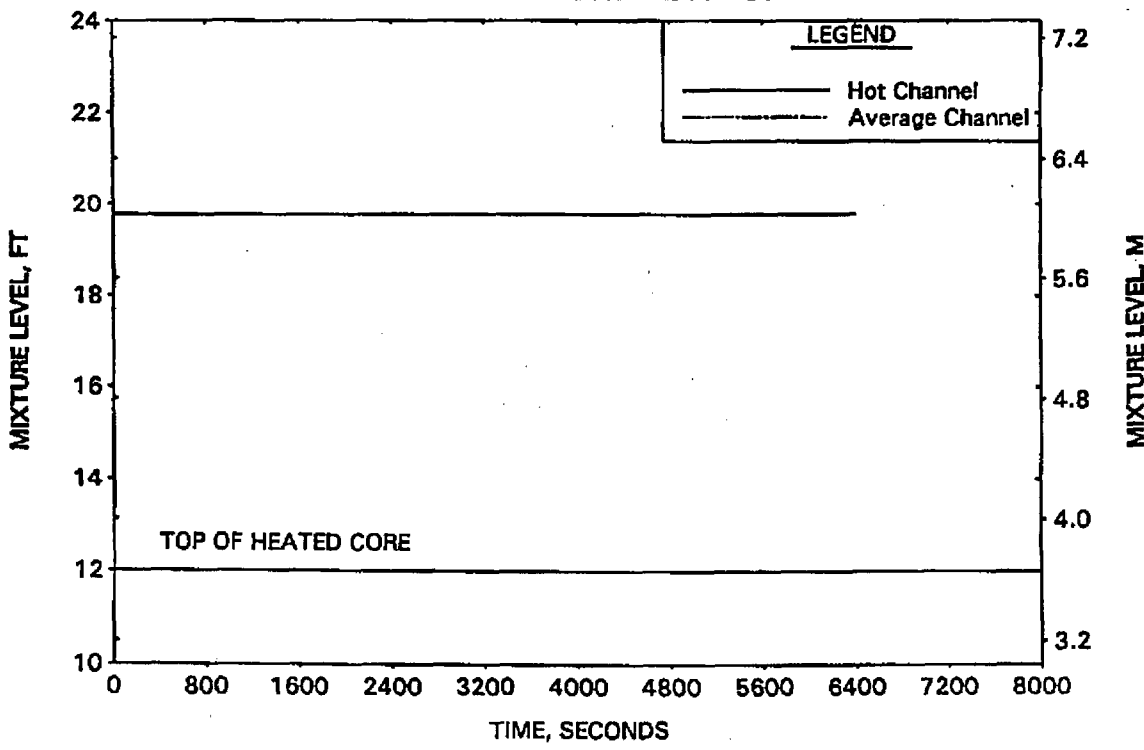


FIGURE A-289. HPI LINE BREAK -
HOT CHANNEL CLAD TEMPERATURES.

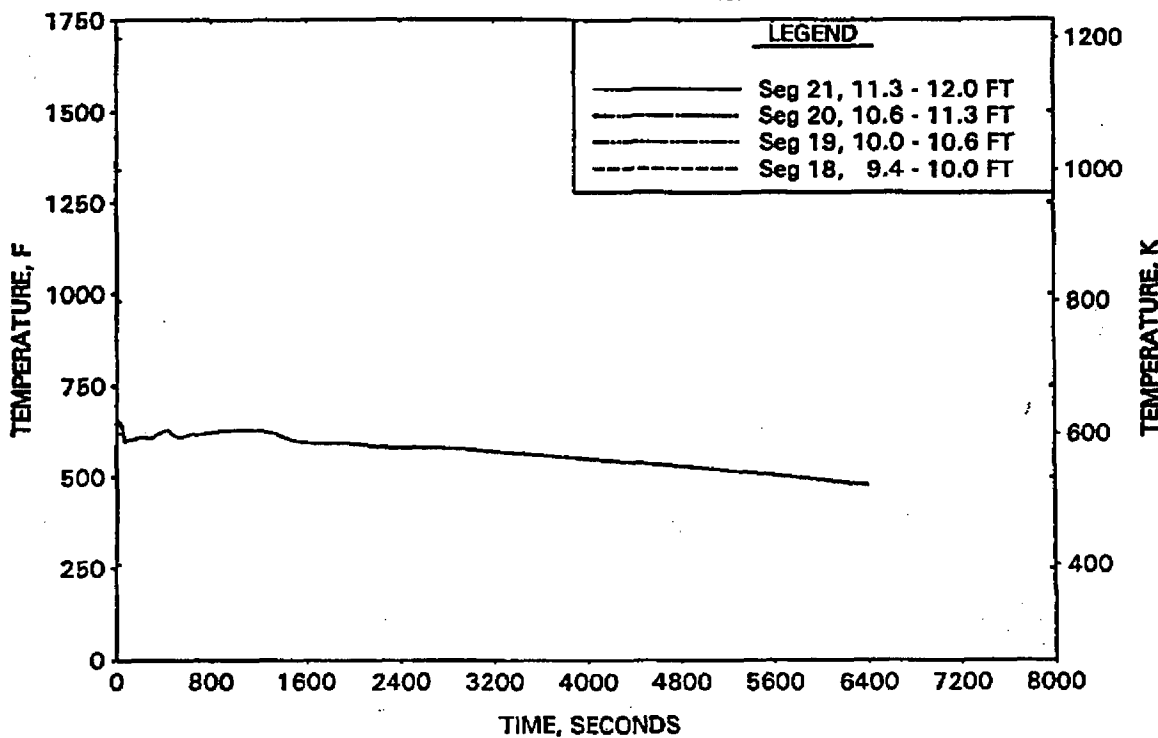


FIGURE A-290. HPI LINE BREAK -
HOT CHANNEL STEAM TEMPERATURES.

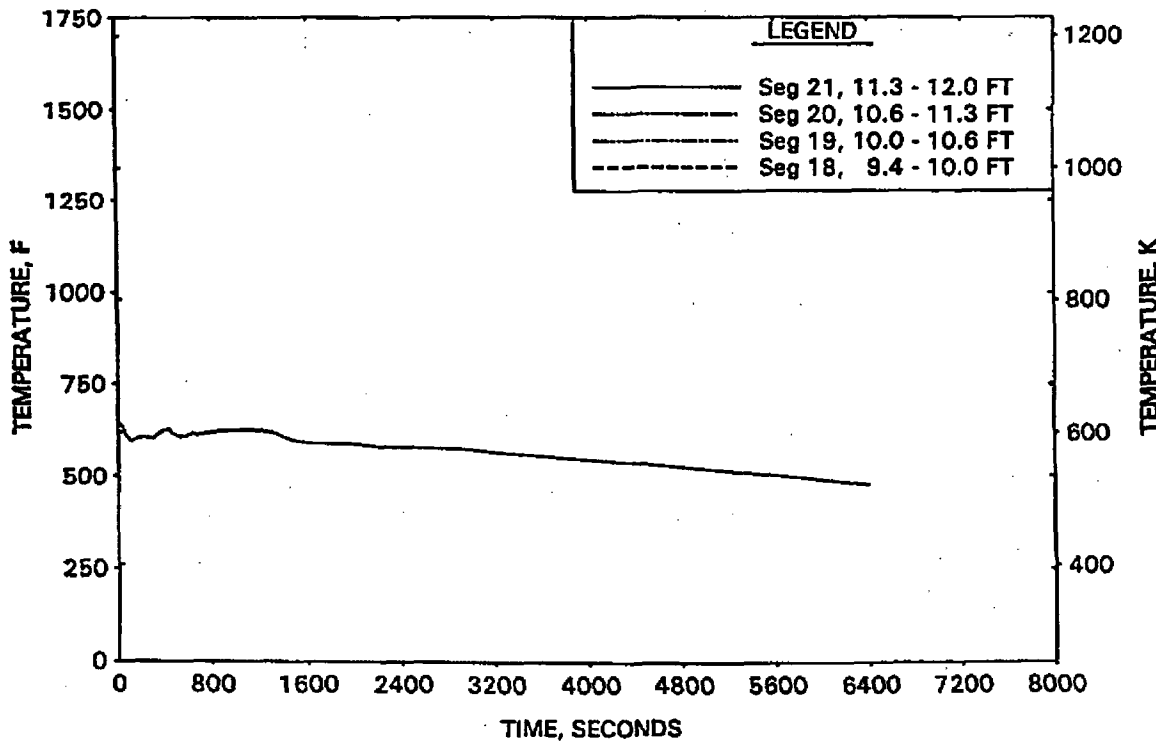


FIGURE A-291. HPI LINE BREAK -
UPPER ELEVATION AVE CHANNEL CLAD TEMPERATURES.

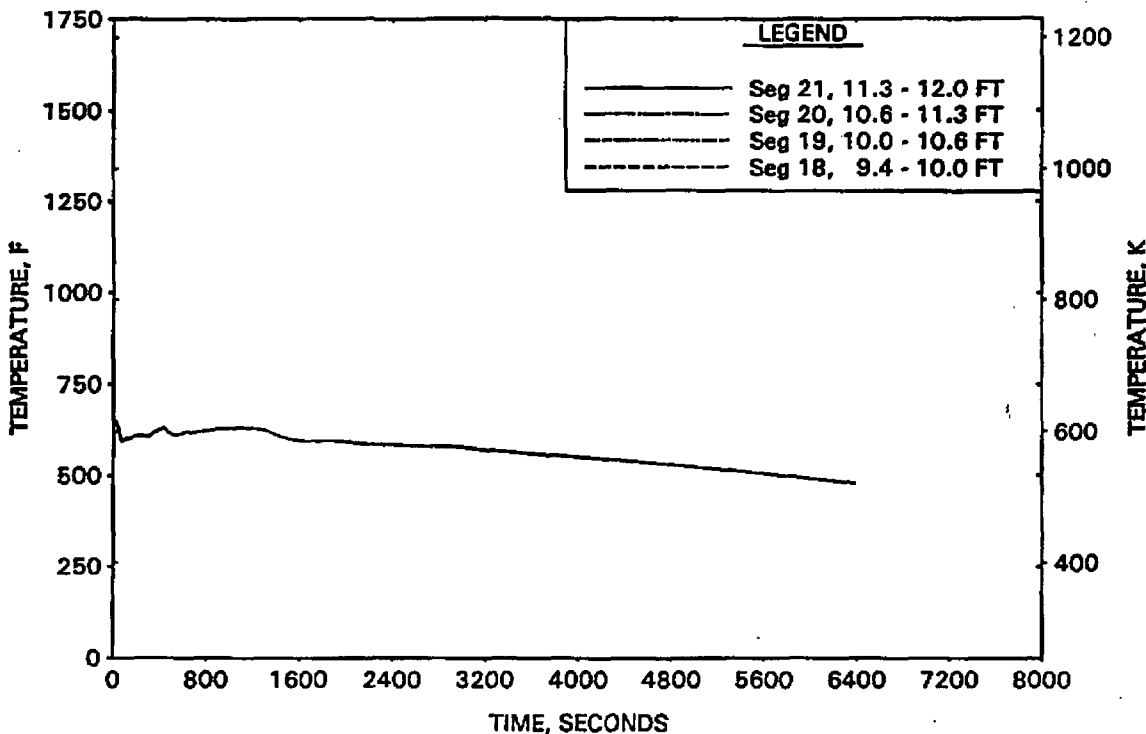


FIGURE A-292. HPI LINE BREAK -
UPPER ELEVATION AVE CHANNEL STEAM TEMPERATURES.

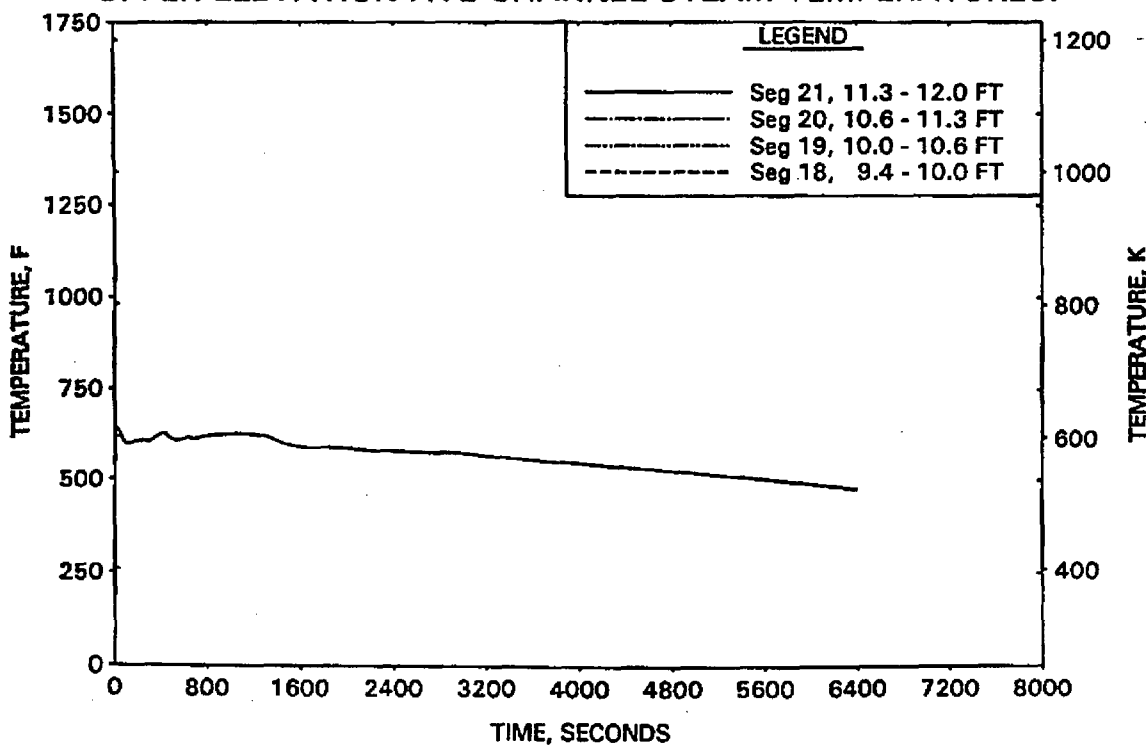
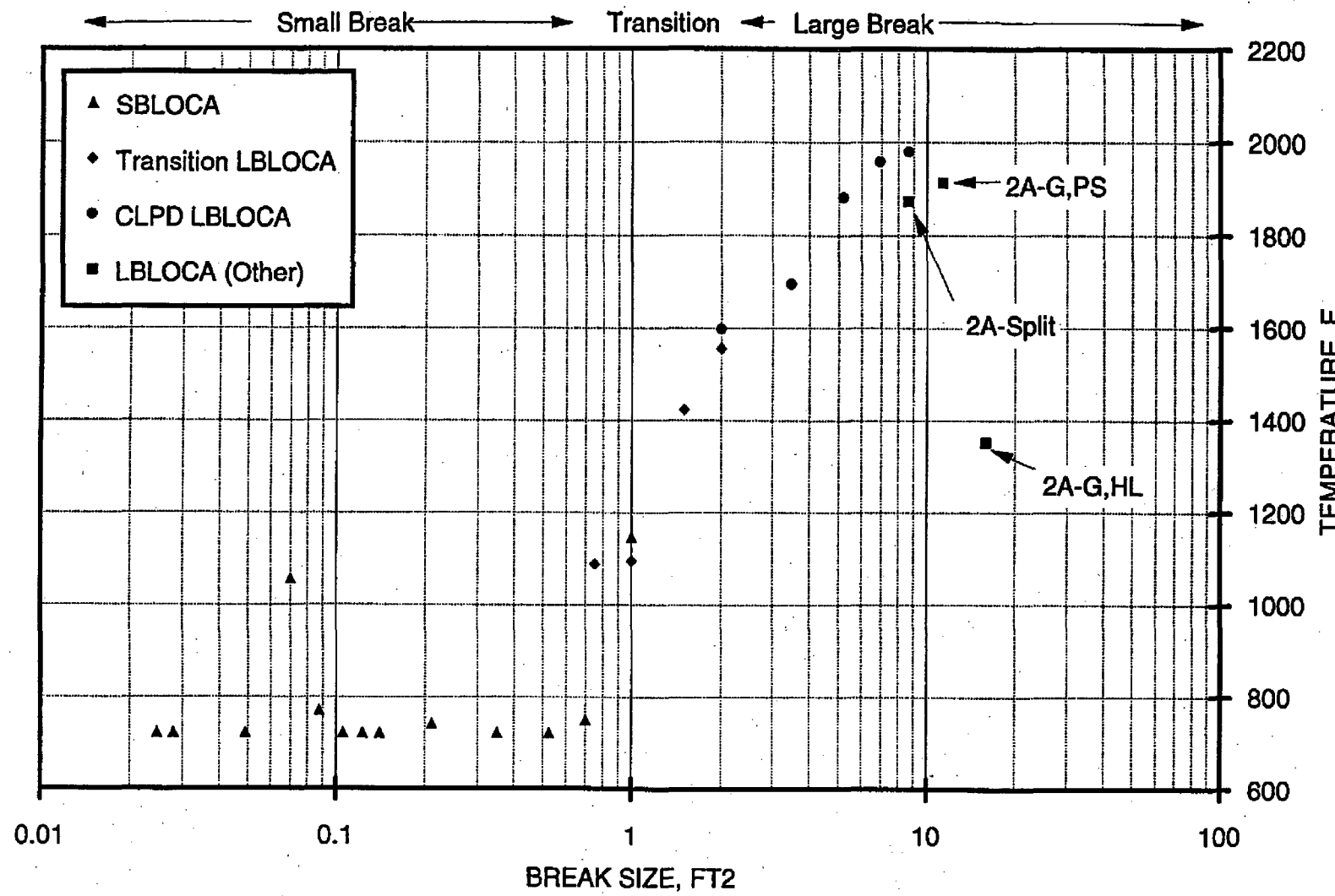


FIGURE A-293. REPRESENTATIVE PCT VERSUS BREAK SIZE.

AREVA NP, INC.

BAW-10192NP-02

This page is intentionally left blank.

FIGURE A-285. HPI LINE BREAK - CLPD COLLAPSED LEVELS.

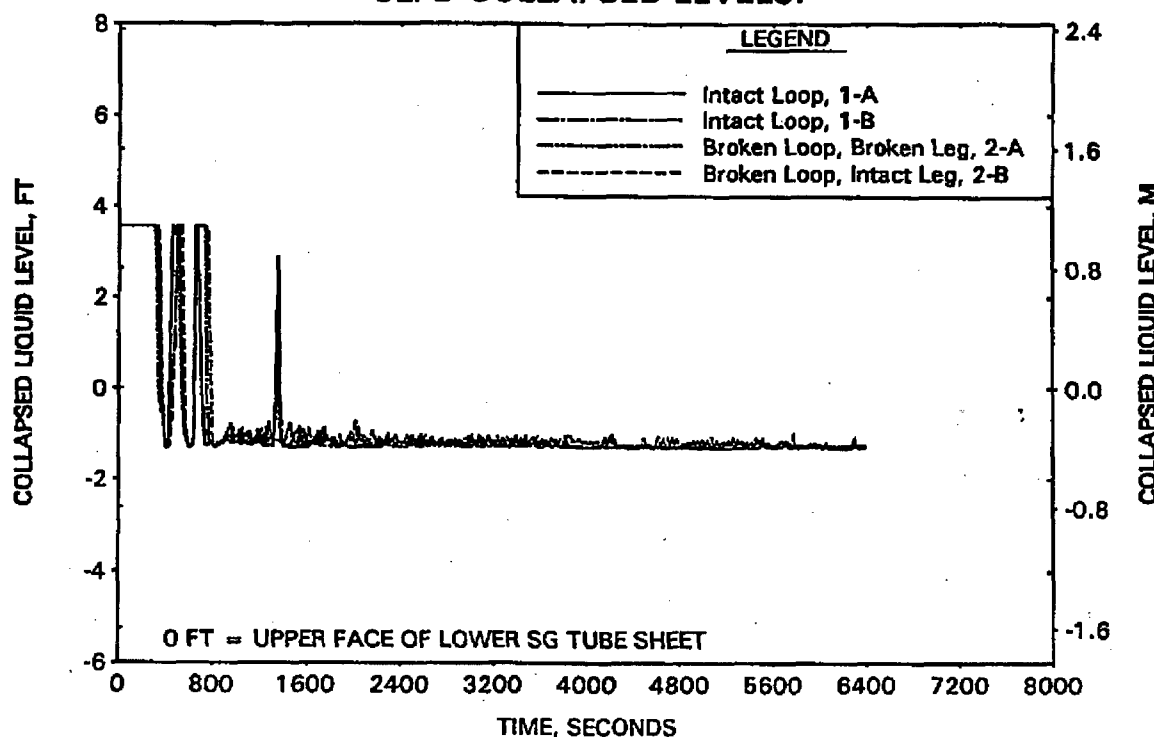


FIGURE A-286. HPI LINE BREAK - CLPS LIQUID VOLUME.

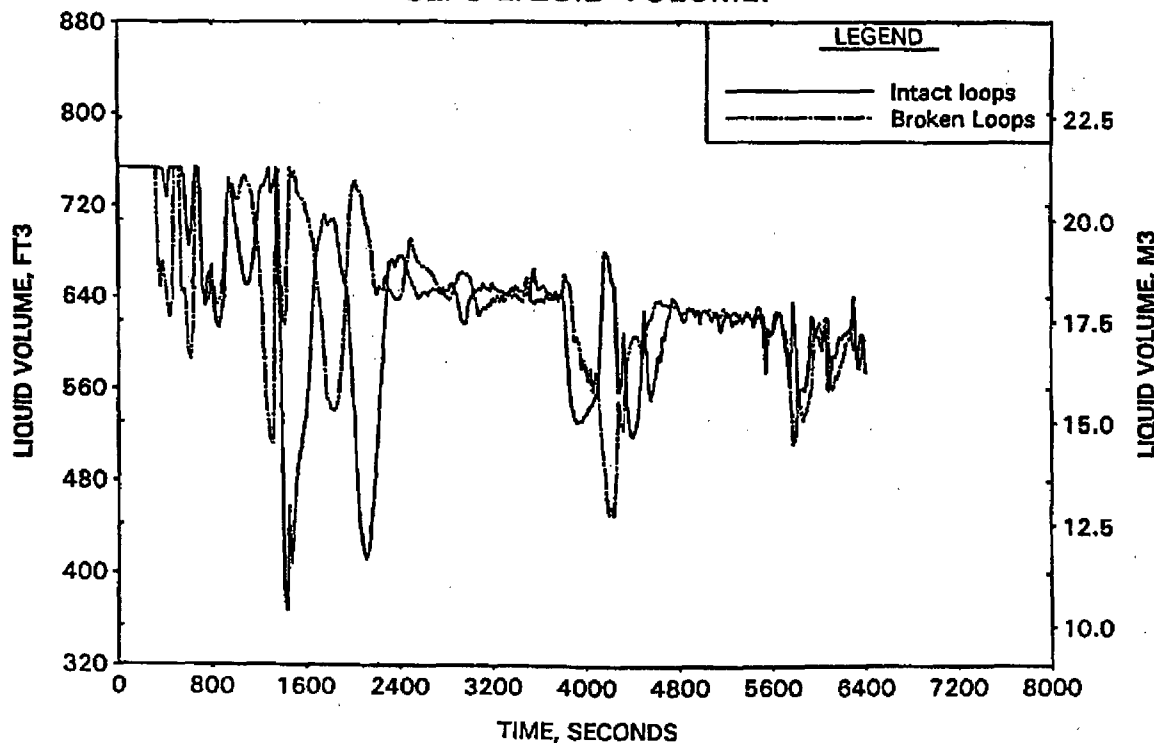


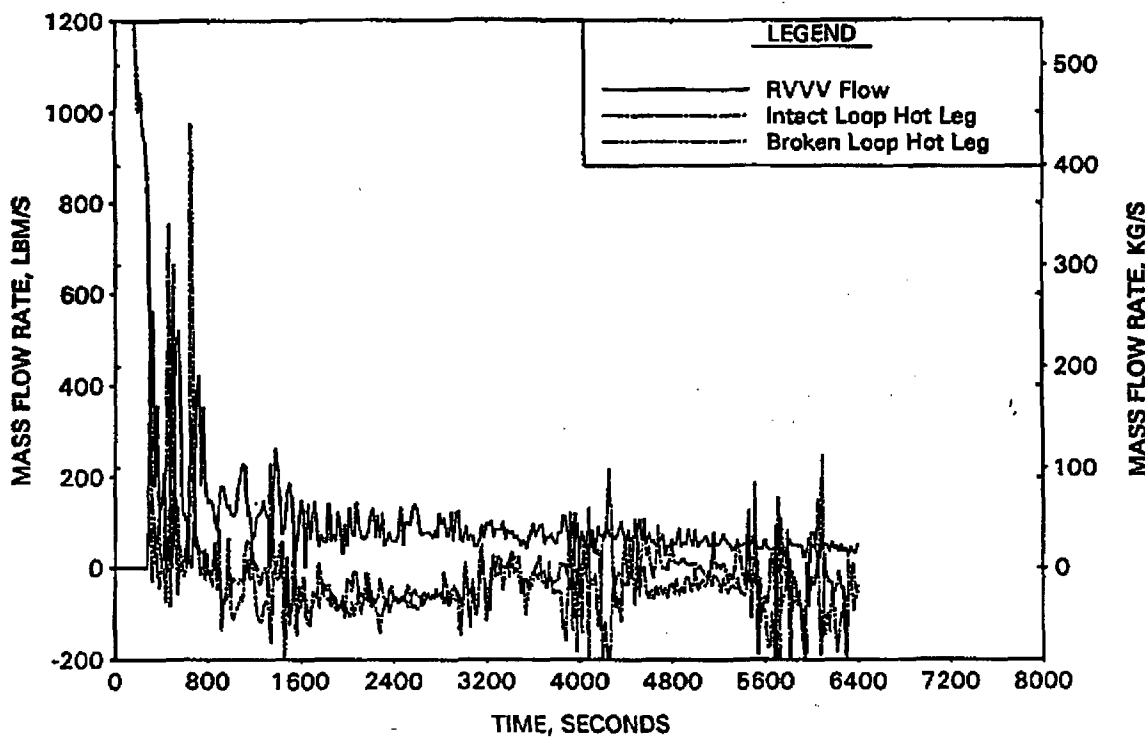
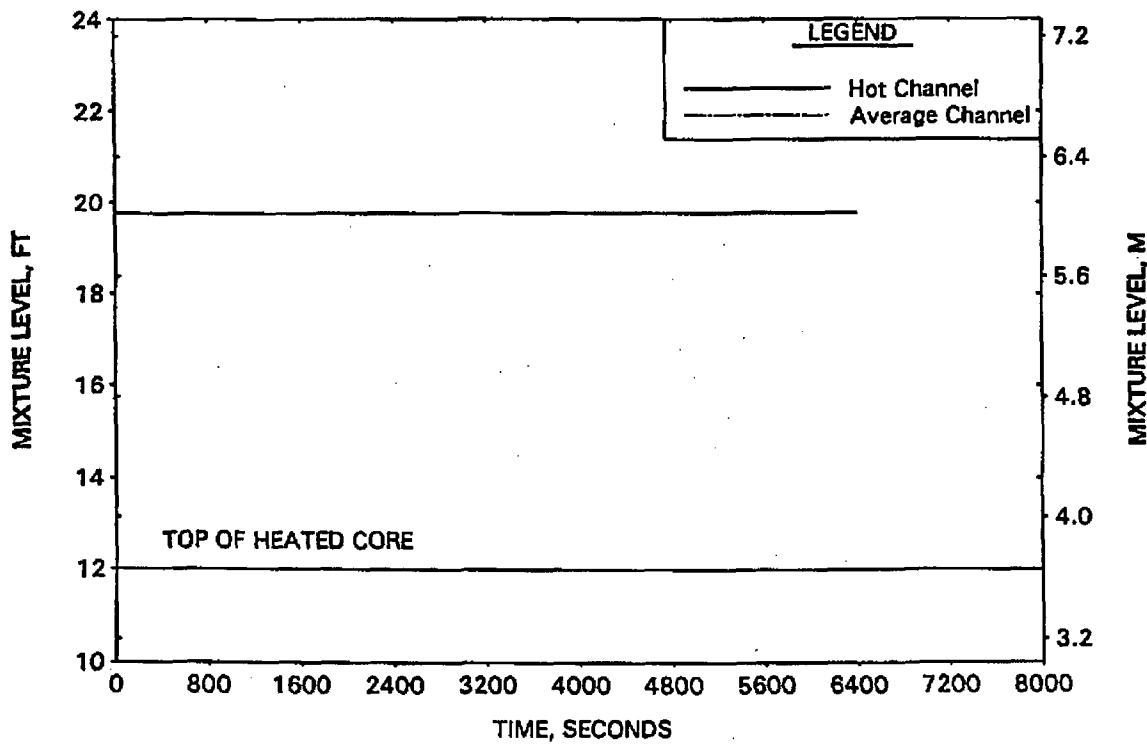
FIGURE A-287. HPI LINE BREAK -
HOT LEG AND RVVV FLOWS.FIGURE A-288. HPI LINE BREAK -
CORE MIXTURE LEVELS.

FIGURE A-289. HPI LINE BREAK -
HOT CHANNEL CLAD TEMPERATURES.

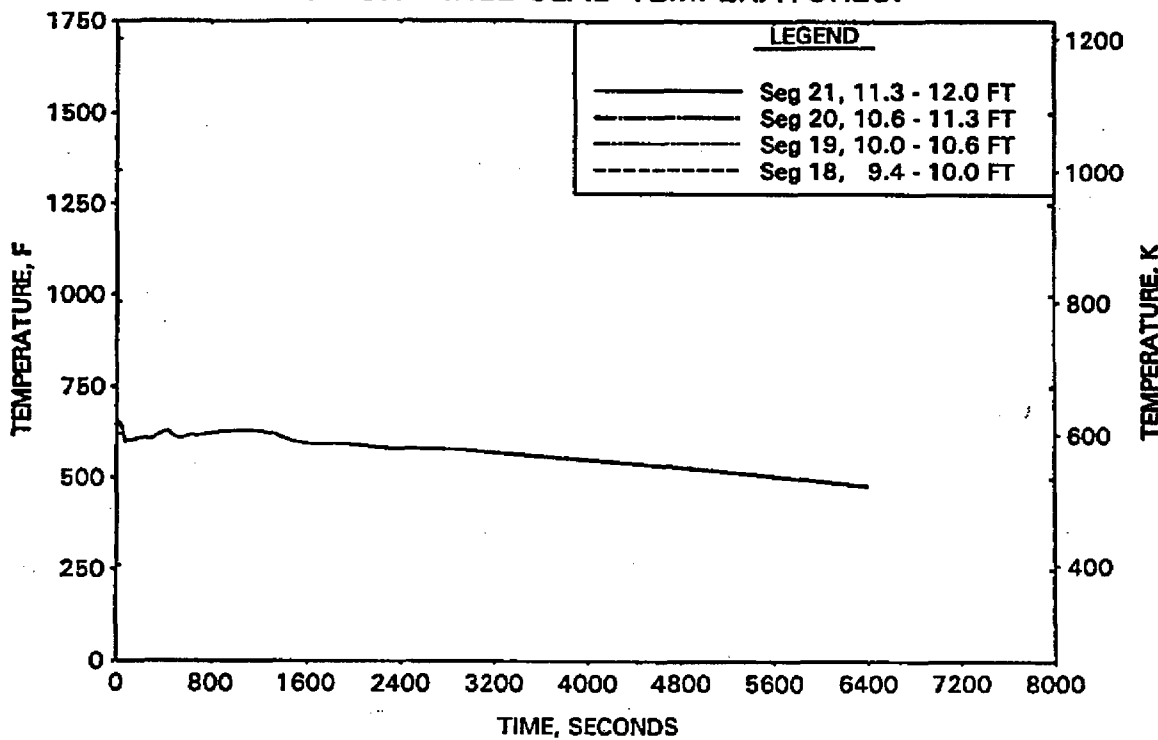


FIGURE A-290. HPI LINE BREAK -
HOT CHANNEL STEAM TEMPERATURES.

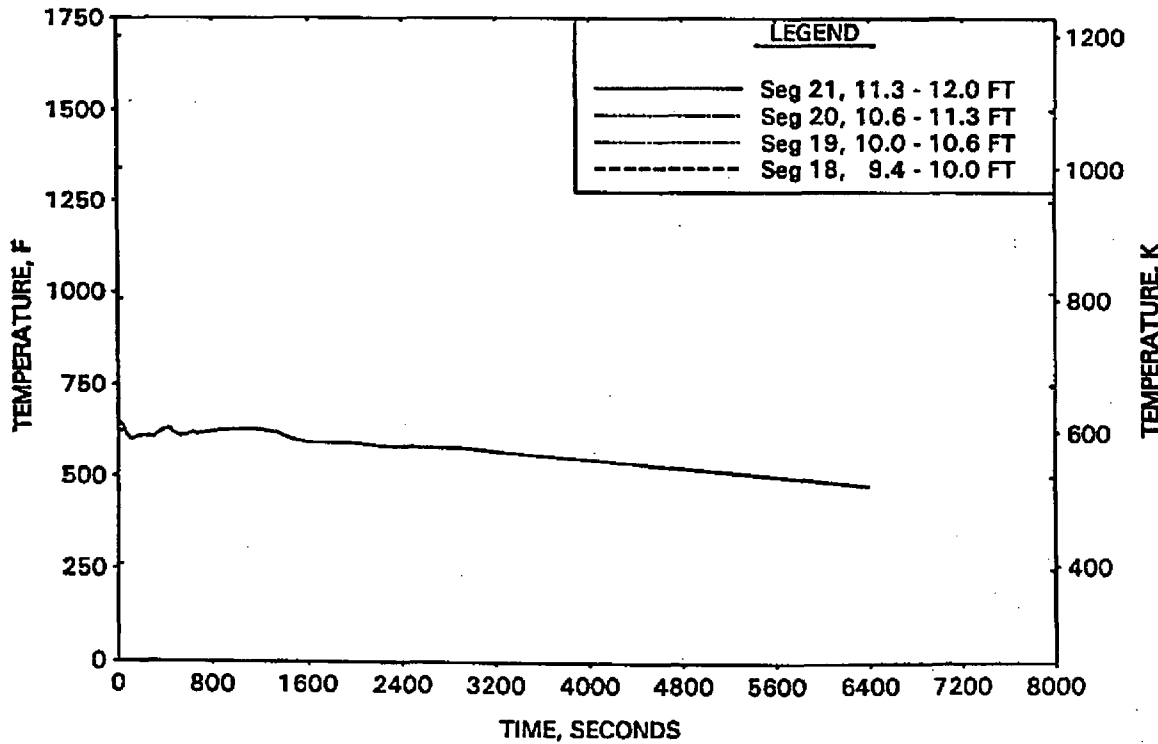


FIGURE A-291. HPI LINE BREAK -
UPPER ELEVATION AVE CHANNEL CLAD TEMPERATURES.

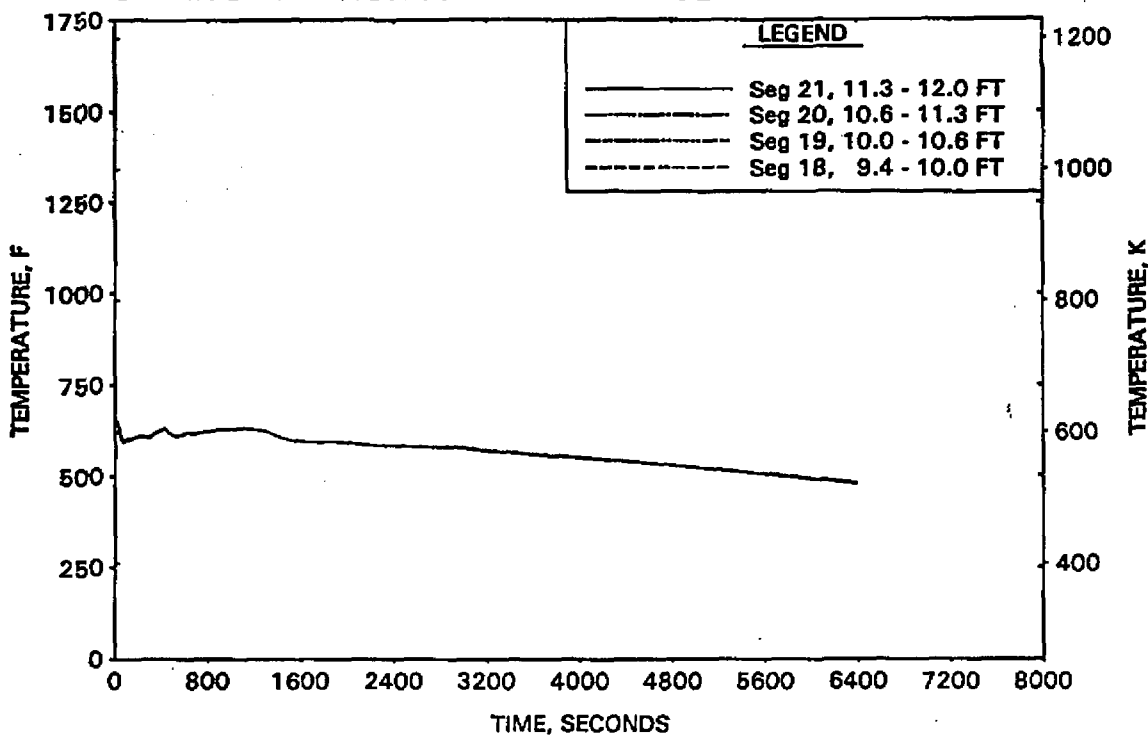


FIGURE A-292. HPI LINE BREAK -
UPPER ELEVATION AVE CHANNEL STEAM TEMPERATURES.

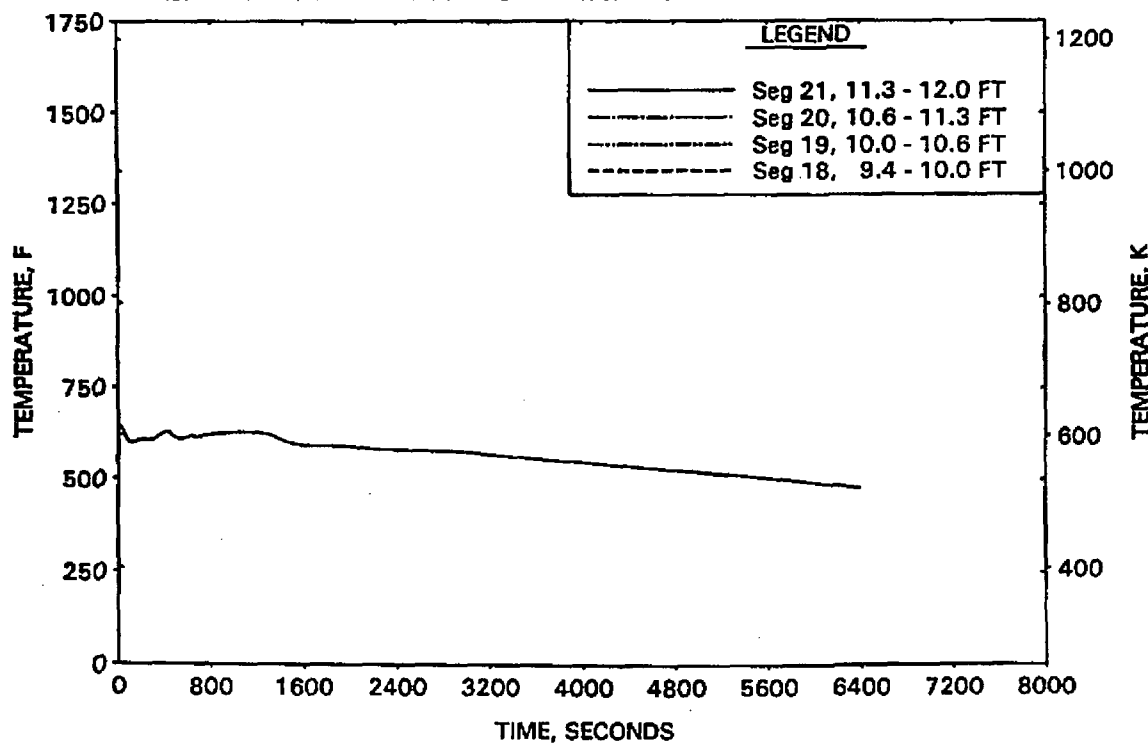
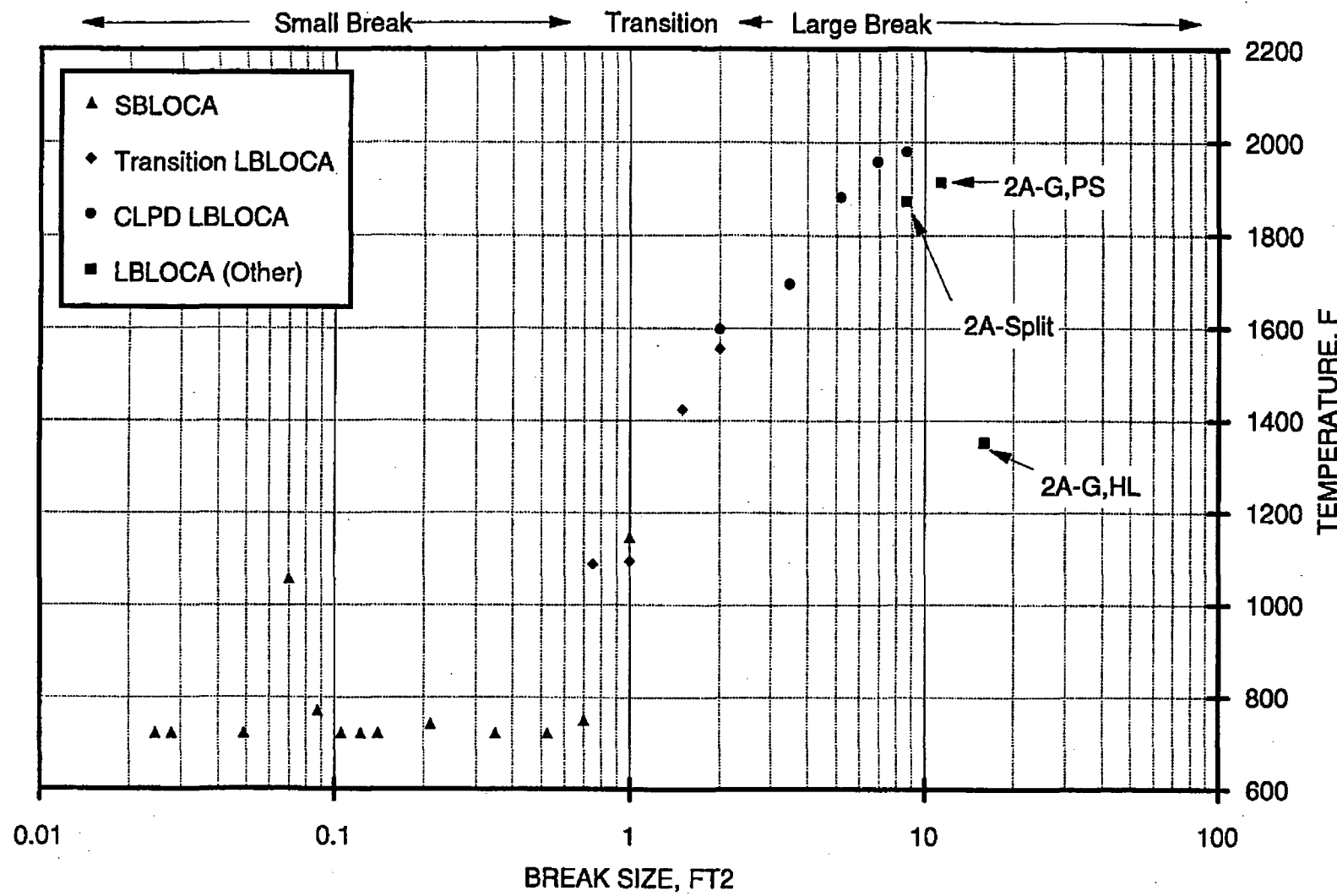


FIGURE A-293. REPRESENTATIVE PCT VERSUS BREAK SIZE.

AREVA NP, INC.

BAW-10192NP-02

This page is intentionally left blank.

AREVA NP, Inc.

BAW-10192NP-02

BAW-10192-A

Topical Report
Revision 0
June 1998

- BWNT LOCA -

BWNT Loss-of-Coolant Accident
Evaluation Model for Once-Through
Steam Generator Plants

Volume III - Licensing Addendum

Framatome Technologies, Inc.
P. O. Box 10935
Lynchburg, Virginia 24506

Framatome Technologies, Inc.
Lynchburg, Virginia 24506

Topical Report BAW-10192-A
Revision 0

June 1998

- BWNT LOCA -

BWNT Loss-of-Coolant Accident
Evaluation Model for Once-Through
Steam Generator Plants

Volume III - Licensing Addendum

Key Words: Large Break, Small Break, LOCA, Transient, Water
Reactors, Evaluation Model

ABSTRACT

This document presents the generic large and small break models to be used by B&W Nuclear Technologies for evaluating the performance of the emergency core cooling systems (ECCS) following a loss-of-coolant accident (LOCA) for all classes of B&W-designed pressurized water reactors (PWR). The large break model is discussed in Volume I and the small break model in Volume II. Volume III is the licensing addendum, which provides a historical record of related correspondence including responses to NRC questions, NRC Safety and Technical Evaluation Reports, and NRC approval letters. The models have been developed and compared with the required and acceptable features contained in Appendix K of the Code of Federal Regulations, 10CFR50. The evaluation models are shown to conform to Appendix K requirements.

AREVA NP, Inc. BAW-10192NP-02

This page is intentionally left blank.

Addendum Purpose and Revision Policy -- BAW-10192A

The Licensing Addendum is provided as a convenient and logical way to provide access to the record of correspondence concerning this report. The material contained in the addendum comprises records of transmittals concerning the report, NRC questions and BWNT responses, NRC Safety and Technical Evaluation Reports (SER and TER) of previous revisions, NRC approval letters of previous revisions, and other material as necessary to present a reasonable record. The records of all revision levels of the report are included in chronological order with a brief descriptive statement provided at the beginning of each. Because the addendum is historical, the material in the addendum is not subject to revision, errors excepted. The addendum will change through additions. No record of revision is, therefore, included in the addendum. The table of contents serves as a complete record of the status of the addendum.

The recorded revision level for the addendum will be kept the same as the most recent revision of the topical report. Unless the current revision of the topical is approved by the NRC, the addendum is not likely to include correspondence on the current revision level. Once NRC approval of a revision has been granted, the report will be reissued as an approved topical with the NRC SER, TER, and approval letter included in this addendum. A statement referencing the location of these reports will be inserted after the report title page (to comply with the regulation that the current SER, TER, and approval letter of an approved report must follow the report title page). No revision level change will be made when releasing the approved version, rather the letter "A" will be appended to the report identification number.

This page is intentionally left blank.

LICENSING ADDENDUM CONTENTS -- BAW-10192-A

1. Transmittal of BAW-10192P, Revision 0, February 1994	LA-1
2. Transmittal Letter for BAW-10192P, James H. Taylor, February 1994	LA-3
3. Affidavit of James H. Taylor.....	LA-5
4. BWNT LOCA EM Topical Question Index.....	LA-11
5. Transmittal Letter for Response to NRC Questions (43-10192Q-00) from James H. Taylor, May 1996.....	LA-15
6. Response to NRC Questions (43-10192Q-00) on BAW-10192P, May 1996	LA-17
7. Transmittal Letter for Response to NRC Questions (43-10192Q-01) from James H. Taylor, October 1996 ..	LA-75
8. Response to NRC Questions (43-10192Q-01) on BAW-10192P, October 1996	LA-77
9. Transmittal Letter for Response to NRC Questions (43-10192Q-02) from James H. Taylor, January 1997 ..	LA-95
10. Affidavit of James H. Taylor on Proprietary Nature of Response to NRC Questions (43-10192Q-02)	LA-97
11. Response to Verbal NRC Question (43-10192Q-02) on BAW-10192P, January 1997	LA-103
12. Transmittal Letter for SER on BAW-10192P, James E. Lyons, February 1997	LA-141
13. SER on BAW-10192P, Revision 00	LA-143
14. TER on BAW-10192P, Revision 00, Prepared by SCIENTECH, Inc.....	LA-165
15. Response to NRC Questions (43-10192Q-03)	LA-189

Transmittal of BAW-10192P, Revision 0

BAW-10192P, Revision 0 was issued for licensing review in proprietary form on February 15, 1994. The report was transmitted to the NRC via the following letter.

J. H. Taylor (BWNT) to R. C. Jones (NRC), JHT/94-18, February 15, 1994.

This page is intentionally left blank.



B&W NUCLEAR TECHNOLOGIES

JHT/94-18
February 15, 1994

3315 Old Forest Road
P.O. Box 10935
Lynchburg, VA 24505-0935
Telephone: 804-385-2000
Telex: 804-385-3663

Mr. Robert C. Jones, Chief
Reactor Systems Branch
Division of Systems Safety and Analysis
U. S. Nuclear Regulatory Commission
Washington, D.C. 20555-0001

Subject: "BWNT LOCA - BWNT Loss-of-Coolant Accident Evaluation
Model for Once-Through Steam Generator Plants",
BAW-10192P.

Dear Mr. Jones:

Enclosed are five copies of the RELAP5/MOD2-B&W-based BWNT LOCA evaluation model applicable to all B&W-designed plants. BWNT intends for the first applications of these LOCA methods to be used for Oconee MARK-B11 fuel reload and Bellefonte plant start-up analyses.

The information in the attachments is considered "Proprietary" as sworn by me as Manager of Licensing Services, B&W Nuclear Technologies, in my affidavit presented with this original topical report submittal, and should be treated as such. Three additional copies of the EM are included with the proprietary information clearly identified for SER reference purposes.

It would be helpful if the NRC's review could be scheduled to provide an SER by February 1, 1995.

If clarification of any of the provided information is needed please contact John Klingenfus at (804) 385-3294.

Very truly yours,

J. H. Taylor, Manager
Licensing Services

JHT/bcc

Enclosures

cc: J. B. Hopkins/NRC
K. L. Bohrer/NRC
R. B. Borsum/BWNT
L. J. Barker/BWNT

This page is intentionally left blank.

AFFIDAVIT OF JAMES H. TAYLOR

- A. My name is James H. Taylor. I am Manager of Licensing Services for B&W Nuclear Technologies (BWNT), and as such I am authorized to execute this Affidavit.
- B. I am familiar with the criteria applied by BWNT to determine whether certain information of BWNT is proprietary and I am familiar with the procedures established within BWNT to ensure the proper application of these criteria.
- C. In determining whether a BWNT document is to be classified as proprietary information, an initial determination is made by the Unit Manager, who is responsible for originating the document, as to whether it falls within the criteria set forth in Paragraph D hereof. If the information falls within any one of these criteria, it is classified as proprietary by the originating Unit Manager. This initial determination is reviewed by the cognizant Section Manager. If the document is designated as proprietary, it is reviewed again by Licensing personnel and other management within BWNT as designated by the Manager of Licensing Services to assure that the regulatory requirements of 10 CFR Section 2.790 are met.
- D. The following information is provided to demonstrate that the provisions of 10 CFR Section 2.790 of the Commission's regulations have been considered:
 - (i) The information has been held in confidence by BWNT. Copies of the document are clearly identified as proprietary. In addition, whenever BWNT transmits the

AFFIDAVIT OF JAMES H. TAYLOR (Cont'd.)

information to a customer, customer's agent, potential customer or regulatory agency, the transmittal requests the recipient to hold the information as proprietary. Also, in order to strictly limit any potential or actual customer's use of proprietary information, the following provision is included in all proposals submitted by BWNT, and an applicable version of the proprietary provision is included in all of BWNT's contracts:

"Purchaser may retain Company's proposal for use in connection with any contract resulting therefrom, and, for that purpose, make such copies thereof as may be necessary. Any proprietary information concerning Company's or its Supplier's products or manufacturing processes which is so designated by Company or its Suppliers and disclosed to Purchaser incident to the performance of such contract shall remain the property of Company or its Suppliers and is disclosed in confidence, and Purchaser shall not publish or otherwise disclose it to others without the written approval of Company, and no rights, implied or otherwise, are granted to produce or have produced any products or to practice or cause to be practiced any manufacturing processes covered thereby.

Notwithstanding the above, Purchaser may provide the NRC or any other regulatory agency with any such proprietary information as the NRC or such other agency may require; provided, however, that Purchaser shall first give Company written notice of such proposed disclosure and Company shall have the right to amend such proprietary information so as to make it non-proprietary. In the event that Company cannot amend such proprietary information, Purchaser

AFFIDAVIT OF JAMES H. TAYLOR (Cont'd.)

shall, prior to disclosing such information, use its best efforts to obtain a commitment from NRC or such other agency to have such information withheld from public inspection.

Company shall be given the right to participate in pursuit of such confidential treatment."

- (ii) The following criteria are customarily applied by BWNT in a rational decision process to determine whether the information should be classified as proprietary. Information may be classified as proprietary if one or more of the following criteria are met:
- a. Information reveals cost or price information, commercial strategies, production capabilities, or budget levels of BWNT, its customers or suppliers.
 - b. The information reveals data or material concerning BWNT research or development plans or programs of present or potential competitive advantage to BWNT.
 - c. The use of the information by a competitor would decrease his expenditures, in time or resources, in designing, producing or marketing a similar product.
 - d. The information consists of test data or other similar data concerning a process, method or component, the application of which results in a competitive advantage to BWNT.
 - e. The information reveals special aspects of a process, method, component or the like, the exclusive use of which results in a competitive advantage to BWNT.

AFFIDAVIT OF JAMES H. TAYLOR (Cont'd.)

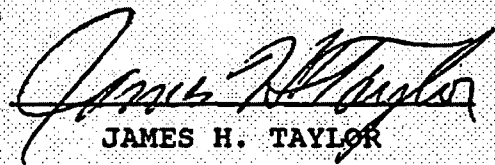
- f. The information contains ideas for which patent protection may be sought.

The document(s) listed on Exhibit "A", which is attached hereto and made a part hereof, has been evaluated in accordance with normal BWNT procedures with respect to classification and has been found to contain information which falls within one or more of the criteria enumerated above. Exhibit "B", which is attached hereto and made a part hereof, specifically identifies the criteria applicable to the document(s) listed in Exhibit "A".

- (iii) The document(s) listed in Exhibit "A", which has been made available to the United States Nuclear Regulatory Commission was made available in confidence with a request that the document(s) and the information contained therein be withheld from public disclosure.
- (iv) The information is not available in the open literature and to the best of our knowledge is not known by Combustion Engineering, EXXON, General Electric, Westinghouse or other current or potential domestic or foreign competitors of BWNT.
- (v) Specific information with regard to whether public disclosure of the information is likely to cause harm to the competitive position of BWNT, taking into account the value of the information to BWNT; the amount of effort or money expended by BWNT developing the information; and the ease or difficulty with which the information could be properly duplicated by others is given in Exhibit "B".
- E. I have personally reviewed the document(s) listed on Exhibit "A" and have found that it is considered proprietary by BWNT because it contains information which falls within one or more of the

AFFIDAVIT OF JAMES H. TAYLOR (Cont'd.)

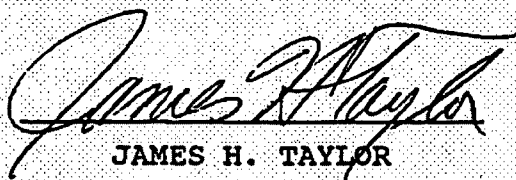
criteria enumerated in Paragraph D, and it is information which is customarily held in confidence and protected as proprietary information by BWNT. This report comprises information utilized by BWNT in its business which afford BWNT an opportunity to obtain a competitive advantage over those who may wish to know or use the information contained in the document(s).



JAMES H. TAYLOR

State of Virginia)
) SS. Lynchburg
City of Lynchburg)

James H. Taylor, being duly sworn, on his oath deposes and says that he is the person who subscribed his name to the foregoing statement, and that the matters and facts set forth in the statement are true.



JAMES H. TAYLOR

Subscribed and sworn before me
this 15th day of February 1994.

Brenda C. Cardosa
Notary Public in and for the City
of Lynchburg, State of Virginia.

My Commission Expires July 31, 1995.

EXHIBITS A & B

EXHIBIT A

BWNT Proprietary Topical Report BAW-10192P, Rev. 0, "BWNT LOCA - BWNT Loss-of-Coolant Accident Evaluation Model for Once-Through Steam Generator Plants", February 1994.

EXHIBIT B

The above listed document contains information which is considered Proprietary in accordance with Criteria b, c, and d of the attached affidavit.

BWNT LOCA EM Topical Question Index for Revision 00

**Initial Questions
BWNT LOCA Requests for Additional Information**

Volume I - LBLOCA

<u>Question #</u>	<u>Topic</u>	<u>Page #</u>
1.	LPI and CFT noding locations	LA-17
2.	HPI noding location	LA-20
3.	RVVV modeling for LBLOCA	LA-20
4.	Partial and complete end of bypass	LA-20
5.	REFLOD3B input to BEACH, FLECHT correlation .	LA-25
6.	Friction factors for transient flow in REFLOD3B	LA-26
7.	Transition LOCA bypass models	LA-26
8.	Steady-state fuel temp. for LOCA analyses ...	LA-29
9.	Reflood rate and steam-water interaction for hot leg or transition LOCAs	LA-29
10.	Amount of water in cold leg piping at EOB ...	LA-30
11.	RELAP5/MOD2-B&W time step sensitivity	LA-31
12.	Integrated accumulator injection	LA-32
13.	PCT at EOB for break noding study	LA-32
14.	Cross-flow modeling	LA-33
15.	Format of blank pages	LA-37
16.	BEACH time step convergence and ramped inlet subcooling	LA-37
17.	BEACH calculation time frame	LA-51
18.	Oxidation increase for sensitivity studies ..	LA-51
19.	RCS pressure history in Figure A-11	LA-52
20.	Pin burnup effect on clad and fuel temperatures	LA-53
21.	Integrated break flow corrections to Tables A-19, A-20 and A-22.	LA-53
22.	Average oxidation increase in Table A-21	LA-55
23.	Target PCT range	LA-55
24.	Mass and energy release at EOB and start of reflood	LA-55
25.	Filtering of heat transfer coefficient for plots	LA-56

Verbal Requests for Additional Information

26.	BEACH steam only cooling, Appendix K requirements	LA-57
-----	--	-------

BWNT EM LOCA Topical Question Index for Revision 00
(continued)

Initial Questions
BWNT LOCA Requests for Additional Information

Volume II - SBLOCA

Question #	Topic	Page #
1.	RCPs 'on' versus 'off'	LA-58
2.	Containment pressure and use of CONTEMPT	LA-59
3.	Analysis power levels greater than 1.02 times licensed power	LA-59
4.	Steady-state fuel temp. effect on PCT	LA-59
5.	Actinide decay heat level	LA-60
6.	Definition of thermal center	LA-60
7.	Fictitious break volume and location	LA-61
8.	CLPD break entrainment criteria	LA-62
9.	Increase in CFT line resistance	LA-62
10.	Mixture level sensitivity relative to control volume height	LA-63
11.	SBLOCA time-in-life sensitivity studies	LA-64
12.	RVvv modeling with time-dependent junctions .	LA-66
13.	Calculation of amount of oxide thickness per mass basis	LA-67
14.	ECCS fluid temperatures	LA-67
15.	RV mixture and collapsed liquid levels	LA-68
16.	Filtering RVvv and hot leg mass flow rates for plots	LA-68
17.	Clad temp. and core mixture level sensitivity to time step	LA-69
18.	Transient termination for SBLOCA cases	LA-69
19.	Break size distribution used in SBLOCA analyses	LA-70
20.	Anomalous increase in break flow for base case	LA-70
21.	RELAP5 user reported errors and void fraction decreases	LA-71
22.	Break volume void fraction history	LA-72
23.	RCS elevation datum	LA-72
24.	Cold leg liquid volume and collapsed level ..	LA-74

BWNT EM LOCA Topical Question Index for Revision 00
(continued)

Second Round of Questions (43-10192Q-01)
BWNT LOCA Requests for Additional Information

<u>Question #</u>	<u>Topic</u>	<u>Page #</u>
1.	Radial vs. axial peak compliance with Appendix K	LA-77
2.	Hot leg/transition method compliance with Appendix K	LA-90
3.	Calculation of CLPS loop seal reformation ...	LA-91
4.	Plant fuel reload core operating limits LOCA analyses	LA-92
Unsolicited clarification for Question 5, Volume II (SBLOCA), 43-10192Q-00.		
5.	Actinide decay heat level	LA-94

Third Round of Questions (43-10192Q-02)
BWNT LOCA Requests for Additional Information

<u>Topic</u>	<u>Page #</u>
Sample LBLOCA EM calculation for 177-FA LL plants	LA-103

Fourth Round of Questions (43-10192Q-03)
BWNT LOCA Requests for Additional Information

<u>Topic</u>	<u>Page #</u>
Unsolicited clarification for Question 21, Volume I (LBLOCA), 43-10192Q-00.	
Response to a Typographical Error in Discussion Of the Three-Operating Reactor Coolant Pump Study	LA-189

This page is intentionally left blank.



Integrated Nuclear Services

JHT/96-33
May 6, 1996

Document Control Desk
U. S. Nuclear Regulatory Commission
Washington, DC 20555-0001

Subject: Responses to Request for Additional Information on BWNT LOCA - BWNT Loss-of-Coolant Accident Evaluation Model for Once-Through Steam Generator Plants, BAW-10192P.

Gentlemen:

Attached are responses to the formal questions, including one verbal request, for additional information on the original release of Topical Report BAW-10192P, "BWNT LOCA, BWNT Loss-of-Coolant Accident Evaluation Model for Once-Through Steam Generator Plants." These responses were previously sent as a draft for consideration by the NRC reviewer. The material adequately addresses the reviewer's questions, therefore, the identical responses are being transmitted officially for inclusion in the SER material.

Some information in the attached responses (specifically LBLOCA Questions 3, 4, 7, 14, and 16, and SBLOCA Question 12) is considered "Proprietary" as sworn by me as Manager of Licensing Services, Framatome Technologies, Incorporated (formerly B&W Nuclear Technologies) in my affidavit presented with the February 15, 1994 submittal of the topical report, and should be treated as such. If clarification of any of the provided information is needed, please contact John Klingenfus at (804) 832-3294.

Very truly yours,

A handwritten signature in cursive ink that reads "J. H. Taylor/bcc".

J. H. Taylor, Manager
Licensing Services

JHT/bcc
Attachment

c: L. Lois/NRC
R. B. Borsum/FTI
R. J. Schomaker/FTI
J. A. Klingenfus/FTI

(LA-15)

This page is intentionally left blank.

Requests for Additional Information
BAW-10192P, Revision 0

"BWNT Loss-of-Coolant Accident Evaluation Model
For Once-Through Steam Generator Plants"

Volume I - Large Break

1. (Section 4.3.1, Figure 4-3) The low pressure injection system and the core flood tanks are connected directly to the vessel as shown in Figure 4-3. Does this reflect the actual arrangement in the plant or are these connections to the cold leg several feet upstream of the vessel? If the connections are to the cold leg in the actual design, please discuss the reasons for the nodalization shown in Figure 4-3 and the impact on the large break LOCA results.

One unique design feature of the B&W-designed plants is the direct vessel injection of the CFT and LPI. The LPI piping connects into the CFT line just upstream of the vessel. The CFT enters the downcomer horizontally through one of two nozzles at an elevation two feet above the nozzle belt centerline. Check-valves prevent backflow into the CFT or LPI lines during steady-state or transient operation. This arrangement is shown in the LBLOCA model presented in Figure 4-3. Supplementary Figures 1-1 and 1-2 show this geometrical arrangement for the B&W-designed lowered-loop plants.

Figure 1-1. REACTOR COOLANT SYSTEM ELEVATION ARRANGEMENT.

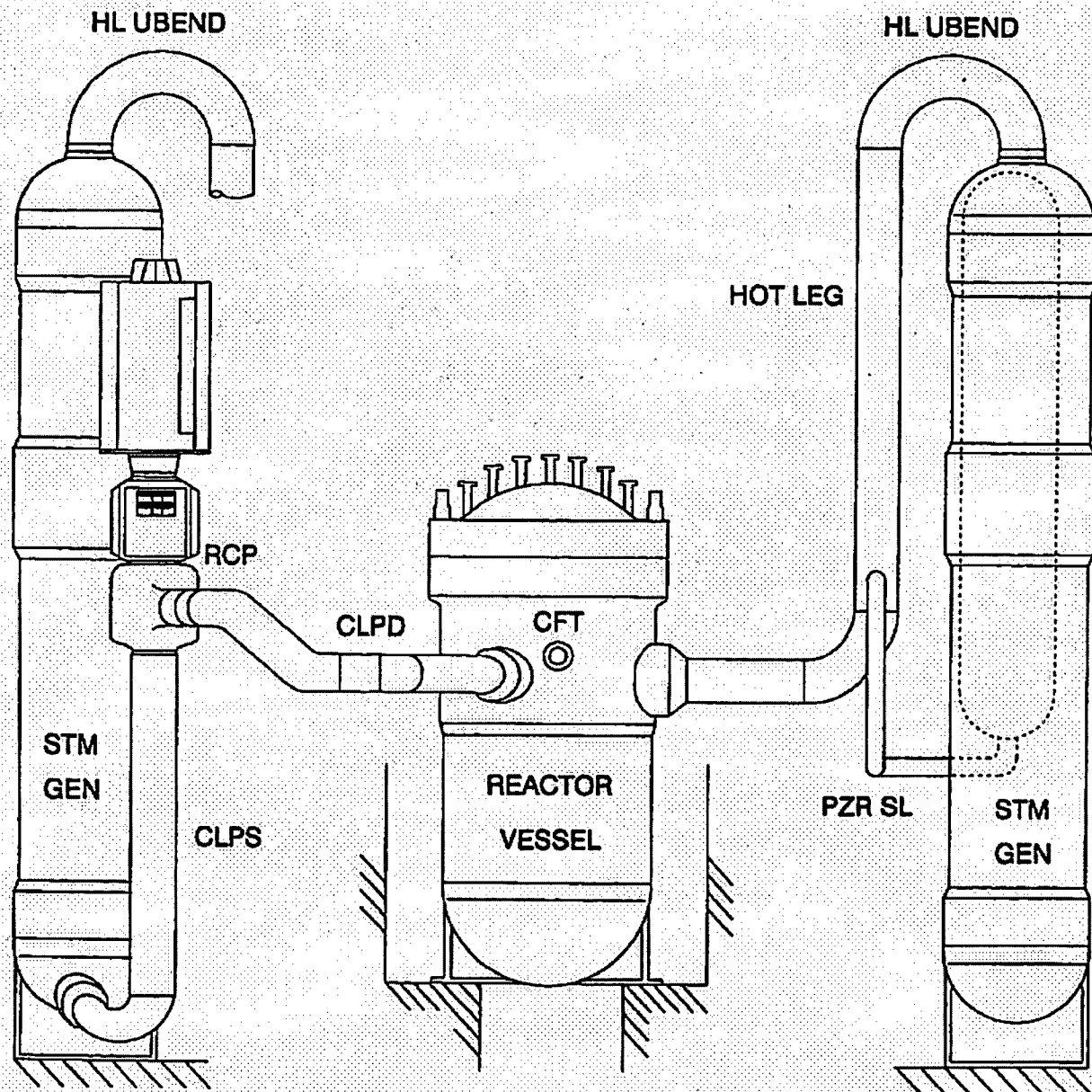
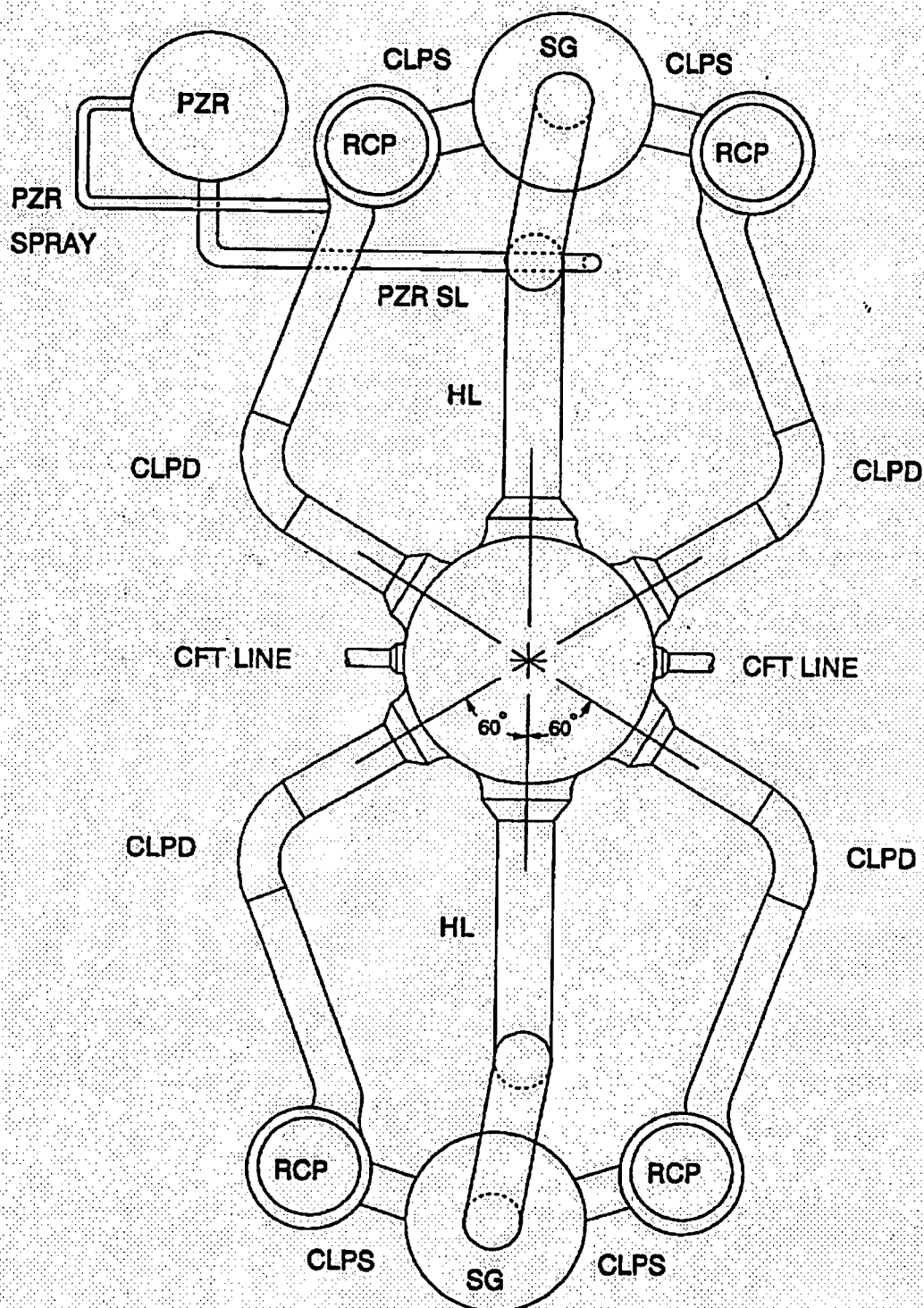


Figure 1-2. REACTOR COOLANT SYSTEM ARRANGEMENT - TOP VIEW.



2. (Section 4.3.1, Figure 4-4) In Figure 4-4, the high pressure injection system is shown as being connected to Volume (271) just downstream of the break (during normal operation). Please discuss the impact (if any) of moving the HPI connection to Volume 270.

The blowdown phase of a limiting LBLOCA transient lasts between 20 and 25 seconds. Typical conservative assumptions used in LBLOCA include a loss of offsite power coincident with break opening. Therefore, initiation of pumped ECCS flow into the RCS is delayed by the emergency diesel startup time plus any conservative time delays needed to account for the emergency safety features actuation signal, signal delays, pump start and spin-up, and alignment of valves in the ECCS piping system. Generally, this total delay time is between 32 and 45 seconds, which precludes the initiation of pumped ECCS flow before the end of blowdown. Also, the broken cold leg HPI connection (Figure 4-4) is included for consistency. For analysis of a postulated double-ended guillotine break, it is assumed that the HPI line is severed; thus, all HPI flow to that leg would spill directly to containment. Therefore, since no HPI flow is available, or allowed to flow into the broken cold leg, there is no effect in moving the HPI connection to Volume 270 in the LBLOCA model.

3. (Section 4.3.1) Please explain how the reactor vessel vent valves are modelled in the large break model (This question is related to Question 12 in the small break LOCA section).

For LBLOCA applications, all of the plant RVVVs are lumped into a single trip valve junction that is open when the pressure differential across the RVVVs is greater than [C,D]. If the pressure differential is less than this value the valves are closed.

4. (Page 4-20) You refer to both partial and complete end of bypass. Explain how each of these variables is calculated, how the model was validated against relevant experimental data and how the requirements of Appendix K, Section I.C.c. are satisfied. In particular, explain how use of a partial end of bypass and a fractional penetration satisfy the Appendix K requirement that "for postulated cold leg breaks, all emergency cooling water injected into the inlet lines or the reactor vessel during the bypass period shall in the calculations be subtracted from the reactor vessel calculated inventory".

Further discussion of end of bypass is also given on page A-16. There is no mention of partial end of bypass in this

section. Is the partial bypass model included in the final EM? The discussion on page A-16 should be consistent with that on Page 4-20.

With respect to ECCS bypass, the cold leg LBLOCA blowdown transient can be characterized by three phases: total bypass, partial bypass, and no bypass. Characterization of the phenomena and discussion of these phases is provided to support of the EM methods and demonstrate how these methods comply with the Appendix K requirements.

The total bypass phase begins when the RCS pressure drops below the CFT fill pressure, and CFT flow initiates (this typically begins 12 to 14 seconds after break opening for the largest or most-limiting breaks). At this time, the break discharge dominates and controls the RCS depressurization. The flashing and boiling of the remaining RCS liquid inventory produces high steam velocities in the upper downcomer region. These velocities are sufficient to entrain all the CFT liquid and carry it out of the broken cold leg. The break flows continue to decrease in proportion to the RCS pressure decline. As the ECCS flows increase and break flows decline, there comes a point at which the steam velocities are no longer sufficient to entrain all ECCS liquid injected into the upper downcomer. Some portion of the CFT flow, particularly that injected through the CFT nozzle farthest removed (opposite side of the downcomer) from the broken cold leg, begins to penetrate the lower downcomer region and the lower plenum. This penetration of the ECCS liquid begins the partial-bypass period. Further depressurization of the RCS by both break flow and ECCS condensation, continues to decrease the break flow and reduces the break flow carryout potential. At some point, the condensation by the CFT flow is sufficient to condense all the steam that flows into the upper downcomer region. At this point, the steam velocities are insufficient to entrain and carry CFT liquid out of the break. This is the beginning of the total end-of-bypass period.

Appendix K requires all the ECCS injected during the bypass period to be subtracted from the reactor vessel inventory. During the RELAP5/MOD2-B&W blowdown analyses, the non-mechanistic ECCS bypass model performs this bypass function throughout refill period by removing all the ECCS injected during the blowdown phase. At the same time, a set of control variables contained in the code input model checks for an end-of-bypass condition. Once end of bypass is predicted, the ECCS flow fraction that should not have been bypassed is integrated such that it can be reintroduced into the lower plenum at the beginning of reflood. The criteria for predicting the time at which the total ECCS bypass ends and the fraction of ECCS liquid retained are determined based on experimental data obtained from tests performed at the Upper Plenum Test Facility (UPTF) (Ref. 4-1).

C,D,E

From a strict EM interpretation, the end-of-bypass is the earliest time at which either the partial-bypass or the end-of-bypass criteria are met. After the partial-bypass is predicted, a conservative integration of the ECCS fraction that reaches the lower plenum is performed. After the end-of-bypass criteria are met, all ECCS liquid will reach the lower plenum. These partial- and end-of-bypass criteria are conservatively determined based on data from prototypical UPTF refill tests. The parameter ranges from the EM analyses are enveloped by the ranges used in the UPTF tests. Therefore, the methods used in the BWNT EM are

conservative with respect to the UPTF data, and comply with the ECCS bypass requirements imposed by Appendix K.

References for Question 4

- 4-1. "Reactor Safety Issues Resolved by the 2D/3D Program", NUREG/IAO-0127, GRS-101, MPR-1346, July 1993.
- 4-2. 2D/3D UPTF Quick Look Report, "Test No.22, Downcomer Injection Test with Vent Valves, E314/91/008", Siemens AG KWU, March 1991.

**Table 4-1. Reactor Vessel Lower Plenum Refilling Measured in
UPTF Direct Downcomer Injection Tests with RVVVs.**

C, D

5. (Page 4-29) Is it correct that the REFLOD3B results are used to establish boundary conditions for BEACH? Explain how use of the FLECHT correlation at a constant flooding rate, constant fuel conductivity and constant gap conductance satisfy Appendix K requirements. In general, the role of this model needs to be better explained so that it is clear what is conservative, e.g. why one would model to "maximize heat removal from the core".

This EM is structured with three primary codes. RELAP5/MOD2-B&W performs the system blowdown thermal-hydraulics and hot pin response in a single, coupled analysis. The adiabatic heatup (refill) and reflood system thermal-hydraulics are performed by REFLOD3B. The REFLOD3B analysis calculates the core inlet flooding rate, core inlet temperature, and core exit pressure boundary conditions that are used in time-dependent components supplied as input to the BEACH hot pin analysis. These REFLOD3B and BEACH analyses are run independently, without coupling or feedback from BEACH to REFLOD3B. Therefore, the analyses are combined with methods that show conservatism, both individually and in the combined EM method. The individual conservatisms include the use of an average channel flooding rate in BEACH and overprediction of the steam binding effects to minimize the average channel flooding rate calculated by REFLOD3B. When combined, these individual code conservatisms produce higher PCTs and delay the time of core quench.

The primary conservatism contained in the REFLOD3B boundary conditions used in the BEACH hot pin solution is low core-average flooding rate. Hot pin cooling is conservatively predicted because the average core flooding rate is used in a decoupled hot channel. That is, no flooding rate augmentation is allowed when the hot channel radial power difference causes its collapsed level to lag behind that of the average core channel. This average core flooding rate is produced by the NRC-approved REFLOD3B code. REFLOD3B calculates a conservative core flooding rate by minimizing the flooding rate potential, that is the manometric pressure differential between the downcomer and core. High core steam production increases the steam binding or over-pressure effects in the upper plenum. One of the steam production sources is the core heat transfer, which is conservatively predicted through the FLECHT correlation with an equivalent constant flooding rate of 3 inches/sec. This heat transfer rate as a function of time is adjusted in time, based on the integration of the calculated variable flooding rate predicted by REFLOD3B. Since the average flooding rates are less than 3 inches/sec, the heat transfer is predicted at earlier times with higher decay heat. This method overpredicts the surface heat transfer and consequently produces more steam that minimizes the predicted flooding rate provided to BEACH. Also, REFLOD3B uses a boundingly high constant fuel and gap conductivity to hasten the heat removal from the rods and produce additional steam binding. These methods maximize the steam

binding effects in REFLOD3B, which results in the prediction of a lower core average flooding rate. BEACH calculates the hot rod thermal response with this conservative core average flooding rate boundary condition, which minimizes the fuel pin surface heat transfer.

The dynamic gap conductance requirements in Appendix K are satisfied by the RELAP5/MOD2-B&W pin model, which calculates variable fuel, gap, and cladding conductivities during the blowdown transient. It also accounts for the presence of fission gases consistent with the fuel rod burnup state. The BEACH code uses the same pin model to continue the dynamic fuel rod temperature predictions during refill and reflood. The gap conductivity is adjusted in these codes using fuel thermal expansion and cladding thermal and mechanical expansion. The NUREG-0630 plastic swell and rupture models are used to determine the deformed cladding geometry. Since RELAP5/MOD2-B&W and BEACH codes are used to predict the hot rod thermal performance, the requirements of Appendix K are satisfied in the hot pin PCT analysis.

6. (Page 4-32) Please provide a more detailed explanation of the approach which calculates the friction factors for transient flow. Is this a two-phase correction or some other type of adjustment?

The REFLOD3B transient friction factors are calculated from the steady-state friction factors adjusted using Colebrook's expression for turbulent friction as a function of Reynolds Number (Eqn 2-4 and 2-5 of BAW-10171P). This friction factor is further adjusted via a two-phase friction multiplier, which is determined by the Martinelli-Nelson model. Section 2.2.1.1 of the NRC-approved REFLOD3B code topical (BAW-10171P) provides the details of the Colebrook and Martinelli-Nelson calculations used during the reflood transient. These adjustments adequately translate the steady-state friction factor to the appropriate value based on the thermal-hydraulic fluid conditions as required by Appendix K.

7. (Page 4-36) In section 4.3.7.1 item 3 states that the ECCS non mechanistic bypass model is deactivated and that the code determines bypass flows. Prediction of bypass flow is further discussed in A.6.4.1. What is the basis for concluding that the bypass was properly simulated? There are no comparisons to experimental data, or even presentations of the amount of bypass predicted.

The requirements of 10 CFR 50.46 and Appendix K dictate the acceptance criteria and the methods used to determine the consequences from a postulated RCS pipe rupture. LOCA analyses are required to bound a spectrum of break sizes and locations anywhere in the RCS. The break sizes range from the full double-ended rupture of hot or cold leg pipes to the smallest area that the pumped ECCS injection capacity cannot exceed. If an ideal LOCA thermal-hydraulic code existed, it could analyze any LOCA without change in models or methods, but this is currently not the case. Instead, code packages and methods are specifically tailored to address certain classes of breaks. Typically, the most limiting LBLOCA is a full double-ended guillotine break in cold leg pump discharge piping. This class of breaks minimizes the core flow during blowdown and has the potential to bypass some of the ECCS fluid injected during the early portion of refill. The BWNT LBLOCA EM is specifically tailored to analyze the core and RCS response to these postulated breaks. These same codes and methods are not applicable--indeed, they are not suitable--for small LOCA analysis. Accordingly, Volume II of the BWNT LOCA EM was written specifically to address SBLOCA analysis. The LBLOCA and SBLOCA EMs combine to address the most limiting break locations and sizes in the large and small categories. Nonetheless, there is still a transition region between them that may not be adequately covered by either of the methods. The transition LOCA method uses elements of each EM to address this break range. The large hot leg break is another example that is not adequately covered by the LBLOCA EM method. The CLPD LBLOCA methods, that conform to Appendix K requirements, are modified slightly to analyze these breaks that are not limiting from a PCT perspective, but still fall under 10 CFR 50.46 consideration.

It is also true that Appendix K methods and requirements may not be rigidly applicable to all classes of breaks. For example, ECCS bypass or carryout during core reflood is not a pertinent to SBLOCA (The ECCS slowly refills the core and quenches any elevated fuel pin temperatures.) This is also the case with the hot leg and transition LOCA methods. The required demonstrations or justifications listed in Appendix K may not be as all encompassing as with the break classes that produce the limiting or near-limiting PCTs. The significant required conservatisms in Appendix K (i.e., 1.2 ANS 1971, maximum fuel stored energy, Baker-Just metal-water reaction, etc.) provide ample margin to cover analyses that are judged to be better estimate in other areas.

In the case of the transition LOCA method, a benchmark was presented in Section A.6.4.1 to demonstrate that the non-mechanistic bypass model (LBLOCA EM) and the RELAP5 calculation of mechanistic bypass (transition LOCA) will produce the same general RCS behavior during the refill and reflood periods. It was further shown that the calculated PCTs were similar between the two methods. While it is true that the bypass flow was not given, it can be inferred from the break flow differences and also the bottom of core recovery time. Because there are

differences in [

C,E

] These variations can be accounted for and used to approximate the ECCS bypass predictions.

C,E

Although extensive evidence of strict compliance and determination of the Appendix K conservatisms may not been provided for the transition LOCA methods, the similarity between and combination of the large and small break EM methods for use in these non-limiting LOCAs has been demonstrated. The transition LOCA method was directly benchmarked to the LBLOCA EM method to provide a comparison by which these methods can be judged as reasonable within the general guidelines and interpretations of Appendix K. This demonstration case and the other transition LOCA break sizes have been provided to demonstrate the continuity of results over the entire spectrum of break sizes. Since these postulated break sizes do not significantly challenge the acceptance criteria in 10 CFR 50.46, the adequacy of these methods can be judged based on the similarity of the methods to the EM and the results of the demonstration cases.

8. (Page 4-39) Under A.1, how is the stored energy or calculated PCT maximized as required by Appendix K? This is not discussed in 4.3.2.3.

Section 4.3.2.3 states that an NRC-approved steady-state fuel pin code will be used to provide the values used for fuel pin initializations for LOCA analyses. Currently, TACO3 (BAW-10162P-A) is the code that is used. TACO3 is a best-estimate fuel performance code that uses conservative fuel rod power histories and includes a multiplicative uncertainty factor on the stored energy of 1.1151 to account for a 95/95 tolerance interval considering code and manufacturing uncertainties. Section 4.5 of the TACO3 SER states that "...the B&W approach for LOCA initialization is considered to be acceptable with respect to fuel temperatures and rod pressures."

9. (Page 4-43) In items D.3 and D.4 the requirements of Appendix K cited apply regardless of what code is used. The phenomenology not the code determines whether the requirements apply. State how Appendix K is satisfied in these areas when only RELAP5 is used.

As stated in the response to Question 7, the EM methods and calculations specifically designed to comply with Appendix K calculations for the most limiting break conditions may not be applicable to all classes or locations of breaks. Different methods and models are used between the large and small break LOCA EM analyses specifically to address the requirements for vastly differing and typically limiting transients that challenge the 10 CFR 50.46 acceptance criteria. Neither the hot leg nor the transition LOCA will produce a limiting transient from the maximum PCT standpoint, but they may produce limiting mass and energy releases for containment design considerations or limiting pipe restraining loads for plants licensed with leak-before-break considerations. For these reasons, methods that produce reasonable results for these special classes of LOCAs may be needed for future analyses. BWNT has chosen to provide these methods, a comparison benchmark, and sample analyses for review in the BWNT LOCA EM.

For these special breaks, RELAP5/MOD2-B&W and BEACH were used to perform the entire transient. These breaks cannot be analyzed accurately with an EM that is structured to conservatively predict the PCT for the classic, limiting double-ended cold leg breaks. The blowdown and refill phases can and will overlap each other such that the typical blowdown, refill, and reflood periods cannot be distinguished with the same definitions used for cold leg LBLOCAs. As the fraction of ECCS bypassed directly out of the break decreases, the lower plenum can be refilled, sometimes

even before the end of blowdown. Therefore, the altered transition EM and hot leg break methods were devised.

Because these breaks are not limiting, determination of the required extent of Appendix K compliance falls with the NRC reviewer. The compliance is provided though use of NRC-approved computer codes RELAP5/MOD2-B&W and BEACH that are used for the same generalized thermal-hydraulic simulation regardless of break size or location. The code models were formulated for predicting the overall RCS and core response to any LOCA event. Small break analyses benchmark the overall RCS behavior, including the ECCS steam-water interactions at a variety of pressures and flow conditions. BEACH analyses (BAW-10166, Appendix G) benchmark the core reflooding rates and carry-out predictions for a wide variety of reflooding rates and conditions provided in FLECHT, SCTF, CCTF, G2, and REBEKA tests. By combining these benchmarks, it is easy to demonstrate that RELAP5/MOD2 and BEACH can successfully predict the ECCS bypass, core reflooding rate, and ECCS steam-water interactions for transition LOCAs. These LOCAs predict limited ECCS bypass similar to the SBLOCA analyses in which RELAP5/MOD2 was primarily formulated for and appropriately predicts the overall RCS response. Further, the transition LOCAs were successfully benchmarked against the EM methods that used RELAP5, REFLOD3B, and BEACH for the 2 ft² break (See Section A.6.4.1 and response to Question 7). This benchmark supports both the overall system responses as well as the hot channel PCT evaluation and provides a basis for showing that Appendix K requirements are met during these analyses.

For hot leg breaks, refill and reflood can begin before the end of blowdown is reached. Because of the break location, no ECCS is lost directly out of the break. The ECCS flows through the core, cooling the fuel rods before exiting via the break. The reflooding rate and steam interaction with the ECCS is calculated with the same code models that were used in the transition LOCA analyses. Because the hot leg LOCA, like the transition LOCA, is not limiting from a PCT perspective, additional benchmarks or justification to show Appendix K requirements is unnecessary. The validity of the approach is demonstrated in the representative hot leg break analysis provided in Section A.6.5.

10. (Section A.2) On Tables A-5 and A-6, please clarify the meaning of the parameter "Amount of RV water in cold leg piping at EOB." Are these values the amount of water in the cold leg and the vessel?

This is the volume of RCS water that remained in the vessel and cold legs at the end of blowdown. The majority of the remaining liquid was located in the lower head of the reactor vessel. This liquid mass is added to the ECCS liquid that should not have been bypassed and placed in the reactor vessel lower plenum at the

initiation of the REFL0D3B analysis. Appropriate time delays are used to account for the gravity drop time.

11. (Page A-6) The time step sensitivity for the blowdown period demonstrates that the time step selection for the base case is converged, but doesn't demonstrate that the internal time step selection option adequately controls time step size selection after the first two seconds. Other RELAP5 users have found that the internal time step selection algorithm does not assure converged solutions unless a maximum time step size close to the converged value is specified. Specification of too large a maximum time step size will cause the code to abort on a physical properties error. The code is unable to reduce the time step size quickly enough when destabilizing events (eg. node filling solid or emptying of liquid) are calculated. With a suitably chosen maximum time step size near the converged value, the code will run satisfactorily.

No justification has been provided for maximum time step sizes greater than that specified in the base case, and certainly not for a maximum of 0.025 seconds. While such larger maximum time steps may be suitable for transition breaks or some other events, use of a larger maximum requires a case-specific convergence demonstration. The writeup should be revised to reflect that convergence has been demonstrated for the base case maximum time step selection, and that further increases in the maximum will be justified by case specific convergence demonstrations.

The results of the time step sensitivity study demonstrate that the code time step control algorithm worked well for the LBLOCA blowdown phase. For the base case, the requested time step was 0.01 seconds between 2 and 20 seconds as shown in Table A-2. The code internal time step control cut the time step back at approximately 6 seconds and then again at 12 and 18 seconds. The results for the minimum time step size of 0.002 seconds and 0.010 seconds are nearly identical, which indicates convergence of the solution and adequacy of the time step control algorithm. While it is true that a case using 0.025 seconds was not run, the code has shown it can cut the time step back appropriately.

For the purpose of analyzing the most limiting cold leg breaks, this EM will restrict the maximum requested time step size to 0.01 seconds. Most cases will use the base case requested time. Special break analyses, such as the transition, and perhaps medium to small hot leg breaks, will restrict the maximum time step size to 0.025 seconds or less.

12. (Section A.2) In some of the results that are presented, there is a variation in the integrated accumulator injection as the sensitivity parameter being evaluated is varied. The core crossflow study results from Table A-5, for example, show 10 to 15 percent more accumulator injection for $K_{cross}=5$ and $K_{cross}=500$ than for the other cases. A corresponding increase in the water inventory ("Amount of RV water in cold leg piping at EOB") is shown. Similar results are seen in Table A-6 where the amount of accumulator injection for cases "MC=AC Power" and "MC=90% of HC Power" is higher relative to the other cases. Please discuss the reasons for the variation in accumulator injection for these cases.

Near the end of blowdown, the CFT flow rate is in the range of 100 to 110 ft³/sec. At this rate, a variation in the end-of-blowdown time will produce a difference in the integrated accumulator (or CFT) injection at the end of blowdown. The variations noted are consistent with the end-of-blowdown time differences and support the conclusions drawn in the sensitivity studies.

13. (Page A-8, Table A-4 and Figures A-13 through A-17) Table A-4 heading refers to a 5 node case, whereas the discussion on page A-8 and Figures A-13 through A-17 refer to a 4 node case. Are these the same cases, or are results in Table A-4 for a different case.

Please also explain why PCT at EOB is included in the Table, rather than global PCT. It would seem that global PCT is a more significant parameter.

The title in Table A-4 is in error. It should have been "Four Node" rather than "Five Node." The noding arrangement shown in Figure A-12 is the four-node configuration that was analyzed and reported in the table and figures.

The break noding study reported here was a RELAP5/MOD2 blowdown study, and the key end-of-blowdown parameters supplied in the table were provided to confirm the consistency of the plotted results. The tabular values and plots indicate that the same qualitative results are obtained with either the base model or the four-node model. The key parameters that can influence the overall or global PCT are the end of blowdown stored energy in the rod hot spot, water level in the lower plenum, and ECCS flow rates into the reactor vessel. Since the results of the blowdown study were nearly identical, and the key parameters determining the core heatup during the refill and reflood portions of the analyses were consistent at the end of blowdown, the global PCT

analysis was not explicitly calculated. The global PCT, if calculated, would simply have given the same response for both cases, because the governing parameters from the end of blowdown were nearly identical between the two cases.

14. (Page A-11) The core noding study illustrates that the cross flow into and/or out of the hot bundle is sensitive to modeling of the surrounding fuel. This is consistent with observations for subchannel codes such as COBRA and VIPRE as evidenced by the following statement from Reference 1, "As long as at least one full row of subchannels are placed to completely surround the hot channel to adequately resolve the details of the flow field in the vicinity of the hot channel, the hot channel flow conditions are very insensitive to the core radial layout or how the rest of the hot bundle and core are modeled."

Since PCT increases for all of the models tested in the sensitivity study compared to the base case, the base case appears to be nonconservative as regards the radial nodalization. This indicates that the base model is overpredicting the cross flow. Provide a demonstration that the cross flow is being modeled in a best estimate or a conservative manner.

Ref. 1. USNRC Letter from C. E. Rossi to J. A. Blaisdell, UGRA Executive Committee, "Acceptance for Referencing of Licensing Topical report, EPRI NP-2511-CCM, VIPRE-01: A Thermal-Hydraulic Analysis Code for Reactor Cores", Volumes 1, 2, 3 and 4", May 1, 1986.

The leak flows from postulated LBLOCAs produce significant core pressure gradients that dominate the axial flow. As the transients progress, there are several flow reversals. When axial flows are large, core crossflow has little effect. During the flow reversals, however, the core crossflow model can slightly influence the results. The topical report acknowledges that the EM analyses will produce PCT changes that are proportional to the core cross-flow resistance.

C,D,E

Framatome Technologies Inc.

43-10192Q-00

C,D,E

**18
(LA-34)**

C,D,E

Reference for Question 14

- 14-1. Idel'chik, I.E., Handbook of Hydraulic Resistance, 3rd Edition, CRC Press, 1994.

Table 14-1. Two-Channel Model Pin Temperatures

	C,D				
EOB time (sec)	19.990	19.52	19.46	19.53	20.16
EOB Clad Temp (F)	1600.9	1605.3	1613.5	1613.3	1643.2
EOB Fuel Temp (F)	1702.0	1707.8	1721.2	1727.4	1749.7
Adj time (sec)	20.4	20.4	20.4	20.4	20.4
Adj Clad Temp (F)	1609.9	1624.7	1634.2	1632.4	1648.5
Adj Fuel Temp (F)	1711.0	1727.2	1741.9	1736.5	1755.0

Table 14-2. Three-Channel Model Pin Temperatures

	2-Chan (Base)	MC=AC	MC=0.8HC	MC=0.9HC	MC=HC
EOB time (sec)	19.46	20.42	19.45	20.23	19.48
EOB Clad Temp (F)	1613.5	1644.6	1631.1	1648.6	1626.5
EOB Fuel Temp (F)	1721.2	1747.3	1749.8	1755.7	1745.0
Adjusted Time (sec)	20.4	20.4	20.4	20.4	20.4
Adj Clad Temp (F)	1634.2	1644.5	1652.0	1652.3	1646.7
Adj Fuel Temp (F)	1741.9	1747.2	1770.7	1759.4	1765.2

15. (Pages A-22, A-42, and A-52) These pages are blank or missing. If a blank, a statement "Intentionally Blank" and a page number should be provided.

Style guides for standard two-sided publications suggest that major sections should begin on an odd numbered page. The EM followed this style guide and began all major sections of the report (ie. 1., 2., A.XX, etc.) were begun on an odd page. If the previous section or group ended on an odd page, the back side (even page) was left blank and no header or page number was included. In Volume 1, blank pages follow this list of pages: 1-3, 3-1, 4-57, 5-1, 6-3, 7-1, A-1, A-21, A-41, A-51, A-55, A-57, A-59, and A-81. Blank pages in Volume 2 follow these pages: 1-3, 3-1, 4-35, 5-1, 7-1, A-1, A-13, A-19, A-21, A-39, and A-203.

16. (Page A-23) The time step convergence studies should be run with a larger decrease between the cases to illustrate convergence. The time step sizes used differ only over a relatively short period and may not be sufficiently different to demonstrate time step convergence. Please justify the time steps used or run additional cases to demonstrate that convergence has been achieved.

The BEACH time step studies have been rerun as requested with significantly larger variations among the relative time step sizes, and with the differing time steps applied over virtually the entire transient. The key parameters and results are presented in tables and figures attached to this response. In

C,E

C,E

Framatome Technologies Inc.

43-10192Q-00

C,E

(LA-39)²³

C,E

References for Question 16

16-1 "Reactor Safety Issues Resolved by the 2D/3D Program",
NUREG/IA0-0127, GRS-101, MPR-1346, July 1993.

16-2 "2D/3D UPTF Quick Look Report, Test No.24, Integral Test
with Vent Valves," E314/90/21, Siemens AG KWU, November
1990.

16-3 "Evaluation Report on SCTF Core-III Tests S3-14, S3-15, and
S3-16," JAERI-memo-62-329, Japan Atomic Energy Research
Institute, September 1987.

Table 16-1. Most Severe Break Case with and without the Inlet Subcooling Model Adjustments.

<u>Parameter</u>	<u>REFLOD3B Subcooling Base Case</u>	<u>Adjusted Subcooling Case</u>
CFT Flow Begins, s	12.8	12.8
End-of-Bypass, s	18.59	18.59
End-of-Blowdown, s	21.045	21.045
Liquid Mass in RV LP at EOB, lbm	15799.8	15799.8
Integrated CFT flow at EOB, lbm	48956.7	48956.7
Integrated Mass Removed at EOB, lbm		
Break	549268.	549268.
ECCS Bypass	47796.8	47796.8
Integrated break energy at EOB, BTU	3.5151×10^8	3.5151×10^8
RV LP Filled, s	27.552	27.552
LPI Flow Begins, s	40.060	40.060
CFTs Empty, s	45.136	45.136
Clad Rupt Time, s	21.195	21.195
Unruptured Segment:		
PCT, F	10	10
Time, s	2015.2	2020.4
	66.245	67.75
Ruptured Segment:		
PCT, F	11	11
Time, s	1967.2	1954.8
	~30.4	~30.6
Average Oxidation Increase, %		
Hot Channel	0.84	0.85
Average Channel	0.076	0.080
Whole-Core Hydrogen Generation, %	0.36	0.37
Average Channel Quench Time, s	253.4	255.62

Table 16-2. BEACH User Requested Time Step Sizes for the Revised Time Step Study.

<u>Interval</u>	<u>0.001 sec Base Case</u>	<u>Increased 0.05 sec Time Step</u>	<u>Decreased 0.0005 sec Time Step</u>
EOB - BOCR (21 - 27 s)	0.05	0.05	0.05
27.0 - 35.0 s	0.001	0.05	0.0005
35.0 - 40.0 s	0.001	0.05	0.0005
40.0 - 45.0 s	0.0025	0.05	0.0008
45.0 - 80.0 s	0.005	0.05	0.0008
80.0 - 300.0 s	0.005	0.05	0.005

Table 16-3. BEACH Parameter Comparison for the Revised Time Step Study.

<u>Parameter</u>	<u>0.001 sec Base Case</u>	<u>0.05 sec Time Step</u>	<u>0.0005 sec Time Step</u>
RV Lower Plenum Filled, s	27.6	27.6	27.6
LPI Flow Begins, s	40.06	40.06	40.06
CFTs Empty, s	45.33	45.33	45.33
Clad Rupture Time, s	21.20	21.20	21.20
Unruptured Segment:	10	10	10
PCT, F Time, s	2020.4 67.75	2031.8 68.44	2011.9 67.36
Ruptured Segment:	11	11	11
PCT, F Time, s	1954.8 -30.6	1961.6 -30.8	1954.5 -30.4
Average Oxidation Increase, %			
Hot Channel	0.85	0.88	0.84
Average Channel	0.080	0.081	0.080

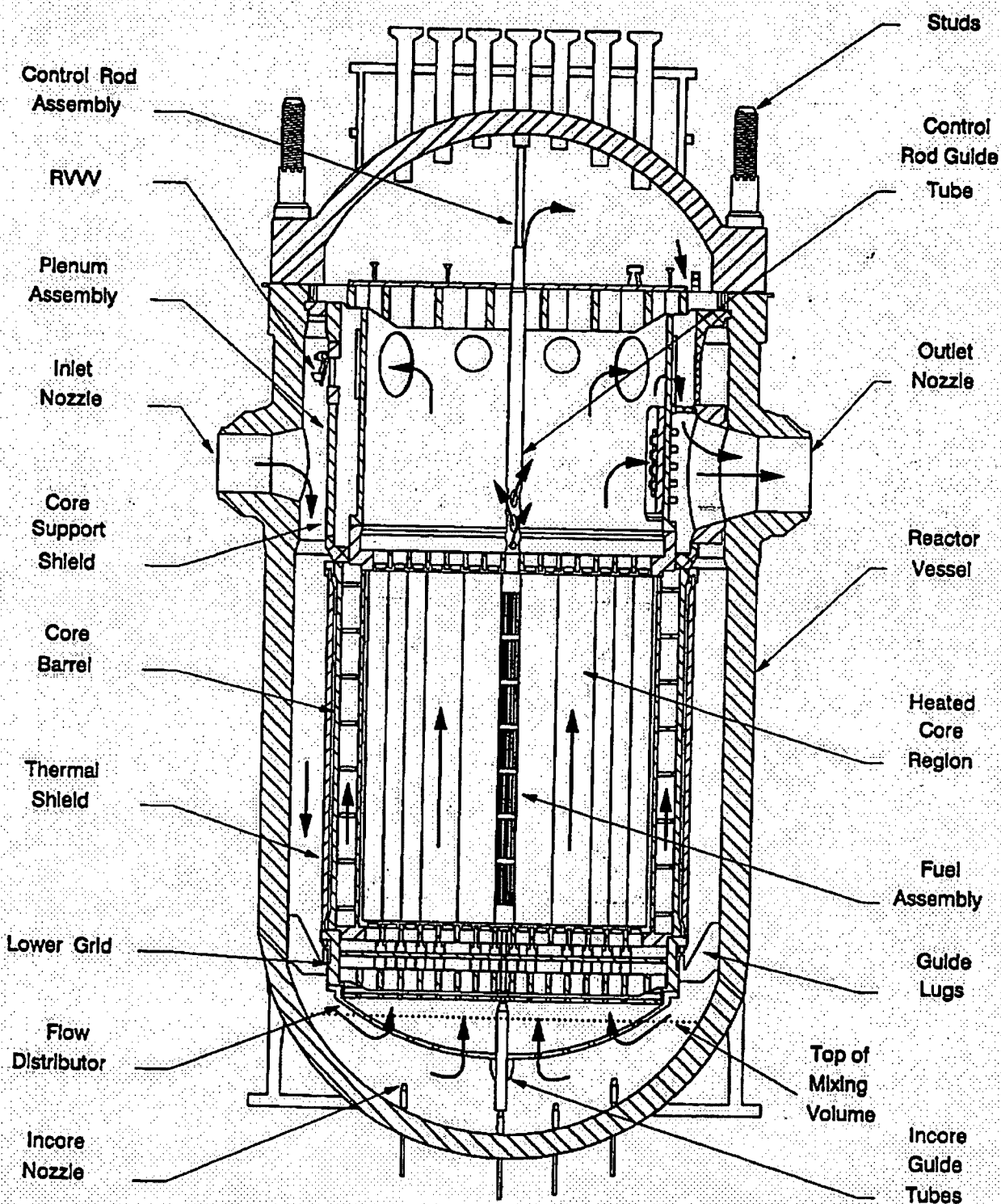
FIGURE 16-1. REACTOR VESSEL ARRANGEMENT.

FIGURE 16-2. BEACH INLET SUBCOOLING STUDY -
COMPARISON OF INLET SUBCOOLING PROFILES.

C, D

FIGURE 16-3. BEACH INLET SUBCOOLING STUDY -
COMPARISON OF RUPTURED NODE HC CLAD TEMPERATURES.

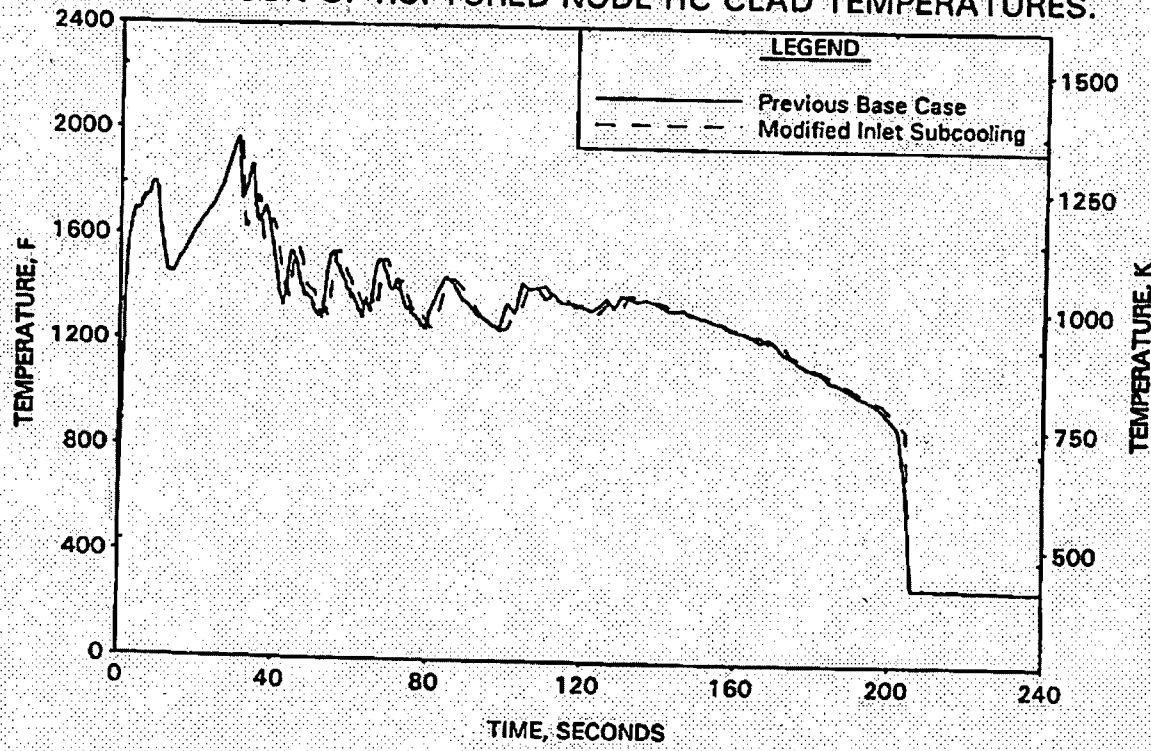


FIGURE 16-4. BEACH INLET SUBCOOLING STUDY -
COMPARISON OF UNRUPTURED NODE HC CLAD TEMPERATURES.

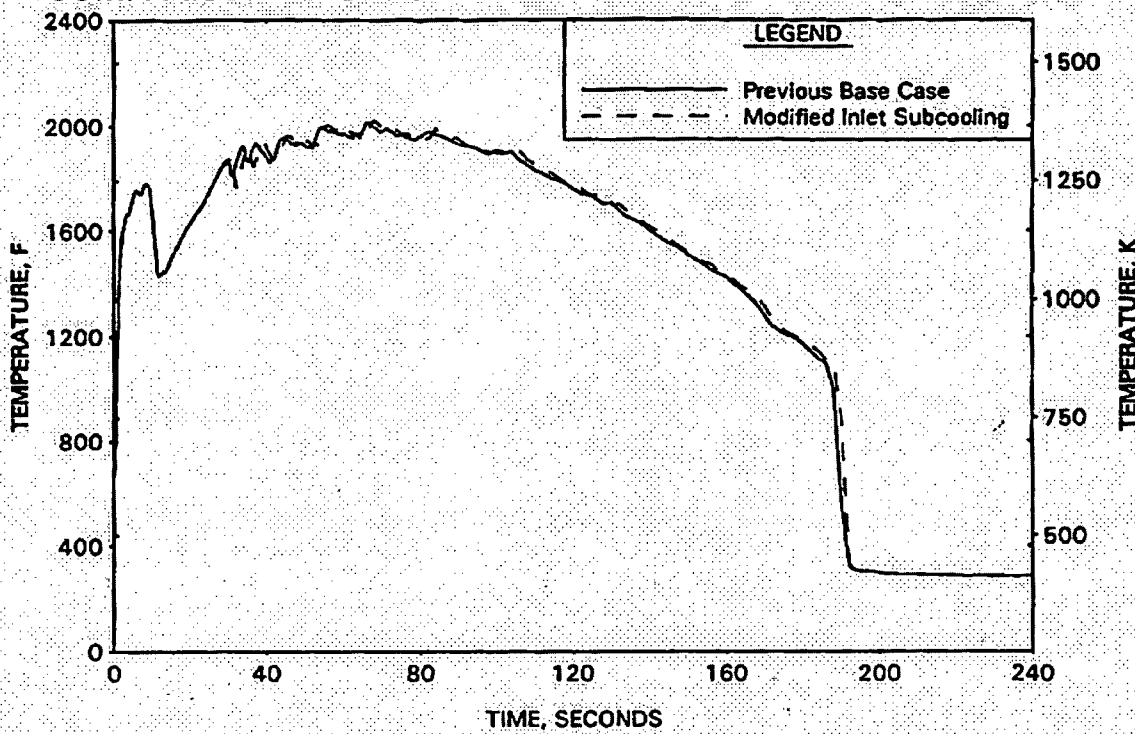
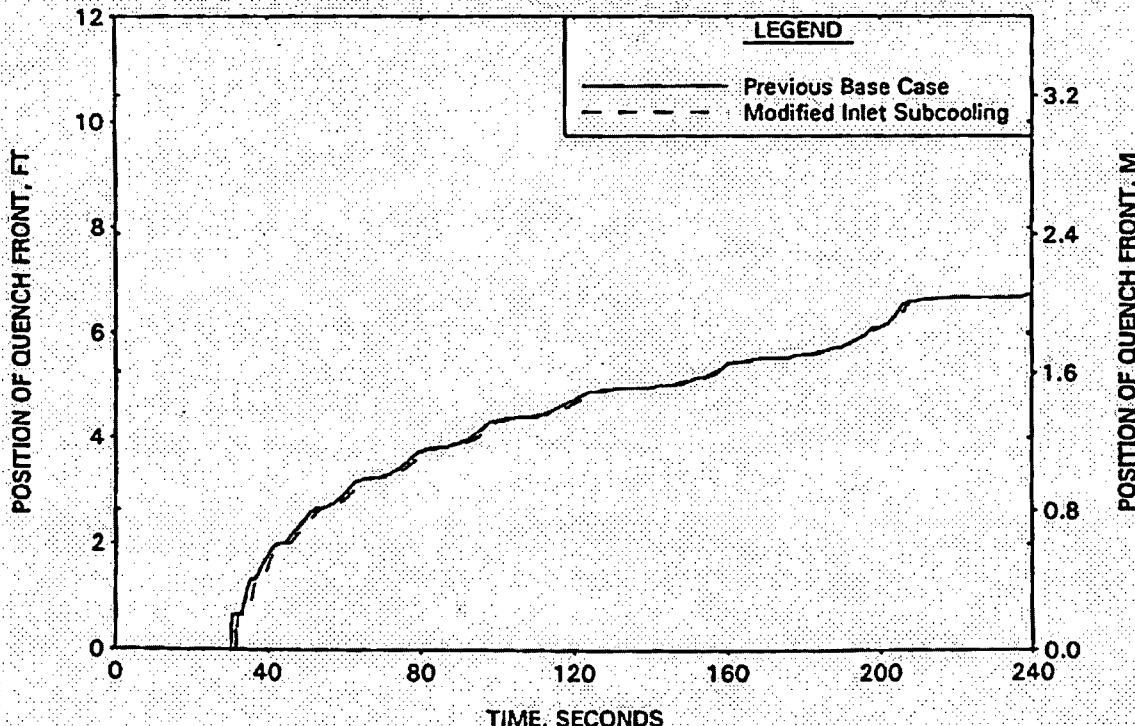


FIGURE 16-5. BEACH INLET SUBCOOLING STUDY -
COMPARISON OF HOT CHANNEL QUENCH FRONT ADVANCEMENT.



(LA 30
46)

FIGURE 16-6. REVISED BEACH TIME STEP STUDY -
REQUESTED TIME STEP ADVANCEMENTS.

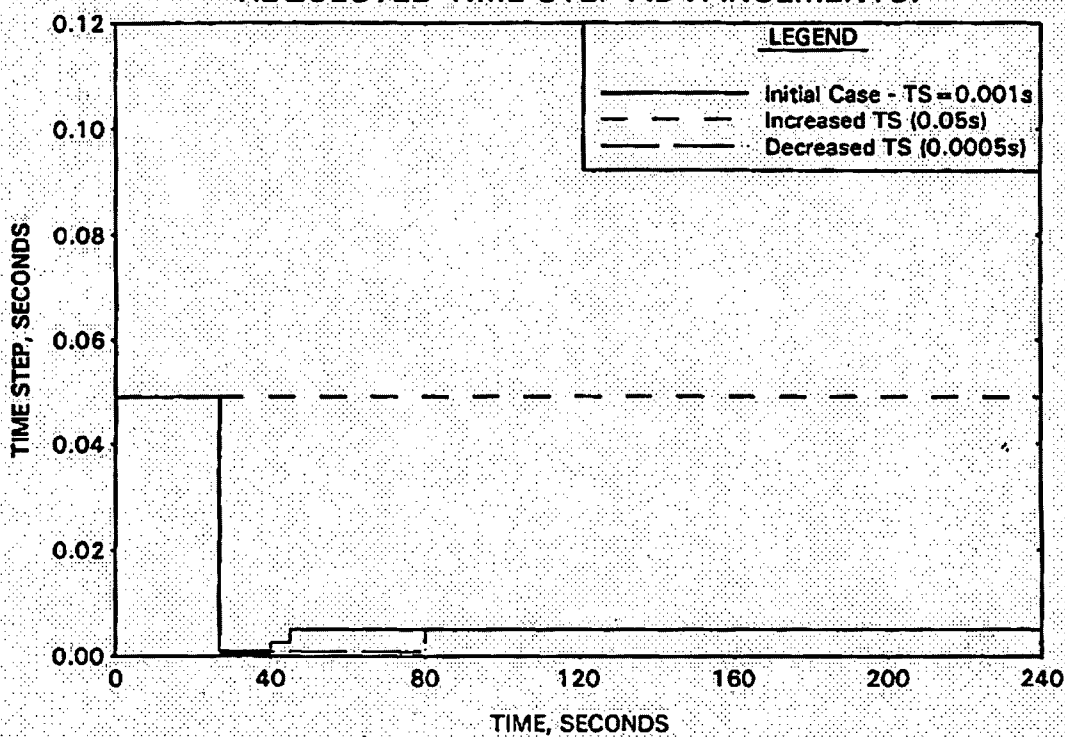


FIGURE 16-7. REVISED BEACH TIME STEP STUDY -
ACTUAL TIME STEP ADVANCEMENTS.

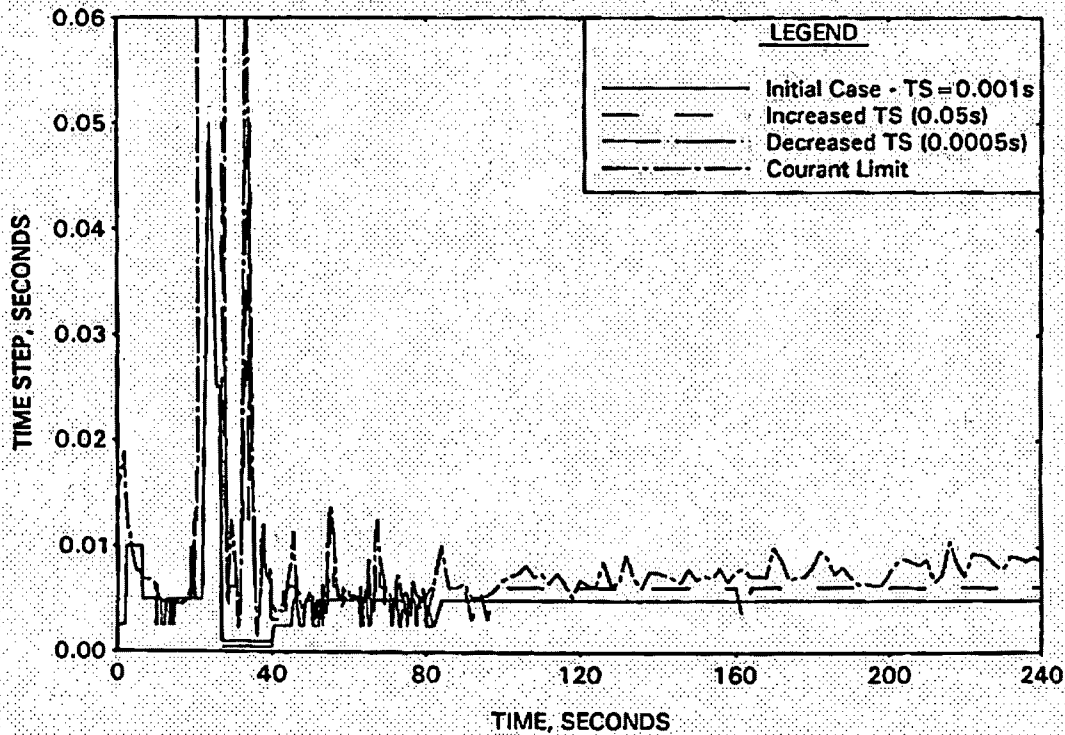


FIGURE 16-8. REVISED BEACH TIME STEP STUDY -
HC CLAD TEMP AT RUPTURED LOCATION.

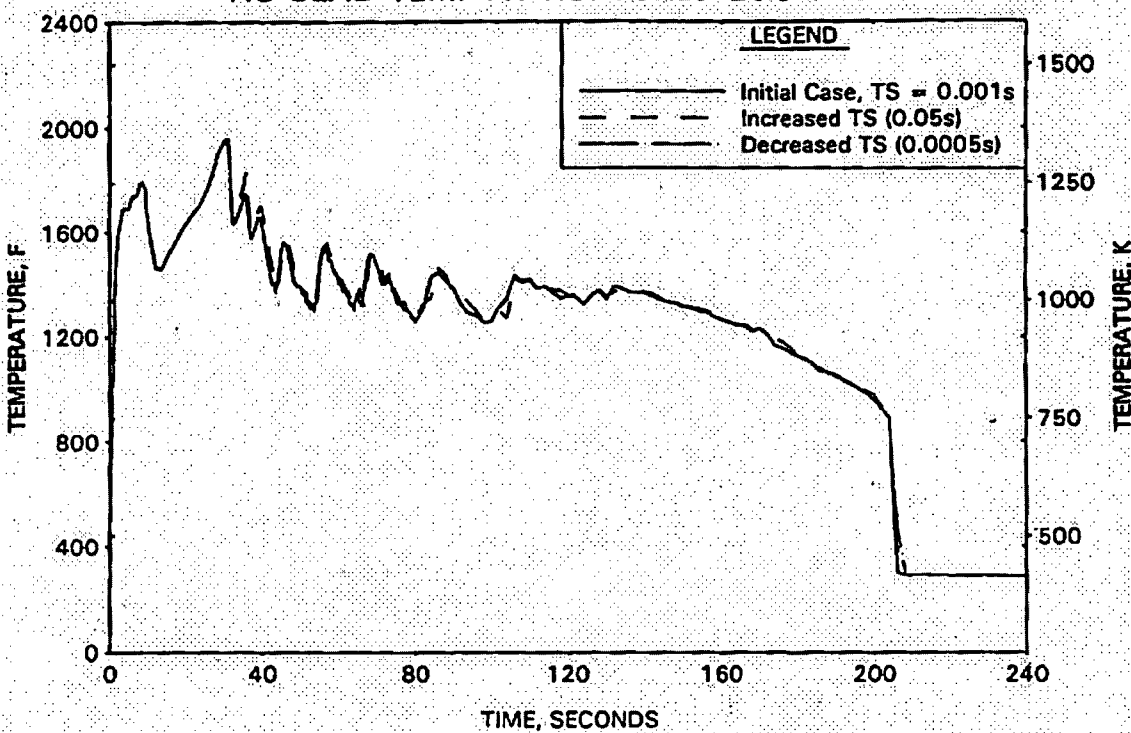


FIGURE 16-9. REVISED BEACH TIME STEP STUDY -
HC CLAD TEMP AT PEAK UNRUPTURED LOCATION.

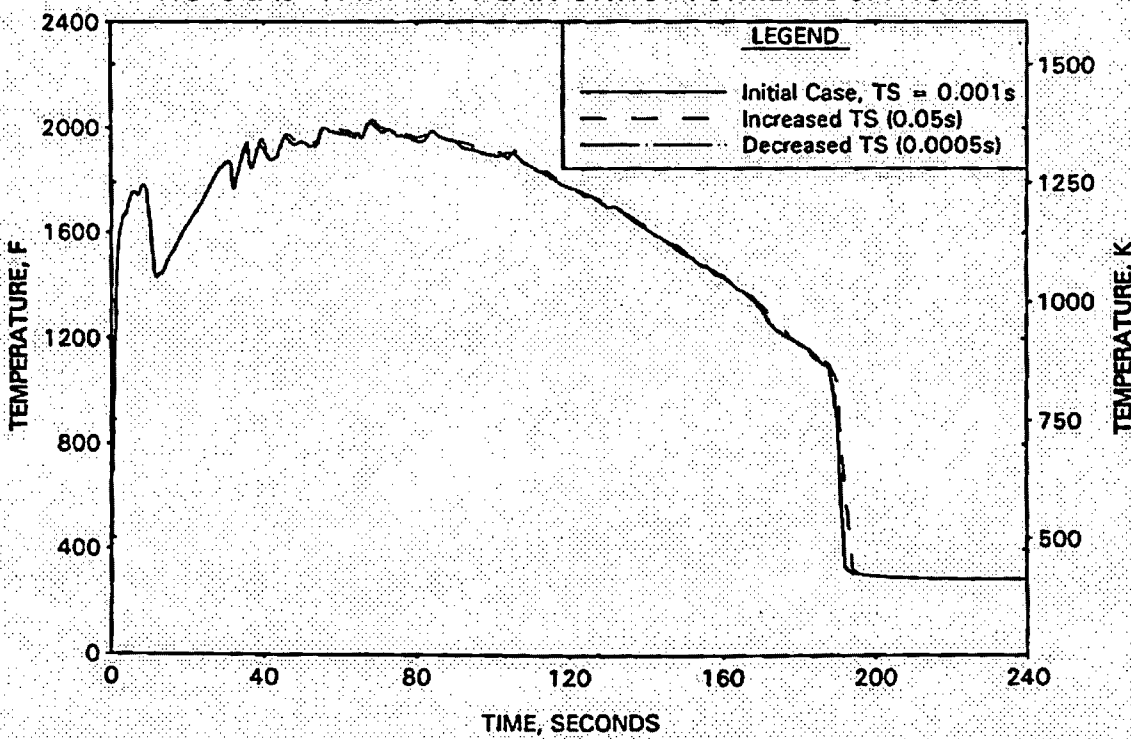


FIGURE 16-10. REVISED BEACH TIME STEP STUDY -
FILTERED HC HTC AT RUPTURED LOCATION.

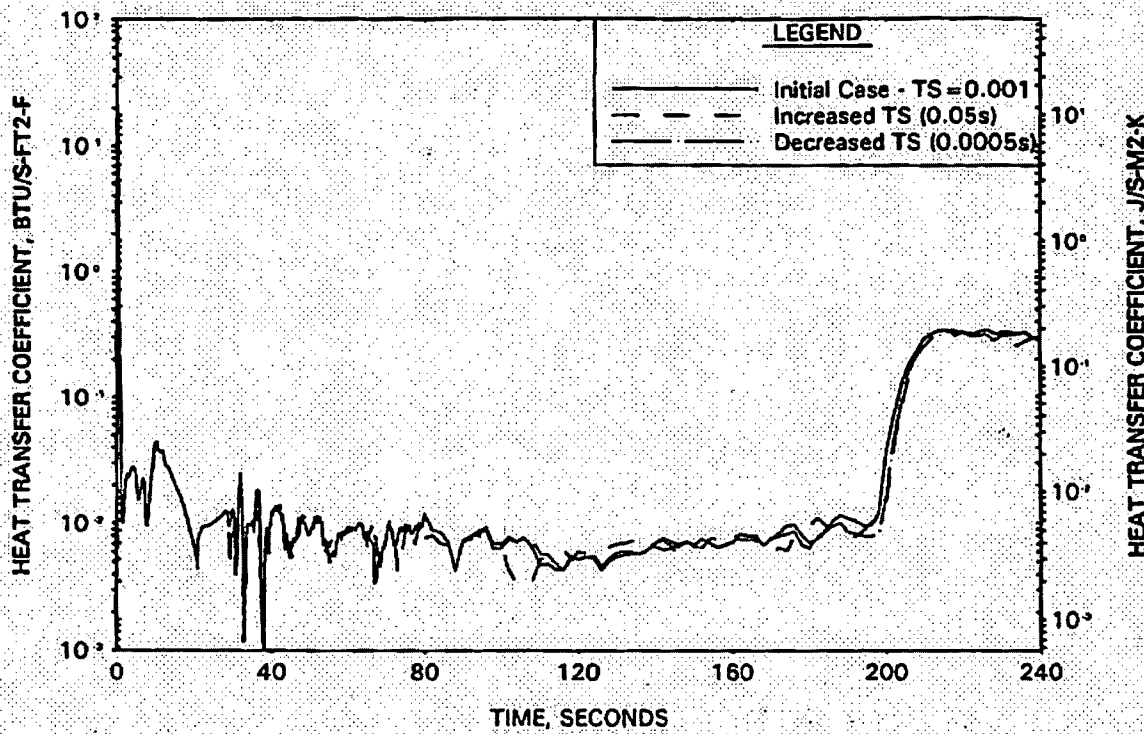


FIGURE 16-11. REVISED BEACH TIME STEP STUDY -
FILTERED HC HTC AT PEAK UNRUPTURED LOCATION.

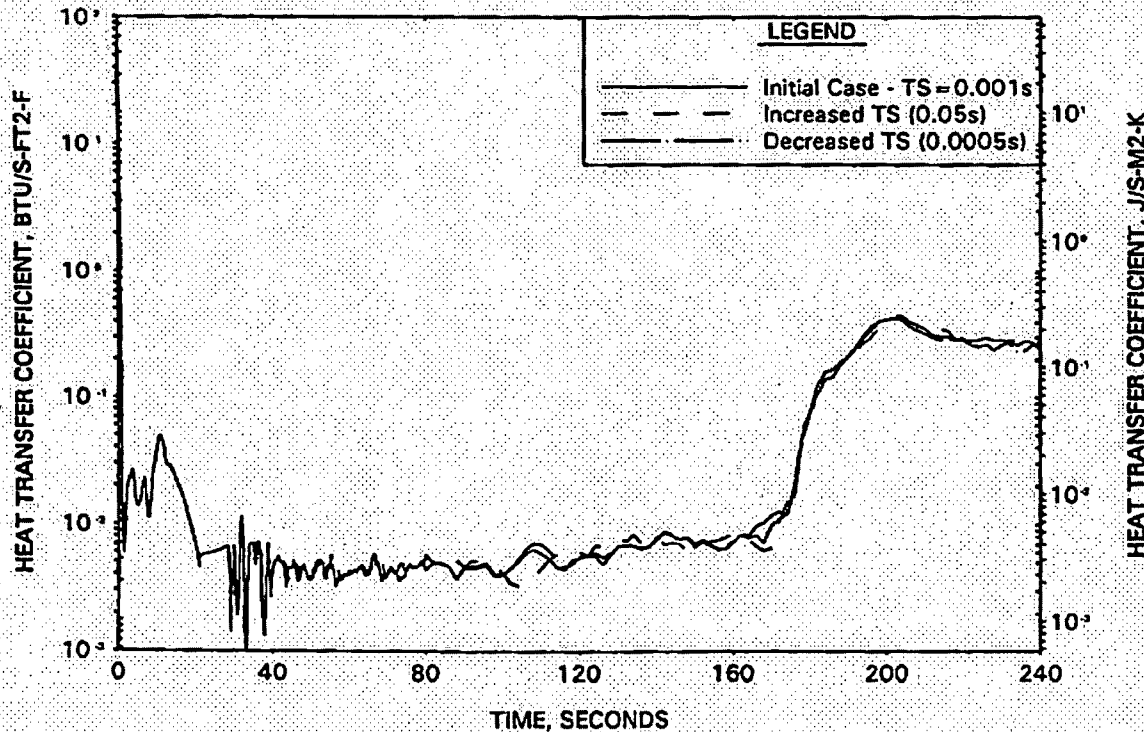


FIGURE 16-12. REVISED BEACH TIME STEP STUDY -
HOT CHANNEL QUENCH FRONT ADVANCEMENT.

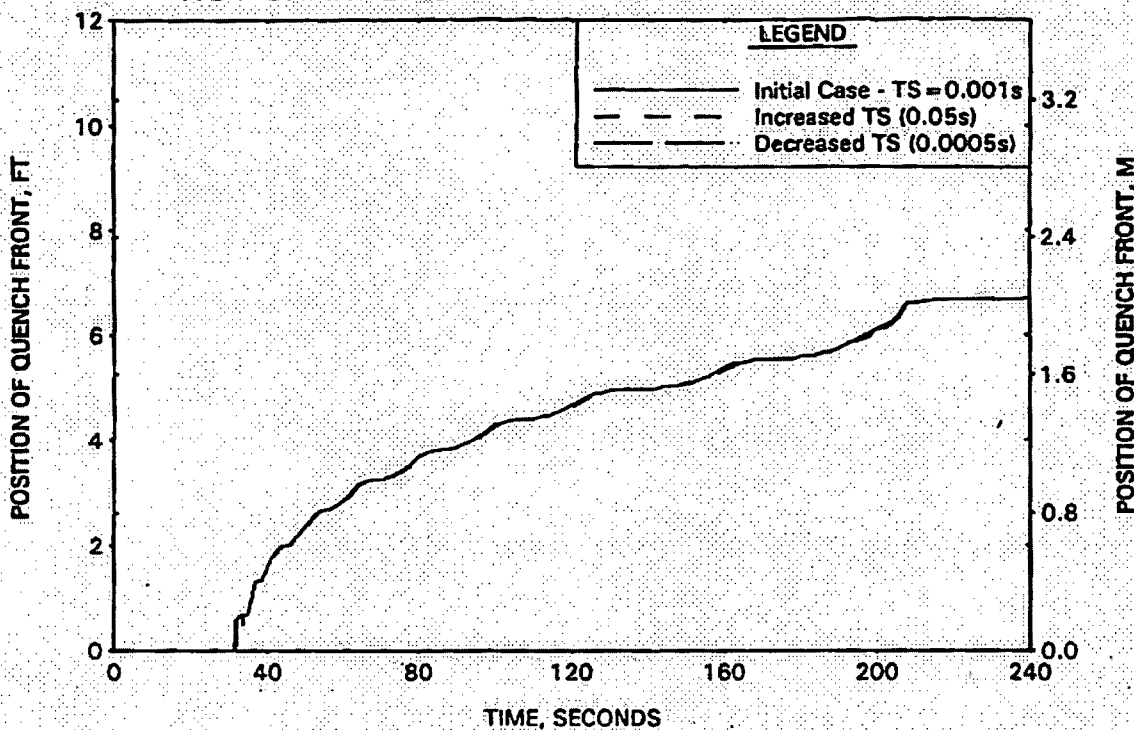
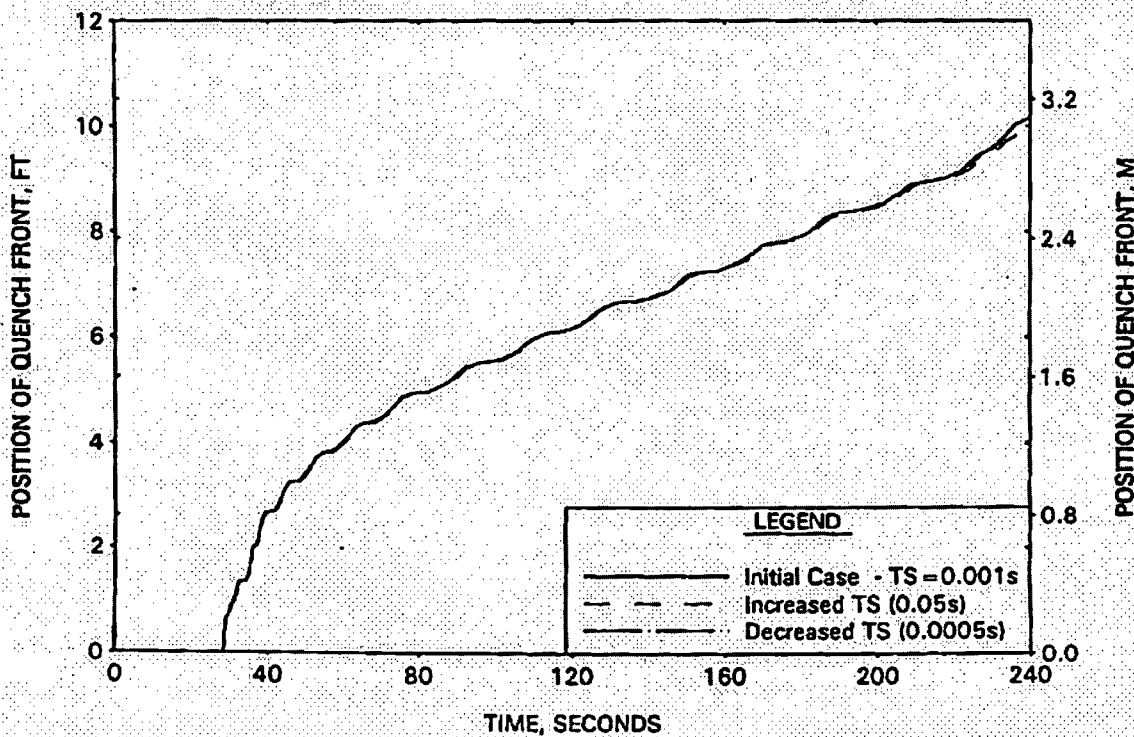


FIGURE 16-13. REVISED BEACH TIME STEP STUDY -
AVERAGE CHANNEL QUENCH FRONT ADVANCEMENT.



17. (Page A-25) In the last paragraph of Section A.4.1, please clarify the time frame for the BEACH calculations. In particular, when does reflood start?

Figure 4-1 (Page 4-45) shows the code interfaces. REFLOD3B performs the refill (adiabatic heatup) and reflood system analyses and determines the time for bottom of core recovery (BOCR). The fine mesh rezoning used in BEACH is activated on the time step after the end of blowdown. The actual reflood phase begins at BOCR.

18. (Page A-27) In this and other sensitivity studies results are given in tabular form for % oxidation increase. How can you support these values when the clad temperatures at the end of the runs remains significantly above the cutoff temperature for the metal-water reaction? This remark applies to a number of the sensitivities.

There were seven complete LOCA simulation studies reported in the topical. They were documented in the radial versus axial core peaking, break spectrum, time-in-life, three-pump, LOCA LHR limit, minimum versus maximum ECCS, and the most severe break case studies. The end of the calculations for these cases was ten seconds after the entire average channel quenched. The metal-water oxidation values from this time were used to perform the oxidation calculations. The calculations are stopped at this point because total core quench has been predicted. In the context of the conservatisms in the EM, the hot channel has been modeled as a closed channel that is reflooded with the average core flooding rate. Because of the hot channel radial power contribution, the isolated hot channel will never fully quench. The core inlet flow can only absorb the lower half of the hot channel decay heat contribution before all the liquid is boiled off. This conservatism is reasonable for PCT evaluations, but must be considered differently from the perspective of whole-core oxidation calculations. In a model with coupled hot and average channels, there will be significant average-to-hot channel liquid flow diversion in the pool region. This flow diversion would allow the hot channel to fully quench at approximately the same time as the average core.

While it is true that some of the hot channel cladding temperatures were still above 1000 F, the maximum temperature of any clad heat structure was approximately 1400 F and rapidly declining. In the topical plots, the end of the plots was shown at 240 seconds for all cases, even though the end of the longest case was 263.4 seconds. Significant oxidation occurs above 1700 F, therefore, there is no potential for an appreciable change in the local oxidation, particularly one that could challenge the local oxidation limits. From a whole-core oxidation perspective,

the hot channel represents ten percent of the core. Since the average channel has completely quenched, any slight oxidation from a limited axial portion of a small radial region will not result in any appreciable increase in the whole-core oxidation. For example, in the most severe case, the maximum hot channel oxidation increase from 160 seconds to 263.4 seconds for any core segment was 0.099 percent. The whole-core contribution increased from 0.352 percent at 160 seconds to 0.358 percent at 263 seconds. It should also be noted that four of hot channel cladding segments were between 1750 F and 1500 at 160 seconds. These four segments accounted for 93 percent of the increased oxidation over the period, despite the fact that six other segments were between 1000 F and 1400 F.

19. (Page A-33) The pressure vs time plots in Figure A-111 for the 1.0 and 0.75 ft² transition breaks appear to show a pressure increase for the first several seconds following the break. Is there a rapid initial drop not evident on the plots? Please explain why pressure is predicted to increase following a pipe break or somehow indicate that there is an initial drop prior to the pressure rise.

The initial RCS pressure was 2249 psia. Following the rapid subcooled depressurization phase, the RCS saturation and core boiling caused the RCS pressure to plateau and undergo a slight repressurization. The repressurization is due primarily to the additional fission power predicted by the reactor kinetics model that does not credit reactor scram. For a full double-ended guillotine break, the break depressurization causes immediate core void generation that provides sufficient negative moderator feedback to shut down the core fission power. For break larger than approximately 1 ft², the additional negative reactivity from the control rods is inconsequential to the core fission power decline. As the break sizes decrease, however, the delayed core void production minimizes the negative reactivity feedback and continues to produce significant core fission power that momentarily repressurizes the RCS. The boiling ultimately produces sufficient negative feedback to shut down the reactor fission power contribution.

The early RCS pressure trend for the transition breaks included in the EM is dictated by the choice of not crediting reactor scram in the analysis. A better representation of the RCS behavior is obtained by crediting the actual reactor scram that will occur for these transition LOCA's. Therefore, the transition methodology should be revised to credit the control rod insertion upon generation of the trip signal and appropriate time delays to account for signal processing and rod drop. Utilization of the reactor scram will prevent the repressurizations noted in the 1.0 and 0.75 ft² analyses.

20. (Page A-40) Provide further explanation of the effects of extended burnup and how this causes an increased difference between clad and fuel temperatures. Clarify the last sentence on this page which lists the consequences of the extended burnup.

Fuel rods are fabricated and initially filled with helium. With burnup, the fissioning process produces xenon, krypton, nitrogen, and oxygen gases. Table A-17 (page A-74) gives the gap gas mole fractions calculated by the NRC-approved TACO3 code. These mole fractions are input to RELAP5/MOD2-B&W for use in the gap conduction model. Of these gases, helium has the highest conductivity followed by oxygen, nitrogen, krypton, and xenon. The oxygen and nitrogen conductivities are roughly one-fifth that of helium, while krypton is less than one-twelfth. Xenon conductivity is less than one-twentieth that of helium. Because of the xenon buildup, the overall gas conductivity decreases as shown in Figure A-136. The gas conductivity change causes the initial fuel temperatures to increase at high burnup and produces an insulating effect between the fuel and clad during the LOCA transient. This decreased conductivity allows the high-burnup hot channel to quench slightly faster than would be the case for a beginning-of-life analysis.

21. (Tables A-19 and A-20) Correct the inconsistency in units for integrated energy out the break at EOB. Clarify break location in Table A-20.

The units in Table A-19 are incorrect by a factor of 100. For the values in the table, the units should have been 100,000,000 BTU. The integrated energy values were reviewed for all cases presented in the EM. The exponent was found to be in error on Table A-22 as well. Corrected versions of these two tables are attached to this response.

The heading in Table A-20 is confusing. The text on page A-43 (second paragraph) clearly identifies that the most severe results were calculated with the inactive pump located in the intact cold leg of the broken loop. This representation, as seen on Figure 4-5 (Page 4-49), makes reactor coolant pump Component 285 inactive.

Table A-19. RELAP5/MOD2 Parameter Comparison for the 3-Pump,
75 Percent Power Study.

<u>Parameter</u>	<u>Base Case</u>	<u>Pump 2B Locked</u>	<u>Pump 2A Locked</u>	<u>Pump 1A Locked</u>
End-of-blowdown (EOB), s	19.460	21.380	22.645	21.415
Peak clad temperature at EOB, F	1613.5	1523.1	1598.6	1581.5
Amount of water in the reactor vessel and cold leg piping at EOB, ft ³	169.703	245.352	297.041	279.147
Integrated accumulator injection at EOB, lbm	48956.7	50176.3	52962.4	50079.5
Integrated mass out the break at EOB, lbm	578160.	549112.	549099.	548583.
Integrated energy out the break at EOB, mBTU	356.317	354.125	352.603	3.52593

Table A-22. Blowdown Mass and Energy Releases for the Minimum Versus Maximum ECCS Cases.

<u>Time, s</u>	<u>Maximum ECCS Injection</u>		<u>Minimum ECCS Injection</u>	
	<u>Int Mass (lbm)</u>	<u>Int Energy (BTU)</u>	<u>Int Mass (lbm)</u>	<u>Int Energy (BTU)</u>
0.0	0.0	0.0	0.0	0.0
2.0	159343.	9.18×10^7	159343.	9.18×10^7
4.0	2.76×10^5	1.61×10^8	2.76×10^5	1.61×10^8
6.0	3.64×10^5	2.16×10^8	3.64×10^5	2.16×10^8
8.0	4.36×10^5	2.62×10^8	4.36×10^5	2.62×10^8
10.0	4.88×10^5	2.97×10^8	4.88×10^5	2.97×10^8
12.0	5.17×10^5	3.22×10^8	5.17×10^5	3.22×10^8
14.0	5.38×10^5	3.39×10^8	5.38×10^5	3.39×10^8
16.0	5.58×10^5	3.49×10^8	5.58×10^5	3.49×10^8
18.0	5.76×10^5	3.55×10^8	5.76×10^5	3.55×10^8
21.045	5.97×10^5	3.59×10^8	5.97×10^5	3.59×10^8

22. (Table A-21) Check the average oxidation increase in the hot channel at the 9.705-ft level for a typographical error. The oxidation should be greatest at this level, as it is for the average channel.

The values in the table are correct. The average channel values increase more in this case because of the increased time at temperature observed in the upper average channel for the 10-ft case. Variations in quench front advancement and corresponding liquid carryout change as the power distributions in the core change. For inlet-skewed peaks, the initial quench front advancement is slow because of the higher pin temperatures and decay heat contributions. In this case the increased liquid carryout limits the temperature increase in the upper elevations, such that the increased oxidation is very low for the average channel. For an exit-skewed peak, the initial quench front advancement is faster, which reduces the liquid carryout. Lower core steam production and less liquid carryout early during the reflood phase force more of the cladding to remain above the threshold temperature for a longer time.

These trends are also observed in the hot channel for these various power shapes. In the case of the hot channel, however, nearly all but the very lowest power end segments increase above the threshold temperature. The integration of time at temperature for the hot channel shows less dramatic changes in the channel average oxidation increase.

23. (Page A-45) A target PCT in the range of 1950 to 2050 F was used. Is this the normal range used for safety analysis? If not, what is the range of values which will be used?

This is the target PCT range for initial LBLOCA LHR limit analyses. This range was selected to provide a reasonable margin to the 10 CFR 50.46 limit of 2200 F, such that there is a limited ability to account for potential plant or fuel rod design changes that would increase the predicted PCT without causing a reduction in the calculated LOCA LHR limit. At the same time, this range is set reasonably high to avoid assigning an overly-restrictive core operating limit.

24. (Tables A-22 and A-23) What mass and energy release are used between the end of blowdown and the start of reflood? How is this calculated?

Between the end of blowdown and the bottom of core recovery, the ECCS condensation overwhelms any RCS steam production. REFLOD3B

assumes that no mass or energy transfer to containment occurs during this adiabatic heatup period.

25. (Figures A-153, A-158, other plots of heat transfer coefficient) Please clarify what is meant by filtering the heat transfer coefficient. Do you mean that you are filtering the flow per Appendix K and then are applying that flow to the determination of the heat transfer coefficient?

The heat transfer coefficient during blowdown and the early reflood phase can oscillate to produce a plot that is not very useful to the reader. A seven-point centrally-weighted average of the calculated value was used to present it as a plot. (Example: The coefficient at time, t , adds the value at time = t to the previous three and trailing three coefficients at the adjoining times and divides by seven.)

During blowdown, the hot channel flow is filtered with a low-pass filter per Appendix K requirements for use in the core heat transfer coefficient determination. The heat transfer used by the code is filtered after the LOCA analysis is completed strictly for plotted presentation.

Verbal Request for Additional Information and Response (LBLOCA)

26. Question: Clarify how the BEACH code complies with Appendix K requirements for steam-only cooling for flooding rates of less than 1.0 in/s.

The BEACH code meets the requirements of 10 CFR 50.46 Appendix K for reflood heat transfer at flooding rates of less than one inch per second. Direct heat transfer above the quench zone, as described in sections 2.2.2.8, 2.2.2.9, and 2.2.2.10 of the BEACH topical BAW-10166, occurs only between the cladding and the vapor. Radiation heat transfer is allowed from the cladding to vapor for single phase flow and from the cladding to both vapor and suspended liquid for two phase flow. Interphase heat transfer between vapor and liquid is allowed under the conditions of two phase flow.

These limitations are applied until the cladding approaches the quench temperature. As quenching occurs--and afterward--the heat transfer package realistically models direct heat flow to liquid even with the flooding rate less than one inch per second. It is FTI's position that the provision of steam-only cooling contained in Appendix K is to be applied at the location of the peak cladding temperature and not to the determination core boundary conditions used to specify the fluid state at the peak. Thus, the use of direct liquid cooling in the lower regions of the core after those regions have peaked in temperature and cooled substantially does not violate Appendix K requirements.

A similar request for additional information (Question 19) was received on the RSG LOCA EM (BAW-10168P, Rev. 1). This response was derived from that previous submittal, since the reflood heat transfer model used in both EM's are identical. This reflood heat transfer model was found to comply to Appendix K as documented in the NRC SER on the RSG LOCA EM (Thadani to Taylor SER Letter dated January 22, 1991).

Volume II - Small Break

1. (Page 4-1) A reference is made to effective cooling with close to total voiding when pumps are on. No pumps on cases are considered. If the model is to be used for this case, present or reference validations against test data or restrict the methodology to the pumps off case.

Plant emergency operating procedures (EOPs) instruct the operators to trip the reactor coolant pumps (RCPs) manually when the core exit subcooling margin is lost. EM calculations generally credit this operator action. In the event that the RCPs are not tripped during a SBLOCA in a reasonable time frame after loss of subcooling margin, the EOPs instruct the operator to keep them powered for the duration of the transient. Provided the RCPs remain in operation, the RCS flow remains homogeneous, with the residual RCS inventory and ECCS injection absorbing core decay heat. The concern lies in the loss of offsite power or other condition that causes the RCPs to trip and coastdown. Should this occur at the minimum RCS inventory, there may not be sufficient liquid remaining in the reactor vessel to provide two-phase mixture level coverage of the entire heated core length. Because continued operation of the RCPs cannot be assured, the EOPs require them to be tripped on loss of subcooling margin.

It is not anticipated that this EM will be used for pumps-on SBLOCA analyses, however, if needed, the current EM would be used. It is true that no pumps-on studies were performed for this EM. An early version of RELAP5/MOD2-B&W was used to benchmark MIST Test 3801AA of the pumps-on conditions during SBLOCA (Ref: Multiloop Integral System Test (MIST): Final Report, NUREG/CR-5395, EPRI/NP-6480, BAW-2078 Volume 10). This post-test benchmark was analyzed to characterize the RCS behavior and two-phase pump performance during SBLOCA. The benchmark comparisons to the test data were reasonable. An underprediction of the leak flows led to an overprediction of the system inventory that increased with time into the transient. The RCS inventory discrepancy made direct comparison of the core inventory at the minimum inventory impossible. Agreements established early during the MIST program set forth rules that did not allow model adjustments, other than operator actions or boundary conditions, to improve the benchmark comparison. The overall RCS behavior calculated by the code, including RCS flow decline and pump cavitation, were demonstrated in the benchmark. Validation of the pumps-on simulation with RELAP5/MOD2-B&W was demonstrated. Within the context of an EM application, the underprediction of leak flow is of little consequence, since a spectrum of breaks would be analyzed to determine the worst case. Validation of the code has been referenced, therefore use of this EM for pumps-on simulation should not be restricted.

2. (Page 4-3) Please justify the use of a high containment pressure as conservative and explain why CONTEMPT analyses are used when the break could unchoke.

The RCS pressure remains sufficiently high during most SBLOCA analyses such that the break flow remains choked throughout the analysis. The minimum core inventory and any cladding temperature escalations as well as the initial core recovery is complete long before the break "unchokes." Therefore, there is no variation on the transient results due to changes in containment backpressure. Use of a high backpressure (i.e., the maximum containment design pressure) would be reasonable (or conservative) so long as the RCS pressures during the calculational period always keep the break choked. SBLOCA transients that are continued to very low RCS pressures need a reasonable containment pressure boundary condition because the leak will unchoke and control RCS pressure and determine the pumped ECCS injection rates. For these cases, a CONTEMPT analysis is one method to determine a reasonable containment pressure.

3. (Page 4-3) What is the purpose of the parenthetical remark in section 4.3.1.1 (or conservatively high). The 1.02 times licensed power is an Appendix K requirement.

There are some situations in which the SBLOCA analyses are performed at a power level higher than the licensed plant power. These analyses may be performed in anticipation of, or as support for, a future plant power increase, or perhaps as a generic analysis that supports several physically similar plants at slightly different power levels. Use of an analysis power level slightly above the licensed power leads to more severe consequences to a postulated SBLOCA transient. In all cases, the power used in the analysis will be increased by 2 percent to account for instrumentation or heat balance uncertainties as required by Appendix K.

4. (Page 4-4) In section 4.3.1.3 it is stated that average fuel temperatures will be adjusted using a pin gap conductance multiplier to match fuel thermal code predictions within 20 F. This is a rather large difference for convergence of models and could have a significant effect on PCT. To determine how much difference is acceptable, the difference in average temperature needs to be translated into an effect on PCT. If the effect on PCT is insignificant, then the value is acceptable.

The effect on SBLOCA PCT is insensitive to initial fuel stored energy. Since the SBLOCA does not lead to initial DNB, the stored energy in the fuel rods is removed by the RCS flow and substantially removed from the RCS due to the primary-to-secondary heat transfer that occurs during the flow coastdown phase. By the time that any fuel or cladding heatup initiates, the fuel and cladding temperatures are slightly above the RCS saturation temperature. The PCT depends on the clad temperature necessary to remove the decay heat for the transient system conditions at the time of the peak. Therefore, the effect on PCT is insignificant, and the 20 F variation in fuel volume-average temperature is acceptable and provides some allowance for fuel rod design changes. Moreover, large or small LOCA the fuel temperatures are 12 percent higher than best-estimate values, and 20 F represents a negligible variation on the fuel temperatures that typically are near an initial value of 2500 F.

5. (Page 4-5, Section 4.3.1.5) Appendix K requires that the actinide decay heat level used in the analysis be for the time in the fuel cycle that yields the highest calculated fuel temperature during a LOCA. Please discuss how this requirement is satisfied.

The actinide decay heat model used in the EM conservatively accounts for the most limiting time-in-life neptunium and plutonium contributions that build up during infinite core operation as required by Appendix K. The actinide decay heat model used in this EM is identical to the model that was approved by the NRC for use in the RSG LOCA EM (BAW-10168P).

6. (Page 4-9) In the second paragraph, what is the meaning of "thermal center"?

The thermal center is a convenient term used to describe the manometric imbalance that dictates the loop natural circulation flow. The thermal center is defined as the elevation at which a partition separating the hot and cold fluids could be placed in a vertical section having a temperature gradient. For example, the thermal center in the uniform radial core with an axial peak at the midplane is at the midplane. The thermal center in the once-through steam generator can vary depending on the feedwater flow rate, injection location, and the secondary pool height. The separation of the tubes wetted by AFW from the remaining tubes allows better simulation of the variations in the primary steam generator density gradients between the wetted and unwetted regions. The result is a better prediction of the steam generator thermal center. The difference between the elevation of the steam generator (or cold side) thermal center and the core

(or hot side) thermal center determines the elevation head that dictates the RCS single phase natural circulation flow rate.

7. (Page 4-10) Why is the area of the junction connecting the loop piping to the fictitious break volume taken as 1/3 of the loop piping area? Why are bottom breaks treated differently from side breaks, in regards to HPI location?

C,E

C,E

8. (Page 4-11) What criteria was used to determine that CLPD break entrainment will not occur for all small breaks? How do you assure that the criteria are met?

C,E

9. (Page 4-17) The factor of [] CFT line resistance will result in a higher pressure differential between the CFT and the primary piping, essentially lowering the primary system

C,D

pressure and the break flow. This artificial increase in friction losses is apparently needed to enhance numerical stability. However, it has the potential to introduce non-conservatism by lowering calculated primary system pressure and break flow. What evaluations has BWNT performed to assure that this approach does not introduce non-conservatisms into the calculations?

C,E

10. (Page 4-19) In section 4.3.2.8, it is stated that mixture level is resolved to within [C,D]. What sensitivity studies have been performed and/or what model features are included to assure that a conservative prediction is obtained. Specifically, when the core liquid level drops, the node which contains the level has a two-phase heat sink, but in actuality the upper portion of the node is above the mixture level. While this will occur for any node size, no matter how small, how do you assure that the effect is small for the node size chosen?

The benchmarks performed to justify the SBLOCA drag model changes in RELAP5/MOD2-B&W (BAW-10164 Rev. 2) show conservative clad temperature predictions using models with the same general noding resolution. The integral system ROSA benchmark in Appendix J produces conservative clad temperatures during the boildown phase. In the ORNL stand-alone core model benchmarks in Appendix H, conservative to best-estimate clad temperatures were predicted. These tests provide assurances that the core noding resolution is reasonable for best-estimate to conservative clad temperature predictions.

Additional conservatisms are included in the EM analyses that use these best-estimate core models. Minimum ECCS flows, 1.2 ANS 1971 decay heat, and a maximum hot channel radial peaking factor reduce the minimum core inventory and maximize the hot pin heatup during periods in which the mixture level is within the core heated region. The core crossflow modeling used in the SBLOCA EM minimizes hot-to-average form loss to restrict the hot channel level swell and maximize hot channel steam flow diversion into the average channel above the mixture level.

RELAP5/MOD2-B&W also tends to underpredict the void fraction in the top volume with two-phase conditions. The interphasic drag at the transition between slug and annular mist allows the liquid to drain rapidly into the next lower volume. This draining occurs as the void fraction increases into the slug/annular mist transition region (50 to 60 percent void fraction). This transition occurs as the actual mixture level begins to fall from the top of the uppermost two-phase control volume. The SBLOCA void profiles (See Figures A-41 and A-42 on page A-77) show this conservative behavior.

The code also does not physically model the localized region just above the mixture level. Within several inches of the mixture level, there is a region of wet steam with small liquid droplets that originate from the spattering and splashing that occurs as the bubbles escape from the pool. This high void region maintains the steam temperatures near saturation for several inches, which is the approximate height of the control volumes.

In summary, RELAP5/MOD2-B&W has been shown to produce best-estimate to conservative clad temperature predictions with models that resolve the mixture level to within approximately [] . The Appendix K assumptions, code crossflow modeling, hot channel radial peaking, and interphasic drag model provide conservatisms that ensure conservative PCT predictions with the axial detail chosen for use in the SBLOCA EM.

11. (Page 4-22) For the consistent time-in-life calculation option of fuel pin heatup, please explain how the time-in-life is specified to assure that the degree of swelling and incidence of rupture are not underestimated.

Appendix K was written with a definite bias toward large break LOCA. In the case in point, the incidence of cladding swell and rupture is significant to a large break transient, but it is typically of little importance for small breaks. Clad rupture during SBLOCA can provide enhanced clad cooling because the cladding surface area for heat transfer increases and the cladding expands away from the pellet. The increased heat transfer and reduced gap coefficient can decrease the peak cladding temperature. The gap effect can temporarily insulate

the fuel pellet, but it can take several hundred seconds for the pellet and cladding to reach a quasi-steady temperature balance. In some cases, the core mixture level may have begun to recover and the cladding heatup arrested before this balance is reached.

Although this is generally the case for most SBLOCAs, there can be an exception that must not be precluded. If clad rupture occurs at high temperatures, the metal-water oxidation rate on the inside and outside clad surfaces may provide a sufficient energy source to offset the increased cladding surface area and the decreased gap coefficient. The rate of oxidation is exponentially dependent on the cladding temperature and inversely dependent on the oxide thickness, thus the effect is strongest when fresh fuel ruptures at the highest possible temperature. If the rupture is at a sufficiently high temperature, most likely somewhere above 2050 F, the reaction may be so strong that the minimal cladding cooling is unable to maintain the cladding temperature within the bounds of 10CFR50.46 criteria. For this reason, it is important to delay the occurrence of rupture until the time that the maximum cladding temperature would occur if rupture were avoided. By doing so, the maximum negative effect of cladding rupture is imposed on the calculated solution. If the rupture occurs earlier, the heat-up of the cladding will be delayed or prevented, and the cladding can gradually oxidize at lower temperatures. A thicker oxide layer reduces the metal-water heat generation rate at the time maximum cladding temperature is reached. The SBLOCA simulation that delays rupture until the highest possible temperature will lead to more favorable SBLOCA performance and lower cladding temperatures for any other pin burnup conditions (pin pressures, oxide thickness, gap gas components, etc.) that result in lower temperature ruptures.

What can be concluded from this discussion is that an iterative process may be required to define the most limiting fuel pin time in life (TIL) because of its relationship to steady-state pin pressure and the time of rupture. For this EM, the process outlined to find the most limiting TIL is first, to maximize the likelihood of pin rupture. This is accomplished by using a set of composite fuel pin inputs with beginning-of-life (BOL) stored energy, gap gas composition, and oxide thickness with an end-of-life (EOL) maximum pin pressure. The BOL gas composition results in the highest gap conductivity for any TIL and the BOL oxide thickness is the smallest. High gap conductivity maintains the best thermal communication between the fuel and cladding temperatures during any cladding heatup period. Use of the BOL oxide thickness maximizes the metal-water energy addition rate and combines with the gap conductance to maximize the unruptured cladding temperature for any TIL. By using an EOL pin pressure, the cladding hoop stresses are maximized such that the lowest conceivable rupture temperature is determined by the NUREG-0630 model. The combination of the highest cladding temperature with lowest rupture temperature maximizes the likelihood of rupture for any TIL of the fuel.

Any SBLOCA case that predicts clad rupture with these assumptions must be further analyzed by adjusting the pin pressure until rupture is avoided, and then to rupture near the time of peak clad temperature from the unruptured case. By adjusting the internal pin pressure (which can be equated to fuel pin burnup), rupture is forced to occur near the time that the cladding temperature reaches its peak. For example, an initial SBLOCA case that uses an internal pin pressure of 3000 psia predicts rupture at the lowest cladding temperature, which is below the threshold for significant metal-water reaction. The case is rerun with a reduced initial pin pressure to allow the cladding temperature excursion to continue. This step is repeated until the internal pin pressure that produces the most-limiting PCT with or without rupture is found. This method assures that the degree of clad swelling and the incidence of rupture have been conservatively estimated for any TIL.

If the SBLOCA analysis shows significantly high PCTs based on the composite pin conditions that were used, the analysis may be rerun using a consistent case that uses oxide thicknesses and gap gas contributions from the most limiting TIL that has been established. This method of specifying the TIL at which to perform a consistent analysis provides a way to remove any artificial conservatism that is imposed by this method that maximizes the calculated PCT for all times in life. It removes some conservatisms from the PCT prediction, but still assures that the degree of swelling and the incidence of rupture have been conservatively estimated.

12. (Page 4-31) Explain why a time dependent junction is used to model the vent valves? These basically function as check valves. What criteria are used to open and close the valves?

C,E

C,E

References for Questions 12

- 12-1 "Internals Vent Valve Evaluation," BAW-10005, July 1969.
12-2 "Model Tests of a 177 Fuel Assembly Two-Loop PWR Progress Report #2 - Vent Valve Tests," BAW-4595, March 1969.

13. (Page 5-1) Explain what is meant by the statement that "the amount of oxide thickness is computed on a mass basis".

In the EM, the oxidation fraction is calculated based on the ratio of the reacted zircaloy volume of the strained clad to the total strained clad volume. Since it represents the volume of zircaloy reacted to the total zircaloy volume, its basis is representative of both a volume and mass ratio. The volume fraction of zircaloy reacted or mass fraction of zircaloy reacted are equivalent.

14. (Page 9-8) For a licensing analysis, ECCS fluid temperatures at the limiting Tech. Spec. value should be used and not nominal yearly average temperatures.

Appendix K does not restrict or limit the choice of the ECCS fluid temperatures. By the same token, BWNT does not ignore the more conservative choice of the highest ECCS temperatures. We have simply chosen to not restrict the ECCS temperatures used in the EM analysis because of the conservatisms already imposed by Appendix K. The Appendix K prescribed conservatisms include: 1.2 times ANS 1971 for infinite core operation, single worst failure, minimum pumped ECCS injection rates, bounding core parameters (stored energy and pin pressure, moderator temperature coefficient, oxide thickness, minimum shutdown reactivities, etc.), and Baker-Just metal-water reaction model. These requirements add significant conservatism to the analyses, which BWNT believes is adequate margin, without applying other bounding parameters such as ECCS temperatures. Certainly, a conservative input can and may be used in the analyses, but will not restrict the temperature to the highest value in the EM. This position is identical to that used in the current NRC-approved EM (BAW-10104,

Rev. 5) for B&W-designed plants and the NRC-approved EM (BAW-10168 Rev. 3) for Recirculating Steam Generator Plants.

15. (Page A-7) The second paragraph refers to RV mixture level and RV collapsed level. Is this the predicted mixture level in the core, or in the vessel? Figures, e.g. A-52, show collapsed level in the downcomer, reactor vessel and core composite. Please describe how these quantities are calculated including any relationships between the three levels.

The predicted mixture levels presented in Appendix A are core mixture levels. The collapsed level in the downcomer is calculated by multiplying the liquid void fraction by the height of each downcomer volume (Control Volumes 300 through 315-4 on Figure 4-3). The liquid level in each volume is then summed to obtain the total collapsed level for the downcomer region. The core composite level consists of the control volumes in the baffle, bypass, hot channel, and average channel regions. The collapsed liquid level is determined for the each region of the core separately. Each of these levels is then weighted by the fraction of the total core area and summed to obtain the core composite collapsed level. The RV collapsed liquid level consists of the core composite level plus the lower plenum, upper plenum, and upper head collapsed levels. The reference elevation for the downcomer, core, and RV collapsed levels depicted in Appendix A is the bottom of the heated core.

16. (Page A-7) Why are filtered RVVV and hot leg mass flow rates plotted for the final cases? Does filtering influence calculations or is it done only for presentation of plots? Explain the need for filtering.

The calculated flows are filtered for plotted presentation. These flows can be quite oscillatory for smaller breaks that have longer flow coastdown or loop draining phases. To help reduce the plot clutter, a seven point centrally-weighted average of the calculated value was used to present it as a plot. This operation is performed after the case is complete so it does not influence the calculations. It does however, assist the reader in interpreting trends. (Example: The flow at time, t , is calculated by adding the code calculated value at time = t to the previous three and training three code-calculated flow rates at the adjoining times and dividing the sum by seven.)

17. (Page A-9) The time step sensitivity studies show very different results for transient clad temperature and core mixture level (Figures A-5 and A-6). Since both the larger and smaller time steps show an earlier quench time (by hundreds of seconds) and the core mixture level differs by several feet, this indicates that time step convergence has not occurred. The .02 time step yields the most conservative results, but time step "convergence" has not been demonstrated as required by Appendix K. This non convergence appears to be related to the anomaly in the base case which is discussed in several places in the Topical and also is the subject of question 21, below.

In addition, the base case should be run for a longer period of time to show recovery of the core and quench of the fuel.

The results of the 10 and 20 millisecond cases show very good agreement in the system response, minimum core inventory, and PCT predictions. There are some minor differences shown at the end of the flow coastdown phase, end of the loop draining phase, and during the post-PCT core recovery phase. These variations are related to slight differences (approximately 20 ft³ out of 10,500 ft³ initially) in core liquid inventory distributions at the minimum inventory time. This convergence is excellent considering the complex nature of the two-phase thermal-hydraulic effects that occur during the SBLOCA transient. The post-PCT variations in the break flow are responsible for the time shift in the core quench, but are not significant in terms of the effect on PCT.

18. (Page A-27) The large break cases were run for only a short period of time at the end of which the collapsed liquid level in the core was near its minimum value. How do you assure that the mixture level continues to increase and cover the entire height of the core and that no subsequent temperature excursions occurs?

We are assuming that this question relates to the large SBLOCA cases from Volume II of the EM. The cases were discontinued after the cladding temperature escalation had been halted and the ECCS flow was of sufficient magnitude to offset the decay heat, wall metal, and flashing contributions. The SBLOCA analyses performed for the EM were stopped at any time after these two criteria were met. Continuous core mixture level coverage is provided by a continuation of the operating HPI pump (using the single worst failure of a train of ECCS), the liquid remaining in the CFTs, and the use of a single LPI pump. Any future application of the EM will be analyzed until all cladding temperatures increases have been quenched and the downcomer

collapsed level is at least recovered to within one foot of the top of the fuel.

19. (Page A-42) The break spectrum results in Figure A-293 show a very localized PCT maximum at a 0.07 ft^2 break size. A slight change in the discharge coefficient for a portion of the transient (Section A.8) results in approximately 90 F increase in PCT as shown in Figure A-244. This is an indication of the sensitive dependence of PCT on break size in this region. In general, the limiting break size will be the one which delays ECCS as long as possible while continuing to empty the coolant inventory. The peak may be very localized as indicated by your results and those of other vendors. There may be multiple peaks corresponding to delaying the different ECCS modes. A complete break spectrum analysis should identify these limiting breaks by a search in the vicinity of the local PCT maximum. Your broad sweep through this critical region is unlikely to have identified the true peak temperature. Provide analyses which demonstrate that your break spectrum sensitivity has identified the true PCT for small breaks.

The break spectrum provided in this EM is for demonstration of the entire range of break sizes. There can be some plant combination of parameters that can lead to localized peaks as you described. The most significant consideration controlling the shape of the range of the break sizes that undergo cladding heatup is the ratio of the core power level to the ECCS capacities and CFT initial conditions. Steam generator secondary level and pressure control can also play a less significant role in determining this profile. Had this been an actual application used for plant licensing, at least two other break sizes would have been analyzed on either side of the 0.07 ft^2 break to ensure that the most limiting break size has been identified. A reasonable break size distribution (with break size variations no greater than approximately twenty percent) will be analyzed in vicinity of the limiting break for specific plant applications.

20. In general there appears to be an anomalous increase in break flow for the base case, which is eliminated by almost any kind of modification, time step size larger or smaller, pressurizer location, different crossflow resistance, etc. The presence of this anomaly in the base case raises the question of whether it is this anomaly that makes the base case most limiting. How do you know that this anomaly did not influence the results of your sensitivity studies?

The anomalous break flow was caused by the artificial entrainment from the downcomer back to the broken leg of HPI that was

injected into the intact loops. The anomaly did occur until slightly after 2300 seconds in the base case. Any results up to this time were not affected. After 2300 seconds, the results are changed, and the magnitude of the change is produced by the fraction of HPI bypassed. The base case break flow, on Figures A-2, A-22, or A-29 (pg A-57, A-67, or A-71), increased by about 5 lbm/s when the anomaly began and increased to approximately 8 lbm/s at 3000 seconds. Using an average HPI loss of 6.5 lbm/s over the last 700 seconds results in a loss of 4550 lbm of reactor vessel inventory. By using an average saturated liquid density of 50.6 lbm/ft³ (500 psia), the volume of liquid loss can be calculated to be approximately 90 ft³. Given that the free flow area in the RV downcomer, core, core baffle, and core bypass is approximately 120 ft², the RV collapsed levels should be approximately 0.75 ft lower due to the HPI bypass, at 3000 seconds. The base case reactor vessel collapsed level deficit, shown in Figures A-3, A-23, or A-28 (pg A-58, A-68, or A-70), is roughly 0.75 ft at 3000 seconds. This deficit delays the post-peak cooldown and ultimate quench time for the PCT location. The validity of the sensitivity studies is not compromised by this anomaly.

21. (Page A-77 and A-78) Both the hot and average channel void fractions show a non physical decrease in void fraction at around the 9 foot elevation. This is indicative of modeling problems and/or code errors which have been identified in other public versions of RELAP5 (see for example Reference 1, attached). The drop in void fraction can be due to use of actual grid spacer flow area as discussed in the attached letter, or to an exceptionally low value of slug-to-annular void transition. Please evaluate this anomalous void profile behavior and provide an explanation. Describe the BWNT procedure for evaluating errors reported by the general RELAP5 user community.

Ref. (1) Letter G. W. Johnsen, INEL to F. Eltawila US NRC, "W6238: Modeling Reactor Core Grid Spacers - GWJ-41-95" June 6, 1995.

The attached reference refers to the rod bundle drag model used in RELAP5/MOD3. This interphase drag model is not used in RELAP5/MOD2, which is the basis for this EM. Therefore, the void distribution is not related to the grid spacer flow area.

The void distribution decrease is related to the transition between the slug and annular or mist regions. Phase separation is modeled within the junctions of RELAP5/MOD2 using the flow regimes determined by the fluid conditions within the control volumes. At the mixture level interface, the upper control volume will be in the annular or mist flow regime which predicts little interphasic drag. The lower control volume will be in the

slug flow regime. When the two are combined at the junction, the result is a higher phase separation. This high phase separation causes the liquid to drain out of the upper volume into the lower volume. The void depression is shown on the figures. The depression is not a result of code errors. It is representative of a discontinuity moving between fixed control volumes of finite size.

This drag model prediction is conservative for use in PCT evaluations because it results in the prediction of a lower mixture level. The drag model changes that were included in the RELAPS/MOD2-B&W code were benchmarked against various tests and shown to be best-estimate to conservative from the standpoint of predicting pool void fraction and mixture level swell. Accordingly, the model review concluded that these changes were appropriate and approved them for use in EM analyses.

Whenever we are apprised of a potential error, regardless of the source (internally within the company or from the worldwide user community) it is reviewed to determine if it is really an error or it can be attributed to a problem with the user's model or use. If a code error is confirmed in the certified code version that would effect the typical or licensed use of the code, it is governed by an FTI internal procedure (BWNT-0902-06) for computer software certification. Should the code error produce an adverse effect on licensing analyses of safety significance to an operating plant, then a preliminary safety concern (BWNT-1707-01) must be written and the concern must be addressed. The procedure for processing the preliminary safety concern is structured to comply with 10CFR21 requirements for NRC notification.

22. (Page A-83), Figure A-54) Please explain why the void fraction does not approach 1.0, but rather never exceeds about 0.97.

Figure A-54 represents the void fraction of the fictitious break volume. The HPI liquid is injected directly into the break volume (See top diagram in Figure 4-5) to ensure complete bypass of the HPI liquid injected into the broken cold leg. A void fraction less than 1.0 in the break volume is representative of the HPI liquid (approximately 20 lbm/sec) passing through the break volume into the containment node.

23. (Page A-84), Figure A-56) Are all of the water levels shown referenced to the same zero (upper face of lower SG tube sheet)? Please explain the large difference between the hot leg riser level and the pressurizer level.

The core, downcomer, and reactor vessel levels are referenced to the bottom of the core. All RCS levels are referenced to upper face of lower SG tube sheet. The bottom of the pressurizer is located slightly below the bottom of the hot leg pipe. The pressurizer empties slightly after 2000 seconds. The pressurizer is simply a trapped water reservoir connected to the hot leg pipe that responds through pressure changes and not level. The following table gives some helpful plant elevations.

Table 23-1. Key Elevations for the Raised-Loop 205-FA Plant

Component	Component Elevation, (ft)	
	Top	Bottom
Hot Leg Riser	67.2	-0.9
Hot Leg Stub & SG Inlet Plenum	67.2	52.1
Steam Generator Tubes	52.1	0.0
SG Exit Plenum and CLPS Stub	0.0	-6.5
CLPS Riser to RCP Spillover	2.9	-6.5
Cold Leg Pump Discharge	2.9	-1.3
RV Downcomer	3.5	-26.5
Reactor Vessel	11.2	-28.0
Reactor Core	-7.1	-19.1
Pressurizer	34.6	-3.8

For this table, the upper face of the lower tube sheet is the datum elevation corresponding to 0.0 ft.

24. (Page A-92) Please explain the relationship between liquid volume and collapsed level shown in Figures A-71 and A-72; in particular, why the liquid volume continues to decrease while the collapsed liquid level remains constant.

Figure A-71 provides a collapsed level plot for the cold leg pump discharge (CLPD) region, while Figure A-72 provides the liquid volume of the cold leg pump suction (CLPS) region. The CLPD piping is empty from 1800 to the end of the transient. The CLPS liquid is gradually declining due to flashing and metal heating.



Integrated Nuclear Services

JHT/96-68
October 11, 1996

Document Control Desk
U. S. Nuclear Regulatory Commission
Washington, DC 20555-0001

Subject: Responses for Verbal Requests of Additional Information on BWNT LOCA -
BWNT Loss-of-Coolant Accident Evaluation Model for Once-Through Steam
Generator Plants.

Gentlemen:

The attachment contains responses to verbal questions and one clarification response for additional information on the original release of Topical Report BAW-10192P, "BWNT LOCA, BWNT Loss-of-Coolant Accident Evaluation Model for Once-Through Steam Generator Plants." These responses were previously sent as a draft for consideration by the NRC reviewer. The material adequately addresses the reviewer's questions, therefore, the identical responses are being transmitted officially for inclusion in the SER material.

Some information in the attached responses (specifically, Question 1) is considered "Proprietary" as sworn by me as Manager of Licensing Services, Framatome Technologies, Inc. in my affidavit presented with the February 15, 1994 submittal of the topical report, and should be treated as such. If clarification of any of the provided information is needed, please contact John Klingensmith at 804-832-3294.

Very truly yours,

A handwritten signature in black ink, appearing to read "J. H. Taylor".

J. H. Taylor, Manager
Licensing Services

JHT/bcc
Attachment

c: L. Lois/NRC
R. B. Borsum/FTI-MD82
R. J. Schomaker/FTI-OF57
J. A. Klingensmith/FTI-OF53

(IA-75)

3315 Old Forest Road, P.O. Box 10935, Lynchburg, VA 24506-0935
Telephone: 804-832-3000 Fax: 804-832-3663

This page is intentionally left blank.

Verbal Requests for Supplemental Information on BAW-10192P, Rev 0**"BWNT Loss-of-Coolant Accident Evaluation Model
For Once-Through Steam Generator Plants"**

During the final NRC review of the BWNT LOCA EM SER, R. C. Jones raised four additional verbal questions. FTI has restated the questions and provided the following written responses.

1. The LBLOCA radial versus axial core power peaking study presented in Volume I Section A.5 shows that the PCT increases for both increases and decreases in the axial peak from the EM specified value of [C,D] [C,D] axial peak complies with the Appendix K requirement included in the following statement. "A range of power distribution shapes and peaking factors representing power distributions that may occur over the core lifetime shall be studied and the one selected should be that which results in the most severe calculated consequences, for the spectrum of postulated breaks and single failures analyzed."

It is impossible to define a single realistic enveloping power distribution that bounds all core operation. If an overly conservative envelope were defined, it would not represent a reasonable combination of power distribution shapes that may occur over the core lifetime. It is possible, however, to evaluate the current core designs and to define achievable radial and axial peaks near the limits of allowed core operation. This process determines the core location and time in life where the power distribution analyses predict the minimum LOCA margins. The radial and axial peaks for the limiting case are used with the maximum core radial peak ($F\Delta h$) and EM conservatisms to standardize a method used for LOCA analysis. This method includes LOCA analyses performed with the core axial shapes peaked at five locations with beginning-of-life (BOL) conditions, five locations with middle-of-life (MOL) conditions, and one bounding end-of-life (EOL) case. This process ensures that the calculated consequences of a postulated LOCA are not underpredicted, and it meets Appendix K requirements by defining the allowed total peak versus core elevation for any time during core operation.

The response to this question will be separated into four parts with a final summary section. First, the calculated variations in PCT for the radial versus axial power study will be discussed. Second, the expected variations in PCT for the core inlet and core exit power peaks will be discussed. Then, the core power distribution analyses will be used to determine the combination of radial and axial peaks that can achieve total peaks similar to values used in the LOCA linear heat rate (LHR) limit analyses.

The final part discusses the EM conservatisms included in the hot assembly radial power. These discussions are designed to elaborate on the thermal-hydraulic effects associated with peaking factor variations and their effect on overall PCT for any elevation in the core. Some of the LOCA analyses are performed

C,D,E

Framatome Technologies Inc.

43-101920-01

C,D,E

Framatome Technologies Inc.

43-101920-01

C,D,E

C,D,E

Framatome Technologies Inc.

43-101920-01

C,D,E

Framatome Technologies Inc.

43-101920-01

C,D,E

Framatome Technologies Inc.

43-101920-01

C,D,E

C,D,E

Table 1-1. Maximum BOL Core Inlet Peaking Factors from Typical
B&W-Designed Plant Core Power Distribution Analyses.

C,D

References for Question 1

- 1-1. BAW-10122A, Rev. 1, Normal Operating Controls, May 1984.
- 1-2. BAW-10104PA, Rev. 5, B&W's ECCS Evaluation Model, Nov. 1986.

Figure 1-1. RADIAL VERSUS AXIAL PCT RELATIONSHIPS FOR THE CORE INLET PEAKS.

10
(LA-86)

Figure 1-2. RADIAL VERSUS AXIAL PCT RELATIONSHIPS FOR THE CORE EXIT PEAKS.

C,D

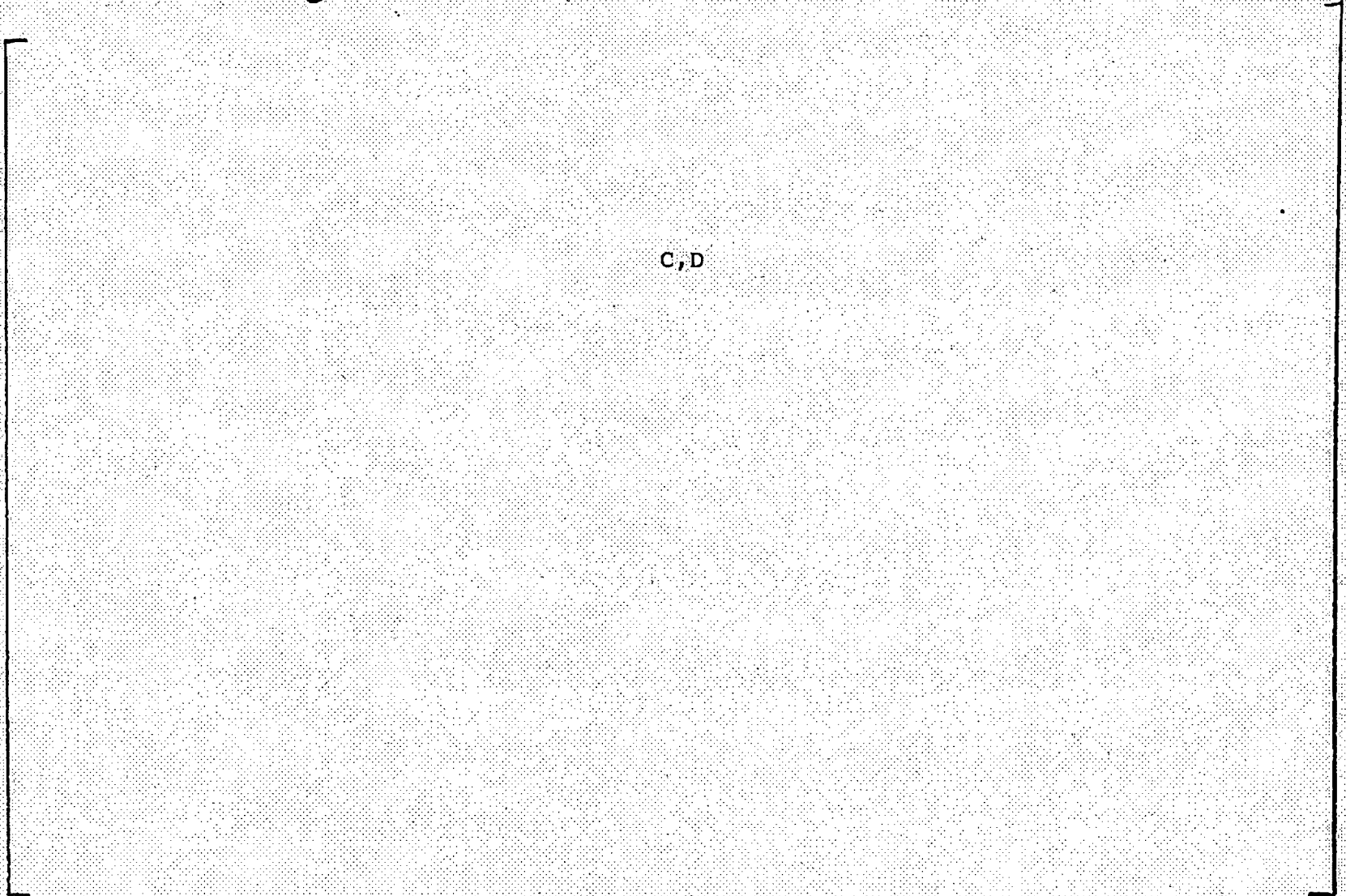
RADIAL VERSUS AXIAL PCT RELATIONSHIPS.

C,D

12

(LA-88)

Figure 1-4. BOL LOCA Margin Versus Offset.



2. Please describe how the hot leg LOCA and transition LOCA methodology complies with the Appendix K requirements.

The consequences of a transition LOCA or hot leg LOCA are not limiting or even close to being limiting from the perspective of demonstrating adequate ECCS performance to show compliance with 10 CFR 50.46 requirements. They are unique in terms of the ECCS bypass and the system conditions at which core reflooding will commence. Classical EM thermal-hydraulic methods that use multiple codes break down during analysis of these break sizes and locations. Historically, crude approximations and physical arguments have been used to describe why analyses of these breaks were unnecessary. In this EM, adjustments of the classical EM methods used for the limiting CLPD LBLOCA analyses were described, and calculations were performed to demonstrate that the transition LOCA methods were adequate for calculating the thermal-hydraulic characteristics of the ECCS bypass and the reflood system analyses encountered during simulations of these smaller break sizes or hot leg locations.

The transition LOCA or hot leg LOCAs methods are a combination of large and small break EM methods that strictly comply with Appendix K. The combination of these methods can raise questions on how Appendix K compliance is demonstrated for ECCS bypass, core carryout during reflood, and ECCS steam interactions. Formal responses applicable to these questions were given in the Requests for Additional Information on LBLOCA Questions 7 and 9. For the hot leg breaks, the break location ensures that direct ECCS bypass will not occur. The CLPD transition LOCA break calculation of ECCS bypass is performed by the RELAP5/MOD2-B&W two-fluid model formulation. The conservative comparisons of the RELAP5-predicted ECCS mass bypassed in Question 7 demonstrate the adequacy of the code and model for these break sizes. The RELAP5 code, with a one-dimensional downcomer model, will calculate higher interphase drag in the downcomer, thereby delaying lower plenum refill. In addition, the UPTF test data indicated that partial end-of-bypass is initiated almost immediately after CFT injection begins for the nozzle farthest removed from the broken cold leg. The EM ECCS bypass methodology conservatively restricted prediction of the partial end-of-bypass until the total steam flows into the upper downcomer were less than 310 kg/s. For breaks of 1.5 ft² or less, the lower plenum steam venting path is never totally cleared, and downcomer upflows never exceed 150 kg/s. At these flows, UPTF data confirms that lower plenum refill (partial end-of-bypass) occurs coincident with CFT actuation.

Compliance was also demonstrated for the core carryout and ECCS steam interaction by direct comparison between the transition LOCA and the LBLOCA EM method for the 2-ft² CLPD break. The LBLOCA EM methods do comply with all of the Appendix K requirements, and the comparison against the transition method is implicit via the comparison predictions. The core collapsed levels on Figure A-108 give an integrated comparison of the core

liquid retention for both methods. The transition methodology under predicted the core liquid retention prior to 85 seconds. After 85 seconds, the transition method advanced faster due to the cross-connection of the hot and average channels. Since the PCT was predicted by 76 seconds, the enhanced liquid retention after 85 seconds was inconsequential.

3. The RELAP5/MOD2-B&W LBLOCA blowdown analysis determines the number of cleared CLPS loop seals that are used in the REFLOD3B model for steam venting. Please clarify how the REFLOD3B code calculates CLPS loop seal reformation versus time during the reflood and long term cooling phase.

REFLOD3B performs the system thermal-hydraulic analyses during the reflood phase of the LBLOCA. The code is formulated with homogeneous, equilibrium conditions in the junctions and volumes, therefore it is unable to predict the formation of a loop seal in the low point of the cold leg pump suction. The formation of a loop seal can potentially be achieved through de-entrainment of liquid that is not vaporized in the steam generator or through backflow of the ECCS liquid injected in the upper downcomer or CLPD piping. Based on the thermal-hydraulic considerations provided in the following text, neither of these mechanisms are plausible prior to total core quench during the LBLOCA.

The REFLOD3B analyses performed for the EM predict complete vaporization of the liquid droplets carried up the hot leg and into the steam generator tubes prior to total core quench. Therefore, there is no liquid to be de-entrained in the CLPS region. This total liquid vaporization increases the steam binding effect, which acts to reduce the core reflooding rate. If a scenario were postulated in which some liquid droplets did pass through the steam generator tubes, the high steam velocities (in excess of 70 ft/s) in the CLPS piping during the core reflooding period are sufficient to atomize and carry the tiny liquid droplets through the pump suction region and pump to the downcomer or break. The RELAP5/MOD2-B&W reflood system calculations performed for the transition LOCA break sizes (0.75 to 2.0 ft²) cleared all four loop seals and did not predict any liquid accumulation during the core reflooding period. The RELAP5/MOD2 non-homogeneous, non-equilibrium formulation provides a more realistic calculation that would not preclude steam generator liquid carryout or de-entrainment in the CLPS piping. Even the small break sizes did not show loop seal formation, therefore, it is not plausible that a CLPS loop seal would form during the core reflooding period.

The cold leg pump discharge piping geometry of the B&W-designed plants is such that the inclined piping prevents any ECCS liquid backflow for the most limiting CLPD LBLOCA. In a less limiting CLPS LBLOCA, some backflow of the ECCS liquid is conceivable once

the downcomer is refilled to near the top of the cold leg nozzle. The additional elevation head in the downcomer increases the core reflooding rate which improves core heat removal and decreases the maximum cladding temperatures. This break location is not limiting, because it results in much less ECCS bypass during the blowdown period, such that the adiabatic heatup period is much shorter. Therefore, although the CLPS break has more potential to calculate ECCS backflow, it is not limiting from a PCT perspective. Also, even if the intact loops are postulated to plug in the long term after the core reflooding is completed, the broken loop and RVVs will continue to provide sufficient steam venting paths such that this break location could not become limiting.

4. Please describe the set of large and small break LOCA analyses that will be performed to provide new LOCA LHR limits that may be referenced in a plant fuel reload core operating limits report (COLR).

A new fuel reload analysis will reference LOCA calculations that are performed in accordance with an NRC-approved EM for the B&W-designed plants. The calculations will be broken into two categories, small break and large break LOCAs. Sufficient analyses will be performed to determine the allowable LOCA LHR limits to justify operation of the fuel throughout the entire fuel cycle. The sensitivity studies included in the EM, or performed using this EM for similar plant classifications, will either be judged to be applicable to the plant and fuel design type or new sensitivity studies will be performed.

The small break LOCA analyses will use the maximum exit-skewed LHR limit in calculations to determine the maximum PCT for the spectrum of most limiting CLPD breaks, including the HPI line break. The SBLOCA spectrum will also include a CFT line break analysis. The fuel pin parameters used as input will bound the fuel over its entire range of operation. The SBLOCA analyses will be performed specifically for each fuel design, or be shown to be bounded by previous NRC-approved EM analyses for a similar fuel design and plant-type classification (ie. 177 fuel-assembly lowered-loop design).

The set of LBLOCA analyses that will be performed, or shown to be bounded by a previous LBLOCA analysis for a similar plant and fuel design, include a mini-spectrum of CLPD guillotine breaks (CDs of 1.0, 0.8, and 0.6), minimum vs maximum ECCS injection study, and reactor coolant pumps powered versus off. Once the most limiting break size and ECCS flow are determined, the LOCA LHR limits will be performed. The cases performed to determine the LOCA LHR limits include five beginning-of-life (BOL) and five middle-of-life (MOL) calculations with the axial peaks located at the midpoint of the grid spans nearest the 2-, 4-, 6-, 8-, and 10-ft elevations. At least one end-of-life (EOL) calculation

will be performed to demonstrate that the consequences of the MOL are bounding for EOL. At least one three-pump LBLOCA analysis will be performed, or shown to be bounded by a previous analysis for the plant and fuel design, to demonstrate that the four-pump LBLOCA limits are bounding for three-pump operation. Should the four-pump LHR limits not bound the three pump operation, a suitable reduction in the four-pump LHR limits will be determined for use in the core operating limits evaluations.

The LOCA LHR limit analyses that will support a specific fuel reload are a complete and comprehensive set of results. The set includes new analyses or applicable reference to plant sensitivity studies, a SBLOCA spectrum, eleven LBLOCA LOCA limit analyses, and a three-pump LBLOCA analysis. The LOCA limits would be reported in the core operating limits report (COLR) and described in the annual ECCS report to the NRC. A LOCA applications topical would not need to be submitted to the NRC review unless there were EM method changes included in the applications.

ACTINIDE ENERGY CONTRIBUTIONS IN BAW-10192

The following information contains an unsolicited clarification of the actinide energy contribution used in BAW-10192. The following question and response was previously sent for Question 5 on Volume II (SBLOCA).

5. (Page 4-5, Section 4.3.1.5) Appendix K requires that the actinide decay heat level used in the analysis be for the time in the fuel cycle that yields the highest calculated fuel temperature during a LOCA. Please discuss how this requirement is satisfied.

The actinide decay heat model used in the EM conservatively accounts for the most limiting time-in-life neptunium and plutonium contributions that build up during infinite core operation as required by Appendix K. The actinide decay heat model used in this EM is identical to the model that was approved by the NRC for use in the RSG LOCA EM (BAW-10168P).

NRC questions on BAW-10168 resulted in a review of the response to the actinide energy contribution used for LBLOCA or SBLOCA for BAW-10192. Upon review, FTI found the wording to be inconsistent with the method used in the EM. The following response is consistent with the EM applications and complies with the Appendix K requirements.

The actinide decay heat model used in the EM conservatively accounts for the energy generated from the radioactive decay of actinides: including neptunium, plutonium, and the isotopes of uranium. The actinide energy contribution will be appropriate for the time in life that produces the highest calculated fuel pin temperatures during the LOCA.



Integrated Nuclear Services

JHT/97-1
January 7, 1997

Document Control Desk
U. S. Nuclear Regulatory Commission
Washington, D.C. 20555-0001

Subject: Response to a Verbal Request for Additional Information on BWNT LOCA -
BWNT Loss-of-Coolant Accident Evaluation Model for Once-Through Steam
Generator Plants

Gentlemen:

Attached is the response to a verbal question for additional information on the original release of Topical Report BAW-10192P, "BWNT LOCA, BWNT Loss-of-Coolant Accident Evaluation Model for Once-Through Steam Generator Plants." Some information in the attached response (specifically, pages 13-18, 20, and 28-33) is considered "Proprietary" as sworn by me as Manager of Licensing Services, Framatome Technologies, Inc. in the attached affidavit.

If clarification of any of the provided information is needed, please call me at 804/832-2817 or John Klingenfus at 804/832-3294.

Very truly yours,

A handwritten signature in black ink, appearing to read "J. H. Taylor".

J. H. Taylor, Manager
Licensing Services

JHT/bcc

Attachment

C: L. Lois/NRC
R. B. Borsum/FTI-MD82
R. J. Schomaker/FTI-OF57
J. A. Klingenfus/FTI-OF53

(LA-95)

3315 Old Forest Road, P.O. Box 10935, Lynchburg, VA 24506-0935
Telephone: 804-832-3000 Fax: 804-832-3663

This page is intentionally left blank.

AFFIDAVIT OF JAMES H. TAYLOR

- A. My name is James H. Taylor. I am Manager of Licensing Services for Framatome Technologies, Inc. (FTI), and as such, I am authorized to execute this Affidavit.
- B. I am familiar with the criteria applied by FTI to determine whether certain information of FTI is proprietary and I am familiar with the procedures established within FTI to ensure the proper application of these criteria.
- C. In determining whether an FTI document is to be classified as proprietary information, an initial determination is made by the Unit Manager, who is responsible for originating the document, as to whether it falls within the criteria set forth in Paragraph D hereof. If the information falls within any one of these criteria, it is classified as proprietary by the originating Unit Manager. This initial determination is reviewed by the cognizant Section Manager. If the document is designated as proprietary, it is reviewed again by Licensing personnel and other management within FTI as designated by the Manager of Licensing Services to assure that the regulatory requirements of 10 CFR Section 2.790 are met.
- D. The following information is provided to demonstrate that the provisions of 10 CFR Section 2.790 of the Commission's regulations have been considered:
 - (i) The information has been held in confidence by FTI. Copies of the document are clearly identified as proprietary. In addition, whenever FTI transmits the information to a customer, customer's agent, potential customer or regulatory agency, the transmittal requests the recipient to hold the information as proprietary. Also, in order to strictly limit any potential or actual customer's use of proprietary information, the substance of the following provision is included in all agreements entered into by FTI, and an equivalent version of the proprietary provision is included in all of FTI's proposals:

AFFIDAVIT OF JAMES H. TAYLOR (Cont'd.)

"Any proprietary information concerning Company's or its Supplier's products or manufacturing processes which is so designated by Company or its Suppliers and disclosed to Purchaser incident to the performance of such contract shall remain the property of Company or its Suppliers and is disclosed in confidence, and Purchaser shall not publish or otherwise disclose it to others without the written approval of Company, and no rights, implied or otherwise, are granted to produce or have produced any products or to practice or cause to be practiced any manufacturing processes covered thereby.

Notwithstanding the above, Purchaser may provide the NRC or any other regulatory agency with any such proprietary information as the NRC or such other agency may require; provided, however, that Purchaser shall first give Company written notice of such proposed disclosure and Company shall have the right to amend such proprietary information so as to make it non-proprietary. In the event that Company cannot amend such proprietary information, Purchaser shall prior to disclosing such information, use its best efforts to obtain a commitment from NRC or such other agency to have such information withheld from public inspection.

Company shall be given the right to participate in pursuit of such confidential treatment."

AFFIDAVIT OF JAMES H. TAYLOR (Cont'd.)

- (ii) The following criteria are customarily applied by FTI in a rational decision process to determine whether the information should be classified as proprietary. Information may be classified as proprietary if one or more of the following criteria are met:
- a. Information reveals cost or price information, commercial strategies, production capabilities, or budget levels of FTI, its customers or suppliers.
 - b. The information reveals data or material concerning FTI research or development plans or programs of present or potential competitive advantage to FTI.
 - c. The use of the information by a competitor would decrease his expenditures, in time or resources, in designing, producing or marketing a similar product.
 - d. The information consists of test data or other similar data concerning a process, method or component, the application of which results in a competitive advantage to FTI.
 - e. The information reveals special aspects of a process, method, component or the like, the exclusive use of which results in a competitive advantage to FTI.
 - f. The information contains ideas for which patent protection may be sought.

AFFIDAVIT OF JAMES H. TAYLOR (Cont'd.)

The document(s) listed on Exhibit "A", which is attached hereto and made a part hereof, has been evaluated in accordance with normal FTI procedures with respect to classification and has been found to contain information which falls within one or more of the criteria enumerated above. Exhibit "B", which is attached hereto and made a part hereof, specifically identifies the criteria applicable to the document(s) listed in Exhibit "A".

- (iii) The document(s) listed in Exhibit "A", which has been made available to the United States Nuclear Regulatory Commission was made available in confidence with a request that the document(s) and the information contained therein be withheld from public disclosure.
 - (iv) The information is not available in the open literature and to the best of our knowledge is not known by Combustion Engineering, EXXON, General Electric, Westinghouse or other current or potential domestic or foreign competitors of FTI.
 - (v) Specific information with regard to whether public disclosure of the information is likely to cause harm to the competitive position of FTI, taking into account the value of the information to FTI; the amount of effort or money expended by FTI developing the information; and the ease or difficulty with which the information could be properly duplicated by others is given in Exhibit "B".
- E. I have personally reviewed the document(s) listed on Exhibit "A" and have found that it is considered proprietary by FTI because it contains information which falls within one or more of the criteria enumerated in Paragraph D, and it is information which is customarily held in confidence and protected as proprietary information by FTI. This report comprises information

AFFIDAVIT OF JAMES H. TAYLOR (Cont'd.)

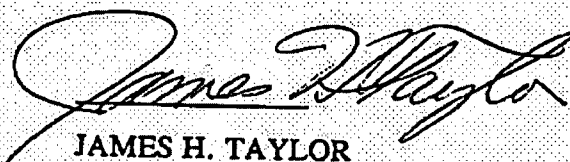
utilized by FTI in its business which afford FTI an opportunity to obtain a competitive advantage over those who may wish to know or use the information contained in the document(s).



JAMES H. TAYLOR

State of Virginia)
) SS. Lynchburg
City of Lynchburg)

James H. Taylor, being duly sworn, on his oath deposes and says that he is the person who subscribed his name to the foregoing statement, and that the matters and facts set forth in the statement are true.



JAMES H. TAYLOR

Subscribed and sworn before me
this 7th day of January 1997.

Brenda C. Cardona
Notary Public in and for the City
of Lynchburg, State of Virginia.

My Commission Expires July 31, 1999

EXHIBITS A & B

EXHIBIT A

Additional Information on BAW-10192P, "BWNT LOCA - BWNT Loss-of-Coolant Accident Evaluation Model for Once-Through Steam Generator Plants," January 7, 1997.

EXHIBIT B

The above listed document contains information which is considered Proprietary in accordance with Criteria b, c, and d of the attached affidavit.

Verbal Requests for Supplemental Information on BAW-10192P, Rev 0**"BWNT Loss-of-Coolant Accident Evaluation Model
For Once-Through Steam Generator Plants"**

The NRC Commission Report on Maine-Yankee contained recommendations that call for demonstration calculations to be contained in EM submittals. The BWNT LOCA EM was developed for three plant classifications: (1) 177-fuel assembly (FA) lowered-loop (LL) plant, (2) 177-FA raised-loop (RL) plant, and (3) 205-FA RL plant. The EM contains demonstration calculations for the 205-FA RL plant. These demonstration cases are directly applicable to the 177-FA RL plant because the only significant difference in the raised-loop designs is the core power density (i.e. 177 15 X 15 pin versus 205 17 X 17 pin fuel assemblies). The NRC has questioned the applicability of the EM to the 177-FA LL plant. The EM identifies the methods used in LOCA analyses and also provides noding arrangements used in constructing the models for the lowered-loop design. Nonetheless, a sample LBLOCA EM calculation on a lowered-loop design has been requested to support the EM approval process.

FTI has performed full LOCA applications for the three Oconee units and for the Three Mile Island Unit 1 (TMI-1) plants in anticipation of receiving NRC approval on the BWNT LOCA EM. These are all Category 1 plants. A summary report was prepared for GPU Nuclear describing the results of the TMI-1 applications. In order to fulfill the requirements from the Maine-Yankee report, portions of the summary report are being sent to the NRC for review in support of completing the SER. Parts of Sections 3, 4, 5, and 6 from that report are attached as the formal response to the NRC request for additional information.

The information included in this submittal describes the lowered-loop or Category 1 plants. Key plant input parameters and RCS initial conditions are provided along with the complete modeling and noding arrangements. The applicability of the generic EM studies is discussed and a summary of the results of Category 1 plant-specific sensitivity studies is provided. The studies identified the most limiting LOCA size, location, and input

parameters that must be used to show compliance with 10 CFR 50.46. The results of one of the beginning-of-life 2.506-ft LOCA limits case is summarized in both tabular and plotted form for a simulated LBLOCA on a Category 1 plant. This is but one case out of the thirty or more (up to fifty if a mixed-core analyses are needed with gadolina fuel pins) plant category-specific analyses that are needed for a complete LBLOCA application for the Category 1 plants.

3. PLANT DESCRIPTION

The TMI-1 nuclear power plant is a Category 1 (Reference 1), lowered-loop nuclear steam supply system designed by B&W. The current licensed operating power level is 2568 MWT (Reference 8), however, the LBLOCA analyses documented in this report consider an uprated core power level of 2772 MWT. The core contains 177 15 x 15 fuel assemblies, each containing 208 active fuel rods. The plant ECCS consists of a conventional combination of pumped high pressure injection (HPI), nitrogen-pressurized core flood tanks (CFT), and pumped low pressure injection (LPI).

3.1. Physical Description

The TMI-1 reactor coolant system is composed of two vertical OTSGs, four shaft-sealed reactor coolant pumps, a reactor vessel, a pressurizer, and interconnecting piping. The system, shown in elevation and plan in Figures 3-1 and 3-2, respectively, is arranged in two heat transfer loops. Each loop has one hot leg pipe, one steam generator, two reactor coolant pumps, and two cold leg pipes. The hot leg connects the exit of the reactor vessel to the inlet plenum of the steam generator. Separate cold leg pump suction (CLPS) pipes extend from the steam generator lower plenum to the centrifugal pump inlets. The pump exits are connected to the reactor vessel inlet nozzles by individual cold leg pump discharge (CLPD) pipes. The pressurizer is connected to the vertical riser of one hot leg by the surge line piping.

The RCS is enclosed entirely within a containment building that is designed to prevent a radioactive release to the atmosphere in the event of a severe accident. This building is equipped with pressure suppression systems (sprays and fan coolers) that activate following a LOCA to prevent over-pressurization of the containment building resulting from mass and energy releases occurring during the transient. Additional containment systems facilitate iodine and hydrogen gas removal and control the reactor building sump pH.

3.1.1. Reactor Vessel

The reactor vessel (RV) configuration is that of a cylindrical shell with a hemispherical bottom head and a removable hemispherical upper head. Major regions of the reactor vessel, shown in Figure 3-3, are the inlet and outlet nozzles, the downcomer, the lower plenum, the core, the upper plenum, and the upper head. Coolant enters the vessel through four inlet nozzles and passes downward through the downcomer into the lower plenum. From the lower plenum, coolant is directed upward, passing either through the core or the baffle/bypass region, to the upper plenum. The coolant flows into the outlet annulus region via one of three paths: (1) the series of small holes in the plenum cylinder that align with each hot leg nozzle, (2) the series of larger holes higher in the plenum cylinder, or (3) into the reactor vessel upper head and back into the top of the outlet annulus though holes in the periphery of the upper support plate. Within the outlet annulus region, the coolant mixes before exiting through the two outlet nozzles. Located in the upper core support shield wall are eight internal reactor vessel vent valves (RVVVs). The valves are closed while the reactor coolant pumps (RCPs) are operating, but open during the course of cold leg break LOCA, providing a core steam relief path to the break.

3.1.2. Reactor Core and Fuel Assembly

The reactor core is comprised of 177 fuel assemblies, each having a 15 x 15 square-pitch arrangement. Each fuel assembly consists of 208 active fuel rods, 16 control rod guide tubes, and one instrument tube. Each fuel rod consists of a 12-foot high stack of fuel pellets contained in a Zr₂Ni clad tube with a gap between the fuel pellet and the clad. The control rod locations accommodate insertion of multi-clustered safety rods, control rods, and axial power shaping rods. These rods are used for power control and fission shutdown capability.

3.1.3. Reactor Coolant Loops

The coolant loop piping is connected to the reactor vessel through six nozzles, all of which are located at the same

elevation, approximately five feet above the top of the core. The outlet piping (hot legs) runs from the reactor vessel in a horizontal plane and bends 90 degrees upward into a long riser pipe. The riser pipe makes a 180-degree bend before it attaches to the steam generator inlet plenum. This inverted U-bend is required to accommodate the unique once-through steam generators in B&W-designed plants.

Two cold leg pump suction pipes are connected to the bottom of each steam generator outlet plenum. Each pipe begins with an inclined descent to a short horizontal run. A 90-degree upward bend leads to a long vertical rise to the pump inlet. Since the TMI-1 plant is a lowered-loop design, the vertical rise of this "J-shaped" piping run is approximately 25 feet.

The pump discharge pipe exits horizontally from the RCP. A downward incline section bends back to a horizontal run that connects to the reactor vessel inlet nozzle. The high pressure injection piping connects to the inclined section of the cold leg pump discharge pipe.

3.1.4. Steam Generators

The TMI-1 steam generators, shown in Figure 3-4, are a straight-tube counter-current flow design. Feedwater enters the top of the downcomer near the middle of the steam generator component. The subcooled feedwater aspirates steam from the interior tube bundle region through ports in the shroud wall. The steam condenses on the feedwater as it travels down the downcomer. The mixed fluid is near saturation as it enters the bottom of the tube region just above the lower tube sheet. The heat transfer in the lower 32 feet of the bundle region boils off nearly all of the liquid before the aspirator port elevation is reached. The heat transfer in the upper 20 feet of the bundle dries and superheats the steam. The steam exits through the steam annulus just below the upper tube sheet.

3.1.5. Pressurizer

The pressurizer is connected to the RCS near the bottom of one of the hot leg riser pipes by the pressurizer surge line. The pressurizer provides capability for controlling the RCS pressure at steady-state operation or during upset conditions. It provides additional RCS liquid inventory available for core cooling in the event of a LOCA. The pressurizer liquid region contains heaters used to maintain system pressure. A spray nozzle is located at the top of the steam region, providing the capability to inject subcooled liquid into the steam space to reduce pressure if needed for steady-state or transient control. Neither the sprays or the heaters are used during LOCA transients.

The pressurizer also contains the connections for the code safety valves and the power operated relief valve (PORV). These valves are connected to the top of the pressurizer. Typically, the valves are not used in LOCA analyses, unless the postulated break is in one of these components.

3.2. Description of Emergency Core Cooling System

The plant ECCS consists of a conventional combination of high and low pressure pumped injection (HPI and LPI, respectively) and pressurized water storage tanks or core flood tanks (CFTs).

The HPI is connected to the reactor coolant piping in the cold leg between the RV and the RC pumps. The CFT line enters directly into the reactor vessel downcomer slightly above the inlet/exit nozzle belt region. The LPI line tees into the CFT line.

The HPI system is capable of injecting above normal operating system pressure. It is part of the makeup and purification system during normal operation. The system includes sufficient redundancy such that at least one full train remains operative under the assumption of a single active failure. Emergency operation is activated automatically after receiving an engineered safeguards actuation system (ESAS) signal. For LOCA,

the occurrence of an ESAS signal indicates a low reactor coolant system pressure or a high containment pressure.

There are two 1400 ft³ core flood tanks, each containing approximately 940 ft³ of borated water nominally pressurized to 600 psig with a nitrogen cover gas. Each tank connects individually to the reactor vessel upper downcomer region approximately 1.5 feet above the nozzle belt centerline. Reverse flow during normal operation is prevented by in-line check valves. The system is, therefore, self-contained, self-actuating, and passive. Flow into the RCS occurs whenever the reactor coolant system pressure falls below the tank pressure.

Low pressure injection is achieved with the decay heat removal (DHR) system pumps. Normally used for decay heat removal when the reactor is in cold shutdown, the system also provides low pressure ECC injection through the two CFT nozzles. In emergency operation, the DHR (commonly referred to as LPI) pumps inject water from the borated water storage tank (BWST). When the BWST low level setpoint is reached, the LPI pumps are aligned to take suction from the containment sump. During this recirculation mode, injection flow is passed through a heat exchanger before being returned to the reactor coolant system. The system contains sufficient redundancy such that it is assumed that one full train is available under a single active failure. Actuation is provided by ESAS on low reactor coolant system pressure or high containment pressure. In its recirculation mode, the decay heat removal pumps provide for long-term core cooling.

In the recirculation mode, only the LPI pump is capable of taking suction from the containment sump. However long-term, high pressure cooling is possible because the HPI pumps can take suction from the LPI pump discharge and deliver coolant through their cold leg connections to the RCS.

3.3. Plant Parameters

The major plant parameters and operating conditions are presented in Table 3-1.

Table 3-1. Plant Parameters and Operating Conditions.

Full Reactor Power	2772 MWT
Heat Balance Error	102 %
Operating Hot Leg Pressure	2170 psia
Minimum System Flow w/ Tube Plugging	137.3×10^6 lbm/hr
Maximum Core Bypass Flow	7.5 %
Average Linear Power Generation Rate	6.4 kW/ft ⁽¹⁾
RCS Average Temperature	579 F
Hot Leg Temperature	605 F
Cold Leg Temperature	553 F
Pressurizer Liquid Level	220±28" / 400" range
Steam Generator Pressure	900 psia
Plant-Average SG Tube Plugging	15 percent
Unit-Maximum SG Tube Plugging	20 percent
Main Feedwater Flow w/ Tube Plugging	1655 lbm/hr BL 1675 lbm/hr IL
Main Feedwater Temperature	465 F
Core Flood Tank Pressure	600±35 psig
Core Flood Tank Liquid Volume	940±45 ft ³
Core Flood Tank Temperature	140 F
BWST Temperature	120 F

NOTES:

- (1) The energy deposition factor was not applied to compute this value. The value therefore represents the average power originating in the fuel pellet at the average power location.

4. LBLOCA ANALYSIS INPUTS AND ASSUMPTIONS

The TMI-1 plant analyses were performed in accordance with the LOCA evaluation model for OTSG plants (Reference 1). This chapter provides a brief discussion of the plant parameters, assumptions, and computer codes used in the analyses. Although the chapter is oriented to the analysis of large breaks, the information supplied applies widely to both large and small break calculations. Specific assumptions for the SBLOCA calculations are provided within Chapter 4 of Volume II.

4.1. LBLOCA Inputs and Assumptions

Table 3-1 identifies the inputs and assumptions specifically used in the TMI-1 LBLOCA analyses. The major plant operating parameters and boundary conditions used in the LOCA codes are:

1. Power Level - The analyses consider that the plant is operating at steady-state conditions with core thermal powers less than or equal to 2827 MWT (102% of 2772 MWT).
2. SG Tube Plugging - The tube flow area is based on the assumption that 20 percent of the broken loop and 10 percent of the intact loop tubes have been plugged on the primary side and removed from service. The higher number of plugged tubes in the broken loop produces increased resistance from the core to the break, which serves to decrease the positive core flows during the first portion of blowdown. The reduced core flows produce less heat transfer from the pins to the fluid resulting in higher fuel and cladding temperatures at the end of blowdown.
3. Total System Flow - The total reactor coolant system (RCS) flow, considering a unit-average tube plugging of 15 percent, is 137.3 Mlbm/hr. The total core bypass flow fraction is 7.5 percent of the RCS flow.
4. Fuel Parameters - The steady-state fuel pin parameters are calculated using a method and code (currently TACO3) that has been approved by the NRC for supplying

inputs to the LOCA analysis (Reference 6). The parameters used are consistent with, or bounded by, the core burnup conditions stated or simulated in the analysis. Parameters supplied to RELAP5/MOD2 as initial steady-state values include fuel volume-average temperatures, hot fuel and cladding dimensions, internal pin pressure, gap gas compositions, fuel radial source factors, fuel-clad mechanical contact pressures, hot pin plenum volumes, and rod average burnup.

5. Emergency Core Cooling System - The ECCS flows are based on the most-limiting case between the assumption of a single active failure and the assumption of no failure. Sensitivity studies, discussed in Chapter 5, confirm that the condition of minimum ECCS (flow from one train) is the most-severe assumption.
6. Core Average Linear Heat Rate (LHR) - The core average LHR for the LOCA analyses performed at 102 percent of 2772 MWT is 6.4 kW/ft.
7. Moderator Density Reactivity - The moderator density reactivity coefficient is based on beginning-of-cycle conditions to minimize negative reactivity contributions. A zero moderator temperature coefficient (MTC) is used for all full-power cases as well as for power levels between 80 and 100 percent full power. For partial-power cases between 50 and 80 percent full power, positive MTCs are used with the full-power LOCA LHR limit. .
8. Cladding Rupture Model - The cladding rupture model is based on NUREG-0630 (see Section 4.3.3.1 of Reference 1).

4.2. LBLOCA Computer Codes and Methods

The LOCA OTSG evaluation model consists of a group of computer codes used in the analysis of cladding temperature transients, local cladding oxidation, and whole-core hydrogen generation. Figure 4-1 illustrates the interrelation among the computer codes used for the large break analyses. The RELAP5/MOD2-B&W code (Reference 2) calculates system thermal-hydraulics, core power

generation, and hot-pin thermal response during blowdown. The system thermal-hydraulic transient calculations are continued with the REFLOD3B code (Reference 3) to determine refill time and core reflooding rates for the remainder of the transient. The BEACH code (Reference 4) is used to determine the hot-pin cladding temperature response during refill and reflood using core flooding rates from REFLOD3B. The containment pressure response is calculated separately by the CONTEMPT code (Reference 5) and provided as an input boundary condition for use in the RELAP5 and REFLOD3B system code calculations.

4.2.1. RELAP5/MOD2-B&W Modeling

The RELAP5/MOD2-B&W computer code is used to analyze RCS thermal-hydraulic behavior during the blowdown phase of a LOCA. RELAP5/MOD2-B&W, a modified version of the INEL RELAP5/MOD2 code, is documented in BAW-10164 (Reference 2). RELAP5 permits the user to select a model representation that results in a suitable finite difference model for the fluid system being analyzed. The nodalization for the plant evaluation, shown in Figures 4-2 and 4-3, was developed in accordance with the LOCA evaluation model.

4.2.2. REFLOD3B Modeling

The REFLOD3B code simulates the thermal-hydraulic behavior of the primary system during the core refill and reflood phases of the LOCA. The nodding, shown in Figure 4-5, is consistent with the LOCA evaluation model and consists of reactor vessel and loop models.

The containment backpressure as a function of time is provided from a CONTEMPT analysis. The CONTEMPT and REFLOD3B calculations are iterated until the pressure and the calculated mass and energy releases converge.

4.2.3. BEACH Modeling

The BEACH code (Reference 4) is used to determine the hot and average fuel rod cladding temperature responses during the refill and reflooding phases of the LOCA. The input model consists of two separated systems, each containing a heated channel and time-dependent inlet and outlet volumes for specification of boundary

data from the REFLOD3B calculations. The core model is identical to the RELAP5/MOD2 blowdown model with the exception that no crossflow is permitted between the hot and average channels. The heated channel length of each fuel rod is divided axially into 20 segments, as shown in Figure 4-6, with variable segment length such that each grid is located at the bottom of a control volume and three volumes are used to cover a grid span.

4.2.4. CONTEMPT MODELING

The containment backpressure is calculated by the CONTEMPT computer code based on mass and energy release calculations from RELAP5/MOD2-B&W and REFLOD3B. The results of the sensitivity study performed for this application indicated that a minimum containment backpressure consistent with minimum ECC injection produced the limiting results for a Category 1 plant.

5. LBLOCA SENSITIVITY STUDIES AND BASE CASE

Various sensitivity studies performed with the evaluation model are required to demonstrate model convergence and conservatism. Most of the studies upon which the analyses in this report are based are generic and were documented in the evaluation model report, BAW-10192 (Reference 1). Studies that are specific to a plant or category of plants are discussed in this report. Section 5.1 provides a discussion of the generic sensitivity studies from the reference evaluation model report. Section 5.2 presents a summary of the sensitivity studies performed for the Oconee plants, which are specifically applicable to TMI-1 because they are all Category 1 plants. Section 5.3 describes the final base case used to perform the LOCA LHR limit analyses.

5.1. LBLOCA Evaluation Model Generic Studies

Of the sensitivity studies presented in the original evaluation model topical report (Reference 1), the majority are generic and apply to any B&W plant analysis. Those studies considered generic demonstrate results that are characteristic of the evaluation model--the codes and interfaces--and are not plant-

C,E

each discussion is referenced to the section in the LBLOCA - evaluation model report where the study is documented.

C,D,E

5.2. LBLOCA Category 1 Plant Sensitivity Studies

Although a considerable portion of the analysis inputs and assumptions are set or controlled by the evaluation model and its sensitivity studies, some parameters are dependent on inputs specific to a plant type and can only be established by separate studies. These studies are performed to identify a limiting case to use in calculating the LOCA LHR limits. This section presents the studies performed with the LOCA evaluation model for the Category 1 plant model configuration used in the LOCA LHR limit analyses.

C,E

C,E

Framatome Technologies Inc.

43-10192Q-02

C,D,E

Framatome Technologies Inc.

43-10192Q-02

C,D,E

6. MARK-B9 LBLOCA LHR LIMITS AT 2772 MWT

The LOCA analyses are performed to show compliance with 10 CFR 50.46 for the limiting core power and peaking conditions that are used to set core operational limits and trip setpoints (i.e. the LOCA limits). These LBLOCA analyses serve as the bases for the allowable local power. Numerous cases are performed to determine a curve of allowable peak linear heat rate (LHR) as a function of core elevation for times in life of fuel operation. This curve is either contained in or referenced by the plant technical specifications. Plant operation is controlled such that the local peaking and power do not exceed these allowable LHR limit values.

The minimum containment pressure, consistent with minimum ECC injection, case was used as the base case for the TMI-1 Mark-B9 LOCA limit analyses. New TACO3 steady-state fuel pin data were obtained for each case based on the assumed axial and radial peaking factors.

The five axial power peaks centered at the middle of the five active-core grid spans (at elevations of 2.506-, 4.264-, 6.021-, 7.779-, and 9.536-ft) were analyzed with a constant axial peak of 1.7; the radial peak was adjusted to obtain an allowable LHR limit. Figure 6-1 identifies the axial power shapes analyzed. Generally, the maximum LOCA LHR limit was established within a PCT range of 1950 F to 2050 F. This PCT range was chosen as reasonable, given the sensitivity of the PCT to the metal-water reaction energy contributions at elevated temperatures.

All five core power peaks are analyzed at the beginning-of-life (BOL) and middle-of-life (MOL) conditions as well as one end-of-life (EOL) case. The results are summarized in tables and eight figures for each case. The figures show (1) the pressure in the upper plenum during blowdown, (2) the mass flow rate through the break during blowdown, (3) the mass flow rate at the ruptured and peak unruptured locations in the hot channel during blowdown, (4) the reflooding rate, (5) the hot channel fuel and clad temperatures at the ruptured location, (6) the hot channel fuel and clad temperatures at the peak unruptured location, (7) the hot channel heat transfer coefficients at the ruptured and peak unruptured locations, and (8) the quench front advancement in the hot and average channels.

6.1. BOL LOCA LHR Demonstration Case

The demonstration case included here is the BOL 2.506-ft core power peak. The hot pin initial conditions are presented in Table 6-1, while the results of the demonstration LOCA limit analysis are tabulated in Table 6-2 and shown in Figures 6-2 through 6-9.

Table 6-1. Mark-B9 Hot Channel Initial Conditions Used for the LOCA LHR Limit Analyses.

Parameter	2.506-ft
BOL Initial Conditions	
Peak LHR, kW/ft	16.2
C,E	

Table 6-2. TMI-1 2772 MWT Mark-B9 BOL LOCA LHR Limit Summary.

<u>Parameter</u>	<u>2.506-ft</u>
HC Peak LHR, kW/ft	16.2
End-of-Bypass, s	18.55
End-of-Blowdown (EOB), s	20.0
Liquid Mass in RV Lower Plenum at EOB, lbm	12691.4
RV Lower Plenum Filled, s	27.60
LPI Flow Begins, s	36.09
CFTs Empty, s	39.84
Clad Rupture Time, s	18.71
Unruptured Segment:	
PCT, F	1926.3
Time, s	32.7
Local Oxidation, %	1.2605
Ruptured Segment:	
PCT, F	2030.5
Time, s	29.54
Local Oxidation, %	2.7927
Average Oxidation Increase, %	
Hot Channel	0.431
Average Channel	0.05
Whole-Core Hydrogen Generation, %	<0.2
Average Channel Quench Time, s	195.8

REFERENCES

1. BAW-10192P, "BWNT LOCA - BWNT Loss-of-Coolant Accident Evaluation Model for Once-Through Steam Generator Plants," Revision 0, B&W Nuclear Technologies, Lynchburg, Virginia, February 1994.
2. J. A. Klingenfus, et al., "RELAP5/MOD2-B&W -- An Advanced Computer Program for Light Water Reactor LOCA and Non-LOCA Transient Analysis," BAW-10164, Revision 3, B&W Nuclear Technologies, Lynchburg, Virginia, October 1992.
3. C. K. Nithianandan, "REFLOOD3B -- Model for Multinode Core Reflooding Analysis," BAW-10171, Revision 3, B&W Nuclear Technologies, Lynchburg, Virginia, September 1989.
4. N. H. Shah, et al., "BEACH -- A Computer Program for Reflood Heat Transfer During LOCA," BAW-10166, Revision 4, B&W Nuclear Technologies, Lynchburg, Virginia, October 1992.
5. Y. H. Hsii, "CONTEMPT - Computer Program for Predicting Containment Pressure-Temperature Response to LOCA," B&W-Revised Version of Phillips Petroleum Co. Program (L. C. Richardson, et al., June 1967), BAW-10095A, Revision 1, Babcock & Wilcox, Lynchburg, Virginia, April 1978.
6. D. A. Wesley, et al., "TACO-3 - Fuel Pin Thermal Analysis Code," BAW-10162P-A, Babcock & Wilcox, Lynchburg, Virginia, November 1989.
7. B. M. Dunn, et al., "B&W's ECCS Evaluation Model," BAW-10104PA, Revision 5, Babcock & Wilcox, Lynchburg, Virginia, November 1986.
8. Three Mile Island Nuclear Station - Unit 1 Final Safety Analysis Report, Update 13, April 1996.

Figure 3-1. REACTOR COOLANT SYSTEM ELEVATION ARRANGEMENT.

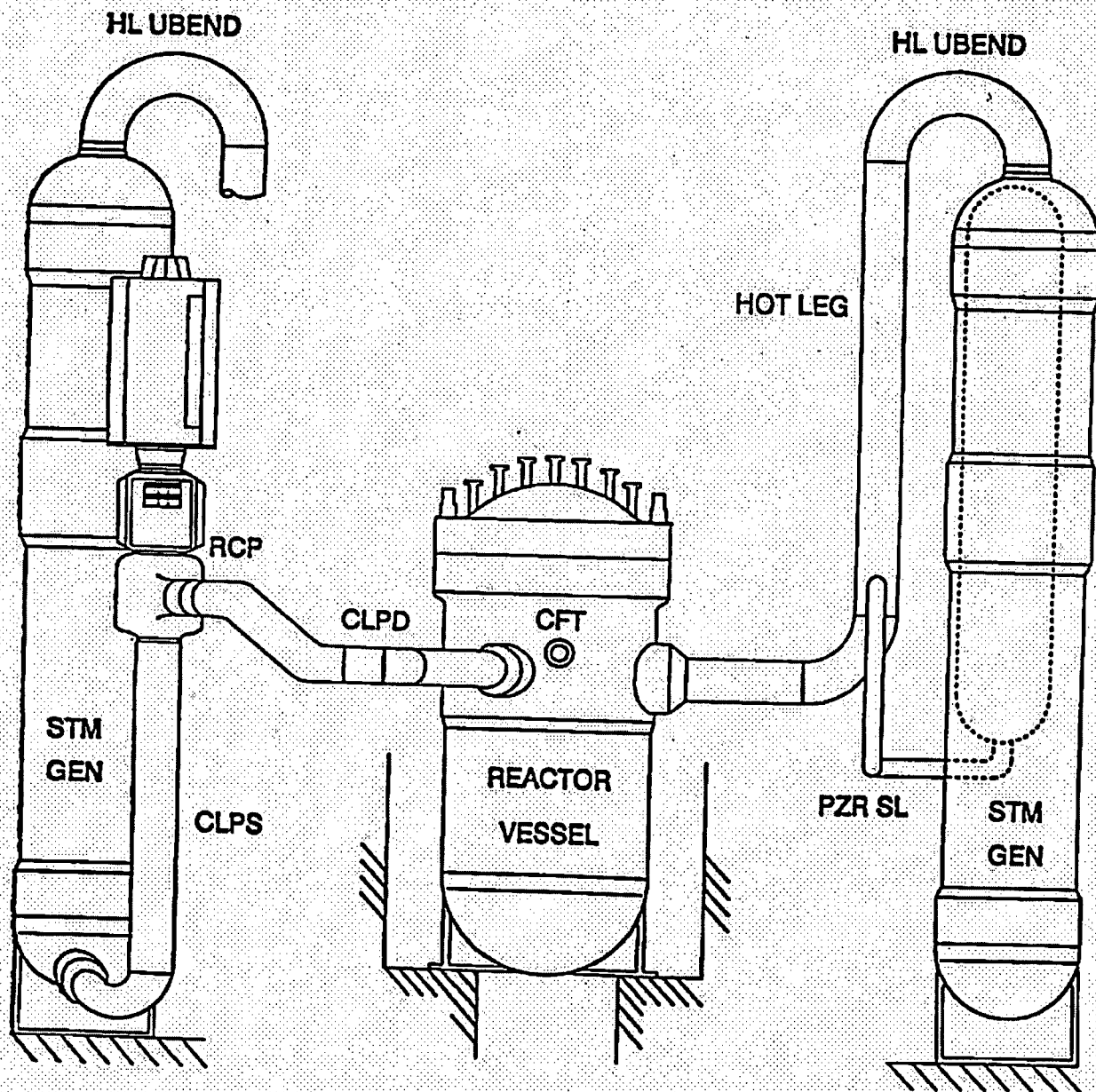


Figure 3-2. REACTOR COOLANT SYSTEM ARRANGEMENT - TOP VIEW.

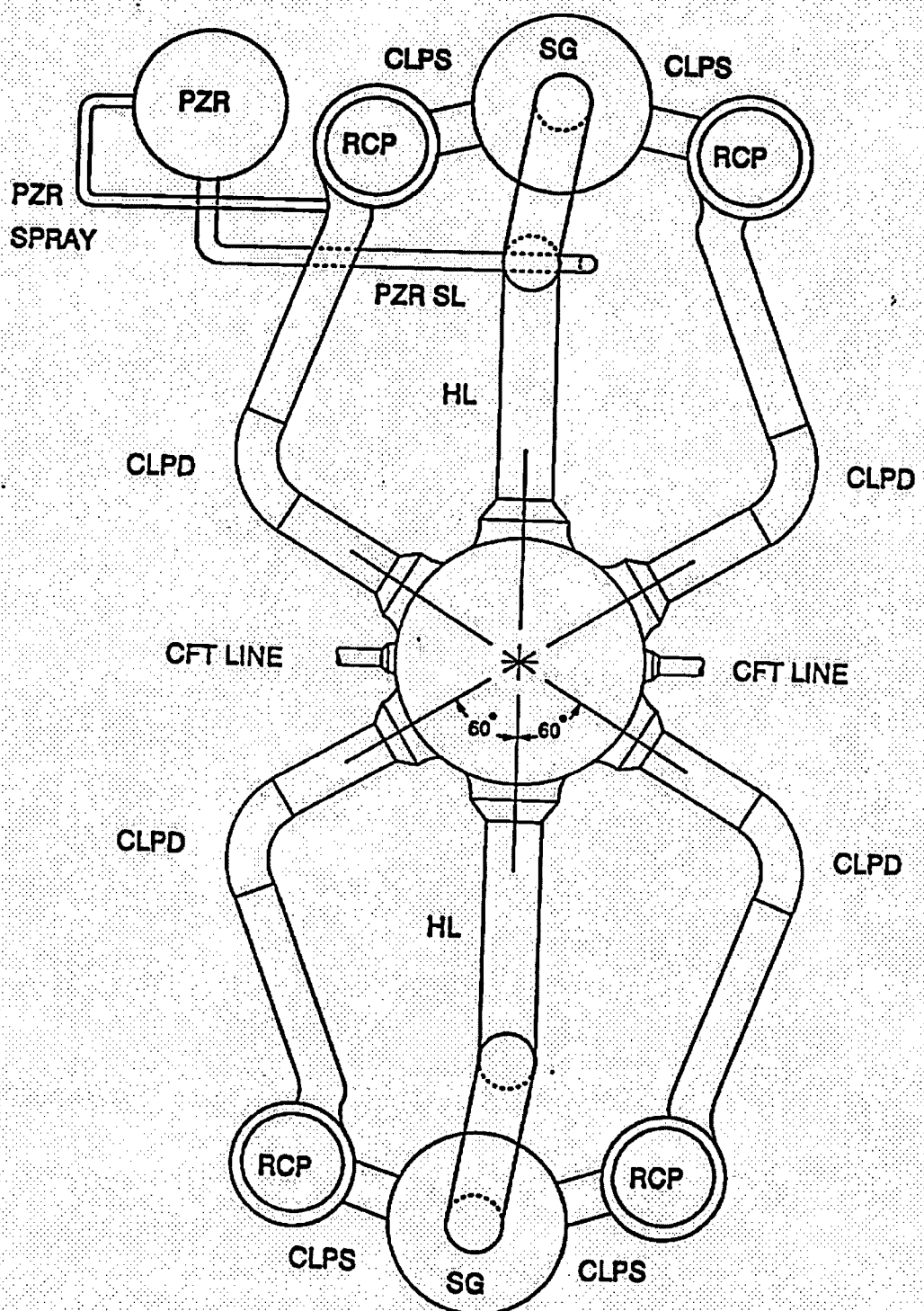


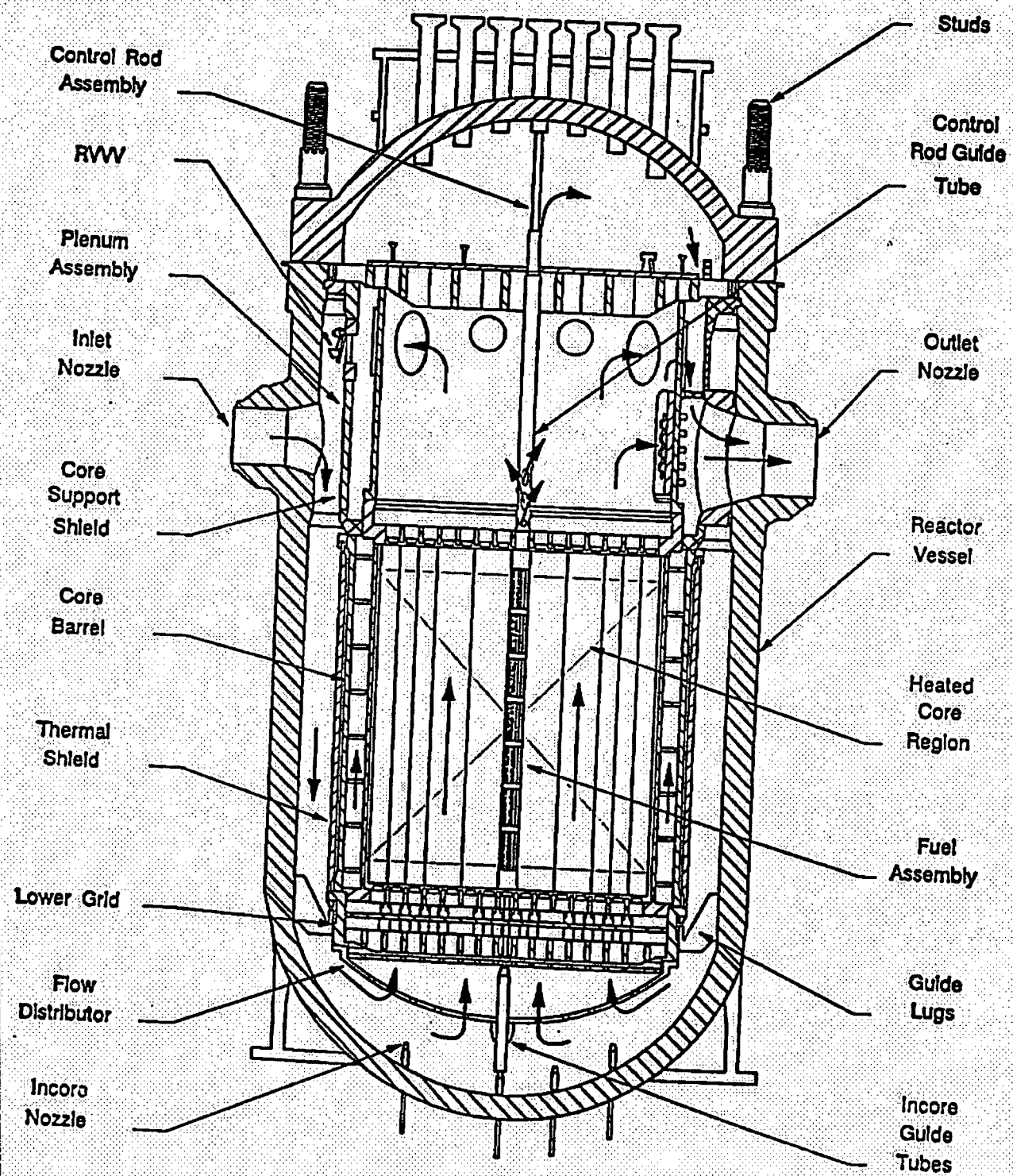
FIGURE 3-3. REACTOR VESSEL ARRANGEMENT.

FIGURE 3-4. ONCE - THROUGH STEAM GENERATOR ARRANGEMENT.

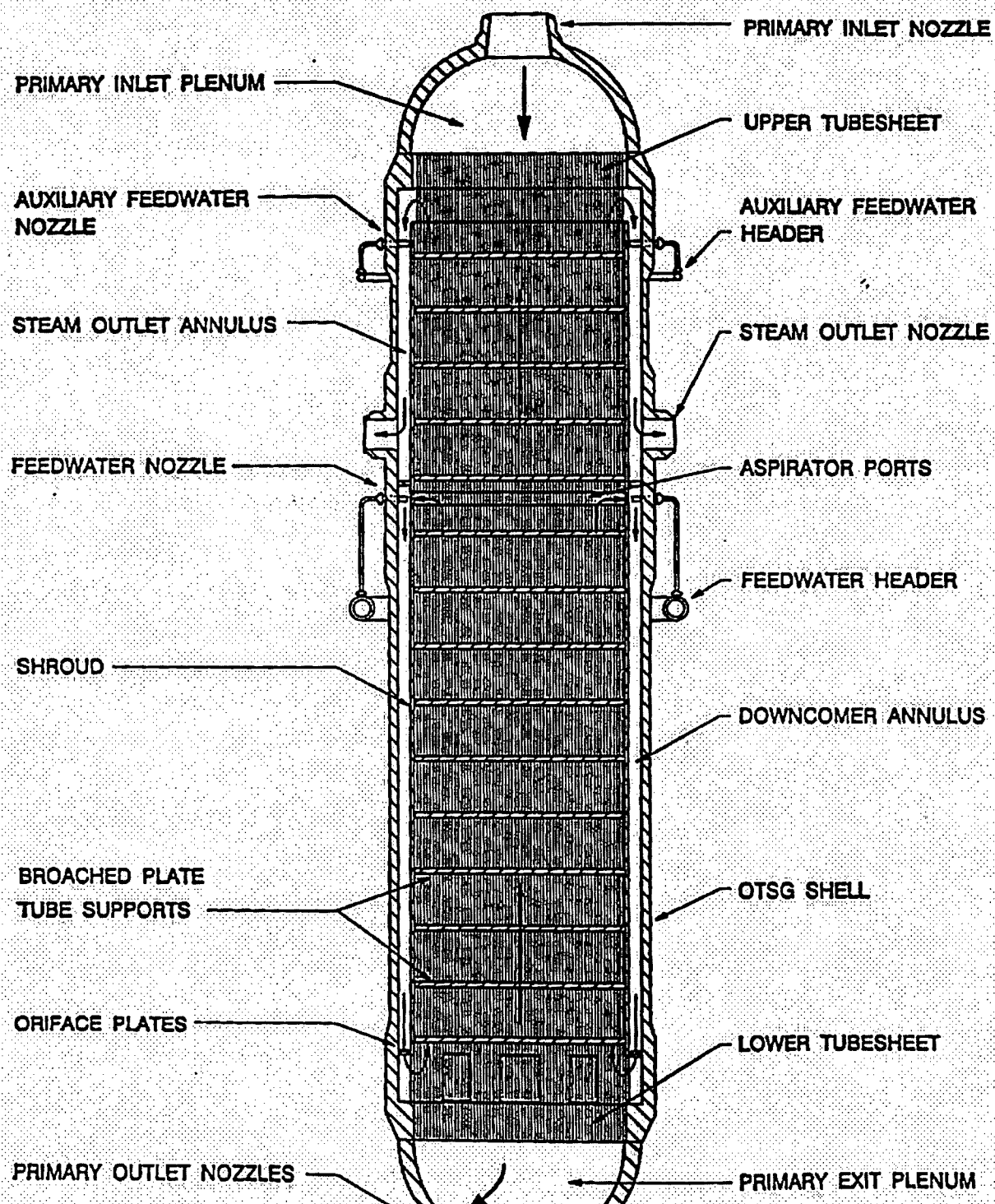


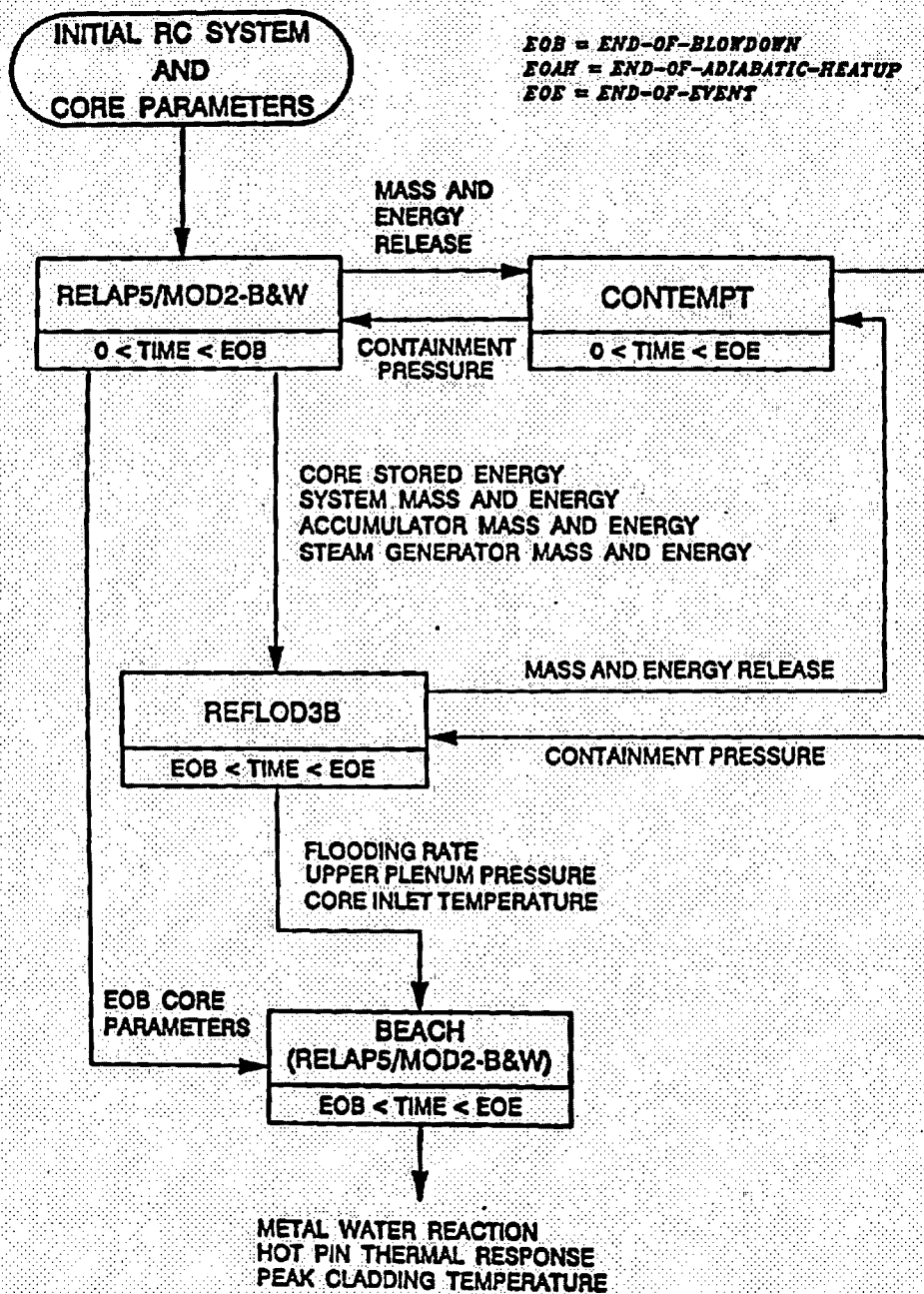
FIGURE 4-1. LARGE BREAK ANALYSIS CODE INTERFACE.

FIGURE 4-2. LBLOCA LOOP NODING ARRANGEMENT (177 LL PLANT).

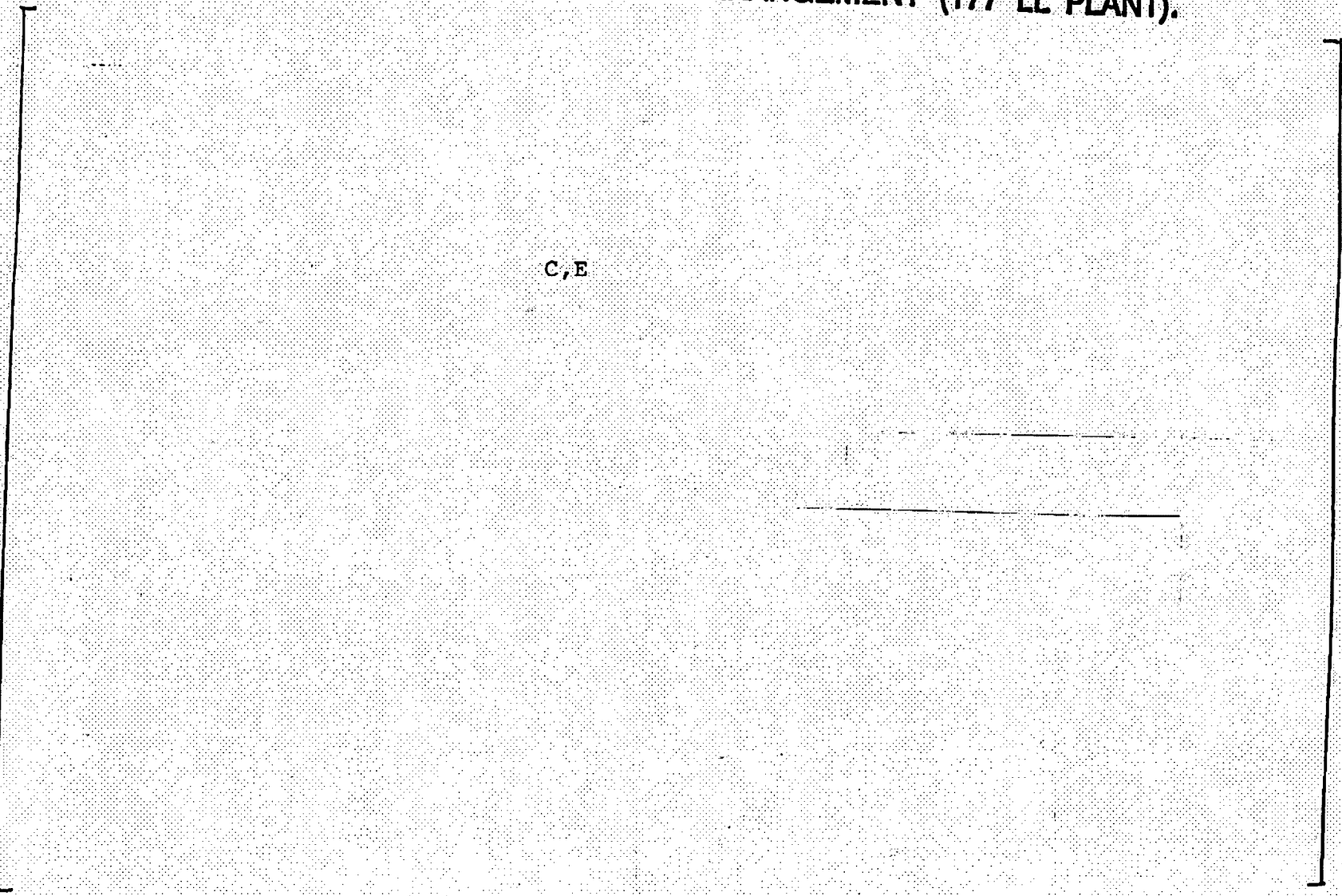


FIGURE 4-3. LBLOCA REACTOR VESSEL NODING ARRANGEMENT (177 LL PLANT).

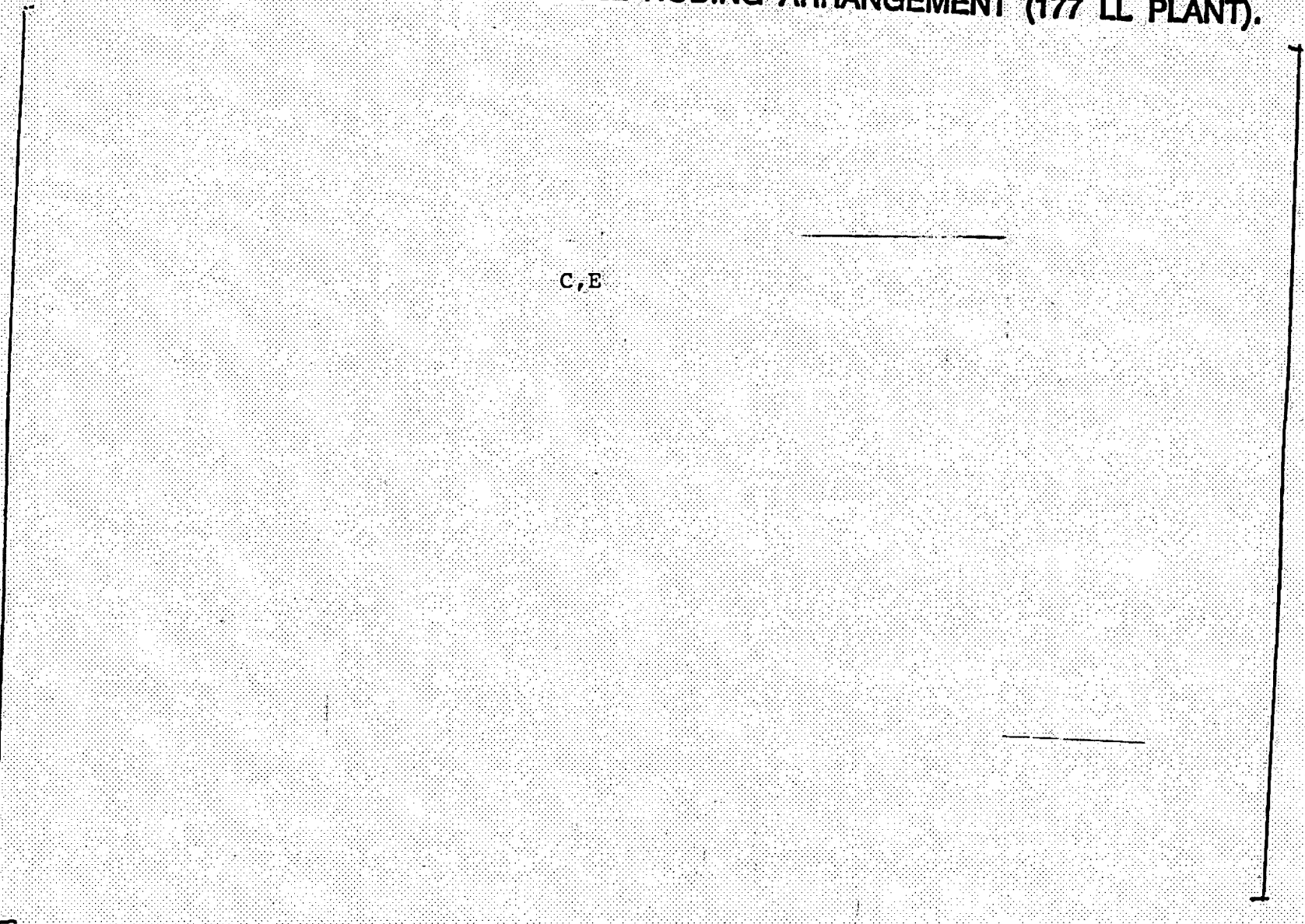


FIGURE 4-4. LBLOCA CLPD BREAK NODING ARRANGEMENT.

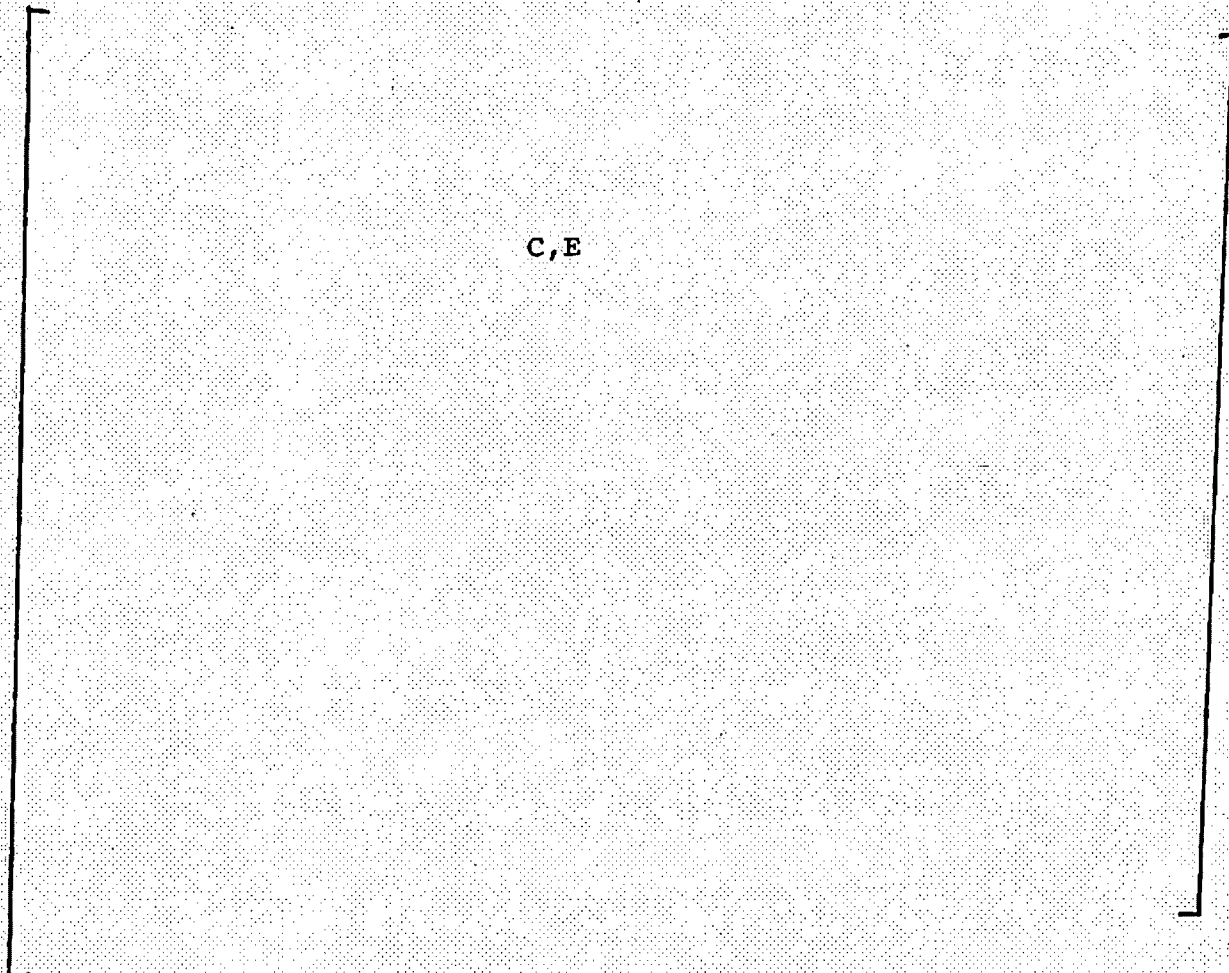


FIGURE 4-5. REFLOD3B NODING ARRANGEMENT (177 LL PLANT).

C,E

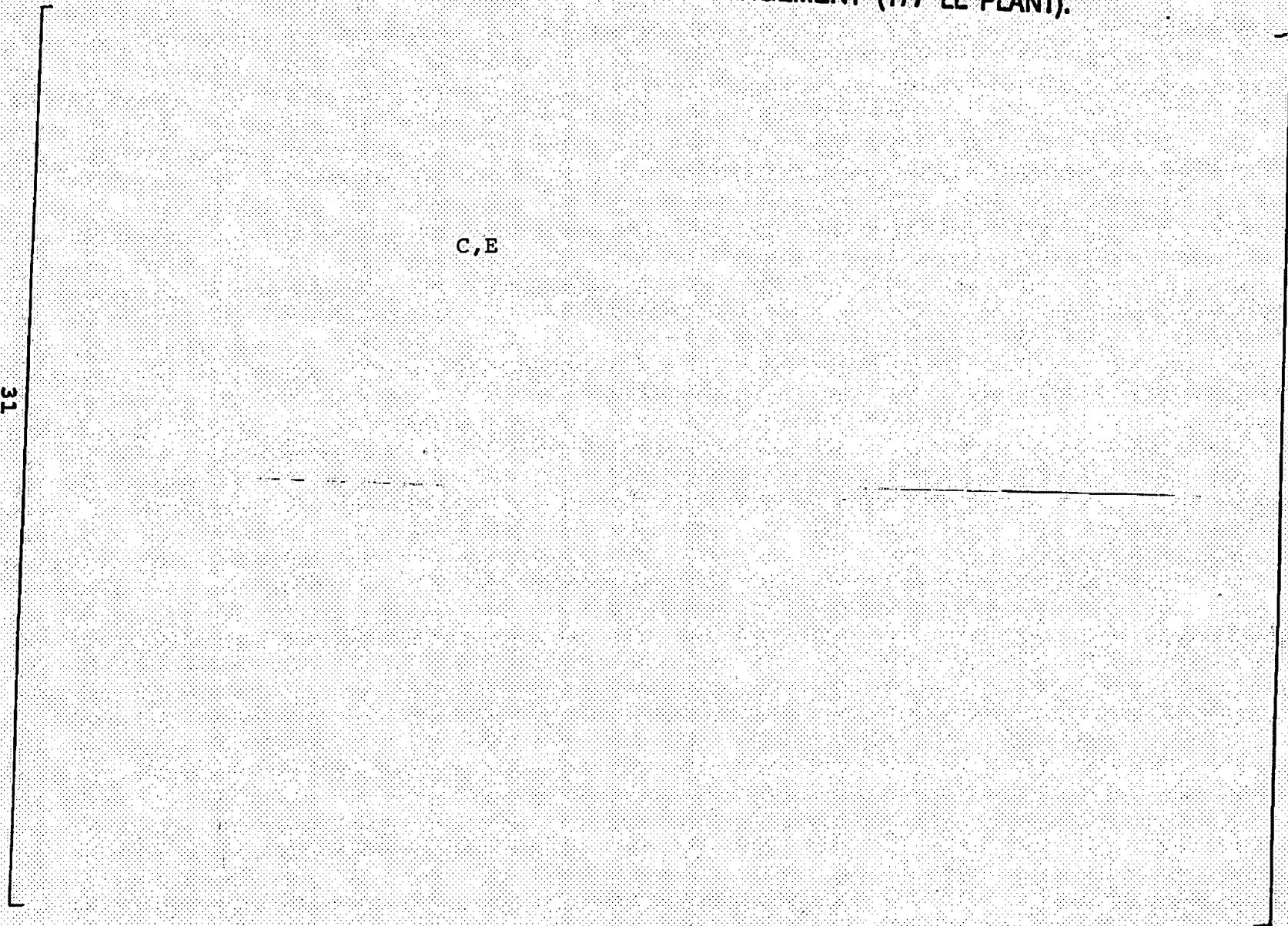


FIGURE 4-6. BEACH NODING ARRANGEMENT (MARK - B FUEL DESIGN).

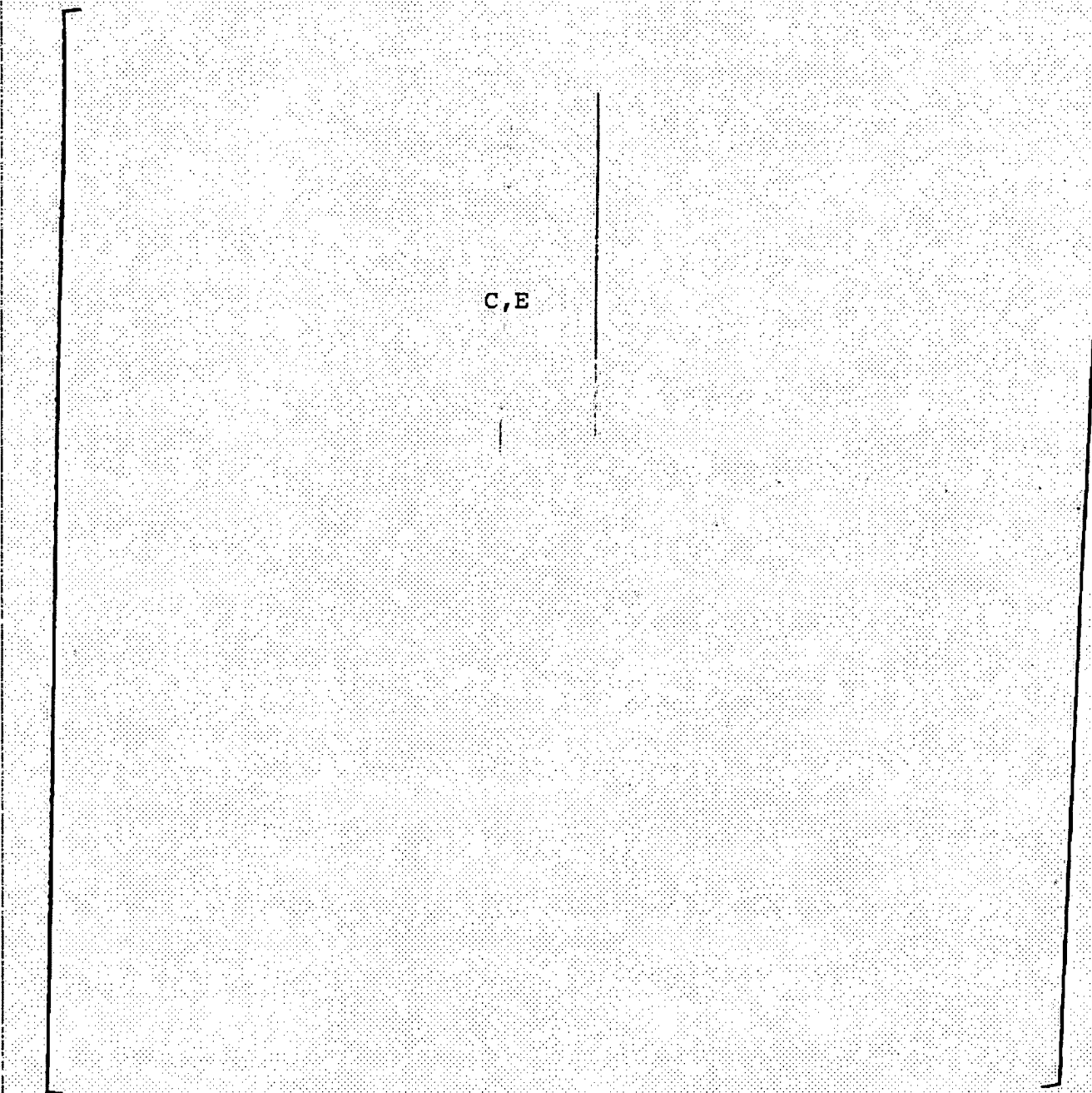
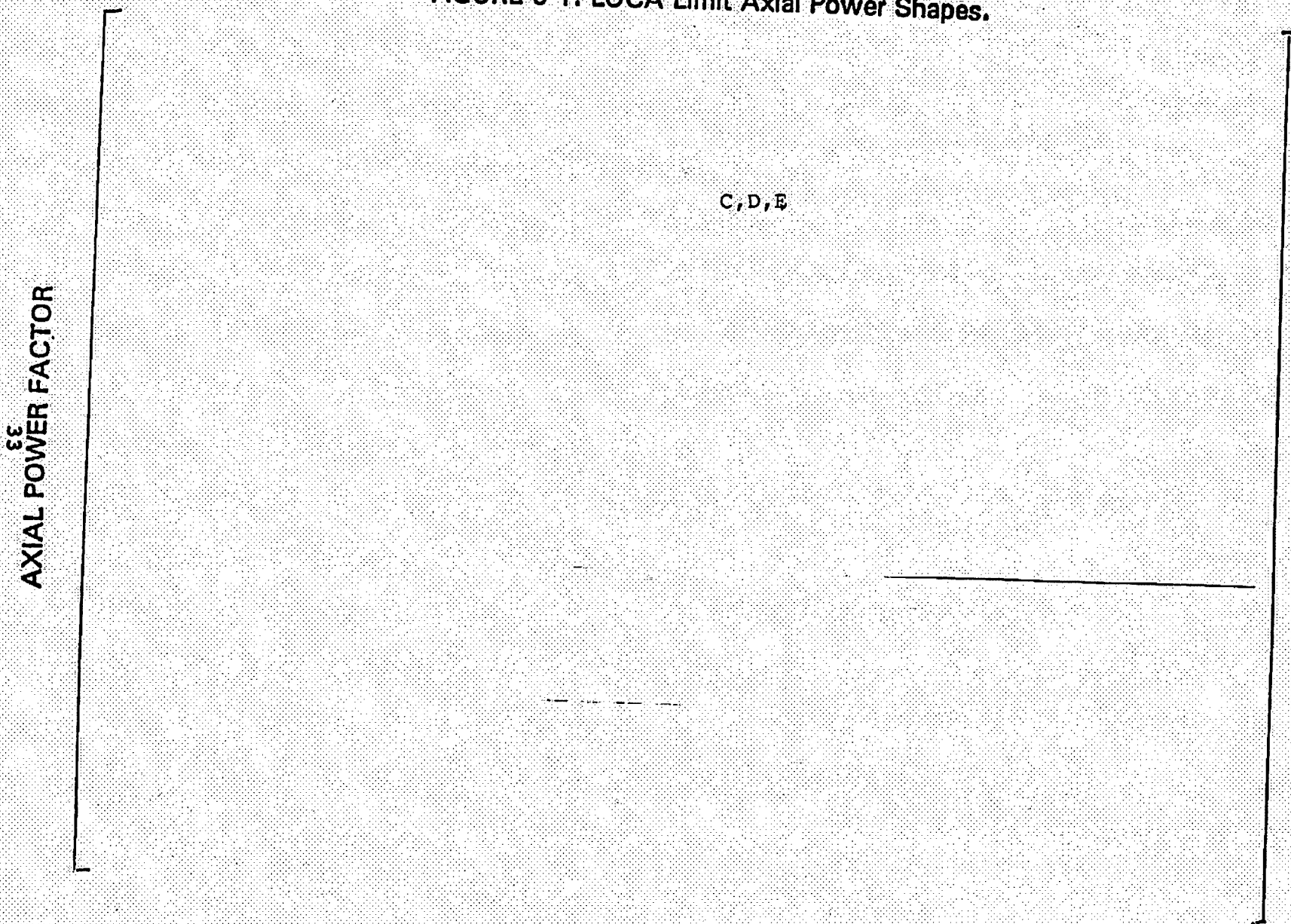


FIGURE 6-1. LOCA Limit Axial Power Shapes.



(SET-ATI)

FIGURE 6-2. 2.506-FT, BOL LOCA LIMIT CASE -
REACTOR VESSEL UPPER PLENUM PRESSURE.

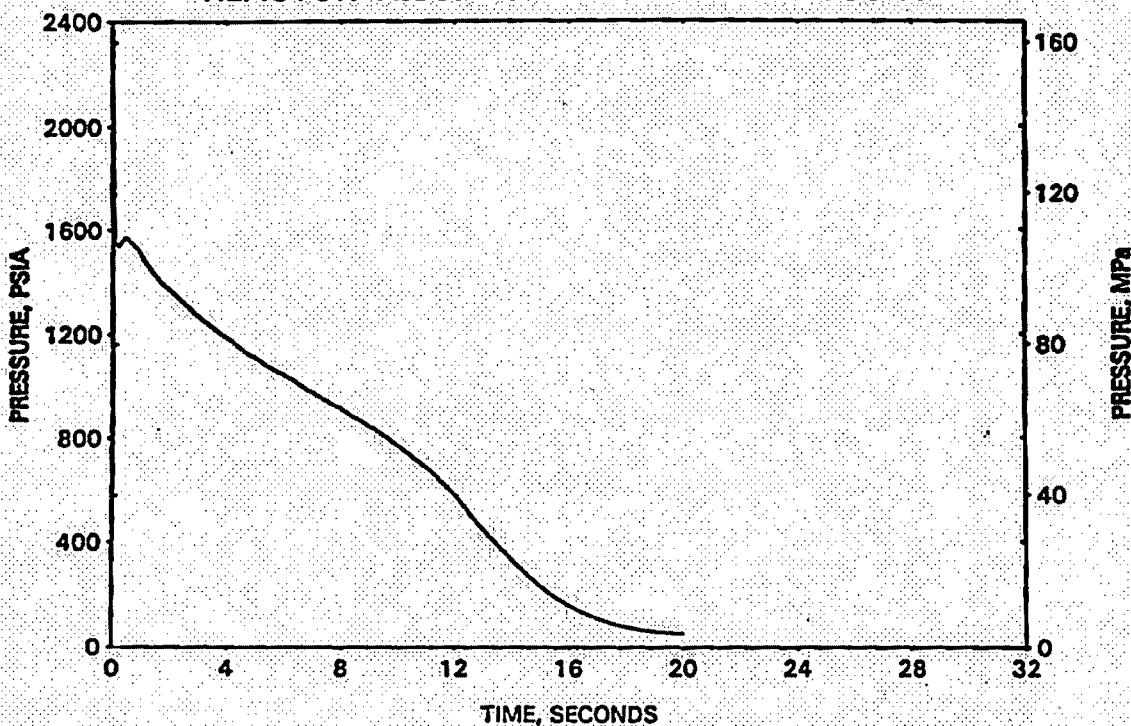


FIGURE 6-3. 2.506-FT, BOL LOCA LIMIT CASE -
BREAK MASS FLOW RATES.

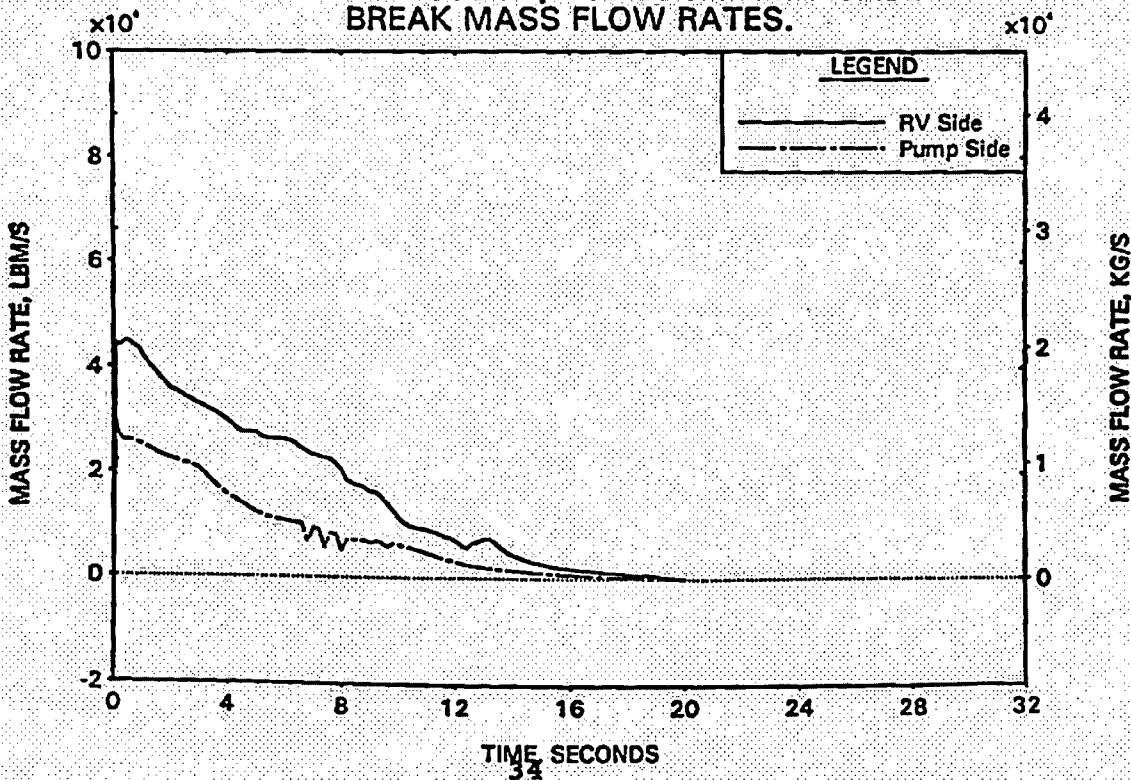


FIGURE 6-4. 2.506-FT, BOL LOCA LIMIT CASE -
HOT CHANNEL MASS FLOW RATES.

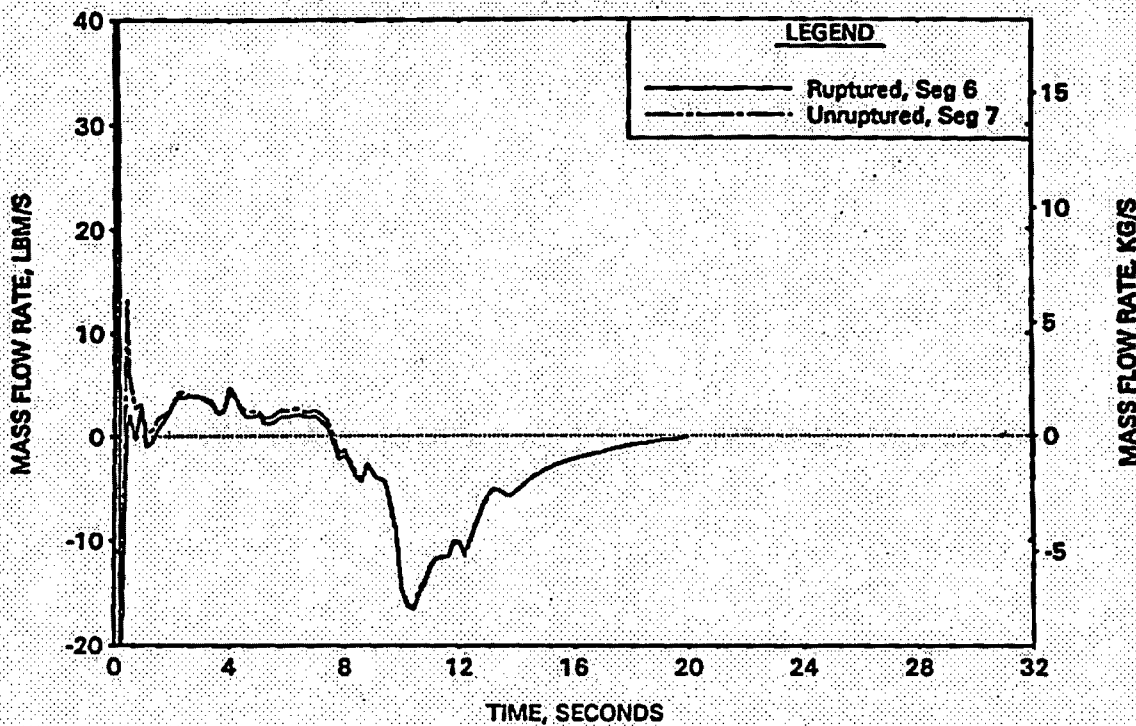


FIGURE 6-5. 2.506-FT, BOL LOCA LIMIT CASE -
CORE FLOODING RATE.

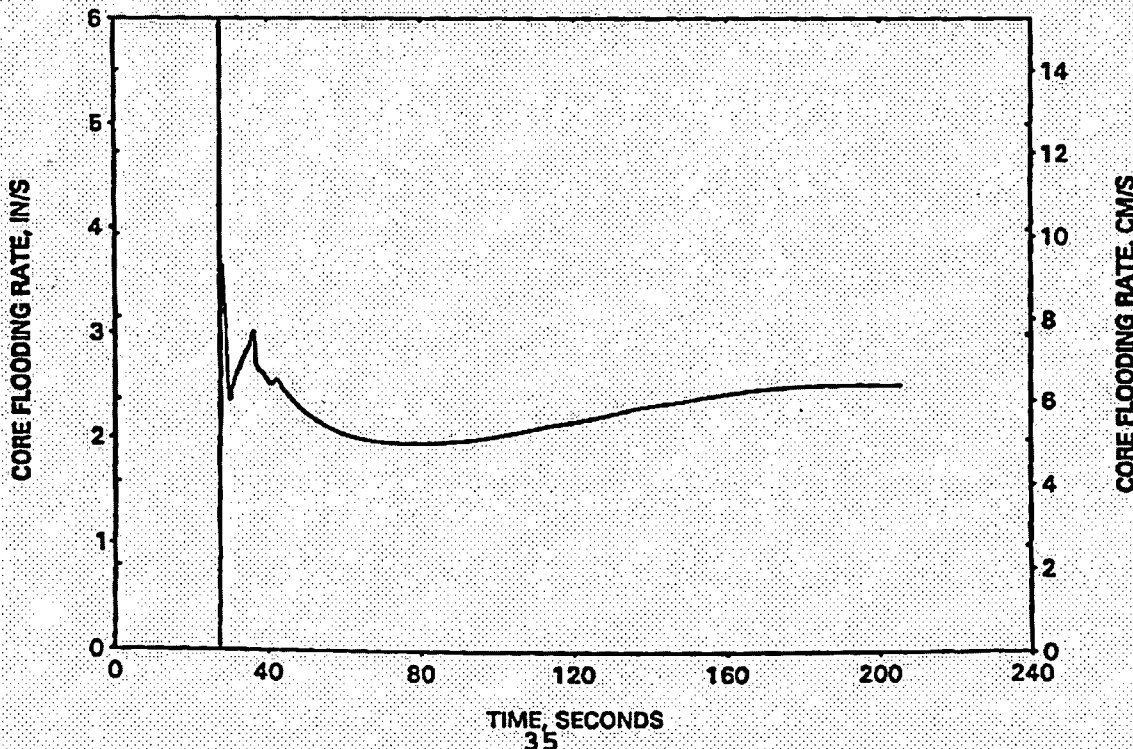


FIGURE 6-6. 2.506-FT, BOL LOCA LIMIT CASE -
HC FUEL & CLAD TEMPERATURES AT RUPTURED LOCATION.

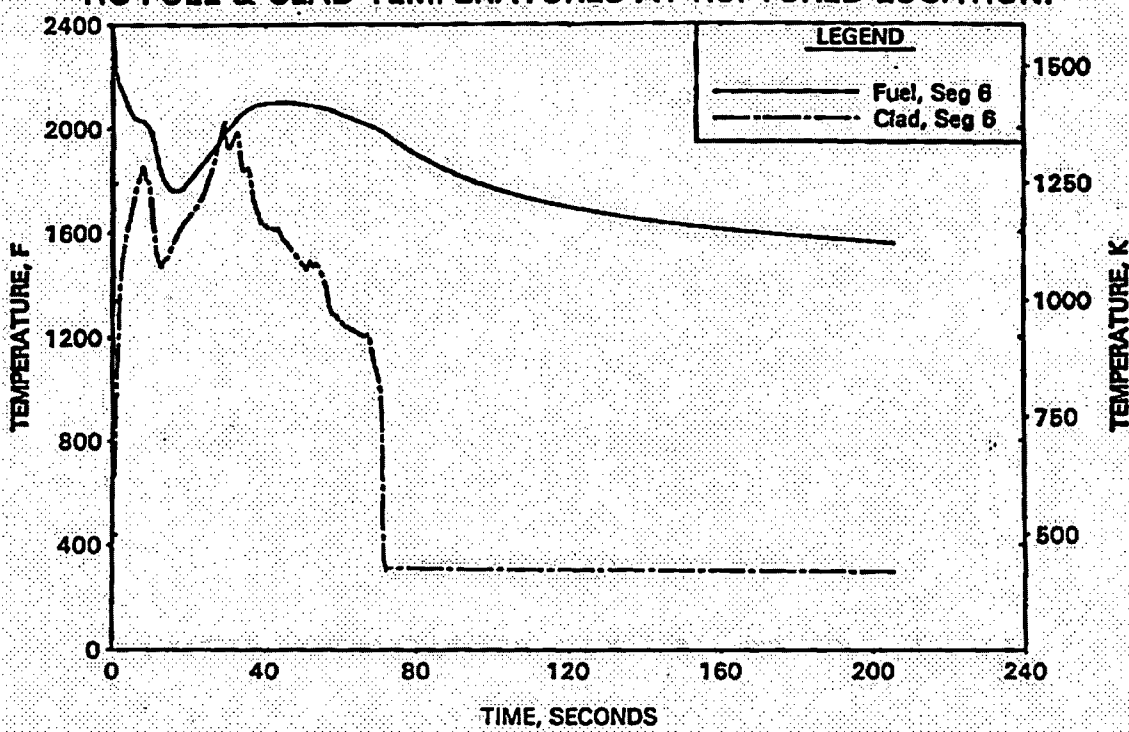


FIGURE 6-7. 2.506-FT, BOL LOCA LIMIT CASE -
HC FUEL & CLAD TEMPERATURES AT PEAK UNRUPTURED LOCATION.

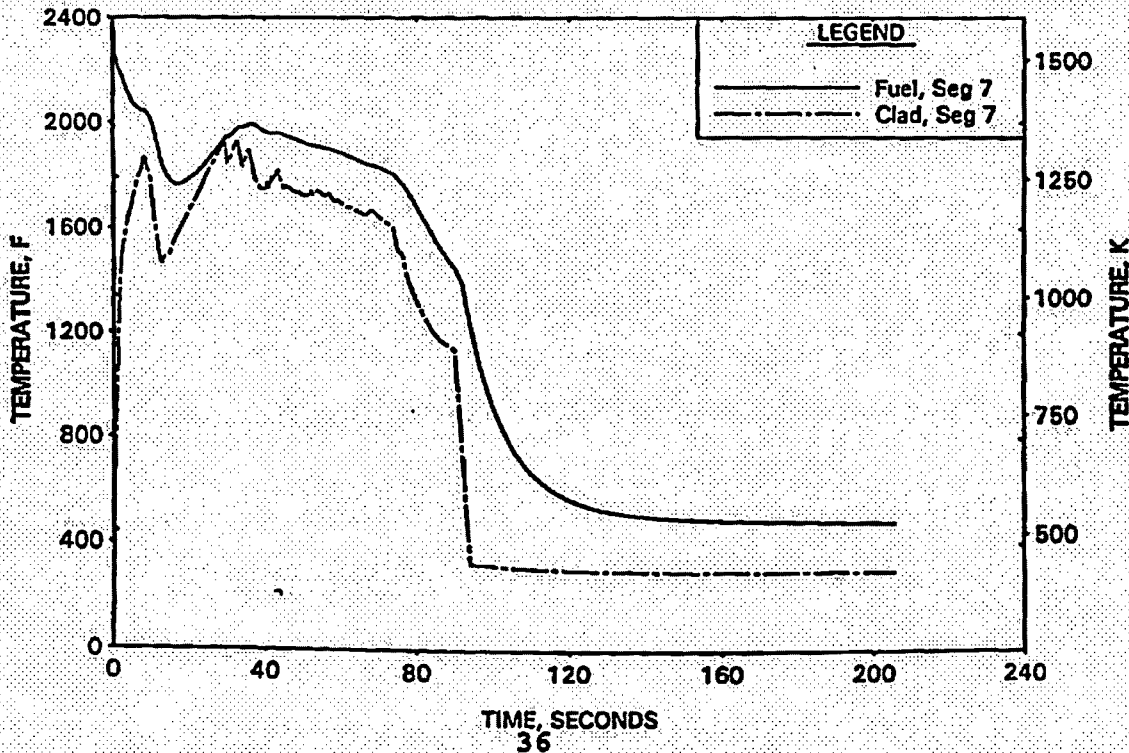
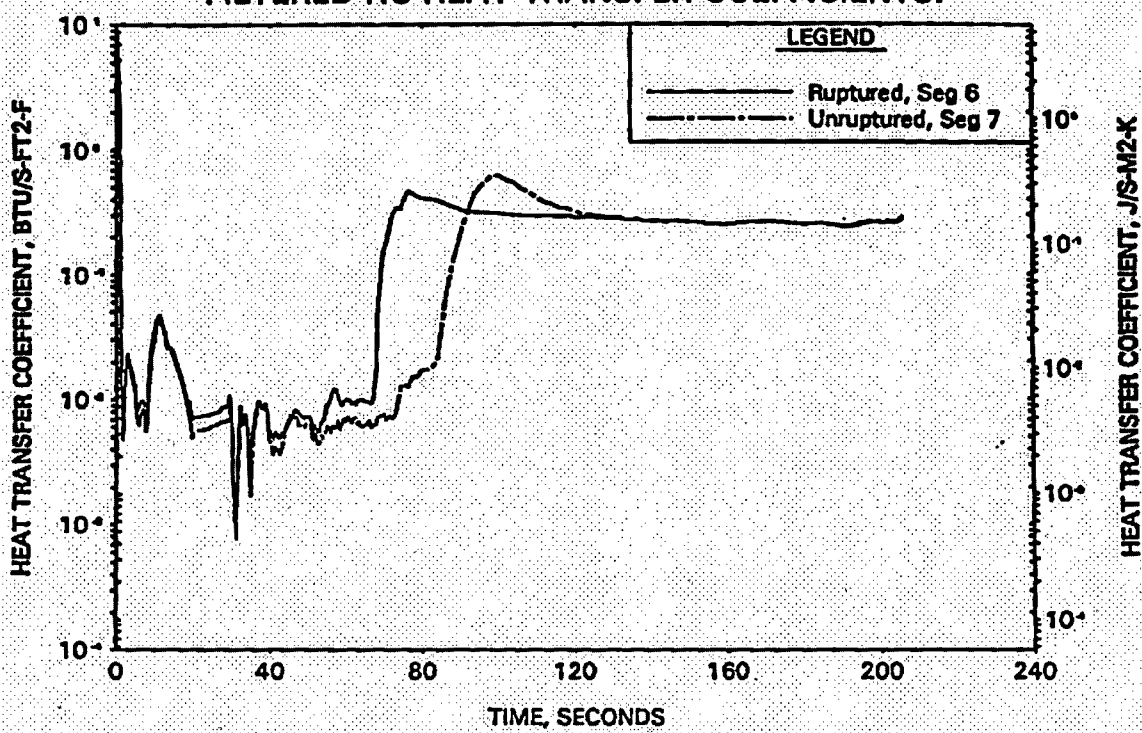
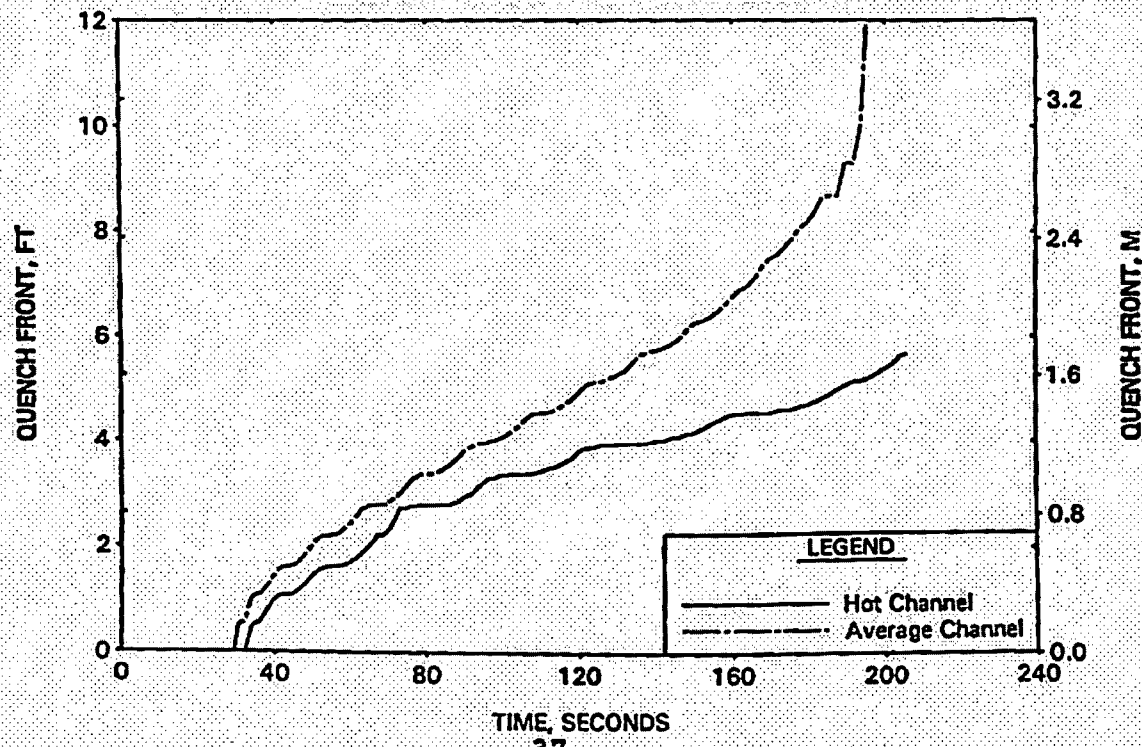


FIGURE 6-8. 2.506-FT, BOL LOCA LIMIT CASE -
FILTERED HC HEAT TRANSFER COEFFICIENTS.FIGURE 6-9. 2.506-FT, BOL LOCA LIMIT CASE -
QUENCH FRONT ADVANCEMENT.

This page is intentionally left blank.



UNITED STATES
NUCLEAR REGULATORY COMMISSION

WASHINGTON, D.C. 20585-0001

February 18, 1997

Mr. J. H. Taylor, Manager
Licensing Services
Framatome Technologies Incorporated
3315 Old Forrest Road
PO Box 10935
Lynchburg, VA 24506-2000

SUBJECT: ACCEPTANCE FOR REFERENCING OF TOPICAL REPORT BAW-10192-P,
"BWNT LOSS-OF-COOLANT ACCIDENT EVALUATION MODEL FOR ONCE-THROUGH
STEAM GENERATOR PLANTS" (TAC NO. M89400)

Dear Mr. Taylor:

We have reviewed the subject topical report of February 1994 and your response of May 6, 1996, to our requests for additional information. On the basis of our review, we conclude that BAW-10192-P is acceptable for referencing in licensing applications in the analysis of loss-of-coolant (LOCA) accidents for once-through steam generator plants. Scientech, Inc., was the staff's consultant in the technical evaluation. The enclosed safety evaluation, gives the basis for and limitations of our approval. The Scientech technical evaluation report is also enclosed.

We will not repeat our review of the matters described in the report and found acceptable when the report appears as a reference in license applications, except to ensure that the material presented applies to the specific plant involved. Acceptance by the Nuclear Regulatory Commission applies only to the matters described in the report. In accordance with procedures established in NUREG 0390, Framatome Technologies, Inc., (previously known as Babcock and Wilcox Nuclear Technologies (BWNT)), should publish accepted versions of this topical report, proprietary and nonproprietary, within 3 months of receipt of this letter. The accepted versions shall include an "-A" (designated accepted) after the report identification symbol.

Should our acceptance criteria or regulations change so that our conclusions as to the acceptability of the report are no longer valid, applicants referencing this topical report will be expected either to revise and resubmit their documentation or to submit justification for the continued applicability of the topical report.

Sincerely,

A handwritten signature in black ink, appearing to read "J. E. Lyons".

James E. Lyons, Acting Chief
Reactor Systems Branch
Division of Systems Safety and Analysis
Office of Nuclear Reactor Regulation

Enclosures: BAW-10192-P:

- Safety Evaluation
- Technical Evaluation Report
(IA-141)

This page is intentionally left blank.

ENCLOSURE 1

SAFETY EVALUATION BY THE OFFICE OF NUCLEAR REACTOR REGULATION
BAW-10192P, REVISION 0, LOSS OF COOLANT ACCIDENT EVALUATION MODEL
FOR ONCE-THROUGH STEAM GENERATOR PLANTS

1 INTRODUCTION

Framatome Technologies, Inc. (FTI), previously known as Babcock and Wilcox Nuclear Technologies (BWNT), submitted Volumes I and II of BAW-10192P, which document generic large and small break loss-of-coolant accident evaluation models, respectively. These reports provide a description of the FTI large and small break LOCA methodology and present the results of benchmarks to demonstrate the methodology. The methodology was reviewed based on the requirements of 10 CFR 50, Appendix K and 10 CFR 50.46 (Reference 1).

The subject topical report describes a methodology which uses a different complement of computer codes than previously approved models for once-through steam generator (OTSG) plants. Currently approved large (Reference 2) and small break (Reference 3) methods for OTSG plants are based upon the CRAFT2 code. The currently approved large break methodology also uses the REFLOD3B and THETA1-B codes. Only the REFLOD3B code is used as a part of the methodology described in this topical report, which is based primarily on the RELAP5/MOD2-B&W code (Reference 4). The BEACH code is also used for the large break analysis. Large and small break ECCS evaluation models for recirculating steam generator (RSG) plants (Reference 5), which use the same suite of codes as the subject methodology, are in use by FTI. These evaluation models have previously received regulatory approval.

This safety evaluation presents the results of an evaluation of the FTI methodology for the large and small break LOCA. Other FTI reports were extensively used in the review as background information. These reports include BAW-10168PA (Reference 5), BAW-10104PA (Reference 2), and BAW-10154A (Reference 3).

Requests for additional information (RAI) were sent to FTI. FTI's responses (which will be included in Volume III of BAW-10192P) were reviewed and evaluated as an integral part of the topical report review process (Reference 6). Responses to the more significant issues raised in the RAI are discussed and evaluated in this report. Any RAI question referenced in the report has a prefix RAI-LB or RAI-SB preceding the question number, denoting whether the question pertains to the large break or small break LOCA. FTI also provided written responses to four questions raised during the Nuclear Regulatory Commission (NRC) management review. Responses to these questions are referenced with the prefix RAI-MR.

FTI also provided an application of the methodology to comply with the requirements of the "Maine Yankee Lessons Learned" (Reference 13). Evaluation of this application is in Section 6 of this review.

2 SUMMARY OF THE LARGE BREAK LOCA ANALYSIS METHODS, BAW-10192P, VOLUME I

Volume I of BAW-10192 presents the generic large break LOCA methodology to be used by FTI for evaluating the performance of the emergency core cooling systems (ECCS's) following a large break LOCA for all classes of B&W-designed plants. The report describes the methods used for large break LOCA analysis and demonstrates the capability of the models through a series of benchmarks. The FTI report also discusses compliance with Appendix K to 10 CFR Part 50 and 10 CFR 50.46.

The FTI methodology for large break LOCA analysis utilizes the RELAP5/MOD2-B&W, REFL0D3B, BEACH, and CONTEMPT computer programs. Revision 3 of the RELAP5/MOD2-B&W code (Reference 4), which is based on the RELAP5/MOD2 code (Reference 7) developed by the Idaho National Engineering Laboratory, was approved for use in the analysis of both large break and small break LOCAs for both

once-through and recirculating steam generator plants. The RELAP5/MOD2 B&W program is used to predict system thermal hydraulics, core power generation, and clad temperature response during blowdown. The REFL0D3B (Reference 8) program is used to determine the length of the vessel refill period and the core flooding rate during reflood. The BEACH (Reference 9) program uses input from REFL0D3B to determine the clad temperature response during the reflood period. The BEACH program has been reviewed and approved for use in LOCA reflood analysis, as has REFL0D3B. The CONTEMPT (Reference 10) code is used if containment response calculations are required. Since the computer models used by FTI have been previously reviewed and approved by the NRC, this evaluation focuses on the techniques and assumptions used in developing a model and evaluating ECCS performance during a LOCA. FTI had previously used the CRAFT2 (Ref. 11) computer code for OTSG plant ECCS evaluation model calculations. The benchmarks that have been performed to demonstrate the large break LOCA methodology are discussed in BAW-10192P, Volume 1 which includes sensitivity studies for the RELAP5/MOD2-B&W, REFL0D3B, and BEACH computer codes. An evaluation of each sensitivity study is presented in Section 3 of this report. The base case for large breaks in the FTI LOCA methodology is a double-ended guillotine rupture of the cold leg pump discharge (CLPD) pipe. This is also the peak clad temperature (PCT) limiting case as determined by a break spectrum study.

A transition break methodology has been developed to analyze hot leg breaks and cold leg breaks in the range 0.75 ft^2 to 2.0 ft^2 . For small breaks the core flow remains upward, the lower plenum does not void, and reflood begins at the end of blowdown, so there is no refill period. Transition breaks include all hot leg breaks and the range of cold leg break sizes between those exhibiting this typical small break behavior ($\leq 0.75 \text{ ft}^2$) and those exhibiting typical large break behavior ($\geq 2.0 \text{ ft}^2$). Because the behavior for small and large breaks is quite different, the large and small break methods do not overlap for any break sizes. FTI developed the transition methodology in order to provide an accurate representation of the physical phenomena occurring for these breaks. Results show a continuous variation of PCT as a function of cold leg break size.

The transition break methodology differs from the full large break LOCA methodology in several respects:

1. Bypass flow is calculated using the RELAP5/MOD2-B&W computer code rather than a nonmechanistic model.
2. The REFL0D3 code is not used; rather the entire transient is analyzed using the RELAP5/MOD2-B&W and BEACH codes. Since no adjustment of lower plenum inventory is necessary, a single code is used.
3. The nonhomogeneous flow model is used for core junctions.

Noding for the transition breaks is the same as for large breaks. There are three classes of B&W designed plants to which the large break LOCA methodology will be applied. Most domestic operating plants are of the lowered loop design with 15 x 15 fuel bundles and eight reactor vessel vent valves (RVVV). A second class of plants has a raised loop design, with the same fuel type, and four RVVVs. This class of plants also differs from the others by virtue of its low head high pressure injection (HPI) system. There is a third design with 17 x 17 fuel, raised loop and eight RVVVs. Differences between the classes of plants are handled by changing the noding schemes in the computer codes used.

3 EVALUATION OF THE LARGE BREAK LOCA ANALYSIS METHODS, BAW-10192P, VOLUME I

This section discusses the review of the FTI large break LOCA methodology, including the modeling features and sensitivity studies performed to select the base case, time step size, nodalization, and other modeling options. The large break model, including the modifications for transition break sizes, was determined to comply with the requirements of Appendix K to 10 CFR Part 50. The sequence of events for a large break LOCA is relatively well known and the OTSG plant response is similar to that of other PWRs during blowdown and refill, so there is no need to repeat this information. The only significant difference in the OTSG plants is the RVVVs, which act to reduce steam binding during reflood. This review emphasized areas in which the OTSG plants differ from the recirculating steam generator plants, for which the methodology has already been approved.

3.1 Base Case Selection

The double-ended guillotine break in the cold leg pump discharge was the most limiting break, and was therefore selected as the base case. The sample analysis was performed for the 205 FA plant with 17 x 17 fuel and raised loops. The base case selected, namely a double-ended guillotine break in the cold leg on a 205 FA plant, is acceptable for demonstrating model sensitivities and convergence. Analyses must still be performed for each plant type to demonstrate compliance with 10 CFR 50.46 acceptance criteria.

For B&W-designed plants, the RVVVs provide the primary path for the steam to reach the break. When the loop seal clears, a second path for the steam to reach the break is opened. FTI has demonstrated the ability of the RELAP5/MOD2-B&W code to predict loop seal clearing by comparing to experimental data from the ROSA large scale test facility and from the Semiscale MOD1 facility. Appendices G and J of Reference 5 contain the benchmarks to ROSA small break LOCA test SB-CL-18. The base case model is a

raised loop plant, which has the loop seal at a higher elevation than a lowered loop plant. The benchmarks indicate that RELAP5/MOD2-B&W is generally capable of predicting loop seal clearing. FTI should include any noding changes necessary to adequately model loop seal clearing in the lowered loop plant model.

The possibility that a loop seal could clear initially and then refill was addressed in the FTI response to RAI-MR Question 3. Although unlikely, this possibility cannot be completely ruled out for all event scenarios.

Therefore, for each plant type where credit is taken for steam flow through the open loop seal, FTI is required to run the RELAP5/MOD2-B&W system model until whole-core quench, to confirm that the loop seal does not refill.

3.2 Time Step Sensitivity Studies

Separate time step convergence studies were performed for the blowdown and reflood portions of the base case event. FTI refers to the time step sensitivity for the blowdown period as the RELAP5/MOD2-B&W time step study and to the reflood period study as the BEACH time step sensitivity. For the RELAP5/MOD2-B&W time step study, the maximum time step size was decreased by a significant amount and there was no significant change in the calculated response, indicating convergence. The final BEACH time step convergence study was performed in response to RAI-LB Question 16. To achieve acceptable convergence, FTI changed the manner of calculating core inlet subcooling, a boundary condition for BEACH determined from REFL0D3B results. Rather than changing the core inlet temperature from saturation to the REFL0D3B-calculated lower plenum volume average temperature, which is significantly subcooled, FTI modified the calculation procedure to ramp the inlet temperature. FTI calculates a mixed mean temperature at bottom of core recovery (BOCR) based on a smaller mixing volume below the uppermost hole in the flow distribution plate. The core inlet temperature used in BEACH is held at this value for 1 second following BOCR and then ramped to the REFL0D3B-calculated value over a period of up to 5 seconds. The ramp time is calculated to be the time required for the temperature interface to travel from the top of the flow distribution plate to the heated core inlet. Experimental data from the Upper Plenum Test Facility (UPTF) and Slab Core Test Facility (SCTF) test programs were used to guide and justify the modeling changes. Since the base model was changed, FTI reconsidered the time step sensitivity studies run with the previous base model. Runs were made with both significantly increased and significantly decreased maximum time step sizes, and the results were essentially the same, demonstrating that the solution is converged.

There was very little difference in calculated fuel clad temperatures with the revised inlet subcooling model. The PCT was only slightly increased using the revised method, which exhibits significantly improved time step convergence. Basically, this revision smooths a discontinuity in a conservative manner and improves calculational stability. FTI considered the potential effect of this change on previously completed sensitivity studies and determined that the conclusions of those studies would not be affected. This observation is reasonable, given the insignificant effect of the change on the values of the key calculational result, namely peak clad temperature.

3.3 Pressurizer Location Study

The base case assumes that the pressurizer is connected to the intact loop hot leg. A sensitivity study was performed with the pressurizer surge line connected to the broken loop hot leg. Only the blowdown portion of the event was simulated, since the pressurizer is emptied and hence does not play a significant role later in the event. The peak clad temperature (PCT) at end of blowdown was lower and more liquid remained in the lower plenum, i.e., results were less conservative. Therefore, the base model retains the pressurizer on the intact loop.

3.4 Break Area Noding Sensitivity Study

Past experience with RELAP5 has indicated that noding detail in the vicinity of the break can affect results. Therefore, FTI performed a sensitivity study to demonstrate that the noding used in the base model is adequate for predicting break flow. An additional node was used at each end of the pipe at the break location. The case was run for the blowdown only, since this is the period when more detailed modeling of break flow may be important. Only small differences in results were found with the more detailed nodalization, thus demonstrating convergence of the base model.

3.5 Core Cross Flow Sensitivity Study

Section I.C.7.a of Appendix K to 10 CFR Part 50 requires that the effect of cross flow in the core be considered. To determine appropriate values to use for cross flow resistance, FTI first estimated a value based upon the core geometry and then performed a sensitivity study to establish the effect of varying the cross flow resistance on calculated PCT. Only small effects were seen for rather large variations in assumed cross flow resistance. Increasing cross flow resistance was shown to be conservative. However, this increased PCT by causing departure from nucleate boiling (DNB) to be calculated earlier. Early calculation of DNB is known to be one of the more significant conservatisms in the evaluation model, so additional conservatism in this area is not needed. Appendix K to 10 CFR Part 50 requires only that the effects of cross flow be modeled realistically. FTI has used a realistic model for cross flow and has shown that the results vary only slightly with changes in cross flow resistance. Therefore, use of the nominal estimated cross flow resistance is acceptable.

3.6 Core Noding Study

In addition to the cross flow resistance sensitivity, FTI considered radial core nodalization and its effect on cross flow. An additional parallel channel, referred to by FTI as the middle channel, was added to represent the eight fuel bundles surrounding the hot bundle. The radial peaking factor for these eight bundles was varied to determine the effect on calculated fuel and clad temperatures. A wide range of radial peaking factors covering the spectrum of possibilities was considered. The effect on fuel and clad temperatures at the end of blowdown was shown to be small. As with the cross flow sensitivity study, the various radial peaking factors influenced fuel temperatures by slightly changing the time of DNB, which is predicted to occur

early. There is no need to select a case which predicts the earliest DNB, since all of the cases predict DNB much earlier than expected. In response to RAI-LB Question 14, FTI provided evidence that the base model predicts more conservative temperatures than one using best estimate cross flow resistance and radial peaking factor. These extensive sensitivity studies demonstrate that the FTI model adequately addresses the effect of cross flow in the core region.

3.7 Pump Degradation Study

In addition to the base model, two different pump two-phase degradation models were tested in a sensitivity study. A curve referred to by FTI as the M1 curve yielded more conservative results and was incorporated into a revised base model. Use of this more conservative model is acceptable.

3.8 Pump Power Study

For ECCS evaluation calculations, a loss of off-site power is assumed concurrent with the LOCA. The main coolant pumps will then be unpowered and will coast down. FTI demonstrated that this assumption is conservative by running the pumps powered case and showing that it yields lower fuel and clad temperatures.

3.9 ECCS Bypass Study

Initially, FTI used a mechanistic ECCS bypass model for the large break. That is, the flow of ECCS to the break was calculated using RELAP5/MOD2-B&W. A sensitivity study was performed using a nonmechanistic model, which removed all ECCS liquid injected prior to the calculated end of bypass. It was determined that the amount of liquid calculated to be resident in the lower plenum at end of blowdown was virtually identical for the two methods. FTI used the nonmechanistic model in its base methodology and all subsequent large break sensitivity studies (See RAI-LB Question 4). Therefore, only the nonmechanistic model is acceptable for large break calculations. The nonmechanistic model has the advantage of producing less calculated oscillatory behavior.

In the nonmechanistic model both a partial end of bypass and an end of bypass are calculated. Appendix K, Section I.C.1.c. does not prescribe how end of bypass is to be calculated. It lists two acceptable methods, but does not limit the definitions to these methods. The partial end of bypass model has been developed based upon relevant Upper Plenum Test Facility (UPTF) data. It satisfies Appendix K requirements for modeling end of bypass.

The transition methodology uses a mechanistic model for predicting bypass flow. Since Appendix K requirements for bypass flow modeling apply only for cold leg breaks, this approach is acceptable for hot leg breaks. For cold leg breaks less than 2.0 ft² (that is, those analyzed with the transition methodology), the mechanistic model is also used. FTI showed that for the 2.0 ft² cold leg break, the mechanistic model underpredicts the lower plenum inventory at the time of PCT, compared to the large break model which uses the nonmechanistic bypass model. On the basis of this comparison and the small

break LOCA benchmarking of the RELAP5/MOD2-B&W code against LOFT Experiment L3-5 reported in Reference 5, the mechanistic model is acceptable for transition breaks.

3.10 REFL0D3B Loop Noding Sensitivity Study

As part of the sensitivity studies performed for REFL0D3B, a loop nodding study was performed by doubling the number of nodes in the loops in the REFL0D3B model and comparing the results to the base model results. FTI compares key results for the core inlet flooding rate, core and downcomer water levels, and carryout rate fraction and found little difference, indicating convergence of the base model.

3.11 REFL0D3B Pump Resistance Sensitivity Study

A locked rotor is assumed in the base REFL0D3B model. To demonstrate that this assumption is conservative, FTI computed form loss coefficients for the pump which correspond to the free-spinning impeller condition. The pump pressure drop formulation in RELAP5/MOD2-B&W was used to determine a loss coefficient for the free-spinning rotor condition. The results show that the free-spinning impeller case results in a higher core flooding rate because of a reduction of steam binding in the upper plenum. Thus the locked rotor assumption is conservative and appropriate for the base model.

3.12 BEACH Axial Fuel Segmentation Study

FTI performed a study to determine the sensitivity of the PCT to a change in the maximum number of axial rezoning segments used in the BEACH analysis. The fine mesh rezoning feature in BEACH adjusts the number of axial mesh points to be used in each heat structure based on user input and criteria programmed into the code. The base case utilizes eight fine mesh rezoning increments. Sensitivity cases with 16 and 32 fine mesh zoning increments were run. The BEACH results for peak clad temperature and average oxidation increase in the hot and average channels are similar, indicating that the base model is converged.

3.13 Axial Versus Radial Core Peaking Factor Study

Section I.A of Appendix K to 10 CFR Part 50 requires that "a range of power distribution shapes and peaking factors representing power distributions that may occur over the core lifetime shall be studied and the one selected should be that which results in the most severe calculated consequences, for the spectrum of postulated breaks and single failures analyzed." FTI performed the axial versus radial core peaking factor study to determine whether significant variations in peak clad temperature or whole-core hydrogen generation would result from different combinations of the radial and axial peaking factors. In this sensitivity study, results for axial peaking factors of 1.6 and 1.8 are generated and compared to the base case, which employs a factor of 1.7. In both cases, the radial peaking factor is adjusted to conserve the peak linear heat generation rate. Both cases produced an increase in the PCT of less than 50 °F.

In response to RAI-MR1 and RAI-MR4, FTI provided a detailed explanation of how the axial and radial peaking factors for the LOCA analysis are determined. The set of power distributions which can actually be achieved is established by a maneuvering analysis which includes non-LOCA imposed limitations. Over most of the range of power distributions, the limitations imposed by the maneuvering analysis are considerably tighter than those imposed by the LOCA linear heat generation rate (LHGR) limit. For certain ranges of the power distribution, in particular core inlet skewed peaks, the margin between the maneuvering analysis limitations and the LOCA limitations, approaches a minimum. For these power distributions the axial and radial peaking factors are approximately equal. Therefore, FTI uses a 1.7 axial peaking factor and sets the radial peaking to reach the LHGR limit.

For the limiting break, five different axial offsets (axial location of the power peak) are then run at both beginning of life (BOL) and middle of life (MOL) conditions, in addition to one end of life (EOL) case to show that MOL conditions bounds EOL conditions. These cases establish the LOCA limit. The cases to be considered are selected from among the infinite number of possibilities to lower the distribution of power shapes which are achievable based upon the constraints imposed by the maneuvering analysis. The cases analyzed are those covering a range of conditions where the margin between the maneuvering analysis limitations and the LOCA limitations are at a minimum. Therefore, use of an axial peaking factor of 1.7 is appropriate as the base case for sensitivity studies in this report. If the maneuvering analysis for a new fuel type or application indicates that the minimum margins occur for power distributions other than those analyzed in this topical report, the axial peaking factor used should be adjusted so that the cases analyzed remain in the range of the minimum margin.

3.14 Break Spectrum Study

To satisfy the requirements of Appendix K to 10 CFR Part 50, a spectrum of 12 large breaks was analyzed, including double-ended breaks located in the hot leg and cold leg pump suction, and split breaks at various locations and of various sizes. The spectrum of breaks considered by FTI in this demonstration is sufficiently inclusive to be used for specific applications of the methodology. The LOCA spectrum results are reviewed in the following sections.

3.14.1 CLPD Guillotine Breaks

For the cold leg pump discharge (CLPD) double-ended guillotine break, discharge coefficients of 1.0, 0.8, 0.6, and 0.4 were analyzed. The results show that the maximum temperature is predicted for a discharge coefficient of 1.0 and that peak clad temperature decreases with decreasing discharge coefficient (or break size). FTI attributes this trend to increases in core upflow during the early phases of blowdown, increased core flooding rate due to lower pin temperatures, and decreased refill time due to earlier end of bypass predictions. In all cases, the temperature is below the 2200 °F temperature limit in 10 CFR 50.46. The results presented by FTI show that the base case, which is a double-ended guillotine break with a discharge coefficient of 1.0, will produce the most limiting results.

3.14.2 CLPD Split Breaks

In the large break LOCA (LBLOCA) spectrum study, several break scenarios involving a split break in the pump discharge piping were analyzed. A split break with an area double the discharge pipe cross sectional area was analyzed using the LBLOCA methodology. An analysis was performed for a 2 ft² split break using both the LBLOCA and transition methodologies. The transition break methodology was used to analyze additional cases involving split breaks with areas of 1.5, 1.0, and 0.75 ft². The CLPD double area split break resulted in lower cladding temperatures than in the base case, which is attributed to predictions of higher core downflow during the later portion of the blowdown phase.

Analysis of the 2 ft² split break using both the base LBLOCA and transition methodologies showed the overlap of the transition LOCA methodology with the large break methodology. FTI presented comparative results using the two methods and noted that the results from the LBLOCA and transition LOCA methodology match well. There is some difference in the collapsed liquid level later in the transient. FTI attributes this to the higher refill rate predicted by the transition methodology than in the LBLOCA methodology. In both cases, the peak clad temperature is predicted to be lower than the base case.

The transition methodology results for the 1.5, 1.0, and 0.75 ft² split breaks show the expected trends in pressure and break mass flow behavior. The peak clad temperature decreases with decreasing break size. FTI notes that the RVEVs pass all of the core steam production to the break for the 1 ft² and 0.75 ft² breaks. Total core dryout was not predicted in these cases. In the case of the 1.5 ft² break, FTI noted that the RVEVs were unable to handle the flow to the break. The lower plenum cleared of liquid in this case, resulting in an additional path for steam venting. Core quenching occurred at approximately the same time for all three cases. In all cases, the peak clad temperature is predicted to be lower than in the base case.

3.14.3 CLPS Break

Analysis of a double-ended guillotine break in the pump suction piping with a discharge coefficient of 1.0 resulted in a lower peak clad temperature prediction than in the base case. FTI attributes this to retention of a significant amount of ECC water during blowdown, which shortened the adiabatic heatup period. Break flow rate is also lower than in the base case because of increased pump resistance due to the changed break location.

3.14.4 Hot Leg Break

The double-ended guillotine break in the hot leg with a discharge coefficient of 1.0 resulted in a lower peak clad temperature than in the base case. FTI attributes this to the mostly positive flow through the core, enhancing core heat transfer. Also, the lower plenum was not predicted to empty during the event, resulting in a shortened adiabatic heatup period.

3.15 Time in Life Study

LOCA limits must be determined by a specific application of the methodology described in this report. The purpose of the analysis described in this section is to provide a demonstration of the methodology to be used. Calculations were performed at four times in life using the full model, i.e., RELAP5/MOD2-B&W, REFLOD-3B and BEACH, along with TACO3 for fuel rod initial conditions. The event selected for analysis was the base case double-ended CLPD break with a center peaked axial power shape.

The demonstration established that BOL conditions should be used in the average channel while burnup is advanced in the hot channel. Based upon the demonstration calculation, it is expected that the linear heat rate will be maintained out to approximately 45,000 MWD/MTU, after which it will need to be decreased. While more than four burnup points will generally be needed for specific applications, the methodology presented in this section adequately demonstrates the approach for determining time-in-life limits.

3.16 Three Operating RC Pumps at Seventy-Five Percent Full Power Study

The purpose of this analysis is to demonstrate that the LOCA limits for four pump operation will cover three pump operation at the 75 percent power level. Since LOCA limits can only be established by a specific application, it follows that limits for three pump operation can also only be established by a specific application. In such an application, the factor of 1.02 will need to be applied to the power to satisfy the requirements of Appendix K to 10 CFR Part 50. To justify operation at 75 percent power will require that the analysis be performed at $75 \times 1.02 = 76.5$ percent power. Depending upon the status of the inoperable pump, it may also be necessary to consider cases in addition to the locked rotor.

3.17 LOCA Limit Demonstration Cases

A demonstration calculation for LOCA limits determination was performed to illustrate the FTI approach. The base CLPD break was simulated with various axial power shapes. In an actual application of the complete methodology, calculations will be performed with the peak power location assumed to occur at five different elevations in the core. For this demonstration calculations were performed with the axial peak of 1.7 at three different locations, and the radial peaking factor was set to obtain the maximum LHGR. In an actual application, five different axial peak locations will be analyzed at BOL and MOL conditions, in addition to one case at EOL to demonstrate that MOL is more limiting. The general approach is acceptable for demonstrating the LOCA limits methodology. However, for a new fuel type or application FTI should demonstrate that the minimum LOCA margins occur for the range of power distributions analyzed.

3.18 Minimum/Maximum ECCS Injection Study

The base case has minimum pumped ECCS injection in the REFLOD3B calculations together with a containment back pressure based upon maximum ECCS pumped injection. Pumped ECCS injection does not occur during the blowdown so

RELAP5/MOD2 calculations are not affected. To determine whether the base case is conservative, two additional cases were run with minimum ECCS injection and maximum ECCS injection in both the REFL0D3B and containment calculations. The maximum ECCS case proved to be the most conservative, although by a very small amount: 32 °F increase in PCT compared to the base case and 35 °F greater than the minimum ECCS case. These calculations showed that it will be necessary to perform this sensitivity study for each specific application to determine the limiting case. The procedure used to perform the sensitivity study is acceptable. Also, the difference in PCT compared to the base case is small enough that sensitivity studies performed with the base case model are acceptable.

4 SUMMARY OF THE SMALL BREAK LOCA ANALYSIS METHODS, BAW-10192P, VOLUME II

Volume II of BAW-10192 presents the generic small break LOCA methodology to be used by FTI for evaluating the performance of the emergency core cooling systems following a small break LOCA for all classes of B&W-designed plants. The report describes the methods used for small break LOCA analysis and demonstrates the capability of the models through a series of benchmarks. The FTI report also discusses compliance with Appendix K to 10 CFR Part 50 and 10 CFR 50.46.

The FTI methodology for small break LOCA analysis utilizes the RELAP5/MOD2-B&W computer code. As noted in Section 2 the RELAP5/MOD2-B&W computer code, which is based on the RELAP5/MOD2 code, was approved for use in the analysis of both large break and small break LOCAs for both once-through and recirculating steam generator plants. The RELAP5/MOD2 B&W program is used to predict system thermal hydraulics, the average core and hot channel void distributions, and the hot and average core cladding temperature response for the entire transient.

The benchmarks that have been performed to demonstrate the small break LOCA methodology are discussed in BAW-10192P, Volume II, which includes sensitivity studies for relevant parameters for the RELAP5/MOD2 B&W computer code. An evaluation of each sensitivity study is presented in Section 5 of this report. The base case chosen for small break sensitivity studies was a 0.1 ft² break at the bottom of the cold leg pump discharge pipe.

The three classes of B&W designed plants to which the small break LOCA methodology will be applied are discussed in Section 3. Differences between the classes of plants are handled by changing the noding schemes in the computer codes used.

5 EVALUATION OF THE SMALL BREAK LOCA ANALYSIS METHODS, BAW-10192P, VOLUME II

The small break ECCS evaluation methodology described in Volume II of BAW-10192P was reviewed to determine compliance with the requirements of Appendix K to 10 CFR Part 50. Based upon this review, the methodology was determined to be in compliance with Appendix K requirements as they apply for small break loss-of-coolant accidents.

This section discusses the methodology used for the small break and the sensitivity studies performed to support the methodology.

5.1 Base Model Selection

A preliminary break spectrum analysis, combined with the results from previously approved evaluation models, was used to select the initial base case for the sensitivity studies. The choice was confirmed by a final break spectrum analysis. Initially a 0.1 ft^2 break in the bottom of the cold leg pump discharge leg was selected as the base case. The analyses were all performed for the 205 FA plant with 17×17 fuel and raised loops. Axial power shape for the base case was selected as a 1.7 peaking factor at the 9.705 ft elevation and a peak LHGR of 16.5 kW/ft. All of the sensitivity studies were performed by varying selected portions of this base model.

To assure that a heatup of the fuel was predicted, it was necessary for FTI to introduce more conservatism into the calculations than normally required for a design basis analysis. The core flood tank (CFT) pressure was reduced from 615 psia to 515 psia to artificially delay coolant flow from the CFTs. If this conservatism is not introduced, no fuel heatup is predicted for the small break LOCA, and convergence effects on the key fuel temperature result cannot be evaluated. For purposes of demonstrating sensitivities and convergence, this approach is acceptable since it is conservative. Following completion of the sensitivity studies, a final base case was run which incorporated changes made as a result of the sensitivity studies.

The definition of the base case using the 0.1 ft^2 break in the bottom of the cold leg in a 205 FA plant is acceptable for demonstrating model sensitivities and convergence. In the RELAP5 code, break flow area (A) and discharge coefficient (C_d) are equivalent multiplicative factors in the break flow calculation. That is, the calculated mass flux is multiplied by $C_d A$ to get the mass flow rate. Separate values of the discharge coefficient can be input for subcooled, two-phase, and superheated conditions at the break inlet. During the course of the sensitivity studies, the break discharge coefficient for void fractions greater than 70 percent was changed from 0.7 to 1.0. This results in a redefinition of the base case so that the break area with the revised discharge coefficient corresponds to a 0.07 ft^2 break. Sensitivity studies performed with the discharge coefficient of 0.7 remain valid since the characteristics of the responses such as convergence and the relative differences in key parameter values are not expected to change appreciably with this small difference in break size.

5.2 Time Step Sensitivity Studies

FTI ran the base case with maximum time steps of .01, .02 and .025 seconds. As indicated in RAI-SB Question 17 on Volume II, the cases with 0.01 and 0.02 maximum time step size had different core mixture level and quench time. FTI correctly points out in its response that there is good agreement in the key predictions of PCT and minimum core mixture level. FTI attributes differences in core mixture level and quench time to variations in the predicted break flow after PCT occurs. For purposes of calculating PCT, FTI has demonstrated convergence in this case.

5.3 Pressurizer Location Study

A sensitivity study was performed starting with the base case small break event, but relocating the break to the loop with the pressurizer attached. The differences were small (18 °F lower PCT) for the sensitivity run. Therefore, the base case was not modified and the pressurizer remains connected to the intact loop.

5.4 Core Cross Flow Sensitivity Study

Section I.C.7.a of Appendix K to 10 CFR Part 50 requires that "the hot channel shall not be greater than the size of one fuel assembly." The hot channel in the small break RELAP5 model consists of 12 fuel bundles in a 3 x 4 rectangular array. FTI states that 5 to 10 percent of the fuel bundles have a radial peaking factor similar to that of the hot bundle. To satisfy Appendix K to 10 CFR Part 50, it must be assumed that all 12 bundles in the hot channel have the same radial peaking factor as the hottest bundle in the core. Since the RELAP5/MOD2 B&W calculation also provides the hot pin results, the peaking factor is actually that of the hottest fuel pin. In this case, the results using the 12 fuel bundle model will be more conservative than those for a single bundle hot channel, since there will be less cross flow. This is an acceptable model since it reduces the hot channel to average channel cross flow area compared to a single bundle hot channel. On a per bundle basis, the area for cross flow is reduced when a larger number of bundles is included in the hot channel.

FTI performed a sensitivity study on the effect of cross flow resistance between the 3 x 4 hot channel and the average core. Three different distributions of resistances were considered in addition to the base case. These cases covered a range of resistance values greater than would be expected to occur. The base case produced the highest value of PCT. In the upper part of the core where the PCT will occur, the base case uses a high value for resistance to flow from the average into the hot channel, and a low value of resistance for flow out of the hot and into the average channel. Hence it is relatively difficult for water to enter from the cooler average channel into the hot channel when the pressure difference would allow flow in this direction. At the same time, when the pressure gradient permits it is easy for steam to leave the hot channel, decreasing in steam velocity and becoming cooler. This is the most likely reason why the base case produced more conservative results than cases with both larger and smaller cross flow resistance.

Appendix K to 10 CFR Part 50 requires that the effect of cross flow in the core be considered. The model used by FTI for cross flow resistance gives more conservative PCT predictions than models with either larger or smaller cross flow resistances. Use of the base model is acceptable since it produces results which bound those of a wide range of cross flow models.

5.5 Core Noding Sensitivity Study

A sensitivity study was performed increasing the number of bundles in the hot channel from 12 to 24. There was no significant change in results. This

indicates that the 12 bundle model is acceptable. As discussed in Section 5.4 above, decreasing the number of fuel bundles included in the hot channel will increase the cross flow area per bundle, leading to increased cross flow and less conservative results. Therefore it was not necessary to run a case with a lesser number of fuel bundles in the hot channel.

5.6 CFT Line Resistance Sensitivity Study

The base case has the nominal (best estimate) CFT line resistance increased by a factor of 100. FTI uses this increased CFT line resistance for all small breaks except the CFT line break, where a nominal value of resistance is used. Increased CFT line resistance promotes calculational stability by eliminating predicted wide swings in CFT injection flow.

To demonstrate that use of this increased resistance is acceptable, FTI ran three sensitivity cases. First, the base case 0.1 ft^2 CLPD break was modified to run with nominal CFT line resistance. Predicted PCT was 20°F lower than the base case, indicating that the use of a high CFT line resistance is conservative. This is the expected trend since the higher resistance results in lower CFT flow for a given primary system to CFT pressure drop, and so decreases flow from the CFT, as is further demonstrated by the second and third sensitivity runs, the 1.0 ft^2 CLPD break with nominal and increased CFT line resistance. There was no fuel heatup for these cases so PCT was the same for both runs. The minimum core mixture level was similar, but the nominal resistance case recovered core level more quickly, indicating that the increased resistance case is more conservative.

Use of a CFT line resistance greater than nominal was shown to be conservative. This practice also leads to increased numerical stability, a desirable outcome. Therefore, use of increased CFT line resistance for the spectrum of small breaks is acceptable.

5.7 Break Discharge Coefficient Study

This sensitivity study resulted in a change being made to the small break modeling approach. In the initial studies, a discharge coefficient of 0.7 was used for break volume void fractions greater than 70 percent. Two sensitivity cases were run, one for the 0.1 ft^2 and one for the 0.3 ft^2 CLPD break. For these runs, the discharge coefficient was not changed as a function of break node void fraction. To make the runs comparable, the break size was reduced by a factor of 0.7. In each case, the PCT increased for the revised model with constant discharge coefficient. FTI referenced material which indicated that the Moody model provides relatively accurate predictions of flow at high void fractions, suggesting that the discharge coefficient of 1.0 is a more appropriate description of the actual physical behavior. The constant discharge coefficient of 1.0 was hence adopted for the base model. This is the only acceptable model.

As a result of the change in the break discharge coefficient, the break spectrum study was performed using a discharge coefficient of 1.0 for break volume void fractions greater than 70 percent. Previous sensitivity cases performed with a discharge coefficient of 0.7 remain valid since the

characteristics of the responses such as convergence and the relative differences in key parameter values are not expected to change appreciably with this small difference in break size.

5.8 Break Spectrum Study

The purpose of the break spectrum study is to demonstrate how the limiting break size will be determined in specific applications of the methodology. FTI performed calculations for 12 cold leg pump discharge break sizes between 0.04 ft² and 1.43 ft². These events were divided into three categories based upon the response characteristics: small, intermediate, and large CLPD small break LOCA (SBLOCAs). FTI also analyzed double-ended CFT line and high pressure injection (HPI) line breaks. In a specific application of the methodology, additional cases may need to be run to more accurately predict the limiting small break size, as discussed in Section 5.8.1 below. Also, smaller break sizes down to the range of 0.01 ft² will need to be considered.

5.8.1 CLPD Breaks

To obtain a temperature excursion for small breaks, it was necessary for FTI to artificially lower the CFT fill pressure from 615 psia to 515 psia. FTI felt it was necessary to obtain a temperature excursion in order to demonstrate convergence of the clad temperature prediction, even though no excursion is normally predicted for licensing applications. With this artificial conservatism, there is a break size which yields a maximum calculated PCT. This break size can be characterized as the one which allows the most fluid to drain from the reactor vessel before the pressure drops to the HPI setpoint. In this demonstration application, FTI identified the 0.1 ft² CLPD break as a limiting SBLOCA. PCT for this case was higher than for slightly smaller and slightly larger breaks. In response to RAI-SB Question 19, FTI stated that its methodology for a specific application would identify the break size which yields the local maximum PCT to within an approximately 20 percent variation in break size. One concern with this approach is that for an actual application, a broad sweep through the spectrum may not show any sign of a peak, possibly because the peak is very localized. Because of the different possible behaviors of the local maximum, FTI should justify its choice of break sizes in each application to assure that either there is no local maximum, or the size yielding the maximum local PCT has been found.

Four small CLPD breaks in the intermediate category were also analyzed: 0.15, 0.175, 0.2, and 0.3 ft². None of these break sizes yielded a significant fuel temperature excursion. In an actual application, the local PCT maximum at 0.3 ft² would warrant additional attention.

Breaks analyzed in the large category of small CLPD breaks included 0.4, 0.75, 1.0, and 1.43 ft². The PCTs calculated for these breaks increase with break size and merge with the transition break results in a reasonable fashion. This indicates that the PCT will be more limiting for larger break sizes than those analyzed using the small break methods.

5.8.2 CFT Line Break

A double-ended rupture of the CFT flood line at the reactor vessel nozzle is the initiator for this event. Break flow area is limited to that of the nozzle insert, 0.44 ft^2 , placing this event in the category of a small break. The break location and ECCS availability are different than for other small breaks, since one CFT and one low pressure injection (LPI) are unavailable before the single failure criterion is applied. As for a number of the small CLPD breaks of similar size, no clad temperature excursion was predicted for this event. FTI has correctly included this case in the spectrum of events to be considered and should continue to do so for specific applications of the methodology.

5.8.3 HPI Line Break

This event is initiated by the rupture of the HPI line at the cold leg connection. Break area is 0.02463 ft^2 , which corresponds to the nozzle area without a thermal sleeve insert. As with the CFT line break, no clad temperature excursion is predicted for this case. Nevertheless, due to the reduced ECCS availability, including this event in the break spectrum analysis is appropriate.

6 APPLICATION

The "Maine Yankee Lessons Learned" team made a number of recommendations (not yet issued) regarding procedures and practices in the review and approval of licensee codes to be used for licensing actions. One such recommendation requires that proposed code documentation should include an application for an actual plant classification for which it is intended. Partial (by chapter) applications shown in this submittal were based on a 205 fuel assembly plant proposed to be built which, however, does not exist at this time. The staff requested that the applicant supplement the submittal with an application section dealing with an actual plant category, i.e. 177 fuel assembly raised or lowered loop plant. Reference 13 includes FTI's response for a lowered loop plant.

Important plant parameters and RCS initial conditions are provided along with the modeling and noding arrangements. The submittal (Reference 13) discusses the applicability of the evaluation model and results of plant specific sensitivity studies which identified the size, location and input parameters for the most limiting LOCA to show compliance with 10 CFR 50.46. This was submitted as a sample of the type of sensitivity analyses performed for each plant application.

Plant description covered: the reactor vessel, reactor core and fuel assembly, reactor coolant pumps, steam generators, the pressurizer and the emergency core cooling system. The plant parameters specified the plant operating conditions.

The application inputs and assumptions included the following:

- power level at 102% of the plant rated power

- steam generator tube plugging was assumed at 20% for the broken loop and 10% for the intact
- total RCS flow was estimated for an average tube plugging of 15% and a total core bypass fraction of 7.5%
- the steady state fuel pin parameters were calculated using TACO3, an NRC approved code
- the ECCS were for conditions of the minimum flow assuming a single active failure
- the core average linear heat rate was assumed at 102% of the nominal value
- the moderator density reactivity coefficient was based on beginning of cycle conditions to minimize negative reactivity contributions
- a zero temperature moderator coefficient was used for full power runs
- the cladding rupture model is based on NUREG-0630.

The LOCA evaluation model consists of a number of codes used in the analysis of cladding temperature transients, local cladding oxidation and whole core hydrogen generation. RELAP5/MOD2 calculates the system thermal hydraulics, core power generation and hot-pin thermal response during blowdown. REFL00D3B continues the thermal hydraulic transient to determine refill time reflooding rates. The BEACH code is used to determine the hot pin cladding temperature response during refill and reflood. Finally, the CONTEMPT code is used to provide containment pressure response which is provided as input to the RELAP5 and REFL00D3B calculations.

Generic sensitivity studies applied in this application included time step (RELAP5 and BEACH), pressurizer location, break noding, core crossflow, core noding, pump degradation, bypass, loop noding, locked vs spinning rotor, fuel axial segmentation and axial vs radial peaking factors. Plant specific application sensitivity studies (Oconee and TMI-1) confirmed that the cold leg pump suction loop refill will not occur for raised loop plants and would not reform for lower loop plants before core quench. Five active core power peaks at elevations from 2.506 ft to 9.536 ft of the active core were analyzed with a constant axial peak of 1.7. All power shapes were analyzed for the beginning, the middle, and the end of cycle conditions. The resulting peak clad temperatures are lower than 2050 °F. In addition, the application demonstrated that the solution is stable and converging.

7 CONCLUSIONS AND LIMITATIONS

The Framatome Technologies LOCA methodology, as documented in BAW-10192P, Volumes I through III, has been reviewed and evaluated. Both the large and small break methods, documented in Volumes I and II respectively, have been determined to comply with the requirements of Appendix K to 10 CFR Part 50. The applicant was informed of the following limitations to the application of BAW-10192P and provided a letter of compliance (Reference 12).

Based on the information presented and the responses provided to RAIs, the use of this methodology for reference in licensing applications involving large and small break LOCA analysis for plants with once-through steam generators is acceptable subject to the following conditions:

1. The LOCA methodology should include any NRC restrictions placed on the individual codes used in the evaluation model (EM).
2. The guidelines, code options, and prescribed input specified in Tables 9-1 and 9-2 in both Volume I and Volume II of BAW-10192P should be used in LBLOCA and SBLOCA evaluation model applications, respectively.
3. The limiting linear heat rate for LOCA limits is determined by the power level and the product of the axial and radial peaking factors. An appropriate axial peaking factor for use in determining LOCA limits is one that is representative of the fuel and core design and that may occur over the core lifetime. The radial peaking factor is then set to obtain the limiting linear heat rate. For this demonstration, calculations were performed with the axial peak of 1.7. The general approach is acceptable for demonstrating the LOCA limits methodology. However, as future fuel or core designs evolve, the basic approaches that were used to establish these conclusions may change. FTI must revalidate the acceptability of the evaluation model peaking methods if: (1) significant changes are found in the core elevation at which the minimum core LOCA margin is predicted or (2) the core maneuvering analyses radial and axial peaks that approach the LOCA LHR limits differ appreciably from those used to demonstrate Appendix K compliance.
4. The mechanistic ECCS bypass model is acceptable for cold leg transition (0.75 ft^2 to 2.0 ft^2) and hot leg break calculations. The nonmechanistic ECCS bypass model must be used in the large cold leg break ($\geq 2.0 \text{ ft}^2$) methodology since the demonstration calculations and sensitivities were run with this model.
5. Time-in-life LOCA limits must be determined with, or shown to be bounded by, a specific application of the NRC-approved evaluation model.
6. LOCA limits for three pump operation must be established for each class of plants by application of the methodology described in this report. An acceptable approach is to demonstrate that three pump operation is bounded by four pump LHR limits.
7. The limiting ECCS configuration, including minimum versus maximum ECCS, must be determined for each plant or class of plants using this methodology.
8. For the small break model, the hot channel radial peaking factor to be used should correspond to that of the hottest rod in the core, and not to the radial peaking factor of the 12 hottest bundles.

9. The constant discharge coefficient model (discharge coefficient = 1.0) referred to as the "High or Low Break Voiding Normalized Value," should be used for all small break analyses. The model which changes the discharge coefficient as a function of void fraction, i.e., the "Intermediate Break Voiding Normalized Value", should not be used unless the transient is analyzed with both discharge models and the intermediate void method produces the more conservative result.
10. For a specific application of the FTI small break LOCA methodology, the break size which yields the local maximum PCT must be identified. In light of the different possible behaviors of the local maximum, FTI should justify its choice of break sizes in each application to assure that either there is no local maximum or the size yielding the maximum local PCT has been found. Break sizes down to 0.01 ft² should be considered.
11. B&W-designed plants have internal reactor vessel vent valves (RVVs) that provide a path for core steam venting directly to the cold legs. The BWNT LOCA evaluation model credits the RVVV steam flow with the loop steam venting for LBLOCA analyses. The possibility exists for a cold leg pump suction seal to clear during blowdown and then reform during reflood before the evaluation model analyses predict average core quench. Since the REFLOOD3B code cannot predict this reformation of the loop seal, FTI is required to run the RELAP5/MOD2-B&W system model until the whole core quench, to confirm that the loop seal does not reform. This demonstration should be performed at least once for each plant type (raised loop and lowered loop) and be judged applicable for all LBLOCA break sizes.

8 REFERENCES

1. U.S. Code of Federal Regulations. "Domestic Licensing of Production and Utilization Facilities," Part 50, Chapter I, Title 10, "Energy"
2. Babcock and Wilcox, Inc., "B&W's ECCS Evaluation Model", BAW-10104PA, Revision 5, November, 1986
3. Babcock and Wilcox, Inc., "B&W's Small-Break LOCA ECCS Evaluation Model", BAW-10154-A, July, 1985
4. B&W Nuclear Technologies, "RELAP5/MOD2-B&W -- An Advanced Computer Program for Light Water Reactor LOCA and non-LOCA Transient Analysis", BAW-10164P, Revision 3, October 1992.
5. B&W Nuclear Technologies, "BWNT Loss-of-Coolant Accident Evaluation Model for Recirculating Steam Generator Plants, BAW-10168PA, Revision 2", October, 1992
6. Letters from J.H. Taylor Framatome to USNRC: (1) "Responses to Request for Additional Information on BWNT LOCA - BWNT Loss-of-Coolant Accident Evaluation Model for Once-Through Steam Generator Plants, BAW-10192P" dated May 6, 1996, (2) "Responses to Verbal Requests of Additional Information on BWNT LOCA - BWNT Loss-of-coolant Accident Evaluation Model for Once-Through Steam Generator Plants" dated October 10, 1996.
7. V.H. Ransom, et. al., "RELAP5/MOD2 Code Manual -- Volume 1: Code Structures, System Models and Solution Methods and Volume 2: Users Guide and Input Requirements" NUREG/CR-4312 - Volume 1, August, 1985 and NUREG/CR-4312 - Volume 2, December 1985.
8. B&W Nuclear Technologies, "REFLOOD3B -- Model for Multinode Core Reflooding Analysis", BAW-10171P, Revision 3, September 1989.
9. B&W Nuclear Technologies, "BEACH -- Best Estimate A Computer Code for Reflood Heat Transfer During LOCA", BAW-10166PA, Revision 4, October 1992.
10. Babcock and Wilcox, Inc., "CONTEMPT- Computer Program for Predicting Containment Pressure-Temperature Response to a LOCA", BAW-10095A, Revision 1, April, 1978
11. J.J. Cudlin, M.I. Meerbaum, and J.A. Klingensmith, "CRAFT-2 - FORTRAN Program for Digital simulation of a Multinode Reactor During Loss of Coolant, BAW-10092", Revision 3, Babcock and Wilcox, October, 1982.
12. Letter from J.H. Taylor Framatome Technologies Inc. to USNRC, "BAW-10192P, BWNT LOCA - BWNT Loss-of-Coolant Accident Evaluation Model for Once-Through Steam Generator Plants SER Limitations" dated October 21, 1996

13. Letter from J.H. Taylor Framatome Technologies Inc. to USNRC, "Response to a Verbal Request for Additional Information on BWNT LOCA-BWNT Loss-of-Coolant Accident Evaluation Model for Once-Through Steam Generator Plants" January 7, 1997.

This page is intentionally left blank.

ENCLOSURE 2

SCIE-NRC-243-96

TECHNICAL EVALUATION REPORT

- BWNT LOCA -

**BWNT Loss-of-Coolant Accident Evaluation Model
for Once-Through Steam Generator Plants
BAW-10192P, Revision 0**

Prepared for

**U. S. Nuclear Regulatory Commission
Washington, D. C. 20555**

**Contract No. NRC-03-95-026
Task Order 203**

Prepared by

**D. A. Prelewicz
W. C. Arcieri**

September 1996

**SCIENTECH, Inc.
11140 Rockville Pike, Suite 500
Rockville, Maryland 20852
(LA-165)**

SUMMARY

Framatome Technologies, Inc. (formerly BWNT) submitted Volumes I and II of BAW-10192P which document the generic large and small break loss-of-coolant accident evaluation models, respectively, for USNRC review. These evaluation models are intended for application to all classes of B&W designed once-through steam generator plants. Volume III is a licensing addendum which will contain licensing data, responses to NRC questions, SER's, and other relevant data. The ECCS evaluation models are developed to meet the requirements of Appendix K to 10 CFR Part 50. The models make use of the RELAPS/MOD2-B&W, BEACH, and REFLOD3B computer programs, which have previously been accepted for LOCA calculations. The CONTEMPT code, which has also been accepted by the NRC, is used in the event that containment response calculations are required. This Topical Report documents the methodology for both large and small break ECCS analysis of OTSG plants using the computer codes listed above.

In the subject Topical Report, Framatome Technologies, Inc. (FTI) presents information which describes how the LOCA analyses will be performed for small and large breaks and includes a break spectrum analysis showing the overlap of results for intermediate break sizes. The large break methodology is used for cold leg breaks larger than 2.0 ft². For all sizes of hot leg breaks and cold leg breaks between 0.75 ft² and 2.0 ft², a transition methodology is used. The small break methodology is used for all breaks less than 0.75 ft².

The methodology described in the Topical Report is generic in that it covers the application of computer models and the manner of developing input for the models. Sensitivity studies are documented for nodalization and time step size, plus choice of model options. Sample base model applications are also included. In response to questions in the Request for Additional Information (RAI) and to questions raised during NRC management review, FTI has provided technical responses which adequately address specific issues raised during the review process.

The methodology reviewed complies with the requirements of Appendix K to 10 CFR Part 50. It is therefore recommended that the methodology described in BAW-10192P, be accepted for use in licensing calculations, subject to the restrictions enumerated in Section 6 of this report.

TABLE OF CONTENTS

<u>Section</u>	<u>Title</u>	<u>Page</u>
	SUMMARY	i
1.0	INTRODUCTION	1
2.0	SUMMARY OF THE LARGE BREAK LOCA ANALYSIS METHODS, BAW-10192P, VOLUME I	2
3.0	EVALUATION OF THE LARGE BREAK LOCA ANALYSIS METHODS, BAW-10192P, VOLUME I	4
3.1	Base Case Selection	4
3.2	Time Step Sensitivity Studies	4
3.3	Pressurizer Location Study	5
3.4	Break Area Noding Sensitivity Study	5
3.5	Core Cross Flow Sensitivity Study	6
3.6	Core Noding Study	6
3.7	Pump Degradation Study	6
3.8	Pump Power Study	6
3.9	ECCS Bypass Study	7
3.10	REFLOD3B Loop Noding Sensitivity Study	7
3.11	REFLOD3B Pump Resistance Sensitivity Study	7
3.12	BEACH Axial Fuel Segmentation Study	8
3.13	Axial Versus Radial Core Peaking Factor Study	8
3.14	Break Spectrum Study	9
3.14.1	CLPD Guillotine Breaks	9
3.14.2	CLPD Split Breaks	9
3.14.3	CLPS Break	10
3.14.4	Hot Leg Break	10
3.15	Time in Life Study	10
3.16	Three Operating RC Pumps at 75% Full Power Study	10
3.17	LOCA Limit Demonstration Cases	11
3.18	Minimum/Maximum ECCS Injection Study	11
4.0	SUMMARY OF THE SMALL BREAK LOCA ANALYSIS METHODS, BAW-10192P, VOLUME II	12
5.0	EVALUATION OF THE SMALL BREAK LOCA ANALYSIS METHODS, BAW-10192P, VOLUME II	13
5.1	Base Model Selection	13
5.2	Time Step Sensitivity Studies	14
5.3	Pressurizer Location Study	14

TABLE OF CONTENTS

<u>Section</u>	<u>Title</u>	<u>Page</u>
5.4	Core Cross Flow Sensitivity Study	14
5.5	Core Noding Sensitivity Study	15
5.6	CFT Line Resistance Sensitivity Study	15
5.7	Break Discharge Coefficient Study	15
5.8	Break Spectrum Study	16
5.8.1	CLPD Breaks	16
5.8.2	CFT Line Break	17
5.8.3	HPI Line Break	17
6.0	CONCLUSIONS AND LIMITATIONS	18
7.0	REFERENCES	20

TECHNICAL EVALUATION REPORT - BWNT LOCA

BWNT Loss-of-Coolant Accident Evaluation Model for Once-Through Steam Generator Plants BAW-10192P, Revision 0

1.0 INTRODUCTION

Framatome Technologies Incorporated (FTI), previously known as Babcock and Wilcox Nuclear Technologies (BWNT), submitted Volumes I and II of BAW-10192P which documents generic large and small break loss-of-coolant accident evaluation models, respectively, for USNRC review. These reports provide a description of the FTI large and small break LOCA methodology and present the results of benchmarks to demonstrate the methodology. The methodology was reviewed based on the requirements of 10-CFR-50, Appendix K and 10-CFR-50.46 (Reference 1).

The subject Topical Report describes a methodology which uses a different complement of computer codes than previously approved models for Once-Through Steam Generator (OTSG) plants. Currently approved large (Reference 2) and small break (Reference 3) methods for OTSG plants are based upon the CRAFT2 code. The currently approved large break methodology also uses the REFLOD3B and THETA1-B codes. Only the REFLOD3B code is used as a part of the methodology described in this Topical Report, which is based primarily on the RELAP5/MOD2-B&W code (Reference 4). The BEACH code is also used for the large break analysis. Large and small break ECCS evaluation models for Recirculating Steam Generator (RSG) plants (Reference 5), which use the same suite of codes as the subject methodology, are in use by FTI, having previously received regulatory approval.

This Technical Evaluation Report presents the results of an evaluation of the FTI methodology for the large and small break LOCA. Other FTI reports were extensively used as part of the review for background information. These reports include BAW-10168PA (Reference 5), BAW-10104PA (Reference 2), and BAW-10154A (Reference 3).

A Request for Additional Information (RAI) was submitted to Framatome Technologies. Their responses, which will be included in Volume III of BAW-10192P, were reviewed and evaluated as an integral part of the Topical Report review process. Many of the questions requested clarification of specific sections in the Topical Report. Responses to the more significant issues raised in the RAI are discussed and evaluated in this report. Any RAI question referenced in the report has a prefix RAI-LB or RAI-SB preceding the question number, denoting whether the question pertains to the large break or small break LOCA. FTI also provided written responses to four questions raised during the NRC management review. Responses to these questions are referenced with the prefix RAI-MR.

2.0 SUMMARY OF THE LARGE BREAK LOCA ANALYSIS METHODS, BAW-10192P, VOLUME I

Volume I of BAW-10192 presents the generic large break LOCA methodology to be used by FTI for evaluating the performance of the emergency core cooling systems following a large break LOCA for all classes of B&W designed plants. The report describes the methods used for large break LOCA analysis and demonstrates the capability of the models through a series of benchmarks. The FTI report also discusses compliance with Appendix K to 10 CFR Part 50 and 10 CFR 50.46.

The FTI methodology for large break LOCA analysis utilizes the RELAPS/MOD2-B&W, REFLOD3B, BEACH and CONTEMPT computer programs. Revision 3 of the RELAPS/MOD2-B&W code (Reference 4), which is based on the RELAPS/MOD2 code (Reference 6) developed by the Idaho National Engineering Laboratory, was approved for use in the analysis of both large break and small break LOCAs for both once through and recirculating steam generator plants. The RELAPS/MOD2 B&W program is used to predict system thermal hydraulics, core power generation, and clad temperature response during blowdown. The REFLOD3B (Reference 7) program is used to determine the length of the vessel refill period and the core flooding rate during reflood. The BEACH (Reference 8) program is used to determine the clad temperature response during the reflood period using input from REFLOD3B. The BEACH program has been reviewed and approved for use in LOCA reflood analysis, as has REFLOD3B. The CONTEMPT (Reference 9) code is used should containment response calculations be required. Since the computer models used by FTI have been previously reviewed and approved by the USNRC, this technical evaluation report (TER) focuses on the techniques and assumptions used in developing a model and evaluating ECCS performance during a LOCA. FTI had previously used the CRAFT2 (Reference 10) computer code for OTSG plant ECCS evaluation model calculations.

The benchmarks that have been performed to demonstrate the large break LOCA methodology are discussed in BAW-10192P, Volume 1 including sensitivity studies for the RELAPS/MOD2-B&W, REFLOD3B, and BEACH computer codes. An evaluation of each sensitivity study is presented in Section 3 of this report. The base case for large breaks in the FTI LOCA methodology is a double ended guillotine rupture of the cold leg pump discharge (CLPD) pipe. This is also the peak clad temperature (PCT) limiting case as determined by a break spectrum study.

A transition break methodology has been developed to analyze hot leg breaks and cold leg breaks in the range 0.75 ft^2 to 2.0 ft^2 . For small breaks the core flow remains upward, the lower plenum does not void and reflood begins at the end of blowdown, so there is no refill period. Transition breaks include all hot leg breaks and the range of cold leg break sizes between those exhibiting this typical small break behavior ($\leq 0.75 \text{ ft}^2$) and those exhibiting typical large break behavior ($\geq 2.0 \text{ ft}^2$). Because the behavior for small and large breaks is quite different, the large and small break methods do not overlap for any break sizes. FTI developed the transition methodology in order to provide an accurate representation of the physical phenomena occurring for these breaks. Results show a continuous variation of PCT as a function of cold leg break size.

The transition break methodology differs from the full large break LOCA methodology in a number of respects, including the following:

1. Bypass flow is calculated using the RELAPS/MOD2-B&W computer code rather than a non-mechanistic model.
2. The REFLOD3 code is not used, but rather the entire transient is analyzed using the RELAPS/MOD2-B&W and BEACH codes. Since no adjustment of lower plenum inventory is necessary, a single code is used.
3. The nonhomogeneous flow model is used for core junctions.

Noding for the transition breaks is the same as for large breaks.

There are 3 classes of B&W designed plants to which the large break LOCA methodology will be applied. Most domestic operating plants are of the lowered loop design with 15 x 15 fuel bundles and 8 Reactor Vessel Vent Valves (RVVV). A second class of plants has a raised loop design, with the same fuel type, and 4 RVVVs. This class of plants also differs from the others by virtue of its low head high pressure injection (HPI) system. There is a third design with 17 x 17 fuel, raised loop and 8 RVVVs. Differences between the classes of plants are handled by changing the noding schemes in the computer codes used.

3.0 EVALUATION OF THE LARGE BREAK LOCA ANALYSIS METHODS, BAW-10192P, VOLUME I

This section discusses the review of the FTI Large Break LOCA methodology, including the modeling features and sensitivity studies performed to select the base case, time step size, nodalization, and other modeling options. The large break model, including the modifications for transition break sizes, was determined to comply with the requirements of Appendix K to 10 CFR Part 50. The sequence of events for a large break LOCA is relatively well known and the OTSG plant response is similar to that of other PWRs during blowdown and refill, so there is no need to reiterate this information. The only significant difference with the OTSG plants is the RVVVs which act to reduce steam binding during reflood. In this review, emphasis was placed on areas which differ from the recirculating steam generator plants, for which the methodology has already been approved.

3.1 Base Case Selection

The double ended guillotine break in the cold leg pump discharge was the most limiting break, and was therefore selected as the base case. The sample analysis was performed for the 205 FA plant with 17 x 17 fuel and raised loops. The base case selected, namely a double ended guillotine break in the cold leg on a 205 FA plant, is acceptable for demonstrating model sensitivities and convergence. Analyses must still be performed for each plant type to demonstrate compliance with 10 CFR 50.46 acceptance criteria.

For B&W designed plants, the RVVVs provide the primary path for the steam to reach the break. When the loop seal clears, a second path for the steam to reach the break is opened. FTI has demonstrated the ability of the RELAPS/MOD2-B&W code to predict loop seal clearing by comparing to experimental data from the ROSA large scale test facility and from the Semiscale MOD1 facility. Appendices G and J of Reference 5 contain the benchmarks. The base case models a raised loop plant which has the loop seal at a higher elevation than a lowered loop plant. The benchmarks indicate that RELAPS/MOD2-B&W is generally capable of predicting loop seal clearing. FTI should include any nodding changes which are necessary to adequately model loop seal clearing in the lowered loop plant model.

The possibility that a loop seal could clear initially and then refill was addressed in the FTI response to RAI-MR Question 3. While this is not a likely occurrence, it is difficult to completely rule out this possibility for all event scenarios. Therefore, for each plant type where credit is taken for steam flow through the open loop seal, FTI is required to run the RELAPS/MOD2-B&W system model to the time of whole core quench, to confirm that the loop seal does not refill.

3.2 Time Step Sensitivity Studies

Separate time step convergence studies were performed for the blowdown and reflood portions of the base case event. FTI refers to the time step sensitivity for the blowdown period as the RELAPS/MOD2-B&W time step study and to the reflood period study as the BEACH time step sensitivity. For the RELAPS/MOD2-B&W time step study, the maximum time step size was

decreased by a significant amount and there was no significant change in the calculated response, indicating convergence. The final BEACH time step convergence study was performed in response to RAI-LB Question 16. To achieve acceptable convergence, FTI made changes in the manner of calculating core inlet subcooling, a boundary condition for BEACH determined from REFLOD3B results. Rather than changing the core inlet temperature from saturation to the REFLOD3B calculated lower plenum volume average temperature, which is significantly subcooled, FTI modified the calculation procedure to ramp the inlet temperature. FTI calculates a mixed mean temperature at bottom of core recovery (BOCR) based on a smaller mixing volume below the uppermost hole in the flow distribution plate. The core inlet temperature used in BEACH is held at this value for one second following BOCR and then ramped to the REFLOD3B calculated value over a period of up to 5 seconds. The ramp time is calculated to be the time required for the temperature interface to travel from the top of the flow distribution plate to the heated core inlet. Experimental data from the Upper Plenum Test Facility (UPTF) and Slab Core Test Facility (SCTF) test programs were used to guide and justify the modeling changes. Since the base model was changed, FTI reconsidered the time step sensitivity studies run with the previous base model. Runs were made with both significantly increased and significantly decreased maximum time step sizes, and the results were essentially the same, demonstrating that the solution is converged.

There was very little difference in calculated fuel clad temperatures with the revised inlet subcooling model. The PCT was only slightly increased using the revised method, which exhibits significantly improved time step convergence. Basically, this revision smooths a discontinuity in a conservative manner and improves calculational stability. FTI considered the potential effect of this change on previously completed sensitivity studies and determined that the conclusions of those studies would not be affected. This observation is reasonable, given the insignificant effect of the change on the values of the key calculational result, namely peak clad temperature.

3.3 Pressurizer Location Study

The base case assumes that the pressurizer is connected to the intact loop hot leg. A sensitivity study was performed with the pressurizer surge line connected to the broken loop hot leg. Only the blowdown portion of the event was simulated, since the pressurizer is emptied and hence does not play a significant role later in the event. The peak clad temperature (PCT) at end-of-blowdown was lower and more liquid remained in the lower plenum, i.e. results were less conservative. Therefore, the base model retains the pressurizer on the intact loop.

3.4 Break Area Noding Sensitivity Study

Past experience with RELAPS has indicated that noding detail in the vicinity of the break can affect results. Therefore, FTI performed a sensitivity study to demonstrate that the noding used in the base model is adequate for predicting break flow. An additional node was used at each end of the pipe at the break location. The case was run for the blowdown only, since this is the period when more detailed modeling of break flow may be important. Only small differences in results were found with the more detailed nodalization, thus demonstrating convergence of the base model.

3.5 Core Cross Flow Sensitivity Study

Section I.C.7.a of Appendix K to 10 CFR Part 50 requires that the effect of cross flow in the core be considered. To determine appropriate values to use for cross flow resistance, FTI first estimated a value based upon the core geometry and then performed a sensitivity study to establish the effect of varying the cross flow resistance on calculated PCT. Only small effects were seen for rather large variations in assumed cross flow resistance. It was shown to be conservative to increase cross flow resistance. However, this increased PCT by causing DNB to be calculated earlier. Early calculation of DNB is known to be one of the more significant conservatisms in the evaluation model, so additional conservatism in this area is not needed. Appendix K to 10 CFR Part 50 requires only that the effects of cross flow be included in a realistic manner. FTI has used a realistic model for cross flow and has shown that the results vary only slightly with changes in cross-flow resistance. Therefore, use of the nominal estimated cross flow resistance is acceptable.

3.6 Core Noding Study

In addition to the cross flow resistance sensitivity, FTI considered radial core nodalization and its effect on cross flow. An additional parallel channel, referred to by FTI as the middle channel, was added to represent the eight fuel bundles surrounding the hot bundle. The radial peaking factor for these eight bundles was varied to determine the effect on calculated fuel and clad temperatures. A wide range of radial peaking factors covering the spectrum of possibilities was considered. The effect on fuel and clad temperatures at the end-of-blowdown was shown to be small. As with the cross flow sensitivity study, the various radial peaking factors influenced fuel temperatures by slightly changing the time of DNB, which is known to be predicted to occur early. There is no need to select a case which predicts the earliest DNB, since all of the cases predict DNB much earlier than expected.

In response to RAI-LB Question 14, FTI provided evidence that the base model predicts more conservative temperatures than one using best estimate cross-flow resistance and radial peaking factor. These extensive sensitivity studies demonstrate that the FTI model adequately addresses the effect of cross flow in the core region.

3.7 Pump Degradation Study

In addition to the base model, two different pump two-phase degradation models were tested in a sensitivity study. A curve referred to by FTI as the M1 curve yielded more conservative results and was incorporated into a revised base model. Use of this more conservative model is acceptable.

3.8 Pump Power Study

For ECCS evaluation calculations, a loss of off-site power is assumed concurrent with the LOCA. The main coolant pumps will then be unpowered and will coast down. FTI demonstrated that this assumption is conservative by running the pumps powered case and showing that it yields lower fuel and clad temperatures.

3.9 ECCS Bypass Study

Initially, FTI used a mechanistic ECCS bypass model for the large break. That is, the flow of ECCS to the break was calculated using RELAP5/MOD2-B&W. A sensitivity study was performed using a non mechanistic model, which removed all ECCS liquid injected prior to the calculated end-of-bypass. It was determined that the amount of liquid calculated to be resident in the lower plenum at end-of-blowdown was virtually identical for the two methods.

FTI used the non mechanistic model in its base methodology and all subsequent large break sensitivity studies (See RAI-LB Question 4). Therefore, only the non mechanistic model is acceptable for large break calculations. The non mechanistic model has the advantage of producing less calculated oscillatory behavior.

In the non mechanistic model both a partial end of bypass and an end of bypass are calculated. Appendix K, Section 1.C.1.c, does not prescribe how end of bypass is to be calculated. It lists two acceptable methods, but does not limit the definitions to these methods. The partial end of bypass model has been developed based upon relevant Upper Plenum Test Facility (UPTF) data. It satisfies Appendix K requirements for modeling end of bypass.

The transition methodology uses a mechanistic model for predicting bypass flow. Since Appendix K requirements for bypass flow modeling apply only for cold leg breaks, this approach is acceptable for hot leg breaks. For cold leg breaks less than 2.0 ft², that is those analyzed with the transition methodology, the mechanistic model is also used. FTI showed that for the 2.0 ft² cold leg break, the mechanistic model underpredicts the lower plenum inventory at the time of PCT compared to the large break model which uses the non mechanistic bypass model. Based upon this comparison and the small break LOCA benchmarking of the RELAP5/MOD2-B&W code against LOFT Experiment L3-5 reported in Reference 5, the mechanistic model is acceptable for transition breaks.

3.10 REFLOD3B Loop Noding Sensitivity Study

As part of the sensitivity studies performed for REFLOD3B, a loop noding study was performed by doubling the number of nodes in the loops in the REFLOD3B model and comparing the results to the base model results. Key results for the core inlet flooding rate, core and downcomer water levels, and carryout rate fraction were compared by FTI and little difference was found, indicating convergence of the base model.

3.11 REFLOD3B Pump Resistance Sensitivity Study

A lock rotor assumption is used in the base REFLOD3B model. To demonstrate that this is conservative, FTI computed form loss coefficients for the pump which correspond to the free-spinning impeller condition. The pump pressure drop formulation in RELAP5/MOD2-B&W was used to determine a loss coefficient for the free-spinning rotor condition. The results show that the free spinning impeller case results in a higher core flooding rate because of a reduction of steam binding in the upper plenum. Thus the locked rotor assumption is conservative and appropriate for the base model.

3.12 BEACH Axial Fuel Segmentation Study

FTI performed a study to determine the sensitivity of the PCT to a change in the maximum number of axial rezoning segments used in the BEACH analysis. The fine mesh rezoning feature in BEACH adjusts the number of axial mesh points to be used in each heat structure based on user input and criteria programmed into the code. The base case utilizes 8 fine mesh rezoning increments. Sensitivity cases with 16 and 32 fine mesh zoning increments were run. The BEACH results for peak clad temperature and average oxidation increase in the hot and average channels are similar, indicating that the base model is converged.

3.13 Axial Versus Radial Core Peaking Factor Study

Section I.A of Appendix K to 10 CFR Part 50 requires that "A range of power distribution shapes and peaking factors representing power distributions that may occur over the core lifetime shall be studied and the one selected should be that which results in the most severe calculated consequences, for the spectrum of postulated breaks and single failures analyzed." FTI performed the axial versus radial core peaking factor study to determine whether significant variations in peak clad temperature or whole-core hydrogen generation would result from different combinations of the radial and axial peaking factors. In this sensitivity study, results for axial peaking factors of 1.6 and 1.8 are generated and compared to the base case which employs a factor of 1.7. In both cases, the radial peaking factor is adjusted to conserve the peak linear heat generation rate. Both cases produced an increase in the PCT of less than 50 °F.

In response to RAI-MR1 and RAI-MR4, FTI provided a detailed explanation of how the axial and radial peaking factors for the LOCA analysis are determined. The set of power distributions which can actually be achieved is set by a maneuvering analysis which includes non-LOCA imposed limitations. Over most of the range of power distributions, the limitations imposed by the maneuvering analysis are considerably tighter than those imposed by the LOCA LHGR limit. For certain ranges of the power distribution, in particular core inlet skewed peaks, the margin between the maneuvering analysis limitations and the LOCA limitations, approaches a minimum. For these power distributions the axial and radial peaking factors are approximately equal. Therefore, FTI uses a 1.7 axial peaking factor and sets the radial peaking to reach the LHGR limit.

For the limiting break, five different axial offsets (axial location of the power peak) are then run at both BOL and MOL conditions, in addition to one EOL case to show that MOL conditions bounds EOL conditions. These cases establish the LOCA limit. The manner of selecting the cases to be considered from among the infinite number of possibilities considers the distribution of power shapes which are achievable based upon the constraints imposed by the maneuvering analysis. The cases analyzed are those covering a range of conditions where the margin between the maneuvering analysis limitations and the LOCA limitations are at a minimum. Therefore, use of an axial peaking factor of 1.7 is appropriate as the base case for sensitivity studies in this report. Should the maneuvering analysis for a new fuel type or application indicate that the minimum margins occur for power distributions other than those analyzed herein, the axial peaking factor used should be adjusted so that the cases analyzed remain in the range of the minimum margin.

3.14 Break Spectrum Study

To satisfy the requirements of Appendix K to 10 CFR Part 50, a spectrum of twelve large breaks was analyzed, including double-ended breaks located in the hot leg and cold leg pump suction, and split breaks at various locations and of various sizes. The spectrum of breaks considered by FTI in this demonstration is sufficiently inclusive to be used as a format for specific applications of the methodology. A review of the LOCA spectrum results is presented in the following sections.

3.14.1 CLPD Guillotine Breaks

For the CLPD double ended guillotine break, discharge coefficients of 1.0, 0.8, 0.6, and 0.4 were analyzed. The results show that the maximum temperature is predicted for a discharge coefficient of 1.0 and that peak clad temperature decreases with decreasing discharge coefficient (or break size). FTI attributes this trend to increases in core upflow during the early phases of blowdown, increased core flooding rate due to lower pin temperatures and decreased refill time due to earlier end of bypass predictions. In all cases, the temperature is below the 2200 °F temperature limit in 10 CFR 50.46. The results presented by FTI show that the base case, which is a double-ended guillotine break with a discharge coefficient of 1.0 will produce the most limiting results.

3.14.2 CLPD Split Breaks

In the LBLOCA spectrum study, several break scenarios involving a split break in the pump discharge piping were analyzed. A split break with an area double the discharge pipe cross sectional area was analyzed using the LBLOCA methodology. An analysis was performed for a 2 ft² split break using both the LBLOCA and transition methodologies. The transition break methodology was used to analyze additional cases involving split breaks with areas of 1.5, 1.0, and 0.75 ft². The CLPD double area split break resulted in lower cladding temperatures relative to the base case, which is attributed to predictions of higher core downflow during the later portion of the blowdown phase.

Analysis of the 2 ft² split break using both the base LBLOCA and transition methodologies showed the overlap of the transition LOCA methodology with the large break methodology. FTI presented comparative results using the two methods and noted that the results from the LBLOCA and transition LOCA methodology match well. There is some difference in the collapsed liquid level later in the transient. FTI attributes this to the higher refill rate predicted by the transition methodology relative to the LBLOCA methodology. In both cases, the peak clad temperature is predicted to be lower than the base case.

The transition methodology results for the 1.5, 1.0, and 0.75 ft² split breaks show the expected trends in pressure and break mass flow behavior. The peak clad temperature decreases with decreasing break size. FTI notes that the RVEVs pass all of the core steam production to the break for the 1 ft² and 0.75 ft² breaks. Total core dryout was not predicted in these cases. In the case of the 1.5 ft² break, FTI noted that the RVEVs were unable to handle the flow to the break. The lower plenum cleared of liquid in this case, resulting in an additional path for steam venting. Core quenching occurred at approximately the same time for all three cases. In all cases, the peak clad temperature is predicted to be lower than the base case.

3.14.3 CLPS Break

Analysis of a double ended guillotine break in the pump suction piping with a discharge coefficient of 1.0 resulted in a lower peak clad temperature prediction than the base case. FTI attributes this to retention of a significant amount of ECC water during blowdown, which shortened the adiabatic heatup period. Break flow rate is also reduced relative to the base case because of increased pump resistance due to the changed break location.

3.14.4 Hot Leg Break

The double ended guillotine break in the hot leg with a discharge coefficient of 1.0 resulted in a lower peak clad temperature relative to the base case. FTI attributes this to mostly positive flow through the core which enhances core heat transfer. Also, the lower plenum was not predicted to empty during the event, resulting in a shortened adiabatic heatup period.

3.15 Time in Life Study

LOCA limits must be determined by a specific application of the methodology described in this report. The purpose of the analysis described in this section is to provide a demonstration of the methodology to be used. Calculations were performed at four times in life using the full model, i.e. RELAPS/MOD2-B&W, REFLOD-3B and BEACH, along with TACO3 for fuel rod initial conditions. The event selected for analysis was the base case double-ended CLPD break with a center peaked axial power shape.

The demonstration established that BOL conditions should be used in the average channel while burnup is advanced in the hot channel. Based upon the demonstration calculation, it is expected that the linear heat rate will be maintained out to approximately 45,000 MWD/MTU, after which it will need to be decreased. While more than four burnup points will generally be needed for specific applications, the methodology presented in this section adequately demonstrates the approach for determining time-in-life limits.

3.16 Three Operating RC Pumps at 75% Full Power Study

The purpose of this analysis is to demonstrate that the LOCA limits for four pump operation will cover three pump operation at the 75% power level. Since LOCA limits can only be established by a specific application, it follows that limits for three pump operation can also only be established specific application. In such an application, the factor of 1.02 will need to be applied to the power to satisfy the requirements of Appendix K to 10 CFR Part 50. To justify operation at 75% power will require that the analysis be performed at $75 \times 1.02 = 76.5\%$ power.

Depending upon the status of the inoperable pump, it may also be necessary to consider cases in addition to the locked rotor.

3.17 LOCA Limit Demonstration Cases

A demonstration calculation for LOCA limits determination was performed to illustrate the FTI approach. The base CLPD break was simulated with various axial power shapes. In an actual

(LA-178)

application of the complete methodology, calculations will be performed with the peak power location assumed to occur at five different elevations in the core. For this demonstration, calculations were performed with the axial peak of 1.7 at three different locations, and the radial peaking factor was set to obtain the maximum LHGR. In an actual application, five different axial peak locations will be analyzed at BOL and MOL conditions, in addition to one case at EOL to demonstrate that MOL is more limiting. The general approach is acceptable for demonstrating the LOCA limits methodology. However, for a new fuel type or application FTI should demonstrate that the minimum LOCA margins occur for the range of power distributions analyzed.

3.18 Minimum/Maximum ECCS Injection Study

The base case has minimum pumped ECCS injection in the REFLOD3B calculations together with a containment back pressure based upon maximum ECCS pumped injection. Pumped ECCS injection does not occur during the blowdown so RELAP5/MOD2 calculations are not affected. To determine whether the base case is conservative, two additional cases were run with minimum ECCS injection and maximum ECCS injection in both the REFLOD3B and containment calculations. The maximum ECCS case proved to be the most conservative although by a very small amount; 32 °F increase in PCT compared to the base case and 35 °F greater than the minimum ECCS case. These calculations showed that it will be necessary to perform this sensitivity study for each specific application to determine the limiting case. The procedure used to perform the sensitivity study is acceptable. Also, the difference in PCT compared to the base case is small enough that sensitivity studies performed with the base case model are acceptable.

4.0 SUMMARY OF THE SMALL BREAK LOCA ANALYSIS METHODS, BAW-10192P, VOLUME II

Volume II of BAW-10192 presents the generic small break LOCA methodology to be used by FTI for evaluating the performance of the emergency core cooling systems following a small break LOCA for all classes of B&W designed plants. The report describes the methods used for small break LOCA analysis and demonstrates the capability of the models through a series of benchmarks. The FTI report also discusses compliance with Appendix K to 10 CFR Part 50 and 10 CFR 50.46.

The FTI methodology for small break LOCA analysis utilizes the RELAPS/MOD2-B&W computer code. The RELAPS/MOD2-B&W computer code, which is based on the RELAPS/MOD2 code, was approved for use in the analysis of both large break and small break LOCAs for both once through and recirculating steam generator plants as noted in Section 2. The RELAPS/MOD2 B&W program is used to predict system thermal hydraulics, the average core and hot channel void distributions, and the hot and average core cladding temperature response for the entire transient.

The benchmarks that have been performed to demonstrate the small break LOCA methodology are discussed in BAW-10192P, Volume II including sensitivity studies for relevant parameters for the RELAPS/MOD2 B&W computer code. An evaluation of each sensitivity study is presented in Section 5 of this report. The base case chosen for small break sensitivity studies was a 0.1 ft² break at the bottom of the cold leg pump discharge pipe.

The three classes of B&W designed plants to which the small break LOCA methodology will be applied are discussed in Section 3. Differences between the classes of plants are handled by changing the noding schemes in the computer codes used.

5.0 EVALUATION OF THE SMALL BREAK LOCA ANALYSIS METHODS, BAW-10192P, VOLUME II

Review of the small break ECCS evaluation methodology described in Volume II of BAW-10192P, was performed to determine compliance with the requirements of Appendix K to 10 CFR Part 50. Based upon this review, the methodology was determined to be in compliance with Appendix K requirements as they apply for small break loss-of-coolant accidents.

This section discusses the methodology used for the small break and the sensitivity studies which were performed to support the methodology.

5.1 Base Model Selection

A preliminary break spectrum analysis combined with the results from previously approved evaluation models were used to select the initial base case for the sensitivity studies. The choice was confirmed by a final break spectrum analysis. Initially a 0.1 ft² break in the bottom of the cold leg pump discharge leg was selected as the base case. The analyses were all performed for the 205 FA plant with 17 x 17 fuel and raised loops. Axial power shape for the base case was selected as a 1.7 peaking factor at the 9.705 ft elevation and a peak LHGR of 16.5 kW/ft. All of the sensitivity studies were performed by varying selected portions of this base model.

To assure that a heatup of the fuel was predicted, it was necessary for FTI to introduce conservatism into the calculations beyond those normally required for a design basis analysis. The core flood tank (CFT) pressure was reduced from 615 psia to 515 psia to artificially delay coolant flow from the CFTs. If this conservatism is not introduced, no fuel heatup is predicted for the small break LOCAs and convergence/effects on the key fuel temperature result cannot be evaluated. For purposes of demonstrating sensitivities and convergence, this approach is acceptable since it is conservative. Following completion of the sensitivity studies, a final base case was run which incorporated changes made as a result of the sensitivity studies.

The definition of the base case using the 0.1 ft² break in the bottom of the cold leg in a 205 FA plant is acceptable for demonstrating model sensitivities and convergence. In the RELAP5 code, break flow area (A) and discharge coefficient (C_D) are equivalent multiplicative factors in the break flow calculation. That is, the calculated mass flux is multiplied by $C_D A$ to get the mass flow rate. Separate values of the discharge coefficient can be input for subcooled, two-phase and superheated conditions at the break inlet. During the course of the sensitivity studies, the break discharge coefficient for void fractions greater than 70 percent was changed from 0.7 to 1.0. This results in a redefinition of the base case so that the break area with the revised discharge coefficient corresponds to a 0.07 ft² break. Sensitivity studies performed with the discharge coefficient of 0.7 remain valid since the characteristics of the responses such as convergence and the relative differences in key parameter values are not expected to change appreciably with this small difference in break size.

5.2 Time Step Sensitivity Studies

FTI ran the base case with maximum time steps of .01, .02 and .025 seconds. As indicated in RAI-SB Question 17 on Volume II, there were differences in core mixture level and quench time between the cases with 0.01 and 0.02 maximum time step size. FTI correctly points out in their response that there is good agreement in the key predictions of PCT and minimum core mixture level. FTI attributes differences in core mixture level and quench time to variations in the prediction of break flow which occur following the time of PCT. For purposes of calculating PCT, FTI has demonstrated convergence in this case.

5.3 Pressurizer Location Study

A sensitivity study was performed starting with the base case small break event, but relocating the break to the loop with the pressurizer attached. The differences were small (18 °F lower PCT) for the sensitivity run. Therefore, the base case was not modified and the pressurizer remains connected to the intact loop.

5.4 Core Cross Flow Sensitivity Study

Section 1.C.7.a of Appendix K to 10 CFR Part 50 requires that "the hot channel shall not be greater than the size of one fuel assembly". The hot channel in the small break RELAP5 model consists of 12 fuel bundles in a 3 x 4 rectangular array. FTI states that 5 to 10 percent of the fuel bundles have a radial peaking factor similar to that of the hot bundle. To satisfy Appendix K to 10 CFR Part 50, it must be assumed that all twelve bundles in the hot channel have the same radial peaking factor as the hottest bundle in the core. Since the RELAP5/MOD2 B&W calculation also provides the hot pin results, the peaking factor is actually that of the hottest fuel pin. In this case, the results of using the 12 fuel bundle model will be more conservative than those for a single bundle hot channel, since there will be less cross flow. This is an acceptable model since it reduces the hot channel to average channel cross flow area compared to a single bundle hot channel. On a per bundle basis, the area for cross flow is reduced when a larger number of bundles is included in the hot channel.

FTI performed a sensitivity study on the effect of cross flow resistance between the 3 x 4 hot channel and the average core. Three different distributions of resistances were considered in addition to the base case. These cases covered a range of resistance values greater than would be expected to occur. The base case produced the highest value of PCT. In the upper part of the core where the PCT will occur, the base case uses a high value for resistance to flow from the average into the hot channel, and a low value of resistance for flow out of the hot and into the average channel. Hence it is relatively difficult for water to enter from the cooler average channel into the hot channel when the pressure difference would allow flow in this direction. At the same time, it is easy for steam to leave the hot channel when the pressure gradient permits, resulting in a decrease in steam velocity and consequently steam cooling. This is the most likely reason why the base case produced conservative results relative to cases with both larger and smaller cross flow resistance.

Appendix K to 10 CFR Part 50 requires that the effect of cross flow in the core be considered. FTI has used a model for cross flow resistance which gives conservative PCT predictions compared to models with either larger or smaller cross flow resistances. Therefore, use of the base model is acceptable since it produces results which bound those of a wide range of cross flow models.

5.5 Core Noding Sensitivity Study

A sensitivity study was performed increasing the number of bundles in the hot channel from 12 to 24. There was no significant change in results. This indicates that the 12 bundle model is acceptable. As discussed in Section 5.4 above, decreasing the number of fuel bundles included in the hot channel will increase the cross flow area per bundle leading to increased cross flow and less conservative results. Therefore it was not necessary to run a case with a lesser number of fuel bundles in the hot channel.

5.6 CFT Line Resistance Sensitivity Study

The base case has the nominal (best estimate) CFT line resistance increased by a factor of 100. FTI uses this increased CFT line resistance for all small breaks except the CFT line break where a nominal value of resistance is used. Increased CFT line resistance promotes calculational stability by eliminating predicted wide swings in CFT injection flow.

To demonstrate that use of this increased resistance is acceptable, FTI ran three sensitivity cases. First, the base case 0.1 ft^2 CLPD break was modified to run with nominal CFT line resistance. Predicted PCT was 20°F lower than the base case indicating that the use of a high CFT line resistance is conservative. This is the expected trend since the higher resistance results in lower CFT flow for a given primary system to CFT pressure drop, and hence decreased flow from the CFT. This is further demonstrated by the second and third sensitivity runs, the 1.0 ft^2 CLPD break with nominal and increased CFT line resistance. There was no fuel heatup for these cases so PCT was the same for both runs. The minimum core mixture level was similar but the nominal resistance case recovered core level more quickly, indicating that the increased resistance case is more conservative..

Use of a CFT line resistance greater than nominal was shown to be conservative. This practice also leads to increased numerical stability, a desirable outcome. Therefore, use of increased CFT line resistance for the spectrum of small breaks is acceptable.

5.7 Break Discharge Coefficient Study

This sensitivity study resulted in a change being made to the small break modeling approach. In the initial studies, a discharge coefficient of 0.7 was used for break volume void fractions greater than 70%. Two sensitivity cases were run, one for the 0.1 ft^2 and one for the 0.3 ft^2 CLPD break. For these runs, the discharge coefficient was not changed as a function of break node void fraction. To make the runs comparable, the break size was reduced by a factor of 0.7. In each case, the PCT increased for the revised model with constant discharge coefficient. FTI referenced material which indicated that the Moody model provides relatively accurate predictions of flow at

high void fractions, suggesting that the discharge coefficient of 1.0 is a more appropriate description of the actual physical behavior. The constant discharge coefficient of 1.0 was hence adopted for the base model. This is the only acceptable model.

As a result of the change in the break discharge coefficient, the break spectrum study was performed using a discharge coefficient of 1.0 for break volume void fractions greater than 70 percent. Previous sensitivity cases performed with a discharge coefficient of 0.7 remain valid since the characteristics of the responses such as convergence and the relative differences in key parameter values are not expected to change appreciably with this small difference in break size.

5.8 Break Spectrum Study

The purpose of the break spectrum study is to demonstrate how the limiting break size will be determined in specific applications of the methodology. FTI performed calculations for 12 cold leg pump discharge break sizes between 0.04 ft^2 and 1.43 ft^2 . These events were divided into three categories based upon the response characteristics; small, intermediate and large CLPD SBLOCAs. FTI also analyzed double ended CFT line and HPI line breaks. In a specific application of the methodology additional cases may need to be run to more accurately predict the limiting small break size, as discussed in Section 5.8.1 below. Also, smaller break sizes down to the range of 0.01 ft^2 will need to be considered.

5.8.1 CLPD Breaks

To obtain a temperature excursion for small breaks, it was necessary for FTI to artificially lower the CFT fill pressure from 615 psia to 515 psia. FTI felt it was necessary to obtain a temperature excursion in order to demonstrate convergence of the clad temperature prediction, even though no excursion is normally predicted for licensing applications. With this artificial conservatism, there is a break size which yields a maximum calculated PCT. This break size can be characterized as the one which allows the most fluid to drain from the reactor vessel prior to the pressure dropping to the HPI setpoint. In this demonstration application, FTI identified the 0.1 ft^2 CLPD break as a limiting SBLOCA. PCT for this case was higher than for slightly smaller and slightly larger breaks. In response to RAI-SB Question 19, FTI stated that its methodology for a specific application would identify the break size which yields the local maximum PCT to within an approximately 20% variation in break size. One concern with this approach is that for an actual application, a broad sweep through the spectrum may not show any sign of a peak, possibly because the peak is very localized. Because of the different possible behaviors of the local maximum, FTI should justify its choice of break sizes in each application to assure that either there is no local maximum, or the size yielding the maximum local PCT has been found.

Four small CLPD breaks in the intermediate category were also analyzed; 0.15 , 0.175 , 0.2 and 0.3 ft^2 . None of these break sizes yielded a significant fuel temperature excursion. In an actual application, the local PCT maximum at 0.3 ft^2 would warrant additional attention.

Breaks analyzed in the large category of small CLPD breaks included 0.4 , 0.75 , 1.0 and 1.43 ft^2 . The PCTs calculated for these breaks increase with break size and merge with the transition break

results in a reasonable fashion. This indicates that the PCT will be more limiting for larger break sizes than those analyzed using the small break methods.

5.8.2 CFT Line Break

A double-ended rupture of the CFT flood line at the reactor vessel nozzle is the initiator for this event. Break flow area is limited to that of the nozzle insert, 0.44 ft^2 , placing this event in the category of a small break. The break location and ECCS availability differ compared to other small breaks, since one CFT and one LPI are unavailable prior to applying the single failure criteria. Like a number of the small CLPD breaks of similar size, no clad temperature excursion was predicted for this event. FTI has correctly included this case in the spectrum of events to be considered and should continue to do so for specific applications of the methodology,

5.8.3 HPI Line Break

This event is initiated by the rupture of the HPI line at the cold leg connection. Break area is 0.02463 ft^2 , which corresponds to the nozzle area without a thermal sleeve insert. As with the CFT line break, no clad temperature excursion is predicted for this case. Nevertheless, due to the reduced ECCS availability, including this event in the break spectrum analysis is appropriate.

6.0 CONCLUSIONS AND LIMITATIONS

The Framatome Technologies LOCA methodology as documented in BAW-10192P, Volumes I through III, has been reviewed and evaluated. Both the large and small break methods, documented in Volumes I and II respectively, have been determined to comply with the requirements of Appendix K to 10 CFR Part 50. Based on the information presented and the responses to RAI provided, the use of this methodology for reference in licensing applications involving large and small break LOCA analysis for plants with once-through steam generators is acceptable subject to the following conditions:

1. The LOCA methodology should include any NRC restrictions placed on the individual codes used in the EM.
2. The guidelines, code options, and prescribed input specified in Tables 9-1 and 9-2 in both Volume I and Volume II of BAW-10192P should be used in LBLOCA and SBLOCA evaluation model applications, respectively.
3. The limiting linear heat rate for LOCA limits is determined by the power level and the product of the axial and radial peaking factors. An appropriate axial peaking factor for use in determining LOCA limits is one that is representative of the fuel and core design, and which may occur over the core lifetime. The radial peaking factor is then set to obtain the limiting linear heat rate. For this demonstration, calculations were performed with the axial peak of 1.7. The general approach is acceptable for demonstrating the LOCA limits methodology. However, for a new fuel type or application, FTI should demonstrate that the minimum LOCA margins occur for the range of power distributions analyzed.
4. The mechanistic ECCS bypass model is acceptable for cold leg transition (0.75 ft^2 to 2.0 ft^2) and hot leg break calculations. The non mechanistic ECCS bypass model must be used in the large cold leg break ($\geq 2.0 \text{ ft}^2$) methodology since the demonstration calculations and sensitivities were run with this model.
5. Time in life LOCA limits must be determined with, or shown to be bounded by, a specific application of the NRC-approved evaluation model.
6. LOCA limits for three pump operation must be established for each class of plants by application of the methodology described in this report. An acceptable approach is to demonstrate that three-pump operation is bounded by four-pump LHR limits.
7. Determination of the limiting ECCS configuration, including minimum versus maximum ECCS, must be determined for each plant or class of plants using this methodology.
8. For the small break model, the hot channel radial peaking factor to be used should correspond to that of the hottest rod in the core, and not to the radial peaking factor of the 12 hottest bundles.

9. The constant discharge coefficient model (discharge coefficient = 1.0) referred to as the "High or Low Break Voiding Normalized Value" should be used for all small break analyses. The model which changes the discharge coefficient as a function of void fraction, i.e. the "Intermediate Break Voiding Normalized Value" should not be used, unless the transient is analyzed with both discharge models and the intermediate void method produces the more conservative result.
10. For a specific application of the FTI small break LOCA methodology, the break size which yields the local maximum PCT must be identified. In light of the different possible behaviors of the local maximum, FTI should justify its choice of break sizes in each application to assure that either there is no local maximum, or the size yielding the maximum local PCT has been found. Break sizes down to 0.01 ft² should be considered.
11. FTI should include any noding changes which are necessary to adequately model loop seal clearing in the lowered loop plant model.
12. The possibility that a loop seal could clear initially and then refill. While this is not a likely occurrence, it is difficult to completely rule out this possibility for all event scenarios. Therefore, for each plant type where credit is taken for steam flow through the open loop seal, FTI is required to run the RELAP5/MOD2-B&W system model to the time of whole core quench, to confirm that the loop seal does not refill.

7.0 REFERENCES

1. U.S. Code of Federal Regulations, "Domestic Licensing of Production and Utilization Facilities," Part 50, Chapter I, Title 10, "Energy"
2. Babcock and Wilcox, Inc., B&W's ECCS Evaluation Model, BAW-10104PA, Revision 5, November, 1986
3. Babcock and Wilcox, Inc., B&W's Small-Break LOCA ECCS Evaluation Model, BAW-10154-A, July, 1985
4. B&W Nuclear Technologies, RELAPS/MOD2-B&W -- An Advanced Computer Program for Light Water Reactor LOCA and non-LOCA Transient Analysis, BAW-10164P, Revision 3, October 1992.
5. B&W Nuclear Technologies, BWNT Loss-of-Coolant Accident Evaluation Model for Recirculating Steam Generator Plants, BAW-10168PA, Revision 2, October, 1992
6. V.H. Ransom, et. al., RELAPS/MOD2 Code Manual -- Volume 1: Code Structures, System Models and Solution Methods and Volume 2: Users Guide and Input Requirements, NUREG/CR-4312 - Volume 1, August, 1985 and NUREG/CR-4312 - Volume 2, December 1985.
7. B&W Nuclear Technologies, REFLOOD3B -- Model for Multinode Core Reflooding Analysis, BAW-10171P, Revision 3, September 1989.
8. B&W Nuclear Technologies, BEACH -- Best Estimate A Computer Code for Reflood Heat Transfer During LOCA, BAW-10166PA, Revision 4, October 1992.
9. Babcock and Wilcox, Inc., CONTEMPT- Computer Program for Predicting Containment Pressure-Temperature Response to a LOCA, BAW-10095A, Revision 1, April, 1978
10. J.J. Cudlin, M.I. Meerbaum, and J.A. Klingensus, CRAFT-2 - FORTRAN Program for Digital simulation of a Multinode Reactor During Loss of Coolant, BAW-10092, Revision 3, Babcock and Wilcox, October, 1982.

43-10192-Q-03



FTI-98-1794
June 10, 1998

Document Control Desk
U. S. Nuclear Regulatory Commission
Washington, DC 20555-0001

Subject: Response to a Typographical Error in BWNT LOCA - BWNT Loss-of-Coolant Accident Evaluation Model for Once-Through Steam Generator Plants, BAW-10192P

- References:**
- 1) Letter (JHT/94-18) from J. H. Taylor (B&W Nuclear Technologies) to Robert C. Jones (US NRC), dated February 15, 1994; Subject: "BWNT LOCA – BWNT Loss-of-Coolant Accident Evaluation Model for Once-Through Steam Generator Plants," BAW-10192P.
 - 2) Letter from James E. Lyons (US NRC) to J. H. Taylor (Framatome Technologies), dated February 18, 1997; Subject: Acceptance for Referencing of Topical Report BAW-10192-P, "BWNT Loss-of-Coolant Accident Evaluation Model for Once-through Steam Generator Plants"

Gentlemen:

Framatome Technologies, Inc. (FTI) has discovered a typographical error in the NRC-approved version of the Topical Report BAW-10192-P, BWNT LOCA (Reference 2). The error was discovered in the Large Break Loss-Of-Coolant Accident (LBLOCA) text discussion of the three-operating Reactor Coolant Pump (RCP) study. The purpose of the study was to validate that the four-reactor coolant pump LOCA linear heat rate (LHR) limits were applicable and bounded the three-pump limits. FTI performed the cold leg pump discharge LOCA blowdown study with all possible orientation differences between the break and the inoperable reactor coolant pump. The most limiting blowdown results were continued through the refill and reflood phases of the event to demonstrate that the calculated three-pump consequences were less severe than the corresponding four-pump case consequences. The most severe three-pump case was calculated when the break was located in the cold leg with the inoperable pump. This orientation is inconsistent with the text included in the topical report. Therefore, replacement pages for the original release of Topical Report BAW-10192P (Reference 1) and BAW-10192NP are included.

(LA-189)

3315 Old Forest Road, P.O. Box 10935, Lynchburg, VA 24506-0935
Telephone: 804-832-3000 Fax: 804-832-3663
Internet: <http://www.framatech.com>

This error, discovered by FTI, is found in the text (page A-43, Volume 1, BWNT LOCA) describing the results of the study. The text stated that:

The case with the locked rotor in the *intact leg of the broken loop* produced the most severe cladding temperatures at the end of blowdown.

This miscommunication was also found in two other places. The first was in the title of the second case identified in Table A-20 (page A-77) of Volume 1, *Break in Unaffected Cold Leg*. The second was in the response to Request for Additional Information (letter JHT/96-33, dated May 6, 1996); specifically, Question 21 in Volume I, which pointed the reviewers back to the text on page A-43 for clarification of the break and inoperable RCP.

Upon review of the calculation files that support the three-pump study, it has been confirmed that the case with the locked rotor in the broken leg produces the most severe results. (It should be noted that Table A-19 correctly identifies that the case with the inactive pump in loop 2A produces the most severe results.) Further, the case identified on Table A-20 has this configuration, and the title of the third column should be "Inoperable Pump in Broken Cold Leg."

FTI is enclosing corrections to these text errors. The changes to the text on page A-43 and Table A-20 of Volume I of the BWNT LOCA topical are identified by change bars in the right margin. Further, the response to Question 21, Volume I, of the Requests for Additional Information (attachment to letter JHT/96-33, May 6, 1996) is incorrect. The second paragraph of that response should have read:

The heading in Table A-20 is confusing. The text on revised page A-43 (second paragraph) identifies that the most severe results were calculated with the inactive pump located in the broken leg. This representation, as seen on Figure 4-5 (Page 4-49), makes reactor coolant pump Component 265 inactive.

The errors noted do not alter the conclusions that the consequences of the four-pump LOCA analyses are more severe than those for the three-pump. The four-pump limits remain bounding for the three-pump limits. FTI also reviewed all LOCA analyses to determine if any three-pump LOCA analyses had been performed incorrectly. A three-pump LOCA analysis was completed for the lowered-loop 177-fuel assembly plant type. That study correctly placed the inoperable pump in the broken cold leg. Therefore, although the topical text was incorrect, the analyses and application studies were performed correctly.

-3-

Eight (8) copies of the two corrected topical report pages are enclosed for replacement in the five (5) Proprietary and three (3) Non-Proprietary copies sent to the NRC with the Reference 1 letter. In accordance with the original designation of the report, these pages should be considered "Proprietary." An affidavit supporting that classification is included. The change pages will also be included in the accepted versions of the Proprietary and Non-Proprietary "BWNT LOCA" topical report.

If you have any questions regarding this material, please contact John Klingenfus at (804) 832-3294.

Very truly yours,


J. J. Kelly, Manager
B&W Owners Group Services

JJK/bcc

c: L. Lois/NRC
 J. L. Birmingham/NRC
 J. A. Klingenfus/FTI-OF53
 D. R. Page/FTI-OF53
 R. J. Schomaker/FTI-OF57

AFFIDAVIT OF JOSEPH J. KELLY

- A. My name is Joseph J. Kelly. I am Manager of B&W Owners Group Services for Framatome Technologies, Inc. (FTI), and as such, I am authorized to execute this Affidavit.
- B. I am familiar with the criteria applied by FTI to determine whether certain information of FTI is proprietary and I am familiar with the procedures established within FTI to ensure the proper application of these criteria.
- C. In determining whether an FTI document is to be classified as proprietary information, an initial determination is made by the Unit Manager, who is responsible for originating the document, as to whether it falls within the criteria set forth in Paragraph D hereof. If the information falls within any one of these criteria, it is classified as proprietary by the originating Unit Manager. This initial determination is reviewed by the cognizant Section Manager. If the document is designated as proprietary, it is reviewed again by me to assure that the regulatory requirements of 10 CFR Section 2.790 are met.
- D. The following information is provided to demonstrate that the provisions of 10 CFR Section 2.790 of the Commission's regulations have been considered:
 - (i) The information has been held in confidence by FTI. Copies of the document are clearly identified as proprietary. In addition, whenever FTI transmits the information to a customer, customer's agent, potential customer or regulatory agency, the transmittal requests the recipient to hold the information as proprietary. Also, in order to strictly limit any potential or actual customer's use of proprietary information, the substance of the following provision is included in all agreements entered into by FTI, and an equivalent version of the proprietary provision is included in all of FTI's proposals:

AFFIDAVIT OF JOSEPH J. KELLY (Cont'd.)

"Any proprietary information concerning Company's or its Supplier's products or manufacturing processes which is so designated by Company or its Suppliers and disclosed to Purchaser incident to the performance of such contract shall remain the property of Company or its Suppliers and is disclosed in confidence, and Purchaser shall not publish or otherwise disclose it to others without the written approval of Company, and no rights, implied or otherwise, are granted to produce or have produced any products or to practice or cause to be practiced any manufacturing processes covered thereby.

Notwithstanding the above, Purchaser may provide the NRC or any other regulatory agency with any such proprietary information as the NRC or such other agency may require; provided, however, that Purchaser shall first give Company written notice of such proposed disclosure and Company shall have the right to amend such proprietary information so as to make it non-proprietary. In the event that Company cannot amend such proprietary information, Purchaser shall prior to disclosing such information, use its best efforts to obtain a commitment from NRC or such other agency to have such information withheld from public inspection.

Company shall be given the right to participate in pursuit of such confidential treatment."

AFFIDAVIT OF JOSEPH J. KELLY (Cont'd.)

- (ii) The following criteria are customarily applied by FTI in a rational decision process to determine whether the information should be classified as proprietary. Information may be classified as proprietary if one or more of the following criteria are met:
- a. Information reveals cost or price information, commercial strategies, production capabilities, or budget levels of FTI, its customers or suppliers.
 - b. The information reveals data or material concerning FTI research or development plans or programs of present or potential competitive advantage to FTI.
 - c. The use of the information by a competitor would decrease his expenditures, in time or resources, in designing, producing or marketing a similar product.
 - d. The information consists of test data or other similar data concerning a process, method or component, the application of which results in a competitive advantage to FTI.
 - e. The information reveals special aspects of a process, method, component or the like, the exclusive use of which results in a competitive advantage to FTI.
 - f. The information contains ideas for which patent protection may be sought.

AFFIDAVIT OF JOSEPH J. KELLY (Cont'd.)

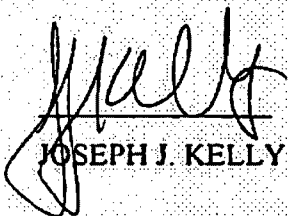
The document(s) listed on Exhibit "A", which is attached hereto and made a part hereof, has been evaluated in accordance with normal FTI procedures with respect to classification and has been found to contain information which falls within one or more of the criteria enumerated above. Exhibit "B", which is attached hereto and made a part hereof, specifically identifies the criteria applicable to the document(s) listed in Exhibit "A".

- (iii) The document(s) listed in Exhibit "A", which has been made available to the United States Nuclear Regulatory Commission was made available in confidence with a request that the document(s) and the information contained therein be withheld from public disclosure.
- (iv) The information is not available in the open literature and to the best of our knowledge is not known by ABB CE, EXXON, General Electric, Westinghouse or other current or potential domestic or foreign competitors of FTI.
- (v) Specific information with regard to whether public disclosure of the information is likely to cause harm to the competitive position of FTI, taking into account the value of the information to FTI; the amount of effort or money expended by FTI developing the information; and the ease or difficulty with which the information could be properly duplicated by others is given in Exhibit "B".

E. I have personally reviewed the document(s) listed on Exhibit "A" and have found that it is considered proprietary by FTI because it contains information which falls within one or more of the criteria enumerated in Paragraph D, and it is information which is customarily held in confidence and protected as proprietary information by FTI. This report comprises

AFFIDAVIT OF JOSEPH J. KELLY (Cont'd.)

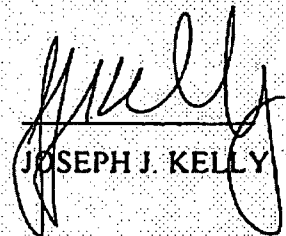
Information utilized by FTI in its business which afford FTI an opportunity to obtain a competitive advantage over those who may wish to know or use the information contained in the document(s).



JOSEPH J. KELLY

State of Virginia)
) SS. Lynchburg
City of Lynchburg)

Joseph J. Kelly, being duly sworn, on his oath deposes and says that he is the person who subscribed his name to the foregoing statement, and that the matters and facts set forth in the statement are true.



JOSEPH J. KELLY

Subscribed and sworn before me
this 10th day of June 1998.

Brenda C. Cardona
Notary Public in and for the City
of Lynchburg, State of Virginia.

My Commission Expires July 31, 1999

EXHIBITS A & B

EXHIBIT A

Two corrected pages from BWNT Proprietary Report BAW-10192P, "BWNT LOCA - BWNT Loss-of-Coolant Accident Evaluation Model for Once-Through Steam Generator Plants"

- Page A-43 A.8. Three Operating RC Pumps at 75 Percent Full Power Study.
- Page A-77 Table A-20. Parameter Comparison for the 3-Pump, 75 Percent Power Study.

EXHIBIT B

The above listed documents contain information which is considered Proprietary in accordance with Criteria b, c and d of the attached affidavit.

A.8. Three Operating RC Pumps at 75 Percent Full Power Study

A LBLOCA analysis was performed with initial conditions based on three operational pumps, with a core power set to 75 percent full power. This study was performed to provide a basis for selection of the most-limiting input parameters and to determine if the four-pump LOCA limits can apply to the three-pump condition. The base case peak linear heat rate of 16.5 kW/ft was used in these three-pump analyses. The base case radial peak was increased from 1.626 to 2.168 to preserve the peak linear heat rate.

Three blowdown calculations were made with the locked rotor located in (1) the broken leg pump (Pump 2A), (2) the intact leg pump of the broken loop (Pump 2B), or (3) one of the intact loop pumps (Pump 1A). A comparison of blowdown results is presented in Figures A-137 through A-141 and in Table A-19. The three-pump case EOB times were all 1.9 to 3.2 seconds longer than the four-pump base case. The case with the locked rotor in the broken leg produced the most severe cladding temperatures at the end of blowdown. This EOB temperature was 15 F below the base case value. It is expected that this case will have lower clad temperatures during reflood due to lower core decay heat and less stored fuel pin energy.

To confirm that the base case remains limiting, the REFLOD3B and BEACH calculations were performed for the worst three-pump operation case. The results are presented in Figures A-142 through A-146 and summarized in Table A-20. They show that the PCT of 1886 F was predicted in an unruptured segment. This peak is 97 F lower than the peak predicted by the base EM case. The higher flooding rates reduced the peak significantly. Therefore, the LOCA limits established for four-pump operation at full power are bounding for three-pump operation at 75 percent power.

43-10192Q-03
BWNT PROPRIETARY

Table A-20. Parameter Comparison for the 3-Pump, 75 Percent Power Study.

<u>Parameter</u>	<u>Base Case</u>	<u>Inoperable Pump In Broken Cold Leg</u>
CFT Flow Begins, s	12.8	13.4
End-of-Bypass, s	18.59	19.45
End-of-Blowdown (EOB), s	21.045	22.645
Liquid Mass in RV Lower Plenum at EOB, lbm	15799.8	17331.5
Integrated accumulator injection at EOB, lbm	48956.7	52962.4
Integrated Mass Removed at EOB, lbm		
Break	549268.	549099.
ECCS Bypass	47796.8	52074.0
Integrated energy out the break at EOB, BTU	3.5151x10 ⁸	3.5260x10 ⁸
RV Lower Plenum Filled, s	27.666	28.998
LPI Flow Begins, s	40.060	40.060
CFTs Empty, s	45.330	46.204
Clad Rupture Time, s	21.195	25.095
Unruptured Segment:		
PCT, F	10	10
Time, s	1958.8	1886.2
	~63.0	58.805
Ruptured Segment:		
PCT, F	11	11
Time, s	1983.4	1752.9
	30.473	~30.6
Average Oxidation Increase, %		
Hot Channel	0.70	0.51
Average Channel	0.066	0.048
Whole-Core Hydrogen Generation, %	0.30	0.22
Average Channel Quench Time, s	232.2	162.2

Table A-21. Parameter Comparison for the 2-, 6-, and 10-ft LOCA Limit Demonstration Cases.

<u>Parameter</u>	<u>2.865-ft</u>	<u>6.285-ft</u>	<u>9.705-ft</u>
CFT Flow Begins, s	12.8	12.8	12.6
End-of-Bypass, s	18.67	18.59	18.50
End-of-Blowdown (EOB), s	21.130	21.045	20.985
Liquid Mass in RV Lower Plenum at EOB, lbm	15529.9	15799.8	15311.8
Integrated accumulator injection at EOB, lbm	49164.7	48956.7	49053.5
Integrated Mass Removed at EOB, lbm			
Break	549139.	549268.	549628.
ECCS Bypass	48004.0	47796.8	47687.4
Integrated energy out the break at EOB, BTU	3.5217x10 ⁸	3.5151x10 ⁸	3.5144x10 ⁸
RV Lower Plenum Filled, s	27.694	27.666	27.588
LPI Flow Begins, s	40.060	40.060	40.060
CFTs Empty, s	44.333	45.330	45.213
Clad Rupture Time, s	20.070	21.195	21.585
Unruptured Segment:			
PCT, F	7	10	16
Time, s	1959.5	1958.8	2020.7
	-54.0	-63.0	71.140
Ruptured Segment:			
PCT, F	6	11	18
Time, s	1986.7	1983.4	1888.1
	30.002	30.473	-36.0
Average Oxidation Increase, %			
Hot Channel	0.68	0.70	0.67
Average Channel	0.039	0.066	0.091
Whole-Core Hydrogen Generation, %	0.28	0.30	0.30
Average Channel Quench Time, s	219.8	232.2	239.1